ABSTRACT

Title of Document: AIRSIDE PASSIVE HEAT TRANSFER ENHANCEMENT, USING MULTI-SCALE ANALYSIS AND SHAPE OPTIMIZATION, FOR COMPACT HEAT EXCHANGERS WITH SMALL CHARACTERISTIC LENGTHS

Daniel Fernandes Bacellar, Doctor of Philosophy, 2016

Directed By: Reinhard Radermacher, Professor
Department of Mechanical Engineering

The study of compact heat exchangers (HX) is a very common, although broad topic that draws interest from many engineering applications. Most technologies contain at least one HX serving as a fundamental component for the proper system functioning. The rapid worldwide population growth, increasing demand for energy resources, widespread environmental concerns, space exploration efforts and economy are all good reasons for developing smaller, lighter and more efficient HX's. This research sheds the light on the next generation of heat exchangers, with a focus on air-to-fluid applications.

For incompressible flows and low-pressure applications, the HX's airside thermal resistance is the major limitation to overall thermal conductance. On conventional surfaces fins are required, but bring many drawbacks. Among these include being prone to fouling/frosting, reduced heat transfer coefficient, higher friction resistance, and more material consumption. Tubes by nature provide more valuable heat transfer than do fins; there is little focus on tubes in the literature.

The first objective of this work is to discuss the fundamental aspects of primary (tubes) and secondary (fins) surfaces, with the aid of numerical analyses. The latter demonstrates how the reduction of characteristic length and novel shapes impact surface performance and compactness of finless and finned tubes. A further discussion is presented arguing that conventional fin concepts are not always beneficial.

The second objective of this work entails developing a comprehensive multi-scale analysis with topology and shape optimization methodology leveraging automated CFD simulations and approximation assisted optimization. Novel finless air-to-fluid HX concepts were developed, for single-phase and two-phase applications, and achieved more than 20% reduction in size, 20% better performance and 20% less material than state-of-the-art HX's including microchannel HX's. Two prototypes (one manufactured in metal 3D printing) were tested in an in-house wind tunnel. The numerical predictions agree with the experimental results in less than 5% deviation for total capacity, 10% for airside heat transfer coefficient and 20% for air pressure drop.

Finally, the last objective is to present the development of robust and computationally inexpensive tools that can accurately predict CFD simulation responses for conventional tube and fin surfaces using small diameter tubes (<5.0mm).

AIRSIDE PASSIVE HEAT TRANSFER ENHANCEMENT, USING MULTI-SCALE ANALYSIS AND SHAPE OPTIMIZATION, FOR COMPACT HEAT EXCHANGERS WITH SMALL CHARACTERISTIC LENGTHS

By

Daniel Fernandes Bacellar

Dissertation submitted to the Faculty of the Graduate School of the
University of Maryland, College Park, in partial fulfillment
of the requirements for the degree of
Doctor of Philosophy
2016

Advisory Committee:
Professor Reinhard Radermacher, Chair
Professor James Baeder (Dean's Representative)
Professor Jungho Kim
Professor Bao Yang
Professor Marino diMarzo
Dr. Vikrant Aute

Dedication

To Heather and Julia.

Acknowledgements

First and foremost, I would like to express my lifetime gratitude to Professor Reinhard Radermacher who believed in my potential when few did. It was a privilege being part of this world class research team, thank you Professor!

I would like to thank Dr. Vikrant Aute who was to me an advisor, a mentor and a role model. This research could have never happened without his assistance. I probably haven’t shown enough appreciation for everything he has done.

I would also like to thank all of my professors during my PhD, in particular the members of this committee: Dr. Jungho Kim, Dr. Bao Yang, Dr. James Baeder and Dr. Marino di Marzo.

I want to thank Dr. Jiazhen Ling for his help with numerical analysis and for having a broad knowledge of engineering faculties that have helped me in many ways; Mr. Jan Muehlbauer for his unmatched experience in the lab and contributions to the novel heat exchanger designs; Zhiwei Huang for all of her effort in testing the heat exchangers and providing the data that successfully validated my work; and Mr. Yoram Shabtay for his relentless effort in finding manufacturing solutions to the novel heat exchangers.

I want to acknowledge my predecessors in the quest for the next generation of heat exchangers: Dr. Khaled Saleh and Dr. Omar Abdelaziz who, not only provided the baseline framework for this research, but also gave me invaluable advices on CFD modeling and optimization.

I hold in high regards Dr. Hongtao Qiao and Dr. Long Huang - whom I also had the privilege of collaborating with – for sharing their knowledge and expertise that were fundamental for my growth as a researcher. I would also like to mention a few colleagues and friends who also had an influence on my graduate life experience, either directly or indirectly to my research: Dr. Sahil Popli, Dr. Mohamed Beshr, Ms. Radia Eldeeb, Dr. Moon Soo Lee, Ms. Camli Badrya, Dr. Ayan Moitra, Mr. Viren Bhanot and Zhenning Li.

I would also like to thank Mary Baugher and Tanya Pringle; their administrative and paper editing support are amongst the key reasons for the center's and students' successful achievements. I am very grateful for all of their support throughout these years.

I grew up in an environment where I had great role models of academic excellence and high standards; I attribute my pursuit for this degree in great part to my mother, Dr. Flora Fernandes, and step-father, Dr. Sergio Matioli. I'd like to thank my father, Flavio Bacellar, for always encouraging me not to be step away from challenges and seeking what is best for me. I must also acknowledge the endless support from my grandparents Marialba Bacellar, Mariano Bacellar and Adhemar Fernandes.

Last (but definitely not the least!), I'd like to thank my wife, Heather Sutton, for her patience and emotional support during this long and winding road.

This work was supported by the United States Department of Energy Grant Number DE-EE0006114 and the Modeling and Optimization Consortium of the Center for Environmental Energy Engineering at the University of Maryland.

Table of Contents

Chapter 1: Introduction 1

1.1 Motivation 1

1.2 Literature Review 3

1.2.1 Airside Heat Transfer 3

1.2.2 Computational Fluid Dynamics (CFD) 7

1.2.3 Numerical Optimization 10

1.2.4 Performance Evaluation Criteria (PEC) 12

1.2.5 Airside Heat Transfer and Friction Characterization in Crossflow 19

1.2.6 Fabrication of Heat Exchangers with Complex Surfaces 25

1.2.7 Literature Gaps 26

Chapter 2: Research Objectives 29

2.1 Summary 29

2.2 Dissertation Organization 30

Chapter 3: Theoretical Background 34

3.1 Airside Modeling 34

3.1.1 CFD Modeling and Simulation 34

3.1.2 CFD Data Reduction 39

3.1.3 CFD Grid Uncertainty Analysis 41

3.1.4 Non-Uniform Rational B-Splines (NURBS) 44

3.2 Heat Exchanger Modeling 46

3.3 Numerical Optimization 48

3.3.1 Design of Experiments 50
3.3.2 Kriging Metamodeling 50
3.3.3 Multi-Objective Optimization 51
Chapter 4: First & Second Order Analyses 52
4.1 First Order Analysis 52
4.2 Second Order Analysis 53
4.2.1 Surface Level Analysis 54
Chapter 5: Multi-Scale Analysis and Shape Optimization 62
5.1 Design Framework 62
5.2 Concept Surfaces 62
5.2.1 Round Tube Heat Exchangers (RTHX & FTHX) 63
5.2.2 NURBS Tube Heat Exchangers (NTHX) 71
5.2.3 Webbed-NURBS Tube Heat Exchangers (WTHX) 74
5.2.4 Airfoil-Shaped Tube Heat Exchangers (AFHX) 76
5.3 Design Problems (DP) 78
5.3.1 DP I: 1.0kW Single-Phase Heat Exchangers 78
5.3.2 DPII: 10.0kW Single-Phase Heat Exchangers 98
5.3.3 DP III: Two-Phase Heat Exchangers 101
Chapter 6: CFD-Based Correlation Development 106
6.1 Round Finless Tubes 107
6.1.1 Data Reduction 108
6.1.2 Correlations 108
6.1.3 Verification 113

6.2 Plain Fin-and-Tubes....114
6.2.1 Data Reduction.... 115
6.2.2 Correlation 115
6.3 Wavy Fin-and-Tubes 117
6.3.1 CFD model.... 118
6.3.2 Correlation 121
Chapter 7: Surface Optimization Study 124
7.1 Optimization Results....126
7.1.1 Discussion 130
Chapter 8: Conclusions 134
8.1 Summary of Contributions....134
8.2 List of Publications 139
8.3 Recommendations for Future Work....143
Appendices.... 148
Appendix A – Non-Uniform Rational B-Spline C# code 148
Appendix B – NTHX-001 Stress Analysis 150
Appendix C – Optimum HX Designs 154
RTHX.... 154
FTHX 183
NTHX 189
WTHX.... 194
AFHX.... 198
Appendix D – Experimental Materials, Methods and Data 203

Appendix E – Correlation Data....210

Wavy Fin Correlation Coefficients Matrices.... 210

Appendix F – Optimum Heat Transfer Surfaces 214

Surface Optimization Study Results.... 214

Appendix G - Performance Evaluation Criteria Analysis....245

Introduction.... 245

HX Evaluation Criteria 249

HX Design 252

List of Tables

Table 1. Summary of HX optimization methods (adapted from Huang et al. [85]) ... 10

Table 2. PEC for single-phase HX (adapted from Webb and Kim [90]).................... 14

Table 3. Selected correlations for finless tube bundle. 22

Table 4. Most relevant fin-and-tube airside correlations in the literature.................. 23

Table 5. Design variable types. 63

Table 6. RTHX and FTHX Design space. 65

Table 7. NTHX Design space. 72

Table 8. WTHX Design space. 75

Table 9. AFHX Design space. 77

Table 10. 1.0kW Baseline MCHX. 78

Table 11. NTHX-001 Numerical results compared to the baseline MCHX. 81

Table 12. RTHX-001 Numerical results compared to the baseline MCHX. 83

Table 13. Baseline cycle verification. 101

Table 14. Two-Phase HX’s operating conditions. 102

Table 15. Finless tubes correlations design space. 109

Table 16. Correlations I coefficients. 110

Table 17. Correlations II coefficients. 110

Table 18. Correlations III coefficients. 111

Table 19. Round finless tubes correlations fitness. 112

Table 20. Flat fin and tube correlations design space. 115

Table 21. Fin-and-tube correlations coefficients. 116

Table 22. Flat fin-and-tube correlations fitness. 117

Table 23. Wavy fin-and-tube correlation design space. 118

Table 24. Air thermophysical properties for wavy fin correlations. 122

Table 25. Wavy fins correlations fitness... 122

Table 26. Parametric Variables. 125

Table 27. Surface Optimization Study Computational Cost. 125

Table 28. Material yield strength (SolidWorks® database). 153

Table 29. NTHX-001 Stress analysis results. 153

Table 30. Optimum RTHX dimensions. 154

Table 31. Optimum RTHX performance and operating conditions. 169

Table 32. FTHX optimum designs dimensions. 184

Table 33. Optimum FTHX performance and operating conditions. 186

Table 34. NTHX dimensions. 189

Table 35. NTHX performances and operating conditions. 191

Table 36. WTHX dimensions. 194

Table 37. WTHX performance and operating conditions. 196

Table 38. AFHX dimensions. 199

Table 39. AFHX performance and operating conditions. 201

Table 40 – Specifications of test facility.. 203

Table 41 - Accuracy of every sensor of airside. 206

Table 42 - Uncertainty calculation of airside (courtesy from Zhiwei Huang).......... 206

Table 43. RTHX-001 Test data.. 207

Table 44. NTHX-001 Test data. 207

Table 45. RTHX-468 Test data.. 208

Table 46. Herringbone correlation: parameters power matrices. 210

Table 47. Herringbone correlation: coefficients arrays. 211

Table 48. Smooth correlation: parameters power matrices. 212

Table 49: Smooth correlation: coefficients arrays. 213

Table 50. WFTS Optimum designs dimensions. 219

Table 51. WFTS optimum designs performance. 228

Table 52. RFTS Optimum designs dimensions. 237

Table 53. RFTS optimum designs performance. 241

Table 54: Optimization Problem. 252

List of Figures

Figure 1. Local heat transfer coefficient. 4

Figure 2. Boundary layer disruption – attachment sites on various fin surfaces: a) Plain; b) Louver; c) Slit; d) Perforated. 5

Figure 3. Streamwise periodic flow computational domain: a) 2-Dimension; b) 3-Dimension. 9

Figure 4. Dissertation organization workflow. 33

Figure 5. Typical CFD 2-D computational domain. 36

Figure 6. Two-dimensional computational domain mesh schemes: a) triangle; b) quadrilateral. 37

Figure 7. Three-dimensional computational domain. 37

Figure 8. Dry air properties as function of temperature. 39

Figure 9. Sequentially increasing grid resolutions. 42

Figure 10. 3rd degree NURBS curve and base functions example from Piegl and Tiller [157]. 44

Figure 11. Tube shape parameterization. 46

Figure 12. Air-to-fluid cross flow HX's. 46

Figure 13. HX Temperature profile illustration. 47

Figure 14. Numerical optimization framework. 49

Figure 15. Parallel Parameterized CFD (PPCFD) framework. 49

Figure 16. Space sampling example: a) biased; b) unbiased (LHS). 50

Figure 17. First order analyses I: compactness, material utilization and internal volume. 53

Figure 18. First order analyses II: fin-to-tube surface ratio. 53

Figure 19. Second order analysis I: thermal-hydraulic characteristics. 54

Figure 20. Thermal characteristics for same Reynolds and different diameters......... 55

Figure 21. Hydraulic characteristics for same Reynolds and different diameters 55

Figure 22. Thermal characteristics for same velocities and different diameters. 55

Figure 23. Hydraulic characteristics for same velocities and different diameters. 56

Figure 24. Momentum boundary layer over different tube diameters and air velocities. 57

Figure 25. Normalized temperature and velocity profiles within the boundary layer at 25% of the tube surface for same velocity. 57

Figure 26. Surface temperature gradient over different tube diameters and air velocities. 58

Figure 27. Surface velocity gradient over different tube diameters and air velocities. 58

Figure 28. Momentum boundary layer over different tube diameters and Reynolds. 58

Figure 29. Normalized temperature and velocity profiles within the boundary layer at 25% of the tube surface for same Reynolds number. 59

Figure 30. Surface temperature gradient over different tube diameters and Reynolds. 59

Figure 31. Surface velocity gradient over different tube diameters and Reynolds. 59

Figure 32. Tube shapes: a) Round; b) Ellipse; c) Eye; d) Airfoil leading edge; e) Airfoil trailing edge. 60

Figure 33. Thermal-hydraulic characteristics of airflow over different shapes. 61

Figure 34. Heat exchanger design framework. 64

Figure 35. Round finless tubes (RTHX): a) In-line; b) Staggered. 65

Figure 36. Flat fin and tube HX (FTHX) 65

Figure 37. RTHX computational domain and mesh: a) staggered; b) in-line. 66

Figure 38. CFD GCI Analysis for BTHX in staggered and in-line arrangements. 66

Figure 39. FTHX Computational domain and mesh. 67

Figure 40. CFD GCI Analysis for FTHX. 67

Figure 41. Example of contour plots on different grid resolutions for the FTHX. 67

Figure 42. Heat transfer coefficient metamodel verification for RTHX in staggered and in-line arrangements for 50 random samples. 68

Figure 43. Pressure drop metamodel verification for RTHX in staggered and in-line arrangements for 50 random samples. 68

Figure 44. Metamodel verification for FTHX for 50 random samples. 69

Figure 45. Equivalent round tube arrangements. 69

Figure 46. In-line vs. Staggered. 70

Figure 47. Contours of velocity angle. 71

Figure 48. Local heat transfer coefficient and skin friction coefficient at the tube wall. 71

Figure 49. NTHX surface concept. 72

Figure 50. NTHX Profile parameterization. 72

Figure 51. NTHX Computational domain. 73

Figure 52. NTHX GCI Analysis. 73

Figure 53. NTHX Metamodel verification against 961 random samples. 74

Figure 54. WTHX Surface concept. 74

Figure 55. WTHX Profile parameterization. 75

Figure 56. WTHX Computational domain. 75

Figure 57. WTHX Metamodel verification. 76

Figure 58. AFHX Concept. 77

Figure 59. AFHX Computational domain. 77

Figure 60. AFHX Metamodel verification. 78

Figure 61. CFD Results for the NTHX-001: a) velocity; b) pressure; c) temperature. 80

Figure 62. Proof-of-concept NTHX-001 dimensions. 80

Figure 63. DP I: RTHX & FTHX Optimization results. 82

Figure 64. RTHX-001 CFD verification contour plots: a) velocity; b) pressure; c) temperature. 83

Figure 65. DP I: NTHX Optimization results I. 84

Figure 66. DP I: NTHX Optimization results II. 85

Figure 67. DP I: NTHX Metamodel verification for the optimum designs. 85

Figure 68. DP I: WTHX & AFHX Optimization results. 86

Figure 69. DP I HX Optimization map I. 87

Figure 70. DP I Optimization map II. 88

Figure 71. Velocity magnitude and angle contour plots for selected designs for DP I: a) RTHX-001; b) NTHX-001; c) NTHX-030; d) WTHX-011; e) AFHX-001. 89

Figure 72. Static pressure and temperature contour plots for selected designs for DP I: a) RTHX-001; b) NTHX-001; c) NTHX-030; d) WTHX-011; e) AFHX-001. 90

Figure 73. DP I: Airside performance parametric analysis.. 92

Figure 74. RTHX-001 Prototype drawing. 94

Figure 75. Stainless steel RTHX-001 sample images.. 94

Figure 76. NTHX-001 Prototype drawing. 95

Figure 77. NTHX-001 sample images. 95

Figure 78. Experimental validation: energy balance and overall capacity. 96

Figure 79. Experimental validation: airside heat transfer coefficient and pressure drop.

.... 97

Figure 80. NTHX-001 CFD Validation: contour plots. 97

Figure 81. DP II: Optimization results... 99

Figure 82. RTHX-468 Prototype. 99

Figure 83. RTHX-468 Experimental capacity results.. 100

Figure 84. Thermal imaging on RTHX-468 prototype. 100

Figure 85. System level study for COP improvement. 102

Figure 86. HX Pass configurations. 103

Figure 87. DP III: Optimization results. 104

Figure 88. DP III: System level analysis. 105

Figure 89. CFD-Based correlation development. 106

Figure 90. Correlations I, II and III verification against source data........................ 112

Figure 91. Correlations I and III verification against random samples. 112

Figure 92. Correlations I verification against experimental data............................. 113

Figure 93. Flat fin. 114

Figure 94. Flat fin and tube contour plots: a) velocity; b) temperature; c) pressure. 114

Figure 95. Flat fin correlations verification against source data. 116

Figure 96. Wavy fin-and-tube surface: a) Herringbone; b) Smooth (Sinusoidal). ... 117

Figure 97. Wavy fin computational domain and mesh. 119

Figure 98. Equivalent wavy fins: a) Herringbone; b) Smooth. 119

Figure 99. Sample velocity contour plots: a) Herringbone and b) smooth wavy fins. 120

Figure 100. Sample temperature contour plots: a) Herringbone and b) smooth wavy fins.. 120

Figure 101. Sample pressure contour plots: a) Herringbone and b) smooth wavy fins. 120

Figure 102. Grid resolution uncertainty for wavy fins: a) fine; b) base; c) coarse meshes. 121

Figure 103. Wavy fin correlations verification against source data. 122

Figure 104. Herringbone correlations verification against 120 random samples. 123

Figure 105. Herringbone correlation comparison. 123

Figure 106. Finless tubes surface optimization results I: tube diameter. 126

Figure 107. Finless tubes surface optimization results II: tube diameter. 126

Figure 108. Finless tubes surface optimization results I: hydraulic diameter........... 127

Figure 109. Finless tubes surface optimization results II: hydraulic diameter. 127

Figure 110. Finless tubes surface optimization results I & II: pitch ratio................ 128

Figure 111. Wavy fin surface optimization results I: tube diameter........................ 128

Figure 112. Wavy fin surface optimization results II: tube diameter. 129

Figure 113. Wavy fin surface optimization results I: hydraulic diameter. 129

Figure 114. Wavy fin surface optimization results II: hydraulic diameter. 130

Figure 115. Wavy fin surface optimization results I and II: pitch ratio. 130

Figure 116. Selected surface optimization case. 132

Figure 117. Equivalent surfaces (same D_h) under wide range of Reynolds numbers. 133

Figure 118. Winglets on high-performance tube shape. 144

Figure 119. High-performance tube and extended surface shapes. 145

Figure 120. Extension of the multi-scale analysis and shape optimization methodology. 145

Figure 121. Fan-coil single unit concept [169]. 146

Figure 122. Stress analysis problem setup. 150

Figure 123. Isotropic stress components and stress-strain engineering curve. 151

Figure 124. NTHX-001 Cut views.. 151

Figure 125. NTHX-001 Header and tubes cross sections. 152

Figure 126. NTHX-001 Header and tube meshes. 152

Figure 127. VonMises stress contour plots for the NTHX-001 tube. 152

Figure 128. Deformation contour plots for the NTHX-001 tube. 153

Figure 129. Round finless tubes (BTHX): a) in-line; b) staggered.......................... 154

Figure 130. Flat fin and tube HX (FTHX). 183

Figure 131. NTHX surface concept. 189

Figure 132. WTHX concept.. 194

Figure 133. AFHX Concept. 198

Figure 134 - Schematic diagram of air-side test facility. 203

Figure 135 - Schematic of cold water loop (top), glycol water loop (middle), hot water loop (bottom) (courtesy from Zhiwei Huang). 204

Figure 136 - Schematic diagram of water/brines system loop................................. 204

Figure 137 - Schematic diagram of refrigerant system with oil loop. 205

Figure 138 - Schematic diagram of refrigerant system without oil loop (courtesy from Zhiwei Huang). 205

Figure 139. Surface optimization results (D_h=0.5mm). 214

Figure 140. Surface optimization results (D_h=1.0mm). 215

Figure 141. Surface optimization results (D_h=1.5mm). 216

Figure 142. Surface optimization results (D_h=2.5mm). 217

Figure 143. Surface optimization results (D_h=3.0mm). 218

Figure 144. Wavy fin surface segment. 219

Figure 145. RFTS Segment... 237

Figure 146: HX surface types: a) RTHX; b) WTHX... 252

Figure 147: HX Design results: a) RTHX; b) WTHX... 253

Figure 148: Entropy Generation: a)RTHX; b) WTHX.. 254

Nomenclature

A_{cs}	Cross section area	m^2
A_c	Minimum free flow area (σA_{fr})	m^2
A_{fin}	Fin surface area	m^2
A_{fr}	Frontal face area	m^2
A_o	Total surface area	m^2
A_t	Tube surface area	m^2
C	Heat capacitance rate	W/K
C_f	Skin friction coefficient	-
c_p	Specific heat	J/kg.K
d	Depth	mm
D_h	Tube hydraulic diameter	m
D_{hin}	In-tube hydraulic diameter	mm
D_{hs}	Surface hydraulic diameter	mm
D_o	Outer diameter	mm
e	Absolute relative difference	-
f	Friction factor	-
FPI	Fins Per Inch	1/in
F_s	Grid factor of safety	-
GCI	Grid Convergence Index	-
h	Heat transfer coefficient	$W/m^2.K$
h_t	Tube height	mm

h_x	Local heat transfer coefficient	W/m².K
k	Thermal conductivity	W/m.K
k	Turbulent kinetic energy	m²/s
L	Tube length	mm
L_c	Characteristic length	mm
$\dot{m}$	Mas flow rate	g/s
N_r	Number of tube rows (transverse)	-
N_t	Number of tube rows (longitudinal)	-
Nu	Nusselt number	-
p	Spatial order of accuracy	-
p^*	Observed order of accuracy	-
p^{**}	Effective order of accuracy	-
P	Pressure	Pa
P	Curve length (tube perimeter)	mm
P_l	Tube longitudinal pitch	mm
P_r	Prandtl Number	-
P_t	Tube transverse pitch	mm
Q	Heat transfer rate	W
r	Grid refinement ratio	-
Re	Reynolds Number	-
r_{Pl}	Longitudinal pitch ratio (Pl/Do)	-
r_{Pt}	Transverse pitch ratio (Pt/Do)	-

T	Temperature	K
u	Velocity	m/s
UA	Thermal conductance	W/K
u_c	Mean velocity at minimum free flow area	m/s
u_{oo}	Uniform velocity	m/s
$\dot{W}''$	Friction power per unit area	W/m^2
w_t	Tube width	mm
x_{cp}	x coordinate Control point	mm
y_{cp}	y coordinate Control point	mm
ΔP	Pressure drop	Pa
j	Colburn j factor	-
f	Darcy friction factor	-
NTU	Number of Transfer Units	-
B	Exergy flow rate	W
s	Specific entropy	J/kg.K
S	Entropy flow rate	W/K
N_s	Number of entropy generation units	-
F_p	Fin pitch	mm
ΔT_{lm}	Logarithmic Mean Temperature Difference	K
V	Volume	cm^3
COP	Coefficient of Performance	-

Greek Letters

δ_t	Tube thickness	mm
δ_f	Fin thickness	mm
ε_M	Eddy diffusivity	m^2/s
μ	Dynamic viscosity	Pa.s
ρ	Density	kg/m^3
σ	Contraction ratio (u/u_{max})	-
α	Thermal diffusivity	m^2/s

Acronyms

AAO	Approximation Assisted Optimization
AFHX	Airfoil Heat Exchanger
CFD	Computational Fluid Dynamics
FTHX	Flat Fin and Tube Heat Exchanger
HX	Heat Exchanger
MCHX	Microchannel Heat Exchanger
NTHX	NURBS Finless Tube Heat Exchanger
PPCFD	Parallel Parameterized CFD
RFTS	Round Finless Tube Surface
RTHX	Round Finless Tube Heat Exchanger
WFTS	Wavy Fin Tube Surface
WTHX	Webbed Tube Heat Exchanger

Chapter 1: Introduction

1.1 Motivation

According to the United States Energy Information Administration (EIA) the US end-use energy consumption in both commercial and residential sectors totaled 39.2 quadrillion BTU (quad) in 2013 [1]. This number is projected to increase by 6.7% by 2040 [1]. Although the residential energy consumption for space heating and cooling have decreased, they still account for 47% (in 2009) energy use in the nation. Nevertheless, the biggest consumers by some extent are those transferring heat, and thus need to use Heat eXchangers (HX).

Westphalen et al. [2] suggested that potential of annual energy savings by heat transfer enhancement of air-cooled HX's could reduce as much as 7 quads, and between 0.7 to 1.1 quads in air-conditioning and refrigeration systems, respectively. These amounts correspond to 20% of the energy consumed by commercial and residential sectors.

One must maximize the overall HX conductance (UA) by Approach Temperature reduction in air-to-fluid HX's to achieve energy conservation. A common way of increasing UA is by increasing surface area; however, such method entails more material consumption and increase of the HX size. This often results in the HX becoming over-sized.

There are many consequences of having over-sized HX's in HVAC&R (Heating, Ventilation, Air-Conditioning and Refrigeration) applications including: a) operate in cycling mode more often (i.e. part-load), thus reducing the COP for being out of the design operating condition; b) installation site may have size limitations; c) extra refrigerant charge is required; d) may have higher costs associated with the extra material needed.

From an environmental perspective resource consumption is a negative impact, thus should be limited as much as possible. Additionally, the additional refrigerant charge poses serious environmental threats (leakage and disposal) due to Global Warming Potential (GWP) and Ozone Depletion Potential (ODP). Therefore, there is an increasing need for reducing the use of such refrigerants, which can be translated in charge reduction in the HX.

The use of compact heat exchangers with high-performance surfaces is a very common (although broad) research topic that draws interests from many engineering applications, and are not exclusive to the HVAC&R industry. Most technologies contain at least one heat exchanger serving as a fundamental component for proper system functioning. The world's rapid population growth, never ending demand for energy resources, dire environmental concerns, expanded space exploration, and goals for increased economic growth are all good motivators for developing smaller, lighter and more efficient HX's.

As computer power and manufacturing technologies (e.g. additive manufacturing) evolve, paradigm shifting is inevitable. A next generation of heat transfer surfaces in smaller scales and complex shapes are starting to take place over conventional HX geometries in order to address the above discussion. This research entails shedding the light on the next generation of heat exchangers, with focus on air-to-fluid applications.

1.2 Literature Review

1.2.1 Airside Heat Transfer

The passive HTE aims more compact surfaces (hydraulic diameters smaller than 6.0mm [3]) and higher thermal-hydraulic ratio [4, 5] without the assistance of any external power. A well-known way of reaching out to these goals is using extended secondary heat transfer surfaces (fins) which, in spite the benefits, bring many drawbacks. Fins will naturally provide additional viscous resistance and have a lower heat transfer potential due to temperature gradient. Furthermore, on the gas side, the fins reduce the mixing and the actual heat transfer coefficient on fins are smaller than the tubes; the resulting overall heat transfer coefficient can be as low as 40% [5] than finless surfaces. Such impact on the thermal resistance is compensated by the additional surface area the fins provide. Fins are also susceptible to performance degradation under fouling or frosting conditions, in particular for enhanced surface fins [6]. Lastly, fins inevitably require additional material consumption, resulting in heavier HX’s, and higher manufacturing costs.

The reason fins are necessary in conventional gas-to-fluid HX’s (tube diameter >5.0mm) is that the primary surfaces cannot provide a minimum thermal resistance that allow the HX to deliver the required capacity within practical dimensions. The idea of a compact high-performance surface [7, 8, 4, 5] is usually associated to the fins, hence, researchers are heavily investing on fins and less on tubes.

The principle of passive HTE is to leverage the developing boundary layer. For simplicity, the reader should follow this discussion assuming a Prandtl number of 1.0 to avoid qualifications as to which boundary layer is being referred to. According to the thermal transport within the boundary layer we know that the local heat transfer coefficient is proportional to the temperature gradient at the surface (equation 1). The thickness of a developing boundary layer is smaller thus resulting in a higher temperature gradient (Figure 1), i.e. higher heat transfer coefficient.

$$h_x\left(T_\infty - T_w\right) = -k\left.\frac{\partial T}{\partial y}\right)_w \tag{1}$$

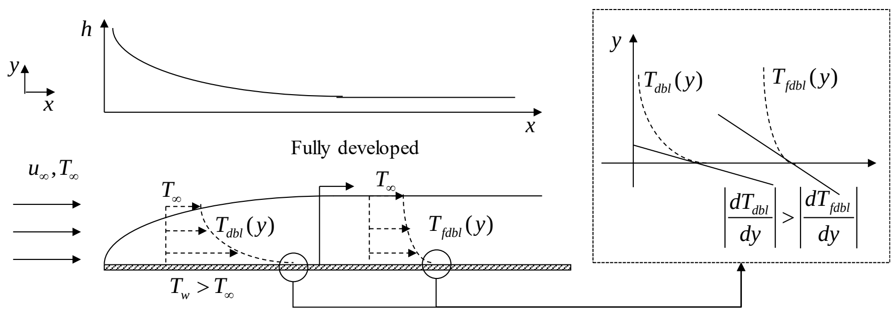

Figure 1. Local heat transfer coefficient.

Typically for on fins, this mechanism is usually exploited with discontinuous surfaces (Figure 2) resulting in a significant improvement over plain flat (Figure 2a) or even wavy fins. Louvered fins (Figure 2b) have been exhaustively investigated, numerically and experimentally, and they are one of the most common types [9, 10, 11, 12, 13, 14, 15, 16, 17, 18] [19]. Slit fins (Figure 2c) [7, 12, 20, 21, 8, 22] are basically fins with offset strips that, unlike louvers, are not rotated thus not redirecting the flow. Perforated fins (Figure 2d) [7, 8, 23, 24] differ from slits and louvers on two matters; on the one hand, it has reduced surface area due to material removal from perforation, on the other hand, there are much less stagnation points resulting in reduced friction resistance [7].

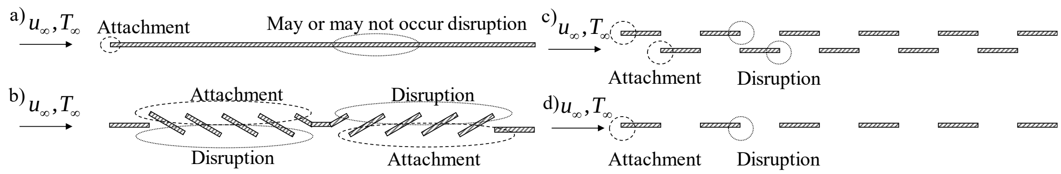

Figure 2. Boundary layer disruption – attachment sites on various fin surfaces: a) Plain; b) Louver; c) Slit; d) Perforated.

In contrast, wavy fins [25, 4, 26, 27] are not a discontinuous surface, but they provide additional surface area for the same volume and can promote chaotic flow [28, 29] which result in enhanced heat transfer. Although wavy fins have lower performance than the discontinuous fin types, they are preferred in some applications where frosting may occur since they are less prone to performance degradation [30, 31]. More recently fins have been improved by addition of winglets, or vortex generators [8, 32, 33, 34, 35, 36, 27, 37], which result in induced turbulence within the boundary layer (or even its disruption), thus enhancing the thermal performance.

The small diameter bare tubes result in high-performance surfaces with sufficiently low thermal resistance that can outperform conventional finned heat exchangers. There are many studies [38, 39, 40, 41, 42, 43] investigating the use of small round finless tubes for HX design, and they have demonstrated great potential for performance enhancement. A major shortcoming of round tubes, however, is the friction resistance, which is also increased with the reduction of the tube size. The consequence is that in order to satisfy a minimum of pressure losses, such surface requires low velocity and relatively short depth. For constant airflow rate this means larger face area [41], which is in many cases, undesirable or prohibitive.

The limitation on friction resistance for round tubes can be addressed by employing alternate shapes. Min and Webb [44] presented a numerical analysis on different tube shapes namely round, oval and flat and the impact on thermal-hydraulic performance of a wavy fin and tube surface, with tube diameters above 6.0mm. Their analyses showed that the flat and oval can have as low as 50% of the pressure drop compared to round tube, while reducing 10-20% the thermal performance. Such reduction in pressure drop is leveraged when combining these alternate tubes with enhanced fins [27, 14, 45, 36]. In fact, flat, multi-port tube and fin heat exchangers have become a high-performance and state-of-the-art. They are commonly called microchannel heat exchangers (MCHX). This type of HX not only has good airside performance, but has mostly, excellent refrigerant side performance. Tuckerman and Pease [46] obtained a factor of 10 in the heat dissipation of integrated chips using a MCHX and have since then, changed the electronics, automotive and aerospace industries [47]. On HVAC&R applications, Kandlikar [48] showed that is a potential of reducing the refrigerant thermal resistance by a factor of 10 with same order reduction in the port size, in addition to significant reduction in refrigerant charge. Huang et al. [49] developed a variable geometry MCHX to address flow mal-distributions and optimizing material usage and localized thermal-hydraulic performance. Although these HX's still require fins, their performance and compactness — but most importantly their low cost and relative ease of manufacturing — are yet to be outdone. Other relevant studies on alternate tube shapes in crossflow include polymer tubes with three different teardrop shapes [50], and cam-shaped tubes [51, 52, 53].

Another significant branch of research is the shape optimization, which has many applications in various engineering problems. Perhaps the most common application is wings and airfoil design within aerospace field. The shape parametrization and optimization for such applications are comprehensively presented in the literature [54, 55], and they can be useful on heat transfer applications as well. High-performing aerodynamic airfoil profiles have been studied on gas-engines [56] and intercooled gas turbines [57]. Other shape optimization studies include convective periodic channels [58, 59, 60, 61], internally enhanced tubes [62, 63, 64, 65] and, most relevant to this work, the periodic crossflow over a tube bundle from Hilbert et al. [66] and Ranut et al. [67]. Their work was limited to the shape optimization while fixing scale and topology parameters. The results are mostly an exercise of their optimization tools and methods but have little use to actual HX design.

1.2.2 Computational Fluid Dynamics (CFD)

Numerical modeling is a fundamental piece to the design and optimization of high-performance HX's. The advances in numerical software have opened new opportunities to researchers worldwide [68]. Computational Fluid Dynamics (CFD), in particular, has become a powerful and reliable tool for HX design and performance prediction.

Some still regard CFD with skepticism [68], and understandably so due to its intrinsic numerical uncertainty, which could possibly lead to significant under or over prediction. There are comprehensive methods that can reliably quantify the uncertainty associated to the model discretization. One standard approach is the five-step Grid Convergence Index (GCI)) method [69, 70, 71], which quantifies the uncertainty of a metric of interest (φ) associated with the grid resolution for at least three mesh sizes. One can perform educated metric modification to the models as the uncertainty is substantially reduced, ensuring that reliable models and consistent simulations. Furthermore, the ultimate verification relies on a model accuracy assessment with experimental data, with which many have claimed to have found good agreements between their CFD simulations and the tested prototypes. Abdelaziz et al. [72] and Xioping et al. [73] verified their CFD models within 10% from experimental data, while Taler and Oclon [74] obtained at most a deviation of 4%. In summary, CFD simulations are a common practice in HX design and optimization and, in spite the uncertainties associated, successful results have been achieved thus shall be continuously used and improved.

1.2.2.1Airside HX Modeling

For HX airside modeling the streamwise periodic flow numerical approach introduced by Pantakar [75] is extensively used in CFD due to the reduction of the computational cost by adequately reducing the HX into a small segment for a computational domain without losing the physical meaning. Typically, the end-effects can be neglected and the thermal-hydraulic characteristics of a surface can be determined by a segment of the HX, where the lower, upper and longitudinal boundaries can be assumed periodic or symmetric. In the literature, the numerical analysis on finless surfaces commonly employ two-dimensional (Figure 3a) computational domains [38, 41, 44, 66, 67], which makes the simulations much lighter and the results are very reliable. On the other hand, if the HX has a discontinuous surface (fins) on the transverse direction then a three-dimensional (Figure 3b) computational domain types [10, 14, 16, 17] are often necessary.

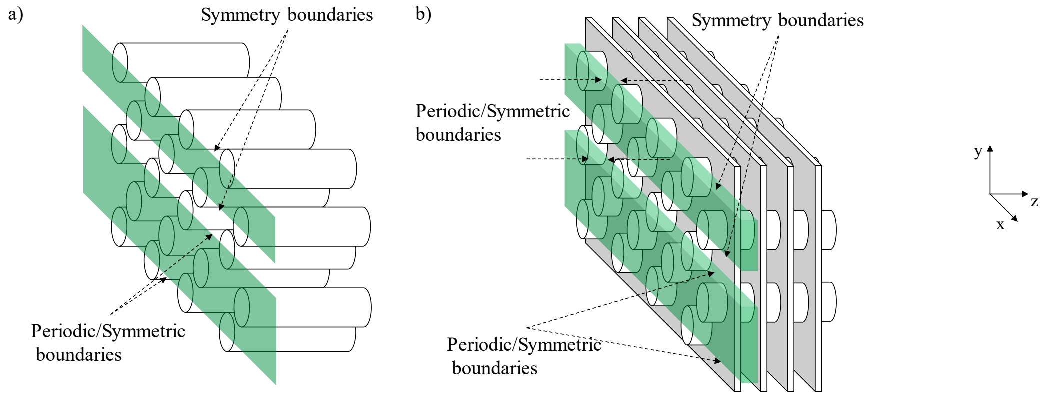

Figure 3. Streamwise periodic flow computational domain: a) 2-Dimension; b) 3-Dimension.

1.2.2.2Automation

Although CFD provides new opportunities in HX design it also entails high costs in engineering time. The traditional manual procedure in building a CFD model is, in many times, a cumbersome task that consumes time which can become prohibitive if one wants to use CFD to perform optimization. Commercial CFD software allows high level parametrization limited to scaling variables only. Topology and shape change often requires new CFD models and cannot easily be done with available tools. One way to address that issue is to use CFD automation methods. The structure behind is a low-level programming language code that can assess every step including: geometry and mesh generation, CFD simulations (including all the settings for governing equations and boundary conditions), to, finally, post-processing the metrics of interest. The model and simulation can take placed either in a commercial software environment, or within a tailored CFD code.

The ANSYS® platform is commonly used due to its journaling and scripting access from the user that allows the automation to happen. Although obsolete, Gambit® is a very robust tool for this kind of application. As for the CFD simulation environment, Fluent® is traditionally an excellent tool, but others can be equally good. Hilbert et al. [66] first presented this approach using a C code that was later used by Ranut et al. [67] for a similar study. Abdelaziz et al. [76, 77] called this method Parallel Parameterized CFD (PPCFD), which was many times used later by their colleagues [40, 78, 79]. These automation techniques potentially save in more than 90% of engineering time compared to conventional CFD modeling [76].

1.2.3 Numerical Optimization

Numerical optimization of HX's has become quite common with the rapid evolution of computational power and numerical methods. Hedderich et al. [80] presented what is most likely the first numerical optimization tool for fin-and-tube air-cooled HX optimization using traditional deterministic methods such as Feasible Directions [81], and the Augmented Lagrangian Multiplier (ALM) [82]. The traditional methods, however, they are not efficient in handling discrete variables; and cannot be used in parallel computing [83]. The Heuristic methods like Genetic Algorithms (GA's) [83] have proven to be more robust and are computationally less expensive (Table 1) than the traditional methods. Furthermore, GA's have the ability of finding even better designs. Between 2005 and 2007 the average number of publications on heat transfer problems using GA had increased by a factor of five compared to the previous decade [84].

Table 1. Summary of HX optimization methods (adapted from Huang et al. [85])

Approach	Expertise	Relative Computational Cost
Exhaustive Search	Low	100,000
Random Search	Low	10,000
Parametric Analysis	Low	1,000
Gradient-Based Methods	Medium	100
Heuristic Methods (GA, MOGA)	Med.-High	1-10

Many studies are leveraging the computational power to couple numerical solvers such as CFD to GA's [86, 62, 59, 58] in order to investigate an otherwise impossible variety of new concepts. Queipo et al. [86] investigated electronic cooling devices; Fabbri [62, 63, 87] used FEM and GA for longitudinal fin shape design; Hilbert et al. [66] and Ranut et al. [67] optimized tube shape, using Non-Rational B-Splines (NURBS) method in a cross flow HX integrating CFD and GA; Nobile et al. [58] also used NURBS for periodic (longitudinal direction) flow channels; Foli et al. [59] used CFD and GA to optimize the channel shape of a gas-to-gas HX. The cost of coupling, however, can be extremely high depending on the complex of the geometry. More recently some researchers have employed approximation assisted optimization (AAO) techniques, [66, 67, 72] which reduces the number of numerical simulations required, thus saving significant computer time. Metamodeling is a robust approximation method commonly used in several different applications.

A metamodel is a simplified version of an actual physical model, such as CFD, which with reasonable accuracy can predict the outcomes of a CFD simulation at a much lower computational cost. Amongst the metamodeling methods, Kriging [88] is a very effective and robust one and is recommended for design spaces with less than 50 design variables [89].

1.2.4 Performance Evaluation Criteria (PEC)

HX Performance Evaluation Criteria (PEC) comprises of quantifying the "goodness" of a heat transfer surface in terms of compactness and performance [90]. There are two main approaches to assess the HX PEC: a) energy-based (first law of thermodynamics); b) entropy-based (second law of thermodynamics) [91].

1.2.4.1Energy-based PEC

Cowell (1990) [92] summarized the energy-based PEC into four categories. The first, known as "area goodness" factor, is a typical way of evaluating surfaces and HX's, and is simply defined as the ratio of j and f factors (equation 2). The main advantage of such metric is the non-dimensional nature, which allows one to compare surfaces regardless the geometrical scale, particularly the surface hydraulic diameter (equation 4).

$$\frac{j}{f} = \left[\frac{h}{\rho u_c c_p}\mathrm{Pr}^{2/3}\right] \Big/ \left[\frac{2A_c \Delta P}{A_o \rho u_c^2}\right] = K\frac{1}{A_c^2}\frac{NTU}{\Delta P}, \quad K = \frac{\dot{m}^2\,\mathrm{Pr}^{2/3}}{2\rho} \qquad (2)$$

$$\Delta P \propto u_c^m, m > 1.0; \quad h \propto u_c^n, 0.0 < n < 1.0; \quad A_c \propto u_c^{-1} \qquad (3)$$

$$D_{hs} = 4\frac{A_c}{A_o}d \qquad (4)$$

Although it well represents the surface characteristics, it leads to potential skewed evaluation of the HX. The simplified form shows the dependency to the thermal conductance and the inverse of the pressure drop and the square of the minimum free flow area. In other words, this metric can only have some meaning either if the thermal hydraulic ratio is fixed or if the minimum free flow area is fixed, otherwise an infinite combination of the two can result in the same factor.

Furthermore, the general knowledge is that this factor is inversely proportional to the Reynolds number, in which having a relatively low number is undesirable. The reason for this is that the pressure drop and face area (assuming constant flow rate) terms are more sensitive to the variation in velocity than for the thermal conductance (equation 3). If one uses this metric as an optimization objective there is a possibility that the optimizer will search for either low-pressure drop, and/or small face area designs, in detriment of lower thermal resistance.

The second category is the "volume goodness", also described by London (1964), but discussed in other relevant papers including Kays and London (1984), Webb and Kim (2005) and Shah (1978). This category evaluates the dimensioned heat transfer coefficient and pressure drop (in the form of pumping power per surface area as shown in equation 5). The common observation with regards to these metrics is their dependency to the hydraulic diameter, thus in order for one to make a fair comparison between two or more designs they must have the same hydraulic diameters [90, 92, 93, 94]. Additionally, the reduction in pressure drop is usually simpler to obtain instead of improving the heat transfer coefficient, thus normally resulting in large face area designs.

$$\frac{h}{\dot{W}^{"}} = \frac{h}{\Delta P \cdot \dot{V} / A_o} = \left(\frac{c_p \mu}{\mathrm{Pr}^{2/3}} \frac{j \,\mathrm{Re}}{D_{hs}} \right) \Big/ \left(\frac{\mu^3}{2\rho^2} \frac{f \,\mathrm{Re}^3}{D_{hs}^3} \right) = \frac{2 j \rho^2 c_p D_{hs}^2}{f \mu^2 \,\mathrm{Pr}^{2/3} \,\mathrm{Re}^2} \quad (5)$$

The third category is used for a direct comparison between a smooth surface type and an enhanced version of it. There are several relevant publications regarding this category including Bergles et al. [95, 96] , Webb et al. [90, 97]. They define 12 scenarios from a combination of the four HX design objectives and three geometry constraint criteria. The three constraint criteria are: a) fixed geometry (FG) which comprises of fixing the frontal area and aspect ratio; b) fixed flow area (FN) which considers fixed frontal area but variable aspect ratio; and c) variable geometry (VG) which entails having fixed flow rates. All these assume fixed hydraulic diameter; the first two require this constraint given the nature of the criteria; the last one falls into the same issues of the "volume goodness" method. This category is summarized in Table 2.

The last category accounts for all methods that are either of diffusive interpretation, or very particular and by any means extendable to a more general method [92]. A comprehensive summary of all metrics variations for the previous evaluation categories has been described by Shah [98].

Table 2. PEC for single-phase HX (adapted from Webb and Kim [90])

Case	**Fixed Parameters**								**Objective**
	D_h	**N_t**	**L**	**A_{fr}**	**$\dot{m}$**	**$\dot{W}$**	**Q**	**ΔT_i**	
FG-1a	x	x	x	x	x			x	max Q
FG-1b	x	x	x	x	x		x		min ΔT_i
FG-2a	x	x	x	x		x		x	max Q
FG-2b	x	x	x	x		x	x		min ΔT_i
FG-3	x	x	x	x			x	x	min $\dot{W}$
FN-1	x			x	x	x	x	x	min L
FN-2	x			x	x		x	x	min L
FN-3	x			x	x		x	x	min $\dot{W}$
VG-1	x				x	x	x	x	min N_t*L
VG-2a	x	x*	x*		x	x		x	max Q
VG-2b	x	x*	x*		x	x	x		min ΔT_i
VG-3	x	x*	x*		x		x	x	min $\dot{W}$

* Product (N_t * L) constant

Cowell [92] proposed a collection of methods that overcome some of the shortcomings of the previous methods by offering quantitative criteria that allows, amongst other things, varying the hydraulic diameter. The assumptions for the method consist of negligible resistance on the other fluid side, negligible fin efficiencies and constant fluid properties throughout the HX (single-phase flow applications only). Although sometimes criticized [93], the assumptions fit quite well on air-to-fluid HX using small hydraulic diameters.

1.2.4.2Entropy-based PEC

The second PEC approach entails a more fundamental perspective by employing the second law of thermodynamics to determine the most, and least, energy degrader surfaces. The entropy generation (irreversibility) is an elegant way of combining both the finite temperature difference and friction dissipation, which ultimately will determine the heat transfer augmentation and the associated costs to it. Shah [68] states that the thermodynamic approach to HX design is important for two reasons: a) bring light to the important factors affecting qualitatively and quantitatively the HX performance; and b) use the availability B (or exergy) perspective to design the HX within a bigger context such as part of a system.

$$\dot{B}_{in} = \dot{B}_{out} + T_{ref}\dot{S}_{gen} \tag{6}$$

In 1951 McClintock [99] introduced the concept of irreversibility to HX design, which was later formalized by Bejan [100] where he defined the concept of Number of Entropy Generation Units (N_S) as an evaluation metric. His work culminated in the idealization of the Entropy Generation Minimization (EGM) method for broad applications of finite-size systems and finite-time processes [101, 102, 103].

$$N_S = \frac{\dot{S}_{gen}}{C_{\min}} \tag{7}$$

The tradeoff between energy-based and entropy-based approaches comprises of balancing out the HX size and production costs directly for savings in energy degradation (irreversibilities) [100] further down the process. A larger and “more expensive” HX is more thermodynamically efficient [100], and better heat transfer performance does not lead to minimum entropy generation [100, 104, 105]. The previous statements are only true is one does not change the surface type and size, i.e. if there are no other ways to enhance a certain surface, the only way to achieve thermodynamic efficiency is by adding surface area, which consequently increases the HX size.

Another parameter used in this approach is the ratio between the entropy generated due to friction loss and finite temperature difference (irreversibility distribution ratio [104, 106]), which indicates how much degradation is due to either mechanisms. This metric is, however, not useful as a design objective provided the expectations are to minimize both types. Lastly there is the entropy generation augmentation number ($N_{S,a}$), that directly compares the ratio between total entropy generation from an enhanced surface to a baseline, i.e. it is similar to the Bergles et al. [95, 96] method, but using entropy as a parameter. If $N_{S,a} < 1$ the design leads to exergy savings [104] (i.e. minimum entropy generation).

$$N_{S,a} = \frac{\dot{S}_{gen,a}}{\dot{S}_{gen,ref}} \tag{8}$$

$$\phi = \frac{\dot{S}_{gen,\Delta P}}{\dot{S}_{gen,\Delta T}} \tag{9}$$

Zimparov and Vulchanov [91] proposed additional equations derived specifically to employ the entropy-based approach to the three variable geometry constraint criteria (VG) established by Bergles [96].

1.2.4.3 Mixed Approach Analysis

It is important to highlight the importance and relevant applicability of each approach. On the one hand, the First Law analysis results in the non-dimensional ε-NTU relationship used in rating and sizing of HX's [68]. On the other hand, the Second Law establishes the physical limitations and how the HX fits in the energy conservation scenario in a much bigger control volume including other relevant processes. A combination of both approaches is evidently beneficial by broadening perspectives from a decision-making viewpoint. The thermoeconomic analysis [103] attempts to tie everything together by evaluating the capital cost of energy degradation caused by the irreversibility from one or more HX's (or components in general) within a system.

One step before introducing the financial aspect of the overall design is determining the indexes that evaluate the HX bounded by the practical aspects (First Law and design constraints), and the possible liability and reliability of the HX in a system context and in a long term (Second Law).

Bejan [107] first studied the relationship between the Number of Entropy Generation Units (Ns) and the Number of Transfer Units (NTU) for a balanced counter flow HX with no pressure drop. He encountered what was called the "entropy generation paradox" for the Ns went to zero for either NTU = 0 or ∞, but reached a maximum at an intermediate NTU. Shah and Skiepko [108] interpreted such behavior as the irreversibility tend to zero whenever the heat transfer potential is zero; i.e. at NTU = 0 there is no heat flow, thus from the Second Law, S_{gen} has to be zero for it cannot be negative. When NTU $\rightarrow \infty$ the hot and cold stream temperatures approach to the same value, thus nulling the heat transfer potential. Ogiso [109, 110] defined the dimensionless "entropy generation index", and showed that the Bejan's paradox can be eliminated [108] since the index is not defined at NTU = 0 or NTU $\rightarrow \infty$.

$$\frac{1}{\psi} = \frac{N_S}{NTU} = \frac{\dot{S}_{gen}}{UA} \tag{10}$$

Shah and Skiepko [108] developed further analysis on different HX's by evaluating the rate of change in irreversibilities with respect to temperature effectiveness (dS/dP_1), NTU ($dS/dNTU$) and the rate of change at maximum entropy generation ($dP_1/dNTU$ and $d^2P_1/dNTU^2$). They pointed out the importance of the identification of the maximum entropy generation point where temperature crossing may occur, thus supporting the need of combined First and Second Law analyses.

Hermes [111] further developed this analysis by presenting an optimization methodology integrating the ε-NTU and the EGM methods for constant wall temperature HX's. In his work, he formalized a straightforward equation relating N_S and NTU, under pertinent assumptions for this particular case study, which allowed him to optimize a HX accounting for both First and Second Laws.

More recently, Gheorghian et al. [112] proposed the relative exergy destruction rate parameter, that was already somewhat already discussed by Shah [68, 108]. Nevertheless, they showed that such index behaves linearly with N_S.

$$\zeta = \frac{T_0 \dot{S}_{gen}}{\dot{Q}} \tag{11}$$

The concept of "Entransy" [113] was first presented as a new physical quantity that, in analogy to electrical capacitor, is the thermal charge stored by a HX. The claim is that such quantity is fundamental for HX optimization as it better evaluates the potential of a HX to exchange heat. Analogous to exergy, the "entransy" can also be lost or dissipated. The minimization of the latter is said to be an efficient way of designing HX. Many authors, including Bejan [114], strongly oppose to this concept pointing out that it was made use of loose physical assumptions and mathematical tricks to define a physical quantity that is not dimensionally sound [114]. Additionally, the concept of "entransy dissipation minimization" does not bring anything new to the EGM already formulated decades ago. In fact, Guo and Xu [115] used the concept to optimize a shell-and-tube HX and concluded similar remarks as obtained by EGM method such as having larger HX.

1.2.5 Airside Heat Transfer and Friction Characterization in Crossflow

The investigation of airflow over cylinders and tube bundles is not a recent problem and is, likely, one of the most common problem in thermal-fluid engineering due to their wide applicability, in particular to HX's. From the general solutions of the external boundary layer problems [116, 117] the heat transfer and friction are functions of the characteristic length, Reynolds number and Prandtl number (heat transfer only). Typically, they consist of a non-linear power function (equation 12), where the multiplier and exponents are a function of the geometry (design variables) and flow regimes (equation 12c, d, e). In many cases, it also pertinent to assume that the Prandtl number is constant.

$$\begin{aligned}
&Nu = f\left(\mathrm{Re}_{Lc}, \mathrm{Pr}\right) = C \cdot \mathrm{Re}_{Lc}^{m} \cdot \mathrm{Pr}^{n} && \text{(a)} \\
&f = f\left(\mathrm{Re}_{Lc}, \mathrm{Pr}\right) = C \cdot \mathrm{Re}_{Lc}^{m} && \text{(b)} \\
&C = f\left(\underset{\sim}{x}, \mathrm{Re}_{Lc}\right) && \text{(c)} \\
&m = f\left(\underset{\sim}{x}, \mathrm{Re}_{Lc}\right) && \text{(d)} \\
&n = f\left(\mathrm{Re}_{Lc}\right) && \text{(e)}
\end{aligned} \tag{12}$$

For very specific/simple problems, or narrow design space ranges, the terms on equation 12c, and 12d can be approximated to constant values based on analytical solution or experimental data. For more complex problems, however, such terms become more complicated non-linear functions instead. For such situations analytical solutions are not a viable option, and solving this problem requires either a numerical simulation or actual testing.

Many researchers have been putting huge efforts in developing such tools in form of correlations that can reasonably predict the airside thermal-hydraulic characteristics for a given set of design parameters and operating conditions. There is a high interest in the effort of developing these correlations in particular for conventional tube and fin HX's using small diameters (<5.0mm), since there are no existing correlations for such range. The reason for the tube diameter being important is that for same Reynolds numbers, different tube sizes are subject to different velocities. Likewise, for same velocities, different tube diameters have different Reynolds number and, therefore different flow regimes. Each tube diameter will result in a different j and f curves with respect to Reynolds number. In other words, the existing correlations were built for curves at flow regimes corresponding to the particular tube diameter ranges investigated, and cannot be extrapolated.

In the following sub-sections, a literature survey on the most relevant correlations available in the literature for common fin and tube surfaces is presented.

1.2.5.1Finless Tube Heat Exchangers

There are numerous studies on thermal-hydraulic performance of gas flow over tube banks. Grimison [118], then later Žukauskas [119] presented, perhaps, the most comprehensive experimental studies on the subject including the development of empirical correlations. Žukauskas [119] correlations are the most commonly used even nowadays. Starting in the late 1970's numerical approaches became popular, especially as computational capabilities keep on continuously increasing. Launder and Massey [120] proposed a cost-effective computational method for laminar flow prediction over staggered tubes and compared against experimental data from Bergelin et al. [121]. Fujii et al. [122] focused on the in-line configuration for fixed number of tube rows and constant tube pitch ratios, varying only the Reynolds number. Hausen [123] presented modifications to Grimison correlations. You may find other correlations developed for shell-and-tube heat exchangers in Taborek et al. [124] and Gaddis & Gnielinski [125]. Wung and Chen [126, 127] presented a parametric analysis on Prandtl and Reynolds numbers and correlated their numerical data into expressions. Their analysis however did not account for geometry variables. Dhaubhadel et al. [128] solved the same problem as Fujii et al. [122] but for staggered arrangement. Beale and Spalding [129] investigated unsteady flow on both in-line and staggered tube banks. Wilson and Bassiouny [130] studied single row and double row tube banks parameterizing tube pitches and its Reynolds number. They also compared their results with empirical data. Buyruk [131] made a similar study using fine grid resolutions. On an analytical approach Khan et al. [132] developed alternate equations for heat transfer and friction for both inline and staggered arrangements. Their equations are limited to tube pitch ratios ranging from 1.05 to 3. They found good agreement with Grimison [118] and Žukauskas [119] for a 16.4mm tube diameter. Table 3 presents more details on selected correlations.

Table 3. Selected correlations for finless tube bundle.

Author	**Arrangement**	**Applicability range**	**Equation format**
Grimison (1937) [118]	Staggered / In-line	$39.8 \le D_o \le 63.6mm$ $1.2 \le P_l / D_o \le 6.0$ $1.25 \le P_t / D_o \le 3.0$ $N = N / A$ $2 \cdot 10^3 \le Re \le 4 \cdot 10^4$	$Nu = c \cdot \mathrm{Re}_{Do}^m \cdot \mathrm{Pr}_f^n$ $f = k \cdot \mathrm{Re}_{Do}^p$
Žukauskas (1972) [119]	Staggered / In-line	$D_o = N / A$ $1.25 \le P_l / D_o \le 2.5$ $1.25 \le P_t / D_o \le 2.5$ $N = N / A$ $1.0 \le Re \le 2 \cdot 10^6$ $0.7 \le Pr \le 500$	$Nu = c \cdot \mathrm{Re}_{Do,c}^m \cdot \mathrm{Pr}_f^{0.36} \left(\frac{\mathrm{Pr}_f}{\mathrm{Pr}_w} \right)^{0.25}$ $f = k \cdot \mathrm{Re}_{Do,c}^p \cdot z$
Khan et al. (2006) [132]	Staggered / In-line	$D_o = N / A$ $1.05 \le P_l / D_o \le 3.0$ $1.05 \le P_t / D_o \le 3.0$ $N = N / A$ $10^3 \le Re \le 10^5$	$Nu_{in-line} = \left(0.25 + e^{-0.55 P_l / D_o}\right) \cdot \mathrm{Re}_{Do,c}^{1/2} \cdot \mathrm{Pr}_f^{1/3} \cdot \left(\frac{P_l}{D_o} \right)^{0.212} \cdot \left(\frac{P_t}{D_o} \right)^{0.285}$ $Nu_{staggered} = \frac{0.61}{1 - 2e^{-1.09 P_l / D_o}} \cdot \mathrm{Re}_{Do,c}^{1/2} \cdot \mathrm{Pr}_f^{1/3} \cdot \left(\frac{P_l}{D_o} \right)^{0.053} \cdot \left(\frac{P_t}{D_o} \right)^{0.091}$

1.2.5.2 Finned Tube Heat Exchangers

Fins provide a substantial addition to the surface area on a tube bundle at large diameters, allowing reducing thermal resistance. Amongst fin types plain fins have much poorer performance compared to enhanced ones such as louver, slits and perforated. Plain fins are, however, less susceptible to material deposition from the airstream.

Applications such as heat pumps in cold climates face an extra challenge of frosting in the outdoor unit, which ultimately compromises the overall system performance. For these systems, the commonly known high performance fins like slits and louvers are generally not suitable. Researchers have shown empirically that louver fins have a poorer performance compared to plain wavy and flat fins, respectively under frosting/defrosting operating modes [6, 30].

Plain flat fins have become quite uncommon but there are applications which they can be useful. There are few correlations in the literature that predict airside performance on those fins with relative large tube diameters. McQuiston (1978) [133] proposed the first correlations for this application that were later improved by Gray et al. [134], then Webb [135] and Kim et al. [136]. The most recent correlations for plate fin-and-tube heat exchangers include those from Wang et. al. (2000) [137]. The most relevant correlations for all fin types are summarized in Table 4.

Table 4. Most relevant fin-and-tube airside correlations in the literature.

Author	Fin type / Tube Arrangement	Applicability range
McQuiston (1978) [133]	Flat / Staggered	$9.675 \le D_o \le 16.13mm; 25.4 \le P_l \le 50.8mm$ $25.4 \le P_t \le 50.8mm; 4 \le FPI \le 14$ $0.15 \le \delta_t \le 0.25mm; N = N / A$ $1.0 \le u \le 4.0m/s$
Gray (1986) [134]	Flat / Staggered	$9.96 \le D_o \le 16.51mm; 1.7 \le P_l/D_o \le 2.58$ $1.97 \le P_t/D_o \le 2.55; 0.08 \le F_s/D_o \le 0.64$ $0.015 \le \delta_t/D_o \le 0.018; 1 \le N \le 8$ $500 \le \mathrm{Re} \le 24700$
Webb (1990) [135]	Flat & Wavy Herringbone / Staggered	$7.95 \le D_c \le 12.52mm; 1.73 \le P_l/D_c \le 2.31$ $2.0 \le P_t/D_c \le 2.5; 1.96 \le F_s \le 4.09mm$ $0.71 \le P_d \le 3.18mm; 2.0 \le X_f/P_l \le 4.0$ $3 \le N \le 6; 500 \le \mathrm{Re} \le 2.47 \cdot 10^4$
Kim et al. (1999) [136]	Flat / Staggered	$7.3 \le D_o \le 19.51mm; 0.857 \le P_t/P_l \le 1.654$ $1.996 \le P_t/D_o \le 2.881; 0.081 \le F_s/D_o \le 0.641$ $0.15 \le \delta_t \le 0.406mm; 1 \le N \le 6$ $505 \le \mathrm{Re} \le 2.47 \cdot 10^4$
Wang et al. (2000) [137]	Flat / Staggered	$6.35 \le D_o \le 12.7mm; 12.4 \le P_l \le 27.5mm$ $17.7 \le P_t \le 31.75mm; 1.19 \le F_p \le 8.7mm$ $0.115 \le \delta_f \le 0.152mm; 1 \le N \le 6$ $200 \le \mathrm{Re} \le 2 \cdot 10^4$
Kim et al. (1997) [138]	Wavy Herringbone / In-line & Staggered	$9.53 \le D_o \le 12.7mm; 1.73 \le P_l/D_o \le 2.88$ $1.16 \le P_t/P_l \le 1.33; 0.11 \le F_s/D_o \le 0.44$ $0.23 \le P_d/F_s \le 1.21; 1.44 \le X_f/P_d \le 5.65$ $1 \le N \le 8; 500 \le \mathrm{Re} \le 9 \cdot 10^3$
Wang et al. (1997) [139]	Wavy Herringbone / In-line & Staggered	$D_c = 10.3mm; 1.85 \le P_l/D_c \le 2.85$ $2.47 \le P_t/D_c \le 2.85; 1.69 \le F_p \le 4.8mm$ $P_d = 1.5mm(staggered); P_d = 2.0mm(in-line)$ $X_f/P_l = 0.25; \delta_f = 0.12mm(staggered)$ $\delta_f = 0.2mm(in-line); 1 \le N \le 4$ $200 < \mathrm{Re} < 10^4$
Wang et al. (1999) [140]	Wavy Herringbone / Staggered	$8.58 \le D_c \le 10.38mm; 1.84 \le P_l/D_c \le 2.95$ $2.45 \le P_t/D_c \le 2.96; 1.21 \le F_p \le 3.66mm$ $1.18 \le P_d \le 1.68mm; X_f/P_l = 0.25$ $0.115 \le \delta_f \le 0.12mm; 1 \le N \le 6$ $200 < \mathrm{Re} < 10^4$

Author	Fin type / Tube Arrangement	Applicability range
Wang et al. (2002) [141]	Wavy Herringbone / Staggered	$7.66 \le D_c \le 16.85mm; 12.7 \le P_l \le 33mm$ $21.0 \le P_t \le 38.1; 1.21 \le F_p \le 6.43mm$ $0.3 \le P_d \le 1.58mm; X_f / P_l = 0.25$ $0.11 \le \delta_f \le 0.25mm; 1 \le N \le 6$ $300 \le \mathrm{Re} \le 10^4$
Wang et al. (1999) [142]	Louver / Staggered	$6.93 \le D_c \le 10.42mm; 12.7 \le P_l \le 22mm$ $17.7 \le P_t \le 25.4mm; 1.21 \le F_p \le 2.49mm$ $0.9 \le L_h \le 1.4mm; 1.7 \le L_p \le 3.75mm$ $\delta_f = N / A; 1 \le N \le 6$ $100 < \mathrm{Re} < 10^4$
Wang et al. (1999) [143]	Slit / Staggered	$D_c = 10.34mm; P_l = 22mm$ $P_t = 25.4mm; 1.22 \le F_p \le 2.48mm$ $S_{lh} = 11.0mm; S_{ls} = 8.0mm S_w = 2.2mm$ $S_h = 0.99mm; \delta_f = 0.12mm; N_S = 4$ $1 \le N \le 6; 100 < \mathrm{Re} < 10^4$
Wang et al. (1998) [11]	Louver & Wavy Herringbone / Staggered	$D_c = 8.54mm; P_l = 19.05mm$ $P_t = 25.4mm; 1.22 \le F_p \le 2.54mm$ $1 \le N \le 4; 100 < \mathrm{Re} < 10^4$

1.2.6 Fabrication of Heat Exchangers with Complex Surfaces

The urge for developing novel high-performing heat transfer surfaces has been well established and discussed in this chapter. Researchers have been creating innovative HX surface concepts aiming address the limitations the conventional heat transfer surfaces. Often, the challenge is the lack of manufacturing options to build these novel designs.

In particular, metal heat exchangers have additional manufacturing constraints as opposed to other materials such as polymers. T'Joen et al. [144] published a review on the latest developments on Polymer heat exchangers. Due to their low conductivity, limited range of application temperature and low structural resistance, polymers are seldom the preferred material. However, plastics have other advantages, but above all is the ease of manufacturing complex structures that researchers can leverage when investigating novel concepts.

Chang and Van Der Geld [145] validated an air-to-water compact plate HX with rectangular channels using PolyVinyliDene-Fluoride (PVDF). Harris et al. [146] built and tested a radiator with sub-millimeter rectangular air and water channels. Their HX was fabricated in polymethylmethacrylate (PMMA) using the LIGA process [147] for two halves of the HX, then alignment and bonding. Cevallos et al. [148] built a webbed-tube HX inspired by the work of Abdelaziz et al. [72], where they used polytetrafluorethylene (PTFE) and injection molding. Recently, Felber et al. [149] used 3-D printing (additive manufacturing) technique to build a microchannel HX with cylindrical pin fins on the airside in staggered arrangement. Their HX was built in Acrylonitrile Butadiene Styrene (ABS).

Additive manufacturing is likely the next generation of manufacturing technology since it eliminates most of the manufacturing constraints in current technologies. It will widen the design frontiers allowing the fabrication of countless innovative designs. Felber et al. [149] used this technology to build on plastic, Arie [150] designed a novel microchannel HX and built it on metal.

Metal additive manufacturing is already available with some restrictions, but the possibilities are vast. As the HX design concepts evolves, it will potentially be undertaken by a pronounced paradigm shift.

1.2.7 Literature Gaps

The previous sections in this dissertation covered the main background used in this work, and pointed out potential literature gaps which this research intends to fill. There are three main gaps summarized in the following subsections that will be addressed in this thesis.

1.2.7.1High-Performance Compact Finless Heat Exchangers

There is a gap in the literature with respect to comprehension of the underlying physics of small characteristic lengths on airside heat transfer, and how different scales affect the performance and the need for extended surfaces (fins). For this reason, the mainstream research heavily focuses on enhancing fins instead evaluating the potential improvement on primary surfaces.

The literature shows a great deal of work on fins, some work on finless micro tubes, and other work on tube shapes. The last two have not been comprehensively studied together, and much of the work is limited to theoretical analysis only, and are not applied to a full-scale design of a HX.

1.2.7.2Multi-Scale and Shape Optimization Methodology

HX optimization studies are commonly studied in literature. Most of them however, either focus on conventional HX's using computationally affordable tools to evaluate performance, or investigate novel surfaces that require computationally expensive tools such as CFD and FEM. The latter however, is usually not applied to a HX context due to the increase in computational efforts that make it a waste of time. Abdelaziz et al. [72] presented a highly cost-effective multi-scale optimization that allows one to investigate and optimize novel HX concepts in a computationally affordable manner. The gap missing is the shape optimization which allows the optimizer to not only optimize the HX, but also find the best surface performance altogether.

1.2.7.3Airside Heat Transfer and Friction Correlations for Small Diameter Tubes

In the literature review it was presented a survey on the most relevant correlations for airside on conventional tube-fin HX's, and explained the need for computationally inexpensive tools. There are no explicit evidences that the available equations in the literature can predict the thermal-hydraulic performances for tube banks using small tube diameters (below 7.0mm). Currently, the only way to determine the thermal-hydraulic characteristics of fin-and-tube HX's is by using small diameter tubes (either experimentally or numerically). Doing this requires computationally expensive tools. There is a demand for computationally inexpensive tools that can aid the design of new HX's using small diameter tubes.

Chapter 2: Research Objectives

2.1 Summary

This dissertation will approach the design of a new generation of HX's with a set of objectives, reaching from fundamental analysis to tool development and finally, design, optimization & validation.

1- The first objective of this work is to discuss with, aid of numerical analyses, the fundamental aspects of airflow over primary (tubes) and secondary (fins) surfaces. Such analyses will serve to demonstrate how the reduction of characteristic length and optimizing shape impact finned and finless heat transfer surfaces and the trade-offs limiting each.

2- The second objective of this research entails developing a comprehensive Multi-Scale analysis with Topology and Shape Optimization Methodology applied to air-to-fluid HX's design. The novel HX's developed with this methodology are significantly superior in performance, size and material usage compared to current state-of-the art with minimal or no use of fins. Furthermore, these HX's will provide additional material to support the first objective in the above paragraph, by proving that fins are unattractive or even necessary under certain scales. This methodology should serve as foundations for a HX design platform where one can leverage computational power to let the optimizer "create" and "invent" new HX's with high design freedom.

3- The third, and last, objective, entails developing computationally inexpensive tools that can accurately predict CFD simulation responses for conventional tube and fin surfaces using small diameter tubes. One aspect of this objective is to fulfill the gap where there are no correlations available in the literature that can be used for small diameter tubes. Therefore, the contribution will be a computationally inexpensive set of tools that replace the need for CFD, which can potentially mean cost savings as well. Additionally, these tools are used to optimize equivalent finned and finless surfaces using different tube diameters. With this additional study will refer back to the first objective and narrow down the trade-offs and the advantages and limitations of finned and finless surfaces.

2.2 Dissertation Organization

These objectives are developed and achieved across the next five Chapters in this dissertation. The dissertation organization workflow (Figure 4) summarizes the following Chapter general task list:

Chapter 2:

- Provide all the fundamental and technical background required in this dissertation.

Chapter 3:

- Present fundamental (first and second order) analyses on surface compactness and thermal-hydraulic performance when varying characteristics such as length and exploring alternate shapes.

- Discuss the advantages and limitations of finned and finless surfaces.
- Provide the solid foundations that justify the work of to the following chapters.

  Chapter 4:

- Present a comprehensive HX design framework that includes design concept, airside modeling and simulation, design and optimization, verification and validation.
- Propose a shape parameterization method to integrate the multi-scale analysis with topology and shape optimization methodology.
- Leverage automated CFD simulations, approximation assisted optimization, and robust air-to-fluid HX simulation tool to explore novel concepts.
- Present novel HX's that outperform state-of-the art HX's in more than 20% performance improvement, size reduction and material usage.
- Design 1.0kW and 10kW air-to-water HX's.
- Explore alternate manufacturing technologies, such as metal additive manufacturing, to build proof-of-concept prototypes.
- Present experimental validations for two distinct design concepts for the 1.0kW air-to-water design.
- Present a road map containing all the novel HX's and how they compare with current state-of-the-art, and discuss potential guidelines for the next generation of HX's based upon lessons learned.

- Design condensers and evaporators for a three ton air-conditioning system achieving 10%+ improvement in COP and 30%+ charge reduction.

Chapter 5:

- Present a comprehensive correlation development framework that leverages automated CFD simulations.
- Present six novel correlations for finless and finned tubes, with different fin types, that addresses the use of small diameter tubes (<5.0mm).
- Present preliminary experimental verification with available test data for one of the prototypes in Chapter 4.

Chapter 6:

- Present a surface optimization analysis with parameterization of key metrics that will allow an additional comprehensive analysis on finned and finless surfaces.
- Demonstrate the robustness of these novel correlations.

Chapter 7: Conclusions

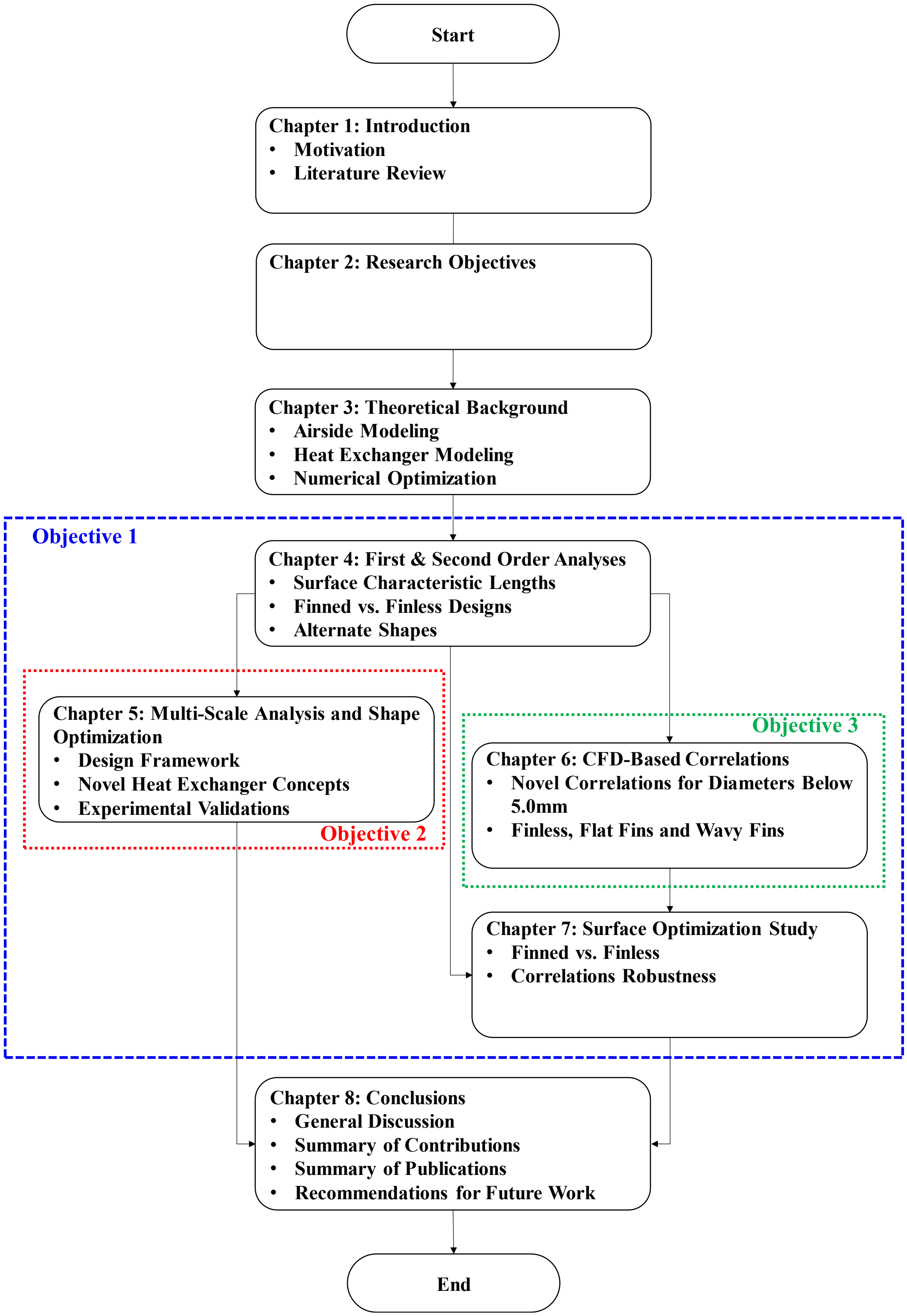

Figure 4. Dissertation organization workflow.

Chapter 3: Theoretical Background

3.1 Airside Modeling

The stream wise periodic flow numerical method introduced by Pantakar [75] is extensively used in Computational Fluid Dynamics (CFD) for heat exchanger problems. CFD is now a required tool in such applications, in spite the criticism regarding the numerical uncertainty associated with it. Shah [68] argued the uncertainties related to CFD simulations can be, in many cases, comparable to performance improvement obtained. For this reason, CFD uncertainty analysis and validations must be carried out.

3.1.1 CFD Modeling and Simulation

The method proposed by Pantakar [75] aims reducing the computational cost by adequately reducing the computational domain without losing physical meaning. Typically, the end-effects can be neglected and the thermal-hydraulic characteristics of a surface can be determined by a segment of the HX where the lower, upper and longitudinal boundaries are assumed periodic or symmetric. In the literature the numerical analysis on finless surfaces commonly employ 2-dimensional computational domains [38, 41, 44, 66, 67], however, finned computational domains must be 3-D.

3.1.1.1CFD Physics and Settings

When using CFD for heat transfer applications the three fundamental set of equations must be solved: momentum (Navier-Stokes) (equation 13), continuity (equation 14) and energy (equation 15). The assumptions used in this work include:

a) steady-state flow; b) non-existent energy and mass sources nor external forces; c) negligible gravitational effects; d) pressure work and kinetic energy are negligible. The physical model is then reduced to convection-diffusion problem with no external components. The resulting governing equations are described below.

$$\nabla\left(\rho \underset{\sim}{u}\right)=0 \tag{13}$$

$$\left(\underset{\sim}{u}\cdot\nabla\right)\left(\rho \underset{\sim}{u}\right)=-\nabla P+\mu\nabla^2\underset{\sim}{u} \tag{14}$$

$$\underset{\sim}{u}\cdot\nabla\left(\rho c_p T\right)-k\cdot\nabla^2 T=0 \tag{15}$$

There are three important aspects regarding this type of CFD simulation that are seldom discussed in detail including the near wall meshing, flow regime models and thermophysical properties.

Both thermal diffusion and viscous resistance within the boundary layer are function of the temperature and velocity gradient at the surface (equations 16 and 17). One must consider a much finer mesh near the wall in order to better capture the boundary layer physics. Hilbert et al. [66] illustrated their computational domain with an unstructured pave mesh with uniform element size, however no refinement near the tube wall. In this work, we consider a two dimensional computational domain (Figure 5) with pave meshing scheme as well, however the near wall region mesh is a fine map scheme with growing layers at a ratio of at most 1.2.

$$h_x\left(T_\infty-T_w\right)=-k\left.\frac{\partial T}{\partial y}\right)_w \tag{16}$$

$$C_f = \frac{\tau_w}{1/2\rho u_\infty^2} = \frac{1}{1/2\rho u_\infty^2}\left(\alpha + \varepsilon_M\right)\frac{\partial \bar{u}}{\partial r}\bigg)_w \tag{17}$$

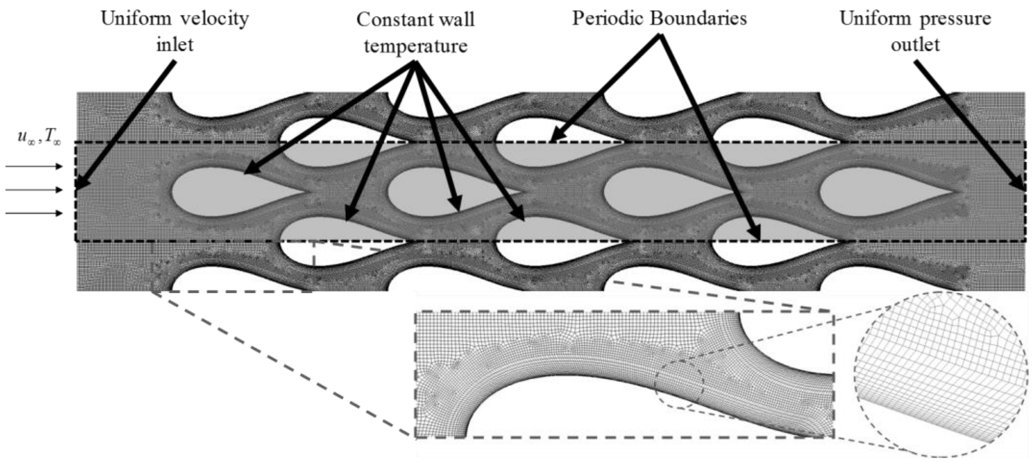

Figure 5. Typical CFD 2-D computational domain.

For the two-dimensional computational domain, both triangle and quadrilateral mesh schemes were used depending upon the geometry.

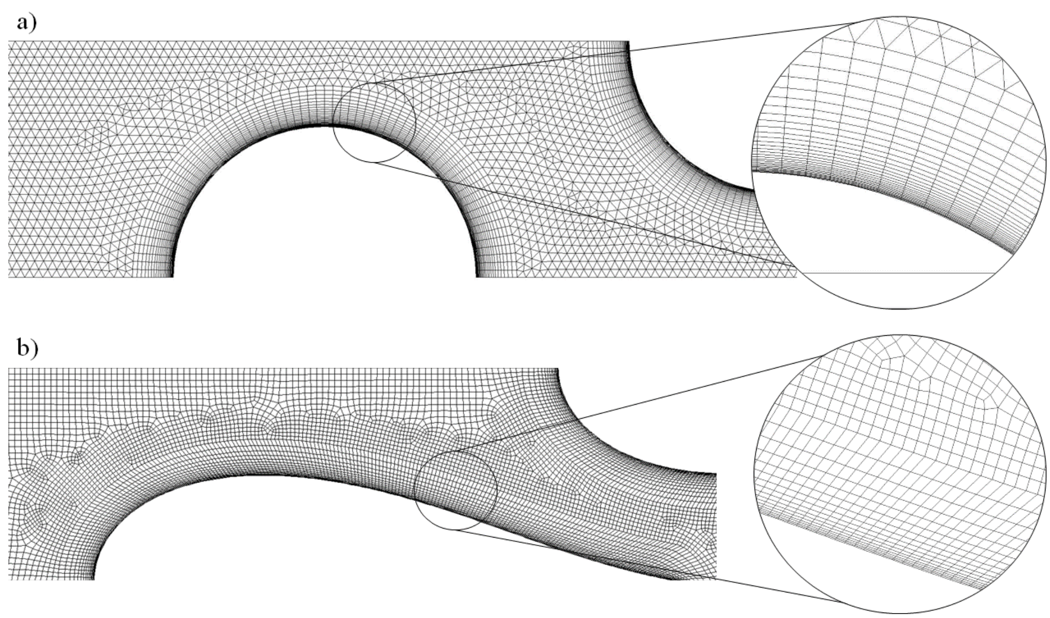

Figure 6. Two-dimensional computational domain mesh schemes: a) triangle; b) quadrilateral.

Hexahedron elements using Cooper scheme is the most efficient way of modeling 3-D computational domain. The periodicity requires mesh link between periodic boundaries and Cooper scheme becomes convenient since it uses a source face to project the mesh onto parallel faces.

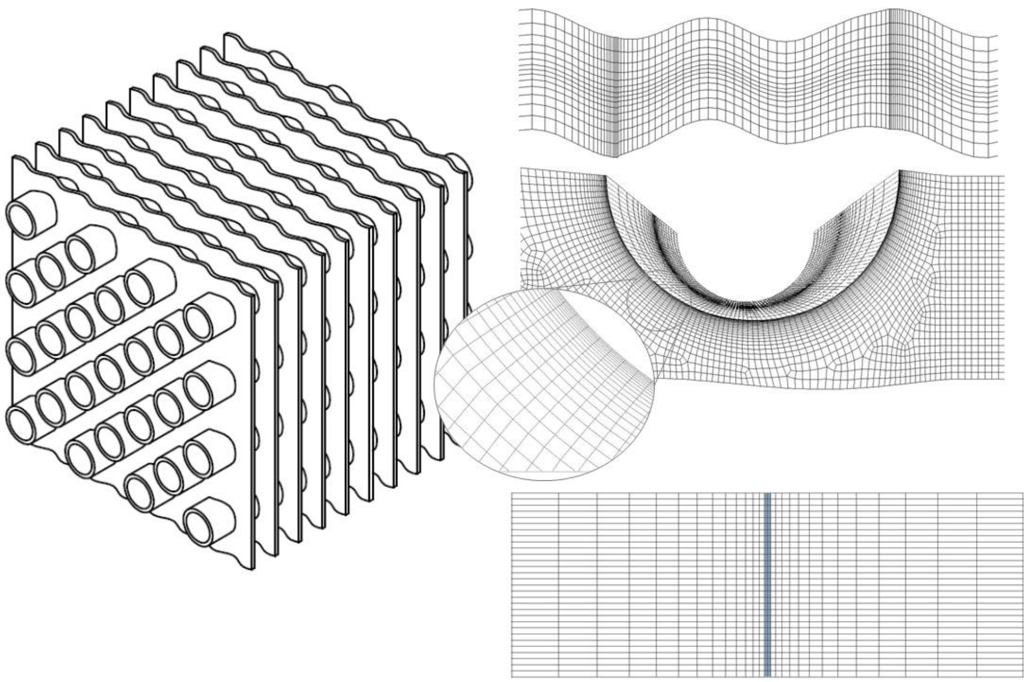

Figure 7. Three-dimensional computational domain.

Flow regimes models are a very debatable issue. For instance both Hilbert et al. [66] and Ranut et al. [67] used laminar flow with the argument that the Reynolds number was low (~160). There are two considerations to their statement. One, they defined the Reynolds number based on the tube vertical spacing (which is fixed in their model), although the most adequate would be using the surface hydraulic diameter (equation 5), which for different shapes it can vary. Second, the same Reynolds number for different surfaces can result in different flow regimes; i.e., eddies can be developed in the inevitable flow separation, generating wakes affecting the flow regime of subsequent tube banks, even if the first tube has a laminar flow. Although turbulence models are known to over predict heat transfer and friction for truly laminar flows, they can better solve a broader range of problems. This is preferable when one has to simulate a large number of samples using common CFD settings. There are many turbulence models available in commercial CFD packages. The two-equation k-ε realizable (RKE) [151] has proven to be a very robust model. The RKE ensures the solution obeys the non-negativity of turbulent normal stress [152], thus they are realistic (when converged) from the physical viewpoint. Additionally, the authors have observed a higher rate of convergence when using RKE for a large number of CFD simulations compared to other models, including laminar.

The thermophysical properties also have an impact to the outcomes of the CFD simulations. In many heat transfer applications, the fluid flow is significantly subsonic ($Ma \ll 0.3$) which characterizes as incompressible flow. Many authors simplify the problem by using constant properties [66, 67]. The temperature, however, may have a significant impact particularly on density, conductivity and viscosity (Figure 8). There are consequences on both momentum and heat transfer. As the airstream gets warmer, the constant density assumption leads to under prediction of the accelerating airflow, the constant conductivity under predicts the thermal diffusion within the boundary layer and the constant viscosity over predicts the shear stress at the surface. Therefore, the ideal-gas model is reasonable for density, whereas the other thermophysical properties can easily be estimated with polynomial curve fits as function of temperature (Figure 8).

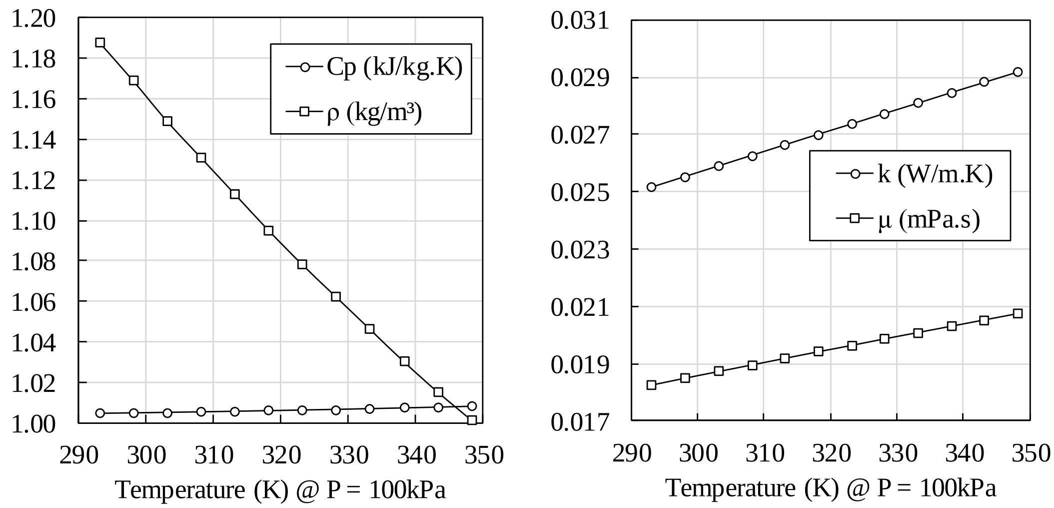

Figure 8. Dry air properties as function of temperature.

Finally, the simulation convergence criteria are set to a maximum residual of 10^{-5} for momentum and continuity, 10^{-6} for energy and 10^{-3} (default) for turbulence. If the simulation does not meet the criteria, however it stabilizes into a solution, we assume that if the standard deviation of the last 100 iterations is less than 0.5% of the average of those same 100 iterations, then it is converged.

3.1.2 CFD Data Reduction

This type of problem is convenient to define uniform wall temperature (Figure 5) allowing one to easily calculate the heat transfer coefficient from the UA-LMTD method (equation 18 and 19). It is also of interest, in particular when studying surface performance, to determine the non-dimensional heat transfer (Colburn j factor) as per equation 20.

$$\dot{Q} = \dot{m} \cdot \bar{c}_p \left(T_o - T_i\right) = \eta_o h \cdot A_o \cdot \Delta T_{ml} \tag{18}$$

$$\eta_o h = \frac{\dot{m}\cdot\bar{c}_p}{A_o}\cdot\frac{(T_o - T_i)}{\Delta T_{ml}} = \frac{\dot{m}\cdot\bar{c}_p}{A_o}\cdot\frac{T_o - T_i}{\frac{\left[(T_w - T_i)-(T_w - T_o)\right]}{\ln\left[(T_w - T_i)/(T_w - T_o)\right]}} = \frac{\dot{m}\cdot\bar{c}_p}{A_o}\cdot\ln\left[\frac{(T_w - T_i)}{(T_w - T_o)}\right] \quad (19)$$

$$j = \frac{h}{\bar{\rho}\cdot u_c\cdot\bar{c}_p}\cdot\mathrm{Pr}^{2/3} \quad (20)$$

For finless designs the fin effectiveness (η_o) is logically equal to unity, however when that is not the case, the fin efficiency / effectiveness and heat transfer coefficient are calculated using Schmidt [153] approach and iteratively using Newton-Raphson method [154].

$$\eta_o = 1 - \frac{A_{fr}}{A_o}(1-\eta) \quad (21)$$

$$\eta = \frac{\tanh(0.5\cdot mD_o\phi)}{0.5\cdot mD_o\phi} \quad (22)$$

$$m = \left(\frac{2h}{k_f\delta_f}\right)^{0.5} \quad (23)$$

$$\phi = (R_{eq}-1)\left[1+0.35\ln(R_{eq})\right] \quad (24)$$

$$X_L = \frac{1}{2}\left(\frac{P_t^2}{4}+P_l^2\right)^{0.5} \quad (25)$$

$$R_{eq} = 1.27\frac{P_t}{D_o}\left(\frac{2X_L}{P_t}-0.3\right)^{0.5} \quad (26)$$

The Newton-Raphson iteratively calculates the heat transfer coefficient for the following set of equations.

$$h^n = h^{n-1} - \frac{\beta(h^{n-1})}{\beta'(h^{n-1})} \quad (27)$$

$$\beta(h^{n-1}) = (UA)_a - \left[1 - \frac{A_{fr}}{A_o}\left(1 - \frac{\tanh\left(0.5 \cdot \left(\frac{2h^{n-1}}{k_f \delta_f}\right)^{0.5} D_o \phi\right)}{0.5 \cdot \left(\frac{2h^{n-1}}{k_f \delta_f}\right)^{0.5} D_o \phi}\right)\right] \cdot h^{n-1} \quad (28)$$

For the pressure drop it is convenient to set the outlet boundary at uniform atmospheric pressure (0.0 gauge). Additionally, the dynamic pressure difference between inlet and outlet can be assumed insignificant compared to the static pressure difference. Lastly, the buoyance term is also negligible for gases, therefore the pressure drop is simply retrieved according to equation 29. Similarly, one can also obtain the non-dimensional pressure drop neglecting local effects (equation 30).

$$\Delta P = P_{in} - P_{out} + \frac{1}{2}\rho_{in} u_{in}^2 \left(1 - \frac{\rho_{out}}{\rho_{in}}\right) \quad (29)$$

$$f = \frac{\Delta P}{\bar{\rho} u_c^2} \cdot \frac{D_{hs}}{2d} \quad (30)$$

3.1.3 CFD Grid Uncertainty Analysis

One standard approach to evaluating the CFD model uncertainty is the 5-step Grid Convergence Index (GCI) method [69, 70, 71]. Grid Convergence Index (GCI) [71] is a formal methodology, developed based on Richardson Extrapolation, to estimate the grid convergence error of a metric of interest (φ) [155].

Step 1: define the average element length of the grid (equation 31 and 32), determined as follows for two-dimensional and three-dimensional computational domains respectively.

$$\delta_{2D} = \left[\frac{\sum \Delta A_i}{N} \right]^{1/2} \tag{31}$$

$$\delta_{3D} = \left[\frac{\sum \Delta V_i}{N} \right]^{1/3} \tag{32}$$

Step 2: select at least three grid resolutions (equation 33) where the element size ratio between subsequent grid resolutions is equal or greater than 1.3. The procedure is simplified when using constant refinement ratio (r) since it eliminates the iterative calculations [69].

$$r_{i+1,\mathrm{i}} = \frac{\delta_{i+1(coarse)}}{\delta_{i(fine)}} \geq 1.3 \tag{33}$$

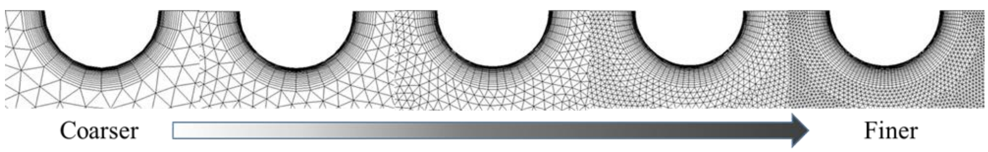

Figure 9. Sequentially increasing grid resolutions.

Step 3: calculate the observed order of accuracy (p*) (equation 34). When the observed order of accuracy (p*) deviates in more than 10% from the formal (p) spatial discretization order of accuracy then the effective value (p**) (equation 37) must be bounded by a minimum of 0.5 and the formal value [156].

$$p^* = \left(\frac{1}{\ln r_{21}} \right) \left(\ln \left| \frac{\varepsilon_{32}}{\varepsilon_{21}} \right| + \ln \left(\frac{r_{21}^p - s}{r_{32}^p - s} \right) \right) \tag{34}$$

$$s = \frac{\varepsilon_{21}/\varepsilon_{32}}{\left|\varepsilon_{21}/\varepsilon_{32}\right|} \tag{35}$$

$$\varepsilon_{21} = \varphi_2 - \varphi_1 \tag{36}$$

$$p^{**} = \min\left\{\max\left[0.5, p\right], p^*\right\} \tag{37}$$

Step 4: calculate the extrapolated values (equation 38)

$$\varphi_{ext}^{21} = \frac{r_{21}^{p}\varphi_1 - \varphi_2}{\left|r_{21}^{p} - 1\right|} \tag{38}$$

Step 5: Calculate and report the estimated extrapolation error (equation 39) and the grid convergence index (GCI) (equation 40)

$$e_{ext}^{21} = \left|\frac{\varphi_{ext}^{21} - \varphi_1}{\varphi_{ext}^{21}}\right| \tag{39}$$

$$GCI_{fine}^{21} = \frac{F_s \cdot e_a^{21}}{r_{21}^{p^{**}} - 1} \tag{40}$$

If p* deviates in more than 10% from p then the factor of safety (F_s) must be set to 3.0 [71], otherwise a value of 1.25 [71] is considered acceptable.

In order to quantify the CFD uncertainty associated with an entire design space the premise that at the boundaries of the design space the uncertainties are fundamentally larger than for any other sample is assumed. The reason for that is that the combinations of lower and upper bounds yield the most skewed computational domains, thus having a higher potential for poorer mesh elements in terms of size and aspect ratios. For every surface investigated, the GCI method is employed for the 2^n samples represented by all variable combinations of 0's and 1's for an n-dimension design space (e.g. n = 5, 2^5 = 32 samples).

3.1.4 Non-Uniform Rational B-Splines (NURBS)

Non-Uniform Rational B-Splines (NURBS) [157] are very common in shape optimization problems [58, 59, 60, 66, 67]. Several algorithms are available, however the most efficient is perhaps the one developed by Piegl and Tiller [157]. NURBS can be applied to both curves and surfaces. A NURBS curve (equation 41) is usually presented in a vector format and is described by the rational piecewise base functions. The base functions are defined on u ∈ [0,1].

$$C(u) = \sum R_{i,p}(u) P_i = \sum \frac{N_{i,p}(u) w_i}{\sum N_{j,p}(u) w_j} P_i, \quad a \le u \le b \tag{41}$$

The P_i are the control points, w_i is the weight vector and N_i are the p^{th}-degree B-Spline base functions defined on the non-uniform knot vector (U).

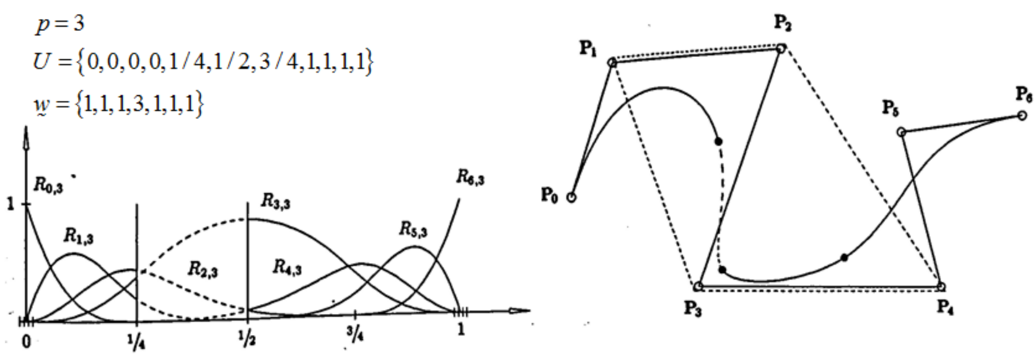

Figure 10. 3rd degree NURBS curve and base functions example from Piegl and Tiller [157].

Piegl and Tiller [157] define 14 properties of NURBS curves from which four are of most interest in this work.

- Any NURBS curve have their first and last point coinciding with the first and last control point; i.e. C(0)=P_0 and C(1)=P_n.

- All derivatives of $R_{i,p}(u)$ exist, i.e. C(u) is infinitely differentiable on the knot span and p-k differentiable at a knot of multiplicity k.
- If the weight vector is unitary, the rational base functions are simply B-Spline base functions. If the B-Spline degree is equal to the number of control points minus one, then it is simply a Bezier curve, which has the base functions as the Bernstein polynomials. This property shows that NURBS contains both rational and non-rational B-Splines and Bezier curves, thus allowing one to describe almost any type of curve.
- Local approximation: a change in a control point or a weight affects only portion of the curve.

The method can essentially be applied to design any type of heat transfer surface; from tubes to fins. In a cross flow HX a tube shape can be described by compounding two or more curves, it can be symmetrical or asymmetrical and it can define a round shape or an airfoil shape.

In this work, 4^{th} and 5^{th} order NURBS curves (equation 13) are considered where the coordinates of the control points are normalized between 0 and 1. The leading edge (le) and trailing edge (te) points are fixed to the (0,0) and (1,0), and the three mid-points are the shape design variables. The x-coordinate of the mid control points are bounded by equally spaced slices in order to avoid self-intersecting curves (Figure 11).

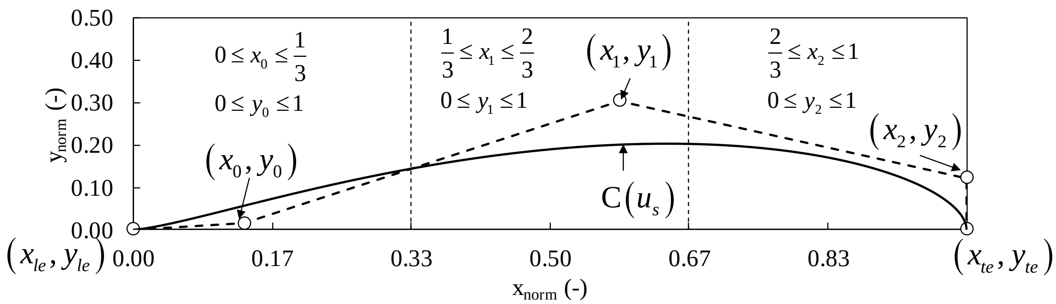

Figure 11. Tube shape parameterization.

Refer to Appendix A for C# codes based on Piegl and Tiller [157] algorithms used in this work.

3.2 Heat Exchanger Modeling

This section presents a brief overview on fluid-to-fluid HX in cross flow modeling. The two common, and equivalent, approaches are the ε-NTU and UA-ΔT_{ml}. Each method has its advantages and disadvantages; the first is well suited for sizing a HX for a determined capacity, however the effectiveness (ε) depends on knowing flow arrangement and passes configurations. If inlet and outlet conditions are known the second method is becoming simpler since the temperature difference can be easily calculated, otherwise additional information regarding the geometry must be known beforehand as well. The two models are detailed through the rest of this section.

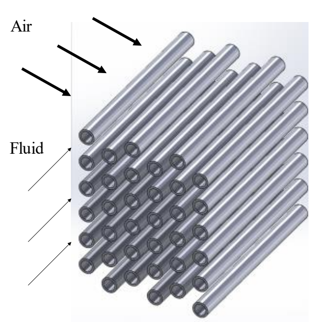

Figure 12. Air-to-fluid cross flow HX's.

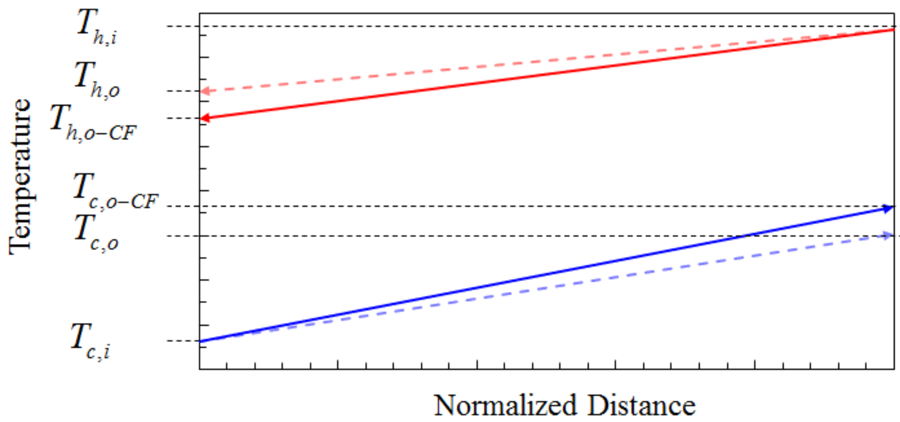

Figure 13. HX Temperature profile illustration.

$$\dot{Q} = \dot{m} c_p \Delta T \tag{42}$$

$$\dot{Q} = UA \cdot F \cdot \Delta T_{\text{ml,max}} = UA \cdot \Delta T_{\text{ml}} \tag{43}$$

Where the maximum temperature difference refers to counter flow HX configuration, and F is the correction factor applied to other flow configurations. On the other hand, if one knows all temperatures then the temperature difference can be readily calculated without needing to use the correction factor.

$$\Delta T_{ml,\max} = \frac{\left[\left(T_{h,i} - T_{c,o-CF}\right) - \left(T_{h,o-CF} - T_{c,i}\right)\right]}{\ln\left[\left(T_{h,i} - T_{c,o-CF}\right) / \left(T_{h,o-CF} - T_{c,i}\right)\right]} \tag{44}$$

$$\Delta T_{ml} = \frac{\left[\left(T_{h,i} - T_{c,o}\right) - \left(T_{h,o} - T_{c,i}\right)\right]}{\ln\left[\left(T_{h,i} - T_{c,o}\right) / \left(T_{h,o} - T_{c,i}\right)\right]} \tag{45}$$

The overall HX thermal conductance (UA) is composed by the fluid thermal resistances, tube thermal resistance and other parasitic resistances such as contact and fouling. Essentially the fluid thermal resistances are significantly larger and, therefore, the parasitic resistances are assumed negligible.

$$\frac{1}{UA} = \frac{1}{(\eta_o hA)_a} + \frac{\delta}{2k \ln(D_o/D_i)} + \frac{1}{(\eta_o hA)_r} \quad (46)$$

Equivalently the metrics described previously can be found using the ε-NTU method.

$$\varepsilon = \frac{\dot{Q}}{\dot{Q}_{\max}} = \frac{\dot{Q}}{(\dot{m}c_p)_{\min}(T_{h,i} - T_{c,i})} = \frac{\dot{Q}}{C_{\min}\Delta T_{\max}} \quad (47)$$

$$NTU = \frac{UA}{C_{\min}} \quad (48)$$

The relations between effectiveness and NTU will depend on flow arrangement and the heat capacity ratio (C_{min}/C_{max}) as summarized by Incropera et al. [158].

In this work the airside performance will be evaluated using the UA-ΔT_{ml} from the CFD simulations, explained previously, whereas the overall HX model is evaluated using the segmented ε-NTU method from Jiang et al. [159].

In the HX model the momentum and energy equations are decoupled, i.e. the thermal and hydraulic characteristics are solved independently.

3.3 Numerical Optimization

Abdelaziz et al. [72] introduced a very cost-effective multi-scale analysis and optimization method for novel air-to-refrigerant HX's, which the framework (Figure 14) foundations are used in this work. Their method consisted of an approximation assisted optimization (AAO) using Parallel Parameterized CFD (PPCFD) [72], Kriging metamodeling [88], and Multi-Objective Genetic Algorithm (MOGA). The entire CFD modeling and simulation occur within

ANSYS® platform, where geometry and meshing are built in Gambit 2.4.6 and the simulations are performed in Fluent 14.5. All other input/output and processed data occur within an external C# code tailored for the specific problem.

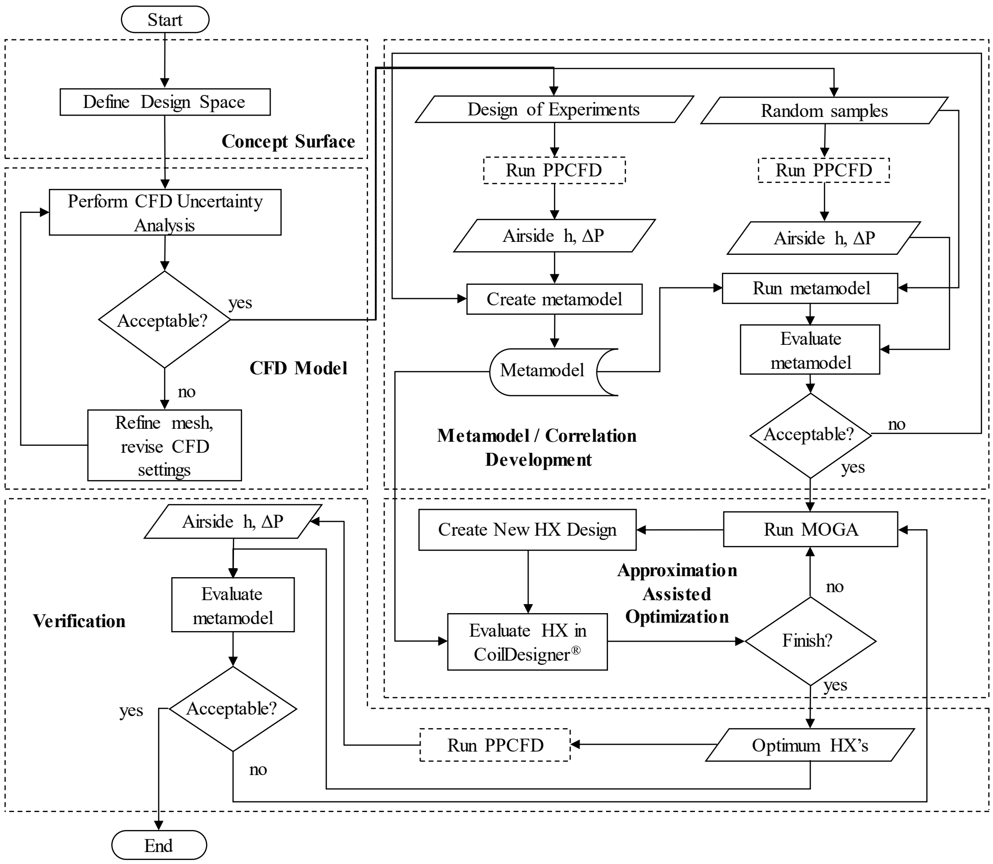

Figure 14. Numerical optimization framework.

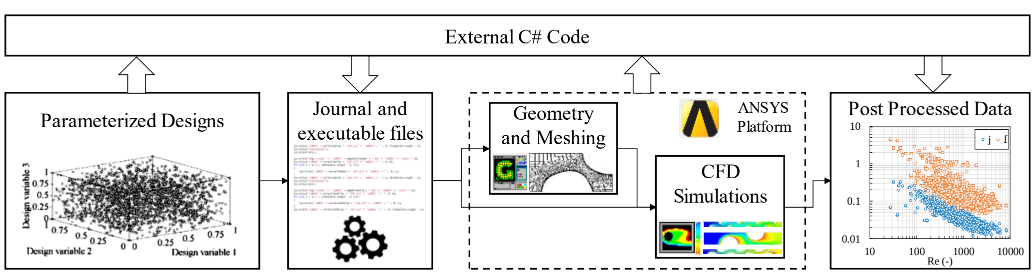

Figure 15. Parallel Parameterized CFD (PPCFD) framework.

3.3.1 Design of Experiments

The Design of Experiments consists of a systematic approach for appropriately sampling the design space in order to retrieve the highest quality of information that will truly portray the impact each design variable has over the simulations responses. Such step is crucial to develop a good metamodel without biasing. There are different methods for space sampling, from which in this work both the Maximum Entropy Sampling (MES) [160] and Latin Hypercube Sampling LHS) [161] are used.

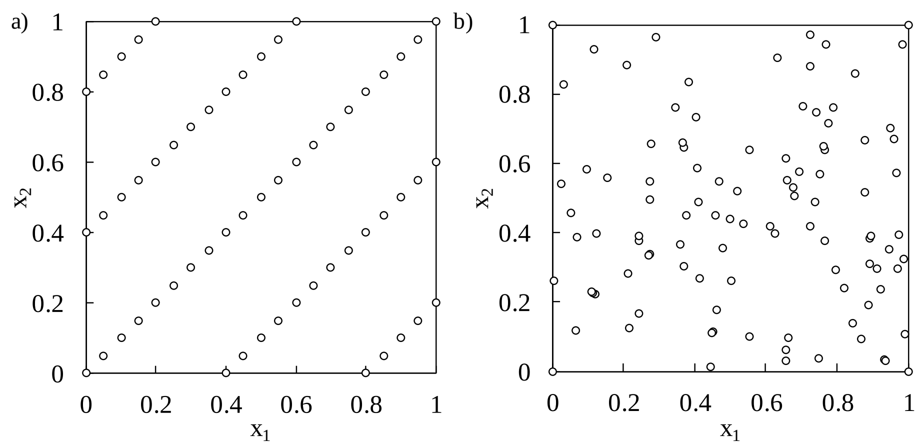

Figure 16. Space sampling example: a) biased; b) unbiased (LHS).

3.3.2 Kriging Metamodeling

Kriging is a metamodeling technique that predicts the response of an unknown design based on its linear distance from known designs and their response values through a stochastic process (i.e. random distributions) [88]. According to Wang and Shan [89] stochastic metamodels have superior performance over their counterpart deterministic methods, especially for non-linear problems. Kriging is recommended when the design space has 50 or less variables making it suitable for the application in this work.

Metamodeling is a simplified version of an actual physical model, such as CFD, with reasonable prediction accuracy. The last is measured by the metamodel's ability to predict ($\hat{y}_i$) the simulation responses (y_i) from random samples within a preset threshold deviation (e_{th}) (usually 5% to 10%). The metamodel is considered accurate (**M**aximum **A**cceptance **S**core) if the percentage of the random predicted responses within e_{th} is higher than the remainder of 1 - e_{th} (equation 49).

$$MAS = 100 \times \frac{\sum_{i=1}^{N} j_i}{N};\ j_i = \begin{cases} 1, & \text{if } e_i \le e_{th} \\ 0, & \text{if } e_i > e_{th} \end{cases};\ e_i = \frac{|\hat{y}_i - y_i|}{y_i};\ MAS_{e_{th}} \ge 1 - e_{th} \quad (49)$$

3.3.3 <u>Multi-Objective Optimization</u>

Multi-Objective optimization problem (equation 50) typically consists of 2 or more objective functions, subject to a set of equality and inequality constrains, and the design space boundaries.

$$\begin{aligned} \min\ & f_m(\underset{\sim}{x}) && m = 1, \dots M \\ s.t.\ & g_j(\underset{\sim}{x}) && j = 1, \dots J \\ & h_i(\underset{\sim}{x}) && i = 1, \dots I \\ & \underset{\sim}{x}_{lower} \le \underset{\sim}{x} \le \underset{\sim}{x}_{upper} \end{aligned} \quad (50)$$

The problem above represented can be suitably solved using Multi-Objective Genetic Algorithms (MOGA) [83].

Chapter 4: First & Second Order Analyses

4.1 First Order Analysis

As previously stated, for conventional tube sizes, fins are an undesired necessity for it provides sufficient surface area to attend the thermal performance required. However, first and second order analyses can readily show the benefits of moving towards smaller diameters. The following analyses are undertaken assuming, for all surfaces: same refrigerant side cross section area, same tube pitch ratios, same number of tube banks, constant airflow rate and velocities. Additionally, all results are based on numerical simulations using the modeling approach described in this section.

Figure 17 shows the compactness (surface-to-volume ratio), material utilization (surface to material volume ratio) and internal volume as a function of diameter for finless finned (plain fins) tubes. The reduction of internal volume translates into less refrigerant charge which will consequently reduce the weight and potential environmental concerns depending on the on the working fluid used. Moreover, the fin-to-tube surface ratio is linearly proportional to the diameter, thus the contribution to the total surface area from fins is significantly reduced for smaller diameters (Figure 18).

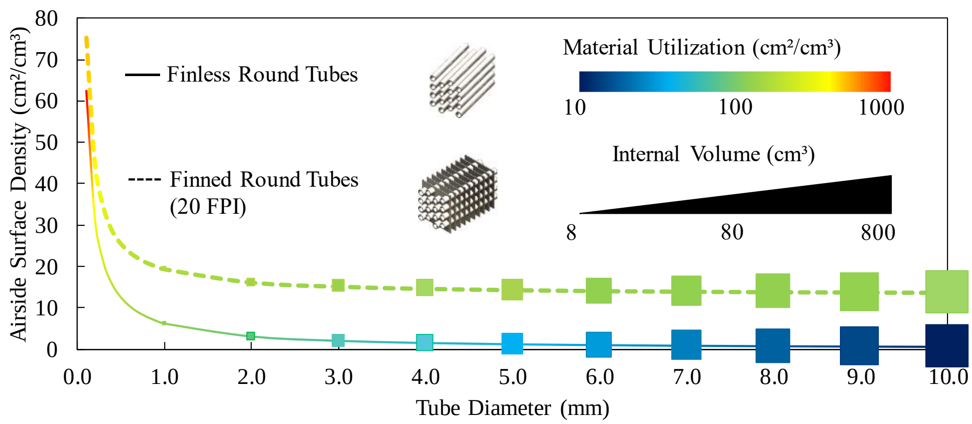

Figure 17. First order analyses I: compactness, material utilization and internal volume.

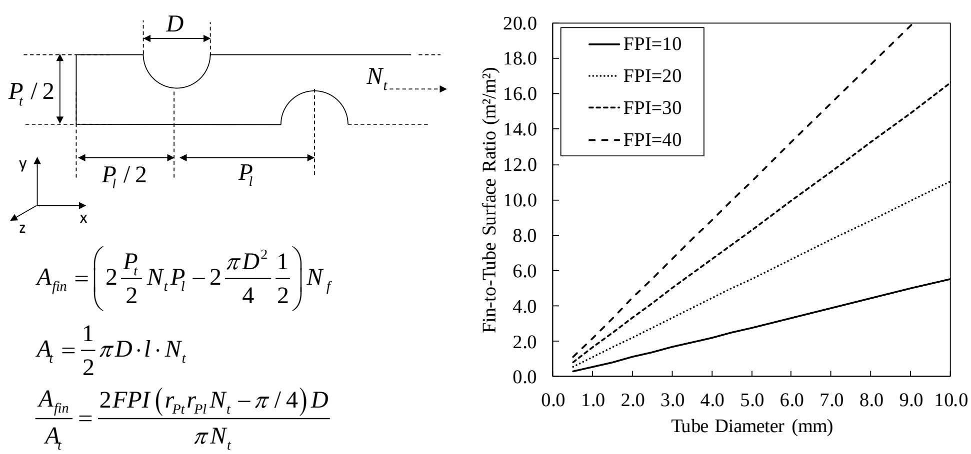

$$A_{fin} = \left(2\frac{P_t}{2} N_t P_l - 2\frac{\pi D^2}{4}\frac{1}{2} \right) N_f$$

$$A_t = \frac{1}{2}\pi D \cdot l \cdot N_t$$

$$\frac{A_{fin}}{A_t} = \frac{2FPI\left(r_{Pt} r_{Pl} N_t - \pi/4\right)D}{\pi N_t}$$

Figure 18. First order analyses II: fin-to-tube surface ratio.

4.2 Second Order Analysis

The reduction of the tube size has, most importantly, a significant impact on heat transfer coefficient. The relation between Nusselt and Reynolds numbers shows that as the characteristic length is reduced the heat transfer coefficient is increased [38] (equation 51). Additionally, the rate at which the heat transfer coefficient increases with respect to pumping power is much higher as the tube diameter is reduced for finless tubes compared to finned tubes. For larger tube diameters the finned surface is preferred as for the same heat transfer coefficient the pumping power cost is lower; however, as the diameter decreases the thermal-hydraulic ratio is favorable to finless surfaces (Figure 20).

$$Nu = \frac{h \cdot L_c}{k} \propto \mathrm{Re}_L^m \rightarrow h \propto L_c^{m-1}; 0 < m < 1 \tag{51}$$

4.2.1 <u>Surface Level Analysis</u>

Typically, we understand that the relationship between Reynolds number and the heat transfer and friction characteristics as fixed for the same type of geometry, i.e. the scale has no impact since Reynolds is a dimensionless number. Under same Reynolds numbers the flow over different diameters have different velocities; i.e. a higher velocity over smaller tubes will have a direct effect on the developing boundary layer over the tube surface, thus yielding different heat transfer and hydraulic characteristics (Figure 20 and Figure 20).

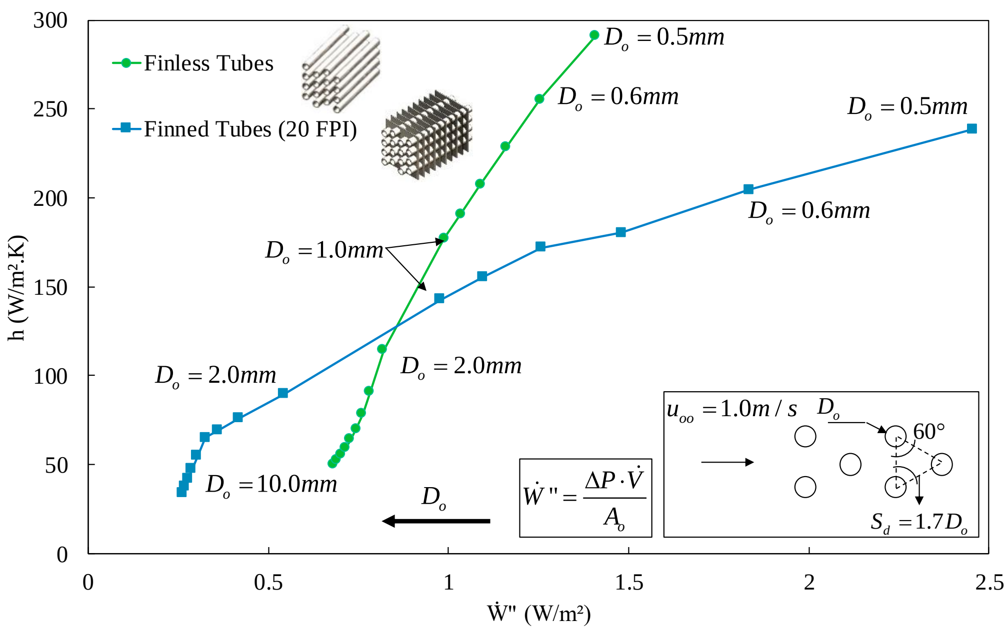

Figure 19. Second order analysis I: thermal-hydraulic characteristics.

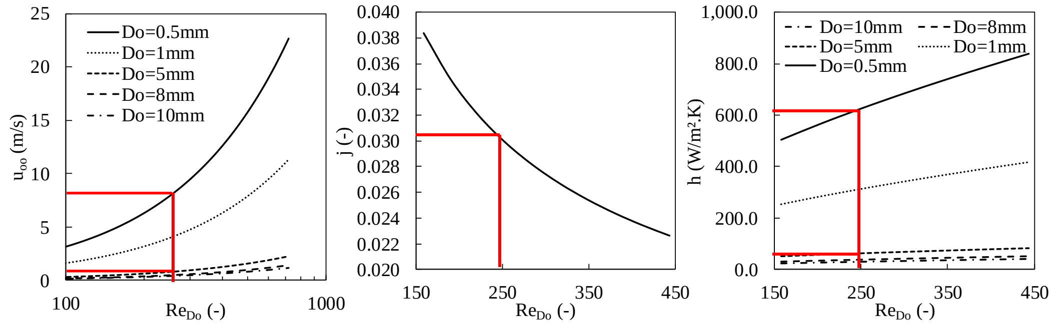

Figure 20. Thermal characteristics for same Reynolds and different diameters.

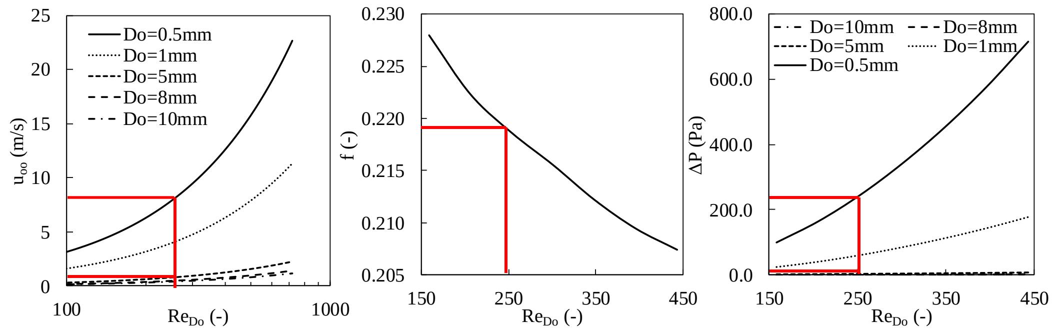

Figure 21. Hydraulic characteristics for same Reynolds and different diameters

Under same velocities the flow over different diameters are in different regimes, or, at least, different regions of the same regime which will result in higher heat transfer and friction for smaller tubes (Figure 22 and Figure 23).

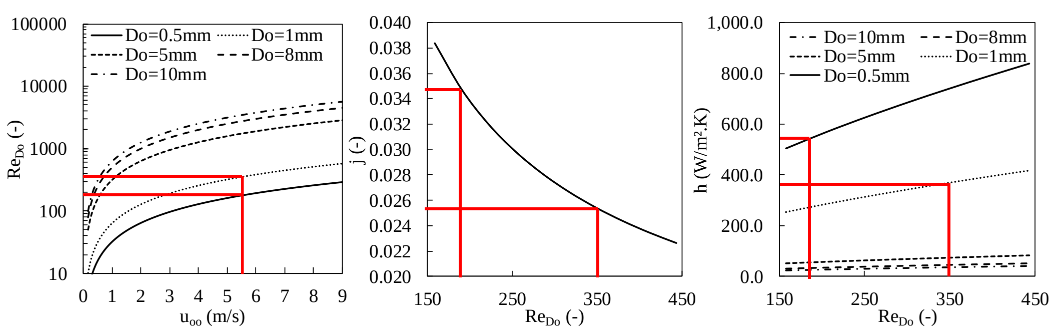

Figure 22. Thermal characteristics for same velocities and different diameters.

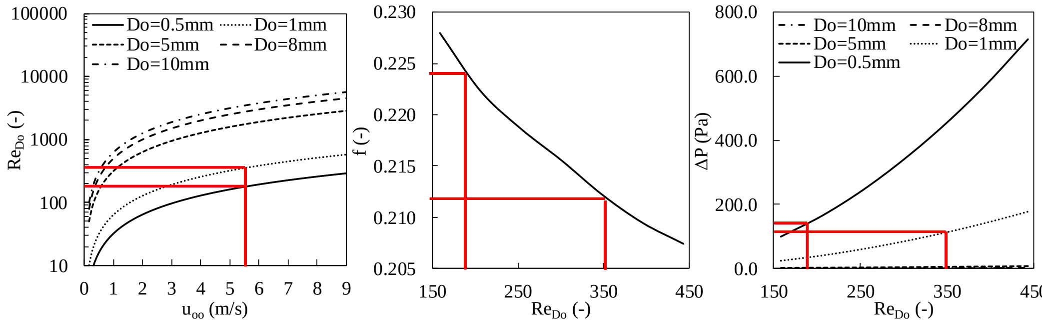

Figure 23. Hydraulic characteristics for same velocities and different diameters.

This section intends to provide a detailed perspective at the surface level using numerical simulations according to the procedures described in the previous section (3.1). The following study comprises of a parametric analysis on a single cylinder with air in cross flow while varying the diameter and cross-section shapes. The numerical and visualization results shall provide good insights on the underlying physics behind it and help understand Figure 20, Figure 20, Figure 22 and Figure 23.

4.2.1.1Round Tube with Parameterized Diameter

The first parametric analysis consists of varying the tube diameter and evaluating the performance characteristics for three different velocities. The normalized momentum boundary layer (Figure 24) is much thinner for smaller tubes which will result in higher velocity gradient, in particular for lower velocities. Likewise, the temperature gradient is much higher (Figure 25) since air has Prandtl number of ~0.7, therefore its development grows at similar rate. The local heat transfer and friction characteristics are show in Figure 26and Figure 27, respectively.

At higher velocities the flow regime on larger tube diameters change to fully turbulent, which result in a higher enhancing effect on smaller tubes. At 1.0m/s the 0.63mm diameter tube has Reynolds of ~40, while the 10mm diameter has ~634 and the average velocity and temperature gradients have a factor of ~4 between the two. For 15m/s, on the other hand, the respective Reynolds numbers raise to ~600 and 9500 and the enhancing factor increases to ~5-6.

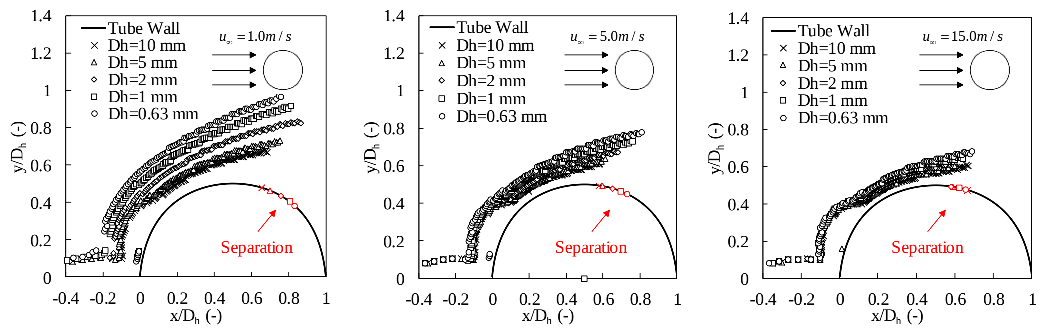

Figure 24. Momentum boundary layer over different tube diameters and air velocities.

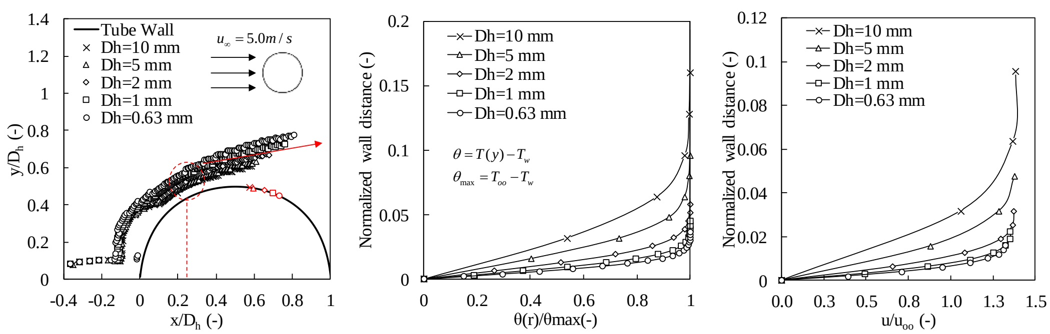

Figure 25. Normalized temperature and velocity profiles within the boundary layer at 25% of the tube surface for same velocity.

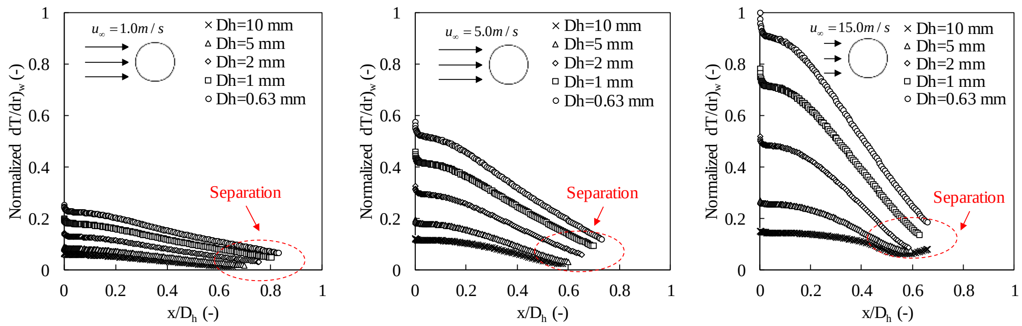

Figure 26. Surface temperature gradient over different tube diameters and air velocities.

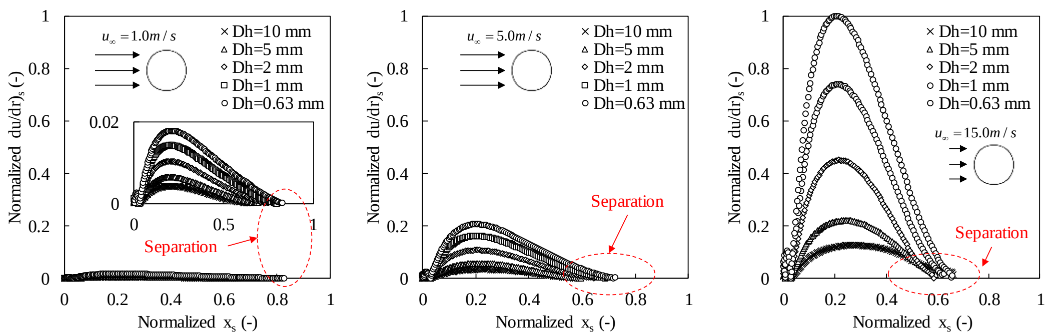

Figure 27. Surface velocity gradient over different tube diameters and air velocities.

The second parametric analysis consists of varying the tube diameter and evaluating the performance characteristics for three different Reynolds numbers (Figure 28). Even for the same Reynolds number, both the temperature and velocity profiles (Figure 29) change at much higher rate for the smaller diameters.

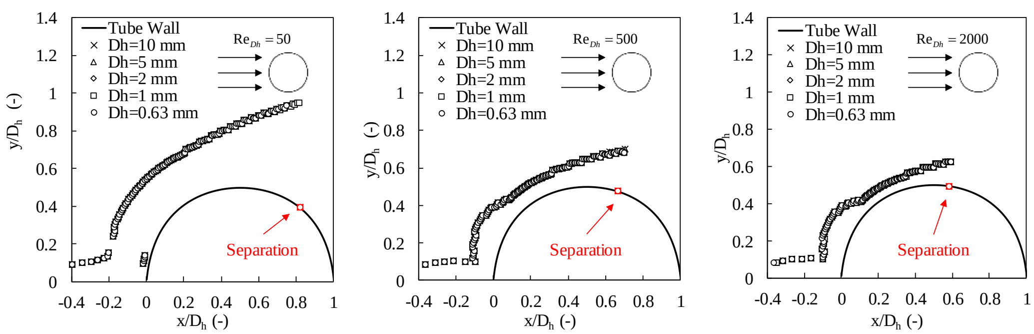

Figure 28. Momentum boundary layer over different tube diameters and Reynolds.

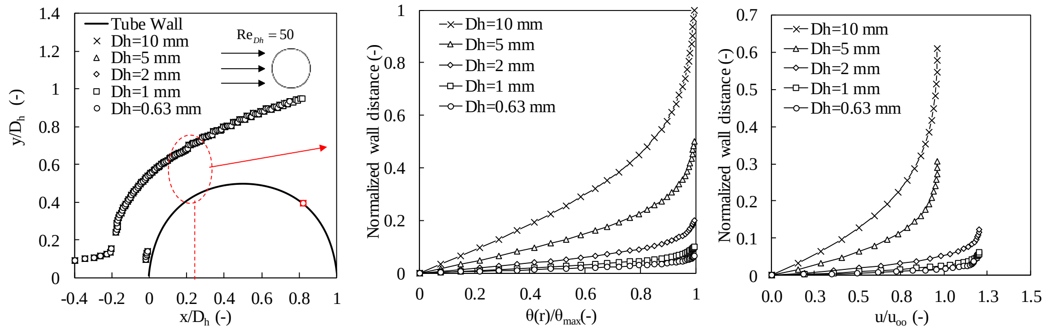

Figure 29. Normalized temperature and velocity profiles within the boundary layer at 25% of the tube surface for same Reynolds number.

The purpose is to demonstrate how the thermal-hydraulic characteristics change as function of the diameters (Figure 30 and Figure 31).

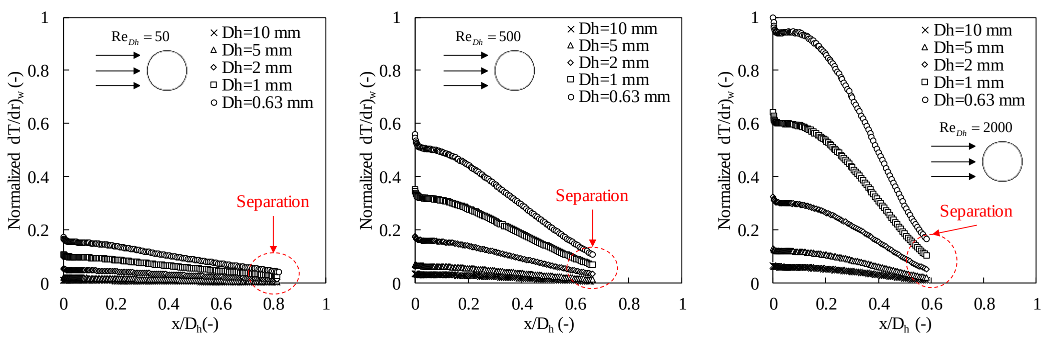

Figure 30. Surface temperature gradient over different tube diameters and Reynolds.

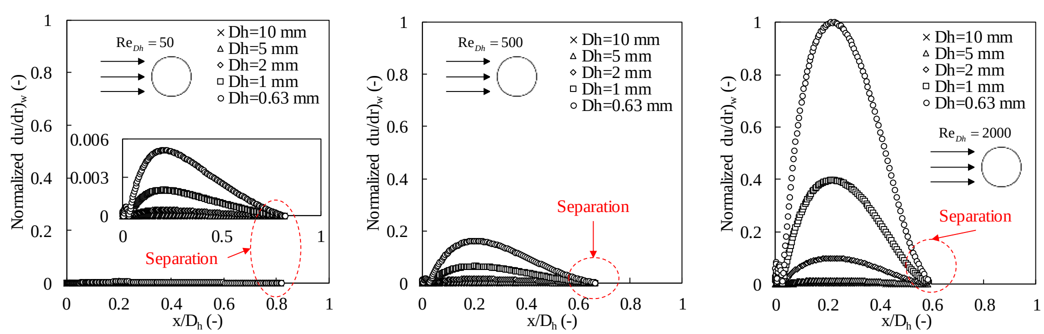

Figure 31. Surface velocity gradient over different tube diameters and Reynolds.

4.2.1.2Alternate Shapes

The impact of the tube shape on the performance can be significant, as demonstrated in the literature. In this section we present a brief analysis for the tube shapes on Figure 32 on how they perform, for the same hydraulic diameter (1.0mm), in a wide range of air velocities. The purpose is to evaluate whether different shapes will indeed impact positively on the thermal-hydraulic performance.

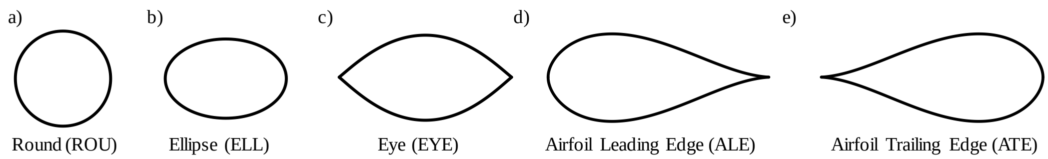

Figure 32. Tube shapes: a) Round; b) Ellipse; c) Eye; d) Airfoil leading edge; e) Airfoil trailing edge.

The top two plots in Figure 33 clearly indicate that ROU shape yields both the highest heat transfer and hydraulic resistance. The ratio of j over f, however, indicates a better balance for the ALE, ATE and EYE shapes.

The non-symmetric shapes with respect to the longitudinal axis to the flow, have a clear advantage over the other shapes. The j/f curves and the dimensioned heat transfer and friction power per unit area suggest a great overall performance improvement.

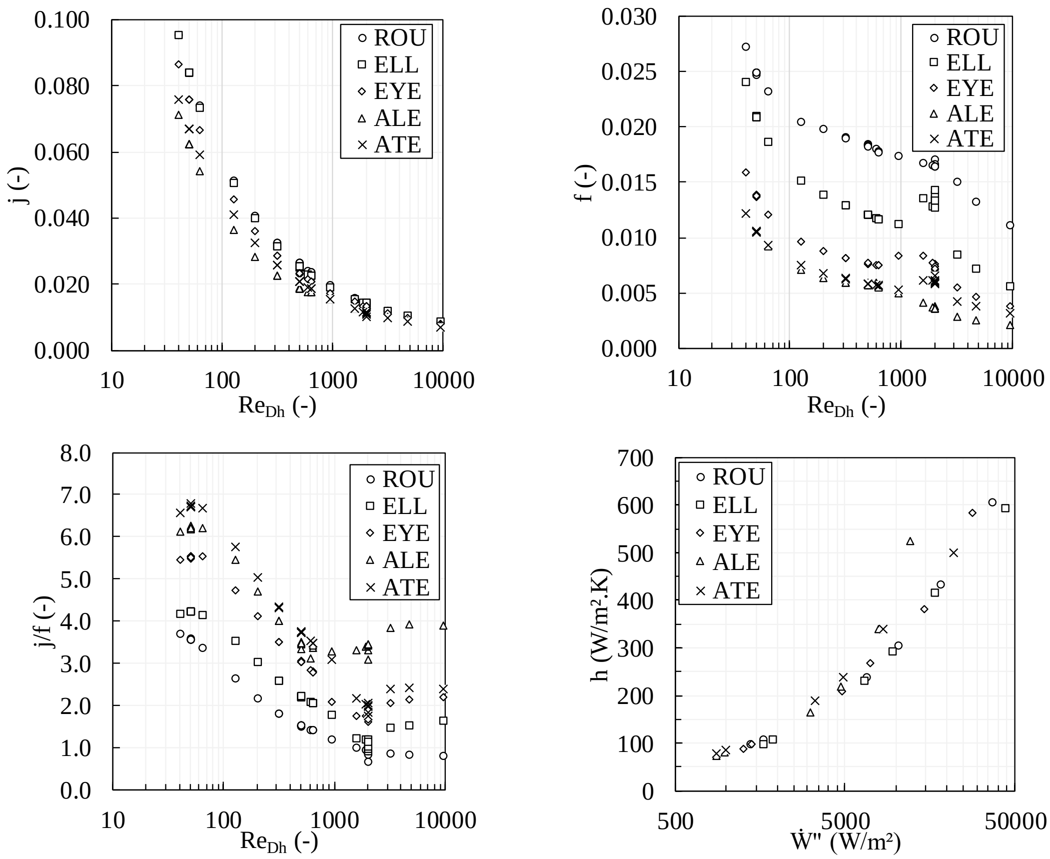

Figure 33. Thermal-hydraulic characteristics of airflow over different shapes.

Chapter 5: Multi-Scale Analysis and Shape Optimization

5.1 Design Framework

The HX design framework (Figure 34) employed in this work consists of six main sub-groups. The first - airside characterization - includes the 3 first sub-steps from the numerical optimization (Figure 14) (surface concept, CFD model and metamodeling). The second entails defining the problem, i.e. flow arrangements and operating conditions. The third step is the actual design and optimization using the approximation assisted optimization (AAO) methodology. The following step consists in the evaluation of the optimum designs with respect to manufacturability and potentially including multi-physics analysis such as mechanical stress evaluation, noise and vibration etc. The fifth step is conditional as to whether the HX was designed for a system level application, where the system performance is evaluated. The last step is the prototyping and experimental validation. On Appendix B stress analysis for one of the key HX's from this analysis is presented. The detailed dimensions and performance characteristics for every HX investigated in this work is disclosed in Appendix C. All details with respect to experimental facility, procedures, uncertainties and data are presented in Appendix D.

5.2 Concept Surfaces

Four types of design variables are defined in this work with which represent all investigated surfaces, however not all concepts will make use of the four types.

The first type, named “Scaling Variables”, which contain all variables that have absolute dimensions range pre-established.

The second type, “Topology Variables”, quantify relative dimensions that are function of the “Scaling Variables”. The third type, “Operating Variables”, i.e. any quantity related to the flow operating conditions or physical state of the fluid. Lastly, the “Shape Variables”, which define the surface shape independent from the other variable types.

Table 5. Design variable types.

Type	**Characteristic**	**Examples**
Scaling	Quantifiable	Diameter, height, length, width, rows of tubes, fin density, fin thickness
Topology	Non-Dimensional	Longitudinal / transverse pitch ratios, wall thickness ratio, corrugation angle
Operating	Fluid related	Velocity, temperature, pressure
Shape	Non-Dimensional	Spline control points, polynomial coefficients / order

5.2.1 Round Tube Heat Exchangers (RTHX & FTHX)

The simplest HX surface is the round tube bundle. From the first and second order analyses in Chapter 3 we observed great potential for such HX’s when using very small diameters. In this research, investigate finless round tube bundle in both staggered and in-line arrangement (Figure 35) using diameters ranging from 0.5mm up to 2.0mm are investigated. In addition to the finless version, tube bundle in staggered arrangement with low fin densities is also studied.

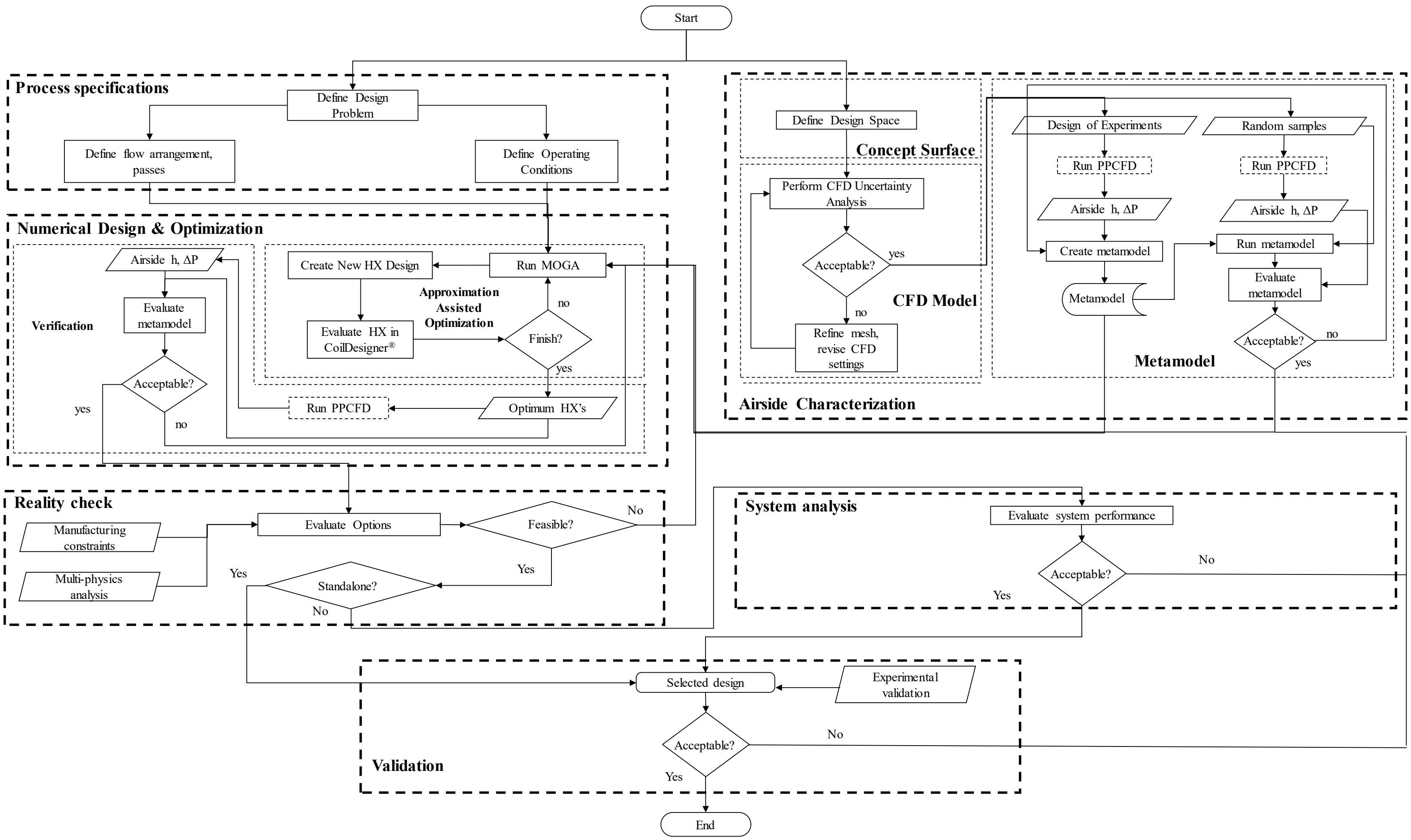

Figure 34. Heat exchanger design framework.

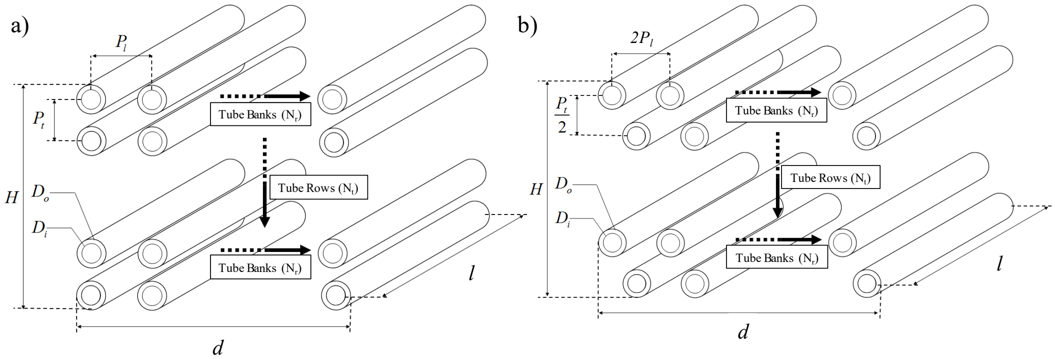

Figure 35. Round finless tubes (RTHX): a) In-line; b) Staggered.

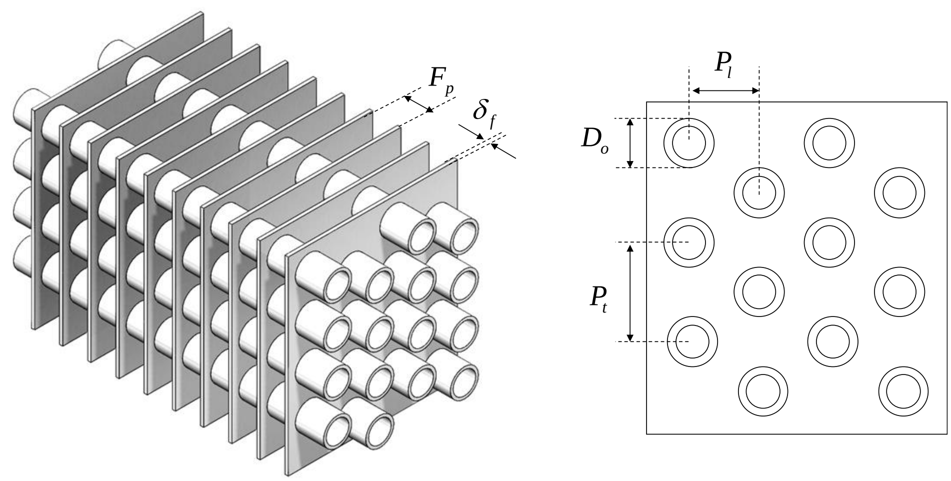

Figure 36. Flat fin and tube HX (FTHX)

Table 6. RTHX and FTHX Design space.

Variable Type	Design Variable	Unit	RTHX	FTHX
Scaling	D_o	mm	0.5 – 2.0	0.5 – 2.0
	FPI	in^{-1}	N/A	5 – 10
	Fin Thickness	mm	N/A	0.115
	Nr	-	2 – 20	2 – 10
Topology	P_t ratio (D_o)	-	1.2 – 4.0	1.5 – 3.0
	P_l ratio (D_o)	-	1.2 – 4.0	1.5 – 3.0
Operating	u	m/s	0.5-3.0	0.5-3.0

5.2.1.1 CFD Model

The CFD model for BTHX consists a 2-D computational domain (Figure 37) with symmetric boundaries on top and bottom. The GCI analysis (Figure 38) used constant refinement ratio of 1.3 and a factor of safety of 3.0 for all samples. Unlike the BTHX model, the FTHX model requires a 3-D computational domain (Figure 39) with symmetric boundaries on top and bottom, and periodic boundaries on the sides. The GCI settings are the same as for the BTHX models.

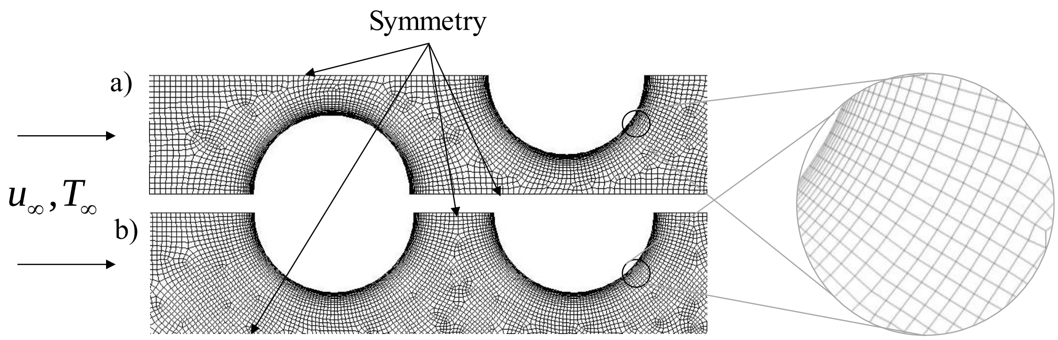

Figure 37. RTHX computational domain and mesh: a) staggered; b) in-line.

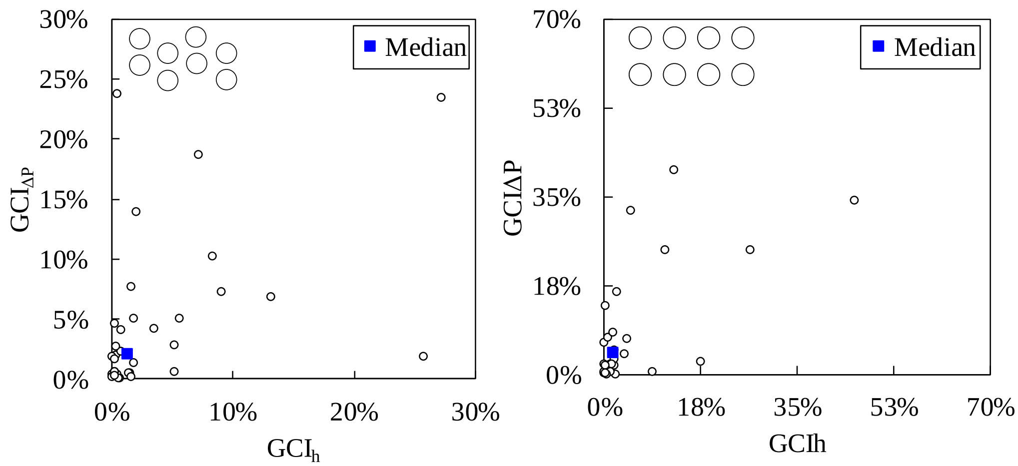

Figure 38. CFD GCI Analysis for BTHX in staggered and in-line arrangements.

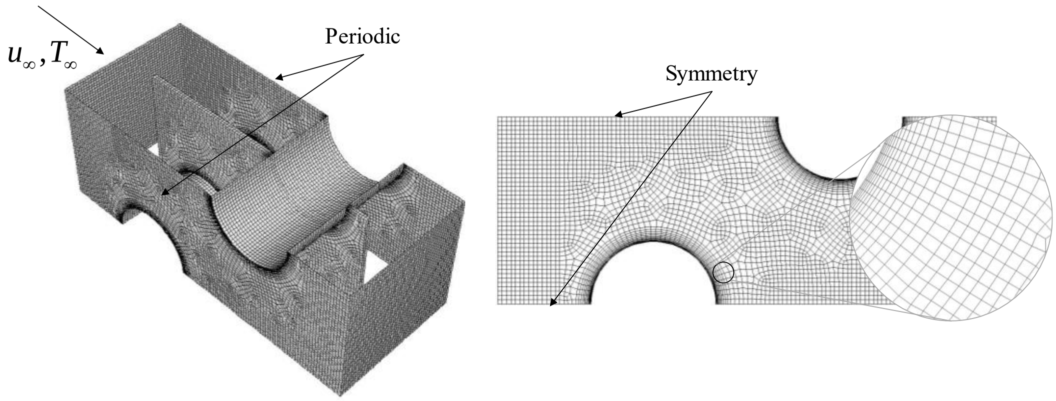

Figure 39. FTHX Computational domain and mesh.

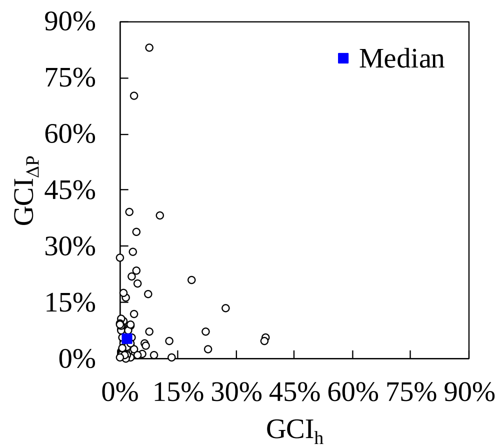

Figure 40. CFD GCI Analysis for FTHX.

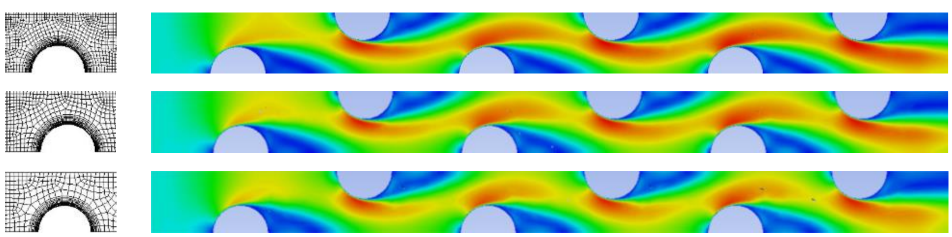

Figure 41. Example of contour plots on different grid resolutions for the FTHX.

5.2.1.2Metamodel Verification

The following plots (Figure 42 and Figure 43) show the metamodel verifications.

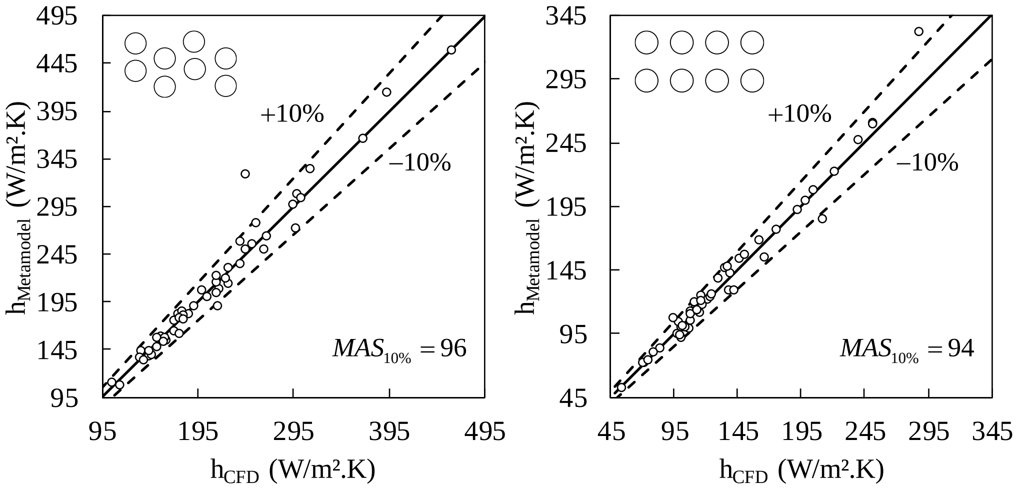

Figure 42. Heat transfer coefficient metamodel verification for RTHX in staggered and in-line arrangements for 50 random samples.

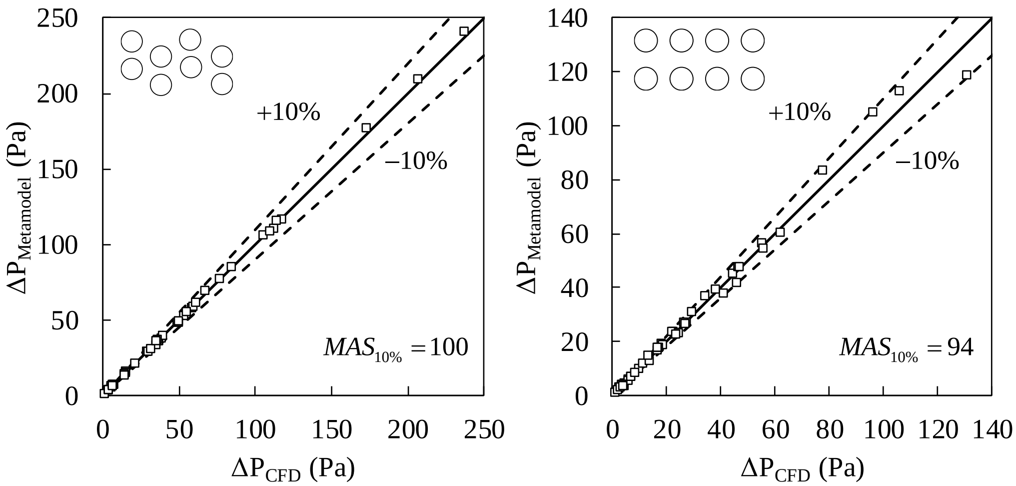

Figure 43. Pressure drop metamodel verification for RTHX in staggered and in-line arrangements for 50 random samples.

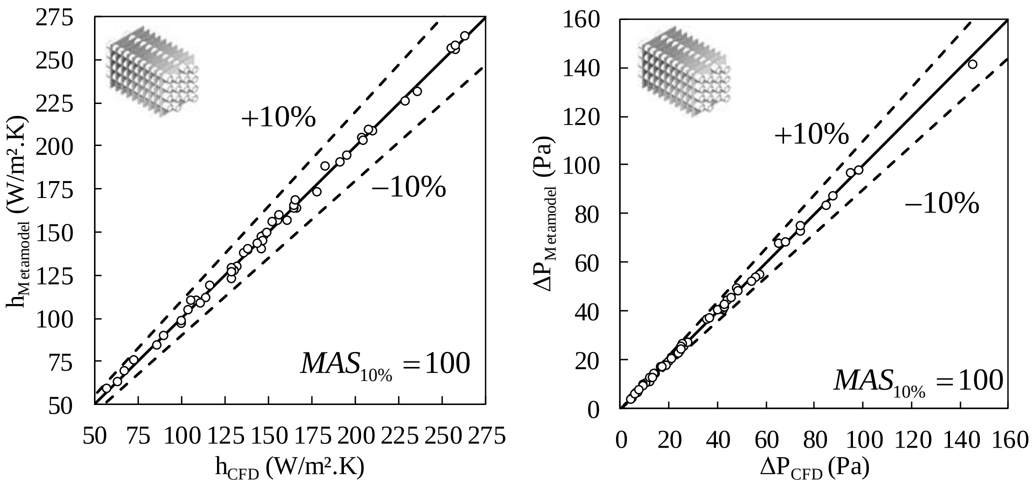

Figure 44. Metamodel verification for FTHX for 50 random samples.

5.2.1.3 RTHX Preliminary Analysis

In this section is presented a brief analysis comparing staggered and inline arrangements with a discussion of the benefits from each. The common sense always points to staggered arrangement as the best option for having higher heat transfer coefficient. On the other hand, it is also expected a higher hydraulic resistance. Zukauskas [119] had pointed out that there are certain configurations and operating conditions where the in-line may outperform the staggered version.

The analysis here presented is for an arbitrary design where both in-line and staggered arrangement have equivalent geometries; i.e. same hydraulic diameter, same surface area and so forth.

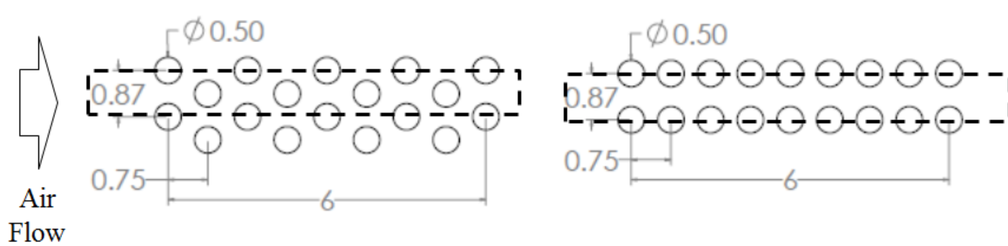

Figure 45. Equivalent round tube arrangements.

The designs above are evaluated under same velocity spectrum. The thermal hydraulic performance of each design, with respect to velocity is shown in Figure 46.

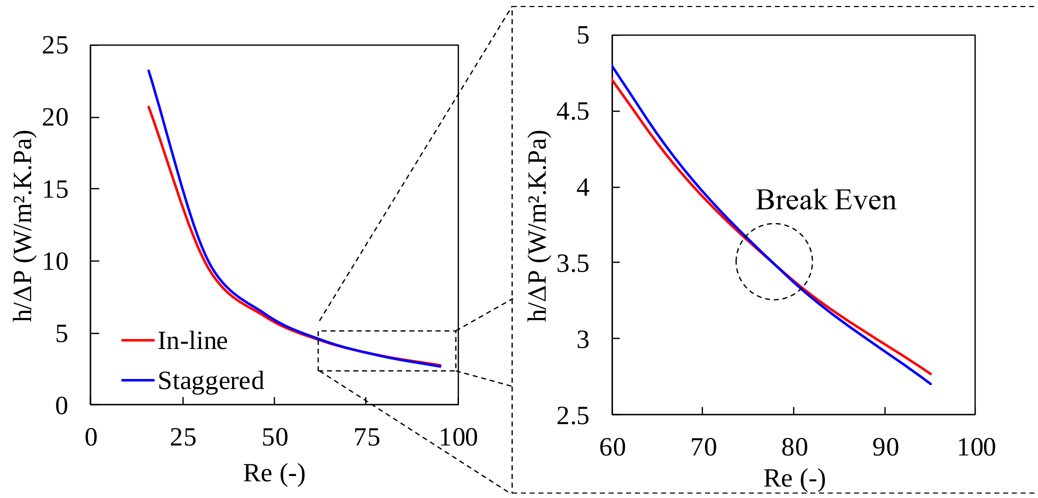

Figure 46. In-line vs. Staggered.

Figure 46 clearly shows how the staggered arrangement has both higher heat transfer coefficient and hydraulic resistance. The thermal-hydraulic performance of the in-line arrangement is less sensitive as velocity increases; the ratio between in-line over staggered decreases from 0.6-0.7 to 0.4-0.5 on both h and ΔP. The underlying physics behind was discussed in section 4.3. The staggered arrangement has an abrupt flow impingement in every tube; furthermore, aside from the first tube bank, all other banks have an accelerated flow impinging on them due to the tube arrangement. The main differences between the two arrangements can be observed in Figure 47 and Figure 48 showing detailed results for one frontal velocity.

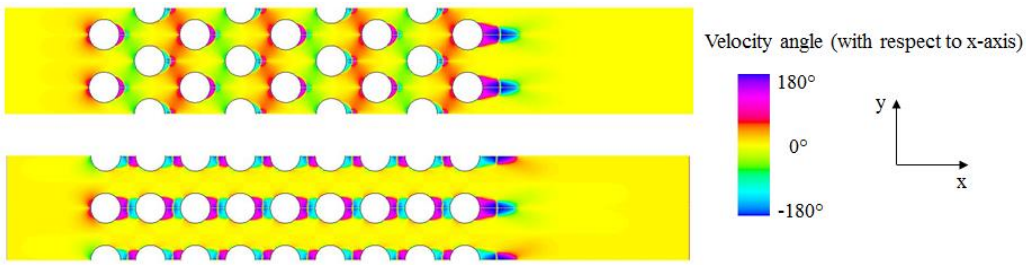

Figure 47. Contours of velocity angle.

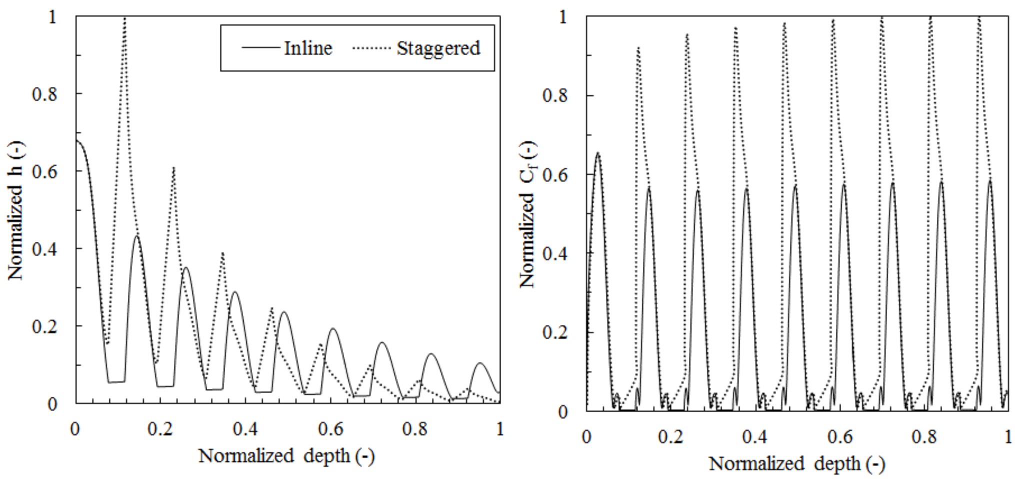

Figure 48. Local heat transfer coefficient and skin friction coefficient at the tube wall.

5.2.2 <u>NURBS Tube Heat Exchangers (NTHX)</u>

The NURBS Tube Heat Exchanger (NTHX) concept (Figure 49) is essentially equivalent to the round finless tube bundle in staggered arrangement, with the addition of the shape variables that describe the cross section profile of the tube. The design space consists of 12 design variables (Table 7) from which 6 are the x and y normalized coordinates of the control points used to describe the NURBS curve. With two fixed control points demarking the width of the tube over the centerline and the three variable points a 4th order NURBS curve (Figure 50). The waterside tube shape is a function of the constant wall thickness. Preliminary structural analysis showed that a wall thickness equivalent to 20% (NTHX-001 is

30%) of the tube height (Figure 50) is a safe assumption to ensure no deformation nor mechanical collapse for an internal pressure at most of 6.0MPa.

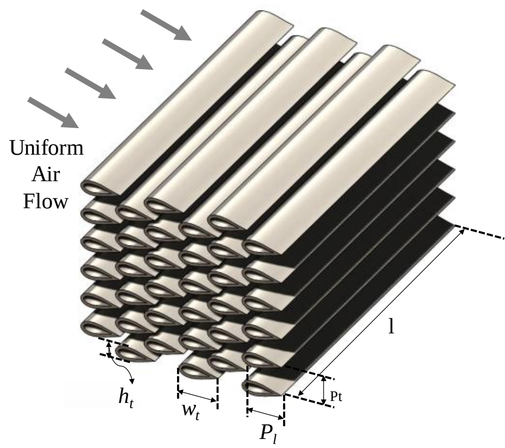

Figure 49. NTHX surface concept.

Table 7. NTHX Design space.

Variable Type	Design Variable	Unit	Range
Scaling	h_t	mm	0.5 - 3.0
	w_t/ h_t	-	1.0 - 3.0
	N_r	-	2 – 20
Topology	P_t/ h_t	-	2.0 - 3.0
	P_l/ w_t	-	0.75 – 3.0
Shape	x_i	-	0.0 – 1.0
	y_i	-	0.0 – 1.0
Fluid	u	m/s	0.5 - 5.0

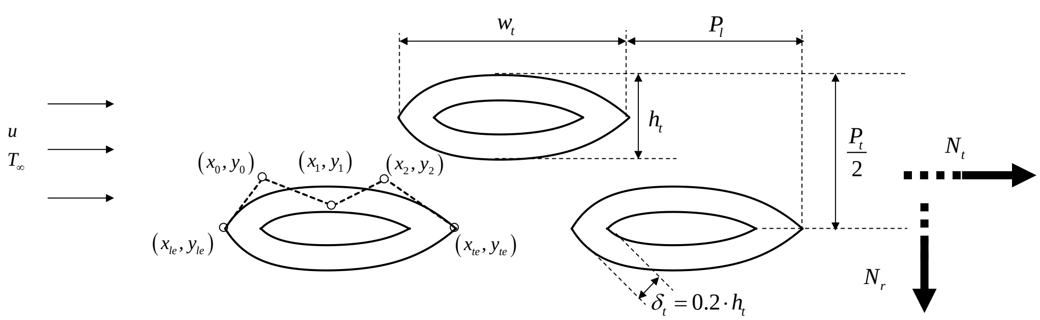

Figure 50. NTHX Profile parameterization.

5.2.2.1 CFD Model

The CFD model for NTHX consists a 2-D computational domain (Figure 51) with symmetric boundaries on top and bottom. The GCI analysis (Figure 52) used constant refinement ratio of 1.3 and a factor of safety of 3.0 for all samples.

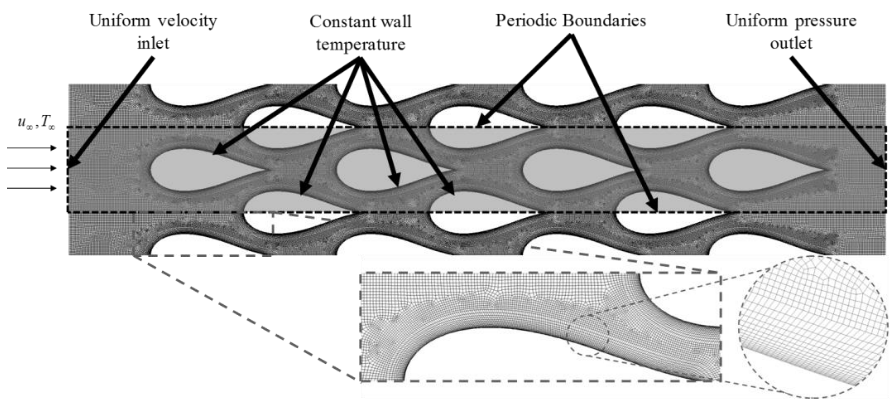

Figure 51. NTHX Computational domain.

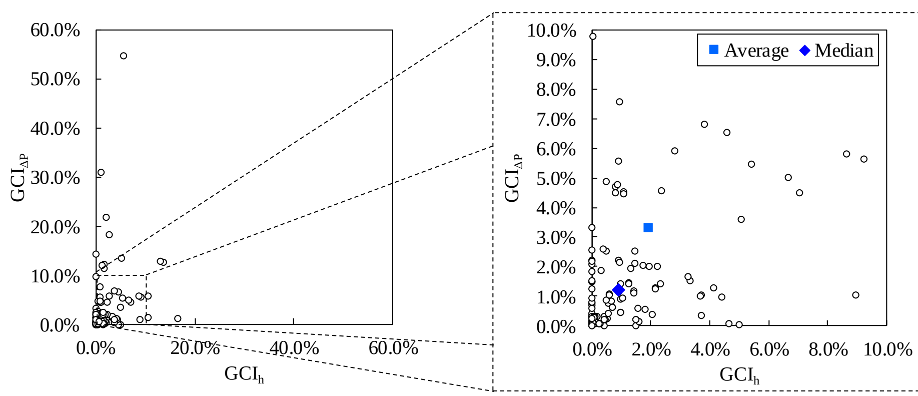

Figure 52. NTHX GCI Analysis.

5.2.2.2Metamodel Verification

A Design of Experiments (DoE) containing 7096 samples generated using Latin Hypercube Sampling (LHS) was simulated using PPCFD. Due to geometry/mesh fails or simulation divergence an effective 3286 samples could be used to create the metamodels. These metamodels were tested against 961 random designs as shown in Figure 53.

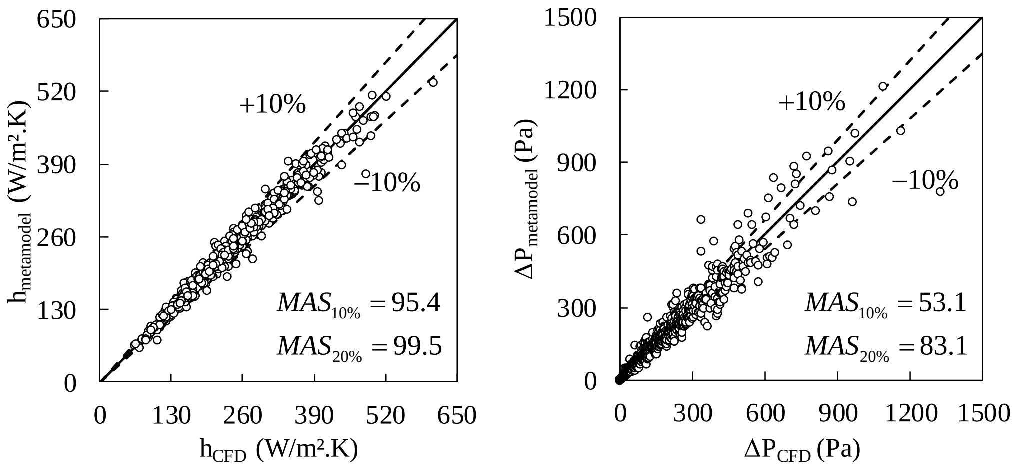

Figure 53. NTHX Metamodel verification against 961 random samples.

5.2.3 Webbed-NURBS Tube Heat Exchangers (WTHX)

Abdelaziz et al. [76] and Cevallos et al. [148] have studied the webbed-round tube surface concept, showing great potential for performance improvement. This work combines the same concept with the NURBS shape parameterization (Figure 54). In this case four variable control points are used as opposed to three, thus resulting in a 5th order NURBS curve (Figure 55).

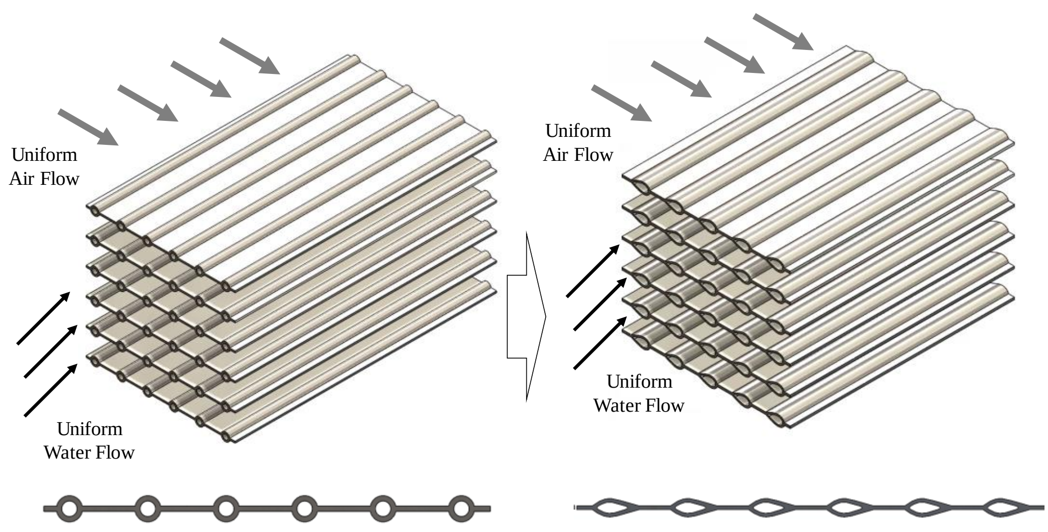

Figure 54. WTHX Surface concept.

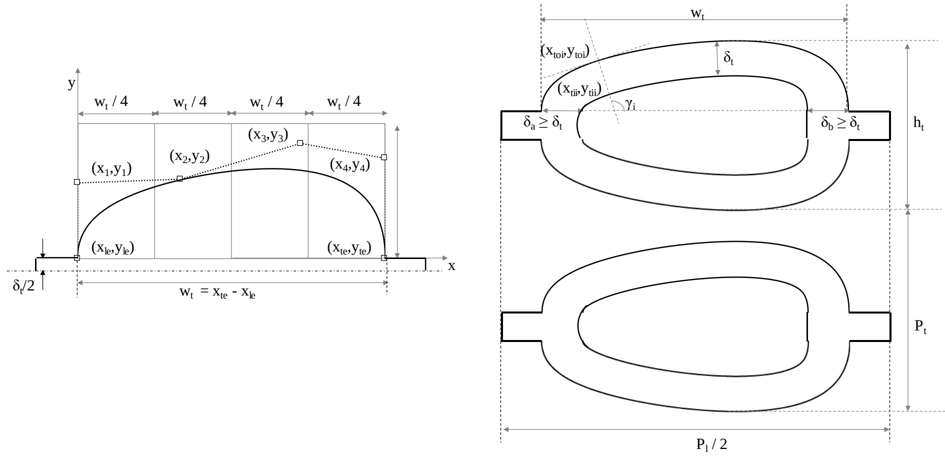

Figure 55. WTHX Profile parameterization.

5.2.3.1 CFD Model

The computational domain (Figure 56) includes one tube only, with periodic boundaries. The mean GCI for heat transfer and pressure drop are 0.7% and 1.8%, respectively. The WTHX design space (Table 8) covers the same type of design variables as the NTHX concept.

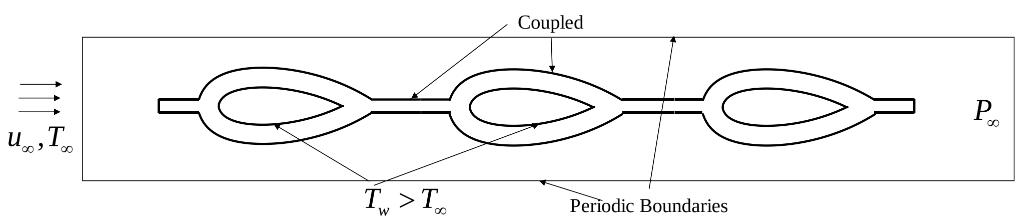

Figure 56. WTHX Computational domain.

Table 8. WTHX Design space.

Variable Type	**Design Variable**	**Unit**	**Range**
Scaling	h_t	mm	0.5 - 3.0
	w_t/ h_t	-	1.0 - 3.0
	N_r	-	2 – 20
Topology	P_t/ h_t	-	2.0 - 3.0
	P_l/ w_t	-	0.75 – 3.0
Shape	x_i	-	0.0 – 1.0
	y_i	-	0.0 – 1.0
Fluid	u	m/s	0.5 - 5.0

5.2.3.2 Metamodel verification

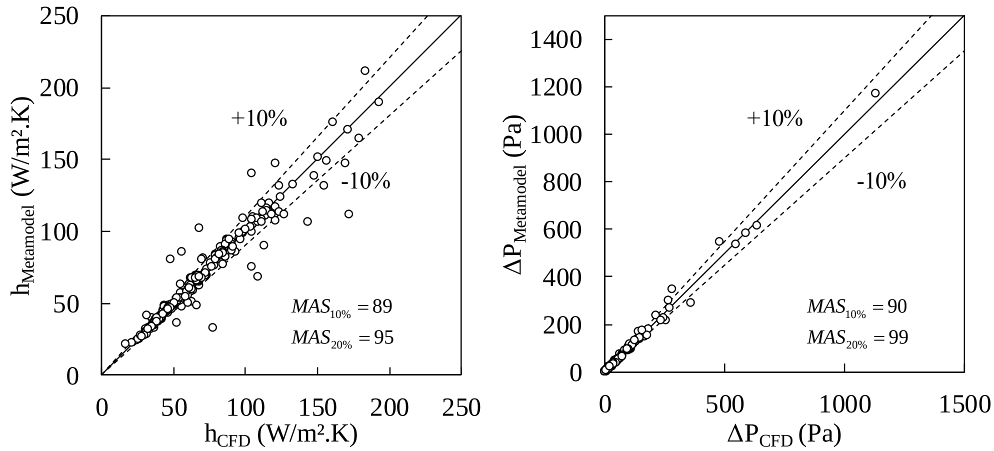

Figure 57. WTHX Metamodel verification.

5.2.4 Airfoil-Shaped Tube Heat Exchangers (AFHX)

The Airfoil-Shaped tube HX (AFHX) is a concept inspired by the rotating air cooler [162]. The latter has the blades arranged as such the air flow passage gap is constant, thus avoiding boundary layer separation. While such characteristic is desirable for lowering pressure drop, the fully developed flow result in lower heat transfer coefficient. The AFHX concept (Figure 58) has two banks where the second is rotated 180° from the first and shifted half the gap. The tube shape, gap passage and leading/trailing edges are all ellipses or part of ellipses, where the radii and coefficients can be the shape design variables. The design space is shown in Table 9.

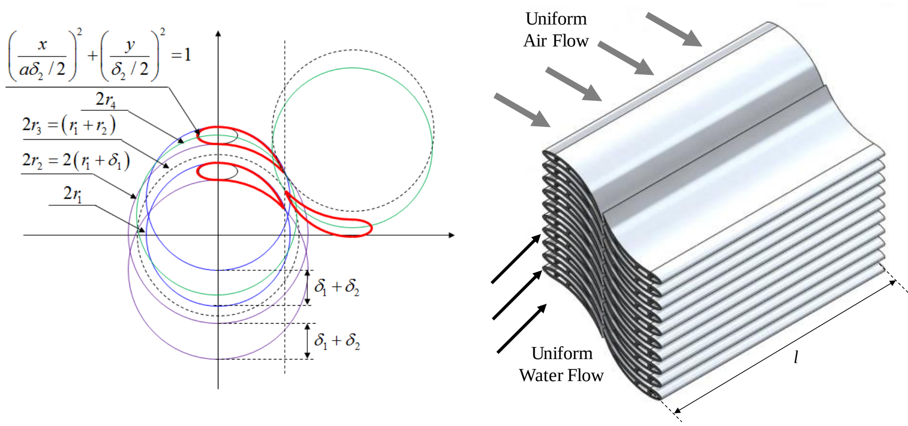

Figure 58. AFHX Concept.

Table 9. AFHX Design space.

Variable Type	Design Variable	Unit	Range
Scaling	r_1	mm	0.5 - 3.0
	δ_1	-	1.0 - 3.0
Topology	δ_2/ δ_1	-	2 – 20
Shape	a	-	2.0 - 3.0
Fluid	u	m/s	0.5 - 5.0

5.2.4.1 CFD Model

The computational domain (Figure 58) is trimmed according to the ellipses at the centerline of the air passage and tubes. The mean GCI for heat transfer and pressure drop are 0.2% and 0.5%, respectively.

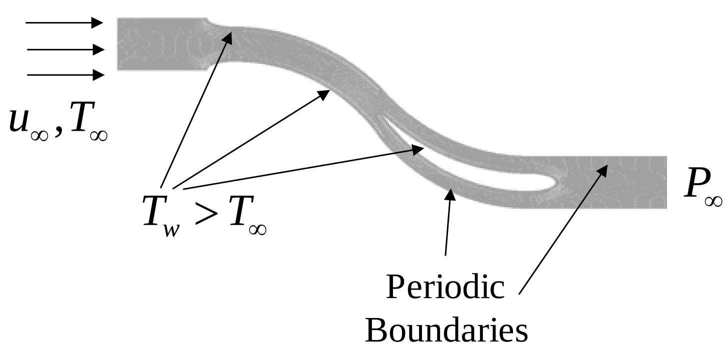

Figure 59. AFHX Computational domain.

5.2.4.2 Metamodel Verification

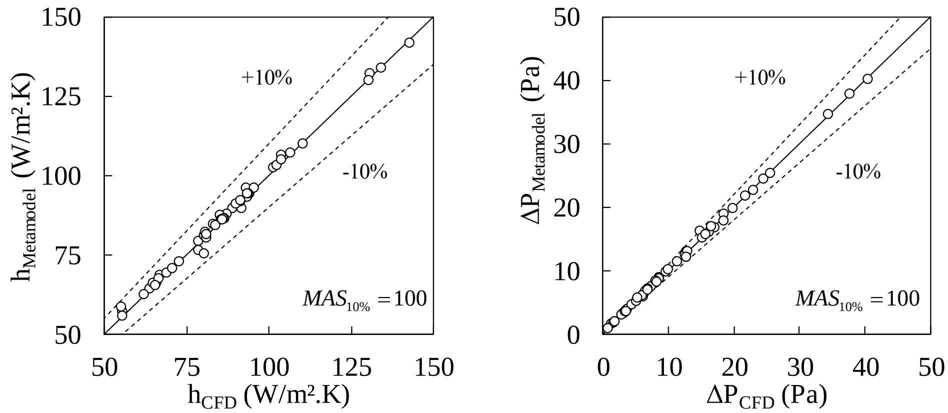

Figure 60. AFHX Metamodel verification.

5.3 Design Problems (DP)

5.3.1 DP I: 1.0kW Single-Phase Heat Exchangers

The first application of the methodology is a 1.0kW air-to-water HX. A MCHX [163] radiator was used as baseline for comparison. This HX is a non-conventional MCHX that was designed to deliver a higher performance than the current state-of-the art MCHX technologies for such application. The HX MCHX is a one slab of 14 tubes with 22 ports each (D_h = 0.75mm), vertically spaced by 4mm; and 18 louvered fins per inch fill the tube spacing. The core volume is 230cm³ with 0.0102m² of face area; the airside hydraulic diameter is 1.64mm.

Table 10. 1.0kW Baseline MCHX.

Metric	**Unit**	**Value**
Air flow rate	m³/s	0.03
Air inlet temperature	K	300
Water flow rate	g/s	25
Water inlet temperature	K	347.5
Heat load	W	1053
Pumping power	W	2.35
Air pressure drop	Pa	78
Air heat transfer coefficient	W/m².K	144
Airside thermal resistance	K/W	0.022

5.3.1.1Proof-of-Concept NTHX-001

The proof-of-concept NTHX-001 was designed to deliver similar capacity as the baseline MCHX while reducing 20% the envelope volume and approximately 20% reduction in airside pressure drop while maintaining the same approach temperature (50K). Additionally, we established the air frontal velocity should be at most 3.0m/s which corresponds to 2% reduction in face area compared to the MCHX. For simplicity, we determined the face area should have aspect ratio equal to 1.0.

The tube shape is similar to the surface ALE from the previous section with minor adjustments to the control point coordinates. Additionally, the available manufacturing option imposed a minimum wall thickness of 0.3mm, tube height of 1.0mm and tube width of 3.0mm.

The airside thermal conductance of the baseline MCHX is approximately 45W/K, therefore a similar value was obtained by the NTHX-001 surface. Several CFD simulations (Figure 61) were carried out in order to find a potential candidate. A final surface with 7 tube banks, 1.1mm tube height, 3.0mm tube width, 2.2mm vertical spacing and 2.4 mm horizontal spacing was found to be a viable candidate (Figure 62). The GCI for this CFD model is 0.1% for heat transfer and 0.397% for pressure drop. The resulting HX then has 315 tubes (7x45) with an airside thermal conductance of 42.2W/K and pressure drop of 64 Pa.

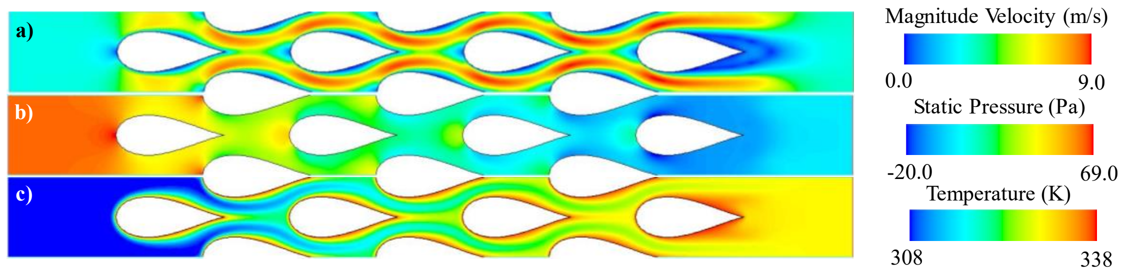

Figure 61. CFD Results for the NTHX-001: a) velocity; b) pressure; c) temperature.

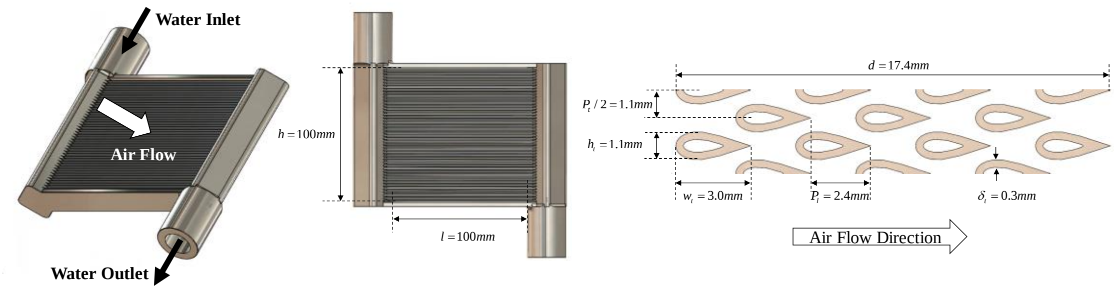

Figure 62. Proof-of-concept NTHX-001 dimensions.

Following the CFD analysis, comes the HX simulation, which occurs within the CoilDesigner® [159] environment. This platform can handle any type of crossflow air-to-fluid HX with either headers or complex tube circuitry. The airside is an external input from CFD, whereas the refrigerant side is handled with existing correlations available in the literature using the equivalent inner hydraulic diameter for round channels. The last is reasonable since these correlations work well for single-phase laminar flows [164, 165]. To account for differences in area and perimeter of the inner the pressure drop on the waterside needs correction (ζ) according to equations (52) and (53). The HX analysis and comparison results against the MCHX are shown in Table 11.

$$\Delta P_w = \zeta \cdot f \frac{l}{D_{h\_in}} \cdot \frac{1}{2} \frac{\dot{m}^2}{\rho \cdot A_{D_{h\_in}}^2} ; \zeta = \left(\frac{A_{D_{h\_in}}}{A_{actual}} \right)^2 \tag{52}$$

$$D_{h\_in} = 4 \frac{A_{actual}}{P} = 4 \frac{\int_{u=0}^{u=1} dC_x(u) \cdot dC_y(u)}{\int_{u=0}^{u=1} \sqrt{1 + \left(\frac{dC_y(u)}{dC_x(u)} \right)^2} \cdot du} \tag{53}$$

Table 11. NTHX-001 Numerical results compared to the baseline MCHX.

Metric	**Unit**	**MCHX**	**NTHX-001**	**Relative Diff.**
Face Area (A_f)	m²	0.0102	0.0100	-2.00%
Water Cross Section Area (A_{cs})	mm²	173	186	7.40%
Airside Heat Transfer Area (A_o)	m²	0.312	0.211	-32.3%
Envelope Volume (V_{HX})	cm³	230	174	-24.3%
Internal Volume (waterside)	cm³	32.9	18.6	-43.5%
Material Volume (tube + fins)	cm³	77.0	46.8	-39.2%
Compactness (A_o/V_{HX})	cm²/cm³	44.3	57.5	29.8%
Air Frontal Velocity (u)	m/s	2.94	3.00	2.00%
Airside Heat Transfer Coefficient (h_{air})	W/m².K	144	200	38.9%
Airside Pressure Drop (ΔP_{air})	Pa	78	64	-17.9%
Airside Conductance (UA_{air})	W/K	44.9	42.2	-5.90%
Heat Load (Q)	W	1109	1072	-3.30%

5.3.1.2 Design and Optimization – RTHX

Two optimization problems (equation 54) were investigated, where the second comprised of fixed diameter tubes due to the availability of tubes to build a prototype. The final results are displayed in Figure 63. The proof-of-concept RTHX-001 was verified against CFD (Figure 41) to evaluate the metamodel prediction, which exhibited 0.6% deviation in heat transfer coefficient, and 3.88% in pressure drop. The uncertainty analysis resulted in GCI of 1.64% for heat transfer coefficient and 2.21% for pressure drop, for the group of the finest meshes from 5 grid resolutions.

$$
\begin{array}{ll}
\text{Optimization I:} & \text{Optimization II: :} \\
\min \Delta P_{air} & \min \Delta P_{air} \\
\min V_{HX} & \min V_{HX} \\
s.t. & s.t. \\
1.0 \le \dot{Q} \le 1.1kW & 1.0 \le \dot{Q} \le 1.1kW \\
\Delta P_{air} \le 0.8 \cdot \Delta P_{air\_baseline} & \Delta P_{air} \le 0.8 \cdot \Delta P_{air\_baseline} \\
\Delta P_{water} \le 1.0kPa & \Delta P_{water} \le 1.0kPa \\
V_{HX} \le 0.8 \cdot V_{HX\_baseline} & V_{HX} \le 0.8 \cdot V_{HX\_baseline} \\
 & D_o = 0.8mm
\end{array}
\tag{54}
$$

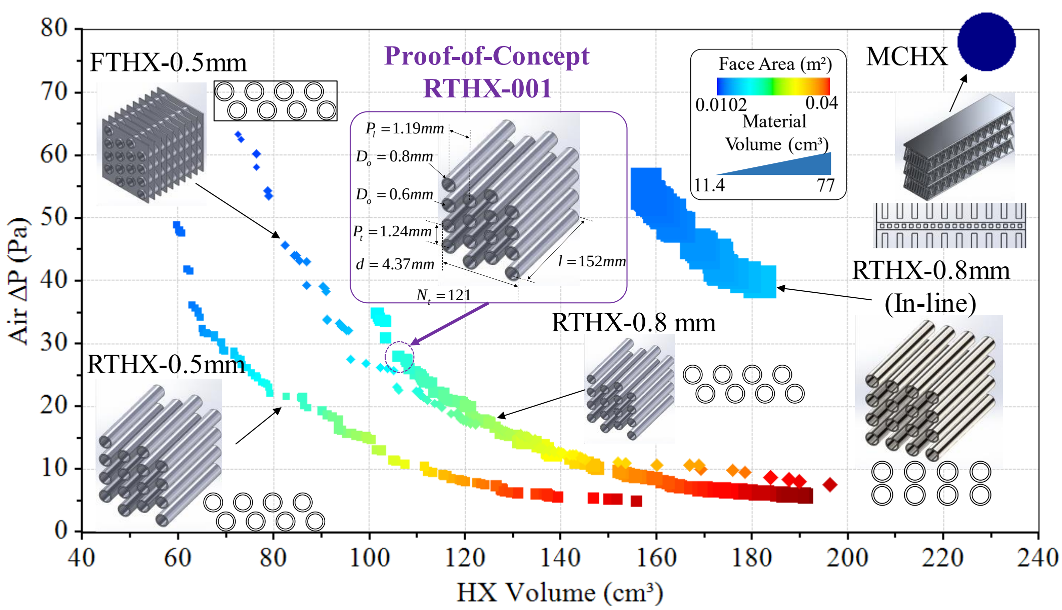

Figure 63. DP I: RTHX & FTHX Optimization results.

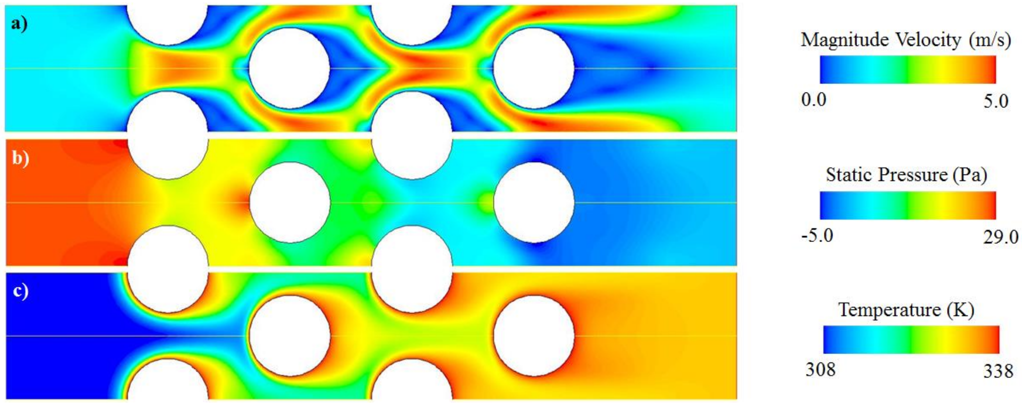

Figure 64. RTHX-001 CFD verification contour plots: a) velocity; b) pressure; c) temperature.

The numerical results compared against the baseline are displayed in Table 12.

Table 12. RTHX-001 Numerical results compared to the baseline MCHX.

Metric	**Unit**	**MCHX**	**RTHX-001**	**Relative Difference**
Face Area (A_f)	m²	0.0102	0.0228	123.53%
Water Cross Section Area (A_{cs})	mm²	173	137	-20.90%
Airside Heat Transfer Area (A_o)	m²	0.312	0.185	-40.74%
Envelope Volume (V_{HX})	cm³	230	109	-52.61%
Internal Volume (waterside)	cm³	77	16.2	-78.99%
Material Volume (tube + fins)	cm³	32.9	20.8	-36.78%
Compactness (A_o/V_{HX})	cm²/cm³	13.57	16.96	25.05%
Air Frontal Velocity (u)	m/s	2.94	1.32	-55.25%
Airside Heat Transfer Coefficient (h_{air})	W/m².K	144	308	113.89%
Airside Pressure Drop (ΔP_{air})	Pa	78	27	-65.38%
Airside Conductance (UA_{air})	W/K	44.9	56.9	26.83%
Heat Load (Q)	W	1109	1200	8.21%

5.3.1.3 Design and Optimization – NTHX

Three optimization problems (equation 55) are investigated each including additional constraints in a stepwise manner, bridging the gap between theoretical and real (i.e. NTHX-001). The last optimization problem entails finding optimum designs with similar manufacturing constraints imposed to the NTHX-001, with a thinner wall thickness.

$$
\begin{array}{lll}
\text{Optimization I:} & \text{Optimization II:} & \text{Optimization III:} \\
\min \Delta P_{air} & \min \Delta P_{air} & \min \Delta P_{air} \\
\min V_{HX} & \min V_{HX} & \min V_{HX} \\
s.t. & s.t. & s.t. \\
1.0 \le \dot{Q} \le 1.1kW & 1.0 \le \dot{Q} \le 1.1kW & 1.0 \le \dot{Q} \le 1.1kW \\
\Delta P_{air} \le 0.8 \cdot \Delta P_{air\_baseline} & \Delta P_{air} \le 0.8 \cdot \Delta P_{air\_baseline} & \Delta P_{air} \le 0.8 \cdot \Delta P_{air\_baseline} \\
\Delta P_{water} \le 1.0kPa & \Delta P_{water} \le 1.0kPa & \Delta P_{water} \le 1.0kPa \\
V_{HX} \le 0.8 \cdot V_{HX\_baseline} & V_{HX} \le 0.8 \cdot V_{HX\_baseline} & V_{HX} \le 0.8 \cdot V_{HX\_baseline} \\
 & A_f \le A_{f\_baseline} & A_f \le A_{f\_baseline} \\
 & & h_t \ge 1.0mm \\
 & & w_t / h_t \ge 3.0
\end{array}
\tag{55}
$$

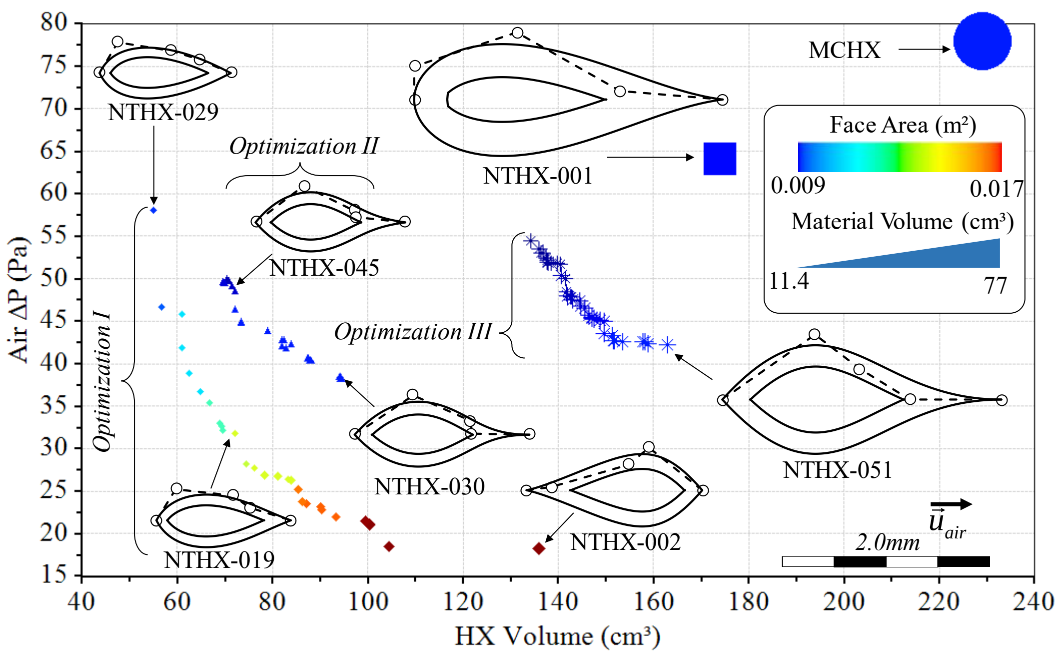

Figure 65. DP I: NTHX Optimization results I.

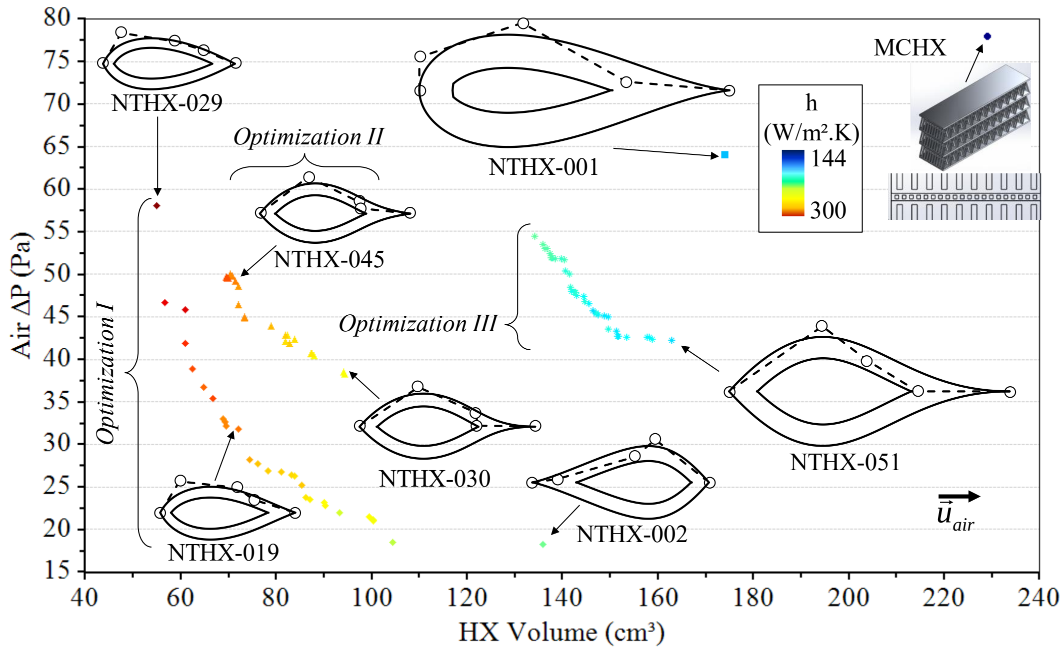

Figure 66. DP I: NTHX Optimization results II.

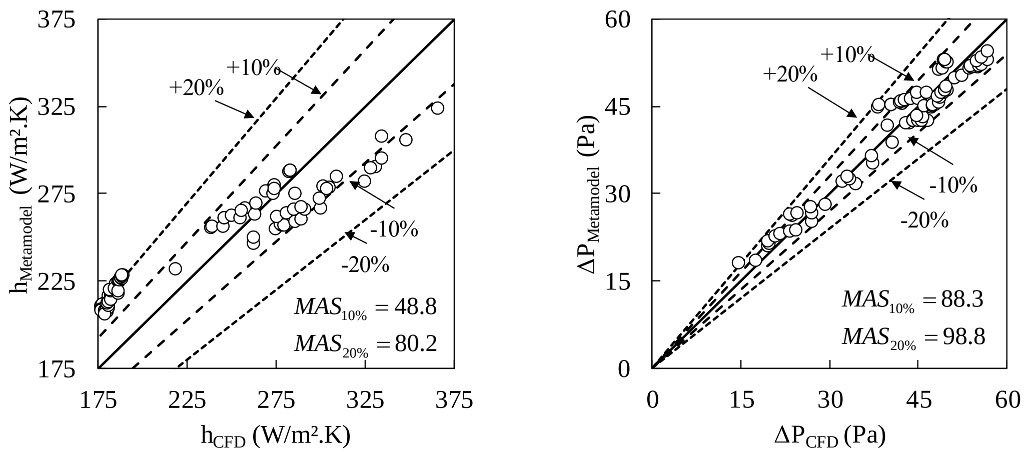

Figure 67. DP I: NTHX Metamodel verification for the optimum designs.

5.3.1.4Design and Optimization – WTHX & AFHX

For the AFHX and WTHX surfaces only one optimization problem was investigated (equation 56). The results are shown in Figure 68.

$$
\begin{aligned}
&\text{Optimization I:}\\
&\min \Delta P_{air}\\
&\min V_{HX}\\
&s.t.\\
&1.0 \le \dot{Q} \le 1.1kW\\
&\Delta P_{air} \le 0.8 \cdot \Delta P_{air\_baseline}\\
&\Delta P_{water} \le 1.0kPa\\
&V_{HX} \le 0.8 \cdot V_{HX\_baseline}\\
&A_f < A_{f\_baseline}
\end{aligned} \tag{56}
$$

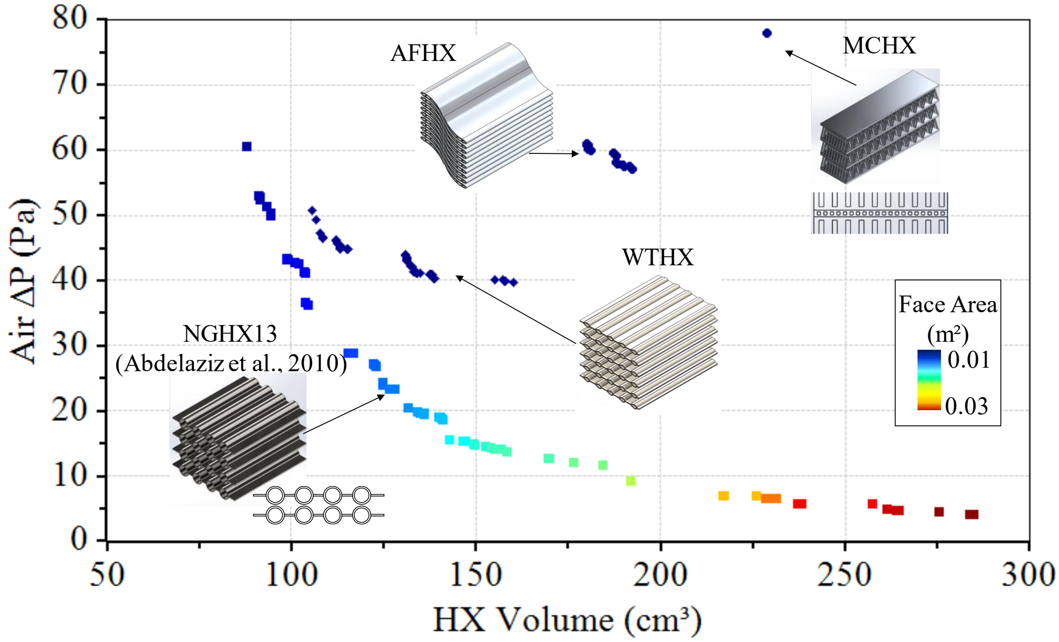

Figure 68. DP I: WTHX & AFHX Optimization results.

5.3.1.5 Heat Exchanger Optimization Map

In this section, the most relevant optimum designs are combined in single optimization maps (Figure 69 and Figure 70) showing different metrics and how they compare overall. The following CFD results (Figure 71 and Figure 72) show contour plots for selected designs at their operating design point.

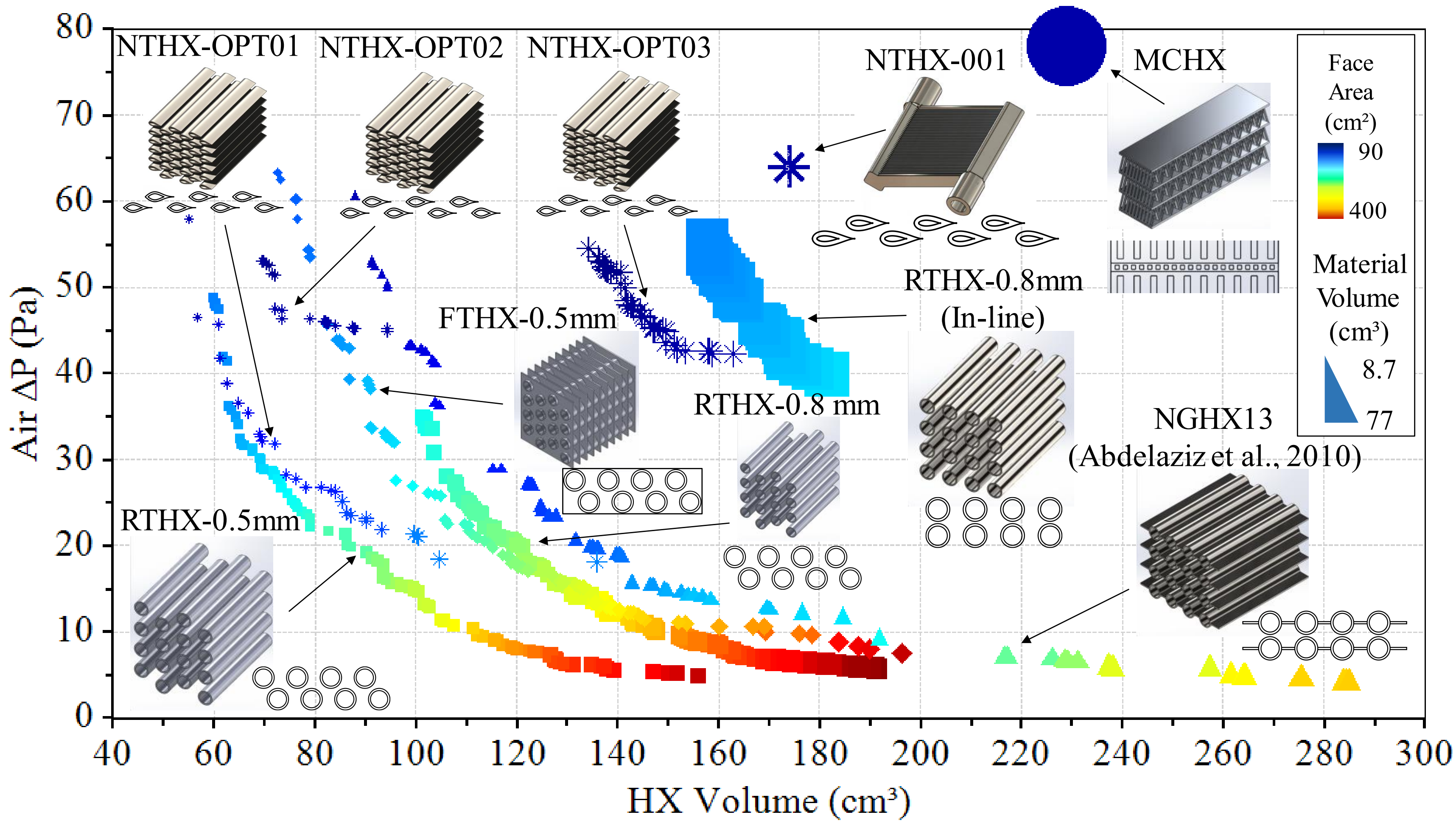

Figure 69. DP I HX Optimization map I.

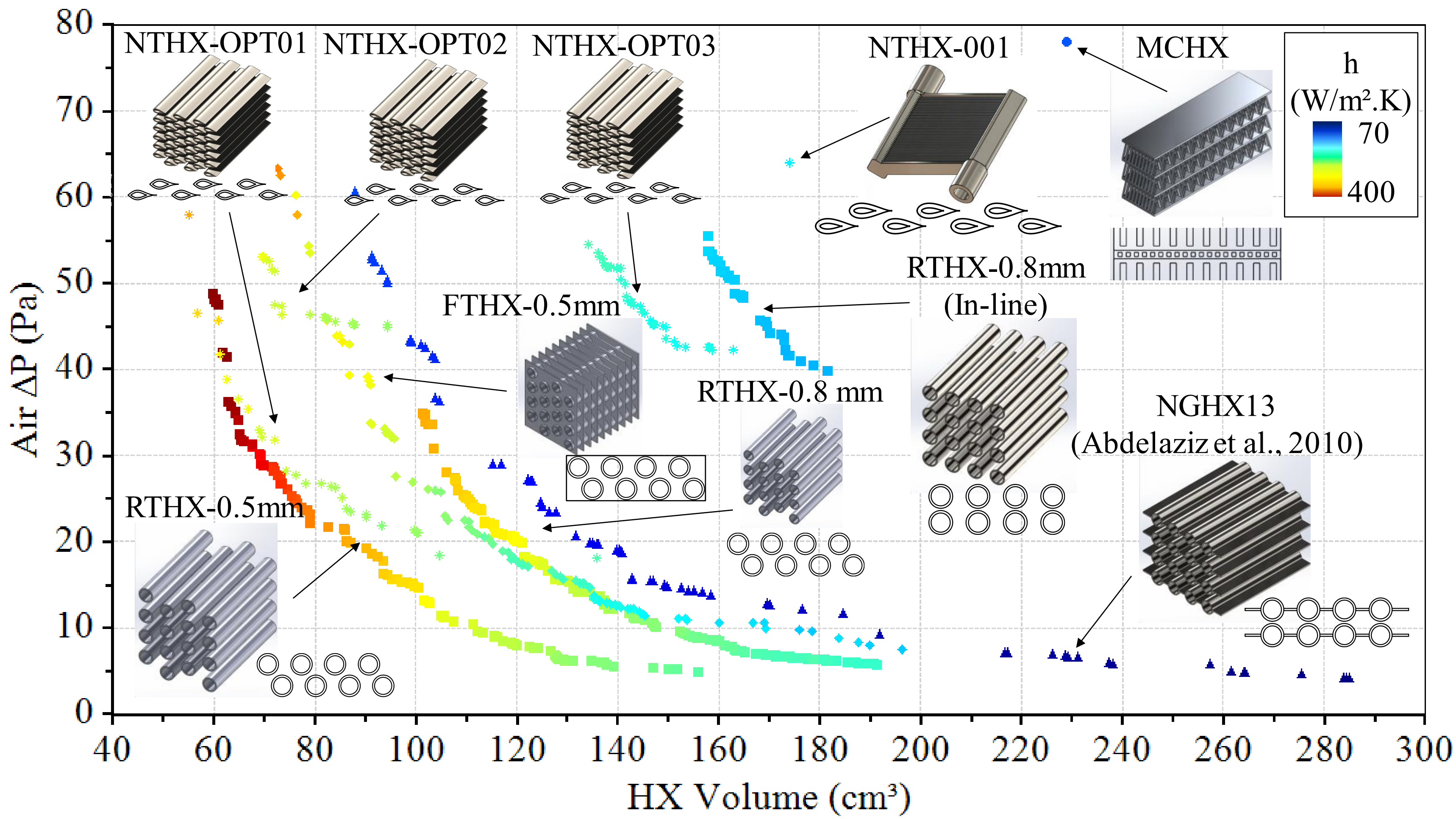

Figure 70. DP I Optimization map II.

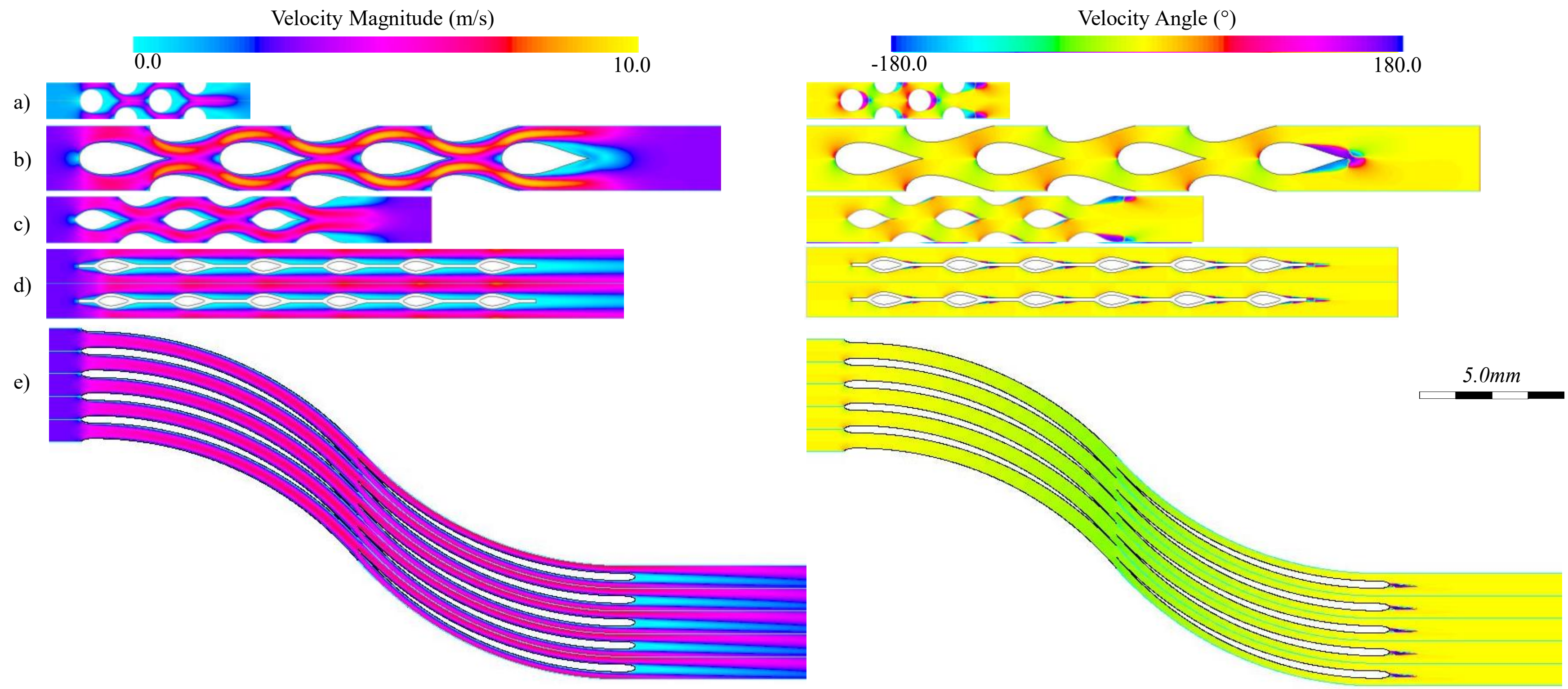

Figure 71. Velocity magnitude and angle contour plots for selected designs for DP I: a) RTHX-001; b) NTHX-001; c) NTHX-030; d) WTHX-011; e) AFHX-001.

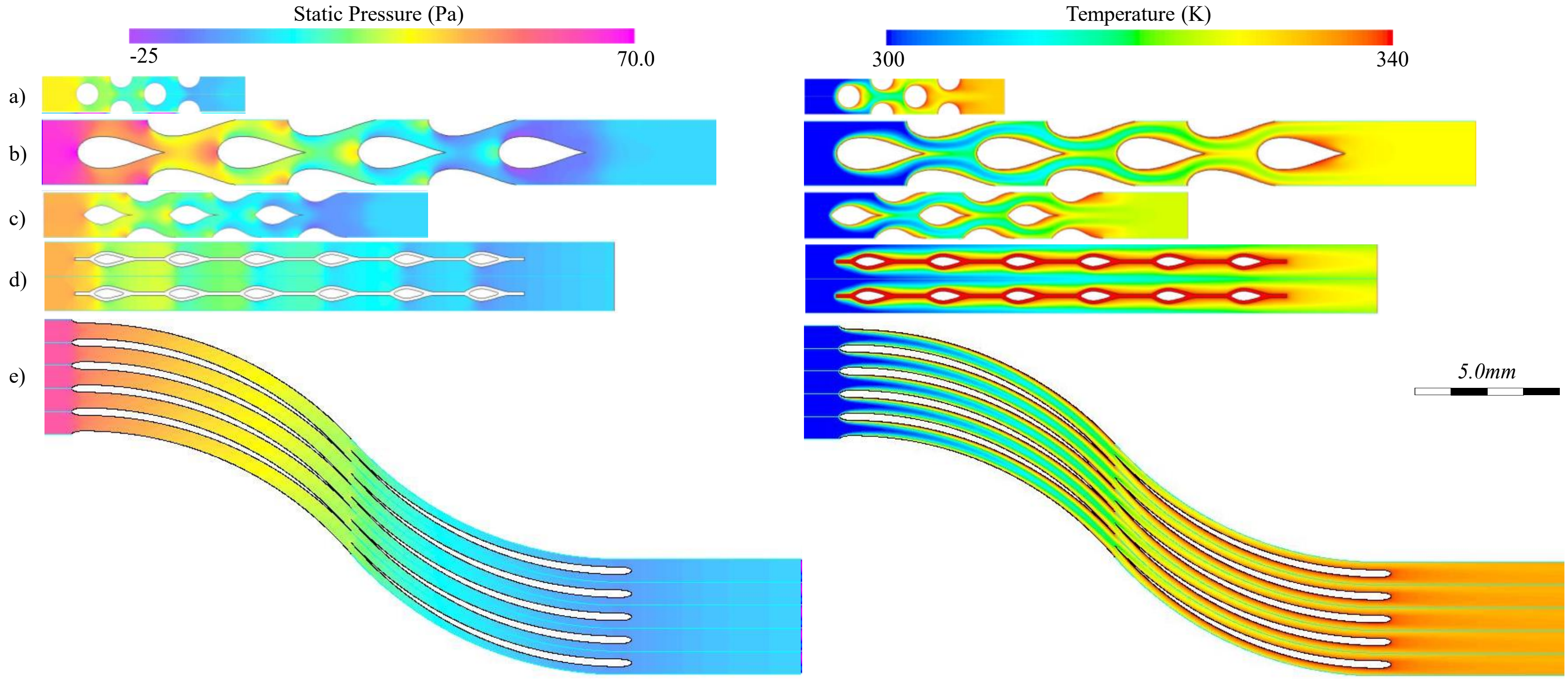

Figure 72. Static pressure and temperature contour plots for selected designs for DP I: a) RTHX-001; b) NTHX-001; c) NTHX-030; d) WTHX-011; e) AFHX-001.

From Figure 71 on the left hand side plot, one can observe a much more streamlined flow over the alternate shape designs compared to the round tube. The right hand side plot in the same figure illustrates the intensity of the stagnation point and flow separation. The latter is much less intense with the optimum shapes which, in combination to the bundle effect, reduce the vortex shed region, thus reducing the flow resistance per unit depth (Figure 72). On the other hand, the high circulation regions for round tubes promotes higher mixing, therefore enhancing the heat transfer. The round tube design has much lower frontal velocity and much shorter flow passage, allowing an overall low pressure drop. The shape optimization allows more flexibility to the thermal-hydraulic compromise compared to the round shape tubes.

5.3.1.6 Discussion

The optimization map in Figure 70 show the heat transfer coefficients of each design. The most important message from this map is to show that most of the concepts developed in this work resulted in an actual heat transfer enhancement, i.e. higher heat transfer coefficients. In a HX scale, having high heat transfer coefficients mean needing less surface area. The concept proposed by Abdelaziz et al. [76] has similar or lower heat transfer coefficient than the baseline, in other words it requires similar or more surface area. The only way to achieve the desired capacity in a small envelope is by greatly reducing tube diameter in order to attain enough compactness as illustrated in Figure 17.

5.3.1.7 Parametric Analysis

In this section includes a parametric analysis (Figure 73) over a wide range of Reynolds number comparing the airside performance between the baseline MCHX, RTHX-001 and NTHX-001/2/30 designs.

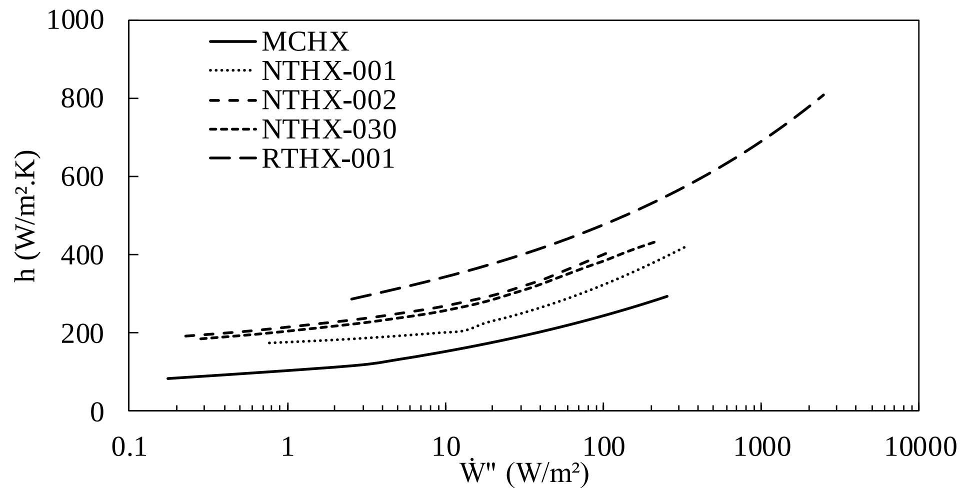

Figure 73. DP I: Airside performance parametric analysis.

Although there are many ways to evaluate a heat transfer surface performance as discussed in chapter 2, the particular analysis above brings some useful insights. First, the curve for the RTHX-001 is evidently higher in the y-axis compared to the others, however significantly shifted to the right. This is the characteristic of surfaces with high heat transfer performance with high friction costs, such as round tubes. To the other end, there is the MCHX which is the lowest curve, but the closest to the y-axis. This is the characteristic of lower friction cost surfaces, which can be partially attributed to the flat shape nature of the MCHX tube. In between, there are the three NTHX surfaces showing the balancing between heat transfer performance and friction cost. The optimized NTHX surfaces resulted in higher and leaning to the left curves, i.e. overall improvement.

5.3.1.8 Prototypes and Experimental Validations

The proof-of-concepts RTHX-001 and NTHX-001 were prototyped and tested in the wind tunnel facility built in the University lab. The details on the facility, data acquisition uncertainty analysis and details on the test matrices are presented in the Appendix D at the end of this manuscript. Two versions of the RTHX-001 concept (Figure 74 and Figure 75) were fabricated; one using stainless steel tubes brazed to a stainless steel header while the second using copper tubes and headers. The first was successfully tested and validated. The NTHX-001 prototype (Figure 76 and Figure 77) was fabricated using metal additive manufacturing technique. The prototype is a single piece component printed in Titanium grade 5.

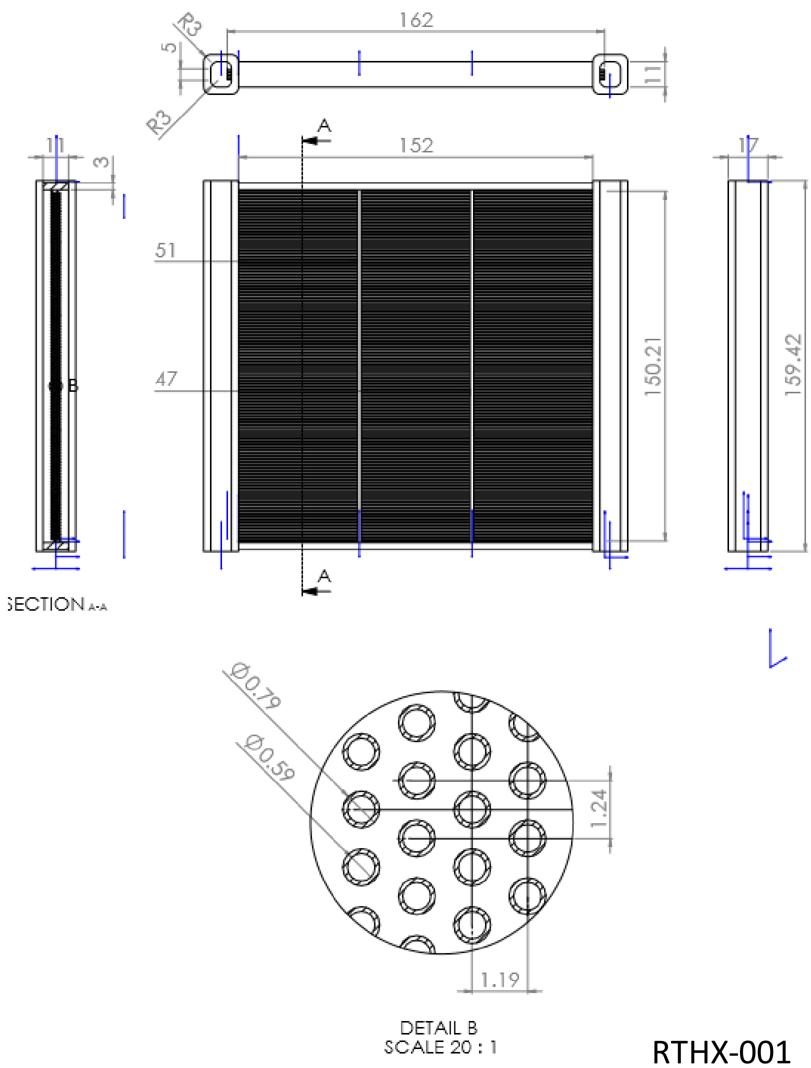

Figure 74. RTHX-001 Prototype drawing.

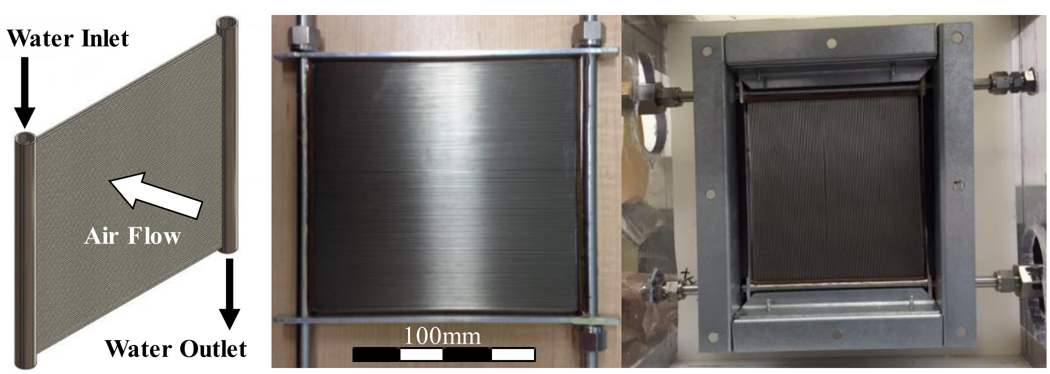

Figure 75. Stainless steel RTHX-001 sample images.

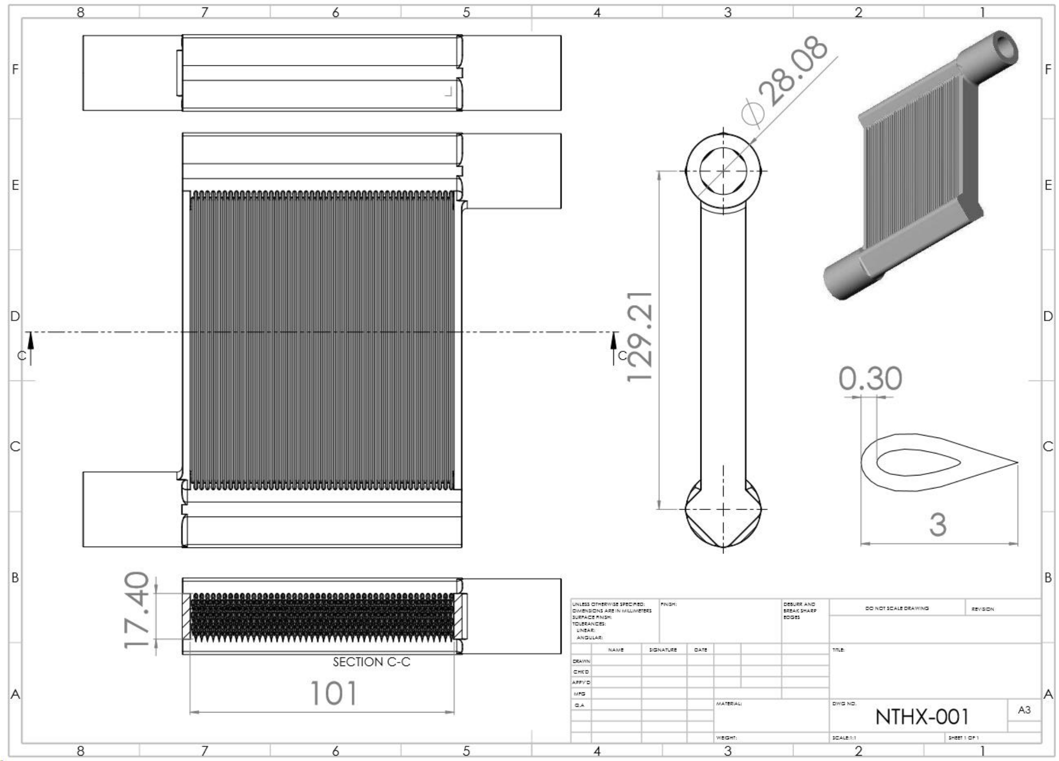

Figure 76. NTHX-001 Prototype drawing.

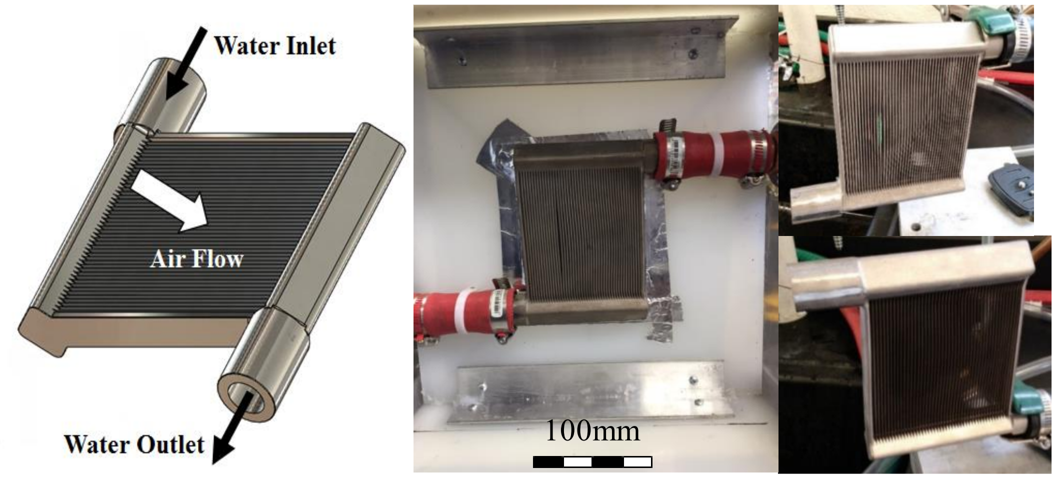

Figure 77. NTHX-001 sample images.

Both prototypes were tested for 15 operating conditions consisting of 5 air flow rates and 3 water flow rates. The inlet approach temperature was kept at 25K which corresponds to 50% of the design approach temperature, thus resulting in lower capacities (<1.0kW). The average experimental capacities were compared to the HX simulation in CoilDesigner® [159], agreeing in less than 5% (Figure 78). The experimental data was reduced using Wilson plot method and the heat transfer coefficients obtained matched within 10%, while the pressure drop matched within 20% (Figure 79 and Figure 80). The latter was particularly off for the RTHX-001 surface, likely due to the turbulence model that over predicted the friction resistance. For the NTHX-001, the good agreement to the pressure drop may have been a combination of factors; the CFD models could have over predicted the pressure drop. An inherited aspect from the printing process is higher roughness, which could have balanced out the numerical prediction. Nevertheless, the results are very encouraging and satisfactory from a validation viewpoint.

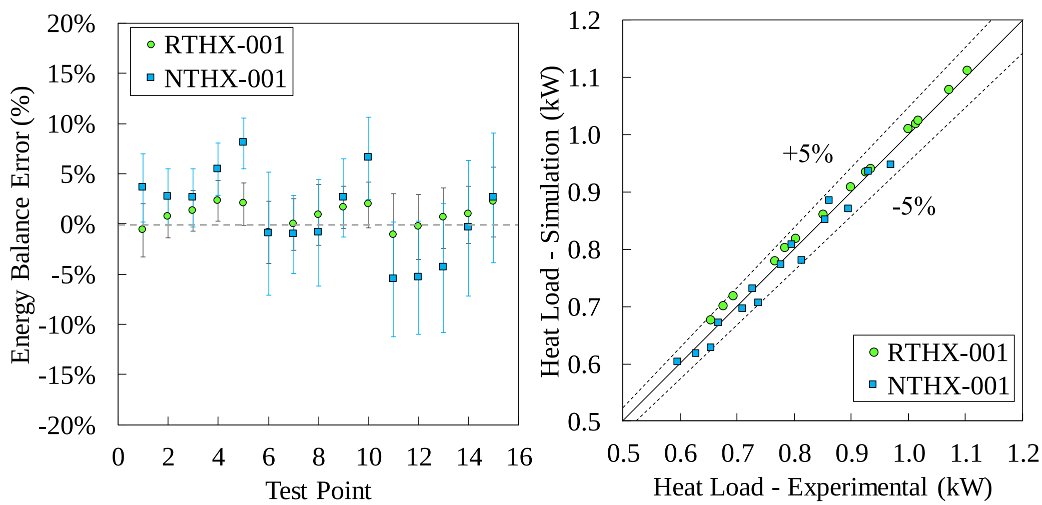

Figure 78. Experimental validation: energy balance and overall capacity.

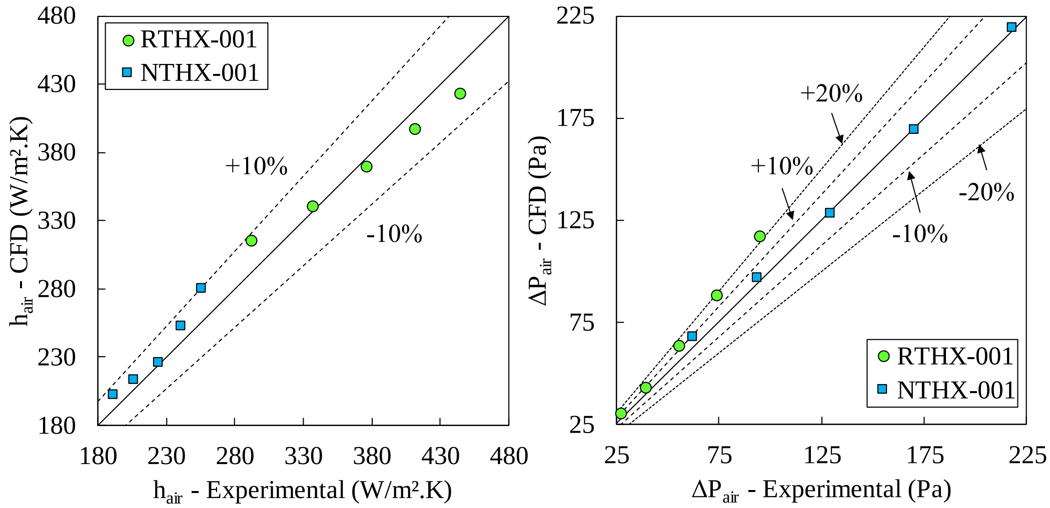

Figure 79. Experimental validation: airside heat transfer coefficient and pressure drop.

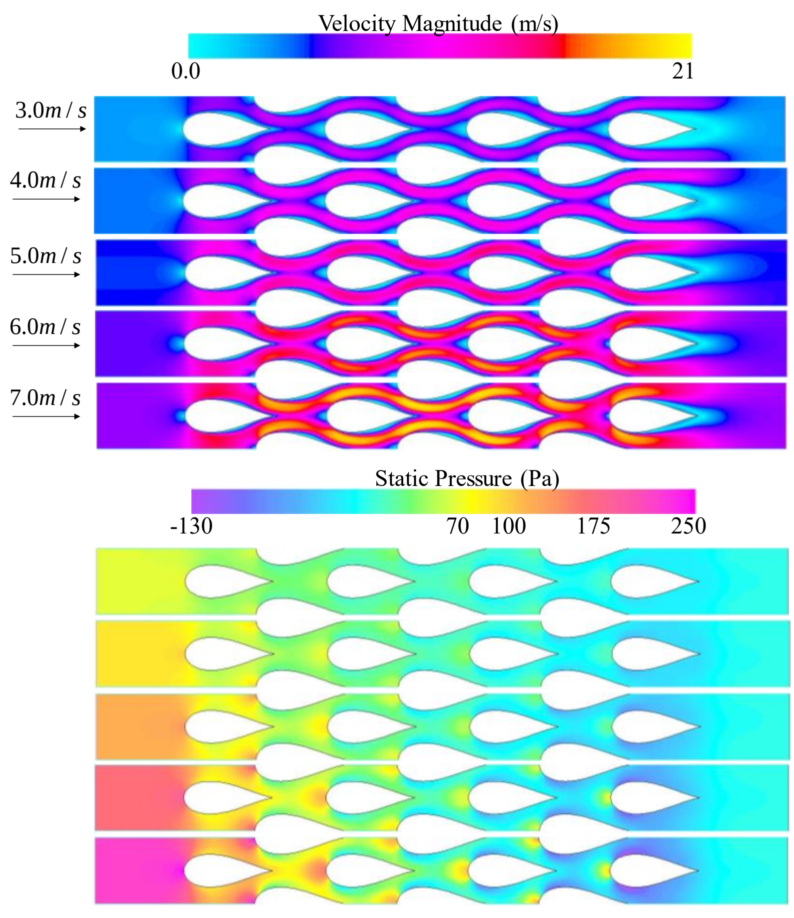

Figure 80. NTHX-001 CFD Validation: contour plots.

5.3.2 DPII: 10.0kW Single-Phase Heat Exchangers

The second design problem (DP II) is a scaled version of the DP I for a 10.0kW application. The general optimization formulation and operating conditions are scaled based on the 1.0kW baseline. The main difference between this application and the previous is the water side pressure drop, which naturally will increase since longer tubes will be required. A maximum of 5kPa was established as a reasonable constraint as opposed to the 1.0kPa from the previous problem. For this application only the RTHX surface was studied with the purpose of prototyping. Since the tubes for the RTHX-001 were available, a similar optimization problem (equation 57) from DP I was performed for DP II applied to the RTHX for fixed tube diameter. The optimization results (Figure 81) are presented as such the geometrical aspects are per unit capacity so that the different scales can be put side by side. The design RTHX-468 indicated in the optimization plot (Figure 81) was selected for prototyping.

$$\begin{aligned}
&\min\ \Delta P_{air} \\
&\min\ V_{HX} \\
&s.t. \\
&\Delta P_{air} \le 62Pa \\
&\Delta P_{water} \le 5.0kPa \\
&V_{HX} \le 1800cm^3 \\
&10 \le \dot{Q} \le 11kW \\
&D_o = 0.8mm
\end{aligned} \tag{57}$$

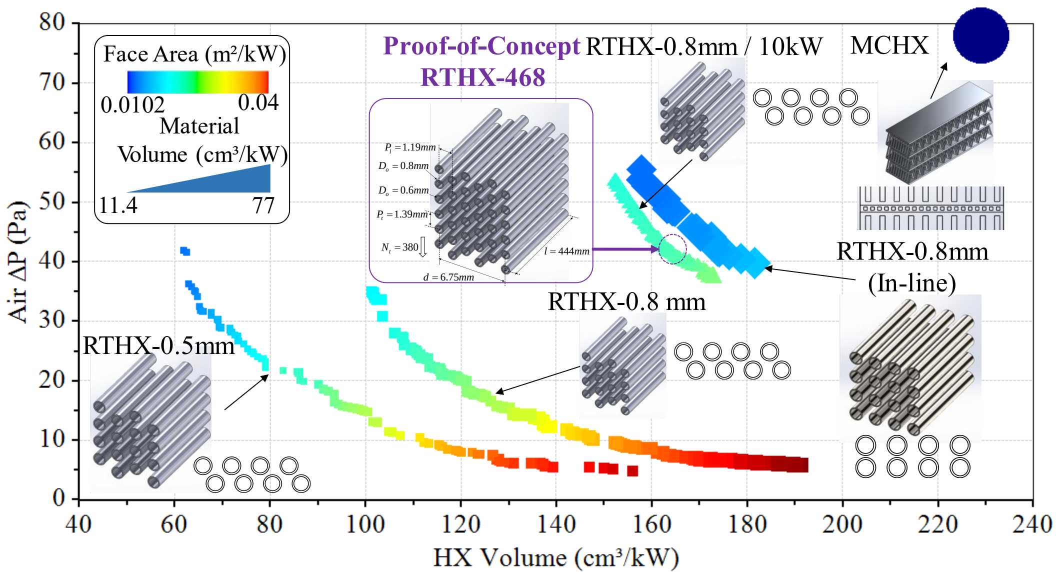

Figure 81. DP II: Optimization results.

5.3.2.1 Prototype RTHX-468

A prototype of the design RTHX-468 (Figure 82) was fabricated using copper tubes brazed to the copper headers. This prototype was tested and resulted in a consistent 50% over prediction compared to experimental data (Figure 83). Thermal imaging tests (Figure 84) revealed that a good portion of the tubes were blocked, thus compromising the overall performance. The details on experimental data are included in Appendix D.

Figure 82. RTHX-468 Prototype.

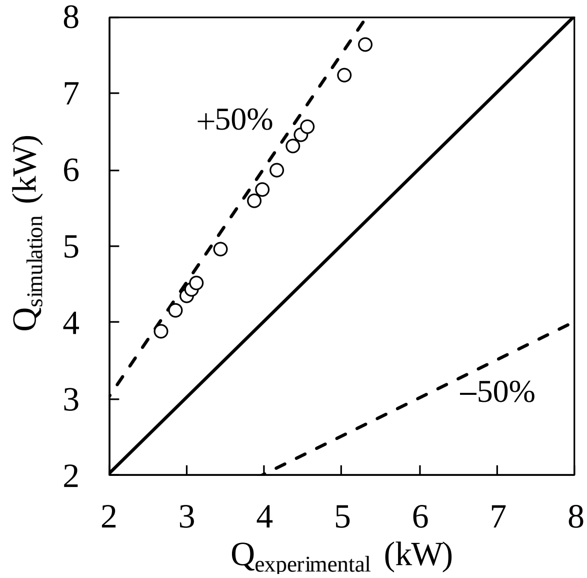

Figure 83. RTHX-468 Experimental capacity results.

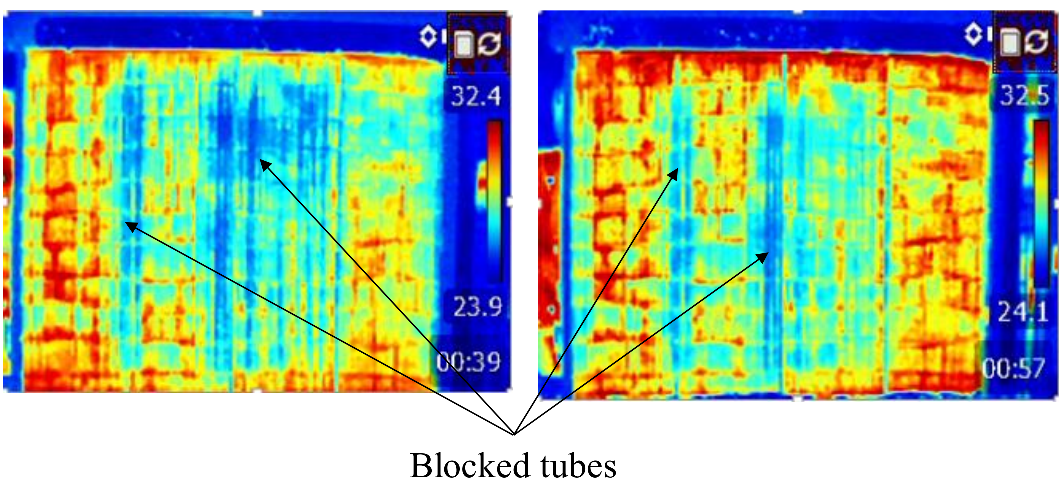

Figure 84. Thermal imaging on RTHX-468 prototype.

Although the results did not match at the 45° line (Figure 83), they line up quite well over the 50% line, which suggests a strong correlation between simulation and the real system. The blockage results suggest that the deviations were likely due to the faulty HX instead of potentially poor numerical prediction.

5.3.3 DP III: Two-Phase Heat Exchangers

This study comprised of optimizing HX's to deliver a 3.0Ton (~10kW) capacity in a Heat Pump / Air-Conditioning Unit. The baseline system is a rated SEER (Seasonal Energy Efficiency Ratio) 16, using R410A as working fluid. For this study the cooling operating mode was considered. The cycle was modeled and verified (Table 13) against the rated performance using VapCyc® [166]. The HX's were modeled in CoilDesigner® [159] according to the manufacturer specifications. The compressor was modeled using the manufacturer 10-coefficient model for mass flow rate and power predictions.

Table 13. Baseline cycle verification.

Cycle	COP*	COP	Q	Sub-cooling	Super heating	Ref. $\dot{m}$	Evap. AFR	Cond. AFR
	-	-	kW	K	K	kg/s	m^3/s	m^3/s
Baseline (rated)	4.507	3.900	10.029	5.447	3.890	0.06224	0.505	1.84
Baseline (simulated)	4.506	3.858	10.025	5.445	3.901	0.06040	0.505	1.84

* *w/o fan power*

Using Engineering Equation Solver (EES®) the potential of reducing the pressure lift was investigated, while maintaining the sub cooling, superheating, air flow rates and assuming constant isentropic efficiency for the compressor. The approach temperatures were monitored to avoid potential Second Law violations. The new HX specifications were retrieved from the EES model according to a theoretical COP (Coefficient of Performance) improvement of 15% and outlet approach temperatures near 1.0°C (Figure 85).

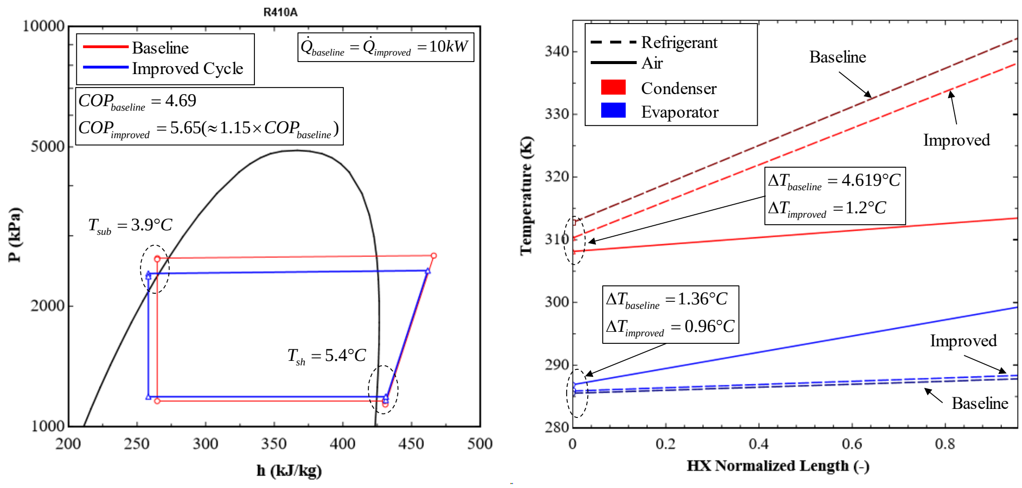

Figure 85. System level study for COP improvement.

5.3.3.1 HX Design and Optimization

The baseline HX's have conventional tube and fins with tube diameters of 7.0mm and 9.5mm in the outdoor and indoor units, respectively. The fins are enhanced with louvers and slits. The HX operating conditions for both the baseline cycle and the expected improved cycle are presented in Table 14.

Table 14. Two-Phase HX's operating conditions.

HX	**Evaporator**					**Condenser**				
Metric	P_{sat} kPa	x_{in} -	V_{air} m³/s	$T_{air,in}$ K	ΔP_{air} Pa	P_{sat} kPa	T_{in} K	V_{air} m³/s	$T_{air,in}$ K	ΔP_{air} Pa
Baseline	1159	0.22	0.505	299.8	57.2*	2675	345.1	1.84	308.2	4.0**
Improved	1179	0.19	0.505	299.8	---	2488	339.7	1.84	308.2	---

** Rated value ** Estimated using Wang et al. correlation* [167]

The fan power is estimated based on the total power to move air through both HX's. For design and optimization purposes the baseline condenser pressure drop of 4.0Pa is highly restrictive, thus the optimizer was allowed to go up to 10Pa. The evaporator pressure drop, however, was constrained as such the total fan power is no higher than the baseline. The optimization problem (equation 58) applied to each HX has the air pressure drop and volume as objective functions, while constraining capacity, refrigerant pressure drop and the rebalanced air pressure drops.

$$
\begin{array}{ll}
\textit{Evaporator} & \textit{Condenser} \\
\min \Delta P_{air} & \min \Delta P_{air} \\
\min V_{HX} & \min V_{HX} \\
s.t. & s.t. \\
\dot{Q} \geq 10.0kW & \dot{Q} \geq 11.8kW \\
\Delta P_{air} \leq 35Pa & \Delta P_{air} \leq 10Pa \\
\Delta P_{ref} \leq \Delta P_{ref,baseline} & \Delta P_{ref} \leq \Delta P_{ref,baseline}
\end{array}
\tag{58}
$$

In addition to the design variables used in the DP I and II the pass configuration (Figure 86) was introduced. For the evaporator two passes are considered as such the design variable indicates the fraction of the tubes as inlet whilst the remainder being the outlet. The condenser has three passes where two design variables define the fraction of the inlet tubes and the mid-section tubes respectively.

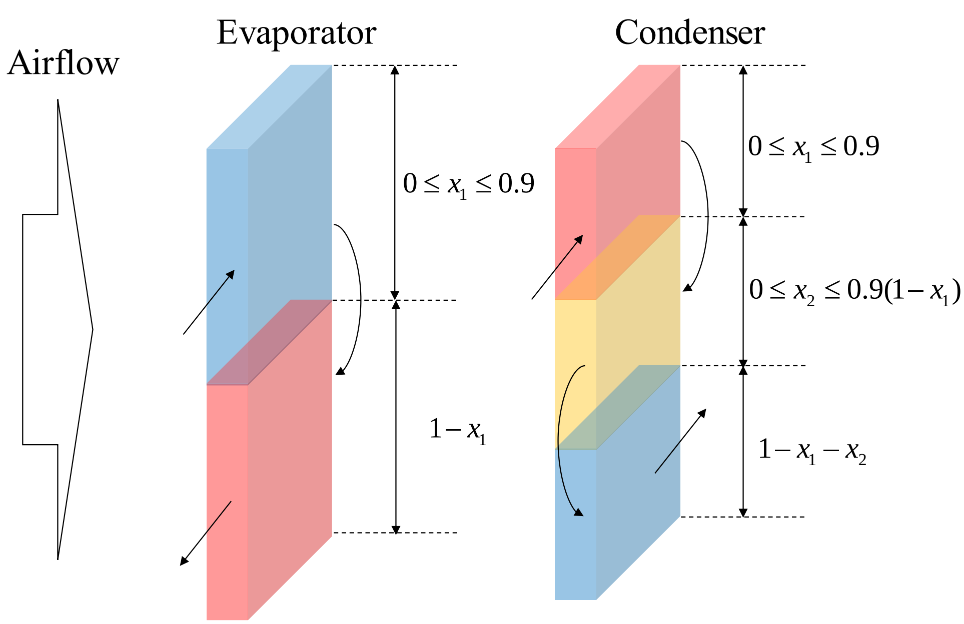

Figure 86. HX Pass configurations.

This study considered only the RTHX concept both in in-line and staggered arrangements. In addition to the optimum designs and the baseline HX's, as reference, the optimization performed for a 3Ton SEER 13 unit [168] with HX's using tube diameters of 3, 4 and 5mm was included. Optimization results are shown in Figure 87.

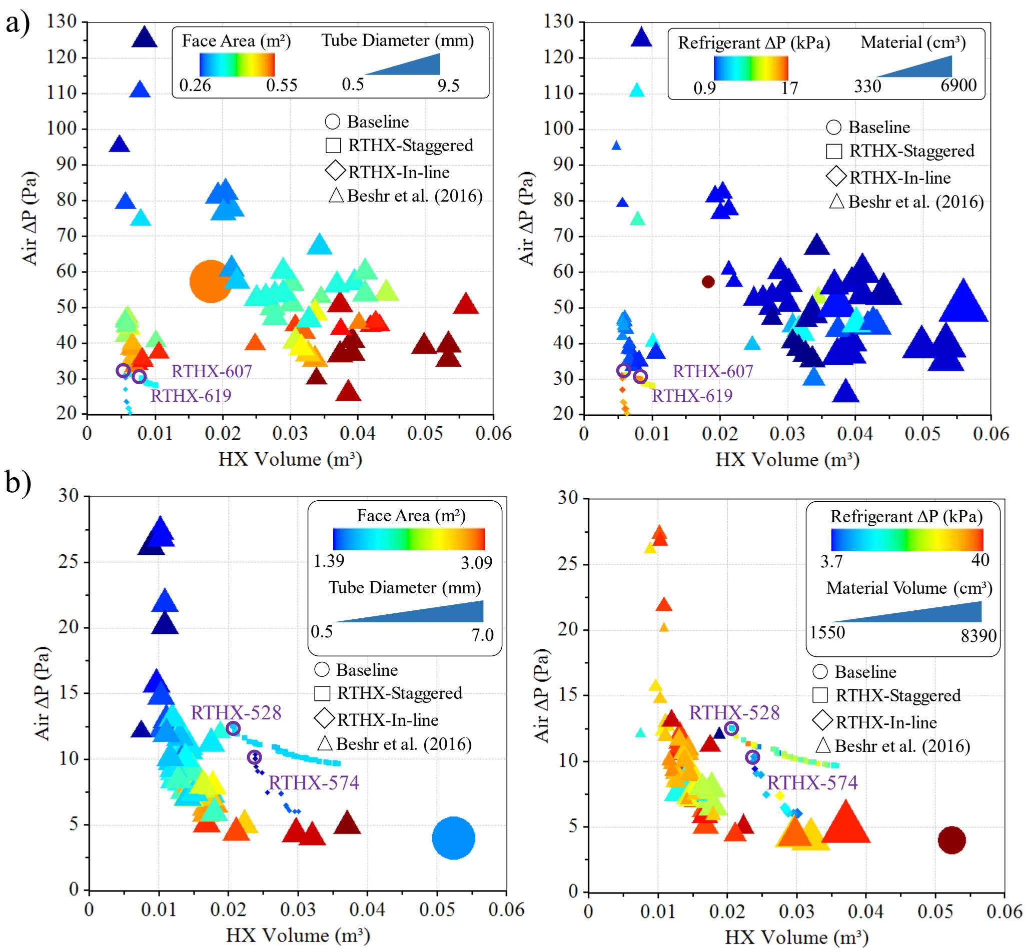

Figure 87. DP III: Optimization results.

5.3.3.2 System Level Analysis

The designs RTHX-528, 574, 607 and 619 indicated in Figure 87 were selected for the system level analysis. Two novel cycles were simulated in

VapCyc® [166]; Cycle I with the RTHX-528 and RTHX-607 designs and Cycle II with RTHX-574 and RTHX-619 designs. Both cycles resulted in significant reduction of refrigerant charge; approximately 50% reduction in the condenser, and up to 90% in the evaporator. The overall charge reduction in the system reached approximately 30%-40% reduction. From a performance perspective the COP was improved in up to 14% with these new HX's. Additionally, these charge reductions in the HX's result in the pipes accumulating a more relative amount of charge. The system results are summarized in Figure 88.

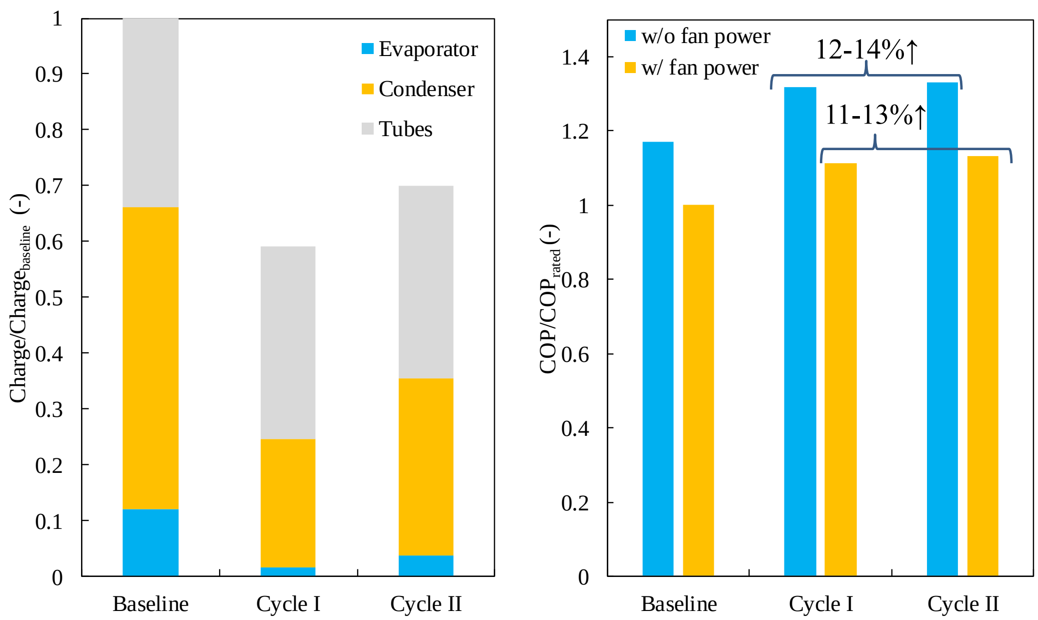

Figure 88. DP III: System level analysis.

Chapter 6: CFD-Based Correlation Development

The procedure to develop the CFD-based correlations follows the similar framework (Figure 89) to develop the metamodels used in the AAO, following three main parts. The first consists of defining the design space within which the correlation will be valid for; next, the CFD uncertainty analysis following the GCI procedure explained in the Chapter 2; last, with the aid of PPCFD a large DoE is simulated and the post-processed data is further used in the correlation development. Additional random samples are simulated and used for final verification.

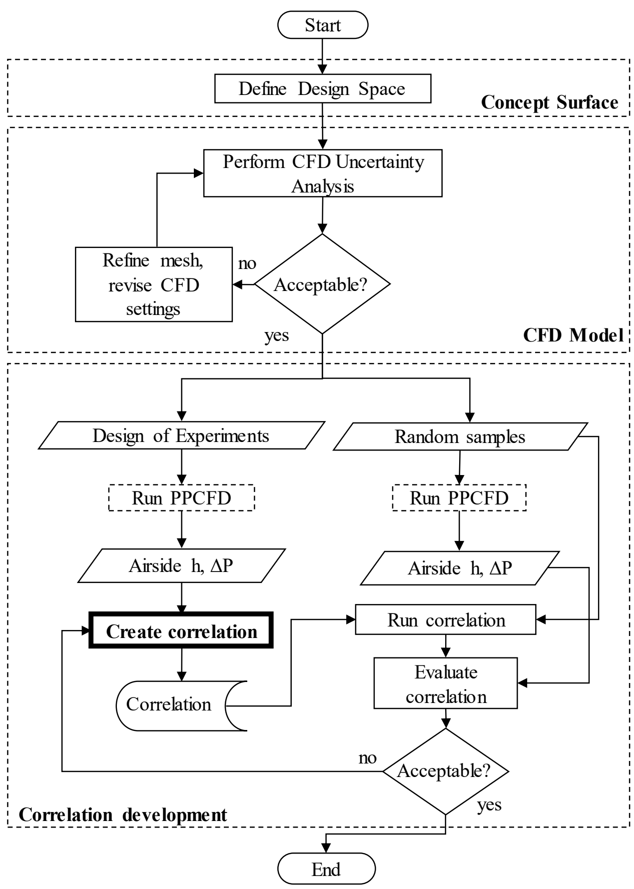

Figure 89. CFD-Based correlation development.

Two correlation approaches are investigated in this work. One (equations 59 to 62), where a non-linear equation form is defined as a function of the geometry and operating conditions, and use an optimization algorithm to find the coefficients of the present equation that result in the minimum square error compared to the CFD source data. Alternatively, (equation 63) the correlation can be found using a stepwise linear regression algorithm which is very robust, although it results in a very large expression. The matrix M contains the power value of each parameter (columns of M) for each of the regression term (rows of M), and the array c contains the coefficients of each term. Both approaches are employed within the Matlab® environment using its built-in optimization and regression engines.

$$f(\underset{\sim}{x}) = \sum_{i=0}^{n} \left(\phi_{corr,i}(\underset{\sim}{x}) - \phi_{CFD,i} \right)^2 \tag{59}$$

Where,

$$\phi = h, j, Nu, \Delta P, f \ldots. \tag{60}$$

$$\underset{\sim}{x} = [D_o, P_l, P_t, F_p, \delta_f, N_r, \theta, \mathrm{Re} \ldots.] \tag{61}$$

$$\begin{aligned} &\min f(\underset{\sim}{x}) \\ &s.t. \\ &\underset{\sim}{x}_{lb} \le \underset{\sim}{x} \le \underset{\sim}{x}_{ub} \end{aligned} \tag{62}$$

$$\phi_{corr}(\underset{\sim}{x}) = \sum_{i=1}^{n_{Rows}} c_i \cdot \left(\prod_{j=1}^{n_{Columns}} x_j^{M_{i,j}} \right) \tag{63}$$

6.1 Round Finless Tubes

The previous Chapters in this dissertation discussed and demonstrated the benefits of using small finless diameter tubes. Among current available tools only

CFD can actually be used to predict the thermal-hydraulic performance of such surfaces. This gap is fulfilled by providing computationally affordable correlations that accurately predict the CFD response.

In this section three sets for correlations are presented, including diameters from 0.5mm to 2.0mm for both staggered and in-line arrangements and the staggered arrangement for tube diameters ranging from 2.0mm to 5.0mm.

6.1.1 Data Reduction

Since the CFD models serve to determine the airside thermal and hydraulic resistances, there is no need to account for additional thermal resistances. Thus with constant wall temperature, the capacitance ratio yields $C_{min} / C_{max} = 0$, then the heat transfer coefficient can be easily calculated through ε-N_{tu} method as per equations (64 to 67). The pressure drop is determined as the difference between inlet and outlet static pressures, assuming that local losses are negligible.

$$N_{tu} = -\ln(1-\varepsilon) = -\ln\left[1-(T_{out}-T_{in})/(T_{wall}-T_{in})\right] \tag{64}$$

$$h = UA/A_o = N_{tu} \cdot C_{\min}/A_o \tag{65}$$

$$j = h\,\mathrm{Pr}^{2/3}/(\rho u_c c_p) \tag{66}$$

$$f = \frac{A_c}{A_o}\frac{\rho_m}{\rho_{in}}\left[\frac{2\Delta P \rho_{in}}{(\rho_m u_c)^2} + (1-\sigma^2)\left(\frac{\rho_{in}}{\rho_{out}}-1\right)\right] \tag{67}$$

6.1.2 Correlations

The CFD models and grid uncertainty analysis were carried out in Chapter 4, thus will not be presented in this section again. The design space investigated is presented in Table 15.

Table 15. Finless tubes correlations design space.

Variable Type	Design Variable	Unit	Correlations I	Correlation II	Correlation III
Scaling	D_o	mm	0.5 – 2.0	0.5 – 2.0	2.0 – 5.0
	Nr	-	2 – 40	2 – 40	2 - 20
Topology	P_t ratio (D_o)	-	1.2 – 4.0	1.2 – 4.0	1.5 – 3.0
	P_l ratio (D_o)	-	1.2 – 4.0	1.2 – 4.0	1.5 – 3.0
Operating	u	m/s	0.5 - 7.0	0.5 - 7.0	0.5 – 7.0
Arrangement	-	-	Staggered	In-line	Staggered

The correlations developed for the finless tubes are based on the non-linear equation approach. For correlations I and II there are four sets of equations for each correlation: 2 to 9 banks, 10 to 24 banks, 25 to 34 banks and 35 to 40 banks. The source data for each fin type consisted of a Design of Experiments with 750 samples sampled using Latin Hypercube Sampling method. The correlation III used 500 samples also generated with Latin Hypercube Sampling.

Equations 68 to 74 present the correlations I and II. The coefficients are presented in Table 16 and Table 17.

$$j = c_1 \mathrm{Re}_{D_o,c}^{p_1} N_t^{p_2} \left(\frac{P_l}{D_o}\right)^{p_3} \left(\frac{P_t}{D_o}\right)^{p_4} \left(\frac{P_l}{P_t}\right)^{c_2} \tag{68}$$

$$f = c_1 \mathrm{Re}_{D_o,c}^{p_1} \left(\frac{P_l}{P_t}\right)^{p_2} \left(\frac{P_l}{D_o}\right)^{p_3} \left(\frac{P_t}{D_o}\right)^{p_4} N^{c_2} \tag{69}$$

$$\mathrm{Re}_{D_o,c} = \frac{\rho u_c D_o}{\mu} \tag{70}$$

$$p_1 = c_3 + \frac{c_4 N}{\ln(\mathrm{Re}_{D_o,c})} + c_5 \ln\left[N\left(\frac{P_t}{D_o}\right)^{c_6}\right] \tag{71}$$

$$p_2 = c_7 + \frac{c_8}{\ln(\mathrm{Re}_{D_o,c})}\left(\frac{P_l}{D_o}\right)^{c_9} \tag{72}$$

$$p_3 = c_{10} + \frac{c_{11} N}{\ln(\mathrm{Re}_{D_o,c})} \tag{73}$$

$$p_4 = c_{12} + c_{13} \ln \frac{\mathrm{Re}_{D_{o,c}}}{N} \tag{74}$$

Table 16. Correlations I coefficients.

	j				f			
N	2-9	10-24	25-34	35-40	2-9	10-24	25-34	35-40
c_1	6.5374	6.5490	6.5405	6.5070	1.4559	6.3104	0.0007	0.2559
c_2	0.1193	0.0918	0.0998	0.3534	-0.5227	-0.4716	-0.7261	0.5290
c_3	-0.7805	-0.7731	-0.7672	-1.1185	-0.3987	-0.6044	4.7749	-0.5908
c_4	0.0369	0.0038	0.0033	0.0158	0.0284	-0.0167	0.4822	-0.0553
c_5	0.1202	0.1164	0.1326	0.3026	0.0707	0.0964	-1.7070	0.1430
c_6	1.9813	1.9942	1.9788	1.9948	0.5907	4.2753	0.1779	-0.0107
c_7	-1.2644	-1.0895	-1.2085	-1.7800	-0.4592	0.7463	0.4904	-0.4653
c_8	1.2039	1.2676	1.2227	0.7869	-2.2383	0.5998	-6.9567	3.4932
c_9	0.3549	0.3341	0.3670	0.1953	-1.4243	1.1010	-0.0456	0.3160
c_{10}	-0.3391	-0.3283	-0.3143	0.1690	0.2957	-1.1875	1.8617	-0.0951
c_{11}	-0.0313	-0.0522	-0.0483	-0.1202	0.1688	-0.0203	-0.3269	-0.0532
c_{12}	-0.8338	-0.7955	-0.7895	-0.5598	-0.2976	0.2579	-0.4149	1.6296
c_{13}	-0.1545	-0.1754	-0.2351	-0.9993	0.0571	-0.2939	0.8621	-0.1635

Table 17. Correlations II coefficients.

	j				f			
N	2-9	10-24	25-34	35-40	2-9	10-24	25-34	35-40
c_1	6.808	1.079	4.072	0.059	4.357983	0.834137	3.626557	1.905177
c_2	-0.019	0.283	0.819	0.732	-1.50004	0.159886	-1.2549	-3.4275
c_3	-0.865	-0.694	-1.668	0.300	-0.59284	-0.61397	-0.94665	1.840706
c_4	-0.072	0.018	-0.151	0.025	-0.05845	-0.04546	0.148834	0.308742
c_5	0.215	0.091	0.476	-0.099	0.209748	0.068112	0.080344	-0.61705
c_6	-0.557	-0.671	-0.831	-0.012	-1.5117	2.004688	-4.95244	0.395123
c_7	-1.390	-0.925	-0.362	-0.514	-1.09594	-0.71962	4.49158	0.313471
c_8	2.861	2.297	1.130	0.665	4.546346	0.138192	10	10
c_9	-3.997	0.439	-0.234	1.116	-0.23323	2.779024	-2.03421	-2.73658
c_{10}	-0.114	0.359	-0.584	-0.081	-0.64347	0.733198	8.397073	5.097817
c_{11}	0.696	-0.056	0.446	0.003	0.94127	0.147212	-0.59114	-0.64904
c_{12}	-1.072	-1.739	-0.315	-0.806	0.144438	-1.68447	-3.11616	1.813604
c_{13}	0.285	0.393	0.541	-0.043	0.556941	0.278091	0.321952	-0.22785

Equations 75 to 80 present the correlations III. The coefficients are presented in Table 18.

$$j = c_1 \mathrm{Re}_{D_o}^{P_1} N_t^{P_2} \left(\frac{P_l}{D_o}\right)^{P_3} \left(\frac{P_t}{D_o}\right)^{P_4} \left(\frac{P_l}{P_t}\right)^{c_2} \tag{75}$$

$$f = c_1 \mathrm{Re}_{D_o}^{P_1} N_t^{P_2} \left(\frac{P_l}{D_o}\right)^{P_3} \left(\frac{P_t}{D_o}\right)^{P_4} \left(\frac{P_l}{P_t}\right)^{c_2} \tag{76}$$

$$P_1 = c_3 + \frac{c_4 N_t}{\ln(\mathrm{Re}_{D_o})} + c_5 \ln\left[N_t \left(\frac{P_l}{D_o}\right)^{c_6} \right] \tag{77}$$

$$P_2 = c_7 + \frac{c_8}{\ln(\mathrm{Re}_{D_o})} \left(\frac{P_t}{D_o}\right)^{c_9} \tag{78}$$

$$P_3 = c_{10} + \frac{c_{11} N_t}{\ln(\mathrm{Re}_{D_o})} \tag{79}$$

$$P_4 = c_{12} + c_{13} \ln \frac{\mathrm{Re}_{D_o}}{N_t} \tag{80}$$

Table 18. Correlations III coefficients.

	j	f
c_1	0.4220555168	0.9981645207
c_2	-0.1327145700	0.8632429086
c_3	-0.4550155190	-0.3179116696
c_4	-0.0090645460	-0.0006687375
c_5	-0.0096188420	0.0005922714
c_6	2.4745395710	-9.9249274428
c_7	0.2262063170	0.2550841764
c_8	-0.2659972990	-4.3313552005
c_9	0.5645583060	-2.5323165527
c_{10}	0.2455957950	-1.0237980350
c_{11}	0.0232402000	0.0203235731
c_{12}	0.0021002020	0.5366315096
c_{13}	-0.0163369050	0.1651970285

The correlations verification is respectively shown in Figure 90and Table 19 against source data and Figure 91 against random data.

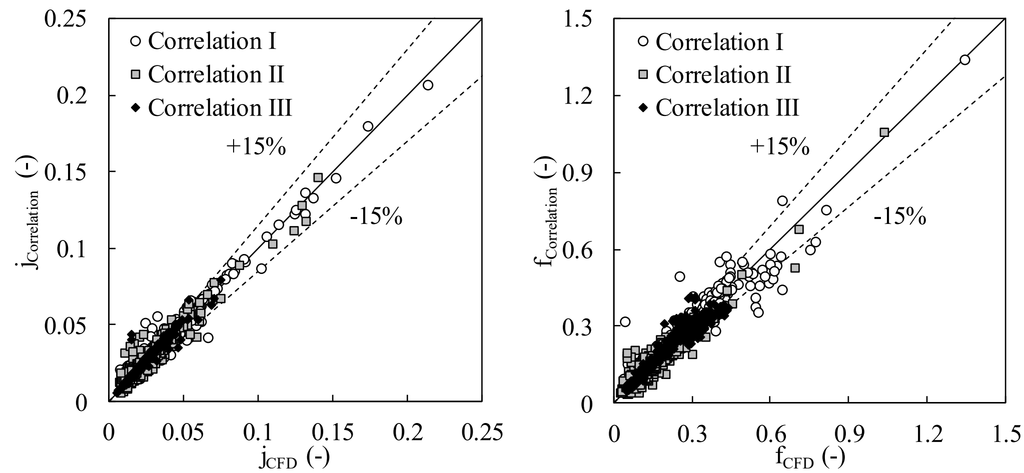

Figure 90. Correlations I, II and III verification against source data.

Table 19. Round finless tubes correlations fitness.

Heat Exchanger	Correlation I		Correlation II		Correlation III	
Air side performance metrics	j	f	j	f	j	f
Predicted data (e=10.0%)	86.9%	79.2%	59.0%	45.7%	91.6%	83.1%
Predicted data (e=15.0%)	92.9%	88.8%	75.2%	62.7%	97.7%	91.3%
Predicted data (e=20.0%)	95.1%	92.9%	83.7%	74.9%	99.1%	95.2%
Predicted data (e=30.0%)	96.9%	96.7%	91.7%	85.7%	99.6%	98.4%
R^2	98.4%	95.8%	95.6%	97.9%	97.6%	97.3%
Mean Absolute Relative Error	6.07%	8.39%	12.41%	17.52%	4.48%	5.55%
Median Absolute Relative Error	2.90%	4.64%	8.15%	10.96%	2.50%	3.39%

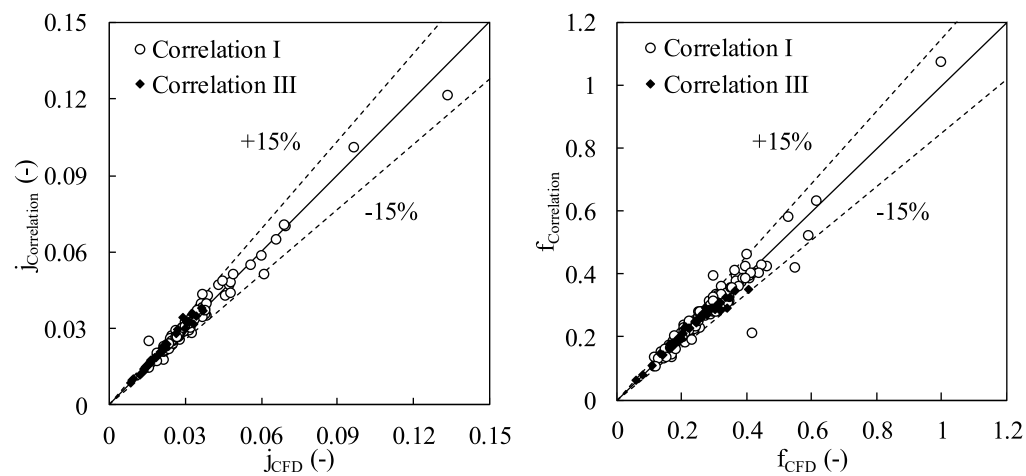

Figure 91. Correlations I and III verification against random samples.

6.1.3 Verification

The proof-of-concept RTHX-001 falls in the correlations I application range. Using the same experimental data for the CFD validations, it was verified that the correlations agree in 10% for the heat transfer coefficient, however they consistently over predict the pressure drop by a factor of 1.64. One reason is the fact that the CFD simulations in this work have consistently over predicted pressure drop, potentially due to the turbulence model used. On the other hand, this consistency suggests that with additional experimental data only small adjustments to the proposed equations might be required.

Furthermore, the experimental verification shows that the proposed equations have significantly better prediction capability when compared to existing correlations in the literature.

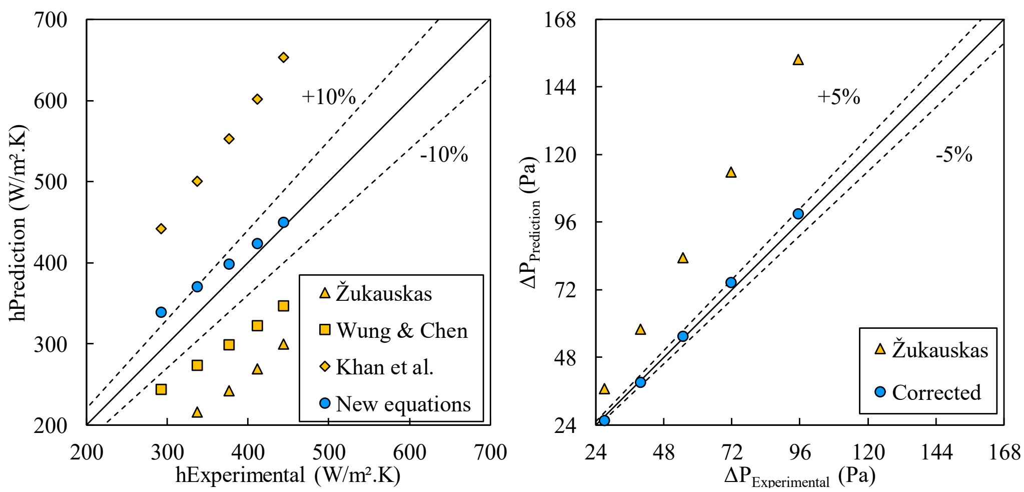

Figure 92. Correlations I verification against experimental data.

6.2 Plain Fin-and-Tubes

The second order analyses in Chapter 3 suggested that for tubes larger than 2.0mm diameter, having fins is performance wise more attractive than finless tubes. In this section correlations for flat fin (Figure 93 and Figure 94) and tubes, with diameters between 2.0mm and 5.0mm are presented.

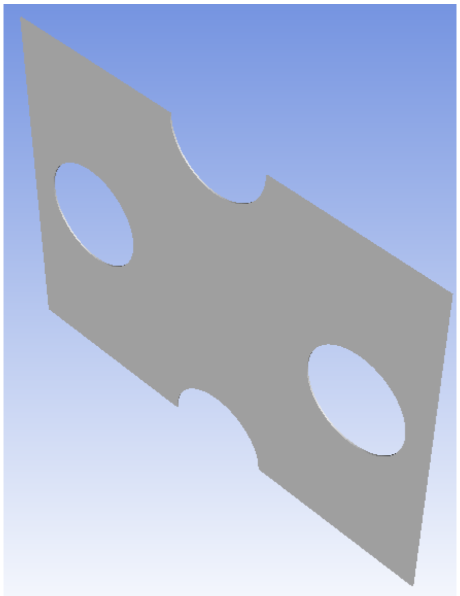

Figure 93. Flat fin.

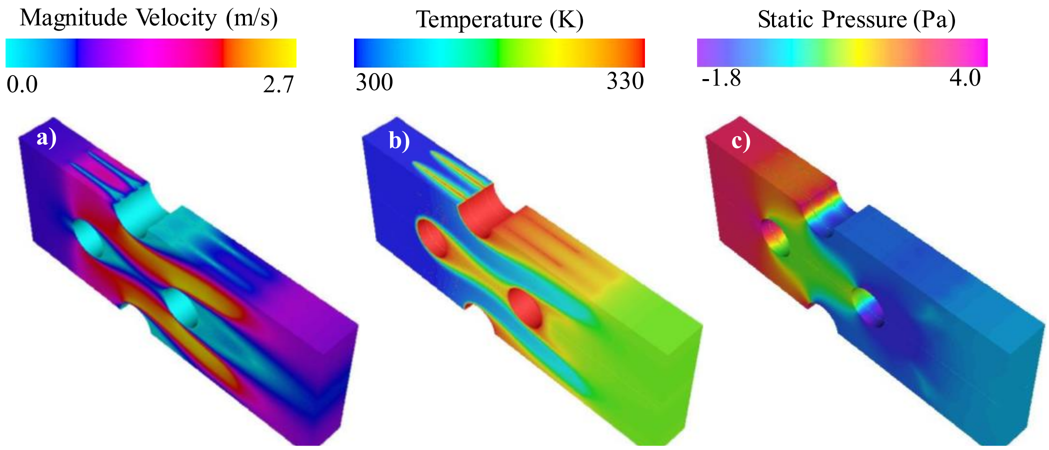

Figure 94. Flat fin and tube contour plots: a) velocity; b) temperature; c) pressure.

The CFD models and grid uncertainty analysis were carried out in Chapter 4, thus will not be presented in this section again. The design space investigated is presented in Table 20.

Table 20. Flat fin and tube correlations design space.

Design Variable	unit	Range
D_o	mm	2.0 - 5.0
P_t ratio (D_o)	-	1.5 - 3.0
P_l ratio (D_o)	-	1.5 - 3.0
N_r	-	2 - 10
FPI	in^{-1}	8 - 24
Air face velocity	m/s	0.5 - 7.0
Fin thickness	mm	0.115 (fixed)

6.2.1 Data Reduction

The heat transfer coefficient can be retrieved using the Schmidt method [153] described in the theoretical background chapter, whilst the friction factor can be calculated the same way for the finless tubes (equation XX).

6.2.2 Correlation

The correlations developed for the finless tubes are based on the non-linear equation approach. The source data for each fin type consisted of a Design of Experiments with 500 samples sampled using Latin Hypercube Sampling method. Equations 81 to 82 present the correlations I and II. The coefficients are presented in Table 21.

$$j = c_1 \mathrm{Re}_{D_o}^{P_1} N_t^{P_2} \left(\frac{F_p}{D_o + 2\delta_f} \right)^{P_3} \left(\frac{P_t}{D_o} \right)^{P_4} \left(\frac{P_l}{D_o} \right)^{c_2} \tag{81}$$

$$f = c_1 \mathrm{Re}_{D_o}^{P_1} N_t^{P_2} \left(\frac{F_p}{D_o + 2\delta_f} \right)^{P_3} \left(\frac{F_p}{D_o} \right)^{P_4} \left(\frac{F_p}{P_t} \right)^{c_2} \tag{82}$$

$$P_1 = c_3 + \frac{c_4 N_t}{\ln(\mathrm{Re}_{D_o})} + c_5 \ln\left[N_t \left(\frac{F_p}{D_o + 2\delta_f} \right)^{c_6} \right] \tag{83}$$

$$P_2 = c_7 + \frac{c_8}{\ln(\mathrm{Re}_{D_o})} \left(\frac{P_t}{D_o} \right)^{c_9} \tag{84}$$

$$P_3 = c_{10} + \frac{c_{11} N_t}{\ln(\mathrm{Re}_{D_o})} \tag{85}$$

$$P_4 = c_{12} + c_{13} \ln \frac{\mathrm{Re}_{D_o+2\delta_t}}{N_t} \tag{86}$$

Table 21. Fin-and-tube correlations coefficients.

	j	*f*
c_1	0.14766977237669	1.71188871245298
c_2	-0.28005133537990	0.92946487673730
c_3	-0.38888826762694	-0.22854500443404
c_4	-0.04370010021825	0.04029790563157
c_5	0.28331914903762	-0.00430627203978
c_6	0.44735912969069	-4.91278551282918
c_7	-2.52843968547746	-0.62616159134051
c_8	5.29660856066235	1.31700831350020
c_9	-0.22444322963679	0.27195519072632
c_{10}	-1.00067471783319	-2.42919816587607
c_{11}	0.30250006880624	0.06332710290257
c_{12}	2.08539578403170	0.97021840449916
c_{13}	-0.27444087385649	0.10375729681002

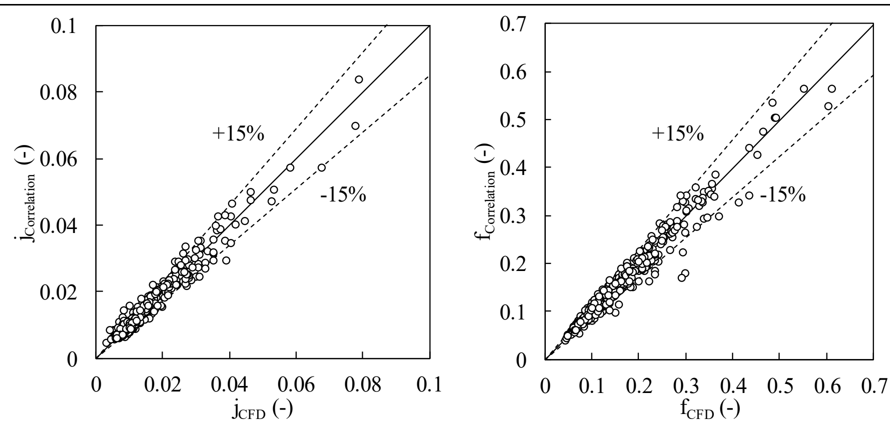

Figure 95. Flat fin correlations verification against source data.

Table 22. Flat fin-and-tube correlations fitness.

Air side performance metrics	j	f
Predicted data (e=10.0%)	64.8%	78.9%
Predicted data (e=15.0%)	82.1%	91.8%
Predicted data (e=20.0%)	91.5%	96.4%
Predicted data (e=30.0%)	96.8%	98.8%
R^2	97.8%	98.0%
Mean Absolute Relative Error	9.51%	6.59%
Median Absolute Relative Error	7.29%	5.07%

6.3 Wavy Fin-and-Tubes

As discussed in the literature review, wavy fins are suitable for applications such as heat pumps in cold climates due to its higher resiliency to performance degradation. Additionally, reducing tube diameters improve performance and for diameters above 2.0mm fins are desirable. This section presents a correlation development for both Herringbone and smooth-wavy fins (Figure 96) using tube diameters from 2.0 to 5.0mm.

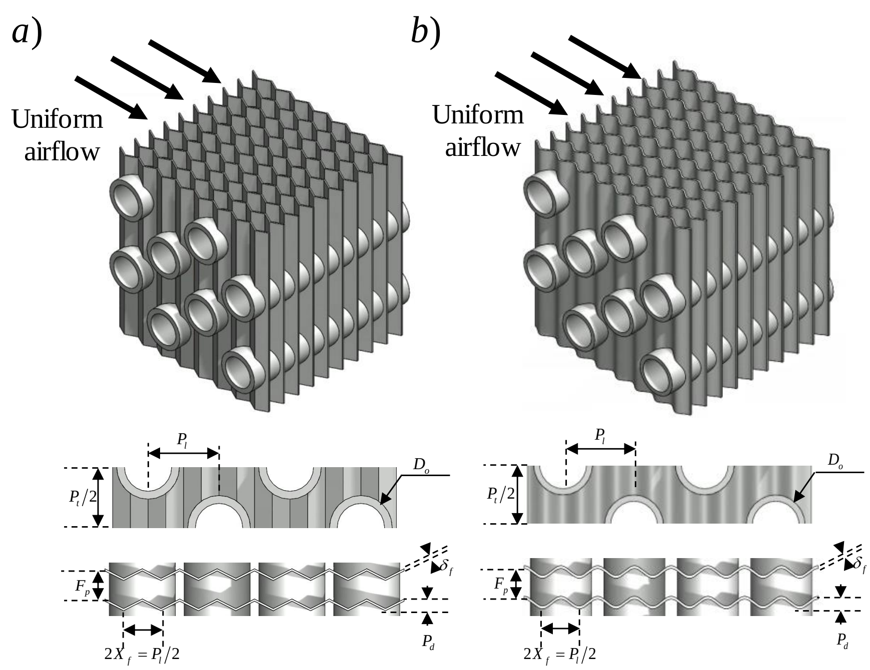

Figure 96. Wavy fin-and-tube surface: a) Herringbone; b) Smooth (Sinusoidal).

Table 23. Wavy fin-and-tube correlation design space.

Variable	Unit	Range
D_o	mm	2.0 - 5.0
P_l/D_o	-	1.25 – 4.0
P_t/D_o	-	1.25 – 4.0
F_p	mm	0.5 – 2.5
P_d/X_f	-	0.088 – 0.84
δ_t	mm	0.05 – 0.1
N_r	-	2-20
u	m/s	0.5 – 7.0

6.3.1 CFD model

The CFD computational domain (Figure 97) is a three dimensional cross section segment of the HX, assuming any end effects to be negligible. The inlet boundary has uniform velocity and uniform temperature (300K), whereas the outlet boundary is at constant atmospheric pressure. The upper and lower boundaries are symmetric, while the lateral boundaries are periodic, and the tube walls are at constant temperature of 340K, whilst the fin walls are coupled to the tubes. The faces parallel to the fins on the sides are periodic. The fluid properties use ideal gas model, and the turbulence is evaluated using the k-ε realizable model. The convergence criteria used is 10^{-5}. The near wall region mesh is a fine map scheme with growing layers at a ratio of 1.2 (Figure 97). The core of the computational domain is a pave mesh scheme with an average element size equal to the last row of the boundary layer mesh.

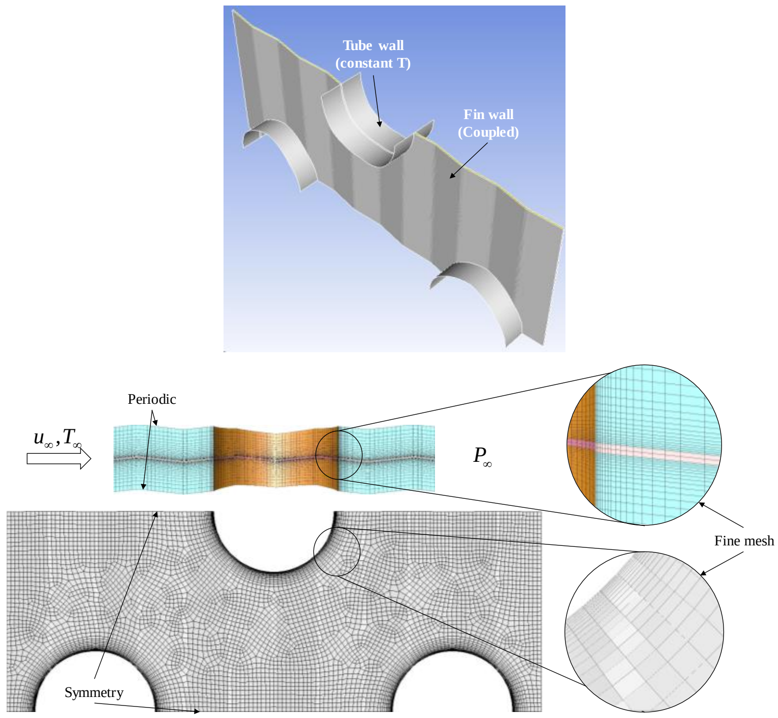

Figure 97. Wavy fin computational domain and mesh.

The following sample CFD results (Figure 98, Figure 99, Figure 100 & Figure 101) show a comparison for an equivalent design using Herringbone and smooth fins.

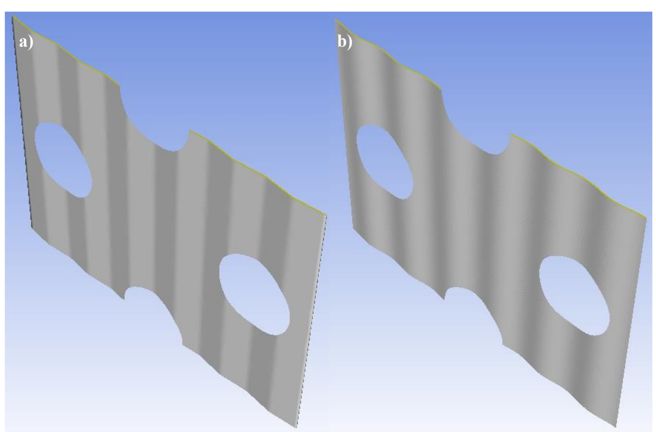

Figure 98. Equivalent wavy fins: a) Herringbone; b) Smooth.

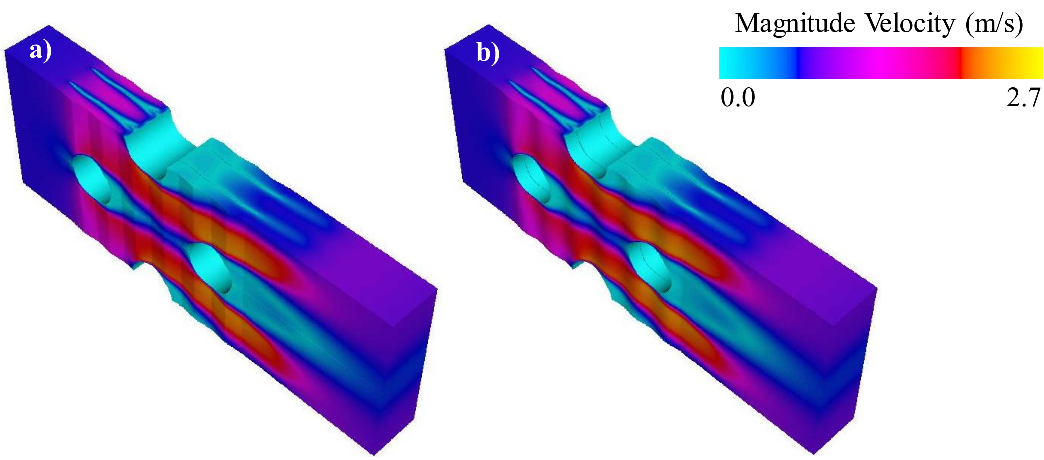

Figure 99. Sample velocity contour plots: a) Herringbone and b) smooth wavy fins.

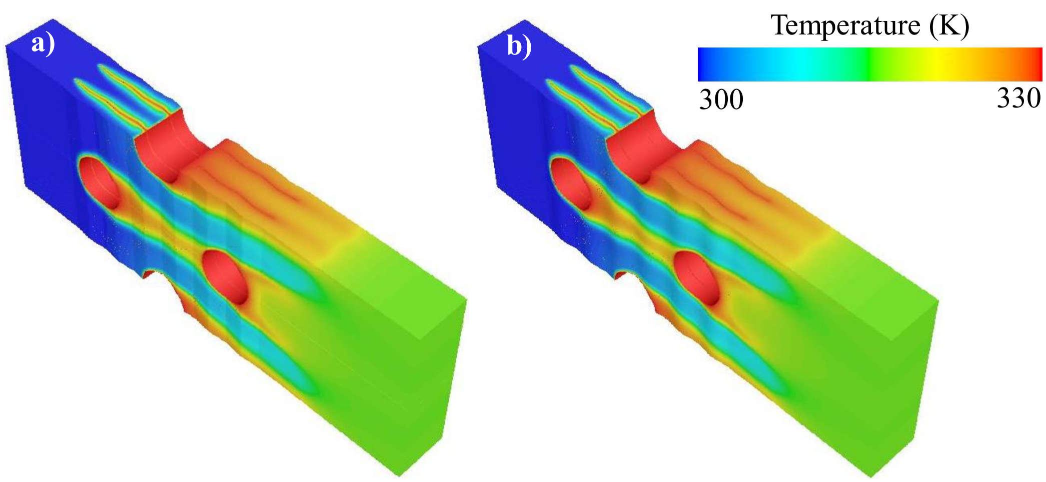

Figure 100. Sample temperature contour plots: a) Herringbone and b) smooth wavy fins.

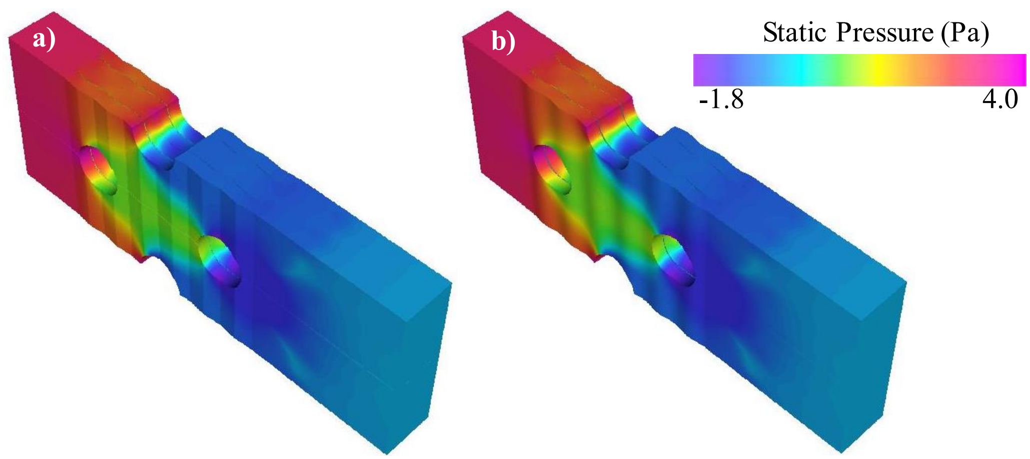

Figure 101. Sample pressure contour plots: a) Herringbone and b) smooth wavy fins.

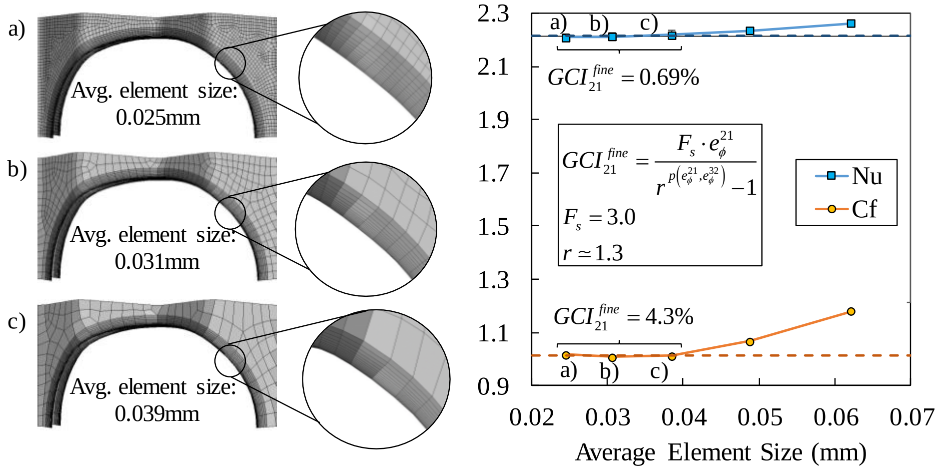

Figure 102. Grid resolution uncertainty for wavy fins: a) fine; b) base; c) coarse meshes.

6.3.2 Correlation

The correlations developed for the wavy fins are based on the multiple regression approach (equation 63). The coefficients and power matrices for the correlations developed are presented in Appendix E. There are two sets of equations for each correlation: one for 2 to 10 tube banks and one for 11 to 20 tube banks. The source data for each fin type consisted of a Design of Experiments with 1300 designs sampled using Latin Hypercube Sampling method.

$$\phi_h = \ln\left(Nu_{Dh}\right), \phi_{\Delta P} = \ln\left(C_f\right) \tag{87}$$

$$\underset{\sim}{x} = \left[\ln\left(F_p/D_o\right), \ln\left(P_l/D_o\right), \ln\left(P_t/D_o\right), \ln\left(P_d/X_f\right), \ln\left(\delta_f/F_p\right), \ln\left(N\right), \ln\left(\mathrm{Re}_{D_o,u_c}\right)\right] \tag{88}$$

$$Nu_{Dh} = hD_h/k \tag{89}$$

$$C_f = \Delta P/\left(0.5\rho u_c^2\right) \cdot D_h/\left(4d\right) \tag{90}$$

$$D_h = 4A_c d/A_o \tag{91}$$

$$\mathrm{Re}_{D_o,u_c} = \rho u_c D_o/\mu \tag{92}$$

The non-dimensional heat transfer and pressure drop are calculated for dry air properties at 300K and 1atm. The property values used are presented in Table 24.

Table 24. Air thermophysical properties for wavy fin correlations.

T (K)	P (kPa)	ρ (kg/m³)	μ (Pa.s)	k (W/m.K)	c_p (J/kg.K)
300	101.325	1.177	1.86E-05	2.57E-02	1005

The correlations verification is respectively shown in Figure 103 and Table 25 against source data and Figure 104 against random data.

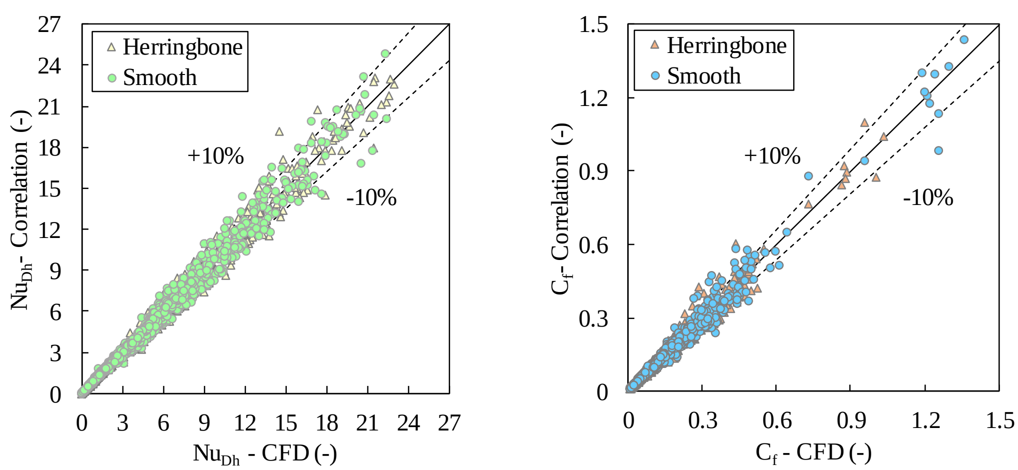

Figure 103. Wavy fin correlations verification against source data.

Table 25. Wavy fins correlations fitness.

Fin Type	Herringbone		Smooth	
Metric	**Nu_{Dh}**	**C_f**	**Nu_{Dh}**	**C_f**
Predicted data (e=10.0%)	84.73%	83.92%	80.84%	81.88%
Predicted data (e=12.5%)	92.63%	91.22%	88.95%	89.43%
Predicted data (e=15.0%)	96.17%	94.54%	94.28%	93.48%
Predicted data (e=20.0%)	99.04%	98.08%	98.97%	97.62%
Predicted data (e=25.0%)	99.56%	99.04%	99.60%	98.97%
R^2	0.9937	0.9881	0.9927	0.9889
Mean Absolute Relative Error	5.344%	5.665%	5.747%	6.038%
Median Absolute Relative Error	3.940%	4.288%	4.253%	4.750%

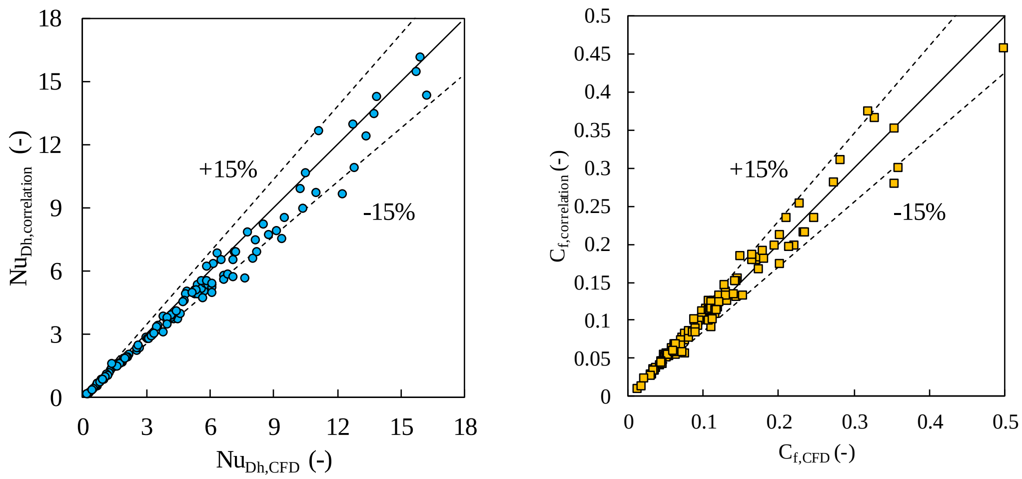

Figure 104. Herringbone correlations verification against 120 random samples.

This section presents a comparison between the proposed correlations with existing ones for the design space investigated (Figure 105). The existing correlations not only largely deviate from the CFD simulations but they are also not consistent, suggesting they cannot and should not be extrapolated.

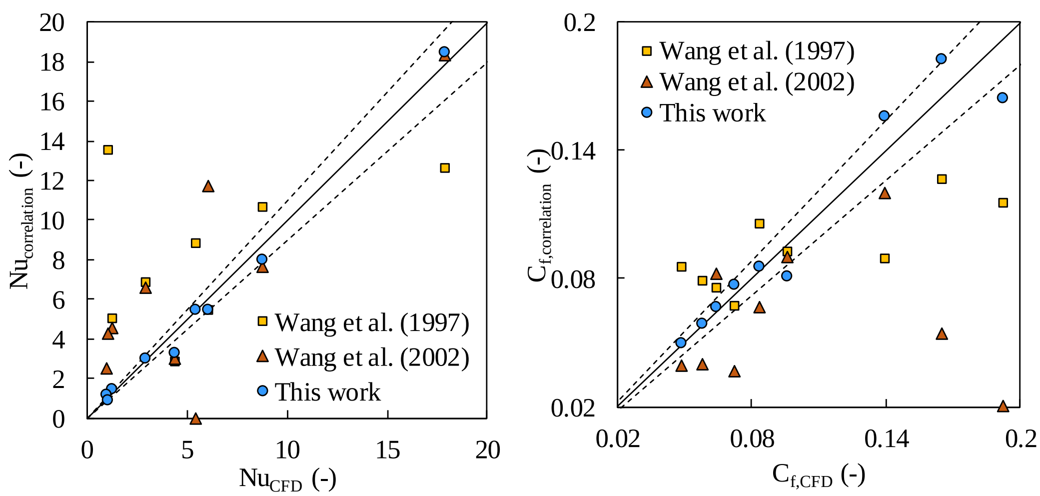

Figure 105. Herringbone correlation comparison.

Chapter 7: Surface Optimization Study

This Chapter is dedicated to surface optimization using the correlations developed in the previous Chapter. The goal is to verify whether optimizing finless and finned surfaces have an actual impact regarding the trade-off shown in Figure 19 from Chapter 3. The study consists of a comprehensive parametric optimization analysis, where the tube diameter, the surface hydraulic diameter and the air frontal velocity are the parametric variables (Table 26), while the other design variables are optimized with respect to heat transfer coefficient and friction power per unit area (equation 93).

$$
\begin{aligned}
&\max h \\
&\min \dot{W}'' \\
&s.t. \\
&D_o = D_o^*; D_o^* \rightarrow parameterized \\
&u = u^*; u^* \rightarrow parameterized \\
&0.99D_h^* \le D_h = 4\frac{A_c}{A_o}d \le 1.01D_h^*
\end{aligned}
\tag{93}
$$

By parameterizing the tube and hydraulic diameters, the evaluation of the characteristic length impact over performance becomes more comprehensive. Additionally, the surface hydraulic diameter is the indication of the surface dimension, thus allowing a fair comparison using dimensioned thermal-hydraulic performance as discussed in the literature review. The detailed dimensions and performance of the investigated surfaces, as well as comparison plots for each combination of parametric variables are presented in Appendix F, whilst the general results are presented in the following sub-section.

Table 26. Parametric Variables.

D_o mm	D_h mm	u m/s
0.5,1, 1.5, 2, 3, 4, 5	0.5, 1.0, 1.5, 2.5, 3.0	1.0, 2.0, 3.0, 5.0

On conventional tube and fin HX's the tubes are typically arranged on an equilateral configuration (square for in-line and triangle for staggered) so the same U-bends can be applied everywhere. In these analyses, the surfaces were optimized with unconstrained tube pitches and constraining them as such the transverse pitch is a function of the longitudinal pitch ensuring the equilateral configuration. Only staggered arrangement is investigated for both finless and wavy Herringbone surfaces.

Another important aspect of this study is to demonstrate the robustness and computational affordability of these correlations. On Table 27 one can see that given the parametric variables the number of parameter combinations total in 300 optimization runs. Typically, for MOGA using 500 iterations and a population of 150 with 10% replacement, the optimizer investigates approximately 5000 designs. Therefore, this study, has investigated approximately 1.5 million designs at a cost of less than 3min per optimization.

Table 27. Surface Optimization Study Computational Cost.

	Finless	**Finned**	**Total**
No. of parametric combinations	140	160	300
No. of correlations (sets) used	2	1	3
No. of correlation calls per optimization (approx..)	5,000	5,000	10,000
Total No. of correlation calls (approx..)	700,000	800,000	1,500,000
Machine time (s)	28,800	24,000	52,800
Time per optimization (s)	205.7	150.0	176.0

7.1 Optimization Results

The following plots include all Pareto sets, i.e. all optimization results from each parametric study are combined in a single plot. For detailed results regarding each optimization study refer to Appendix F.

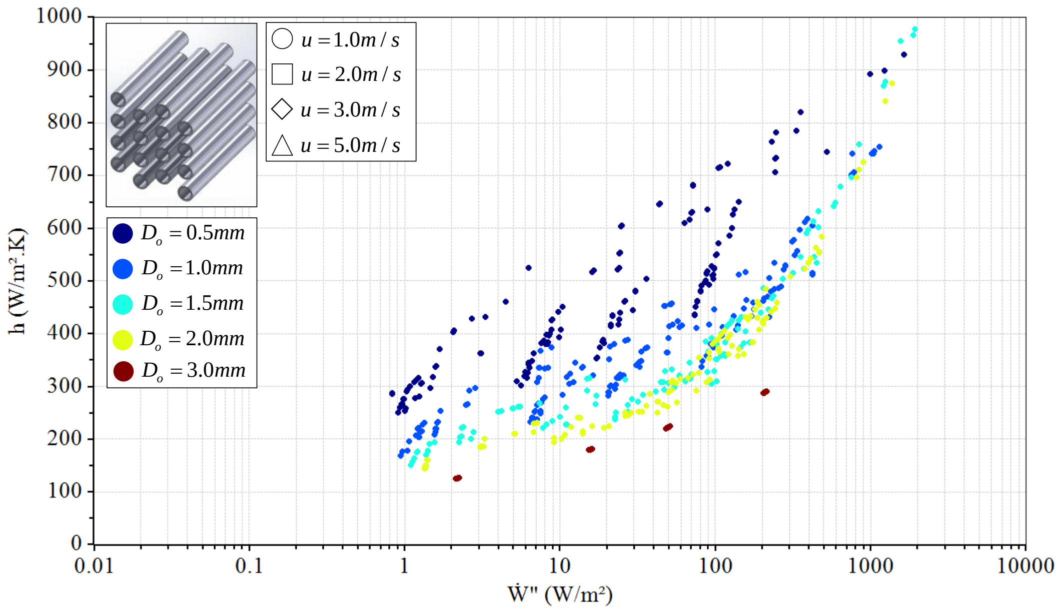

Figure 106. Finless tubes surface optimization results I: tube diameter.

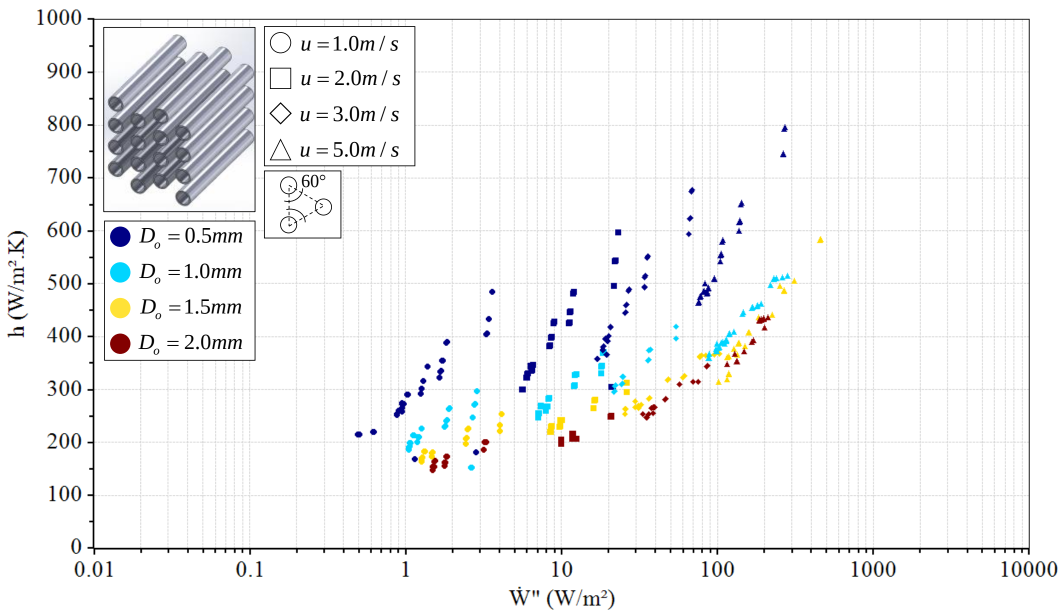

Figure 107. Finless tubes surface optimization results II: tube diameter.

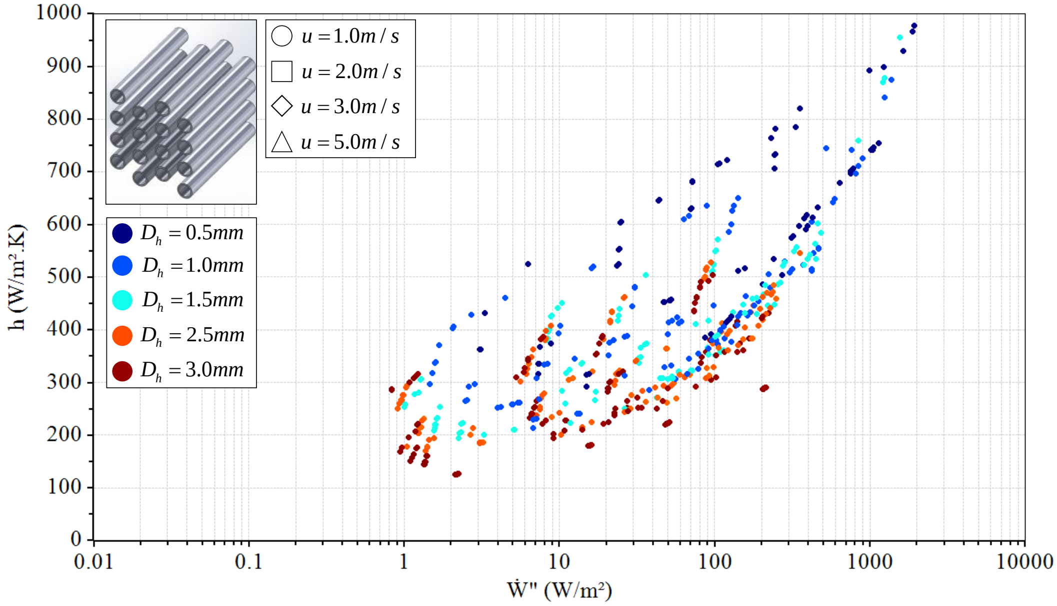

Figure 108. Finless tubes surface optimization results I: hydraulic diameter.

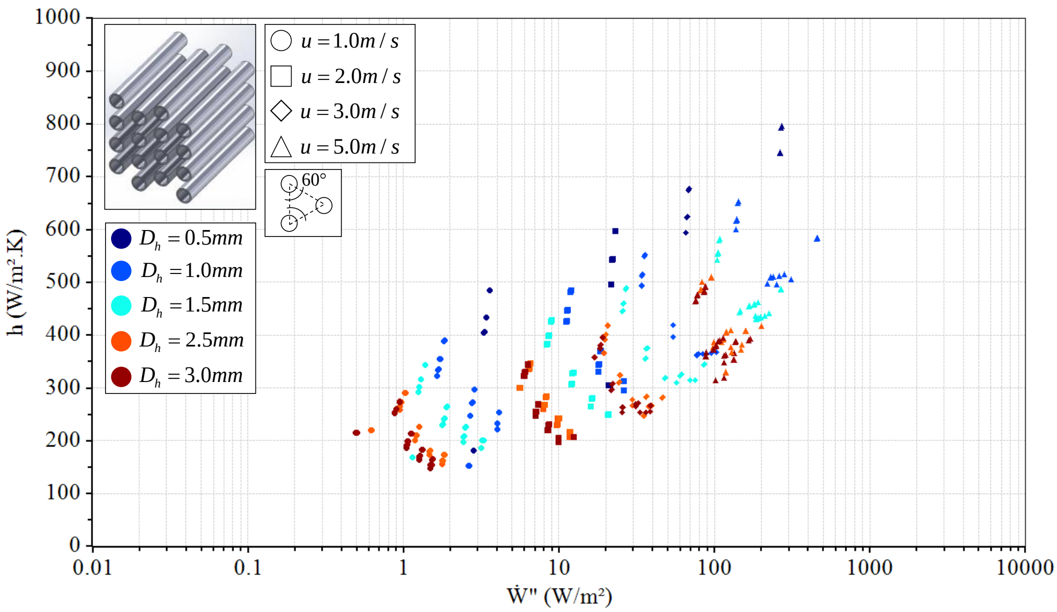

Figure 109. Finless tubes surface optimization results II: hydraulic diameter.

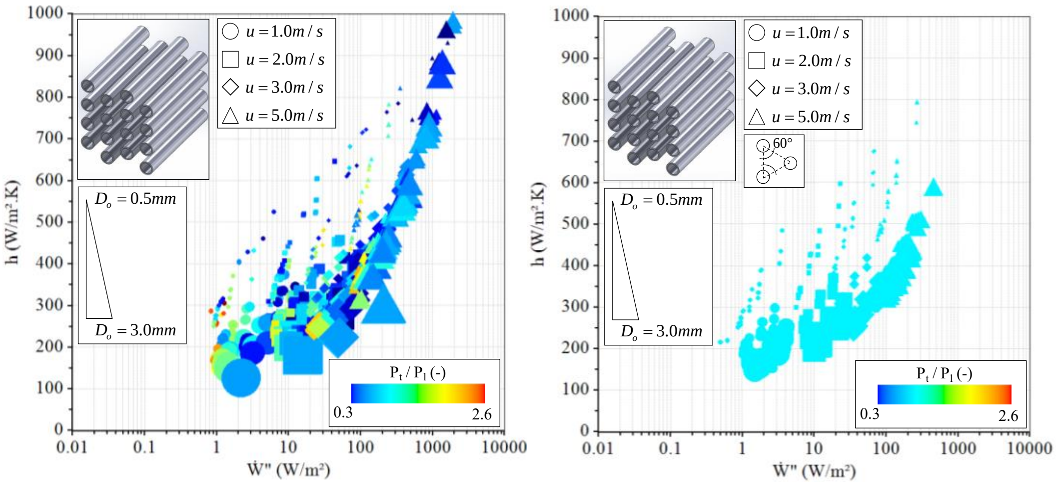

Figure 110. Finless tubes surface optimization results I & II: pitch ratio.

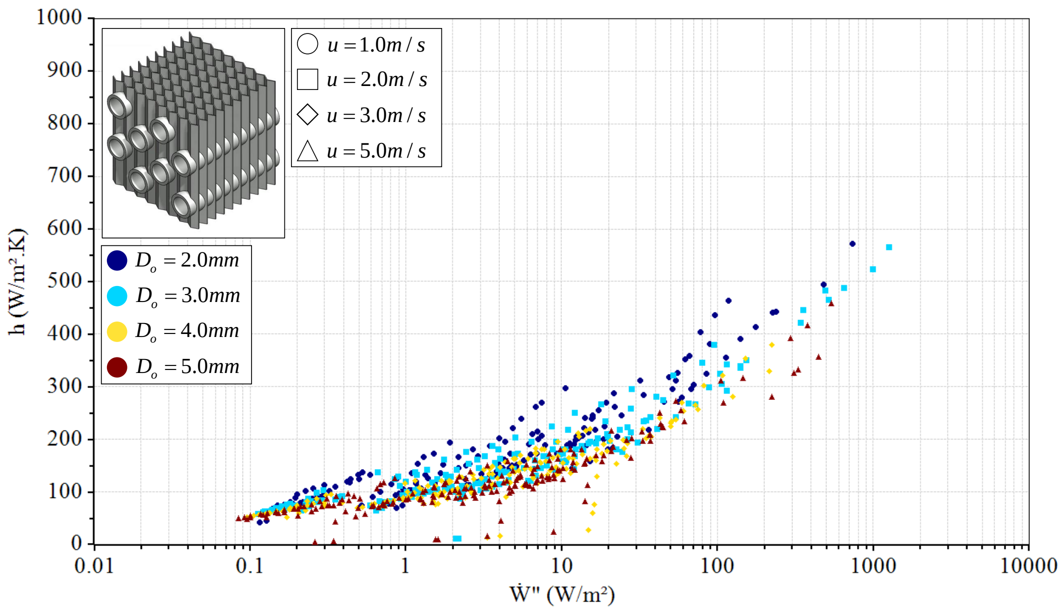

Figure 111. Wavy fin surface optimization results I: tube diameter.

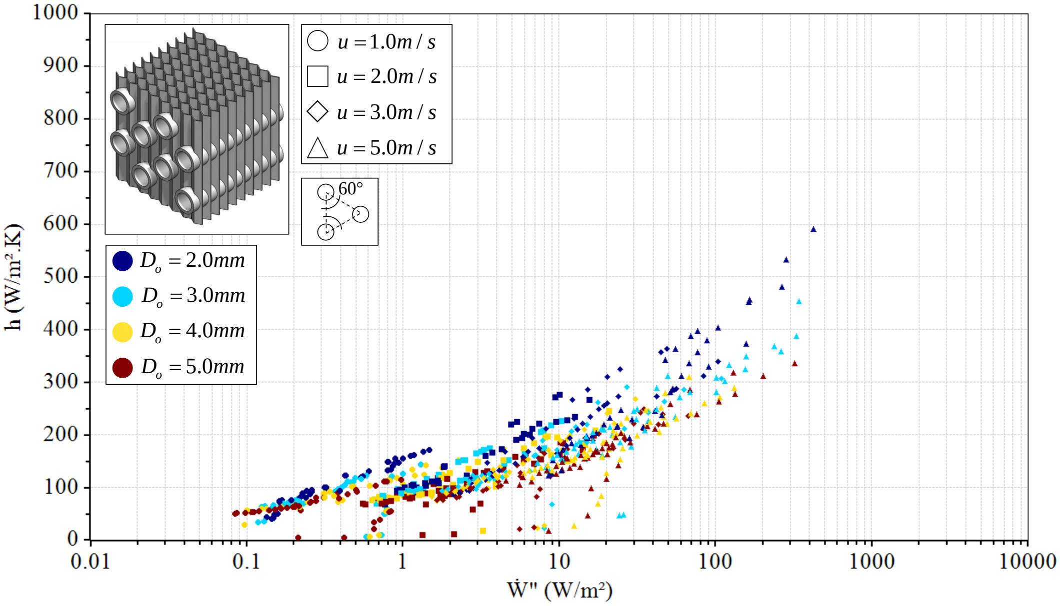

Figure 112. Wavy fin surface optimization results II: tube diameter.

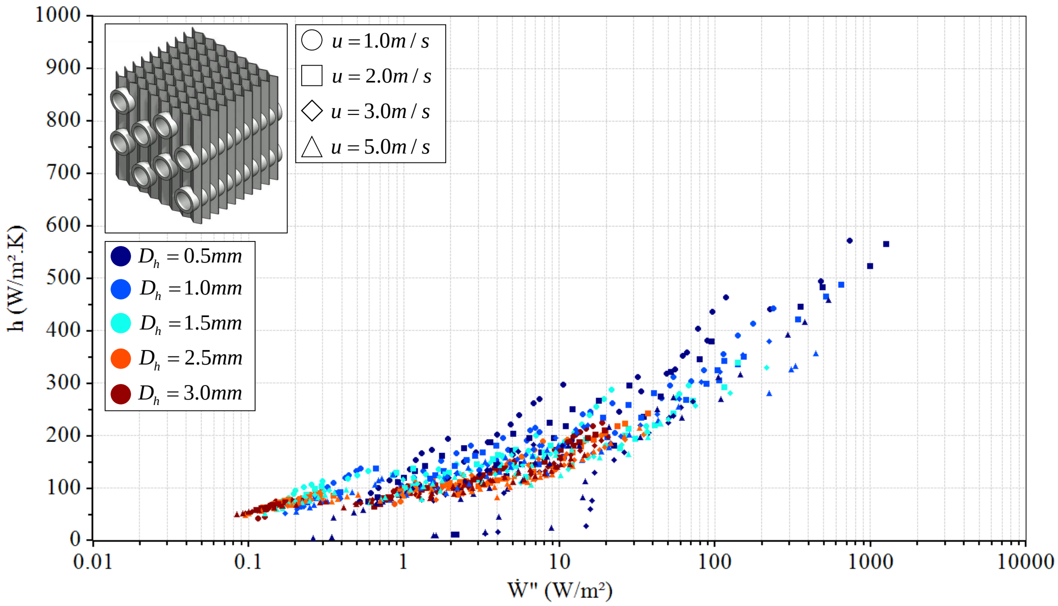

Figure 113. Wavy fin surface optimization results I: hydraulic diameter.

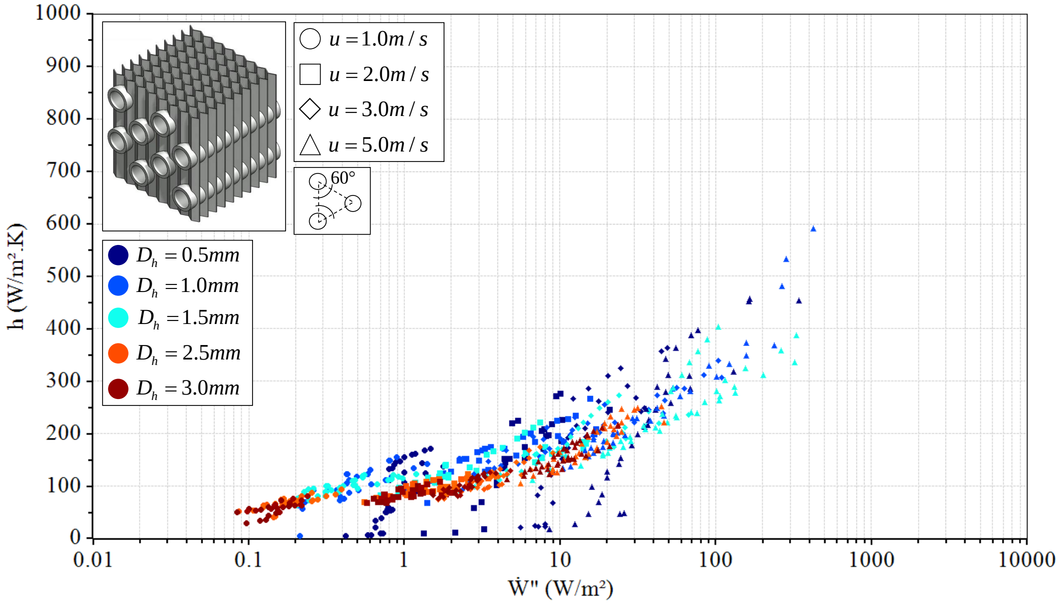

Figure 114. Wavy fin surface optimization results II: hydraulic diameter.

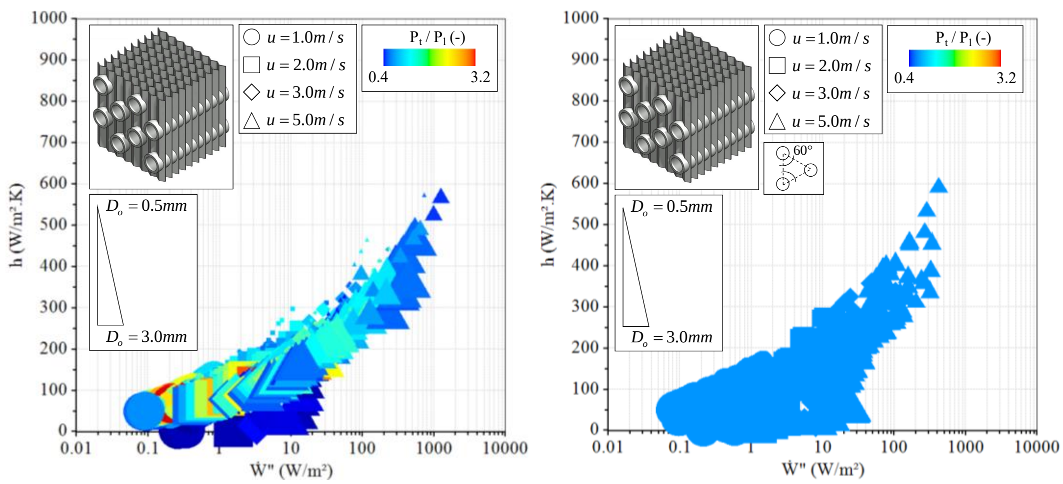

Figure 115. Wavy fin surface optimization results I and II: pitch ratio.

7.1.1 Discussion

The plots shown in Figure 106 to Figure 115 contain a lot of valuable information regarding surface size and surface type. First, again it has been demonstrated that the tube diameter has a clear correlation with heat transfer coefficient, regardless whether the surface is finned or finless; the plots are very stratified, although there is some overlapping, in particular for the finned surface.

Second, the finless surfaces consistently achieve higher heat transfer coefficients than their finned counterparts, for all surface sizes (hydraulic diameters), Additionally, the general trend for finless surfaces show a steeper slope between h and $\dot{W}$”, which has been suggested in the second order analysis presented in Figure 19 from Chapter 3. Therefore, supporting the fact that such trends are an intrinsic characteristic of the surfaces and not to a particular pairwise comparison; the finned surfaces have very small increments in heat transfer coefficient as the diameter is reduced, while the finless tubes benefit greatly from it.

Third, Figure 106 and Figure 107 have an important message regarding the compactness of finless tubes. Although the optimization considered all diameters from 0.5mm to 5.0mm, only 3.0mm or less were found to be feasible. The reason is depicted in Figure 17 from Chapter 3, where the compactness falls abruptly for diameters larger than 2.0mm, in particular for finless tubes; the optimization imposed specific constraints to the hydraulic diameter, which is an indirect way of measuring the compactness. Furthermore, for equilateral tube arrangement (Figure 107) the largest diameter obtained from the optimization was 2.0mm. The main reason for this, however, was not the arrangement itself, but the fact that the correlations for finless tubes ranging from 2.0mm to 5.0mm are limited to pitch ratios down to 1.5, whereas the correlations for smaller tubes are valid for pitch ratios as low as 1.2. Nevertheless, this characteristic only supports the fact that for finless designs the tubes have to be very small, while finned designs don’t have the same limitation.

Finally, a few optimization problems (Figure 116) were selected for one velocity and one hydraulic diameter in order to discuss the impact of tube diameter and surface type under a fair comparison. The first thing that is clear is that the surface types are clustered in very distinct regions of the plot (Figure 116). There is a clear trade-off where for larger diameters the preference is for finned surfaces and the small diameters lean towards finless tubes. Near the 2.0mm is where the plots seem to have similar slopes and are almost continuing, which may also suggest where the breakeven occurs. Not surprisingly this was observed in both Figure 17 and Figure 19 from Chapter 3, where the compactness rapidly increases below 1.0mm to 2.0mm, so does the heat transfer coefficient, since both are inversely proportional to the tube diameter. The non-dominated sorting illustrates very well this trade-off, but also shows that the finless tubes are more sensitive to the heat transfer coefficient, remaining only the 0.5mm diameter designs.

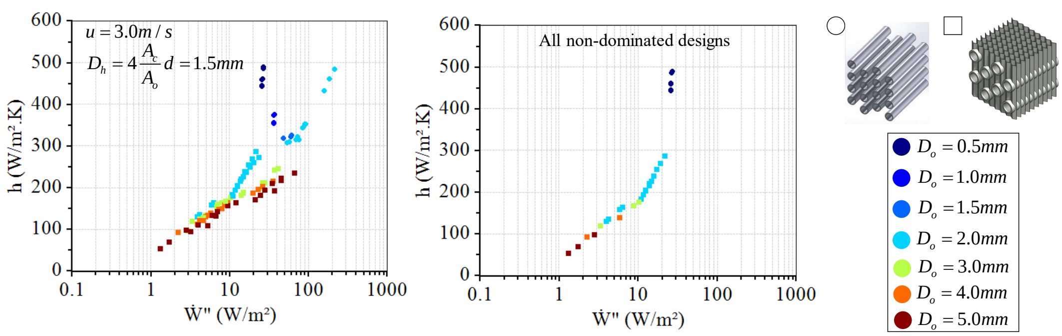

Figure 116. Selected surface optimization case.

A few surfaces form Figure 116 were selected for a further investigation for varying velocity (Figure 117). Since all have same hydraulic diameter varying the velocity results in same Reynolds to all surfaces at same velocities. The curves in Figure 117 show an almost linear increase of the heat transfer coefficient with the log of friction power for the finned surfaces, while the finless show a much faster, non-linear, grow relating the same variables. Additionally, for both surface types, the smaller the tube the higher the rate of heat transfer coefficient. Furthermore, the finless curves show no trade-off with respect to diameter, the smallest diameter always performs better. The finned surfaces, on the other hand, show potential trade-offs of varying diameter. The latter observations were already shown in Figure 116. Lastly, again the 2.0mm diameter seem to be a turning point for either surface types. For the finned surface the 2.0mm curve suggest that at low Reynolds number it actually performs worse than the 3.0mm.

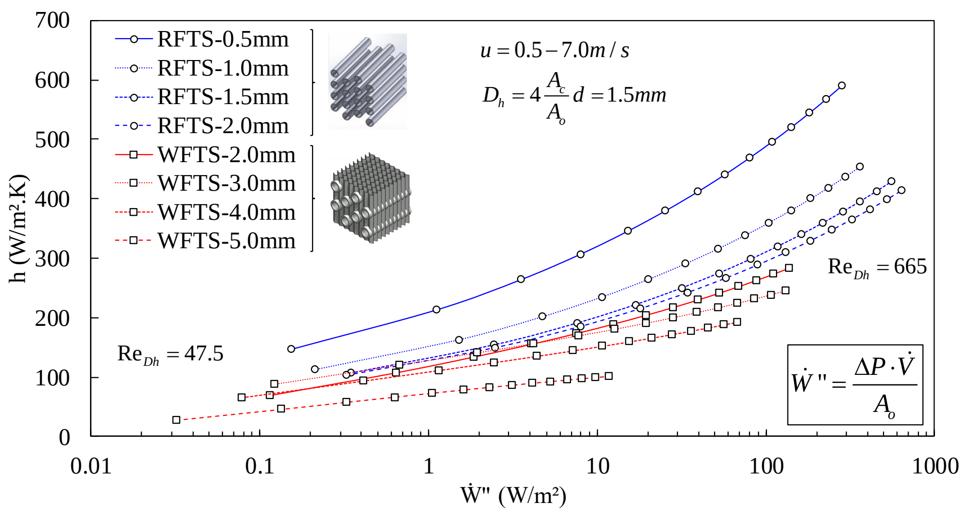

Figure 117. Equivalent surfaces (same D_h) under wide range of Reynolds numbers.

Chapter 8: Conclusions

8.1 Summary of Contributions

The main contributions of this Ph.D. are to shed light on the next generation of heat exchangers, with focus on air-to-fluid applications. The following summary lists the most important aspects of each chapter.

1- Fundamental aspects of air-to-fluid heat exchangers

- Reduction of tube diameter
    - In Chapter 3 it was clearly demonstrated in the first order analysis that regardless the surface type, and that the compactness, material utilization and internal volume are inversely proportional to the tube diameter.
    - Thermal performance is also enhanced when reducing the diameter, as first suggested on Chapter 3, then verified multiple times along the dissertation (Chapters 4 and 6). The surface level analysis showed how the temperature gradient within the boundary layer significantly increases when reducing the tube size. Moreover, the characteristic length has a stronger influence than the flow regime. With either same frontal velocity, or same Reynolds number, the heat transfer coefficient is always higher in smaller tubes.
    - In Chapter 4 it was demonstrated with actual HX applications, the benefits of reducing the tube diameter with novel

HX concepts that outperform current state-of-the art HX's greatly in size, material and performance.

- The reduction of tube size also has an inverse proportionality to the friction resistance, which was highlighted in the second order analysis. It was also highlighted it in the boundary layer analysis, where the velocity gradient grows much faster on smaller tubes. Such characteristic had an impact on the RTHX designs investigated in Chapter 4. All round tube designs with small diameter ended up having larger face area in order to reduce the frontal velocity and satisfy the pressure drop.

- Finned vs. Finless Surfaces
  - The first and second order analyses in Chapter 3 suggested that the contribution from conventional fins are not always beneficial. The fin-to-tube surface ratio is directly proportional to the tube diameter, thus for smaller tubes, the ratio can decrease one or two orders of magnitude.
  - Additionally, the finned surfaces consistently have lower heat transfer coefficients than finless surfaces. Thus at very small diameters fins not only are much less helpful in reducing the thermal resistance, but will still offer additional friction resistance. This was explained in Chapter 4 when the FTHX, with similar tube diameters than the RTHX, resulted in designs with higher pressure drop for the

same volume. Moreover, the heat transfer coefficients were much lower, thus requiring even more tubes than the RTHX

- Chapter 6 also served as an additional comparison, where it was extensively verified the trade-off proposed in Chapter 3 with the second order analysis when comparing optimized finless and finned surfaces.

- Tube shapes
  - The nature of the flow over conventional round shape results in a large wake region due to the flow separation. The latter has a mixing effect which benefits heat transfer, however it naturally increases hydraulic resistance. Alternate shapes such as oval and flat tubes led to reduced flow resistance.
  - In Chapter 3 it was demonstrated with a comprehensive study on various alternate shapes that when the shape has an aspect ratio (i.e. tube height per tube width) less than unity the hydraulic resistance is significantly less. Instead, the round tube has consistently the highest heat transfer coefficient. Shapes with non-symmetric leading and trailing edges (i.e. airfoils) provide much better thermal-hydraulic ratio, despite the lower heat transfer coefficient compared to round tubes.
  - When using airfoil shaped tubes in a scaled HX, the aerodynamics allow the air velocity to increase with less pressure loss penalty, but it also allows packing additional tube banks, which

can provide additional surface area to compensate for the reduction in heat transfer coefficient. The resulting HXs have significantly smaller face areas; the NTHX-001 concept, from Chapter 4, has more than 50% smaller face area than the RTHX-001, while delivering the 1.0kW

2- Multi-Scale analysis with Topology and Shape Optimization Framework

- In Chapter 4 it was presented a comprehensive HX design framework that includes design concept, airside modeling and simulation, design and optimization, verification and validation. The modeling tools leveraged the automated CFD simulations and approximation assisted optimization techniques.
- It was developed a shape parameterization method that was incorporated to the multi-scale analysis and topology design and optimization methodology, which the foundations were first introduced by Abdelaziz et al. [72].
- The methodology was used to optimize air-to-water HX's which are 20% to 80% smaller, with at least 20% better performance and have more than 50% reduction in material compared to a state-of-the-art MCHX.
- Advanced manufacturing techniques were leveraged, such as metal additive manufacturing, to build a prototype of the proof-of-concept NTHX-001

- Two prototypes were tested, RTHX-001 and NTHX-001, and validated it in less than 5% in capacity, 10% in air heat transfer coefficient, and 20% in airside pressure drop.
- This methodology should serve as foundations for a HX design platform where one can leverage computational power to let the optimizer “create” and “invent” new HX’s with high design freedom.
- Finally, it was demonstrated the potential of using small finless tubes in three-ton heat exchangers using R410A as refrigerant. The resulting HX’s can be more than 50% smaller with more than 50% reduction in charge and improving COP in 10-15% of a SEER 16 baseline unit. Furthermore, the reduction in refrigerant charge within the HX’s allows the new system to have more charge in the pipes.

3- <u>CFD-Based correlations for small diameter tubes</u>

- Six novel sets of correlations were developed for airside characterization for finless, flat fin and tube and wavy fin (smooth and Herringbone) and tube surfaces with diameters smaller than 5.0mm, fulfilling the literature gap
- These correlations are a computationally inexpensive set of tools that, at a small accuracy cost, replace the need for CFD or other numerical methods, which can potentially mean cost savings in the event of not having this type of software available. In Chapter 6 it was presented a study with 280 optimization runs using these correlations from which the software made an estimated 1.5 million correlation calls, and the overall time needed

was just 14.7 hours. During the course of this doctorate the amount of CFD simulations performed was two orders of magnitude smaller than the number of correlation calls. In other words, the study in Chapter 6 could have never been made without these correlations.

- All correlations are currently available in the latest version of CoilDesigner® [159] and is ready to be used to evaluate coils with small diameter tubes.

8.2 List of Publications

The following peer-reviewed journal papers were published or submitted as outcomes of this research.

1- Huang, L. Bacellar, D., Aute, V., Radermacher, R., **Variable geometry microchannel heat exchanger modeling under dry, wet, and partially wet surface conditions accounting for tube-to-tube heat conduction**, Science and Technology for the Built Environment (2015) 21, 703–717

2- Bacellar, D., Aute, V., Huang, Z. Radermacher, R, **Airside friction and heat transfer characteristics for staggered tube bundle in crossflow configuration with diameters from 0.5 mm to 2.0 mm**, International Journal of Heat and Mass Transfer, 98, p. 448-454

3- Bacellar, D., Aute, V., Huang, Z., Radermacher, R, **High Performance Compact Air-to-Fluid Heat Exchangers Using Multi-Scale Analysis and Shape Optimization with Experimental Validation of a 3-D Printed Prototype** (Journal: *Science and Technology for the Built Environment*)

4- Huang, Z., Bacellar, D., Aute, V., Radermacher, R, **Air side performance of a novel air-to-refrigerant heat exchange**r, (Journal: *Experimental Thermal and Fluid Sciences*)

5- Bacellar, D., Aute, V., Radermacher, R, **Thermal-hydraulic optimum topology configurations for fin and tube heat exchangers with diameters below 5.0mm**, (Journal: *International Journal of Refrigeration*)

6- Li, Zhenning, Bacellar, D., Aute, V., Radermacher, R, **Review on Correlations for Small Diameter Tube Heat Exchangers**, (Journal: *International Journal of Refrigeration*)

The following peer-reviewed conference papers were published or accepted and resulted from this research.

1- Bacellar, D., Aute, V., Huang, Z. Radermacher, R., **Novel Airside Heat Transfer Surface Designs Using an Integrated Multi-Scale Analysis with Topology and Shape Optimization**, 16th International Refrigeration and Air Conditioning Conference at Purdue, July 11-14, 2016

2- Bacellar, D., Aute, V., Huang, Z. Radermacher, R, **Airside Performance Correlations and Optimal Heat Pump Heat Exchanger Designs Based on 0.5mm-2mm Finless Round Tube Bundles**, 16th International Refrigeration and Air Conditioning Conference at Purdue, July 11-14, 2016

3- Bacellar, D., Aute, V., Radermacher, R**., Performance Evaluation Criteria Analysis of Compact Air-to-Refrigerant Heat Exchangers and Selection Utility Function for Single Phase Applications**, 16th

International Refrigeration and Air Conditioning Conference at Purdue, July 11-14, 2016.

4- Bacellar, D., Aute, V., Radermacher, R., **Wavy Fin Profile Optimization Using NURBS for Air-To-Refrigerant Tube-Fin Heat Exchangers with Small Diameter Tubes**, 16th International Refrigeration and Air Conditioning Conference at Purdue, July 11-14, 2016

5- Bacellar, D., Aute, V., Radermacher, R., **CFD-Based Correlation Development for Air Side Performance of Wavy Fin Tube Heat Exchangers using Small Diameter Tubes**, 16th International Refrigeration and Air Conditioning Conference at Purdue, July 11-14, 2016

6- Bacellar, D., Aute, V., Huang, Z. Radermacher, R., **High Performance Gas-to-Fluid Crossflow Heat Exchangers using Micro Tubes with Round and Novel Shapes**, Thermal Fluids Analysis Workshop (TFAWS16) at NASA-Ames Research Center, August 01-04, 2016

7- Bacellar, D., Aute, V., Radermacher, R., **Verification & Validation of CFD Models Used in Automated Simulations Applied to Novel Air Heat Transfer Surfaces Optimization**, ASME V&V Symposium, 2016, Las Vegas, NV.

8- Bacellar, D., Ling, J., Abdelaziz, O., Aute, V., Radermacher, R., **Design of Novel Air-to-Refrigerant Heat Exchangers Using Approximation Assisted Optimization**, ASME 2014 Verification & Validation Symposium, May 7-9, 2014 – Las Vegas, Nevada.

9- Bacellar, D., Aute, V., Radermacher, R., **CFD-Based Correlation Development for Air Side Performance of Finned and Finless Tube Heat Exchangers with Small Diameter Tubes**, 15th International Refrigeration and Air Conditioning Conference at Purdue, July 14-17, 2014.

10- Bacellar, D., Ling, J., Abdelaziz, O., Aute, V., Radermacher, R., **Multi-scale modeling and approximation assisted optimization of bare tube heat exchangers**, Proceedings of the 15th International Heat Transfer Conference, IHTC-15, August 10-15, 2014, Kyoto, Japan.

11- Bacellar, D., Abdelaziz, O., Aute, V., Radermacher, R., **Novel Heat Exchanger Design using Computational Fluid Dynamics and Approximation Assisted Optimization**, ASHRAE 2015, Winter Conference, January 24-28, 2015 - Chicago, IL.

12- Bacellar, D., Aute, V., Radermacher, R., **A Method for Air-To-Refrigerant Heat Exchanger Multi-Scale Analysis and Optimization with Tube Shape Parameterization**, 24th IIR International Congress of Refrigeration, August 16 – 22, 2015 – Yokohama, Japan.

13- Bacellar, D., Aute, V., Radermacher, R., **CFD-Based Correlation Development for Air Side Performance on Finned Tube Heat Exchangers with Wavy Fins and Small Tube Diameters**, 24th IIR International Congress of Refrigeration, August 16 – 22, 2015 – Yokohama, Japan.

14- Huang, L. Bacellar, D., Aute, V., Radermacher, R., **Fin Performance Analysis for Microchannel Heat Exchangers Under Dry, Wet and**

Partial Wet Conditions, 15th International Refrigeration and Air Conditioning Conference at Purdue, July 14-17, 2014.

15- Bhanot, V., Bacellar, D., Ling, J., Alabdulkarem, A., Aute, V., Radermacher, R., **Steady State and Transient Validation of Heat Pumps Using Alternative Lower-GWP Refrigerants**, 15th International Refrigeration and Air Conditioning Conference at Purdue, July 14-17, 2014

16- Saleh, K., Bacellar, D., Aute, V., Radermacher, R., **An Adaptive Multiscale Approximation Assisted Multiobjective Optimization Applied to Compact Heat Exchangers**, 4th International Conference of Engineering Optimization, EngOpt 2014, September 8-11, Lisbon, Portugal.

The following invention disclosures/provisional patents have been developed as a result of the work presented in this dissertation.

1- **Air-to-Refrigerant Heat Exchangers with Parameterized Tube Shapes**, Invention Disclosure No. PS-2015-112, September/2015

2- **High-Performance Air-to-Refrigerant Heat Exchangers Using Small Round Tubes**, Invention Disclosure No. PS-2015-130, October/2015

3- **Integrated Air-to-Refrigerant Heat Exchanger and Impeller**, Invention Disclosure No. PS-2014-181, Provisional Patent No. 62/264692, December/2015

8.3 Recommendations for Future Work

This work has opened new frontiers to the next generation of heat This work has opened new frontiers to the next generation of heat exchangers and created opportunities to great advances in the art. Future researches can benefit greatly from the fundamentals and technical contributions of this work by addressing the following:

- Although it was demonstrated that conventional fin concepts can become detrimental at a certain scale, the conclusions do not imply that other methods of surface enhancement should not be investigated. My suggestion is to focus on the primary heat transfer surfaces and, in addition to the shape optimization and size reduction, by investigate adding other potential enhancement mechanisms, including, but not limited to:
    - Surface coating/treatment
    - Winglets/vortex generators (Figure 118); such mechanisms, in combination with novel shapes, may contribute to reduce flow separation even more and induce turbulence within the boundary layer to enhance heat transfer
    - Extended surfaces with same shape as the tubes in order to achieve comparable performance and add surface area (Figure 119)

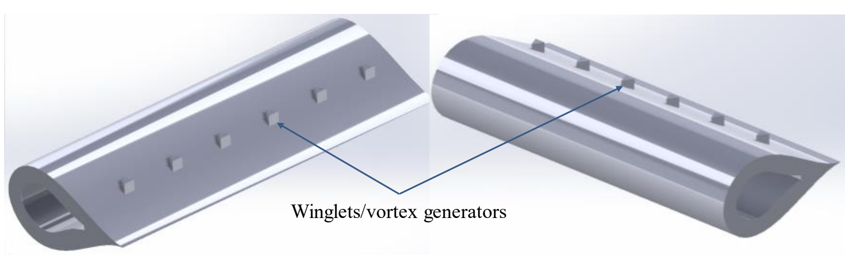

Figure 118. Winglets on high-performance tube shape.

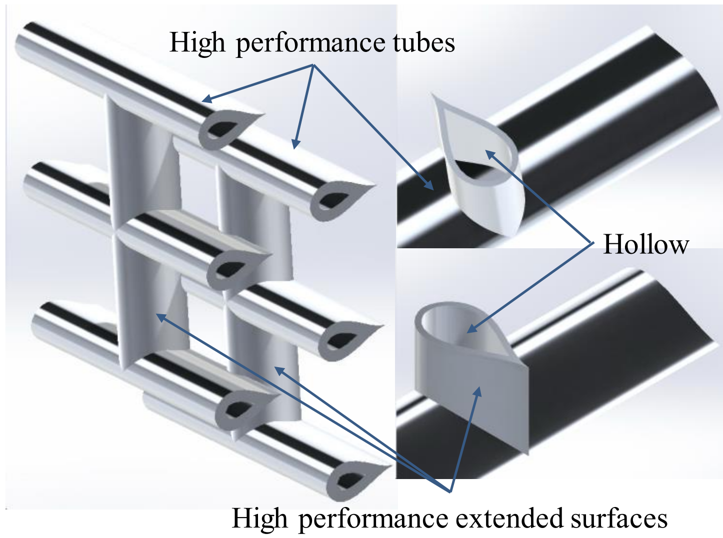

Figure 119. High-performance tube and extended surface shapes.

- Leverage the flexibility and powerful capabilities of the multi-scale analysis and shape optimization methodology
  - Optimization of tube path shape and even tube arrangement shape (Figure 120)
  - Design of coil and fan as single unit, i.e. make the tubes as the fan blades (Figure 121)

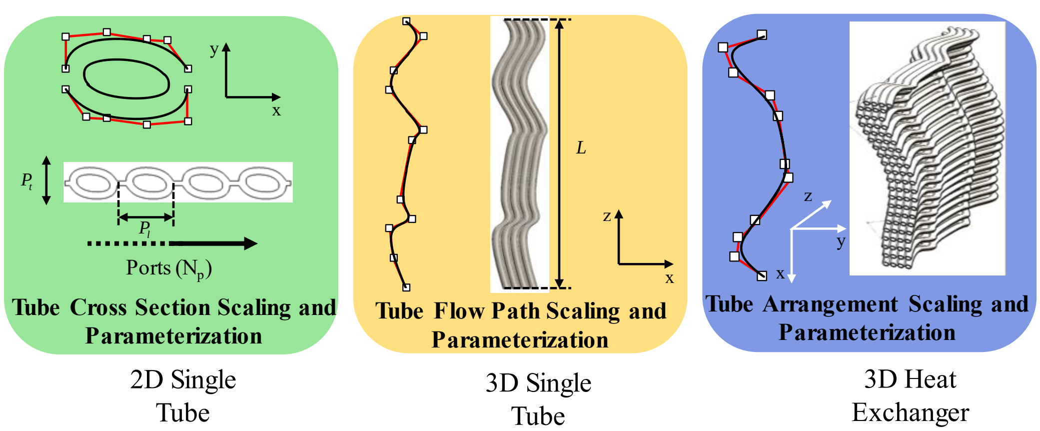

Figure 120. Extension of the multi-scale analysis and shape optimization methodology.

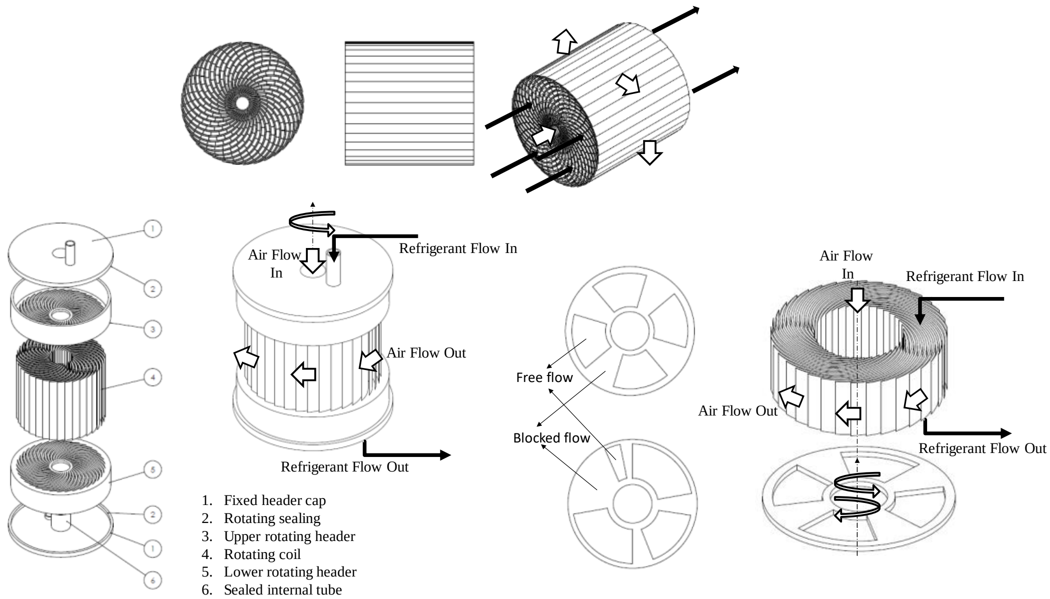

Figure 121. Fan-coil single unit concept [169].

- Address other physics that may have other unforeseen impacts, including: degradation due to fouling/frosting, vibration and noise, static and dynamic stress analysis, and corrosion
- Investigate the physics of in-tube fluid when exploring alternate shapes to ensure the correlations are applicable, in particular to two-phase flows
- Include manufacturing constraints to the optimization problem, but keeping up to date to the new advances and opportunities. Investigate solutions to larger scale HX's that may pose additional challenges when using small tubes including: tube length / bending; tube blockage, tube brazing and others

- Develop a high level platform with a comprehensive User Interface, allowing any user to perform the entire design framework based on their needs
- Investigate the possibility of optimizing an entire HVAC system addressing some of the issues found in this work including: charge migration to pipes, high airside pressure drop in the condenser and manufacturing challenges
- Investigate the possibility of 3D printing the entire HVAC unit (HX's and pipes), including fan blades, and leaving space for fan motor, compressor and valves

As the industry matures small diameter tube HX's may become available for testing which will be a great opportunity to test and improve the CFD-based correlations developed in this work.

Appendices

Appendix A – Non-Uniform Rational B-Spline C# code

Sample Call Function:

```
        public void GetNURBS(double[] xControlPolygon, double[] yControlPolygon,
int p, double[] w, double[] xNURBS, double[] yNURBS)
        // xControlPolygon & yControlPolygon - the coordinates of all control
points (any number); xControlPolygon.Length = yControlPolygon.Length
        // p – interpolation order < xControlPolygon.Length
        // w – weight vector; w.Length = xControlPolygon.Length
        // xNURBS & yNURBS - output
                {
                    int Nv = 201; //Subject to change

                    double t = 0.0;
                    double dt = 1.0 / (Nv - 1);
                    int nCP = xControlPolygon.Length - 1;
                    double[] U = getKnotVector(nCP, p);

                    if(w.Length != xControlPolygon.Length)
                       {
                         w = new double[nCP];
                        for (int i = 0; i <= nCP; i++) w[i] = 1.0;
                }

                    xNURBS = new double[Nv];
                    yNURBS = new double[Nv];

                    for (int i = 0; i < xNURBS.Length; i++)
                    {
                        xNURBS[i] = ratBSpline(t, p, U, w, xControlPolygon);
                        yNURBS[i] = ratBSpline(t, p, U, w, yControlPolygon);
                        t += dt;
                    }
                }
```

Support Functions based on Tiller and Piegl algorithms [157]:

Basis Function

```
        public double[] basisFun(int i, double u, int p, double[] U)
                {
                    double[] N = new double[p + 1];
                    double[] l = new double[p + 1];
                    double[] r = new double[p + 1];
                    double saved = 0.0;
                    double temp;
                    N[0] = 1.0;

                    for (int j = 1; j <= p; j++)
                    {
                        l[j] = u - U[i + 1 - j];
```

```
                r[j] = U[i + j] - u;
                saved = 0.0;
                for (int k = 0; k < j; k++)
                {
                    temp = N[k] / (r[k + 1] + l[k + 1]);
                    N[k] = saved + r[k + 1] * temp;
                    saved = l[j - k] * temp;
                }
                N[j] = saved;
            }
            return N;
        }
```

Find Span (interval) Function

```
        public int findSpan(int p, double u, double[] U)
        {
            int span = 0;
            int count = 0;
            int n = U.Length - p - 1;
            if (Math.Abs(u - U[n + 1]) < 0.0000001) return n - 1;

            double lo = p; double hi = n + 1; int mid =
(int)Math.Floor((0.5 * (lo + hi)));

            do
            {
                if (u < U[mid]) hi = mid;
                else lo = mid;
                mid = (int)Math.Floor((0.5 * (lo + hi)));
                count++;
            } while (u < U[mid] || u >= U[mid + 1]);

            span = mid;
            return span;
        }
```

Rational B-Spline Function

```
        public double ratBSpline(double u, int p, double[] U, double[]
w, double[] x)
        {
            double xCurve = 0.0;
            int n = p + 1;

            int s = findSpan(p, u, U);

            double[] N;
            N = basisFun(s, u, p, U);
            int m = x.Length;
            double[] Nn = new double[m];

            double b = 0.0;

            for (int i = 0; i < n; i++) Nn[s - p + i] = N[i];
            for (int i = 0; i < m; i++) b += Nn[i] * w[i];
            for (int i = 0; i < m; i++) xCurve += Nn[i] * w[i] / b *
x[i];
```

```
                return xCurve;
            }
```

Get Uniform/Non-Uniform Knot Vector Function

```
        public double[] getKnotVector(int n, int p)
            {
                double[] U = new double[2 * (p + 1) + n - p];
                for (int i = U.Length - p - 1; i < U.Length; i++) U[i] =
1.0;
                int midKnots = n - p;
                if (p < n)
                    for (int i = 0; i < midKnots; i++) U[p + 1 + i] =
((double)(i + 1) / ((double)n + 1.0 - (double)p));
                return U;
            }
```

Appendix B – NTHX-001 Stress Analysis

The stress analysis carried entailed evaluating the stress and elastic deformation when submitted to a static uniform internal pressure (6.0MPa) with fixed end supports and no additional loads (Figure 122). The main assumption is isotropic behavior, i.e. the properties are independent to stress direction.

The objective is to evaluate whether the maximum VonMises (equation 94) stress falls within the elastic region, and if so, how far is it from achieving the yield stress. The factor of safety (equation 95) is then defined as the ratio between yield stress and maximum VonMises stress.

The present analysis is performed in ANSYS Mechanic®.

Figure 122. Stress analysis problem setup.

$$\sigma_{VonMises} = \sqrt{\frac{1}{2}\left[\left(\sigma_{11}-\sigma_{22}\right)^2 + \left(\sigma_{22}-\sigma_{33}\right)^2 + \left(\sigma_{33}-\sigma_{11}\right)^2 + 6\left(\sigma_{12}^2+\sigma_{23}^2+\sigma_{31}^2\right)\right]} \quad (94)$$

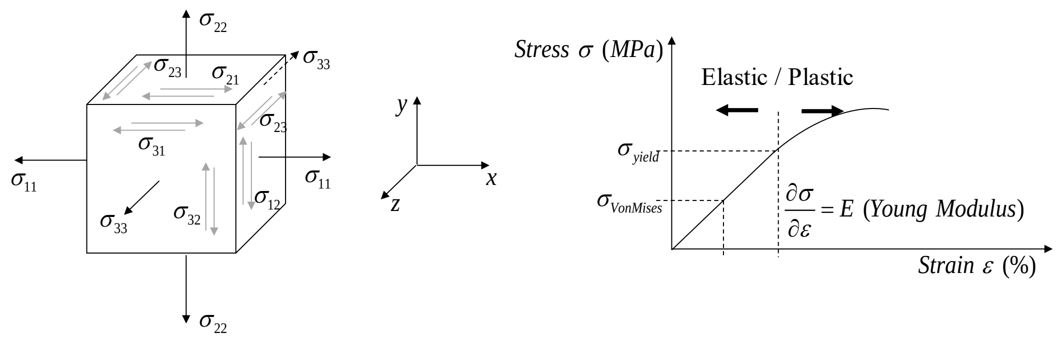

Figure 123. Isotropic stress components and stress-strain engineering curve.

$$FOS = \frac{\sigma_{Yield}}{\sigma_{VonMises,Max}} \quad (95)$$

The analysis described above was performed for the NTHX-001 (Figure 124) header and tube separately. For the latter two alternate inner shapes were studied; the first was a simple ellipse with a minimum distance from the outer shape of 0.3mm. The second was a B-Spline ensuring constant thickness of 0.3mm.

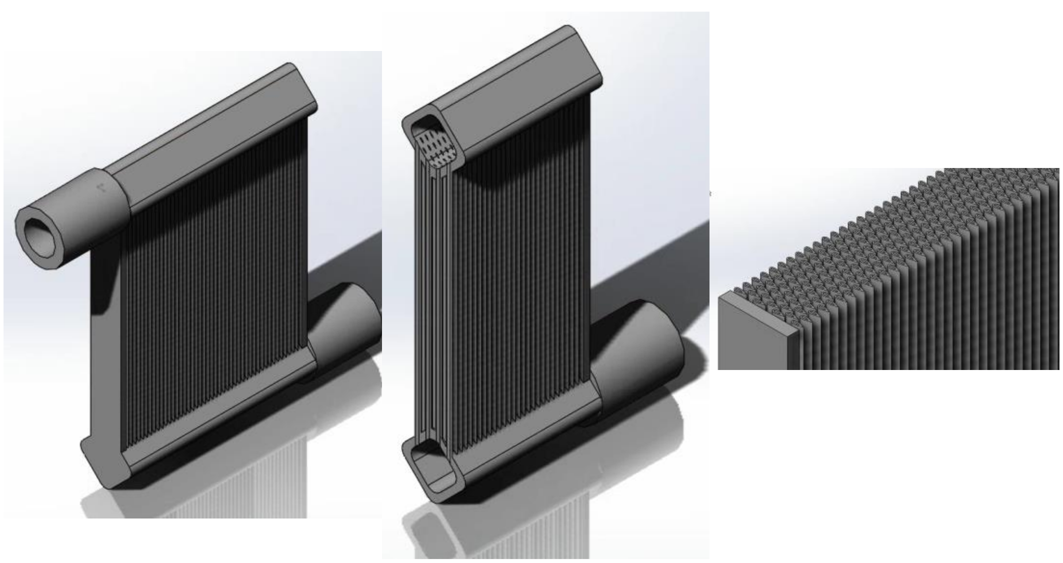

Figure 124. NTHX-001 Cut views.

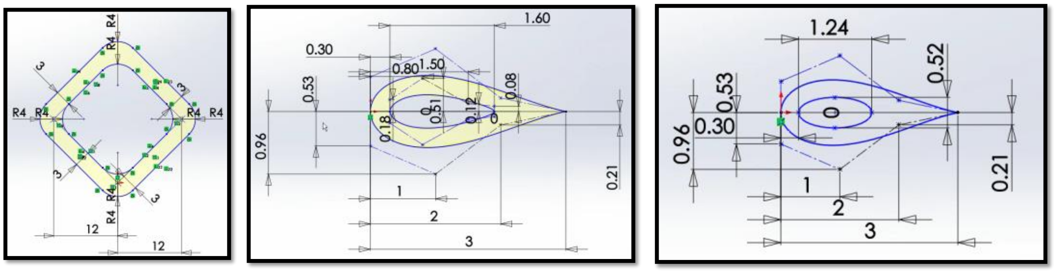

Figure 125. NTHX-001 Header and tubes cross sections.

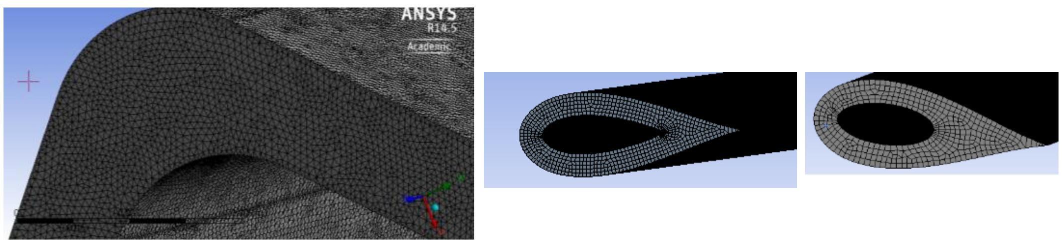

Figure 126. NTHX-001 Header and tube meshes.

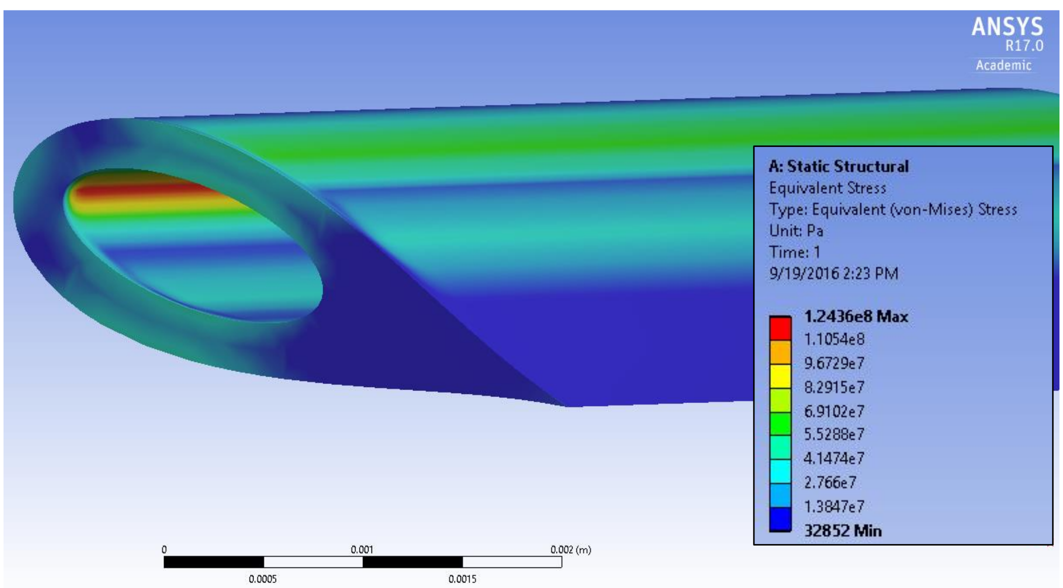

Figure 127. VonMises stress contour plots for the NTHX-001 tube.

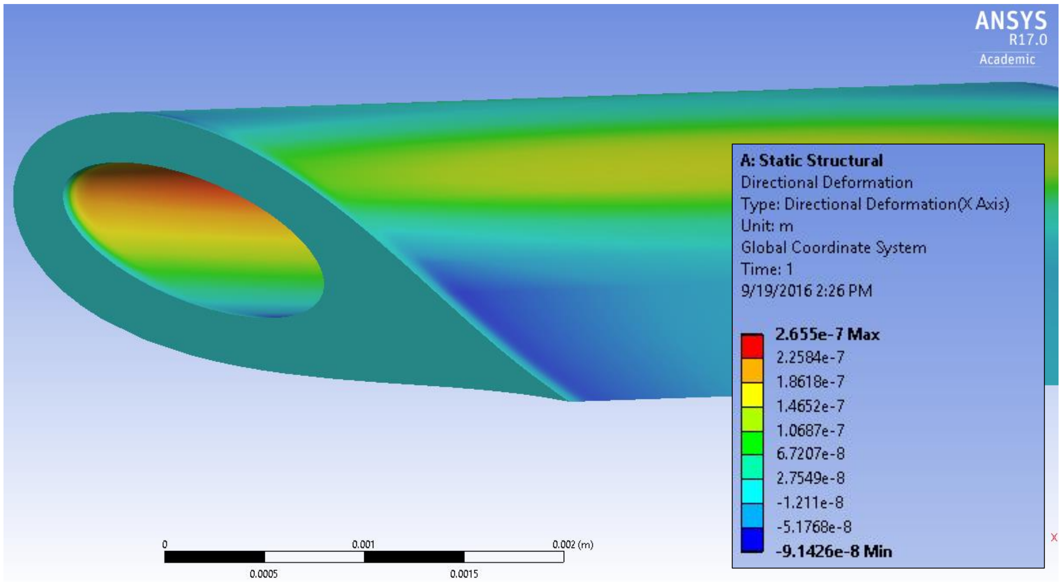

Figure 128. Deformation contour plots for the NTHX-001 tube.

Table 28. Material yield strength (SolidWorks® database).

Yield Strength	MPa
Stainless Steel (304)	207
Copper (99.9%)	70
Aluminum (1060)	27
Titanium (Grade 2)	78
Titanium (Grade 5)	206

Table 29. NTHX-001 Stress analysis results.

		Unit	Header	Tube (Ellipse)	Tube (B-Spline)
Simulation Results	Max. deformation	μm	2.63	0.22	0.53
	Max. Strain	%	0.07	0.04	0.08
	Max. VonMises	MPa	125.7	76.4	150.4
FOS (-)	Stainless Steel (304)	-	1.65	2.71	1.38
	Copper (99.9%)	-	0.56	0.92	0.47
	Aluminum (1060)	-	0.21	0.35	0.18
	Titanium (Grade 2)	-	0.62	1.02	0.52
	Titanium (Grade 5)	-	1.64	2.69	1.37

<u>*RTHX*</u>

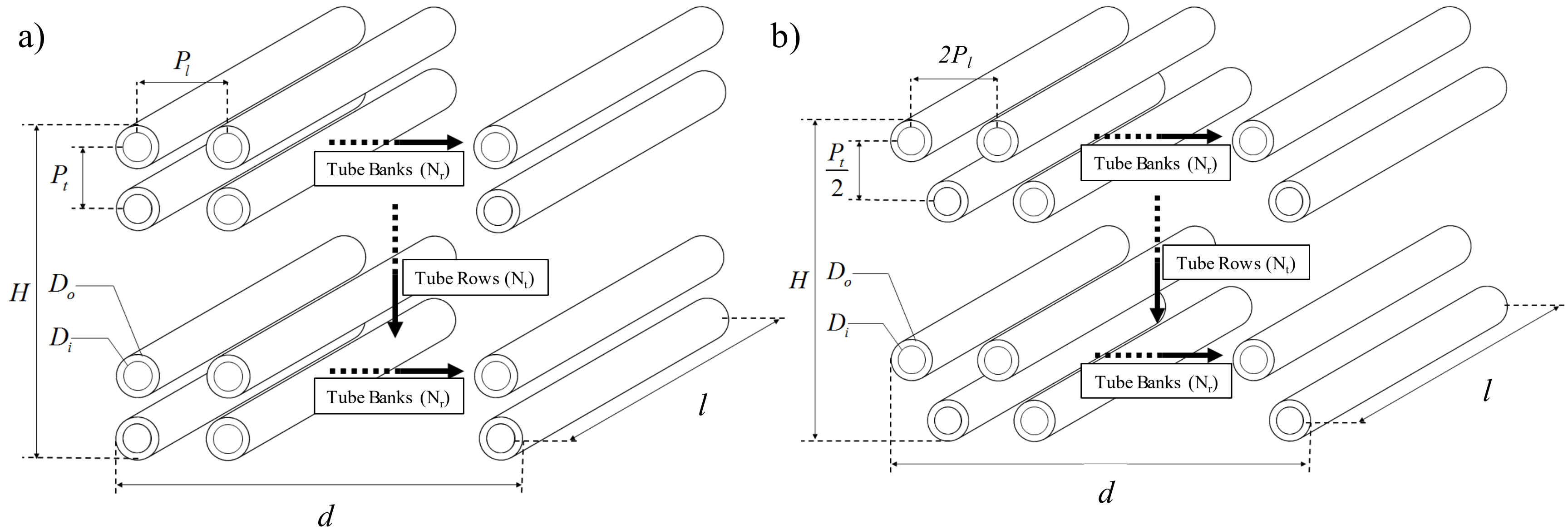

Figure 129. Round finless tubes (BTHX): a) in-line; b) staggered.

Table 30. Optimum RTHX dimensions.

Design Tag	Arrangement	Slabs	D_o	D_i	P_l	P_t	N_r	N_t	Pass Config.	l	H	d	A_f	V	$V_{mat'l}$
	-	-	mm	mm	mm	mm	-	-	%	m	m	m	m^2	cm^3	cm^3
RTHX-001	Staggered	1	0.7920	0.5940	1.1903	1.2379	4	121	100	0.1524	0.1486	0.0048	0.0226	107.81	15.77
RTHX-002	Staggered	1	0.7919	0.5939	1.1901	1.1983	4	101	100	0.1777	0.1198	0.0048	0.0213	101.36	15.31

Design Tag	Arrangement	Slabs	D_o	D_i	P_l	P_t	N_r	N_t	Pass Config.	l	H	d	A_f	V	$V_{mat'l}$
	-	-	mm	mm	mm	mm	-	-	%	m	m	m	m^2	cm^3	cm^3
RTHX-003	Staggered	1	0.7928	0.5946	1.1916	1.1997	4	101	100	0.1777	0.1200	0.0048	0.0213	101.60	15.35
RTHX-004	Staggered	1	0.7936	0.5952	1.1927	1.2008	4	101	100	0.1777	0.1201	0.0048	0.0213	101.79	15.38
RTHX-005	Staggered	1	0.7928	0.5946	1.1916	1.2020	4	101	100	0.1777	0.1202	0.0048	0.0214	101.80	15.35
RTHX-006	Staggered	1	0.7928	0.5946	1.1916	1.2044	4	101	100	0.1777	0.1204	0.0048	0.0214	102.00	15.35
RTHX-007	Staggered	1	0.7916	0.5937	1.1944	1.2049	4	101	100	0.1777	0.1205	0.0048	0.0214	102.28	15.30
RTHX-008	Staggered	1	0.7916	0.5937	1.2037	1.2049	4	101	100	0.1777	0.1205	0.0048	0.0214	103.08	15.30
RTHX-009	Staggered	1	0.7928	0.5946	1.1916	1.2020	4	101	100	0.1803	0.1202	0.0048	0.0217	103.32	15.58
RTHX-010	Staggered	1	0.7922	0.5941	1.1906	1.2243	4	186	100	0.0959	0.2265	0.0048	0.0217	103.47	15.31
RTHX-011	Staggered	1	0.7922	0.5942	1.1907	1.2244	4	186	100	0.0959	0.2265	0.0048	0.0217	103.48	15.31
RTHX-012	Staggered	1	0.7916	0.5937	1.1920	1.2396	4	196	100	0.0919	0.2417	0.0048	0.0222	105.97	15.44
RTHX-013	Staggered	1	0.7916	0.5937	1.1944	1.2396	4	196	100	0.0919	0.2417	0.0048	0.0222	106.17	15.44
RTHX-014	Staggered	1	0.7916	0.5937	1.1943	1.2396	4	196	100	0.0933	0.2417	0.0048	0.0225	107.70	15.66
RTHX-015	Staggered	1	0.7916	0.5937	1.1944	1.2396	4	196	100	0.0933	0.2417	0.0048	0.0225	107.71	15.66
RTHX-016	Staggered	1	0.7919	0.5939	1.1902	1.2378	4	121	100	0.1524	0.1485	0.0048	0.0226	107.79	15.77
RTHX-017	Staggered	1	0.7916	0.5937	1.1943	1.2419	4	196	100	0.0933	0.2422	0.0048	0.0226	107.90	15.66
RTHX-018	Staggered	1	0.7916	0.5937	1.1874	1.2501	4	191	100	0.0959	0.2375	0.0047	0.0228	108.21	15.70
RTHX-019	Staggered	1	0.7916	0.5937	1.1874	1.2501	4	196	100	0.0946	0.2438	0.0047	0.0231	109.52	15.89
RTHX-020	Staggered	1	0.7916	0.5937	1.1874	1.2512	4	196	100	0.0946	0.2440	0.0047	0.0231	109.62	15.89
RTHX-021	Staggered	1	0.7916	0.5937	1.1874	1.2513	4	196	100	0.0946	0.2440	0.0047	0.0231	109.63	15.89
RTHX-022	Staggered	1	0.7922	0.5942	1.1906	1.2522	4	196	100	0.0946	0.2442	0.0048	0.0231	110.01	15.91
RTHX-023	Staggered	1	0.7922	0.5942	1.1907	1.2523	4	196	100	0.0946	0.2442	0.0048	0.0231	110.02	15.91
RTHX-024	Staggered	1	0.7922	0.5942	1.1883	1.2522	4	181	100	0.1032	0.2254	0.0048	0.0233	110.61	16.03
RTHX-025	Staggered	1	0.7908	0.5931	1.1896	1.2534	4	181	100	0.1032	0.2256	0.0048	0.0233	110.83	15.97
RTHX-026	Staggered	1	0.7916	0.5937	1.1897	1.2570	4	181	100	0.1032	0.2263	0.0048	0.0234	111.15	16.00
RTHX-027	Staggered	1	0.7916	0.5937	1.1897	1.2570	4	181	100	0.1032	0.2263	0.0048	0.0234	111.16	16.00
RTHX-028	Staggered	1	0.7917	0.5938	1.1898	1.2572	4	181	100	0.1032	0.2263	0.0048	0.0234	111.19	16.01
RTHX-029	Staggered	1	0.7917	0.5938	1.1899	1.2572	4	181	100	0.1032	0.2263	0.0048	0.0234	111.19	16.01
RTHX-030	Staggered	1	0.7922	0.5942	1.1907	1.2580	4	181	100	0.1032	0.2264	0.0048	0.0234	111.34	16.03
RTHX-031	Staggered	1	0.7923	0.5943	1.1908	1.2582	4	181	100	0.1032	0.2265	0.0048	0.0234	111.37	16.03
RTHX-032	Staggered	1	0.7910	0.5932	1.1888	1.2572	4	106	100	0.1777	0.1320	0.0048	0.0235	111.53	16.04
RTHX-033	Staggered	1	0.7910	0.5932	1.1888	1.2572	4	106	100	0.1777	0.1320	0.0048	0.0235	111.54	16.04
RTHX-034	Staggered	1	0.7916	0.5937	1.1897	1.2593	4	181	100	0.1039	0.2267	0.0048	0.0236	112.07	16.11
RTHX-035	Staggered	1	0.7967	0.5975	1.1974	1.2675	4	181	100	0.1032	0.2281	0.0048	0.0236	112.80	16.21
RTHX-036	Staggered	1	0.7973	0.5979	1.1994	1.2684	4	181	100	0.1032	0.2283	0.0048	0.0236	113.07	16.23
RTHX-037	Staggered	1	0.7922	0.5942	1.1907	1.2743	4	181	100	0.1039	0.2294	0.0048	0.0238	113.50	16.13
RTHX-038	Staggered	1	0.7923	0.5942	1.1908	1.2745	4	181	100	0.1039	0.2294	0.0048	0.0238	113.53	16.14
RTHX-039	Staggered	1	0.7924	0.5943	1.1910	1.2746	4	181	100	0.1039	0.2294	0.0048	0.0238	113.56	16.14
RTHX-040	Staggered	1	0.7924	0.5943	1.2003	1.2746	4	181	100	0.1039	0.2294	0.0048	0.0238	114.45	16.14
RTHX-041	Staggered	1	0.7925	0.5944	1.2003	1.2747	4	181	100	0.1039	0.2294	0.0048	0.0238	114.46	16.14
RTHX-042	Staggered	1	0.7925	0.5943	1.2015	1.2747	4	181	100	0.1039	0.2294	0.0048	0.0238	114.57	16.14
RTHX-043	Staggered	1	0.7958	0.5968	1.2042	1.2800	4	196	100	0.0959	0.2496	0.0048	0.0239	115.33	16.28
RTHX-044	Staggered	1	0.7958	0.5969	1.2065	1.2801	4	196	100	0.0959	0.2496	0.0048	0.0239	115.56	16.28
RTHX-045	Staggered	1	0.7925	0.5943	1.1910	1.2735	4	181	100	0.1059	0.2292	0.0048	0.0243	115.65	16.45
RTHX-046	Staggered	1	0.7913	0.5934	1.1892	1.2785	4	181	100	0.1059	0.2301	0.0048	0.0244	115.92	16.40

Design Tag	Arrangement	Slabs	D_o	D_i	P_l	P_t	N_r	N_t	Pass Config.	l	H	d	A_f	V	$V_{mat'l}$
	-	-	mm	mm	mm	mm	-	-	%	m	m	m	m^2	cm^3	cm^3
RTHX-047	Staggered	1	0.7916	0.5937	1.1897	1.2791	4	181	100	0.1059	0.2302	0.0048	0.0244	116.03	16.42
RTHX-048	Staggered	1	0.7919	0.5939	1.1902	1.2796	4	181	100	0.1059	0.2303	0.0048	0.0244	116.12	16.43
RTHX-049	Staggered	1	0.7925	0.5943	1.1910	1.2805	4	181	100	0.1059	0.2305	0.0048	0.0244	116.28	16.45
RTHX-050	Staggered	1	0.7925	0.5944	1.1910	1.2794	4	186	100	0.1039	0.2367	0.0048	0.0246	117.16	16.59
RTHX-051	Staggered	1	0.7950	0.5962	1.1948	1.2846	4	186	100	0.1032	0.2376	0.0048	0.0245	117.25	16.59
RTHX-052	Staggered	1	0.7950	0.5962	1.1948	1.2834	4	186	100	0.1039	0.2374	0.0048	0.0247	117.89	16.70
RTHX-053	Staggered	1	0.7950	0.5962	1.1948	1.2834	4	186	100	0.1039	0.2374	0.0048	0.0247	117.90	16.70
RTHX-054	Staggered	1	0.7922	0.5941	1.1906	1.2731	4	191	100	0.1032	0.2419	0.0048	0.0250	118.92	16.92
RTHX-055	Staggered	1	0.7922	0.5941	1.1906	1.2754	4	191	100	0.1032	0.2423	0.0048	0.0250	119.14	16.92
RTHX-056	Staggered	1	0.7925	0.5944	1.1922	1.2759	4	191	100	0.1032	0.2424	0.0048	0.0250	119.34	16.93
RTHX-057	Staggered	1	0.7922	0.5942	1.1907	1.2790	4	191	100	0.1032	0.2430	0.0048	0.0251	119.48	16.92
RTHX-058	Staggered	1	0.7925	0.5944	1.1922	1.2794	4	191	100	0.1032	0.2431	0.0048	0.0251	119.67	16.93
RTHX-059	Staggered	1	0.7922	0.5942	1.1907	1.2790	4	186	100	0.1066	0.2366	0.0048	0.0252	120.08	17.01
RTHX-060	Staggered	1	0.7924	0.5943	1.1909	1.2792	4	186	100	0.1066	0.2367	0.0048	0.0252	120.13	17.01
RTHX-061	Staggered	1	0.7924	0.5943	1.1909	1.2792	4	186	100	0.1066	0.2367	0.0048	0.0252	120.13	17.01
RTHX-062	Staggered	1	0.7916	0.5937	1.1897	1.2790	4	191	100	0.1039	0.2430	0.0048	0.0252	120.15	17.00
RTHX-063	Staggered	1	0.7917	0.5938	1.1898	1.2792	4	191	100	0.1039	0.2431	0.0048	0.0253	120.19	17.01
RTHX-064	Staggered	1	0.7972	0.5979	1.1982	1.2882	4	191	100	0.1032	0.2448	0.0048	0.0253	121.10	17.13
RTHX-065	Staggered	1	0.7973	0.5979	1.1982	1.2882	4	191	100	0.1032	0.2448	0.0048	0.0253	121.11	17.14
RTHX-066	Staggered	1	0.7974	0.5981	1.1985	1.2885	4	191	100	0.1032	0.2448	0.0048	0.0253	121.16	17.14
RTHX-067	Staggered	1	0.7910	0.5932	1.1888	1.3001	4	191	100	0.1032	0.2470	0.0048	0.0255	121.26	16.87
RTHX-068	Staggered	1	0.7920	0.5940	1.1903	1.3018	4	191	100	0.1032	0.2473	0.0048	0.0255	121.57	16.91
RTHX-069	Staggered	1	0.7922	0.5941	1.1906	1.3021	4	191	100	0.1032	0.2474	0.0048	0.0255	121.64	16.92
RTHX-070	Staggered	1	0.7917	0.5938	1.1898	1.3048	4	191	100	0.1032	0.2479	0.0048	0.0256	121.81	16.90
RTHX-071	Staggered	1	0.7916	0.5937	1.1909	1.3047	4	191	100	0.1032	0.2479	0.0048	0.0256	121.91	16.89
RTHX-072	Staggered	1	0.7922	0.5941	1.1906	1.3056	4	191	100	0.1032	0.2481	0.0048	0.0256	121.96	16.92
RTHX-073	Staggered	1	0.7919	0.5939	1.1914	1.3052	4	191	100	0.1032	0.2480	0.0048	0.0256	122.00	16.91
RTHX-074	Staggered	1	0.7916	0.5937	1.1909	1.3046	4	186	100	0.1066	0.2414	0.0048	0.0257	122.51	16.98
RTHX-075	Staggered	1	0.7917	0.5938	1.1898	1.3048	4	191	100	0.1039	0.2479	0.0048	0.0258	122.59	17.01
RTHX-076	Staggered	1	0.7922	0.5941	1.1906	1.3056	4	191	100	0.1039	0.2481	0.0048	0.0258	122.75	17.03
RTHX-077	Staggered	1	0.7922	0.5942	1.1906	1.3056	4	191	100	0.1039	0.2481	0.0048	0.0258	122.75	17.03
RTHX-078	Staggered	1	0.7973	0.5979	1.1982	1.3139	4	191	100	0.1032	0.2497	0.0048	0.0258	123.53	17.14
RTHX-079	Staggered	1	0.7973	0.5979	1.1994	1.3139	4	191	100	0.1032	0.2497	0.0048	0.0258	123.65	17.14
RTHX-080	Staggered	1	0.7965	0.5973	1.1970	1.3115	4	191	100	0.1039	0.2492	0.0048	0.0259	123.96	17.21
RTHX-081	Staggered	1	0.7972	0.5979	1.1993	1.3139	4	191	100	0.1039	0.2496	0.0048	0.0259	124.43	17.24
RTHX-082	Staggered	1	0.7902	0.5926	1.1876	1.3012	4	196	100	0.1032	0.2537	0.0048	0.0262	124.43	17.28
RTHX-083	Staggered	1	0.7916	0.5937	1.1897	1.3034	4	196	100	0.1032	0.2542	0.0048	0.0262	124.87	17.34
RTHX-084	Staggered	1	0.7918	0.5938	1.1900	1.3038	4	196	100	0.1032	0.2542	0.0048	0.0262	124.94	17.35
RTHX-085	Staggered	1	0.7917	0.5938	1.1898	1.3048	4	191	100	0.1059	0.2479	0.0048	0.0263	124.94	17.33
RTHX-086	Staggered	1	0.7922	0.5942	1.1918	1.3057	4	196	100	0.1032	0.2546	0.0048	0.0263	125.31	17.37
RTHX-087	Staggered	1	0.7922	0.5942	1.1919	1.3150	4	196	100	0.1032	0.2564	0.0048	0.0265	126.20	17.37
RTHX-088	Staggered	1	0.7916	0.5937	1.1909	1.3290	4	196	100	0.1032	0.2592	0.0048	0.0268	127.45	17.34
RTHX-089	Staggered	1	0.7917	0.5937	1.2003	1.3291	4	196	100	0.1032	0.2592	0.0048	0.0268	128.46	17.34
RTHX-090	Staggered	1	0.7958	0.5969	1.1972	1.3361	4	196	100	0.1032	0.2605	0.0048	0.0269	128.80	17.52

Design Tag	Arrangement	Slabs	D_o	D_i	P_l	P_t	N_r	N_t	Pass Config.	l	H	d	A_f	V	$V_{mat'l}$
	-	-	mm	mm	mm	mm	-	-	%	m	m	m	m^2	cm^3	cm^3
RTHX-091	Staggered	1	0.7971	0.5979	1.1992	1.3383	4	196	100	0.1032	0.2610	0.0048	0.0269	129.23	17.58
RTHX-092	Staggered	1	0.7964	0.5973	1.2074	1.3370	4	196	100	0.1032	0.2607	0.0048	0.0269	129.99	17.55
RTHX-093	Staggered	1	0.7971	0.5979	1.2086	1.3383	4	196	100	0.1032	0.2610	0.0048	0.0269	130.24	17.58
RTHX-094	Staggered	1	0.7922	0.5942	1.1907	1.3417	4	196	100	0.1052	0.2616	0.0048	0.0275	131.12	17.70
RTHX-095	Staggered	1	0.7922	0.5942	1.1907	1.3428	4	196	100	0.1059	0.2619	0.0048	0.0277	132.06	17.81
RTHX-096	Staggered	1	0.7920	0.5940	1.1950	1.3425	4	196	100	0.1059	0.2618	0.0048	0.0277	132.51	17.80
RTHX-097	Staggered	1	0.7920	0.5940	1.1996	1.3424	4	196	100	0.1059	0.2618	0.0048	0.0277	133.02	17.80
RTHX-098	Staggered	1	0.7923	0.5942	1.2094	1.3430	4	196	100	0.1059	0.2619	0.0048	0.0277	134.16	17.82
RTHX-099	Staggered	1	0.7920	0.5940	1.2136	1.3425	4	196	100	0.1059	0.2618	0.0049	0.0277	134.57	17.80
RTHX-100	Staggered	1	0.7922	0.5941	1.1906	1.3428	4	206	100	0.1032	0.2753	0.0048	0.0284	135.34	18.25
RTHX-101	Staggered	1	0.7923	0.5942	1.1908	1.3418	4	201	100	0.1066	0.2684	0.0048	0.0286	136.22	18.39
RTHX-102	Staggered	1	0.7950	0.5962	1.1948	1.3475	4	206	100	0.1032	0.2762	0.0048	0.0285	136.29	18.38
RTHX-103	Staggered	1	0.7923	0.5942	1.1908	1.3430	4	201	100	0.1066	0.2686	0.0048	0.0286	136.33	18.39
RTHX-104	Staggered	1	0.7938	0.5953	1.1930	1.3501	4	206	100	0.1039	0.2768	0.0048	0.0288	137.23	18.45
RTHX-105	Staggered	1	0.7916	0.5937	1.1909	1.3615	4	206	100	0.1032	0.2791	0.0048	0.0288	137.26	18.23
RTHX-106	Staggered	1	0.7922	0.5941	1.1906	1.3637	4	206	100	0.1032	0.2796	0.0048	0.0289	137.44	18.25
RTHX-107	Staggered	1	0.7922	0.5942	1.1907	1.3637	4	206	100	0.1032	0.2796	0.0048	0.0289	137.46	18.26
RTHX-108	Staggered	1	0.7910	0.5932	1.1888	1.3709	4	206	100	0.1032	0.2810	0.0048	0.0290	137.96	18.20
RTHX-109	Staggered	1	0.7911	0.5934	1.1890	1.3711	4	206	100	0.1032	0.2811	0.0048	0.0290	138.01	18.21
RTHX-110	Staggered	1	0.7916	0.5937	1.1909	1.3720	4	206	100	0.1032	0.2813	0.0048	0.0290	138.32	18.23
RTHX-111	Staggered	1	0.7922	0.5942	1.1907	1.3730	4	206	100	0.1032	0.2815	0.0048	0.0291	138.39	18.26
RTHX-112	Staggered	1	0.7922	0.5941	1.1953	1.3730	4	206	100	0.1032	0.2815	0.0048	0.0291	138.92	18.25
RTHX-113	Staggered	1	0.7924	0.5943	1.1909	1.3733	4	116	100	0.1890	0.1579	0.0048	0.0298	142.18	18.76
RTHX-114	Staggered	1	0.7919	0.5939	1.1901	1.3840	4	116	100	0.1890	0.1592	0.0048	0.0301	143.20	18.73
RTHX-115	Staggered	1	0.7920	0.5940	1.1904	1.3843	4	116	100	0.1890	0.1592	0.0048	0.0301	143.25	18.74
RTHX-116	Staggered	1	0.7922	0.5942	1.1906	1.3846	4	116	100	0.1890	0.1592	0.0048	0.0301	143.32	18.75
RTHX-117	Staggered	1	0.7930	0.5948	1.1919	1.3861	4	116	100	0.1890	0.1594	0.0048	0.0301	143.61	18.79
RTHX-118	Staggered	1	0.7922	0.5941	1.1906	1.3846	4	116	100	0.1916	0.1592	0.0048	0.0305	145.32	19.01
RTHX-119	Staggered	1	0.7922	0.5942	1.1906	1.3846	4	116	100	0.1916	0.1592	0.0048	0.0305	145.33	19.01
RTHX-120	Staggered	1	0.7922	0.5942	1.1907	1.3847	4	116	100	0.1916	0.1592	0.0048	0.0305	145.35	19.01
RTHX-121	Staggered	1	0.7922	0.5942	1.1918	1.3846	4	116	100	0.1916	0.1592	0.0048	0.0305	145.47	19.01
RTHX-122	Staggered	1	0.7916	0.5937	1.1898	1.3882	4	116	100	0.1930	0.1596	0.0048	0.0308	146.61	19.11
RTHX-123	Staggered	1	0.7925	0.5943	1.1910	1.3897	4	116	100	0.1930	0.1598	0.0048	0.0308	146.93	19.15
RTHX-124	Staggered	1	0.7922	0.5941	1.1906	1.4020	4	116	100	0.1916	0.1612	0.0048	0.0309	147.15	19.01
RTHX-125	Staggered	1	0.7919	0.5939	1.1901	1.4073	4	116	100	0.1916	0.1618	0.0048	0.0310	147.65	18.99
RTHX-126	Staggered	1	0.7913	0.5935	1.1893	1.4063	4	216	100	0.1059	0.3023	0.0048	0.0320	152.31	19.59
RTHX-127	Staggered	1	0.7916	0.5937	1.1898	1.4068	4	216	100	0.1059	0.3025	0.0048	0.0320	152.43	19.61
RTHX-128	Staggered	1	0.7913	0.5935	1.1892	1.4108	4	216	100	0.1059	0.3033	0.0048	0.0321	152.80	19.59
RTHX-129	Staggered	1	0.7916	0.5937	1.1897	1.4114	4	216	100	0.1059	0.3034	0.0048	0.0321	152.92	19.61
RTHX-130	Staggered	1	0.7916	0.5937	1.1897	1.4160	4	216	100	0.1059	0.3044	0.0048	0.0322	153.42	19.61
RTHX-131	Staggered	1	0.7916	0.5937	1.1897	1.4218	4	216	100	0.1059	0.3057	0.0048	0.0324	154.05	19.61
RTHX-132	Staggered	1	0.7916	0.5937	1.1898	1.4219	4	216	100	0.1059	0.3057	0.0048	0.0324	154.06	19.61
RTHX-133	Staggered	1	0.7916	0.5937	1.1898	1.4231	4	216	100	0.1059	0.3060	0.0048	0.0324	154.19	19.61
RTHX-134	Staggered	1	0.7916	0.5937	1.1898	1.4277	4	216	100	0.1059	0.3070	0.0048	0.0325	154.69	19.61

Design Tag	Arrangement	Slabs	D_o	D_i	P_l	P_t	N_r	N_t	Pass Config.	l	H	d	A_f	V	$V_{mat'l}$
	-	-	mm	mm	mm	mm	-	-	%	m	m	m	m^2	cm^3	cm^3
RTHX-135	Staggered	1	0.7923	0.5943	1.1908	1.4290	4	216	100	0.1059	0.3072	0.0048	0.0325	154.97	19.65
RTHX-136	Staggered	1	0.7913	0.5934	1.1938	1.4270	4	216	100	0.1059	0.3068	0.0048	0.0325	155.15	19.59
RTHX-137	Staggered	1	0.7916	0.5937	1.1909	1.4253	4	111	100	0.2083	0.1568	0.0048	0.0327	155.54	19.73
RTHX-138	Staggered	1	0.7940	0.5955	1.1933	1.4319	4	216	100	0.1059	0.3079	0.0048	0.0326	155.61	19.73
RTHX-139	Staggered	1	0.7938	0.5953	1.1976	1.4316	4	216	100	0.1059	0.3078	0.0048	0.0326	156.14	19.72
RTHX-140	Staggered	1	0.7939	0.5955	1.1944	1.4296	4	111	100	0.2083	0.1573	0.0048	0.0327	156.47	19.85
RTHX-141	Staggered	1	0.7966	0.5975	1.1973	1.4367	4	216	100	0.1059	0.3089	0.0048	0.0327	156.65	19.86
RTHX-142	Staggered	1	0.7910	0.5932	1.1888	1.4265	4	221	100	0.1059	0.3138	0.0048	0.0332	158.03	20.03
RTHX-143	Staggered	1	0.7915	0.5936	1.1895	1.4274	4	221	100	0.1059	0.3140	0.0048	0.0333	158.23	20.06
RTHX-144	Staggered	1	0.7916	0.5937	1.1909	1.4253	4	111	100	0.2136	0.1568	0.0048	0.0335	159.51	20.23
RTHX-145	Staggered	1	0.7920	0.5940	1.1903	1.4261	4	111	100	0.2136	0.1569	0.0048	0.0335	159.52	20.25
RTHX-146	Staggered	1	0.7920	0.5940	1.1915	1.4261	4	111	100	0.2136	0.1569	0.0048	0.0335	159.67	20.25
RTHX-147	Staggered	1	0.7920	0.5940	1.1915	1.4261	4	111	100	0.2136	0.1569	0.0048	0.0335	159.68	20.26
RTHX-148	Staggered	1	0.7923	0.5943	1.1920	1.4267	4	111	100	0.2136	0.1569	0.0048	0.0335	159.81	20.27
RTHX-149	Staggered	1	0.7928	0.5946	1.1927	1.4276	4	111	100	0.2136	0.1570	0.0048	0.0335	160.01	20.30
RTHX-150	Staggered	1	0.7916	0.5937	1.1897	1.4532	4	221	100	0.1059	0.3197	0.0048	0.0339	161.10	20.06
RTHX-151	Staggered	1	0.7948	0.5961	1.1946	1.4592	4	221	100	0.1059	0.3210	0.0048	0.0340	162.44	20.23
RTHX-152	Staggered	1	0.7916	0.5937	1.1897	1.4566	4	221	100	0.1066	0.3205	0.0048	0.0341	162.50	20.19
RTHX-153	Staggered	1	0.7916	0.5937	1.1897	1.4717	4	221	100	0.1059	0.3238	0.0048	0.0343	163.16	20.06
RTHX-154	Staggered	1	0.7916	0.5937	1.1897	1.4717	4	221	100	0.1059	0.3238	0.0048	0.0343	163.16	20.06
RTHX-155	Staggered	1	0.7916	0.5937	1.1898	1.4753	4	221	100	0.1059	0.3246	0.0048	0.0344	163.57	20.07
RTHX-156	Staggered	1	0.7922	0.5941	1.1906	1.4764	4	221	100	0.1059	0.3248	0.0048	0.0344	163.80	20.09
RTHX-157	Staggered	1	0.7916	0.5937	1.1897	1.4752	4	221	100	0.1066	0.3245	0.0048	0.0346	164.57	20.19
RTHX-158	Staggered	1	0.7924	0.5943	1.1886	1.4814	4	221	100	0.1066	0.3259	0.0048	0.0347	165.12	20.23
RTHX-159	Staggered	1	0.7920	0.5940	1.1891	1.4794	4	176	100	0.1358	0.2589	0.0048	0.0352	167.24	20.49
RTHX-160	Staggered	1	0.7904	0.5928	1.1948	1.4810	4	226	100	0.1059	0.3332	0.0048	0.0353	168.65	20.46
RTHX-161	Staggered	1	0.7913	0.5934	1.1892	1.4804	4	116	100	0.2089	0.1702	0.0048	0.0356	169.19	20.67
RTHX-162	Staggered	1	0.7909	0.5932	1.1887	1.4798	4	116	100	0.2103	0.1702	0.0048	0.0358	170.13	20.79
RTHX-163	Staggered	1	0.7913	0.5934	1.1892	1.4804	4	116	100	0.2103	0.1702	0.0048	0.0358	170.27	20.81
RTHX-164	Staggered	1	0.7934	0.5951	1.1925	1.4845	4	116	100	0.2103	0.1707	0.0048	0.0359	171.21	20.92
RTHX-165	Staggered	1	0.7934	0.5951	1.1925	1.4857	4	116	100	0.2103	0.1709	0.0048	0.0359	171.35	20.92
RTHX-166	Staggered	1	0.7958	0.5968	1.1960	1.4889	4	116	100	0.2103	0.1712	0.0048	0.0360	172.23	21.05
RTHX-167	Staggered	1	0.7918	0.5939	1.1878	1.4815	4	116	100	0.2129	0.1704	0.0048	0.0363	172.34	21.10
RTHX-168	Staggered	1	0.7918	0.5939	1.1901	1.4815	4	116	100	0.2129	0.1704	0.0048	0.0363	172.68	21.10
RTHX-169	Staggered	1	0.7928	0.5946	1.1915	1.4833	4	116	100	0.2129	0.1706	0.0048	0.0363	173.11	21.15
RTHX-170	Staggered	1	0.7928	0.5946	1.1916	1.4834	4	116	100	0.2129	0.1706	0.0048	0.0363	173.11	21.15
RTHX-171	Staggered	1	0.7909	0.5932	1.1887	1.4798	4	116	100	0.2142	0.1702	0.0048	0.0365	173.36	21.18
RTHX-172	Staggered	1	0.7916	0.5937	1.1898	1.4811	4	116	100	0.2142	0.1703	0.0048	0.0365	173.66	21.22
RTHX-173	Staggered	1	0.7924	0.5943	1.1910	1.4826	4	116	100	0.2142	0.1705	0.0048	0.0365	174.01	21.26
RTHX-174	Staggered	1	0.7940	0.5955	1.1933	1.4855	4	116	100	0.2142	0.1708	0.0048	0.0366	174.69	21.35
RTHX-175	Staggered	1	0.7946	0.5959	1.1942	1.4867	4	116	100	0.2142	0.1710	0.0048	0.0366	174.97	21.38
RTHX-176	Staggered	1	0.7948	0.5961	1.1946	1.4871	4	116	100	0.2142	0.1710	0.0048	0.0366	175.08	21.39
RTHX-177	Staggered	1	0.7939	0.5955	1.2026	1.4855	4	116	100	0.2142	0.1708	0.0048	0.0366	176.05	21.35
RTHX-178	Staggered	1	0.7940	0.5955	1.2026	1.4855	4	116	100	0.2142	0.1708	0.0048	0.0366	176.06	21.35

Design Tag	Arrangement	Slabs	D_o	D_i	P_l	P_t	N_r	N_t	Pass Config.	l	H	d	A_f	V	$V_{mat'l}$
	-	-	mm	mm	mm	mm	-	-	%	m	m	m	m^2	cm^3	cm^3
RTHX-179	Staggered	1	0.7940	0.5955	1.2026	1.4867	4	116	100	0.2142	0.1710	0.0048	0.0366	176.19	21.35
RTHX-180	Staggered	1	0.7946	0.5959	1.2035	1.4878	4	116	100	0.2142	0.1711	0.0048	0.0367	176.47	21.38
RTHX-181	Staggered	1	0.7904	0.5928	1.1960	1.4764	4	186	100	0.1358	0.2731	0.0048	0.0371	177.45	21.57
RTHX-182	Staggered	1	0.7928	0.5946	1.1916	1.4834	4	186	100	0.1358	0.2744	0.0048	0.0373	177.63	21.71
RTHX-183	Staggered	1	0.7930	0.5947	1.1918	1.4836	4	186	100	0.1358	0.2745	0.0048	0.0373	177.69	21.71
RTHX-184	Staggered	1	0.7931	0.5948	1.1920	1.4839	4	186	100	0.1358	0.2745	0.0048	0.0373	177.76	21.72
RTHX-185	Staggered	1	0.7908	0.5931	1.1886	1.4796	4	116	100	0.2209	0.1702	0.0048	0.0376	178.69	21.84
RTHX-186	Staggered	1	0.7911	0.5934	1.1890	1.4802	4	116	100	0.2209	0.1702	0.0048	0.0376	178.83	21.85
RTHX-187	Staggered	1	0.7928	0.5946	1.1915	1.4833	4	116	100	0.2209	0.1706	0.0048	0.0377	179.59	21.95
RTHX-188	Staggered	1	0.7900	0.5925	1.1943	1.4781	4	186	100	0.1385	0.2734	0.0048	0.0379	180.87	21.97
RTHX-189	Staggered	1	0.7903	0.5927	1.1948	1.4787	4	186	100	0.1385	0.2736	0.0048	0.0379	181.02	21.99
RTHX-190	Staggered	1	0.7904	0.5928	1.1948	1.4787	4	186	100	0.1385	0.2736	0.0048	0.0379	181.03	21.99
RTHX-191	Staggered	1	0.7916	0.5937	1.1897	1.4810	4	121	100	0.2142	0.1777	0.0048	0.0381	181.19	22.14
RTHX-192	Staggered	1	0.7923	0.5943	1.1908	1.4825	4	116	100	0.2235	0.1705	0.0048	0.0381	181.54	22.18
RTHX-193	Staggered	1	0.7925	0.5943	1.1922	1.4827	4	121	100	0.2142	0.1779	0.0048	0.0381	181.78	22.19
RTHX-194	Staggered	1	0.7938	0.5954	1.1930	1.4852	4	121	100	0.2142	0.1782	0.0048	0.0382	182.22	22.27
RTHX-195	Staggered	1	0.7924	0.5943	1.1909	1.4825	4	191	100	0.1365	0.2817	0.0048	0.0384	183.12	22.38
RTHX-196	Staggered	1	0.8021	0.6016	1.2055	1.5007	4	121	100	0.2136	0.1801	0.0048	0.0385	185.46	22.66
RTHX-197	Staggered	1	0.8024	0.6018	1.2059	1.5012	4	121	100	0.2136	0.1801	0.0048	0.0385	185.58	22.68
RTHX-198	Staggered	1	0.8024	0.6018	1.2060	1.5013	4	121	100	0.2136	0.1802	0.0048	0.0385	185.62	22.68
RTHX-199	Staggered	1	0.8021	0.6016	1.2126	1.5007	4	121	100	0.2136	0.1801	0.0049	0.0385	186.55	22.66
RTHX-200	Staggered	1	0.7911	0.5934	1.1890	1.4802	4	121	100	0.2209	0.1776	0.0048	0.0392	186.60	22.80
RTHX-201	Staggered	1	0.7928	0.5946	1.1916	1.4834	4	196	100	0.1358	0.2893	0.0048	0.0393	187.23	22.88
RTHX-202	Staggered	1	0.7922	0.5941	1.1906	1.4798	4	116	100	0.2315	0.1702	0.0048	0.0394	187.65	22.97
RTHX-203	Staggered	1	0.7922	0.5941	1.1906	1.4810	4	116	100	0.2315	0.1703	0.0048	0.0394	187.79	22.97
RTHX-204	Staggered	1	0.7922	0.5942	1.1907	1.4822	4	196	100	0.1365	0.2890	0.0048	0.0394	187.86	22.96
RTHX-205	Staggered	1	0.7922	0.5941	1.1906	1.4822	4	116	100	0.2315	0.1704	0.0048	0.0395	187.94	22.97
RTHX-206	Staggered	1	0.7938	0.5953	1.1930	1.4851	4	196	100	0.1365	0.2896	0.0048	0.0395	188.60	23.05
RTHX-207	Staggered	1	0.7938	0.5953	1.1930	1.4839	4	196	100	0.1371	0.2894	0.0048	0.0397	189.36	23.16
RTHX-208	Staggered	1	0.7916	0.5937	1.1967	1.4810	4	196	100	0.1371	0.2888	0.0048	0.0396	189.57	23.03
RTHX-209	Staggered	1	0.7916	0.5937	1.1967	1.4811	4	196	100	0.1371	0.2888	0.0048	0.0396	189.58	23.03
RTHX-210	Staggered	1	0.7909	0.5932	1.1980	1.4798	4	126	100	0.2142	0.1850	0.0048	0.0396	189.91	23.03
RTHX-211	Staggered	1	0.7916	0.5937	1.1990	1.4811	4	126	100	0.2142	0.1851	0.0048	0.0397	190.24	23.07
RTHX-212	Staggered	1	0.7904	0.5928	1.1948	1.4787	4	196	100	0.1385	0.2884	0.0048	0.0399	190.82	23.18
RTHX-213	Staggered	1	0.7922	0.5942	1.1906	1.4822	4	186	100	0.1464	0.2742	0.0048	0.0402	191.24	23.37
RTHX-214	Staggered	1	0.6217	0.4663	0.9380	1.2616	4	246	100	0.1105	0.3091	0.0038	0.0342	128.21	14.39
RTHX-215	Staggered	1	0.6173	0.4630	0.9296	1.2265	4	251	100	0.1119	0.3066	0.0037	0.0343	127.55	14.65
RTHX-216	Staggered	1	0.6217	0.4663	0.9326	1.1732	4	241	100	0.1099	0.2816	0.0037	0.0309	115.41	14.01
RTHX-217	Staggered	1	0.6672	0.5004	1.0066	1.3754	4	246	100	0.1105	0.3370	0.0040	0.0373	149.99	16.57
RTHX-218	Staggered	1	0.6217	0.4663	0.9362	1.1450	4	236	100	0.1046	0.2691	0.0037	0.0281	105.36	13.05
RTHX-219	Staggered	1	0.6188	0.4641	0.9309	1.0579	4	246	100	0.0893	0.2592	0.0037	0.0231	86.16	11.51
RTHX-220	Staggered	1	0.6188	0.4641	0.9381	1.1532	4	251	100	0.0992	0.2883	0.0038	0.0286	107.37	13.06
RTHX-221	Staggered	1	0.6217	0.4663	0.9362	1.2671	4	246	100	0.1119	0.3104	0.0037	0.0347	130.06	14.56
RTHX-222	Staggered	1	0.6217	0.4663	0.9344	1.0857	4	246	100	0.0992	0.2660	0.0037	0.0264	98.67	12.92

Design Tag	Arrangement	Slabs	D_o	D_i	P_l	P_t	N_r	N_t	Pass Config.	l	H	d	A_f	V	$V_{mat'l}$
	-	-	mm	mm	mm	mm	-	-	%	m	m	m	m^2	cm^3	cm^3
RTHX-223	Staggered	1	0.6202	0.4652	0.9394	1.1159	4	231	100	0.1052	0.2567	0.0038	0.0270	101.49	12.80
RTHX-224	Staggered	1	0.6202	0.4652	0.9304	1.2587	4	246	100	0.1119	0.3084	0.0037	0.0345	128.39	14.49
RTHX-225	Staggered	1	0.6217	0.4663	0.9326	1.2671	4	246	100	0.1119	0.3104	0.0037	0.0347	129.55	14.56
RTHX-226	Staggered	1	0.6217	0.4663	0.9453	1.1212	4	231	100	0.1052	0.2579	0.0038	0.0271	102.61	12.86
RTHX-227	Staggered	1	0.6217	0.4663	0.9362	1.1477	4	236	100	0.1046	0.2697	0.0037	0.0282	105.61	13.05
RTHX-228	Staggered	1	0.6217	0.4663	0.9453	1.1194	4	231	100	0.1052	0.2575	0.0038	0.0271	102.45	12.86
RTHX-229	Staggered	1	0.5938	0.4454	0.8951	0.9543	4	231	100	0.0786	0.2195	0.0036	0.0173	61.80	8.77
RTHX-230	Staggered	1	0.5938	0.4454	0.8942	0.9883	4	231	100	0.0833	0.2273	0.0036	0.0189	67.72	9.29
RTHX-231	Staggered	1	0.6217	0.4663	0.9326	1.2024	4	251	100	0.1066	0.3006	0.0037	0.0320	119.48	14.15
RTHX-232	Staggered	1	0.6202	0.4652	0.9322	1.0868	4	236	100	0.0999	0.2554	0.0037	0.0255	95.14	12.41
RTHX-233	Staggered	1	0.6393	0.4795	0.9646	1.3180	4	246	100	0.1105	0.3229	0.0039	0.0357	137.72	15.21
RTHX-234	Staggered	1	0.6202	0.4652	0.9340	1.0831	4	246	100	0.0999	0.2654	0.0037	0.0265	99.05	12.94
RTHX-235	Staggered	1	0.6202	0.4652	0.9358	1.0868	4	241	100	0.0999	0.2608	0.0037	0.0261	97.55	12.68
RTHX-236	Staggered	1	0.6202	0.4652	0.9340	1.0868	4	246	100	0.0966	0.2663	0.0037	0.0257	96.08	12.51
RTHX-237	Staggered	1	0.6217	0.4663	0.9326	1.1796	4	241	100	0.1099	0.2831	0.0037	0.0311	116.04	14.01
RTHX-238	Staggered	1	0.5968	0.4476	0.8969	1.0037	4	246	100	0.0886	0.2459	0.0036	0.0218	78.17	10.63
RTHX-239	Staggered	1	0.6202	0.4652	0.9304	1.1768	4	241	100	0.1105	0.2824	0.0037	0.0312	116.19	14.03
RTHX-240	Staggered	1	0.5938	0.4454	0.8942	0.9953	4	231	100	0.0806	0.2289	0.0036	0.0185	66.02	8.99
RTHX-241	Staggered	1	0.6173	0.4630	0.9296	1.2292	4	251	100	0.1119	0.3073	0.0037	0.0344	127.83	14.65
RTHX-242	Staggered	1	0.6202	0.4652	0.9358	1.0868	4	246	100	0.0946	0.2663	0.0037	0.0252	94.28	12.25
RTHX-243	Staggered	1	0.5938	0.4454	0.8942	0.9865	4	236	100	0.0833	0.2318	0.0036	0.0193	69.07	9.49
RTHX-244	Staggered	1	0.5953	0.4465	0.8973	0.9977	4	236	100	0.0886	0.2345	0.0036	0.0208	74.57	10.14
RTHX-245	Staggered	1	0.6672	0.5004	1.0066	1.3754	4	241	100	0.1105	0.3301	0.0040	0.0365	146.93	16.23
RTHX-246	Staggered	1	0.6217	0.4663	0.9362	1.2088	4	246	100	0.1119	0.2961	0.0037	0.0331	124.07	14.56
RTHX-247	Staggered	1	0.6217	0.4663	0.9326	1.1440	4	236	100	0.1046	0.2688	0.0037	0.0281	104.86	13.05
RTHX-248	Staggered	1	0.5938	0.4454	0.8942	0.9822	4	246	100	0.0747	0.2406	0.0036	0.0180	64.26	8.87
RTHX-249	Staggered	1	0.5938	0.4454	0.8942	0.9987	4	246	100	0.0747	0.2447	0.0036	0.0183	65.34	8.87
RTHX-250	Staggered	1	0.5982	0.4487	0.8991	1.0061	4	231	100	0.0833	0.2314	0.0036	0.0193	69.32	9.42
RTHX-251	Staggered	1	0.6217	0.4663	0.9380	1.0893	4	236	100	0.1046	0.2560	0.0038	0.0268	100.44	13.05
RTHX-252	Staggered	1	0.6173	0.4630	0.9296	1.1649	4	241	100	0.1079	0.2796	0.0037	0.0302	112.16	13.56
RTHX-253	Staggered	1	0.5938	0.4454	0.8942	0.9317	4	231	100	0.0786	0.2143	0.0036	0.0169	60.28	8.77
RTHX-254	Staggered	1	0.6202	0.4652	0.9358	1.0868	4	246	100	0.0966	0.2663	0.0037	0.0257	96.27	12.51
RTHX-255	Staggered	1	0.6393	0.4795	0.9646	1.2973	4	246	100	0.1099	0.3178	0.0039	0.0349	134.75	15.12
RTHX-256	Staggered	1	0.5938	0.4454	0.8908	0.9857	4	236	100	0.0886	0.2316	0.0036	0.0205	73.13	10.09
RTHX-257	Staggered	1	0.6217	0.4663	0.9362	1.2088	4	251	100	0.1119	0.3022	0.0037	0.0338	126.60	14.86
RTHX-258	Staggered	1	0.5938	0.4454	0.8925	0.9987	4	246	100	0.0886	0.2447	0.0036	0.0217	77.41	10.52
RTHX-259	Staggered	1	0.5938	0.4454	0.8942	0.9987	4	241	100	0.0893	0.2397	0.0036	0.0214	76.54	10.39
RTHX-260	Staggered	1	0.5982	0.4487	0.8991	1.0061	4	246	100	0.0886	0.2465	0.0036	0.0218	78.56	10.68
RTHX-261	Staggered	1	0.5953	0.4465	0.8965	1.0160	4	246	100	0.0886	0.2489	0.0036	0.0221	79.10	10.57
RTHX-262	Staggered	1	0.5938	0.4454	0.8942	0.9317	4	231	100	0.0780	0.2143	0.0036	0.0167	59.77	8.69
RTHX-263	Staggered	1	0.6393	0.4795	0.9646	1.3330	4	246	100	0.1105	0.3266	0.0039	0.0361	139.29	15.21
RTHX-264	Staggered	1	0.5938	0.4454	0.8942	0.9953	4	246	100	0.0747	0.2438	0.0036	0.0182	65.11	8.87
RTHX-265	Staggered	1	0.6276	0.4707	0.9450	1.2202	4	241	100	0.1105	0.2928	0.0038	0.0324	122.37	14.36
RTHX-266	Staggered	1	0.6217	0.4663	0.9362	1.2088	4	241	100	0.1105	0.2901	0.0037	0.0321	120.10	14.09

Design Tag	Arrangement	Slabs	D_o	D_i	P_l	P_t	N_r	N_t	Pass Config.	l	H	d	A_f	V	$V_{mat'l}$
	-	-	mm	mm	mm	mm	-	-	%	m	m	m	m^2	cm^3	cm^3
RTHX-267	Staggered	1	0.5938	0.4454	0.8942	0.9874	4	236	100	0.0833	0.2320	0.0036	0.0193	69.14	9.49
RTHX-268	Staggered	1	0.5938	0.4454	0.8942	0.9874	4	231	100	0.0886	0.2271	0.0036	0.0201	71.98	9.88
RTHX-269	Staggered	1	0.6202	0.4652	0.9358	1.0868	4	231	100	0.0999	0.2500	0.0037	0.0250	93.48	12.15
RTHX-270	Staggered	1	0.6305	0.4729	0.9559	1.0779	4	246	100	0.0893	0.2641	0.0038	0.0236	90.15	11.95
RTHX-271	Staggered	1	0.6202	0.4652	0.9304	1.2514	4	251	100	0.1099	0.3128	0.0037	0.0344	127.93	14.52
RTHX-272	Staggered	1	0.5938	0.4454	0.8942	0.9987	4	241	100	0.0886	0.2397	0.0036	0.0212	75.97	10.31
RTHX-273	Staggered	1	0.6202	0.4652	0.9358	1.0604	4	231	100	0.0999	0.2439	0.0037	0.0244	91.21	12.15
RTHX-274	Staggered	1	0.6202	0.4652	0.9304	1.2587	4	251	100	0.1119	0.3147	0.0037	0.0352	131.01	14.79
RTHX-275	Staggered	1	0.6217	0.4663	0.9362	1.2088	4	246	100	0.1112	0.2961	0.0037	0.0329	123.34	14.47
RTHX-276	Staggered	1	0.6217	0.4663	0.9326	1.1732	4	241	100	0.1079	0.2816	0.0037	0.0304	113.32	13.76
RTHX-277	Staggered	1	0.6217	0.4663	0.9362	1.0629	4	246	100	0.0893	0.2604	0.0037	0.0232	87.06	11.62
RTHX-278	Staggered	1	0.5938	0.4454	0.8925	0.9987	4	246	100	0.0946	0.2447	0.0036	0.0231	82.63	11.23
RTHX-279	Staggered	1	0.6217	0.4663	0.9362	1.0629	4	236	100	0.0999	0.2498	0.0037	0.0250	93.46	12.47
RTHX-280	Staggered	1	0.6804	0.5103	1.0205	1.4186	4	246	100	0.1099	0.3475	0.0041	0.0382	155.89	17.13
RTHX-281	Staggered	1	0.6188	0.4641	0.9318	1.0543	4	236	100	0.0999	0.2478	0.0037	0.0248	92.26	12.36
RTHX-282	Staggered	1	0.6202	0.4652	0.9322	1.0831	4	246	100	0.0992	0.2654	0.0037	0.0263	98.20	12.86
RTHX-283	Staggered	1	0.6217	0.4663	0.9326	1.2024	4	246	100	0.1066	0.2946	0.0037	0.0314	117.09	13.87
RTHX-284	Staggered	1	0.6202	0.4652	0.9358	1.0831	4	246	100	0.0999	0.2654	0.0037	0.0265	99.25	12.94
RTHX-285	Staggered	1	0.6217	0.4663	0.9326	1.0456	4	246	100	0.0899	0.2562	0.0037	0.0230	85.94	11.71
RTHX-286	Staggered	1	0.5938	0.4454	0.8942	0.9813	4	231	100	0.0786	0.2257	0.0036	0.0177	63.49	8.77
RTHX-287	Staggered	1	0.5953	0.4465	0.8965	0.9977	4	231	100	0.0893	0.2295	0.0036	0.0205	73.46	10.00
RTHX-288	Staggered	1	0.6202	0.4652	0.9304	1.1768	4	241	100	0.1099	0.2824	0.0037	0.0310	115.49	13.94
RTHX-289	Staggered	1	0.5938	0.4454	0.8942	0.9813	4	231	100	0.0780	0.2257	0.0036	0.0176	62.95	8.69
RTHX-290	Staggered	1	0.5953	0.4465	0.8965	1.0012	4	241	100	0.0886	0.2403	0.0036	0.0213	76.35	10.36
RTHX-291	Staggered	1	0.5938	0.4454	0.8925	0.9317	4	231	100	0.0786	0.2143	0.0036	0.0169	60.16	8.77
RTHX-292	Staggered	1	0.6393	0.4795	0.9646	1.2964	4	246	100	0.1119	0.3176	0.0039	0.0355	137.10	15.40
RTHX-293	Staggered	1	0.6202	0.4652	0.9358	1.2587	4	246	100	0.1119	0.3084	0.0037	0.0345	129.14	14.49
RTHX-294	Staggered	1	0.5953	0.4465	0.8930	0.9977	4	246	100	0.0800	0.2444	0.0036	0.0195	69.82	9.54
RTHX-295	Staggered	1	0.6217	0.4663	0.9362	1.2024	4	241	100	0.1099	0.2886	0.0037	0.0317	118.74	14.01
RTHX-296	Staggered	1	0.6202	0.4652	0.9358	1.0868	4	246	100	0.0999	0.2663	0.0037	0.0266	99.58	12.94
RTHX-297	Staggered	1	0.5938	0.4454	0.8916	0.9857	4	231	100	0.0886	0.2267	0.0036	0.0201	71.65	9.88
RTHX-298	Staggered	1	0.5938	0.4454	0.8942	0.9326	4	231	100	0.0786	0.2145	0.0036	0.0169	60.34	8.77
RTHX-299	Staggered	1	0.5968	0.4476	0.8987	0.9870	4	231	100	0.0786	0.2270	0.0036	0.0179	64.18	8.85
RTHX-300	Staggered	1	0.5953	0.4465	0.8930	0.9977	4	231	100	0.0893	0.2295	0.0036	0.0205	73.17	10.00
RTHX-301	Staggered	1	0.5953	0.4465	0.8965	1.0012	4	236	100	0.0893	0.2353	0.0036	0.0210	75.32	10.22
RTHX-302	Staggered	1	0.5938	0.4454	0.8908	0.9822	4	236	100	0.0786	0.2308	0.0036	0.0182	64.67	8.96
RTHX-303	Staggered	1	0.6217	0.4663	0.9326	1.1468	4	241	100	0.1086	0.2752	0.0037	0.0299	111.45	13.84
RTHX-304	Staggered	1	0.6672	0.5004	1.0066	1.3754	4	246	100	0.1119	0.3370	0.0040	0.0377	151.79	16.77
RTHX-305	Staggered	1	0.5938	0.4454	0.8916	0.9987	4	246	100	0.0906	0.2447	0.0036	0.0222	79.07	10.76
RTHX-306	Staggered	1	0.5938	0.4454	0.8925	0.9839	4	231	100	0.0886	0.2263	0.0036	0.0201	71.59	9.88
RTHX-307	Staggered	1	0.5938	0.4454	0.8908	0.9874	4	231	100	0.0886	0.2271	0.0036	0.0201	71.70	9.88
RTHX-308	Staggered	1	0.5938	0.4454	0.8908	0.9874	4	241	100	0.0860	0.2370	0.0036	0.0204	72.58	10.00
RTHX-309	Staggered	1	0.5938	0.4454	0.8942	0.9317	4	231	100	0.0793	0.2143	0.0036	0.0170	60.79	8.84
RTHX-310	Staggered	1	0.6202	0.4652	0.9322	1.0868	4	241	100	0.0999	0.2608	0.0037	0.0261	97.17	12.68

Design Tag	Arrangement	Slabs	D_o	D_i	P_l	P_t	N_r	N_t	Pass Config.	l	H	d	A_f	V	$V_{mat'l}$
	-	-	mm	mm	mm	mm	-	-	%	m	m	m	m^2	cm^3	cm^3
RTHX-311	Staggered	1	0.6393	0.4795	0.9721	1.2973	4	246	100	0.1105	0.3178	0.0039	0.0351	136.62	15.21
RTHX-312	Staggered	1	0.6202	0.4652	0.9322	1.1995	4	251	100	0.1066	0.2999	0.0037	0.0320	119.15	14.09
RTHX-313	Staggered	1	0.5938	0.4454	0.8916	0.9953	4	231	100	0.0806	0.2289	0.0036	0.0185	65.83	8.99
RTHX-314	Staggered	1	0.5938	0.4454	0.8942	0.9953	4	246	100	0.0800	0.2438	0.0036	0.0195	69.75	9.50
RTHX-315	Staggered	1	0.5938	0.4454	0.8942	0.9874	4	231	100	0.0833	0.2271	0.0036	0.0189	67.66	9.29
RTHX-316	Staggered	1	0.5938	0.4454	0.8925	0.9865	4	236	100	0.0833	0.2318	0.0036	0.0193	68.94	9.49
RTHX-317	Staggered	1	0.6393	0.4795	0.9646	1.2973	4	246	100	0.1119	0.3178	0.0039	0.0356	137.20	15.40
RTHX-318	Staggered	1	0.6202	0.4652	0.9322	1.0431	4	246	100	0.0899	0.2556	0.0037	0.0230	85.71	11.65
RTHX-319	Staggered	1	0.5968	0.4476	0.9004	0.9590	4	231	100	0.0786	0.2206	0.0036	0.0173	62.48	8.85
RTHX-320	In-line	1	0.7999	0.5999	0.9599	1.0628	11	131	100	0.1422	0.1388	0.0092	0.0197	181.67	45.07
RTHX-321	In-line	1	0.7999	0.5999	0.9599	1.0628	11	113	100	0.1645	0.1200	0.0092	0.0197	181.67	44.98
RTHX-322	In-line	1	0.8000	0.6000	0.9621	1.0629	11	112	100	0.1634	0.1188	0.0092	0.0194	178.68	44.26
RTHX-323	In-line	1	0.7999	0.5999	0.9620	1.0627	11	165	100	0.1107	0.1752	0.0092	0.0194	178.66	44.20
RTHX-324	In-line	1	0.7999	0.5999	0.9620	1.0627	11	165	100	0.1107	0.1752	0.0092	0.0194	178.66	44.20
RTHX-325	In-line	1	0.7999	0.5999	0.9620	1.0627	11	165	100	0.1107	0.1752	0.0092	0.0194	178.66	44.20
RTHX-326	In-line	1	0.7999	0.5999	0.9599	1.0628	11	112	100	0.1614	0.1188	0.0092	0.0192	176.28	43.72
RTHX-327	In-line	1	0.7999	0.5999	0.9598	1.0627	11	129	100	0.1376	0.1376	0.0092	0.0189	174.10	42.93
RTHX-328	In-line	1	0.7999	0.5999	0.9598	1.0627	11	129	100	0.1374	0.1376	0.0092	0.0189	173.83	42.86
RTHX-329	In-line	1	0.7999	0.5999	0.9598	1.0627	11	129	100	0.1374	0.1376	0.0092	0.0189	173.83	42.86
RTHX-330	In-line	1	0.7999	0.5999	0.9620	1.0627	11	112	100	0.1584	0.1188	0.0092	0.0188	173.18	42.91
RTHX-331	In-line	1	0.7999	0.5999	0.9598	1.0452	11	114	100	0.1579	0.1191	0.0092	0.0188	173.03	43.55
RTHX-332	In-line	1	0.8000	0.6000	0.9688	1.0454	11	133	100	0.1346	0.1391	0.0092	0.0187	172.89	43.31
RTHX-333	In-line	1	0.8001	0.6001	0.9623	1.0456	11	113	100	0.1588	0.1179	0.0092	0.0187	172.45	43.41
RTHX-334	In-line	1	0.8001	0.6000	0.9601	1.0455	11	113	100	0.1569	0.1179	0.0092	0.0185	170.20	42.89
RTHX-335	In-line	1	0.8000	0.6000	0.9601	1.0455	11	114	100	0.1553	0.1192	0.0092	0.0185	170.20	42.81
RTHX-336	In-line	1	0.7999	0.6000	0.9599	1.0453	11	113	100	0.1569	0.1179	0.0092	0.0185	170.18	42.89
RTHX-337	In-line	1	0.7999	0.5999	0.9599	1.0453	11	114	100	0.1553	0.1191	0.0092	0.0185	170.18	42.82
RTHX-338	In-line	1	0.7999	0.5999	0.9599	1.0453	11	114	100	0.1553	0.1191	0.0092	0.0185	170.17	42.82
RTHX-339	In-line	1	0.7999	0.5999	0.9598	1.0452	11	113	100	0.1569	0.1179	0.0092	0.0185	170.16	42.90
RTHX-340	In-line	1	0.7999	0.5999	0.9599	1.0365	11	114	100	0.1554	0.1187	0.0092	0.0184	169.66	42.85
RTHX-341	In-line	1	0.8000	0.6000	0.9621	1.0366	11	115	100	0.1549	0.1187	0.0092	0.0184	169.32	43.10
RTHX-342	In-line	1	0.7999	0.5999	0.9621	1.0365	11	114	100	0.1549	0.1187	0.0092	0.0184	169.30	42.73
RTHX-343	In-line	1	0.7999	0.5999	0.9620	1.0365	11	167	100	0.1061	0.1733	0.0092	0.0184	169.29	42.87
RTHX-344	In-line	1	0.7999	0.5999	0.9621	1.0365	11	114	100	0.1540	0.1187	0.0092	0.0183	168.29	42.47
RTHX-345	In-line	1	0.8000	0.6000	0.9600	1.0125	11	158	100	0.1118	0.1605	0.0092	0.0179	164.96	42.71
RTHX-346	In-line	1	0.7999	0.5999	0.9599	1.0124	11	171	100	0.1038	0.1727	0.0092	0.0179	164.95	42.95
RTHX-347	In-line	1	0.7999	0.5999	0.9599	1.0124	11	171	100	0.1038	0.1727	0.0092	0.0179	164.95	42.95
RTHX-348	In-line	1	0.7999	0.5999	0.9621	1.0124	11	114	100	0.1557	0.1150	0.0092	0.0179	164.86	42.94
RTHX-349	In-line	1	0.7999	0.5999	0.9599	1.0124	11	152	100	0.1159	0.1543	0.0092	0.0179	164.47	42.61
RTHX-350	In-line	1	0.7999	0.5999	0.9598	1.0124	11	151	100	0.1168	0.1531	0.0092	0.0179	164.46	42.67
RTHX-351	In-line	1	0.8001	0.6001	0.9601	1.0127	11	152	100	0.1157	0.1543	0.0092	0.0179	164.27	42.53
RTHX-352	In-line	1	0.7999	0.5999	0.9599	1.0124	11	116	100	0.1520	0.1175	0.0092	0.0179	164.23	42.65
RTHX-353	In-line	1	0.7999	0.5999	0.9599	1.0124	11	152	100	0.1157	0.1543	0.0092	0.0179	164.23	42.55
RTHX-354	In-line	1	0.7999	0.5999	0.9599	1.0124	11	115	100	0.1536	0.1162	0.0092	0.0179	164.23	42.73

Design Tag	Arrangement	Slabs	D_o	D_i	P_l	P_t	N_r	N_t	Pass Config.	l	H	d	A_f	V	$V_{mat'l}$
	-	-	mm	mm	mm	mm	-	-	%	m	m	m	m^2	cm^3	cm^3
RTHX-355	In-line	1	0.7999	0.5999	0.9599	1.0125	11	115	100	0.1527	0.1162	0.0092	0.0178	163.29	42.48
RTHX-356	In-line	1	0.7999	0.5999	0.9599	1.0125	11	115	100	0.1527	0.1162	0.0092	0.0178	163.29	42.48
RTHX-357	In-line	1	0.7999	0.5999	0.9599	1.0124	11	115	100	0.1527	0.1162	0.0092	0.0178	163.28	42.48
RTHX-358	In-line	1	0.7999	0.5999	0.9598	1.0124	11	115	100	0.1527	0.1162	0.0092	0.0178	163.27	42.49
RTHX-359	In-line	1	0.7999	0.5999	0.9598	1.0124	11	115	100	0.1527	0.1162	0.0092	0.0178	163.27	42.49
RTHX-360	In-line	1	0.8000	0.6000	0.9600	0.9972	11	126	100	0.1415	0.1252	0.0092	0.0177	163.06	43.14
RTHX-361	In-line	1	0.7999	0.5999	0.9599	0.9971	11	126	100	0.1415	0.1252	0.0092	0.0177	163.04	43.14
RTHX-362	In-line	1	0.7999	0.5999	0.9599	0.9971	11	126	100	0.1416	0.1252	0.0092	0.0177	163.04	43.14
RTHX-363	In-line	1	0.7999	0.5999	0.9599	0.9971	11	126	100	0.1407	0.1252	0.0092	0.0176	162.11	42.90
RTHX-364	In-line	1	0.7999	0.5999	0.9643	0.9971	11	116	100	0.1522	0.1155	0.0092	0.0176	161.94	42.70
RTHX-365	In-line	1	0.7999	0.5999	0.9621	0.9971	11	117	100	0.1506	0.1167	0.0092	0.0176	161.79	42.63
RTHX-366	In-line	1	0.7999	0.5999	0.9599	0.9971	11	116	100	0.1518	0.1155	0.0092	0.0175	161.18	42.58
RTHX-367	In-line	1	0.7999	0.5999	0.9599	0.9971	11	116	100	0.1518	0.1155	0.0092	0.0175	161.18	42.58
RTHX-368	In-line	1	0.7999	0.5999	0.9599	0.9949	11	116	100	0.1519	0.1153	0.0092	0.0175	161.18	42.63
RTHX-369	In-line	1	0.7999	0.5999	0.9599	0.9949	11	116	100	0.1519	0.1153	0.0092	0.0175	161.18	42.63
RTHX-370	In-line	1	0.7999	0.5999	0.9599	0.9971	11	126	100	0.1393	0.1252	0.0092	0.0174	160.50	42.47
RTHX-371	In-line	1	0.7999	0.5999	0.9599	0.9949	11	117	100	0.1497	0.1166	0.0092	0.0174	160.49	42.36
RTHX-372	In-line	1	0.7999	0.5999	0.9599	0.9949	11	116	100	0.1513	0.1153	0.0092	0.0174	160.49	42.44
RTHX-373	In-line	1	0.7999	0.5999	0.9599	0.9949	11	116	100	0.1513	0.1153	0.0092	0.0174	160.49	42.44
RTHX-374	In-line	1	0.7999	0.5999	0.9621	0.9927	11	116	100	0.1512	0.1152	0.0092	0.0174	160.41	42.42
RTHX-375	In-line	1	0.7999	0.5999	0.9620	0.9927	11	134	100	0.1305	0.1335	0.0092	0.0174	160.40	42.31
RTHX-376	In-line	1	0.7999	0.5999	0.9620	0.9927	11	116	100	0.1512	0.1152	0.0092	0.0174	160.40	42.43
RTHX-377	In-line	1	0.7999	0.5999	0.9599	0.9840	11	155	100	0.1140	0.1524	0.0092	0.0174	159.81	42.75
RTHX-378	In-line	1	0.7999	0.5999	0.9643	0.9883	11	110	100	0.1584	0.1089	0.0092	0.0173	158.97	42.14
RTHX-379	In-line	1	0.7999	0.5999	0.9642	0.9883	11	110	100	0.1584	0.1089	0.0092	0.0173	158.97	42.14
RTHX-380	In-line	1	0.8000	0.6000	0.9622	0.9797	11	117	100	0.1505	0.1146	0.0092	0.0173	158.85	42.61
RTHX-381	In-line	1	0.7999	0.5999	0.9621	0.9796	11	118	100	0.1490	0.1158	0.0092	0.0173	158.83	42.53
RTHX-382	In-line	1	0.7999	0.5999	0.9620	0.9795	11	173	100	0.1021	0.1690	0.0092	0.0173	158.82	42.71
RTHX-383	In-line	1	0.7999	0.5999	0.9621	0.9796	11	127	100	0.1386	0.1243	0.0092	0.0172	158.62	42.59
RTHX-384	In-line	1	0.7999	0.5999	0.9599	0.9796	11	155	100	0.1129	0.1521	0.0092	0.0172	158.02	42.35
RTHX-385	In-line	1	0.7999	0.5999	0.9598	0.9796	11	155	100	0.1129	0.1521	0.0092	0.0172	158.02	42.35
RTHX-386	In-line	1	0.7999	0.5999	0.9598	0.9795	11	173	100	0.1016	0.1690	0.0092	0.0172	158.02	42.53
RTHX-387	In-line	1	0.7999	0.5999	0.9620	0.9795	11	98	100	0.1779	0.0964	0.0092	0.0172	157.94	42.18
RTHX-388	In-line	1	0.7999	0.5999	0.9620	0.9795	11	117	100	0.1497	0.1146	0.0092	0.0172	157.94	42.38
RTHX-389	In-line	1	0.7999	0.5999	0.9620	0.9664	11	118	100	0.1506	0.1139	0.0092	0.0172	157.94	42.99
RTHX-390	Staggered	1	0.7921	0.5940	1.1939	1.4099	6	390	100	0.4599	0.5499	0.0072	0.2529	1811.36	236.65
RTHX-391	Staggered	1	0.7922	0.5941	1.1940	1.4101	6	390	100	0.4592	0.5499	0.0072	0.2525	1809.11	236.30
RTHX-392	Staggered	1	0.7921	0.5940	1.1939	1.4099	6	390	100	0.4592	0.5499	0.0072	0.2525	1808.67	236.30
RTHX-393	Staggered	1	0.7922	0.5941	1.1894	1.4101	6	390	100	0.4592	0.5499	0.0071	0.2525	1802.07	236.30
RTHX-394	Staggered	1	0.7921	0.5940	1.1892	1.4099	6	390	100	0.4592	0.5499	0.0071	0.2525	1801.63	236.30
RTHX-395	Staggered	1	0.7921	0.5940	1.1881	1.4099	6	390	100	0.4592	0.5499	0.0071	0.2525	1799.87	236.30
RTHX-396	Staggered	1	0.7922	0.5941	1.1894	1.4054	6	390	100	0.4592	0.5481	0.0071	0.2517	1796.14	236.30
RTHX-397	Staggered	1	0.7921	0.5940	1.1892	1.4053	6	390	100	0.4592	0.5480	0.0071	0.2517	1795.69	236.30
RTHX-398	Staggered	1	0.7922	0.5941	1.1894	1.4043	6	390	100	0.4592	0.5477	0.0071	0.2515	1794.65	236.30

Design Tag	Arrangement	Slabs	D_o	D_i	P_l	P_t	N_r	N_t	Pass Config.	l	H	d	A_f	V	$V_{mat'l}$
	-	-	mm	mm	mm	mm	-	-	%	m	m	m	m²	cm³	cm³
RTHX-399	Staggered	1	0.7920	0.5940	1.1892	1.4029	6	390	100	0.4592	0.5471	0.0071	0.2512	1792.64	236.30
RTHX-400	Staggered	1	0.7922	0.5941	1.1894	1.4043	6	390	100	0.4578	0.5477	0.0071	0.2507	1789.30	235.59
RTHX-401	Staggered	1	0.7997	0.5997	1.2007	1.4234	6	380	100	0.4517	0.5409	0.0072	0.2443	1759.98	226.46
RTHX-402	Staggered	1	0.7990	0.5993	1.1997	1.4223	6	380	100	0.4517	0.5405	0.0072	0.2441	1757.22	226.46
RTHX-403	Staggered	1	0.7950	0.5962	1.1936	1.4151	6	380	100	0.4544	0.5377	0.0072	0.2443	1749.92	227.83
RTHX-404	Staggered	1	0.7944	0.5958	1.1928	1.4141	6	380	100	0.4544	0.5374	0.0072	0.2442	1747.60	227.83
RTHX-405	Staggered	1	0.7944	0.5958	1.1928	1.4130	6	380	100	0.4537	0.5369	0.0072	0.2436	1743.53	227.49
RTHX-406	Staggered	1	0.7944	0.5958	1.1928	1.4141	6	380	100	0.4517	0.5374	0.0072	0.2427	1737.07	226.46
RTHX-407	Staggered	1	0.7950	0.5962	1.1983	1.4151	6	380	100	0.4489	0.5377	0.0072	0.2414	1735.59	225.09
RTHX-408	Staggered	1	0.7949	0.5962	1.1982	1.4150	6	380	100	0.4489	0.5377	0.0072	0.2414	1735.34	225.09
RTHX-409	Staggered	1	0.7949	0.5962	1.1982	1.4149	6	380	100	0.4489	0.5377	0.0072	0.2414	1735.25	225.09
RTHX-410	Staggered	1	0.7950	0.5962	1.1936	1.4151	6	380	100	0.4489	0.5377	0.0072	0.2414	1728.84	225.09
RTHX-411	Staggered	1	0.7950	0.5962	1.1924	1.4151	6	380	100	0.4489	0.5377	0.0072	0.2414	1727.15	225.09
RTHX-412	Staggered	1	0.7947	0.5960	1.1931	1.4145	6	380	100	0.4482	0.5375	0.0072	0.2409	1724.85	224.75
RTHX-413	Staggered	1	0.7944	0.5958	1.1928	1.4141	6	380	100	0.4482	0.5374	0.0072	0.2409	1723.91	224.75
RTHX-414	Staggered	1	0.7922	0.5941	1.1941	1.4101	6	380	100	0.4489	0.5358	0.0072	0.2406	1723.41	225.09
RTHX-415	Staggered	1	0.7922	0.5941	1.1883	1.4101	6	380	100	0.4489	0.5358	0.0071	0.2406	1715.03	225.09
RTHX-416	Staggered	1	0.7922	0.5941	1.1894	1.4101	6	380	100	0.4482	0.5358	0.0071	0.2402	1714.00	224.75
RTHX-417	Staggered	1	0.7920	0.5940	1.1892	1.4099	6	380	100	0.4482	0.5357	0.0071	0.2401	1713.49	224.75
RTHX-418	Staggered	1	0.7922	0.5941	1.1894	1.4101	6	380	100	0.4469	0.5358	0.0071	0.2394	1708.77	224.06
RTHX-419	Staggered	1	0.7915	0.5936	1.1884	1.4089	6	380	100	0.4462	0.5354	0.0071	0.2389	1703.37	223.72
RTHX-420	Staggered	1	0.7915	0.5936	1.1884	1.4089	6	380	100	0.4462	0.5354	0.0071	0.2389	1703.21	223.72
RTHX-421	Staggered	1	0.7915	0.5936	1.1872	1.4089	6	380	100	0.4462	0.5354	0.0071	0.2389	1701.54	223.72
RTHX-422	Staggered	1	0.7909	0.5932	1.1875	1.4078	6	380	100	0.4462	0.5350	0.0071	0.2387	1700.77	223.72
RTHX-423	Staggered	1	0.7909	0.5932	1.1875	1.4078	6	380	100	0.4462	0.5350	0.0071	0.2387	1700.68	223.72
RTHX-424	Staggered	1	0.7908	0.5931	1.1874	1.4077	6	380	100	0.4462	0.5349	0.0071	0.2387	1700.51	223.72
RTHX-425	Staggered	1	0.7915	0.5936	1.1884	1.4043	6	380	100	0.4469	0.5336	0.0071	0.2385	1700.45	224.06
RTHX-426	Staggered	1	0.7913	0.5934	1.1880	1.4038	6	380	100	0.4469	0.5335	0.0071	0.2384	1699.27	224.06
RTHX-427	Staggered	1	0.7921	0.5940	1.1881	1.4053	6	380	100	0.4462	0.5340	0.0071	0.2383	1698.45	223.72
RTHX-428	Staggered	1	0.7919	0.5939	1.1879	1.4050	6	380	100	0.4462	0.5339	0.0071	0.2382	1697.86	223.72
RTHX-429	Staggered	1	0.7915	0.5936	1.1884	1.4043	6	380	100	0.4462	0.5336	0.0071	0.2381	1697.76	223.72
RTHX-430	Staggered	1	0.7915	0.5936	1.1884	1.4042	6	380	100	0.4462	0.5336	0.0071	0.2381	1697.59	223.72
RTHX-431	Staggered	1	0.7914	0.5936	1.1883	1.4042	6	380	100	0.4462	0.5336	0.0071	0.2381	1697.51	223.72
RTHX-432	Staggered	1	0.7915	0.5936	1.1884	1.4042	6	380	100	0.4455	0.5336	0.0071	0.2377	1694.99	223.37
RTHX-433	Staggered	1	0.7914	0.5936	1.1883	1.4042	6	380	100	0.4455	0.5336	0.0071	0.2377	1694.91	223.37
RTHX-434	Staggered	1	0.7912	0.5934	1.1879	1.4037	6	380	100	0.4448	0.5334	0.0071	0.2373	1691.05	223.03
RTHX-435	Staggered	1	0.7909	0.5932	1.1875	1.4032	6	380	100	0.4448	0.5332	0.0071	0.2372	1690.05	223.03
RTHX-436	Staggered	1	0.7909	0.5932	1.1875	1.4032	6	380	100	0.4448	0.5332	0.0071	0.2372	1689.96	223.03
RTHX-437	Staggered	1	0.7908	0.5931	1.1874	1.4031	6	380	100	0.4448	0.5332	0.0071	0.2372	1689.71	223.03
RTHX-438	Staggered	1	0.7915	0.5936	1.1873	1.4031	6	380	100	0.4448	0.5332	0.0071	0.2372	1689.50	223.03
RTHX-439	Staggered	1	0.7909	0.5932	1.1875	1.4020	6	380	100	0.4448	0.5328	0.0071	0.2370	1688.57	223.03
RTHX-440	Staggered	1	0.7908	0.5931	1.1874	1.4019	6	380	100	0.4448	0.5327	0.0071	0.2370	1688.32	223.03
RTHX-441	Staggered	1	0.7908	0.5931	1.1874	1.4019	6	380	100	0.4448	0.5327	0.0071	0.2370	1688.23	223.03
RTHX-442	Staggered	1	0.7908	0.5931	1.1863	1.4019	6	380	100	0.4448	0.5327	0.0071	0.2370	1686.67	223.03

Design Tag	Arrangement	Slabs	D_o	D_i	P_l	P_t	N_r	N_t	Pass Config.	l	H	d	A_f	V	$V_{mat'l}$
	-	-	mm	mm	mm	mm	-	-	%	m	m	m	m^2	cm^3	cm^3
RTHX-443	Staggered	1	0.7903	0.5927	1.1865	1.4009	6	380	100	0.4448	0.5323	0.0071	0.2368	1685.81	223.03
RTHX-444	Staggered	1	0.7909	0.5932	1.1863	1.4020	6	380	100	0.4441	0.5328	0.0071	0.2366	1684.32	222.69
RTHX-445	Staggered	1	0.7909	0.5932	1.1863	1.4020	6	380	100	0.4441	0.5328	0.0071	0.2366	1684.24	222.69
RTHX-446	Staggered	1	0.7908	0.5931	1.1863	1.4019	6	380	100	0.4441	0.5327	0.0071	0.2366	1684.07	222.69
RTHX-447	Staggered	1	0.7906	0.5929	1.1859	1.4015	6	380	100	0.4441	0.5326	0.0071	0.2365	1682.91	222.69
RTHX-448	Staggered	1	0.7909	0.5932	1.1875	1.3986	6	380	100	0.4441	0.5315	0.0071	0.2360	1681.79	222.69
RTHX-449	Staggered	1	0.7906	0.5929	1.1870	1.3980	6	380	100	0.4441	0.5312	0.0071	0.2359	1680.37	222.69
RTHX-450	Staggered	1	0.7903	0.5927	1.1866	1.3975	6	380	100	0.4441	0.5310	0.0071	0.2359	1679.13	222.69
RTHX-451	Staggered	1	0.7902	0.5927	1.1865	1.3974	6	380	100	0.4441	0.5310	0.0071	0.2358	1678.96	222.69
RTHX-452	Staggered	1	0.7907	0.5930	1.1872	1.3959	6	380	100	0.4441	0.5304	0.0071	0.2356	1678.17	222.69
RTHX-453	Staggered	1	0.7909	0.5932	1.1875	1.3940	6	380	100	0.4441	0.5297	0.0071	0.2353	1676.29	222.69
RTHX-454	Staggered	1	0.7908	0.5931	1.1874	1.3938	6	380	100	0.4441	0.5297	0.0071	0.2352	1675.96	222.69
RTHX-455	Staggered	1	0.7914	0.5936	1.1871	1.3937	6	380	100	0.4441	0.5296	0.0071	0.2352	1675.41	222.69
RTHX-456	Staggered	1	0.7909	0.5932	1.1875	1.3928	6	380	100	0.4441	0.5293	0.0071	0.2351	1674.90	222.69
RTHX-457	Staggered	1	0.7909	0.5932	1.1875	1.3928	6	380	100	0.4441	0.5293	0.0071	0.2351	1674.81	222.69
RTHX-458	Staggered	1	0.7908	0.5931	1.1874	1.3927	6	380	100	0.4441	0.5292	0.0071	0.2350	1674.56	222.69
RTHX-459	Staggered	1	0.7907	0.5930	1.1872	1.3925	6	380	100	0.4441	0.5291	0.0071	0.2350	1674.07	222.69
RTHX-460	Staggered	1	0.7907	0.5930	1.1872	1.3924	6	380	100	0.4441	0.5291	0.0071	0.2350	1673.99	222.69
RTHX-461	Staggered	1	0.7921	0.5940	1.1881	1.3913	6	380	100	0.4441	0.5287	0.0071	0.2348	1673.87	222.69
RTHX-462	Staggered	1	0.7909	0.5932	1.1875	1.3893	6	380	100	0.4448	0.5279	0.0071	0.2348	1673.12	223.03
RTHX-463	Staggered	1	0.7909	0.5932	1.1863	1.3893	6	380	100	0.4448	0.5279	0.0071	0.2348	1671.49	223.03
RTHX-464	Staggered	1	0.7914	0.5936	1.1871	1.3902	6	380	100	0.4441	0.5283	0.0071	0.2346	1671.23	222.69
RTHX-465	Staggered	1	0.7909	0.5932	1.1864	1.3893	6	380	100	0.4441	0.5279	0.0071	0.2345	1669.08	222.69
RTHX-466	Staggered	1	0.7909	0.5932	1.1863	1.3893	6	380	100	0.4441	0.5279	0.0071	0.2345	1668.92	222.69
RTHX-467	Staggered	1	0.7909	0.5932	1.1863	1.3881	6	380	100	0.4441	0.5275	0.0071	0.2343	1667.60	222.69
RTHX-468	Staggered	1	0.7909	0.5932	1.1863	1.3881	6	380	100	0.4441	0.5275	0.0071	0.2343	1667.52	222.69
RTHX-469	Staggered	1	0.7901	0.5926	1.1852	1.3868	6	380	100	0.4441	0.5270	0.0071	0.2340	1664.31	222.69
RTHX-470	Staggered	1	0.7901	0.5926	1.1852	1.3856	6	380	100	0.4441	0.5265	0.0071	0.2338	1662.92	222.69
RTHX-471	Staggered	1	0.7915	0.5936	1.1872	1.3810	6	380	100	0.4441	0.5248	0.0071	0.2331	1660.23	222.69
RTHX-472	Staggered	1	0.7909	0.5932	1.1864	1.3800	6	380	100	0.4441	0.5244	0.0071	0.2329	1657.93	222.69
RTHX-473	Staggered	1	0.7907	0.5930	1.1872	1.3774	6	380	100	0.4441	0.5234	0.0071	0.2325	1655.87	222.69
RTHX-474	Staggered	1	0.7909	0.5932	1.1875	1.3754	6	380	100	0.4441	0.5226	0.0071	0.2321	1653.90	222.69
RTHX-475	Staggered	1	0.7908	0.5931	1.1874	1.3753	6	380	100	0.4441	0.5226	0.0071	0.2321	1653.65	222.69
RTHX-476	Staggered	1	0.7907	0.5931	1.1873	1.3751	6	380	100	0.4441	0.5225	0.0071	0.2321	1653.24	222.69
RTHX-477	Staggered	1	0.7907	0.5930	1.1872	1.3751	6	380	100	0.4441	0.5225	0.0071	0.2321	1653.16	222.69
RTHX-478	Staggered	1	0.7907	0.5930	1.1872	1.3750	6	380	100	0.4441	0.5225	0.0071	0.2321	1653.08	222.69
RTHX-479	Staggered	1	0.7915	0.5936	1.1872	1.3717	6	380	100	0.4448	0.5213	0.0071	0.2319	1651.61	223.03
RTHX-480	Staggered	1	0.7914	0.5936	1.1871	1.3717	6	380	100	0.4448	0.5212	0.0071	0.2319	1651.45	223.03
RTHX-481	Staggered	1	0.7909	0.5932	1.1875	1.3708	6	380	100	0.4448	0.5209	0.0071	0.2317	1650.94	223.03
RTHX-482	Staggered	1	0.7909	0.5932	1.1875	1.3707	6	380	100	0.4448	0.5209	0.0071	0.2317	1650.86	223.03
RTHX-483	Staggered	1	0.7909	0.5932	1.1863	1.3707	6	380	100	0.4448	0.5209	0.0071	0.2317	1649.24	223.03
RTHX-484	Staggered	1	0.7908	0.5931	1.1863	1.3706	6	380	100	0.4448	0.5208	0.0071	0.2317	1649.00	223.03
RTHX-485	Staggered	1	0.7914	0.5936	1.1871	1.3717	6	380	100	0.4441	0.5212	0.0071	0.2315	1648.91	222.69
RTHX-486	Staggered	1	0.7909	0.5931	1.1874	1.3707	6	380	100	0.4441	0.5209	0.0071	0.2313	1648.15	222.69

Design Tag	Arrangement	Slabs	D_o	D_i	P_l	P_t	N_r	N_t	Pass Config.	l	H	d	A_f	V	$V_{mat'l}$
	-	-	mm	mm	mm	mm	-	-	%	m	m	m	m^2	cm^3	cm^3
RTHX-487	Staggered	1	0.7908	0.5931	1.1874	1.3706	6	380	100	0.4441	0.5208	0.0071	0.2313	1647.99	222.69
RTHX-488	Staggered	1	0.7901	0.5926	1.1852	1.3694	6	380	100	0.4441	0.5204	0.0071	0.2311	1643.45	222.69
RTHX-489	Staggered	1	0.7909	0.5932	1.1863	1.3649	6	380	100	0.4448	0.5187	0.0071	0.2307	1642.27	223.03
RTHX-490	Staggered	1	0.7909	0.5932	1.1864	1.3650	6	380	100	0.4441	0.5187	0.0071	0.2304	1639.82	222.69
RTHX-491	Staggered	1	0.7909	0.5932	1.1863	1.3649	6	380	100	0.4441	0.5187	0.0071	0.2304	1639.66	222.69
RTHX-492	Staggered	1	0.7907	0.5931	1.1861	1.3647	6	380	100	0.4441	0.5186	0.0071	0.2303	1639.09	222.69
RTHX-493	Staggered	1	0.7903	0.5927	1.1854	1.3638	6	380	100	0.4441	0.5183	0.0071	0.2302	1637.07	222.69
RTHX-494	Staggered	1	0.7909	0.5931	1.1874	1.3614	6	380	100	0.4441	0.5173	0.0071	0.2298	1637.00	222.69
RTHX-495	Staggered	1	0.7908	0.5931	1.1874	1.3614	6	380	100	0.4441	0.5173	0.0071	0.2298	1636.92	222.69
RTHX-496	Staggered	1	0.7906	0.5929	1.1859	1.3609	6	380	100	0.4441	0.5171	0.0071	0.2297	1634.19	222.69
RTHX-497	Staggered	1	0.7915	0.5936	1.1872	1.3578	6	380	100	0.4441	0.5160	0.0071	0.2292	1632.33	222.69
RTHX-498	Staggered	1	0.7914	0.5936	1.1871	1.3577	6	380	100	0.4441	0.5159	0.0071	0.2291	1632.17	222.69
RTHX-499	Staggered	1	0.7909	0.5932	1.1864	1.3569	6	380	100	0.4441	0.5156	0.0071	0.2290	1630.07	222.69
RTHX-500	Staggered	1	0.7909	0.5932	1.1863	1.3568	6	380	100	0.4441	0.5156	0.0071	0.2290	1629.91	222.69
RTHX-501	Staggered	1	0.7915	0.5936	1.1872	1.3532	6	380	100	0.4448	0.5142	0.0071	0.2287	1629.25	223.03
RTHX-502	Staggered	1	0.7909	0.5932	1.1863	1.3522	6	380	100	0.4448	0.5138	0.0071	0.2286	1626.92	223.03
RTHX-503	Staggered	1	0.7908	0.5931	1.1863	1.3521	6	380	100	0.4448	0.5138	0.0071	0.2285	1626.68	223.03
RTHX-504	Staggered	1	0.7909	0.5932	1.1875	1.3522	6	380	100	0.4441	0.5138	0.0071	0.2282	1626.01	222.69
RTHX-505	Staggered	1	0.7909	0.5932	1.1863	1.3522	6	380	100	0.4441	0.5138	0.0071	0.2282	1624.42	222.69
RTHX-506	Staggered	1	0.7906	0.5929	1.1859	1.3516	6	380	100	0.4441	0.5136	0.0071	0.2281	1623.05	222.69
RTHX-507	Staggered	1	0.7905	0.5929	1.1857	1.3515	6	380	100	0.4441	0.5136	0.0071	0.2281	1622.73	222.69
RTHX-508	Staggered	1	0.7906	0.5929	1.1859	1.3493	6	380	100	0.4441	0.5127	0.0071	0.2277	1620.27	222.69
RTHX-509	Staggered	1	0.7906	0.5929	1.1859	1.3470	6	380	100	0.4441	0.5119	0.0071	0.2273	1617.48	222.69
RTHX-510	Staggered	1	0.7915	0.5936	1.1884	1.3439	6	380	100	0.4441	0.5107	0.0071	0.2268	1617.17	222.69
RTHX-511	Staggered	1	0.7915	0.5936	1.1872	1.3439	6	380	100	0.4441	0.5107	0.0071	0.2268	1615.59	222.69
RTHX-512	Staggered	1	0.7909	0.5932	1.1875	1.3429	6	380	100	0.4441	0.5103	0.0071	0.2266	1614.85	222.69
RTHX-513	Staggered	1	0.7909	0.5932	1.1863	1.3429	6	380	100	0.4441	0.5103	0.0071	0.2266	1613.27	222.69
RTHX-514	Staggered	1	0.7909	0.5932	1.1863	1.3429	6	380	100	0.4441	0.5103	0.0071	0.2266	1613.19	222.69
RTHX-515	Staggered	1	0.7909	0.5932	1.1864	1.3406	6	380	100	0.4441	0.5094	0.0071	0.2263	1610.57	222.69
RTHX-516	Staggered	1	0.7909	0.5932	1.1863	1.3383	6	380	100	0.4448	0.5085	0.0071	0.2262	1610.18	223.03
RTHX-517	Staggered	1	0.7908	0.5931	1.1863	1.3382	6	380	100	0.4448	0.5085	0.0071	0.2262	1609.94	223.03
RTHX-518	Staggered	1	0.7909	0.5932	1.1863	1.3382	6	380	100	0.4441	0.5085	0.0071	0.2259	1607.62	222.69
RTHX-519	Staggered	1	0.7493	0.5620	1.7461	2.4639	11	478	67/5/28	1.6647	1.1785	0.0182	1.9618	35724.23	1688.45
RTHX-520	Staggered	1	0.7493	0.5620	1.7276	2.4639	11	471	67/5/28	1.6894	1.1612	0.0180	1.9618	35362.15	1688.44
RTHX-521	Staggered	1	0.7478	0.5609	1.7263	2.4590	11	478	67/22/11	1.6679	1.1762	0.0180	1.9618	35333.10	1685.15
RTHX-522	Staggered	1	0.7463	0.5598	1.7229	2.4542	11	477	66/17/17	1.6747	1.1714	0.0180	1.9618	35263.82	1681.84
RTHX-523	Staggered	1	0.7287	0.5466	1.6823	2.3964	11	478	67/22/11	1.7116	1.1462	0.0176	1.9618	34432.45	1642.19
RTHX-524	Staggered	1	0.7229	0.5422	1.6589	2.3771	11	471	67/5/28	1.7511	1.1203	0.0173	1.9618	33961.26	1628.96
RTHX-525	Staggered	1	0.6994	0.5246	1.6146	2.2999	11	474	61/23/16	1.7984	1.0909	0.0168	1.9618	33046.84	1576.10
RTHX-526	Staggered	1	0.7331	0.5499	1.5821	2.4108	11	477	66/17/17	1.7049	1.1507	0.0166	1.9618	32475.19	1652.10
RTHX-527	Staggered	1	0.7331	0.5499	1.5781	2.4108	11	477	66/17/17	1.7049	1.1507	0.0165	1.9618	32396.46	1652.10
RTHX-528	Staggered	1	0.7302	0.5477	1.5558	2.4072	11	477	66/23/11	1.7074	1.1490	0.0163	1.9618	31953.20	1641.40
RTHX-529	Staggered	1	0.7126	0.5345	1.5202	2.3433	11	477	66/17/17	1.7540	1.1185	0.0159	1.9618	31221.51	1605.85
RTHX-530	Staggered	1	0.7111	0.5334	1.5152	2.3385	11	471	84/8/8	1.7800	1.1021	0.0159	1.9618	31119.08	1602.53

Design Tag	Arrangement	Slabs	D_o	D_i	P_l	P_t	N_r	N_t	Pass Config.	l	H	d	A_f	V	$V_{mat'l}$
	-	-	mm	mm	mm	mm	-	-	%	m	m	m	m^2	cm^3	cm^3
RTHX-531	Staggered	1	0.7126	0.5345	1.5124	2.3297	11	478	67/20/13	1.7605	1.1143	0.0158	1.9618	31068.46	1615.25
RTHX-532	Staggered	1	0.7126	0.5345	1.5124	2.3297	11	477	22/47/31	1.7642	1.1120	0.0158	1.9618	31068.46	1615.25
RTHX-533	Staggered	1	0.7302	0.5477	1.4858	2.4012	11	477	66/17/17	1.7117	1.1461	0.0156	1.9618	30580.92	1645.50
RTHX-534	Staggered	1	0.7126	0.5345	1.4500	2.3433	11	477	66/23/11	1.7540	1.1185	0.0152	1.9618	29844.03	1605.85
RTHX-535	Staggered	1	0.7229	0.5422	1.4313	2.3850	11	471	84/8/8	1.7453	1.1241	0.0150	1.9618	29497.59	1623.56
RTHX-536	Staggered	1	0.7009	0.5257	1.4261	2.3048	11	478	67/29/4	1.7796	1.1024	0.0150	1.9618	29352.77	1579.41
RTHX-537	Staggered	1	0.7229	0.5422	1.4076	2.3771	11	486	45/33/22	1.6971	1.1560	0.0148	1.9618	29031.82	1628.99
RTHX-538	Staggered	1	0.7170	0.5378	1.4021	2.3578	11	477	66/17/17	1.7432	1.1254	0.0147	1.9618	28911.77	1615.76
RTHX-539	Staggered	1	0.7111	0.5334	1.3906	2.3385	11	478	64/22/14	1.7539	1.1185	0.0146	1.9618	28675.27	1602.54
RTHX-540	Staggered	1	0.6994	0.5246	1.3677	2.2999	11	478	67/29/4	1.7833	1.1001	0.0144	1.9618	28202.28	1576.11
RTHX-541	Staggered	1	0.7126	0.5345	1.3642	2.3297	11	478	67/22/11	1.7605	1.1143	0.0144	1.9618	28160.44	1615.25
RTHX-542	Staggered	1	0.6994	0.5246	1.3849	2.3076	11	477	66/20/14	1.7555	1.1014	0.0145	1.9336	28129.83	1548.29
RTHX-543	Staggered	1	0.7126	0.5345	1.3622	2.3277	11	478	67/22/11	1.7620	1.1134	0.0143	1.9618	28122.18	1616.61
RTHX-544	Staggered	1	0.7302	0.5477	1.3199	2.4092	11	478	67/17/16	1.7025	1.1523	0.0139	1.9618	27326.65	1640.04
RTHX-545	Staggered	1	0.7302	0.5477	1.3199	2.4012	11	567	66/19/15	1.4401	1.3622	0.0139	1.9618	27326.65	1645.66
RTHX-546	Staggered	1	0.7287	0.5466	1.3093	2.3964	11	474	22/52/26	1.7260	1.1366	0.0138	1.9618	27115.26	1642.19
RTHX-547	Staggered	1	0.7331	0.5499	1.3252	2.4108	11	478	90/6/4	1.6768	1.1531	0.0140	1.9336	27041.83	1628.35
RTHX-548	Staggered	1	0.7214	0.5411	1.3040	2.3723	11	478	90/5/5	1.7041	1.1347	0.0138	1.9336	26609.16	1602.29
RTHX-549	Staggered	1	0.7302	0.5477	1.1740	2.4092	11	567	66/23/11	1.4354	1.3667	0.0125	1.9618	24464.46	1640.20
RTHX-550	Staggered	1	0.7302	0.5477	1.1720	2.4072	11	567	66/23/11	1.4366	1.3656	0.0125	1.9618	24425.25	1641.57
RTHX-551	Staggered	1	0.7067	0.5301	1.1499	2.3240	11	477	66/5/29	1.7685	1.1093	0.0122	1.9618	23944.09	1592.63
RTHX-552	Staggered	1	0.7111	0.5334	1.1414	2.3385	11	477	66/23/11	1.7576	1.1162	0.0121	1.9618	23787.64	1602.54
RTHX-553	Staggered	1	0.7111	0.5334	1.1356	2.3385	11	461	2/48/50	1.8185	1.0788	0.0121	1.9618	23673.09	1602.51
RTHX-554	Staggered	1	0.6877	0.5158	1.1038	2.2614	11	465	66/23/11	1.8644	1.0522	0.0117	1.9618	23002.89	1549.65
RTHX-555	Staggered	1	0.7302	0.5477	1.0641	2.4092	11	477	21/52/27	1.7060	1.1499	0.0114	1.9618	22308.01	1640.04
RTHX-556	Staggered	1	0.7111	0.5334	1.0091	2.3346	11	461	2/48/50	1.8216	1.0770	0.0108	1.9618	21191.09	1605.18
RTHX-557	Staggered	1	0.6994	0.5246	0.9944	2.2827	11	496	66/17/17	1.7316	1.1329	0.0106	1.9618	20879.10	1588.04
RTHX-558	Staggered	1	0.6994	0.5246	1.0020	2.2616	11	567	32/34/34	1.5070	1.2831	0.0107	1.9336	20726.89	1579.88
RTHX-559	Staggered	1	0.6994	0.5246	0.9944	2.2616	11	567	32/34/34	1.5070	1.2831	0.0106	1.9336	20578.84	1579.88
RTHX-560	In-line	1	0.5293	0.3970	0.8293	1.2828	21	1160	36/54/10	1.1801	1.4886	0.0171	1.7567	30067.74	2767.71
RTHX-561	In-line	1	0.5191	0.3893	0.8132	1.2579	21	1160	36/54/10	1.2035	1.4597	0.0168	1.7567	29484.71	2714.04
RTHX-562	In-line	1	0.5059	0.3794	0.7926	1.2259	21	1160	90/9/1	1.2349	1.4226	0.0164	1.7567	28735.10	2645.04
RTHX-563	In-line	1	0.5000	0.3750	0.7834	1.2008	21	1167	8/56/36	1.2532	1.4018	0.0162	1.7567	28401.94	2638.21
RTHX-564	In-line	1	0.5015	0.3761	0.7802	1.1933	21	1160	87/7/6	1.2686	1.3848	0.0161	1.7567	28292.34	2670.28
RTHX-565	In-line	1	0.5000	0.3750	0.7779	1.1898	21	1160	89/9/2	1.2723	1.3807	0.0161	1.7567	28209.61	2662.47
RTHX-566	In-line	1	0.5015	0.3761	0.7857	1.1796	20	978	8/46/46	1.4739	1.1541	0.0162	1.7011	27584.21	2491.16
RTHX-567	In-line	1	0.5000	0.3750	0.7834	1.1761	20	985	64/30/6	1.4678	1.1590	0.0162	1.7011	27503.55	2483.88
RTHX-568	In-line	1	0.5000	0.3750	0.7779	1.2008	20	1160	90/9/1	1.1414	1.3934	0.0161	1.5905	25540.01	2274.80
RTHX-569	In-line	1	0.5059	0.3794	0.7926	1.1927	21	1160	87/11/2	1.0972	1.3841	0.0164	1.5186	24840.39	2350.22
RTHX-570	In-line	1	0.5000	0.3750	0.7779	1.1789	21	1160	81/10/9	1.0977	1.3680	0.0161	1.5017	24113.76	2297.03
RTHX-571	In-line	1	0.5088	0.3816	0.7972	1.2080	20	1348	66/28/6	0.8920	1.6289	0.0165	1.4530	23904.40	2139.18
RTHX-572	In-line	1	0.5000	0.3750	0.7779	1.1885	22	1160	90/5/5	1.0258	1.3791	0.0168	1.4147	23818.77	2248.87
RTHX-573	In-line	1	0.5000	0.3750	0.7943	1.1789	21	1160	87/11/2	1.0621	1.3680	0.0164	1.4530	23809.22	2222.56
RTHX-574	In-line	1	0.5073	0.3805	0.7935	1.1795	21	1160	84/14/2	1.0615	1.3687	0.0164	1.4530	23795.16	2286.99

Design Tag	Arrangement	Slabs	D_o	D_i	P_l	P_t	N_r	N_t	Pass Config.	l	H	d	A_f	V	$V_{mat'l}$
	-	-	mm	mm	mm	mm	-	-	%	m	m	m	m^2	cm^3	cm^3
RTHX-575	Staggered	2	0.6188	0.4641	1.9094	1.9873	15	404	43/57	0.4568	0.8035	0.0274	0.3670	10038.86	364.19
RTHX-576	Staggered	2	0.6188	0.4641	1.9094	1.9873	15	392	40/60	0.4719	0.7778	0.0273	0.3670	10015.07	363.32
RTHX-577	Staggered	2	0.6173	0.4630	1.9049	1.9826	14	409	42/58	0.4516	0.8127	0.0273	0.3670	10004.05	340.21
RTHX-578	Staggered	2	0.6188	0.4641	1.9026	1.9856	14	392	43/57	0.4708	0.7796	0.0254	0.3670	9307.83	339.91
RTHX-579	Staggered	2	0.6188	0.4641	1.7671	1.9873	15	409	37/63	0.4512	0.8134	0.0251	0.3670	9220.80	364.20
RTHX-580	Staggered	2	0.6188	0.4641	1.7502	1.9873	14	403	20/80	0.4579	0.8015	0.0247	0.3670	9081.55	339.91
RTHX-581	Staggered	2	0.6188	0.4641	1.7231	1.9873	15	409	42/58	0.4512	0.8134	0.0244	0.3670	8942.31	364.20
RTHX-582	Staggered	2	0.6188	0.4641	1.6960	1.9873	14	407	20/80	0.4534	0.8095	0.0243	0.3670	8924.90	339.92
RTHX-583	Staggered	2	0.6188	0.4641	1.6926	1.9873	15	409	43/57	0.4523	0.8115	0.0241	0.3670	8860.34	363.33
RTHX-584	Staggered	2	0.6173	0.4630	1.6802	1.9826	14	403	42/58	0.4579	0.8015	0.0240	0.3670	8803.07	339.91
RTHX-585	Staggered	2	0.6188	0.4641	1.6689	1.9873	14	400	43/57	0.4618	0.7949	0.0238	0.3670	8750.85	340.20
RTHX-586	Staggered	2	0.6188	0.4641	1.6588	1.9856	15	403	88/12	0.4583	0.8008	0.0237	0.3670	8707.34	364.50
RTHX-587	Staggered	2	0.6188	0.4641	1.6503	1.9856	15	410	20/80	0.4501	0.8154	0.0236	0.3670	8646.42	364.20
RTHX-588	Staggered	2	0.6188	0.4641	1.6384	1.9873	15	403	43/57	0.4590	0.7996	0.0235	0.3670	8625.93	363.33
RTHX-589	Staggered	2	0.6173	0.4630	1.6346	1.9826	15	410	20/80	0.4501	0.8154	0.0234	0.3670	8594.20	364.20
RTHX-590	Staggered	2	0.6188	0.4641	1.6283	1.9873	14	392	42/58	0.4943	0.7425	0.0232	0.3670	8531.96	328.73
RTHX-591	Staggered	2	0.5938	0.4454	1.6179	1.8926	15	409	42/58	0.4468	0.8134	0.0234	0.3634	8509.56	360.61
RTHX-592	Staggered	2	0.6188	0.4641	1.6283	1.9873	14	392	42/58	0.4943	0.7425	0.0227	0.3670	8331.51	328.73
RTHX-593	Staggered	2	0.5938	0.4454	1.5789	1.8926	13	404	20/80	0.4780	0.7678	0.0227	0.3670	8329.30	342.94
RTHX-594	Staggered	2	0.6305	0.4729	1.6971	1.8990	13	409	43/57	0.4811	0.7629	0.0227	0.3670	8319.80	336.56
RTHX-595	Staggered	2	0.6188	0.4641	1.6960	1.8637	13	397	42/58	0.4968	0.7387	0.0227	0.3670	8316.21	335.75
RTHX-596	Staggered	2	0.6173	0.4630	1.6954	1.8593	14	409	43/57	0.4789	0.7665	0.0226	0.3670	8310.51	364.17
RTHX-597	Staggered	2	0.6217	0.4663	1.6938	1.8725	13	404	20/80	0.4871	0.7535	0.0226	0.3670	8303.63	336.56
RTHX-598	Staggered	2	0.6188	0.4641	1.6926	1.8637	13	410	20/80	0.4800	0.7647	0.0225	0.3670	8271.31	336.56
RTHX-599	Staggered	2	0.6188	0.4641	1.6859	1.8637	13	409	43/57	0.4823	0.7611	0.0225	0.3670	8251.71	335.76
RTHX-600	Staggered	2	0.6173	0.4630	1.6819	1.8593	13	409	44/56	0.4789	0.7665	0.0225	0.3670	8245.55	338.15
RTHX-601	Staggered	2	0.6217	0.4663	1.6802	1.8725	13	404	42/58	0.4825	0.7607	0.0224	0.3670	8219.19	339.75
RTHX-602	Staggered	2	0.6246	0.4685	1.6745	1.8813	13	409	43/57	0.4811	0.7629	0.0224	0.3670	8206.66	336.56
RTHX-603	Staggered	2	0.6188	0.4641	1.6723	1.8637	13	409	42/58	0.4811	0.7629	0.0222	0.3670	8142.01	336.56
RTHX-604	Staggered	2	0.6188	0.4641	1.6588	1.8637	13	404	42/58	0.4825	0.7607	0.0222	0.3670	8137.61	339.75
RTHX-605	Staggered	2	0.6246	0.4685	1.6574	1.8813	13	404	88/12	0.4871	0.7535	0.0219	0.3670	8045.04	336.56
RTHX-606	Staggered	2	0.6188	0.4641	1.6384	1.8637	13	409	43/57	0.4811	0.7629	0.0219	0.3670	8036.96	336.56
RTHX-607	Staggered	2	0.6188	0.4641	1.6367	1.8637	14	409	43/57	0.4811	0.7629	0.0218	0.3670	8012.71	362.45
RTHX-608	Staggered	2	0.6188	0.4641	1.6317	1.8637	13	409	42/58	0.4811	0.7629	0.0216	0.3670	7939.98	336.56
RTHX-609	Staggered	2	0.6188	0.4641	1.6164	1.8637	14	409	20/80	0.4396	0.8349	0.0168	0.3670	6174.83	331.17
RTHX-610	In-line	2	0.6158	0.4619	0.7424	1.1688	24	306	85/15	0.4368	0.8200	0.0177	0.3581	6335.63	784.74
RTHX-611	In-line	2	0.6276	0.4707	0.7531	1.1705	22	307	85/15	0.4377	0.8223	0.0172	0.3599	6188.33	751.59
RTHX-612	In-line	2	0.6158	0.4619	0.7390	1.1486	22	313	85/15	0.4460	0.8069	0.0169	0.3599	6072.66	724.10
RTHX-613	In-line	2	0.5748	0.4311	0.6897	1.0736	24	339	62/38	0.4277	0.8498	0.0164	0.3634	5974.31	784.86
RTHX-614	In-line	2	0.6158	0.4619	0.7390	1.1486	22	302	85/15	0.4292	0.8069	0.0169	0.3464	5844.66	698.66
RTHX-615	In-line	2	0.6158	0.4619	0.7424	1.1587	23	291	85/15	0.4144	0.8129	0.0169	0.3369	5709.57	708.99
RTHX-616	In-line	2	0.5777	0.4333	0.6933	1.0459	23	338	85/15	0.4264	0.8279	0.0158	0.3530	5587.75	738.06
RTHX-617	In-line	2	0.5748	0.4311	0.6929	1.0406	24	324	74/26	0.4116	0.8185	0.0165	0.3369	5562.35	722.47
RTHX-618	In-line	2	0.5748	0.4311	0.6897	1.0185	22	343	85/15	0.4209	0.8307	0.0157	0.3497	5506.70	711.58

Design Tag	Arrangement	Slabs	D_o	D_i	P_l	P_t	N_r	N_t	Pass Config.	l	H	d	A_f	V	$V_{mat'l}$
	-	-	mm	mm	mm	mm	-	-	%	m	m	m	m²	cm³	cm³
RTHX-619	In-line	2	0.5733	0.4300	0.6880	1.0159	22	344	85/15	0.4220	0.8286	0.0157	0.3497	5492.66	708.20

Table 31. Optimum RTHX performance and operating conditions.

Design Tag	Design Problem	Fluid	Application	V_{air}	u_{air}	$\dot{m}_{fluid}$	$T_{air,in}$	$T_{fluid,in}$	$P_{fluid,in}$	$x_{fluid,in}$	h_{air}	ΔP_{air}	ΔP_{fluid}	Q
	-	-	-	m³/s	m/s	g/s	K	K	kPa	-	W/m².K	Pa	kPa	kW
RTHX-001	DP I	Water	Radiator	0.03	1.32	25.00	300.00	342.00	200.00	Liquid	308.77	27.25	1.035	1.000
RTHX-002	DP I	Water	Radiator	0.03	1.41	25.00	300.00	342.00	200.00	Liquid	323.42	34.92	1.449	1.005
RTHX-003	DP I	Water	Radiator	0.03	1.41	25.00	300.00	342.00	200.00	Liquid	323.02	34.84	1.442	1.005
RTHX-004	DP I	Water	Radiator	0.03	1.41	25.00	300.00	342.00	200.00	Liquid	322.73	34.78	1.437	1.005
RTHX-005	DP I	Water	Radiator	0.03	1.40	25.00	300.00	342.00	200.00	Liquid	322.30	34.41	1.442	1.004
RTHX-006	DP I	Water	Radiator	0.03	1.40	25.00	300.00	342.00	200.00	Liquid	321.59	33.98	1.442	1.003
RTHX-007	DP I	Water	Radiator	0.03	1.40	25.00	300.00	342.00	200.00	Liquid	322.41	33.68	1.451	1.004
RTHX-008	DP I	Water	Radiator	0.03	1.40	25.00	300.00	342.00	200.00	Liquid	321.60	33.65	1.451	1.003
RTHX-009	DP I	Water	Radiator	0.03	1.38	25.00	300.00	342.00	200.00	Liquid	320.24	33.61	1.464	1.008
RTHX-010	DP I	Water	Radiator	0.03	1.38	25.00	300.00	342.00	200.00	Liquid	321.74	30.87	0.422	1.004
RTHX-011	DP I	Water	Radiator	0.03	1.38	25.00	300.00	342.00	200.00	Liquid	321.71	30.87	0.422	1.004
RTHX-012	DP I	Water	Radiator	0.03	1.35	25.00	300.00	342.00	200.00	Liquid	315.74	28.04	0.385	1.001
RTHX-013	DP I	Water	Radiator	0.03	1.35	25.00	300.00	342.00	200.00	Liquid	315.65	28.04	0.385	1.001
RTHX-014	DP I	Water	Radiator	0.03	1.33	25.00	300.00	342.00	200.00	Liquid	313.71	27.41	0.391	1.005
RTHX-015	DP I	Water	Radiator	0.03	1.33	25.00	300.00	342.00	200.00	Liquid	313.71	27.41	0.391	1.005
RTHX-016	DP I	Water	Radiator	0.03	1.33	25.00	300.00	342.00	200.00	Liquid	308.80	27.25	1.035	1.000
RTHX-017	DP I	Water	Radiator	0.03	1.33	25.00	300.00	342.00	200.00	Liquid	312.91	27.09	0.391	1.004
RTHX-018	DP I	Water	Radiator	0.03	1.32	25.00	300.00	342.00	200.00	Liquid	309.91	25.95	0.412	1.001
RTHX-019	DP I	Water	Radiator	0.03	1.30	25.00	300.00	342.00	200.00	Liquid	308.50	25.47	0.396	1.005
RTHX-020	DP I	Water	Radiator	0.03	1.30	25.00	300.00	342.00	200.00	Liquid	308.19	25.33	0.396	1.004
RTHX-021	DP I	Water	Radiator	0.03	1.30	25.00	300.00	342.00	200.00	Liquid	304.81	25.24	0.396	1.000
RTHX-022	DP I	Water	Radiator	0.03	1.30	25.00	300.00	342.00	200.00	Liquid	305.70	25.23	0.395	1.001
RTHX-023	DP I	Water	Radiator	0.03	1.30	25.00	300.00	342.00	200.00	Liquid	305.69	25.22	0.395	1.001
RTHX-024	DP I	Water	Radiator	0.03	1.29	25.00	300.00	342.00	200.00	Liquid	307.09	24.99	0.467	1.006
RTHX-025	DP I	Water	Radiator	0.03	1.29	25.00	300.00	342.00	200.00	Liquid	306.50	24.65	0.470	1.005
RTHX-026	DP I	Water	Radiator	0.03	1.28	25.00	300.00	342.00	200.00	Liquid	305.65	24.34	0.468	1.004
RTHX-027	DP I	Water	Radiator	0.03	1.28	25.00	300.00	342.00	200.00	Liquid	305.65	24.33	0.468	1.004
RTHX-028	DP I	Water	Radiator	0.03	1.28	25.00	300.00	342.00	200.00	Liquid	305.61	24.33	0.468	1.004
RTHX-029	DP I	Water	Radiator	0.03	1.28	25.00	300.00	342.00	200.00	Liquid	305.61	24.33	0.468	1.004
RTHX-030	DP I	Water	Radiator	0.03	1.28	25.00	300.00	342.00	200.00	Liquid	305.43	24.30	0.467	1.004
RTHX-031	DP I	Water	Radiator	0.03	1.28	25.00	300.00	342.00	200.00	Liquid	305.39	24.29	0.467	1.004
RTHX-032	DP I	Water	Radiator	0.03	1.28	25.00	300.00	342.00	200.00	Liquid	302.48	23.93	1.386	1.000
RTHX-033	DP I	Water	Radiator	0.03	1.28	25.00	300.00	342.00	200.00	Liquid	302.48	23.93	1.386	1.000
RTHX-034	DP I	Water	Radiator	0.03	1.27	25.00	300.00	342.00	200.00	Liquid	304.30	23.83	0.472	1.005
RTHX-035	DP I	Water	Radiator	0.03	1.27	25.00	300.00	342.00	200.00	Liquid	303.33	23.77	0.457	1.004

Design Tag	Design Problem	Fluid	Application	V_{air}	u_{air}	$\dot{m}_{fluid}$	$T_{air,in}$	$T_{fluid,in}$	$P_{fluid,in}$	$x_{fluid,in}$	h_{air}	ΔP_{air}	ΔP_{fluid}	Q
	-	-	-	m³/s	m/s	g/s	K	K	kPa	-	W/m².K	Pa	kPa	kW
RTHX-036	DP I	Water	Radiator	0.03	1.27	25.00	300.00	342.00	200.00	Liquid	303.10	23.73	0.455	1.004
RTHX-037	DP I	Water	Radiator	0.03	1.26	25.00	300.00	342.00	200.00	Liquid	300.36	22.29	0.470	1.001
RTHX-038	DP I	Water	Radiator	0.03	1.26	25.00	300.00	342.00	200.00	Liquid	300.32	22.29	0.470	1.001
RTHX-039	DP I	Water	Radiator	0.03	1.26	25.00	300.00	342.00	200.00	Liquid	300.29	22.28	0.469	1.001
RTHX-040	DP I	Water	Radiator	0.03	1.26	25.00	300.00	342.00	200.00	Liquid	299.93	22.25	0.469	1.000
RTHX-041	DP I	Water	Radiator	0.03	1.26	25.00	300.00	342.00	200.00	Liquid	299.91	22.25	0.469	1.000
RTHX-042	DP I	Water	Radiator	0.03	1.26	25.00	300.00	342.00	200.00	Liquid	299.87	22.25	0.469	1.000
RTHX-043	DP I	Water	Radiator	0.03	1.25	25.00	300.00	342.00	200.00	Liquid	299.30	22.09	0.393	1.001
RTHX-044	DP I	Water	Radiator	0.03	1.25	25.00	300.00	342.00	200.00	Liquid	299.21	22.08	0.393	1.001
RTHX-045	DP I	Water	Radiator	0.03	1.24	25.00	300.00	342.00	200.00	Liquid	298.83	21.76	0.478	1.007
RTHX-046	DP I	Water	Radiator	0.03	1.23	25.00	300.00	342.00	200.00	Liquid	297.37	21.14	0.481	1.004
RTHX-047	DP I	Water	Radiator	0.03	1.23	25.00	300.00	342.00	200.00	Liquid	296.87	21.11	0.480	1.004
RTHX-048	DP I	Water	Radiator	0.03	1.23	25.00	300.00	342.00	200.00	Liquid	297.15	21.10	0.480	1.004
RTHX-049	DP I	Water	Radiator	0.03	1.23	25.00	300.00	342.00	200.00	Liquid	296.97	21.08	0.478	1.004
RTHX-050	DP I	Water	Radiator	0.03	1.22	25.00	300.00	342.00	200.00	Liquid	296.49	20.92	0.457	1.007
RTHX-051	DP I	Water	Radiator	0.03	1.22	25.00	300.00	342.00	200.00	Liquid	295.92	20.88	0.448	1.005
RTHX-052	DP I	Water	Radiator	0.03	1.22	25.00	300.00	342.00	200.00	Liquid	295.67	20.79	0.451	1.007
RTHX-053	DP I	Water	Radiator	0.03	1.22	25.00	300.00	342.00	200.00	Liquid	295.48	20.79	0.451	1.007
RTHX-054	DP I	Water	Radiator	0.03	1.20	25.00	300.00	342.00	200.00	Liquid	293.13	20.77	0.443	1.011
RTHX-055	DP I	Water	Radiator	0.03	1.20	25.00	300.00	342.00	200.00	Liquid	292.83	20.56	0.443	1.011
RTHX-056	DP I	Water	Radiator	0.03	1.20	25.00	300.00	342.00	200.00	Liquid	292.68	20.54	0.442	1.011
RTHX-057	DP I	Water	Radiator	0.03	1.20	25.00	300.00	342.00	200.00	Liquid	292.84	20.26	0.442	1.011
RTHX-058	DP I	Water	Radiator	0.03	1.20	25.00	300.00	342.00	200.00	Liquid	291.77	20.21	0.442	1.010
RTHX-059	DP I	Water	Radiator	0.03	1.19	25.00	300.00	342.00	200.00	Liquid	293.20	20.12	0.469	1.013
RTHX-060	DP I	Water	Radiator	0.03	1.19	25.00	300.00	342.00	200.00	Liquid	293.15	20.12	0.469	1.013
RTHX-061	DP I	Water	Radiator	0.03	1.19	25.00	300.00	342.00	200.00	Liquid	293.14	20.12	0.469	1.013
RTHX-062	DP I	Water	Radiator	0.03	1.19	25.00	300.00	342.00	200.00	Liquid	293.15	20.02	0.447	1.014
RTHX-063	DP I	Water	Radiator	0.03	1.19	25.00	300.00	342.00	200.00	Liquid	293.11	20.01	0.447	1.014
RTHX-064	DP I	Water	Radiator	0.03	1.19	25.00	300.00	342.00	200.00	Liquid	289.98	19.88	0.431	1.010
RTHX-065	DP I	Water	Radiator	0.03	1.19	25.00	300.00	342.00	200.00	Liquid	289.97	19.88	0.431	1.010
RTHX-066	DP I	Water	Radiator	0.03	1.19	25.00	300.00	342.00	200.00	Liquid	289.92	19.87	0.431	1.010
RTHX-067	DP I	Water	Radiator	0.03	1.18	25.00	300.00	342.00	200.00	Liquid	286.29	18.30	0.445	1.002
RTHX-068	DP I	Water	Radiator	0.03	1.17	25.00	300.00	342.00	200.00	Liquid	285.95	18.25	0.443	1.002
RTHX-069	DP I	Water	Radiator	0.03	1.17	25.00	300.00	342.00	200.00	Liquid	285.93	18.25	0.442	1.002
RTHX-070	DP I	Water	Radiator	0.03	1.17	25.00	300.00	342.00	200.00	Liquid	286.80	18.04	0.444	1.003
RTHX-071	DP I	Water	Radiator	0.03	1.17	25.00	300.00	342.00	200.00	Liquid	286.02	18.02	0.444	1.002
RTHX-072	DP I	Water	Radiator	0.03	1.17	25.00	300.00	342.00	200.00	Liquid	286.58	18.01	0.442	1.003
RTHX-073	DP I	Water	Radiator	0.03	1.17	25.00	300.00	342.00	200.00	Liquid	285.93	18.00	0.443	1.002
RTHX-074	DP I	Water	Radiator	0.03	1.17	25.00	300.00	342.00	200.00	Liquid	286.36	17.90	0.470	1.004
RTHX-075	DP I	Water	Radiator	0.03	1.16	25.00	300.00	342.00	200.00	Liquid	286.04	17.86	0.446	1.005
RTHX-076	DP I	Water	Radiator	0.03	1.16	25.00	300.00	342.00	200.00	Liquid	284.21	17.79	0.445	1.002
RTHX-077	DP I	Water	Radiator	0.03	1.16	25.00	300.00	342.00	200.00	Liquid	284.11	17.79	0.445	1.002
RTHX-078	DP I	Water	Radiator	0.03	1.16	25.00	300.00	342.00	200.00	Liquid	284.19	17.78	0.431	1.002
RTHX-079	DP I	Water	Radiator	0.03	1.16	25.00	300.00	342.00	200.00	Liquid	284.14	17.77	0.431	1.002

Design Tag	Design Problem	Fluid	Application	V_{air}	u_{air}	$\dot{m}_{fluid}$	$T_{air,in}$	$T_{fluid,in}$	$P_{fluid,in}$	$x_{fluid,in}$	h_{air}	ΔP_{air}	ΔP_{fluid}	Q
	-	-	-	m³/s	m/s	g/s	K	K	kPa	-	W/m².K	Pa	kPa	kW
RTHX-080	DP I	Water	Radiator	0.03	1.16	25.00	300.00	342.00	200.00	Liquid	285.22	17.76	0.436	1.006
RTHX-081	DP I	Water	Radiator	0.03	1.16	25.00	300.00	342.00	200.00	Liquid	283.38	17.60	0.434	1.004
RTHX-082	DP I	Water	Radiator	0.03	1.15	25.00	300.00	342.00	200.00	Liquid	284.51	17.49	0.436	1.010
RTHX-083	DP I	Water	Radiator	0.03	1.14	25.00	300.00	342.00	200.00	Liquid	284.44	17.44	0.433	1.011
RTHX-084	DP I	Water	Radiator	0.03	1.14	25.00	300.00	342.00	200.00	Liquid	284.37	17.43	0.432	1.011
RTHX-085	DP I	Water	Radiator	0.03	1.14	25.00	300.00	342.00	200.00	Liquid	282.16	17.31	0.455	1.007
RTHX-086	DP I	Water	Radiator	0.03	1.14	25.00	300.00	342.00	200.00	Liquid	282.69	17.29	0.431	1.008
RTHX-087	DP I	Water	Radiator	0.03	1.13	25.00	300.00	342.00	200.00	Liquid	280.31	16.62	0.431	1.005
RTHX-088	DP I	Water	Radiator	0.03	1.12	25.00	300.00	342.00	200.00	Liquid	277.94	15.65	0.432	1.002
RTHX-089	DP I	Water	Radiator	0.03	1.12	25.00	300.00	342.00	200.00	Liquid	276.71	15.61	0.432	1.000
RTHX-090	DP I	Water	Radiator	0.03	1.12	25.00	300.00	342.00	200.00	Liquid	276.57	15.49	0.423	1.002
RTHX-091	DP I	Water	Radiator	0.03	1.11	25.00	300.00	342.00	200.00	Liquid	275.71	15.43	0.420	1.001
RTHX-092	DP I	Water	Radiator	0.03	1.11	25.00	300.00	342.00	200.00	Liquid	275.15	15.43	0.422	1.000
RTHX-093	DP I	Water	Radiator	0.03	1.11	25.00	300.00	342.00	200.00	Liquid	274.90	15.40	0.420	1.000
RTHX-094	DP I	Water	Radiator	0.03	1.09	25.00	300.00	342.00	200.00	Liquid	272.37	14.48	0.439	1.002
RTHX-095	DP I	Water	Radiator	0.03	1.08	25.00	300.00	342.00	200.00	Liquid	271.89	14.28	0.442	1.004
RTHX-096	DP I	Water	Radiator	0.03	1.08	25.00	300.00	342.00	200.00	Liquid	271.79	14.27	0.443	1.004
RTHX-097	DP I	Water	Radiator	0.03	1.08	25.00	300.00	342.00	200.00	Liquid	271.63	14.26	0.443	1.004
RTHX-098	DP I	Water	Radiator	0.03	1.08	25.00	300.00	342.00	200.00	Liquid	271.19	14.23	0.442	1.003
RTHX-099	DP I	Water	Radiator	0.03	1.08	25.00	300.00	342.00	200.00	Liquid	271.13	14.23	0.443	1.003
RTHX-100	DP I	Water	Radiator	0.03	1.06	25.00	300.00	342.00	200.00	Liquid	268.84	13.76	0.410	1.010
RTHX-101	DP I	Water	Radiator	0.03	1.05	25.00	300.00	342.00	200.00	Liquid	268.34	13.67	0.434	1.013
RTHX-102	DP I	Water	Radiator	0.03	1.05	25.00	300.00	342.00	200.00	Liquid	268.49	13.67	0.404	1.011
RTHX-103	DP I	Water	Radiator	0.03	1.05	25.00	300.00	342.00	200.00	Liquid	268.62	13.62	0.434	1.013
RTHX-104	DP I	Water	Radiator	0.03	1.04	25.00	300.00	342.00	200.00	Liquid	264.52	13.29	0.409	1.008
RTHX-105	DP I	Water	Radiator	0.03	1.04	25.00	300.00	342.00	200.00	Liquid	263.52	12.72	0.411	1.002
RTHX-106	DP I	Water	Radiator	0.03	1.04	25.00	300.00	342.00	200.00	Liquid	264.13	12.67	0.410	1.004
RTHX-107	DP I	Water	Radiator	0.03	1.04	25.00	300.00	342.00	200.00	Liquid	264.11	12.67	0.410	1.004
RTHX-108	DP I	Water	Radiator	0.03	1.03	25.00	300.00	342.00	200.00	Liquid	263.01	12.27	0.412	1.001
RTHX-109	DP I	Water	Radiator	0.03	1.03	25.00	300.00	342.00	200.00	Liquid	262.96	12.26	0.412	1.001
RTHX-110	DP I	Water	Radiator	0.03	1.03	25.00	300.00	342.00	200.00	Liquid	262.77	12.25	0.411	1.001
RTHX-111	DP I	Water	Radiator	0.03	1.03	25.00	300.00	342.00	200.00	Liquid	262.08	12.22	0.410	1.001
RTHX-112	DP I	Water	Radiator	0.03	1.03	25.00	300.00	342.00	200.00	Liquid	262.48	12.22	0.410	1.001
RTHX-113	DP I	Water	Radiator	0.03	1.01	25.00	300.00	342.00	200.00	Liquid	260.09	11.73	1.337	1.008
RTHX-114	DP I	Water	Radiator	0.03	1.00	25.00	300.00	342.00	200.00	Liquid	254.67	11.19	1.340	1.000
RTHX-115	DP I	Water	Radiator	0.03	1.00	25.00	300.00	342.00	200.00	Liquid	254.62	11.19	1.339	1.000
RTHX-116	DP I	Water	Radiator	0.03	1.00	25.00	300.00	342.00	200.00	Liquid	254.57	11.18	1.338	1.000
RTHX-117	DP I	Water	Radiator	0.03	1.00	25.00	300.00	342.00	200.00	Liquid	254.32	11.16	1.332	1.000
RTHX-118	DP I	Water	Radiator	0.03	0.98	25.00	300.00	342.00	200.00	Liquid	253.72	10.96	1.357	1.005
RTHX-119	DP I	Water	Radiator	0.03	0.98	25.00	300.00	342.00	200.00	Liquid	253.72	10.96	1.357	1.005
RTHX-120	DP I	Water	Radiator	0.03	0.98	25.00	300.00	342.00	200.00	Liquid	253.71	10.96	1.357	1.005
RTHX-121	DP I	Water	Radiator	0.03	0.98	25.00	300.00	342.00	200.00	Liquid	253.28	10.95	1.357	1.004
RTHX-122	DP I	Water	Radiator	0.03	0.97	25.00	300.00	342.00	200.00	Liquid	251.99	10.67	1.370	1.005
RTHX-123	DP I	Water	Radiator	0.03	0.97	25.00	300.00	342.00	200.00	Liquid	251.73	10.65	1.364	1.005

Design Tag	Design Problem	Fluid	Application	V_{air}	u_{air}	$\dot{m}_{fluid}$	$T_{air,in}$	$T_{fluid,in}$	$P_{fluid,in}$	$x_{fluid,in}$	h_{air}	ΔP_{air}	ΔP_{fluid}	Q
	-	-	-	m³/s	m/s	g/s	K	K	kPa	-	W/m².K	Pa	kPa	kW
RTHX-124	DP I	Water	Radiator	0.03	0.97	25.00	300.00	342.00	200.00	Liquid	252.43	10.31	1.357	1.003
RTHX-125	DP I	Water	Radiator	0.03	0.97	25.00	300.00	342.00	200.00	Liquid	250.90	10.10	1.359	1.000
RTHX-126	DP I	Water	Radiator	0.03	0.94	25.00	300.00	342.00	200.00	Liquid	249.39	9.66	0.403	1.012
RTHX-127	DP I	Water	Radiator	0.03	0.94	25.00	300.00	342.00	200.00	Liquid	249.30	9.66	0.402	1.012
RTHX-128	DP I	Water	Radiator	0.03	0.93	25.00	300.00	342.00	200.00	Liquid	246.75	9.48	0.403	1.008
RTHX-129	DP I	Water	Radiator	0.03	0.93	25.00	300.00	342.00	200.00	Liquid	246.66	9.48	0.402	1.008
RTHX-130	DP I	Water	Radiator	0.03	0.93	25.00	300.00	342.00	200.00	Liquid	244.85	9.30	0.402	1.005
RTHX-131	DP I	Water	Radiator	0.03	0.93	25.00	300.00	342.00	200.00	Liquid	246.48	9.15	0.402	1.008
RTHX-132	DP I	Water	Radiator	0.03	0.93	25.00	300.00	342.00	200.00	Liquid	246.47	9.15	0.402	1.008
RTHX-133	DP I	Water	Radiator	0.03	0.93	25.00	300.00	342.00	200.00	Liquid	243.16	9.07	0.402	1.002
RTHX-134	DP I	Water	Radiator	0.03	0.92	25.00	300.00	342.00	200.00	Liquid	245.51	8.97	0.402	1.006
RTHX-135	DP I	Water	Radiator	0.03	0.92	25.00	300.00	342.00	200.00	Liquid	245.22	8.95	0.401	1.006
RTHX-136	DP I	Water	Radiator	0.03	0.92	25.00	300.00	342.00	200.00	Liquid	242.72	8.93	0.403	1.001
RTHX-137	DP I	Water	Radiator	0.03	0.92	25.00	300.00	342.00	200.00	Liquid	242.62	8.90	1.546	1.003
RTHX-138	DP I	Water	Radiator	0.03	0.92	25.00	300.00	342.00	200.00	Liquid	242.09	8.88	0.397	1.002
RTHX-139	DP I	Water	Radiator	0.03	0.92	25.00	300.00	342.00	200.00	Liquid	242.00	8.87	0.398	1.002
RTHX-140	DP I	Water	Radiator	0.03	0.92	25.00	300.00	342.00	200.00	Liquid	241.94	8.85	1.528	1.004
RTHX-141	DP I	Water	Radiator	0.03	0.92	25.00	300.00	342.00	200.00	Liquid	240.90	8.81	0.392	1.001
RTHX-142	DP I	Water	Radiator	0.03	0.90	25.00	300.00	342.00	200.00	Liquid	240.89	8.64	0.394	1.008
RTHX-143	DP I	Water	Radiator	0.03	0.90	25.00	300.00	342.00	200.00	Liquid	241.18	8.64	0.393	1.009
RTHX-144	DP I	Water	Radiator	0.03	0.90	25.00	300.00	342.00	200.00	Liquid	240.83	8.58	1.586	1.011
RTHX-145	DP I	Water	Radiator	0.03	0.90	25.00	300.00	342.00	200.00	Liquid	240.76	8.57	1.583	1.011
RTHX-146	DP I	Water	Radiator	0.03	0.90	25.00	300.00	342.00	200.00	Liquid	240.72	8.57	1.583	1.011
RTHX-147	DP I	Water	Radiator	0.03	0.90	25.00	300.00	342.00	200.00	Liquid	240.71	8.57	1.583	1.011
RTHX-148	DP I	Water	Radiator	0.03	0.90	25.00	300.00	342.00	200.00	Liquid	240.62	8.56	1.580	1.011
RTHX-149	DP I	Water	Radiator	0.03	0.89	25.00	300.00	342.00	200.00	Liquid	240.47	8.55	1.576	1.011
RTHX-150	DP I	Water	Radiator	0.03	0.89	25.00	300.00	342.00	200.00	Liquid	239.55	7.95	0.393	1.006
RTHX-151	DP I	Water	Radiator	0.03	0.88	25.00	300.00	342.00	200.00	Liquid	238.60	7.89	0.387	1.006
RTHX-152	DP I	Water	Radiator	0.03	0.88	25.00	300.00	342.00	200.00	Liquid	239.11	7.79	0.396	1.008
RTHX-153	DP I	Water	Radiator	0.03	0.87	25.00	300.00	342.00	200.00	Liquid	237.11	7.49	0.393	1.002
RTHX-154	DP I	Water	Radiator	0.03	0.87	25.00	300.00	342.00	200.00	Liquid	237.11	7.49	0.393	1.002
RTHX-155	DP I	Water	Radiator	0.03	0.87	25.00	300.00	342.00	200.00	Liquid	236.45	7.40	0.393	1.001
RTHX-156	DP I	Water	Radiator	0.03	0.87	25.00	300.00	342.00	200.00	Liquid	236.28	7.39	0.392	1.001
RTHX-157	DP I	Water	Radiator	0.03	0.87	25.00	300.00	342.00	200.00	Liquid	236.06	7.33	0.396	1.003
RTHX-158	DP I	Water	Radiator	0.03	0.86	25.00	300.00	342.00	200.00	Liquid	235.13	7.21	0.394	1.002
RTHX-159	DP I	Water	Radiator	0.03	0.85	25.00	300.00	342.00	200.00	Liquid	230.90	7.05	0.632	1.000
RTHX-160	DP I	Water	Radiator	0.03	0.85	25.00	300.00	342.00	200.00	Liquid	232.70	6.97	0.387	1.004
RTHX-161	DP I	Water	Radiator	0.03	0.84	25.00	300.00	342.00	200.00	Liquid	229.91	6.89	1.486	1.003
RTHX-162	DP I	Water	Radiator	0.03	0.84	25.00	300.00	342.00	200.00	Liquid	229.59	6.83	1.498	1.005
RTHX-163	DP I	Water	Radiator	0.03	0.84	25.00	300.00	342.00	200.00	Liquid	229.50	6.83	1.496	1.005
RTHX-164	DP I	Water	Radiator	0.03	0.84	25.00	300.00	342.00	200.00	Liquid	228.86	6.79	1.479	1.005
RTHX-165	DP I	Water	Radiator	0.03	0.84	25.00	300.00	342.00	200.00	Liquid	228.68	6.76	1.479	1.004
RTHX-166	DP I	Water	Radiator	0.03	0.83	25.00	300.00	342.00	200.00	Liquid	228.59	6.76	1.462	1.005
RTHX-167	DP I	Water	Radiator	0.03	0.83	25.00	300.00	342.00	200.00	Liquid	228.62	6.70	1.511	1.009

Design Tag	Design Problem	Fluid	Application	V_{air}	u_{air}	$\dot{m}_{fluid}$	$T_{air,in}$	$T_{fluid,in}$	$P_{fluid,in}$	$x_{fluid,in}$	h_{air}	ΔP_{air}	ΔP_{fluid}	Q
	-	-	-	m^3/s	m/s	g/s	K	K	kPa	-	$W/m^2.K$	Pa	kPa	kW
RTHX-168	DP I	Water	Radiator	0.03	0.83	25.00	300.00	342.00	200.00	Liquid	228.49	6.69	1.511	1.009
RTHX-169	DP I	Water	Radiator	0.03	0.83	25.00	300.00	342.00	200.00	Liquid	228.21	6.68	1.503	1.009
RTHX-170	DP I	Water	Radiator	0.03	0.83	25.00	300.00	342.00	200.00	Liquid	228.20	6.68	1.503	1.009
RTHX-171	DP I	Water	Radiator	0.03	0.82	25.00	300.00	342.00	200.00	Liquid	228.76	6.65	1.527	1.011
RTHX-172	DP I	Water	Radiator	0.03	0.82	25.00	300.00	342.00	200.00	Liquid	228.56	6.64	1.522	1.011
RTHX-173	DP I	Water	Radiator	0.03	0.82	25.00	300.00	342.00	200.00	Liquid	228.32	6.63	1.516	1.011
RTHX-174	DP I	Water	Radiator	0.03	0.82	25.00	300.00	342.00	200.00	Liquid	227.86	6.60	1.504	1.011
RTHX-175	DP I	Water	Radiator	0.03	0.82	25.00	300.00	342.00	200.00	Liquid	227.89	6.60	1.499	1.012
RTHX-176	DP I	Water	Radiator	0.03	0.82	25.00	300.00	342.00	200.00	Liquid	227.60	6.59	1.497	1.011
RTHX-177	DP I	Water	Radiator	0.03	0.82	25.00	300.00	342.00	200.00	Liquid	227.57	6.59	1.504	1.011
RTHX-178	DP I	Water	Radiator	0.03	0.82	25.00	300.00	342.00	200.00	Liquid	227.57	6.59	1.504	1.011
RTHX-179	DP I	Water	Radiator	0.03	0.82	25.00	300.00	342.00	200.00	Liquid	227.39	6.56	1.504	1.010
RTHX-180	DP I	Water	Radiator	0.03	0.82	25.00	300.00	342.00	200.00	Liquid	227.20	6.55	1.499	1.010
RTHX-181	DP I	Water	Radiator	0.03	0.81	25.00	300.00	342.00	200.00	Liquid	227.39	6.51	0.604	1.017
RTHX-182	DP I	Water	Radiator	0.03	0.80	25.00	300.00	342.00	200.00	Liquid	226.89	6.44	0.596	1.017
RTHX-183	DP I	Water	Radiator	0.03	0.80	25.00	300.00	342.00	200.00	Liquid	226.86	6.44	0.596	1.017
RTHX-184	DP I	Water	Radiator	0.03	0.80	25.00	300.00	342.00	200.00	Liquid	226.91	6.44	0.595	1.018
RTHX-185	DP I	Water	Radiator	0.03	0.80	25.00	300.00	342.00	200.00	Liquid	231.30	6.42	1.577	1.028
RTHX-186	DP I	Water	Radiator	0.03	0.80	25.00	300.00	342.00	200.00	Liquid	226.20	6.35	1.574	1.020
RTHX-187	DP I	Water	Radiator	0.03	0.80	25.00	300.00	342.00	200.00	Liquid	225.69	6.33	1.560	1.020
RTHX-188	DP I	Water	Radiator	0.03	0.79	25.00	300.00	342.00	200.00	Liquid	226.28	6.30	0.617	1.023
RTHX-189	DP I	Water	Radiator	0.03	0.79	25.00	300.00	342.00	200.00	Liquid	226.17	6.29	0.616	1.023
RTHX-190	DP I	Water	Radiator	0.03	0.79	25.00	300.00	342.00	200.00	Liquid	226.07	6.29	0.616	1.023
RTHX-191	DP I	Water	Radiator	0.03	0.79	25.00	300.00	342.00	200.00	Liquid	225.61	6.24	1.460	1.024
RTHX-192	DP I	Water	Radiator	0.03	0.79	25.00	300.00	342.00	200.00	Liquid	224.99	6.22	1.583	1.023
RTHX-193	DP I	Water	Radiator	0.03	0.79	25.00	300.00	342.00	200.00	Liquid	224.92	6.22	1.453	1.023
RTHX-194	DP I	Water	Radiator	0.03	0.79	25.00	300.00	342.00	200.00	Liquid	224.55	6.20	1.443	1.023
RTHX-195	DP I	Water	Radiator	0.03	0.78	25.00	300.00	342.00	200.00	Liquid	224.79	6.16	0.585	1.027
RTHX-196	DP I	Water	Radiator	0.03	0.78	25.00	300.00	342.00	200.00	Liquid	222.24	6.10	1.380	1.022
RTHX-197	DP I	Water	Radiator	0.03	0.78	25.00	300.00	342.00	200.00	Liquid	222.16	6.10	1.379	1.022
RTHX-198	DP I	Water	Radiator	0.03	0.78	25.00	300.00	342.00	200.00	Liquid	222.14	6.10	1.378	1.022
RTHX-199	DP I	Water	Radiator	0.03	0.78	25.00	300.00	342.00	200.00	Liquid	222.20	6.09	1.380	1.022
RTHX-200	DP I	Water	Radiator	0.03	0.76	25.00	300.00	342.00	200.00	Liquid	223.17	5.97	1.509	1.032
RTHX-201	DP I	Water	Radiator	0.03	0.76	25.00	300.00	342.00	200.00	Liquid	223.15	5.96	0.566	1.033
RTHX-202	DP I	Water	Radiator	0.03	0.76	25.00	300.00	342.00	200.00	Liquid	222.87	5.96	1.642	1.034
RTHX-203	DP I	Water	Radiator	0.03	0.76	25.00	300.00	342.00	200.00	Liquid	222.77	5.94	1.642	1.034
RTHX-204	DP I	Water	Radiator	0.03	0.76	25.00	300.00	342.00	200.00	Liquid	222.93	5.93	0.571	1.034
RTHX-205	DP I	Water	Radiator	0.03	0.76	25.00	300.00	342.00	200.00	Liquid	222.51	5.91	1.642	1.033
RTHX-206	DP I	Water	Radiator	0.03	0.76	25.00	300.00	342.00	200.00	Liquid	222.09	5.90	0.566	1.033
RTHX-207	DP I	Water	Radiator	0.03	0.76	25.00	300.00	342.00	200.00	Liquid	222.26	5.89	0.569	1.036
RTHX-208	DP I	Water	Radiator	0.03	0.76	25.00	300.00	342.00	200.00	Liquid	222.55	5.89	0.575	1.035
RTHX-209	DP I	Water	Radiator	0.03	0.76	25.00	300.00	342.00	200.00	Liquid	222.54	5.89	0.575	1.035
RTHX-210	DP I	Water	Radiator	0.03	0.76	25.00	300.00	342.00	200.00	Liquid	222.53	5.88	1.407	1.035
RTHX-211	DP I	Water	Radiator	0.03	0.76	25.00	300.00	342.00	200.00	Liquid	222.31	5.87	1.402	1.035

Design Tag	Design Problem	Fluid	Application	V_{air}	u_{air}	$\dot{m}_{fluid}$	$T_{air,in}$	$T_{fluid,in}$	$P_{fluid,in}$	$x_{fluid,in}$	h_{air}	ΔP_{air}	ΔP_{fluid}	Q
	-	-	-	m^3/s	m/s	g/s	K	K	kPa	-	$W/m^2.K$	Pa	kPa	kW
RTHX-212	DP I	Water	Radiator	0.03	0.75	25.00	300.00	342.00	200.00	Liquid	222.21	5.82	0.585	1.038
RTHX-213	DP I	Water	Radiator	0.03	0.75	25.00	300.00	342.00	200.00	Liquid	221.67	5.78	0.646	1.039
RTHX-214	DP I	Water	Radiator	0.03	0.88	25.00	300.00	342.00	200.00	Liquid	255.21	6.40	0.968	1.000
RTHX-215	DP I	Water	Radiator	0.03	0.87	25.00	300.00	342.00	200.00	Liquid	259.84	6.79	0.989	1.018
RTHX-216	DP I	Water	Radiator	0.03	0.97	25.00	300.00	342.00	200.00	Liquid	273.17	9.20	0.983	1.015
RTHX-217	DP I	Water	Radiator	0.03	0.81	25.00	300.00	342.00	200.00	Liquid	240.70	5.26	0.730	1.005
RTHX-218	DP I	Water	Radiator	0.03	1.07	25.00	300.00	342.00	200.00	Liquid	284.57	11.41	0.955	1.002
RTHX-219	DP I	Water	Radiator	0.03	1.30	25.00	300.00	342.00	200.00	Liquid	323.28	20.05	0.797	1.000
RTHX-220	DP I	Water	Radiator	0.03	1.05	25.00	300.00	342.00	200.00	Liquid	284.15	10.81	0.868	1.003
RTHX-221	DP I	Water	Radiator	0.03	0.86	25.00	300.00	342.00	200.00	Liquid	254.02	6.19	0.980	1.003
RTHX-222	DP I	Water	Radiator	0.03	1.14	25.00	300.00	342.00	200.00	Liquid	304.91	15.23	0.871	1.024
RTHX-223	DP I	Water	Radiator	0.03	1.11	25.00	300.00	342.00	200.00	Liquid	294.23	13.16	0.992	1.007
RTHX-224	DP I	Water	Radiator	0.03	0.87	25.00	300.00	342.00	200.00	Liquid	255.51	6.34	0.990	1.005
RTHX-225	DP I	Water	Radiator	0.03	0.86	25.00	300.00	342.00	200.00	Liquid	259.30	6.28	0.981	1.012
RTHX-226	DP I	Water	Radiator	0.03	1.11	25.00	300.00	342.00	200.00	Liquid	292.52	12.92	0.982	1.006
RTHX-227	DP I	Water	Radiator	0.03	1.06	25.00	300.00	342.00	200.00	Liquid	283.86	11.28	0.955	1.001
RTHX-228	DP I	Water	Radiator	0.03	1.11	25.00	300.00	342.00	200.00	Liquid	293.04	13.02	0.982	1.007
RTHX-229	DP I	Water	Radiator	0.03	1.74	25.00	300.00	342.00	200.00	Liquid	425.66	41.91	0.882	1.010
RTHX-230	DP I	Water	Radiator	0.03	1.58	25.00	300.00	342.00	200.00	Liquid	389.88	30.99	0.934	1.001
RTHX-231	DP I	Water	Radiator	0.03	0.94	25.00	300.00	342.00	200.00	Liquid	270.89	8.19	0.916	1.016
RTHX-232	DP I	Water	Radiator	0.03	1.18	25.00	300.00	342.00	200.00	Liquid	305.54	15.72	0.922	1.009
RTHX-233	DP I	Water	Radiator	0.03	0.84	25.00	300.00	342.00	200.00	Liquid	248.66	5.71	0.866	1.001
RTHX-234	DP I	Water	Radiator	0.03	1.13	25.00	300.00	342.00	200.00	Liquid	304.83	15.14	0.885	1.025
RTHX-235	DP I	Water	Radiator	0.03	1.15	25.00	300.00	342.00	200.00	Liquid	305.70	15.34	0.903	1.018
RTHX-236	DP I	Water	Radiator	0.03	1.17	25.00	300.00	342.00	200.00	Liquid	306.93	15.65	0.855	1.014
RTHX-237	DP I	Water	Radiator	0.03	0.96	25.00	300.00	342.00	200.00	Liquid	271.81	8.98	0.983	1.013
RTHX-238	DP I	Water	Radiator	0.03	1.38	25.00	300.00	342.00	200.00	Liquid	340.57	23.73	0.914	1.003
RTHX-239	DP I	Water	Radiator	0.03	0.96	25.00	300.00	342.00	200.00	Liquid	272.39	8.95	0.999	1.016
RTHX-240	DP I	Water	Radiator	0.03	1.63	25.00	300.00	342.00	200.00	Liquid	405.20	31.61	0.904	1.002
RTHX-241	DP I	Water	Radiator	0.03	0.87	25.00	300.00	342.00	200.00	Liquid	259.37	6.73	0.989	1.017
RTHX-242	DP I	Water	Radiator	0.03	1.19	25.00	300.00	342.00	200.00	Liquid	308.84	16.13	0.837	1.008
RTHX-243	DP I	Water	Radiator	0.03	1.55	25.00	300.00	342.00	200.00	Liquid	383.01	30.23	0.914	1.003
RTHX-244	DP I	Water	Radiator	0.03	1.44	25.00	300.00	342.00	200.00	Liquid	362.81	26.15	0.963	1.009
RTHX-245	DP I	Water	Radiator	0.03	0.82	25.00	300.00	342.00	200.00	Liquid	245.03	5.46	0.746	1.003
RTHX-246	DP I	Water	Radiator	0.03	0.91	25.00	300.00	342.00	200.00	Liquid	264.24	7.60	0.981	1.019
RTHX-247	DP I	Water	Radiator	0.03	1.07	25.00	300.00	342.00	200.00	Liquid	284.92	11.47	0.955	1.002
RTHX-248	DP I	Water	Radiator	0.03	1.67	25.00	300.00	342.00	200.00	Liquid	418.43	34.91	0.786	1.008
RTHX-249	DP I	Water	Radiator	0.03	1.64	25.00	300.00	342.00	200.00	Liquid	409.51	31.78	0.786	1.000
RTHX-250	DP I	Water	Radiator	0.03	1.56	25.00	300.00	342.00	200.00	Liquid	390.39	29.04	0.907	1.004
RTHX-251	DP I	Water	Radiator	0.03	1.12	25.00	300.00	342.00	200.00	Liquid	302.79	14.72	0.956	1.025
RTHX-252	DP I	Water	Radiator	0.03	0.99	25.00	300.00	342.00	200.00	Liquid	277.10	9.61	0.993	1.011
RTHX-253	DP I	Water	Radiator	0.03	1.78	25.00	300.00	342.00	200.00	Liquid	421.96	48.09	0.882	1.006
RTHX-254	DP I	Water	Radiator	0.03	1.17	25.00	300.00	342.00	200.00	Liquid	306.84	15.64	0.855	1.014
RTHX-255	DP I	Water	Radiator	0.03	0.86	25.00	300.00	342.00	200.00	Liquid	250.41	6.12	0.861	1.001

Design Tag	Design Problem	Fluid	Application	V_{air}	u_{air}	$\dot{m}_{fluid}$	$T_{air,in}$	$T_{fluid,in}$	$P_{fluid,in}$	$x_{fluid,in}$	h_{air}	ΔP_{air}	ΔP_{fluid}	Q
	-	-	-	m³/s	m/s	g/s	K	K	kPa	-	W/m².K	Pa	kPa	kW
RTHX-256	DP I	Water	Radiator	0.03	1.46	25.00	300.00	342.00	200.00	Liquid	361.66	27.55	0.972	1.007
RTHX-257	DP I	Water	Radiator	0.03	0.89	25.00	300.00	342.00	200.00	Liquid	264.05	7.39	0.962	1.027
RTHX-258	DP I	Water	Radiator	0.03	1.38	25.00	300.00	342.00	200.00	Liquid	342.34	23.95	0.933	1.003
RTHX-259	DP I	Water	Radiator	0.03	1.40	25.00	300.00	342.00	200.00	Liquid	347.19	24.50	0.959	1.003
RTHX-260	DP I	Water	Radiator	0.03	1.37	25.00	300.00	342.00	200.00	Liquid	339.71	23.61	0.905	1.003
RTHX-261	DP I	Water	Radiator	0.03	1.36	25.00	300.00	342.00	200.00	Liquid	339.06	22.13	0.923	1.001
RTHX-262	DP I	Water	Radiator	0.03	1.80	25.00	300.00	342.00	200.00	Liquid	422.94	48.86	0.874	1.004
RTHX-263	DP I	Water	Radiator	0.03	0.83	25.00	300.00	342.00	200.00	Liquid	248.94	5.48	0.866	1.002
RTHX-264	DP I	Water	Radiator	0.03	1.65	25.00	300.00	342.00	200.00	Liquid	412.09	32.42	0.786	1.003
RTHX-265	DP I	Water	Radiator	0.03	0.93	25.00	300.00	342.00	200.00	Liquid	268.36	7.90	0.953	1.015
RTHX-266	DP I	Water	Radiator	0.03	0.94	25.00	300.00	342.00	200.00	Liquid	266.98	7.99	0.989	1.009
RTHX-267	DP I	Water	Radiator	0.03	1.55	25.00	300.00	342.00	200.00	Liquid	382.42	30.08	0.914	1.002
RTHX-268	DP I	Water	Radiator	0.03	1.49	25.00	300.00	342.00	200.00	Liquid	366.21	28.17	0.993	1.003
RTHX-269	DP I	Water	Radiator	0.03	1.20	25.00	300.00	342.00	200.00	Liquid	309.86	16.34	0.941	1.005
RTHX-270	DP I	Water	Radiator	0.03	1.27	25.00	300.00	342.00	200.00	Liquid	318.02	19.31	0.739	1.001
RTHX-271	DP I	Water	Radiator	0.03	0.87	25.00	300.00	342.00	200.00	Liquid	257.47	6.49	0.953	1.009
RTHX-272	DP I	Water	Radiator	0.03	1.41	25.00	300.00	342.00	200.00	Liquid	354.28	24.92	0.952	1.008
RTHX-273	DP I	Water	Radiator	0.03	1.23	25.00	300.00	342.00	200.00	Liquid	318.46	18.58	0.942	1.016
RTHX-274	DP I	Water	Radiator	0.03	0.85	25.00	300.00	342.00	200.00	Liquid	254.91	6.16	0.970	1.012
RTHX-275	DP I	Water	Radiator	0.03	0.91	25.00	300.00	342.00	200.00	Liquid	266.10	7.69	0.975	1.019
RTHX-276	DP I	Water	Radiator	0.03	0.99	25.00	300.00	342.00	200.00	Liquid	274.20	9.45	0.965	1.009
RTHX-277	DP I	Water	Radiator	0.03	1.29	25.00	300.00	342.00	200.00	Liquid	321.98	19.86	0.782	1.000
RTHX-278	DP I	Water	Radiator	0.03	1.30	25.00	300.00	342.00	200.00	Liquid	331.47	21.65	0.996	1.018
RTHX-279	DP I	Water	Radiator	0.03	1.20	25.00	300.00	342.00	200.00	Liquid	313.03	17.79	0.913	1.019
RTHX-280	DP I	Water	Radiator	0.03	0.79	25.00	300.00	342.00	200.00	Liquid	234.76	4.88	0.671	1.000
RTHX-281	DP I	Water	Radiator	0.03	1.21	25.00	300.00	342.00	200.00	Liquid	315.32	18.28	0.931	1.020
RTHX-282	DP I	Water	Radiator	0.03	1.14	25.00	300.00	342.00	200.00	Liquid	305.44	15.30	0.879	1.023
RTHX-283	DP I	Water	Radiator	0.03	0.96	25.00	300.00	342.00	200.00	Liquid	271.46	8.43	0.934	1.009
RTHX-284	DP I	Water	Radiator	0.03	1.13	25.00	300.00	342.00	200.00	Liquid	304.74	15.13	0.885	1.025
RTHX-285	DP I	Water	Radiator	0.03	1.30	25.00	300.00	342.00	200.00	Liquid	325.56	21.42	0.788	1.008
RTHX-286	DP I	Water	Radiator	0.03	1.69	25.00	300.00	342.00	200.00	Liquid	419.05	35.71	0.882	1.004
RTHX-287	DP I	Water	Radiator	0.03	1.46	25.00	300.00	342.00	200.00	Liquid	367.31	26.73	0.991	1.008
RTHX-288	DP I	Water	Radiator	0.03	0.97	25.00	300.00	342.00	200.00	Liquid	272.68	9.03	0.993	1.014
RTHX-289	DP I	Water	Radiator	0.03	1.70	25.00	300.00	342.00	200.00	Liquid	419.31	36.20	0.874	1.001
RTHX-290	DP I	Water	Radiator	0.03	1.41	25.00	300.00	342.00	200.00	Liquid	352.73	24.79	0.943	1.007
RTHX-291	DP I	Water	Radiator	0.03	1.78	25.00	300.00	342.00	200.00	Liquid	422.23	48.10	0.882	1.007
RTHX-292	DP I	Water	Radiator	0.03	0.84	25.00	300.00	342.00	200.00	Liquid	250.25	5.99	0.877	1.009
RTHX-293	DP I	Water	Radiator	0.03	0.87	25.00	300.00	342.00	200.00	Liquid	255.27	6.32	0.990	1.004
RTHX-294	DP I	Water	Radiator	0.03	1.53	25.00	300.00	342.00	200.00	Liquid	386.00	28.83	0.834	1.007
RTHX-295	DP I	Water	Radiator	0.03	0.95	25.00	300.00	342.00	200.00	Liquid	271.35	8.30	0.983	1.013
RTHX-296	DP I	Water	Radiator	0.03	1.13	25.00	300.00	342.00	200.00	Liquid	303.48	14.87	0.885	1.024
RTHX-297	DP I	Water	Radiator	0.03	1.49	25.00	300.00	342.00	200.00	Liquid	368.72	28.49	0.994	1.005
RTHX-298	DP I	Water	Radiator	0.03	1.78	25.00	300.00	342.00	200.00	Liquid	421.80	47.82	0.882	1.006
RTHX-299	DP I	Water	Radiator	0.03	1.68	25.00	300.00	342.00	200.00	Liquid	414.49	35.12	0.864	1.002

Design Tag	Design Problem	Fluid	Application	V_{air}	u_{air}	$\dot{m}_{fluid}$	$T_{air,in}$	$T_{fluid,in}$	$P_{fluid,in}$	$x_{fluid,in}$	h_{air}	ΔP_{air}	ΔP_{fluid}	Q
	-	-	-	m^3/s	m/s	g/s	K	K	kPa	-	$W/m^2.K$	Pa	kPa	kW
RTHX-300	DP I	Water	Radiator	0.03	1.46	25.00	300.00	342.00	200.00	Liquid	367.53	26.75	0.991	1.008
RTHX-301	DP I	Water	Radiator	0.03	1.43	25.00	300.00	342.00	200.00	Liquid	357.20	25.33	0.970	1.006
RTHX-302	DP I	Water	Radiator	0.03	1.65	25.00	300.00	342.00	200.00	Liquid	407.22	34.12	0.863	1.002
RTHX-303	DP I	Water	Radiator	0.03	1.00	25.00	300.00	342.00	200.00	Liquid	279.76	10.42	0.972	1.019
RTHX-304	DP I	Water	Radiator	0.03	0.80	25.00	300.00	342.00	200.00	Liquid	239.25	5.16	0.739	1.008
RTHX-305	DP I	Water	Radiator	0.03	1.35	25.00	300.00	342.00	200.00	Liquid	338.04	23.14	0.954	1.008
RTHX-306	DP I	Water	Radiator	0.03	1.50	25.00	300.00	342.00	200.00	Liquid	368.55	28.74	0.994	1.005
RTHX-307	DP I	Water	Radiator	0.03	1.49	25.00	300.00	342.00	200.00	Liquid	366.43	28.18	0.993	1.003
RTHX-308	DP I	Water	Radiator	0.03	1.47	25.00	300.00	342.00	200.00	Liquid	365.06	27.72	0.924	1.007
RTHX-309	DP I	Water	Radiator	0.03	1.77	25.00	300.00	342.00	200.00	Liquid	425.21	47.54	0.890	1.013
RTHX-310	DP I	Water	Radiator	0.03	1.15	25.00	300.00	342.00	200.00	Liquid	305.58	15.34	0.903	1.018
RTHX-311	DP I	Water	Radiator	0.03	0.85	25.00	300.00	342.00	200.00	Liquid	249.90	6.06	0.866	1.003
RTHX-312	DP I	Water	Radiator	0.03	0.94	25.00	300.00	342.00	200.00	Liquid	271.22	8.22	0.924	1.016
RTHX-313	DP I	Water	Radiator	0.03	1.63	25.00	300.00	342.00	200.00	Liquid	408.23	31.68	0.904	1.005
RTHX-314	DP I	Water	Radiator	0.03	1.54	25.00	300.00	342.00	200.00	Liquid	388.67	28.98	0.842	1.009
RTHX-315	DP I	Water	Radiator	0.03	1.59	25.00	300.00	342.00	200.00	Liquid	402.51	31.39	0.934	1.013
RTHX-316	DP I	Water	Radiator	0.03	1.55	25.00	300.00	342.00	200.00	Liquid	383.12	30.24	0.914	1.003
RTHX-317	DP I	Water	Radiator	0.03	0.84	25.00	300.00	342.00	200.00	Liquid	249.82	5.97	0.877	1.008
RTHX-318	DP I	Water	Radiator	0.03	1.31	25.00	300.00	342.00	200.00	Liquid	326.08	21.51	0.796	1.007
RTHX-319	DP I	Water	Radiator	0.03	1.73	25.00	300.00	342.00	200.00	Liquid	424.97	41.50	0.865	1.011
RTHX-320	DP I	Water	Radiator	0.03	1.52	25.00	300.00	342.00	200.00	Liquid	177.22	39.76	0.563	1.018
RTHX-321	DP I	Water	Radiator	0.03	1.52	25.00	300.00	342.00	200.00	Liquid	177.13	39.76	0.753	1.018
RTHX-322	DP I	Water	Radiator	0.03	1.55	25.00	300.00	342.00	200.00	Liquid	177.47	40.46	0.755	1.012
RTHX-323	DP I	Water	Radiator	0.03	1.55	25.00	300.00	342.00	200.00	Liquid	177.52	40.46	0.347	1.012
RTHX-324	DP I	Water	Radiator	0.03	1.55	25.00	300.00	342.00	200.00	Liquid	177.48	40.51	0.347	1.012
RTHX-325	DP I	Water	Radiator	0.03	1.55	25.00	300.00	342.00	200.00	Liquid	177.49	40.51	0.347	1.012
RTHX-326	DP I	Water	Radiator	0.03	1.57	25.00	300.00	342.00	200.00	Liquid	177.81	41.01	0.745	1.008
RTHX-327	DP I	Water	Radiator	0.03	1.59	25.00	300.00	342.00	200.00	Liquid	178.09	41.59	0.549	1.003
RTHX-328	DP I	Water	Radiator	0.03	1.59	25.00	300.00	342.00	200.00	Liquid	178.12	41.66	0.548	1.003
RTHX-329	DP I	Water	Radiator	0.03	1.59	25.00	300.00	342.00	200.00	Liquid	178.12	41.66	0.548	1.003
RTHX-330	DP I	Water	Radiator	0.03	1.59	25.00	300.00	342.00	200.00	Liquid	177.63	42.28	0.732	1.001
RTHX-331	DP I	Water	Radiator	0.03	1.59	25.00	300.00	342.00	200.00	Liquid	179.95	43.44	0.722	1.008
RTHX-332	DP I	Water	Radiator	0.03	1.60	25.00	300.00	342.00	200.00	Liquid	179.61	43.73	0.527	1.006
RTHX-333	DP I	Water	Radiator	0.03	1.60	25.00	300.00	342.00	200.00	Liquid	179.40	44.14	0.733	1.005
RTHX-334	DP I	Water	Radiator	0.03	1.62	25.00	300.00	342.00	200.00	Liquid	180.44	44.23	0.724	1.003
RTHX-335	DP I	Water	Radiator	0.03	1.62	25.00	300.00	342.00	200.00	Liquid	180.41	44.23	0.709	1.003
RTHX-336	DP I	Water	Radiator	0.03	1.62	25.00	300.00	342.00	200.00	Liquid	180.45	44.23	0.724	1.003
RTHX-337	DP I	Water	Radiator	0.03	1.62	25.00	300.00	342.00	200.00	Liquid	180.43	44.23	0.709	1.003
RTHX-338	DP I	Water	Radiator	0.03	1.62	25.00	300.00	342.00	200.00	Liquid	180.43	44.23	0.710	1.003
RTHX-339	DP I	Water	Radiator	0.03	1.62	25.00	300.00	342.00	200.00	Liquid	180.47	44.24	0.725	1.003
RTHX-340	DP I	Water	Radiator	0.03	1.63	25.00	300.00	342.00	200.00	Liquid	181.47	45.13	0.710	1.005
RTHX-341	DP I	Water	Radiator	0.03	1.63	25.00	300.00	342.00	200.00	Liquid	181.20	45.50	0.708	1.004
RTHX-342	DP I	Water	Radiator	0.03	1.63	25.00	300.00	342.00	200.00	Liquid	181.21	45.50	0.708	1.004
RTHX-343	DP I	Water	Radiator	0.03	1.63	25.00	300.00	342.00	200.00	Liquid	181.28	45.50	0.333	1.003

Design Tag	Design Problem	Fluid	Application	V_{air}	u_{air}	$\dot{m}_{fluid}$	$T_{air,in}$	$T_{fluid,in}$	$P_{fluid,in}$	$x_{fluid,in}$	h_{air}	ΔP_{air}	ΔP_{fluid}	Q
	-	-	-	m^3/s	m/s	g/s	K	K	kPa	-	$W/m^2.K$	Pa	kPa	kW
RTHX-344	DP I	Water	Radiator	0.03	1.64	25.00	300.00	342.00	200.00	Liquid	181.32	45.77	0.704	1.001
RTHX-345	DP I	Water	Radiator	0.03	1.67	25.00	300.00	342.00	200.00	Liquid	184.97	48.37	0.374	1.004
RTHX-346	DP I	Water	Radiator	0.03	1.67	25.00	300.00	342.00	200.00	Liquid	184.78	48.37	0.323	1.004
RTHX-347	DP I	Water	Radiator	0.03	1.67	25.00	300.00	342.00	200.00	Liquid	184.78	48.37	0.323	1.004
RTHX-348	DP I	Water	Radiator	0.03	1.68	25.00	300.00	342.00	200.00	Liquid	184.65	48.46	0.727	1.004
RTHX-349	DP I	Water	Radiator	0.03	1.68	25.00	300.00	342.00	200.00	Liquid	185.11	48.52	0.403	1.003
RTHX-350	DP I	Water	Radiator	0.03	1.68	25.00	300.00	342.00	200.00	Liquid	185.13	48.52	0.410	1.003
RTHX-351	DP I	Water	Radiator	0.03	1.68	25.00	300.00	342.00	200.00	Liquid	185.09	48.59	0.402	1.003
RTHX-352	DP I	Water	Radiator	0.03	1.68	25.00	300.00	342.00	200.00	Liquid	185.24	48.59	0.695	1.003
RTHX-353	DP I	Water	Radiator	0.03	1.68	25.00	300.00	342.00	200.00	Liquid	185.12	48.59	0.403	1.003
RTHX-354	DP I	Water	Radiator	0.03	1.68	25.00	300.00	342.00	200.00	Liquid	184.81	48.59	0.709	1.003
RTHX-355	DP I	Water	Radiator	0.03	1.69	25.00	300.00	342.00	200.00	Liquid	184.86	48.89	0.705	1.001
RTHX-356	DP I	Water	Radiator	0.03	1.69	25.00	300.00	342.00	200.00	Liquid	184.86	48.89	0.705	1.001
RTHX-357	DP I	Water	Radiator	0.03	1.69	25.00	300.00	342.00	200.00	Liquid	184.86	48.89	0.705	1.001
RTHX-358	DP I	Water	Radiator	0.03	1.69	25.00	300.00	342.00	200.00	Liquid	184.87	48.89	0.705	1.001
RTHX-359	DP I	Water	Radiator	0.03	1.69	25.00	300.00	342.00	200.00	Liquid	184.87	48.89	0.705	1.001
RTHX-360	DP I	Water	Radiator	0.03	1.69	25.00	300.00	342.00	200.00	Liquid	186.90	50.49	0.603	1.006
RTHX-361	DP I	Water	Radiator	0.03	1.69	25.00	300.00	342.00	200.00	Liquid	186.92	50.49	0.603	1.006
RTHX-362	DP I	Water	Radiator	0.03	1.69	25.00	300.00	342.00	200.00	Liquid	186.92	50.49	0.603	1.006
RTHX-363	DP I	Water	Radiator	0.03	1.70	25.00	300.00	342.00	200.00	Liquid	187.11	50.62	0.599	1.004
RTHX-364	DP I	Water	Radiator	0.03	1.71	25.00	300.00	342.00	200.00	Liquid	186.97	50.87	0.703	1.003
RTHX-365	DP I	Water	Radiator	0.03	1.71	25.00	300.00	342.00	200.00	Liquid	187.07	50.91	0.688	1.003
RTHX-366	DP I	Water	Radiator	0.03	1.71	25.00	300.00	342.00	200.00	Liquid	187.14	51.22	0.701	1.002
RTHX-367	DP I	Water	Radiator	0.03	1.71	25.00	300.00	342.00	200.00	Liquid	187.14	51.22	0.701	1.002
RTHX-368	DP I	Water	Radiator	0.03	1.71	25.00	300.00	342.00	200.00	Liquid	187.37	51.40	0.701	1.003
RTHX-369	DP I	Water	Radiator	0.03	1.71	25.00	300.00	342.00	200.00	Liquid	187.38	51.40	0.702	1.003
RTHX-370	DP I	Water	Radiator	0.03	1.72	25.00	300.00	342.00	200.00	Liquid	186.99	51.46	0.593	1.000
RTHX-371	DP I	Water	Radiator	0.03	1.72	25.00	300.00	342.00	200.00	Liquid	187.44	51.58	0.684	1.001
RTHX-372	DP I	Water	Radiator	0.03	1.72	25.00	300.00	342.00	200.00	Liquid	186.95	52.01	0.698	1.000
RTHX-373	DP I	Water	Radiator	0.03	1.72	25.00	300.00	342.00	200.00	Liquid	186.95	52.01	0.698	1.000
RTHX-374	DP I	Water	Radiator	0.03	1.72	25.00	300.00	342.00	200.00	Liquid	187.20	52.16	0.698	1.001
RTHX-375	DP I	Water	Radiator	0.03	1.72	25.00	300.00	342.00	200.00	Liquid	186.84	52.16	0.521	1.001
RTHX-376	DP I	Water	Radiator	0.03	1.72	25.00	300.00	342.00	200.00	Liquid	187.21	52.16	0.698	1.001
RTHX-377	DP I	Water	Radiator	0.03	1.73	25.00	300.00	342.00	200.00	Liquid	188.66	52.56	0.397	1.004
RTHX-378	DP I	Water	Radiator	0.03	1.74	25.00	300.00	342.00	200.00	Liquid	187.91	52.66	0.772	1.000
RTHX-379	DP I	Water	Radiator	0.03	1.74	25.00	300.00	342.00	200.00	Liquid	187.91	52.66	0.772	1.000
RTHX-380	DP I	Water	Radiator	0.03	1.74	25.00	300.00	342.00	200.00	Liquid	189.23	53.29	0.695	1.003
RTHX-381	DP I	Water	Radiator	0.03	1.74	25.00	300.00	342.00	200.00	Liquid	189.21	53.29	0.681	1.003
RTHX-382	DP I	Water	Radiator	0.03	1.74	25.00	300.00	342.00	200.00	Liquid	188.82	53.29	0.320	1.003
RTHX-383	DP I	Water	Radiator	0.03	1.74	25.00	300.00	342.00	200.00	Liquid	189.02	53.46	0.590	1.002
RTHX-384	DP I	Water	Radiator	0.03	1.75	25.00	300.00	342.00	200.00	Liquid	189.31	53.65	0.393	1.001
RTHX-385	DP I	Water	Radiator	0.03	1.75	25.00	300.00	342.00	200.00	Liquid	189.31	53.65	0.393	1.001
RTHX-386	DP I	Water	Radiator	0.03	1.75	25.00	300.00	342.00	200.00	Liquid	189.03	53.65	0.318	1.001
RTHX-387	DP I	Water	Radiator	0.03	1.75	25.00	300.00	342.00	200.00	Liquid	188.98	53.72	0.976	1.001

Design Tag	Design Problem	Fluid	Application	V_{air}	u_{air}	$\dot{m}_{fluid}$	$T_{air,in}$	$T_{fluid,in}$	$P_{fluid,in}$	$x_{fluid,in}$	h_{air}	ΔP_{air}	ΔP_{fluid}	Q
	-	-	-	m³/s	m/s	g/s	K	K	kPa	-	W/m².K	Pa	kPa	kW
RTHX-388	DP I	Water	Radiator	0.03	1.75	25.00	300.00	342.00	200.00	Liquid	189.34	53.78	0.692	1.001
RTHX-389	DP I	Water	Radiator	0.03	1.75	25.00	300.00	342.00	200.00	Liquid	189.41	55.43	0.696	1.003
RTHX-390	DP II	Water	Radiator	0.30	1.19	250.00	300.00	342.00	200.00	Liquid	262.41	37.29	4.992	10.471
RTHX-391	DP II	Water	Radiator	0.30	1.19	250.00	300.00	342.00	200.00	Liquid	262.48	37.37	4.982	10.467
RTHX-392	DP II	Water	Radiator	0.30	1.19	250.00	300.00	342.00	200.00	Liquid	262.50	37.38	4.984	10.467
RTHX-393	DP II	Water	Radiator	0.30	1.19	250.00	300.00	342.00	200.00	Liquid	262.52	37.38	4.982	10.467
RTHX-394	DP II	Water	Radiator	0.30	1.19	250.00	300.00	342.00	200.00	Liquid	262.55	37.39	4.984	10.467
RTHX-395	DP II	Water	Radiator	0.30	1.19	250.00	300.00	342.00	200.00	Liquid	262.56	37.39	4.984	10.467
RTHX-396	DP II	Water	Radiator	0.30	1.19	250.00	300.00	342.00	200.00	Liquid	263.52	38.00	4.982	10.480
RTHX-397	DP II	Water	Radiator	0.30	1.19	250.00	300.00	342.00	200.00	Liquid	263.57	38.01	4.984	10.480
RTHX-398	DP II	Water	Radiator	0.30	1.19	250.00	300.00	342.00	200.00	Liquid	263.77	38.16	4.982	10.483
RTHX-399	DP II	Water	Radiator	0.30	1.19	250.00	300.00	342.00	200.00	Liquid	264.05	38.33	4.985	10.486
RTHX-400	DP II	Water	Radiator	0.30	1.20	250.00	300.00	342.00	200.00	Liquid	263.95	38.33	4.967	10.475
RTHX-401	DP II	Water	Radiator	0.30	1.23	250.00	300.00	342.00	200.00	Liquid	263.54	39.16	4.841	10.358
RTHX-402	DP II	Water	Radiator	0.30	1.23	250.00	300.00	342.00	200.00	Liquid	263.71	39.22	4.856	10.357
RTHX-403	DP II	Water	Radiator	0.30	1.23	250.00	300.00	342.00	200.00	Liquid	264.30	39.25	4.986	10.370
RTHX-404	DP II	Water	Radiator	0.30	1.23	250.00	300.00	342.00	200.00	Liquid	264.44	39.30	5.000	10.369
RTHX-405	DP II	Water	Radiator	0.30	1.23	250.00	300.00	342.00	200.00	Liquid	264.84	39.56	4.992	10.369
RTHX-406	DP II	Water	Radiator	0.30	1.24	250.00	300.00	342.00	200.00	Liquid	264.94	39.67	4.969	10.353
RTHX-407	DP II	Water	Radiator	0.30	1.24	250.00	300.00	342.00	200.00	Liquid	265.27	39.98	4.926	10.338
RTHX-408	DP II	Water	Radiator	0.30	1.24	250.00	300.00	342.00	200.00	Liquid	265.29	39.99	4.927	10.338
RTHX-409	DP II	Water	Radiator	0.30	1.24	250.00	300.00	342.00	200.00	Liquid	265.29	39.99	4.928	10.338
RTHX-410	DP II	Water	Radiator	0.30	1.24	250.00	300.00	342.00	200.00	Liquid	265.32	39.99	4.926	10.338
RTHX-411	DP II	Water	Radiator	0.30	1.24	250.00	300.00	342.00	200.00	Liquid	265.34	39.99	4.926	10.338
RTHX-412	DP II	Water	Radiator	0.30	1.25	250.00	300.00	342.00	200.00	Liquid	265.55	40.12	4.926	10.334
RTHX-413	DP II	Water	Radiator	0.30	1.25	250.00	300.00	342.00	200.00	Liquid	265.61	40.14	4.931	10.334
RTHX-414	DP II	Water	Radiator	0.30	1.25	250.00	300.00	342.00	200.00	Liquid	266.06	40.26	4.996	10.336
RTHX-415	DP II	Water	Radiator	0.30	1.25	250.00	300.00	342.00	200.00	Liquid	266.12	40.27	4.996	10.337
RTHX-416	DP II	Water	Radiator	0.30	1.25	250.00	300.00	342.00	200.00	Liquid	266.26	40.36	4.988	10.333
RTHX-417	DP II	Water	Radiator	0.30	1.25	250.00	300.00	342.00	200.00	Liquid	266.29	40.38	4.991	10.333
RTHX-418	DP II	Water	Radiator	0.30	1.25	250.00	300.00	342.00	200.00	Liquid	266.55	40.56	4.973	10.325
RTHX-419	DP II	Water	Radiator	0.30	1.26	250.00	300.00	342.00	200.00	Liquid	266.88	40.72	4.982	10.321
RTHX-420	DP II	Water	Radiator	0.30	1.26	250.00	300.00	342.00	200.00	Liquid	266.90	40.72	4.983	10.321
RTHX-421	DP II	Water	Radiator	0.30	1.26	250.00	300.00	342.00	200.00	Liquid	266.91	40.72	4.983	10.321
RTHX-422	DP II	Water	Radiator	0.30	1.26	250.00	300.00	342.00	200.00	Liquid	267.06	40.78	4.997	10.321
RTHX-423	DP II	Water	Radiator	0.30	1.26	250.00	300.00	342.00	200.00	Liquid	267.07	40.78	4.997	10.321
RTHX-424	DP II	Water	Radiator	0.30	1.26	250.00	300.00	342.00	200.00	Liquid	267.08	40.78	4.998	10.321
RTHX-425	DP II	Water	Radiator	0.30	1.26	250.00	300.00	342.00	200.00	Liquid	267.89	41.30	4.989	10.339
RTHX-426	DP II	Water	Radiator	0.30	1.26	250.00	300.00	342.00	200.00	Liquid	267.97	41.33	4.996	10.339
RTHX-427	DP II	Water	Radiator	0.30	1.26	250.00	300.00	342.00	200.00	Liquid	267.91	41.35	4.968	10.336
RTHX-428	DP II	Water	Radiator	0.30	1.26	250.00	300.00	342.00	200.00	Liquid	267.95	41.36	4.972	10.336
RTHX-429	DP II	Water	Radiator	0.30	1.26	250.00	300.00	342.00	200.00	Liquid	268.06	41.40	4.982	10.336
RTHX-430	DP II	Water	Radiator	0.30	1.26	250.00	300.00	342.00	200.00	Liquid	268.08	41.40	4.983	10.336
RTHX-431	DP II	Water	Radiator	0.30	1.26	250.00	300.00	342.00	200.00	Liquid	268.08	41.41	4.983	10.336

Design Tag	Design Problem	Fluid	Application	V_{air}	u_{air}	$\dot{m}_{fluid}$	$T_{air,in}$	$T_{fluid,in}$	$P_{fluid,in}$	$x_{fluid,in}$	h_{air}	ΔP_{air}	ΔP_{fluid}	Q
	-	-	-	m^3/s	m/s	g/s	K	K	kPa	-	$W/m^2.K$	Pa	kPa	kW
RTHX-432	DP II	Water	Radiator	0.30	1.26	250.00	300.00	342.00	200.00	Liquid	268.22	41.50	4.975	10.332
RTHX-433	DP II	Water	Radiator	0.30	1.26	250.00	300.00	342.00	200.00	Liquid	268.23	41.50	4.976	10.332
RTHX-434	DP II	Water	Radiator	0.30	1.26	250.00	300.00	342.00	200.00	Liquid	268.49	41.63	4.975	10.328
RTHX-435	DP II	Water	Radiator	0.30	1.26	250.00	300.00	342.00	200.00	Liquid	268.55	41.66	4.981	10.328
RTHX-436	DP II	Water	Radiator	0.30	1.26	250.00	300.00	342.00	200.00	Liquid	268.56	41.66	4.982	10.328
RTHX-437	DP II	Water	Radiator	0.30	1.26	250.00	300.00	342.00	200.00	Liquid	268.57	41.67	4.983	10.328
RTHX-438	DP II	Water	Radiator	0.30	1.26	250.00	300.00	342.00	200.00	Liquid	268.68	41.77	4.967	10.332
RTHX-439	DP II	Water	Radiator	0.30	1.27	250.00	300.00	342.00	200.00	Liquid	268.86	41.83	4.982	10.332
RTHX-440	DP II	Water	Radiator	0.30	1.27	250.00	300.00	342.00	200.00	Liquid	268.88	41.84	4.983	10.332
RTHX-441	DP II	Water	Radiator	0.30	1.27	250.00	300.00	342.00	200.00	Liquid	268.88	41.84	4.984	10.332
RTHX-442	DP II	Water	Radiator	0.30	1.27	250.00	300.00	342.00	200.00	Liquid	268.89	41.84	4.983	10.332
RTHX-443	DP II	Water	Radiator	0.30	1.27	250.00	300.00	342.00	200.00	Liquid	269.06	41.90	4.998	10.332
RTHX-444	DP II	Water	Radiator	0.30	1.27	250.00	300.00	342.00	200.00	Liquid	269.04	41.94	4.974	10.329
RTHX-445	DP II	Water	Radiator	0.30	1.27	250.00	300.00	342.00	200.00	Liquid	269.04	41.94	4.975	10.329
RTHX-446	DP II	Water	Radiator	0.30	1.27	250.00	300.00	342.00	200.00	Liquid	269.06	41.94	4.976	10.329
RTHX-447	DP II	Water	Radiator	0.30	1.27	250.00	300.00	342.00	200.00	Liquid	269.14	41.97	4.982	10.328
RTHX-448	DP II	Water	Radiator	0.30	1.27	250.00	300.00	342.00	200.00	Liquid	269.94	42.47	4.974	10.340
RTHX-449	DP II	Water	Radiator	0.30	1.27	250.00	300.00	342.00	200.00	Liquid	270.04	42.50	4.983	10.340
RTHX-450	DP II	Water	Radiator	0.30	1.27	250.00	300.00	342.00	200.00	Liquid	270.14	42.53	4.990	10.340
RTHX-451	DP II	Water	Radiator	0.30	1.27	250.00	300.00	342.00	200.00	Liquid	270.15	42.54	4.991	10.340
RTHX-452	DP II	Water	Radiator	0.30	1.27	250.00	300.00	342.00	200.00	Liquid	270.62	42.85	4.979	10.348
RTHX-453	DP II	Water	Radiator	0.30	1.28	250.00	300.00	342.00	200.00	Liquid	271.18	43.19	4.974	10.355
RTHX-454	DP II	Water	Radiator	0.30	1.28	250.00	300.00	342.00	200.00	Liquid	271.20	43.20	4.976	10.355
RTHX-455	DP II	Water	Radiator	0.30	1.28	250.00	300.00	342.00	200.00	Liquid	271.34	43.32	4.961	10.360
RTHX-456	DP II	Water	Radiator	0.30	1.28	250.00	300.00	342.00	200.00	Liquid	271.49	43.37	4.974	10.359
RTHX-457	DP II	Water	Radiator	0.30	1.28	250.00	300.00	342.00	200.00	Liquid	271.50	43.37	4.975	10.359
RTHX-458	DP II	Water	Radiator	0.30	1.28	250.00	300.00	342.00	200.00	Liquid	271.52	43.38	4.976	10.359
RTHX-459	DP II	Water	Radiator	0.30	1.28	250.00	300.00	342.00	200.00	Liquid	271.56	43.39	4.979	10.359
RTHX-460	DP II	Water	Radiator	0.30	1.28	250.00	300.00	342.00	200.00	Liquid	271.56	43.40	4.980	10.359
RTHX-461	DP II	Water	Radiator	0.30	1.28	250.00	300.00	342.00	200.00	Liquid	272.09	43.81	4.946	10.371
RTHX-462	DP II	Water	Radiator	0.30	1.28	250.00	300.00	342.00	200.00	Liquid	272.28	43.83	4.983	10.374
RTHX-463	DP II	Water	Radiator	0.30	1.28	250.00	300.00	342.00	200.00	Liquid	272.29	43.83	4.983	10.375
RTHX-464	DP II	Water	Radiator	0.30	1.28	250.00	300.00	342.00	200.00	Liquid	272.30	43.88	4.962	10.371
RTHX-465	DP II	Water	Radiator	0.30	1.28	250.00	300.00	342.00	200.00	Liquid	272.46	43.93	4.974	10.371
RTHX-466	DP II	Water	Radiator	0.30	1.28	250.00	300.00	342.00	200.00	Liquid	272.48	43.94	4.975	10.371
RTHX-467	DP II	Water	Radiator	0.30	1.28	250.00	300.00	342.00	200.00	Liquid	272.79	44.12	4.975	10.375
RTHX-468	DP II	Water	Radiator	0.30	1.28	250.00	300.00	342.00	200.00	Liquid	272.80	44.13	4.975	10.375
RTHX-469	DP II	Water	Radiator	0.30	1.28	250.00	300.00	342.00	200.00	Liquid	273.05	44.21	4.995	10.375
RTHX-470	DP II	Water	Radiator	0.30	1.28	250.00	300.00	342.00	200.00	Liquid	273.38	44.40	4.995	10.379
RTHX-471	DP II	Water	Radiator	0.30	1.29	250.00	300.00	342.00	200.00	Liquid	274.91	45.42	4.961	10.403
RTHX-472	DP II	Water	Radiator	0.30	1.29	250.00	300.00	342.00	200.00	Liquid	275.10	45.48	4.975	10.403
RTHX-473	DP II	Water	Radiator	0.30	1.29	250.00	300.00	342.00	200.00	Liquid	275.83	45.90	4.981	10.411
RTHX-474	DP II	Water	Radiator	0.30	1.29	250.00	300.00	342.00	200.00	Liquid	276.45	46.28	4.976	10.420
RTHX-475	DP II	Water	Radiator	0.30	1.29	250.00	300.00	342.00	200.00	Liquid	276.47	46.29	4.977	10.420

Design Tag	Design Problem	Fluid	Application	V_{air}	u_{air}	$\dot{m}_{fluid}$	$T_{air,in}$	$T_{fluid,in}$	$P_{fluid,in}$	$x_{fluid,in}$	h_{air}	ΔP_{air}	ΔP_{fluid}	Q
	-	-	-	m^3/s	m/s	g/s	K	K	kPa	-	$W/m^2.K$	Pa	kPa	kW
RTHX-476	DP II	Water	Radiator	0.30	1.29	250.00	300.00	342.00	200.00	Liquid	276.51	46.30	4.980	10.420
RTHX-477	DP II	Water	Radiator	0.30	1.29	250.00	300.00	342.00	200.00	Liquid	276.51	46.31	4.980	10.420
RTHX-478	DP II	Water	Radiator	0.30	1.29	250.00	300.00	342.00	200.00	Liquid	276.52	46.31	4.981	10.420
RTHX-479	DP II	Water	Radiator	0.30	1.29	250.00	300.00	342.00	200.00	Liquid	277.43	46.93	4.970	10.439
RTHX-480	DP II	Water	Radiator	0.30	1.29	250.00	300.00	342.00	200.00	Liquid	277.45	46.94	4.970	10.439
RTHX-481	DP II	Water	Radiator	0.30	1.29	250.00	300.00	342.00	200.00	Liquid	277.62	47.00	4.983	10.439
RTHX-482	DP II	Water	Radiator	0.30	1.29	250.00	300.00	342.00	200.00	Liquid	277.62	47.00	4.984	10.439
RTHX-483	DP II	Water	Radiator	0.30	1.29	250.00	300.00	342.00	200.00	Liquid	277.64	47.00	4.984	10.439
RTHX-484	DP II	Water	Radiator	0.30	1.29	250.00	300.00	342.00	200.00	Liquid	277.66	47.01	4.985	10.439
RTHX-485	DP II	Water	Radiator	0.30	1.30	250.00	300.00	342.00	200.00	Liquid	277.67	47.05	4.963	10.436
RTHX-486	DP II	Water	Radiator	0.30	1.30	250.00	300.00	342.00	200.00	Liquid	277.86	47.12	4.977	10.436
RTHX-487	DP II	Water	Radiator	0.30	1.30	250.00	300.00	342.00	200.00	Liquid	277.87	47.12	4.978	10.436
RTHX-488	DP II	Water	Radiator	0.30	1.30	250.00	300.00	342.00	200.00	Liquid	278.14	47.20	4.996	10.437
RTHX-489	DP II	Water	Radiator	0.30	1.30	250.00	300.00	342.00	200.00	Liquid	279.41	48.06	4.984	10.460
RTHX-490	DP II	Water	Radiator	0.30	1.30	250.00	300.00	342.00	200.00	Liquid	279.64	48.17	4.976	10.458
RTHX-491	DP II	Water	Radiator	0.30	1.30	250.00	300.00	342.00	200.00	Liquid	279.65	48.18	4.977	10.458
RTHX-492	DP II	Water	Radiator	0.30	1.30	250.00	300.00	342.00	200.00	Liquid	279.70	48.20	4.980	10.458
RTHX-493	DP II	Water	Radiator	0.30	1.30	250.00	300.00	342.00	200.00	Liquid	279.89	48.25	4.993	10.458
RTHX-494	DP II	Water	Radiator	0.30	1.31	250.00	300.00	342.00	200.00	Liquid	280.74	48.84	4.978	10.470
RTHX-495	DP II	Water	Radiator	0.30	1.31	250.00	300.00	342.00	200.00	Liquid	280.75	48.84	4.978	10.470
RTHX-496	DP II	Water	Radiator	0.30	1.31	250.00	300.00	342.00	200.00	Liquid	280.87	48.87	4.985	10.471
RTHX-497	DP II	Water	Radiator	0.30	1.31	250.00	300.00	342.00	200.00	Liquid	282.01	49.66	4.963	10.488
RTHX-498	DP II	Water	Radiator	0.30	1.31	250.00	300.00	342.00	200.00	Liquid	282.02	49.66	4.964	10.488
RTHX-499	DP II	Water	Radiator	0.30	1.31	250.00	300.00	342.00	200.00	Liquid	282.22	49.73	4.977	10.488
RTHX-500	DP II	Water	Radiator	0.30	1.31	250.00	300.00	342.00	200.00	Liquid	282.24	49.73	4.978	10.488
RTHX-501	DP II	Water	Radiator	0.30	1.31	250.00	300.00	342.00	200.00	Liquid	283.27	50.46	4.971	10.508
RTHX-502	DP II	Water	Radiator	0.30	1.31	250.00	300.00	342.00	200.00	Liquid	283.50	50.53	4.985	10.508
RTHX-503	DP II	Water	Radiator	0.30	1.31	250.00	300.00	342.00	200.00	Liquid	283.52	50.54	4.987	10.508
RTHX-504	DP II	Water	Radiator	0.30	1.31	250.00	300.00	342.00	200.00	Liquid	283.74	50.65	4.977	10.505
RTHX-505	DP II	Water	Radiator	0.30	1.31	250.00	300.00	342.00	200.00	Liquid	283.76	50.65	4.977	10.506
RTHX-506	DP II	Water	Radiator	0.30	1.32	250.00	300.00	342.00	200.00	Liquid	283.89	50.69	4.986	10.506
RTHX-507	DP II	Water	Radiator	0.30	1.32	250.00	300.00	342.00	200.00	Liquid	283.92	50.70	4.988	10.506
RTHX-508	DP II	Water	Radiator	0.30	1.32	250.00	300.00	342.00	200.00	Liquid	284.67	51.16	4.986	10.515
RTHX-509	DP II	Water	Radiator	0.30	1.32	250.00	300.00	342.00	200.00	Liquid	285.46	51.64	4.986	10.524
RTHX-510	DP II	Water	Radiator	0.30	1.32	250.00	300.00	342.00	200.00	Liquid	286.66	52.49	4.964	10.541
RTHX-511	DP II	Water	Radiator	0.30	1.32	250.00	300.00	342.00	200.00	Liquid	286.67	52.50	4.964	10.541
RTHX-512	DP II	Water	Radiator	0.30	1.32	250.00	300.00	342.00	200.00	Liquid	286.90	52.57	4.978	10.542
RTHX-513	DP II	Water	Radiator	0.30	1.32	250.00	300.00	342.00	200.00	Liquid	286.92	52.57	4.978	10.542
RTHX-514	DP II	Water	Radiator	0.30	1.32	250.00	300.00	342.00	200.00	Liquid	286.92	52.57	4.979	10.542
RTHX-515	DP II	Water	Radiator	0.30	1.33	250.00	300.00	342.00	200.00	Liquid	287.72	53.06	4.978	10.551
RTHX-516	DP II	Water	Radiator	0.30	1.33	250.00	300.00	342.00	200.00	Liquid	288.26	53.44	4.986	10.562
RTHX-517	DP II	Water	Radiator	0.30	1.33	250.00	300.00	342.00	200.00	Liquid	288.28	53.45	4.988	10.562
RTHX-518	DP II	Water	Radiator	0.30	1.33	250.00	300.00	342.00	200.00	Liquid	288.56	53.57	4.979	10.560
RTHX-519	DP III	R410A	Condenser	1.84	0.94	58.30	308.15	339.75	2488.40	Vapor	171.03	9.67	17.852	11.814

Design Tag	Design Problem	Fluid	Application	V_{air}	u_{air}	$\dot{m}_{fluid}$	$T_{air,in}$	$T_{fluid,in}$	$P_{fluid,in}$	$x_{fluid,in}$	h_{air}	ΔP_{air}	ΔP_{fluid}	Q
	-	-	-	m³/s	m/s	g/s	K	K	kPa	-	W/m².K	Pa	kPa	kW
RTHX-520	DP III	R410A	Condenser	1.84	0.94	58.30	308.15	339.75	2488.40	Vapor	172.86	9.70	18.473	11.811
RTHX-521	DP III	R410A	Condenser	1.84	0.94	58.30	308.15	339.75	2488.40	Vapor	172.89	9.70	18.036	11.816
RTHX-522	DP III	R410A	Condenser	1.84	0.94	58.30	308.15	339.75	2488.40	Vapor	173.15	9.70	18.333	11.817
RTHX-523	DP III	R410A	Condenser	1.84	0.94	58.30	308.15	339.75	2488.40	Vapor	175.67	9.75	20.866	11.823
RTHX-524	DP III	R410A	Condenser	1.84	0.94	58.30	308.15	339.75	2488.40	Vapor	177.70	9.78	22.820	11.826
RTHX-525	DP III	R410A	Condenser	1.84	0.94	58.30	308.15	339.75	2488.40	Vapor	180.32	9.83	27.160	11.833
RTHX-526	DP III	R410A	Condenser	1.84	0.94	58.30	308.15	339.75	2488.40	Vapor	187.24	9.95	20.183	11.825
RTHX-527	DP III	R410A	Condenser	1.84	0.94	58.30	308.15	339.75	2488.40	Vapor	187.72	9.96	20.182	11.825
RTHX-528	DP III	R410A	Condenser	1.84	0.94	58.30	308.15	339.75	2488.40	Vapor	189.94	9.96	20.615	11.825
RTHX-529	DP III	R410A	Condenser	1.84	0.94	58.30	308.15	339.75	2488.40	Vapor	192.80	10.04	23.794	11.833
RTHX-530	DP III	R410A	Condenser	1.84	0.94	58.30	308.15	339.75	2488.40	Vapor	193.31	10.05	24.996	11.832
RTHX-531	DP III	R410A	Condenser	1.84	0.94	58.30	308.15	339.75	2488.40	Vapor	194.36	10.16	23.614	11.838
RTHX-532	DP III	R410A	Condenser	1.84	0.94	58.30	308.15	339.75	2488.40	Vapor	194.39	10.16	23.794	11.837
RTHX-533	DP III	R410A	Condenser	1.84	0.94	58.30	308.15	339.75	2488.40	Vapor	199.20	10.16	20.551	11.829
RTHX-534	DP III	R410A	Condenser	1.84	0.94	58.30	308.15	339.75	2488.40	Vapor	202.19	10.21	23.724	11.835
RTHX-535	DP III	R410A	Condenser	1.84	0.94	58.30	308.15	339.75	2488.40	Vapor	205.78	10.23	22.484	11.834
RTHX-536	DP III	R410A	Condenser	1.84	0.94	58.30	308.15	339.75	2488.40	Vapor	204.30	10.25	25.948	11.838
RTHX-537	DP III	R410A	Condenser	1.84	0.94	58.30	308.15	339.75	2488.40	Vapor	209.61	10.35	20.637	11.835
RTHX-538	DP III	R410A	Condenser	1.84	0.94	58.30	308.15	339.75	2488.40	Vapor	209.75	10.35	22.811	11.835
RTHX-539	DP III	R410A	Condenser	1.84	0.94	58.30	308.15	339.75	2488.40	Vapor	210.72	10.37	23.772	11.837
RTHX-540	DP III	R410A	Condenser	1.84	0.94	58.30	308.15	339.75	2488.40	Vapor	212.94	10.40	26.218	11.840
RTHX-541	DP III	R410A	Condenser	1.84	0.94	58.30	308.15	339.75	2488.40	Vapor	215.62	10.55	23.486	11.842
RTHX-542	DP III	R410A	Condenser	1.84	0.95	58.30	308.15	339.75	2488.40	Vapor	211.27	10.57	26.216	11.833
RTHX-543	DP III	R410A	Condenser	1.84	0.94	58.30	308.15	339.75	2488.40	Vapor	216.02	10.57	23.491	11.842
RTHX-544	DP III	R410A	Condenser	1.84	0.94	58.30	308.15	339.75	2488.40	Vapor	224.00	10.58	20.283	11.833
RTHX-545	DP III	R410A	Condenser	1.84	0.94	58.30	308.15	339.75	2488.40	Vapor	224.50	10.64	12.807	11.833
RTHX-546	DP III	R410A	Condenser	1.84	0.94	58.30	308.15	339.75	2488.40	Vapor	226.18	10.67	21.022	11.835
RTHX-547	DP III	R410A	Condenser	1.84	0.95	58.30	308.15	339.75	2488.40	Vapor	225.21	10.91	19.702	11.828
RTHX-548	DP III	R410A	Condenser	1.84	0.95	58.30	308.15	339.75	2488.40	Vapor	227.49	10.95	21.585	11.832
RTHX-549	DP III	R410A	Condenser	1.84	0.94	58.30	308.15	339.75	2488.40	Vapor	252.14	11.12	12.723	11.836
RTHX-550	DP III	R410A	Condenser	1.84	0.94	58.30	308.15	339.75	2488.40	Vapor	252.68	11.14	12.711	11.836
RTHX-551	DP III	R410A	Condenser	1.84	0.94	58.30	308.15	339.75	2488.40	Vapor	254.62	11.20	24.608	11.846
RTHX-552	DP III	R410A	Condenser	1.84	0.94	58.30	308.15	339.75	2488.40	Vapor	257.04	11.25	23.721	11.845
RTHX-553	DP III	R410A	Condenser	1.84	0.94	58.30	308.15	339.75	2488.40	Vapor	258.44	11.28	26.040	11.844
RTHX-554	DP III	R410A	Condenser	1.84	0.94	58.30	308.15	339.75	2488.40	Vapor	262.45	11.32	30.934	11.850
RTHX-555	DP III	R410A	Condenser	1.84	0.94	58.30	308.15	339.75	2488.40	Vapor	278.21	11.63	20.126	11.843
RTHX-556	DP III	R410A	Condenser	1.84	0.94	58.30	308.15	339.75	2488.40	Vapor	291.22	11.94	25.873	11.851
RTHX-557	DP III	R410A	Condenser	1.84	0.94	58.30	308.15	339.75	2488.40	Vapor	294.30	12.08	23.079	11.860
RTHX-558	DP III	R410A	Condenser	1.84	0.95	58.30	308.15	339.75	2488.40	Vapor	295.23	12.54	15.890	11.863
RTHX-559	DP III	R410A	Condenser	1.84	0.95	58.30	308.15	339.75	2488.40	Vapor	297.51	12.58	15.889	11.863
RTHX-560	DP III	R410A	Condenser	1.84	1.05	58.30	308.15	339.75	2488.40	Vapor	100.21	6.03	12.380	11.826
RTHX-561	DP III	R410A	Condenser	1.84	1.05	58.30	308.15	339.75	2488.40	Vapor	101.47	6.05	13.902	11.820
RTHX-562	DP III	R410A	Condenser	1.84	1.05	58.30	308.15	339.75	2488.40	Vapor	103.19	6.07	16.155	11.825
RTHX-563	DP III	R410A	Condenser	1.84	1.05	58.30	308.15	339.75	2488.40	Vapor	105.52	6.33	17.182	11.837

Design Tag	Design Problem	Fluid	Application	V_{air}	u_{air}	$\dot{m}_{fluid}$	$T_{air,in}$	$T_{fluid,in}$	$P_{fluid,in}$	$x_{fluid,in}$	h_{air}	ΔP_{air}	ΔP_{fluid}	Q
	-	-	-	m^3/s	m/s	g/s	K	K	kPa	-	$W/m^2.K$	Pa	kPa	kW
RTHX-564	DP III	R410A	Condenser	1.84	1.05	58.30	308.15	339.75	2488.40	Vapor	107.11	6.49	17.319	11.846
RTHX-565	DP III	R410A	Condenser	1.84	1.05	58.30	308.15	339.75	2488.40	Vapor	107.27	6.50	17.614	11.846
RTHX-566	DP III	R410A	Condenser	1.84	1.08	58.30	308.15	339.75	2488.40	Vapor	110.25	7.38	26.544	11.803
RTHX-567	DP III	R410A	Condenser	1.84	1.08	58.30	308.15	339.75	2488.40	Vapor	110.50	7.38	26.536	11.805
RTHX-568	DP III	R410A	Condenser	1.84	1.16	58.30	308.15	339.75	2488.40	Vapor	109.86	7.50	15.755	11.800
RTHX-569	DP III	R410A	Condenser	1.84	1.21	58.30	308.15	339.75	2488.40	Vapor	114.23	9.00	14.326	11.816
RTHX-570	DP III	R410A	Condenser	1.84	1.23	58.30	308.15	339.75	2488.40	Vapor	115.78	9.07	15.149	11.811
RTHX-571	DP III	R410A	Condenser	1.84	1.27	58.30	308.15	339.75	2488.40	Vapor	114.63	9.47	8.084	11.815
RTHX-572	DP III	R410A	Condenser	1.84	1.30	58.30	308.15	339.75	2488.40	Vapor	117.47	10.03	13.037	11.816
RTHX-573	DP III	R410A	Condenser	1.84	1.27	58.30	308.15	339.75	2488.40	Vapor	116.79	10.09	14.648	11.808
RTHX-574	DP III	R410A	Condenser	1.84	1.27	58.30	308.15	339.75	2488.40	Vapor	118.86	10.37	13.668	11.825
RTHX-575	DP III	R410A	Evaporator	0.51	1.38	58.30	299.82	285.93	1179.76	0.1924	170.88	28.16	10.992	10.002
RTHX-576	DP III	R410A	Evaporator	0.51	1.38	58.30	299.82	285.93	1179.76	0.1924	170.92	28.17	12.094	10.004
RTHX-577	DP III	R410A	Evaporator	0.51	1.38	58.30	299.82	285.93	1179.76	0.1924	171.47	28.21	10.572	10.004
RTHX-578	DP III	R410A	Evaporator	0.51	1.38	58.30	299.82	285.93	1179.76	0.1924	184.79	28.50	11.935	10.010
RTHX-579	DP III	R410A	Evaporator	0.51	1.38	58.30	299.82	285.93	1179.76	0.1924	186.76	28.55	10.570	10.013
RTHX-580	DP III	R410A	Evaporator	0.51	1.38	58.30	299.82	285.93	1179.76	0.1924	189.40	28.64	11.126	10.015
RTHX-581	DP III	R410A	Evaporator	0.51	1.38	58.30	299.82	285.93	1179.76	0.1924	192.92	28.73	10.572	10.014
RTHX-582	DP III	R410A	Evaporator	0.51	1.38	58.30	299.82	285.93	1179.76	0.1924	193.36	28.74	10.729	10.014
RTHX-583	DP III	R410A	Evaporator	0.51	1.38	58.30	299.82	285.93	1179.76	0.1924	194.61	28.79	10.717	10.019
RTHX-584	DP III	R410A	Evaporator	0.51	1.38	58.30	299.82	285.93	1179.76	0.1924	195.75	28.83	11.129	10.016
RTHX-585	DP III	R410A	Evaporator	0.51	1.38	58.30	299.82	285.93	1179.76	0.1924	197.13	28.91	11.348	10.020
RTHX-586	DP III	R410A	Evaporator	0.51	1.38	58.30	299.82	285.93	1179.76	0.1924	198.10	28.95	11.141	10.019
RTHX-587	DP III	R410A	Evaporator	0.51	1.38	58.30	299.82	285.93	1179.76	0.1924	199.90	28.95	10.541	10.017
RTHX-588	DP III	R410A	Evaporator	0.51	1.38	58.30	299.82	285.93	1179.76	0.1924	199.81	28.97	11.283	10.021
RTHX-589	DP III	R410A	Evaporator	0.51	1.38	58.30	299.82	285.93	1179.76	0.1924	201.19	29.00	10.542	10.018
RTHX-590	DP III	R410A	Evaporator	0.51	1.38	58.30	299.82	285.93	1179.76	0.1924	199.26	29.37	15.235	10.077
RTHX-591	DP III	R410A	Evaporator	0.51	1.39	58.30	299.82	285.93	1179.76	0.1924	202.04	29.52	10.459	10.008
RTHX-592	DP III	R410A	Evaporator	0.51	1.38	58.30	299.82	285.93	1179.76	0.1924	204.34	29.53	15.239	10.081
RTHX-593	DP III	R410A	Evaporator	0.51	1.38	58.30	299.82	285.93	1179.76	0.1924	200.19	29.85	11.845	10.005
RTHX-594	DP III	R410A	Evaporator	0.51	1.38	58.30	299.82	285.93	1179.76	0.1924	198.73	29.86	12.754	10.028
RTHX-595	DP III	R410A	Evaporator	0.51	1.38	58.30	299.82	285.93	1179.76	0.1924	198.41	29.87	14.117	10.029
RTHX-596	DP III	R410A	Evaporator	0.51	1.38	58.30	299.82	285.93	1179.76	0.1924	199.36	29.87	12.415	10.023
RTHX-597	DP III	R410A	Evaporator	0.51	1.38	58.30	299.82	285.93	1179.76	0.1924	198.77	29.87	13.182	10.029
RTHX-598	DP III	R410A	Evaporator	0.51	1.38	58.30	299.82	285.93	1179.76	0.1924	199.94	29.89	12.713	10.029
RTHX-599	DP III	R410A	Evaporator	0.51	1.38	58.30	299.82	285.93	1179.76	0.1924	200.26	29.91	12.929	10.030
RTHX-600	DP III	R410A	Evaporator	0.51	1.38	58.30	299.82	285.93	1179.76	0.1924	201.02	29.91	12.415	10.022
RTHX-601	DP III	R410A	Evaporator	0.51	1.38	58.30	299.82	285.93	1179.76	0.1924	202.22	29.93	12.491	10.017
RTHX-602	DP III	R410A	Evaporator	0.51	1.38	58.30	299.82	285.93	1179.76	0.1924	201.62	29.94	12.755	10.027
RTHX-603	DP III	R410A	Evaporator	0.51	1.38	58.30	299.82	285.93	1179.76	0.1924	203.32	29.99	12.756	10.028
RTHX-604	DP III	R410A	Evaporator	0.51	1.38	58.30	299.82	285.93	1179.76	0.1924	204.37	30.00	12.493	10.019
RTHX-605	DP III	R410A	Evaporator	0.51	1.38	58.30	299.82	285.93	1179.76	0.1924	205.53	30.07	13.186	10.030
RTHX-606	DP III	R410A	Evaporator	0.51	1.38	58.30	299.82	285.93	1179.76	0.1924	206.13	30.07	12.758	10.030
RTHX-607	DP III	R410A	Evaporator	0.51	1.38	58.30	299.82	285.93	1179.76	0.1924	206.79	30.09	12.758	10.031

Design Tag	Design Problem	Fluid	Application	V_{air}	u_{air}	$\dot{m}_{fluid}$	$T_{air,in}$	$T_{fluid,in}$	$P_{fluid,in}$	$x_{fluid,in}$	h_{air}	ΔP_{air}	ΔP_{fluid}	Q
	-	-	-	m³/s	m/s	g/s	K	K	kPa	-	W/m².K	Pa	kPa	kW
RTHX-608	DP III	R410A	Evaporator	0.51	1.38	58.30	299.82	285.93	1179.76	0.1924	208.80	30.15	12.760	10.032
RTHX-609	DP III	R410A	Evaporator	0.51	1.38	58.30	299.82	285.93	1179.76	0.1924	283.80	31.19	10.294	10.008
RTHX-610	DP III	R410A	Evaporator	1.51	4.20	58.30	299.82	285.93	1179.76	0.1924	172.23	20.49	11.999	10.129
RTHX-611	DP III	R410A	Evaporator	2.51	6.96	58.30	299.82	285.93	1179.76	0.1924	174.10	21.69	11.859	10.108
RTHX-612	DP III	R410A	Evaporator	3.51	9.74	58.30	299.82	285.93	1179.76	0.1924	175.98	21.77	13.170	10.117
RTHX-613	DP III	R410A	Evaporator	4.51	12.40	58.30	299.82	285.93	1179.76	0.1924	183.15	21.80	13.124	10.196
RTHX-614	DP III	R410A	Evaporator	5.51	15.89	58.30	299.82	285.93	1179.76	0.1924	179.25	23.34	12.736	10.089
RTHX-615	DP III	R410A	Evaporator	6.51	19.31	58.30	299.82	285.93	1179.76	0.1924	178.52	23.64	12.338	10.066
RTHX-616	DP III	R410A	Evaporator	7.51	21.26	58.30	299.82	285.93	1179.76	0.1924	193.58	26.96	13.732	10.194
RTHX-617	DP III	R410A	Evaporator	8.51	25.25	58.30	299.82	285.93	1179.76	0.1924	199.53	30.16	12.864	10.211
RTHX-618	DP III	R410A	Evaporator	9.51	27.18	58.30	299.82	285.93	1179.76	0.1924	202.21	31.08	13.411	10.212
RTHX-619	DP III	R410A	Evaporator	10.51	30.04	58.30	299.82	285.93	1179.76	0.1924	202.51	31.09	13.610	10.213

FTHX

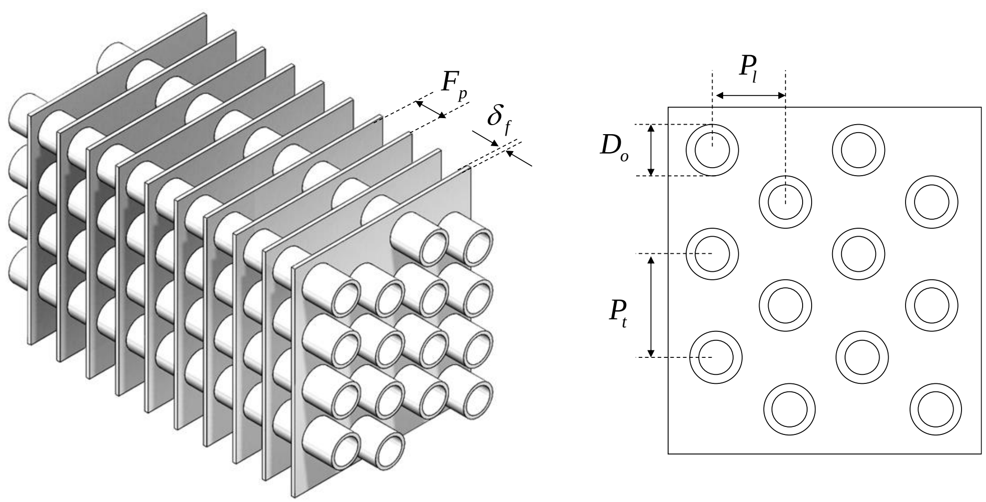

Figure 130. Flat fin and tube HX (FTHX).

Table 32. FTHX optimum designs dimensions.

Design Tag	Arrangement	D_o	D_i	P_l	P_t	FPI	δ_f	N_r	N_t	Passes	l	H	d	A_f	V	$V_{mat'l}$
	-	mm	mm	mm	mm	in^{-1}	mm	-	-	%	m	m	m	m^2	cm^3	cm^3
FTHX-001	Staggered	1	0.4014	0.8067	1.3168	5.3226	0.115	6	245	100	0.0873	0.3226	0.0048	0.028	136.3	15.9
FTHX-002	Staggered	1	0.4014	0.8059	1.2485	5.0098	0.115	6	245	100	0.0820	0.3059	0.0048	0.025	121.2	14.6
FTHX-003	Staggered	1	0.4014	0.8051	1.1096	5.0098	0.115	6	230	100	0.0760	0.2552	0.0048	0.019	93.7	12.4
FTHX-004	Staggered	1	0.3838	0.7713	1.1052	5.3177	0.115	6	245	100	0.0766	0.2708	0.0046	0.021	96.1	12.5
FTHX-005	Staggered	1	0.4025	0.8089	1.1630	6.2708	0.115	6	230	100	0.0800	0.2675	0.0049	0.021	103.8	13.9
FTHX-006	Staggered	1	0.4014	0.8028	1.2430	5.3666	0.115	6	230	100	0.0873	0.2859	0.0048	0.025	120.2	14.8
FTHX-007	Staggered	1	0.3926	0.8013	1.0354	6.2610	0.115	6	230	100	0.0720	0.2381	0.0048	0.017	82.4	11.7
FTHX-008	Staggered	1	0.4014	0.8161	1.3231	5.0538	0.115	6	245	100	0.0873	0.3242	0.0049	0.028	138.5	15.8
FTHX-009	Staggered	1	0.4014	0.8067	1.1598	5.0489	0.115	6	230	100	0.0793	0.2668	0.0048	0.021	102.4	13.1
FTHX-010	Staggered	1	0.4014	0.8036	1.2289	5.6745	0.115	6	230	100	0.0873	0.2826	0.0048	0.025	118.9	14.9
FTHX-011	Staggered	1	0.4190	0.8519	1.3811	5.0489	0.115	6	245	100	0.1086	0.3384	0.0051	0.037	187.7	21.4
FTHX-012	Staggered	1	0.4014	0.8067	1.3231	5.3666	0.115	6	250	100	0.0873	0.3308	0.0048	0.029	139.7	16.3
FTHX-013	Staggered	1	0.4190	0.8519	1.3811	5.0489	0.115	6	245	100	0.0979	0.3384	0.0051	0.033	169.3	19.3
FTHX-014	Staggered	1	0.3937	0.7912	1.1376	5.3324	0.115	6	230	100	0.0800	0.2616	0.0047	0.021	99.3	12.8
FTHX-015	Staggered	1	0.3926	0.7875	1.0838	5.0391	0.115	6	230	100	0.0773	0.2493	0.0047	0.019	91.1	12.1
FTHX-016	Staggered	1	0.4014	0.8028	1.0586	5.0000	0.115	6	230	100	0.0773	0.2435	0.0048	0.019	90.7	12.6
FTHX-017	Staggered	1	0.4014	0.8051	1.1096	5.0000	0.115	6	230	100	0.0773	0.2552	0.0048	0.020	95.3	12.7
FTHX-018	Staggered	1	0.4014	0.8059	1.2360	5.0489	0.115	6	245	100	0.0873	0.3028	0.0048	0.026	127.8	15.5
FTHX-019	Staggered	1	0.4014	0.8161	1.3231	5.0098	0.115	6	245	100	0.0879	0.3242	0.0049	0.029	139.6	15.9
FTHX-020	Staggered	1	0.3926	0.8013	1.1713	5.3617	0.115	6	245	100	0.0806	0.2870	0.0048	0.023	111.2	13.9
FTHX-021	Staggered	1	0.4036	0.8072	1.0644	5.3226	0.115	6	230	100	0.0720	0.2448	0.0048	0.018	85.4	11.9
FTHX-022	Staggered	1	0.4410	0.8966	1.4768	5.4057	0.115	6	250	100	0.0886	0.3692	0.0054	0.033	176.0	20.1
FTHX-023	Staggered	1	0.4014	0.8067	1.3074	6.2610	0.115	6	245	100	0.0873	0.3203	0.0048	0.028	135.3	16.5
FTHX-024	Staggered	1	0.3926	0.8013	1.1713	5.0196	0.115	6	250	100	0.0813	0.2928	0.0048	0.024	114.5	14.1
FTHX-025	Staggered	1	0.4025	0.8050	1.1127	5.0000	0.115	6	230	100	0.0773	0.2559	0.0048	0.020	95.6	12.7
FTHX-026	Staggered	1	0.4014	0.8051	1.1096	5.0049	0.115	6	230	100	0.0766	0.2552	0.0048	0.020	94.5	12.6
FTHX-027	Staggered	1	0.4014	0.8161	1.1897	5.0098	0.115	6	230	100	0.0820	0.2736	0.0049	0.022	109.8	13.6
FTHX-028	Staggered	1	0.4014	0.8036	1.1912	5.0489	0.115	6	235	100	0.0820	0.2799	0.0048	0.023	110.6	13.9
FTHX-029	Staggered	1	0.4014	0.8036	1.3231	5.0880	0.115	6	245	100	0.0899	0.3242	0.0048	0.029	140.6	16.3
FTHX-030	Staggered	1	0.4014	0.8059	1.2485	5.3861	0.115	6	230	100	0.0873	0.2872	0.0048	0.025	121.2	14.8
FTHX-031	Staggered	1	0.3849	0.7758	0.9496	5.3275	0.115	6	230	100	0.0720	0.2184	0.0047	0.016	73.2	10.8
FTHX-032	Staggered	1	0.4190	0.8519	1.4138	5.0391	0.115	6	245	100	0.1072	0.3464	0.0051	0.037	189.8	21.2
FTHX-033	Staggered	1	0.4014	0.8059	1.2462	5.4448	0.115	6	245	100	0.0806	0.3053	0.0048	0.025	119.0	14.6
FTHX-034	Staggered	1	0.4025	0.8152	1.3283	5.0098	0.115	6	245	100	0.0899	0.3254	0.0049	0.029	143.2	16.3
FTHX-035	Staggered	1	0.4014	0.8067	1.0594	5.0196	0.115	6	230	100	0.0766	0.2437	0.0048	0.019	90.4	12.5
FTHX-036	Staggered	1	0.4014	0.8114	1.3231	5.0929	0.115	6	245	100	0.0873	0.3242	0.0049	0.028	137.7	15.8
FTHX-037	Staggered	1	0.4025	0.8089	1.3267	5.0489	0.115	6	245	100	0.0899	0.3250	0.0049	0.029	141.9	16.3
FTHX-038	Staggered	1	0.4014	0.8059	1.2462	5.3666	0.115	6	245	100	0.0873	0.3053	0.0048	0.027	128.9	15.8
FTHX-039	Staggered	1	0.4025	0.8050	1.1127	5.3226	0.115	6	230	100	0.0766	0.2559	0.0048	0.020	94.7	12.8
FTHX-040	Staggered	1	0.4014	0.8059	1.3097	5.1271	0.115	6	245	100	0.0873	0.3209	0.0048	0.028	135.4	15.8
FTHX-041	Staggered	1	0.4014	0.8193	1.1912	5.3226	0.115	6	230	100	0.0820	0.2740	0.0049	0.022	110.4	13.8

Design Tag	Arrangement	D_o	D_i	P_l	P_t	FPI	δ_f	N_r	N_t	Passes	l	H	d	A_f	V	$V_{mat'l}$
	-	mm	mm	mm	mm	in^{-1}	mm	-	-	%	m	m	m	m^2	cm^3	cm^3
FTHX-042	Staggered	1	0.4036	0.8103	1.3303	5.0147	0.115	6	245	100	0.0899	0.3259	0.0049	0.029	142.5	16.4
FTHX-043	Staggered	1	0.4366	0.8774	1.4391	5.0147	0.115	6	245	100	0.0899	0.3526	0.0053	0.032	166.9	19.2
FTHX-044	Staggered	1	0.4212	0.8564	1.4278	5.0196	0.115	6	245	100	0.1092	0.3498	0.0051	0.038	196.3	21.9
FTHX-045	Staggered	1	0.4014	0.8067	1.0657	5.0196	0.115	6	230	100	0.0766	0.2451	0.0048	0.019	90.9	12.5
FTHX-046	Staggered	1	0.4014	0.8067	1.2477	5.0098	0.115	6	245	100	0.0873	0.3057	0.0048	0.027	129.1	15.6
FTHX-047	Staggered	1	0.4014	0.8028	1.0335	9.1153	0.115	6	205	100	0.0773	0.2119	0.0048	0.016	78.9	12.6
FTHX-048	Staggered	1	0.4025	0.8058	1.3259	5.3275	0.115	6	250	100	0.0899	0.3315	0.0048	0.030	144.1	16.8
FTHX-049	Staggered	1	0.4014	0.8036	1.3231	5.3421	0.115	6	245	100	0.0873	0.3242	0.0048	0.028	136.4	15.9
FTHX-050	Staggered	1	0.4410	0.8966	1.4768	5.3617	0.115	6	250	100	0.0899	0.3692	0.0054	0.033	178.6	20.4
FTHX-051	Staggered	1	0.4014	0.8036	1.2226	5.6745	0.115	6	230	100	0.0873	0.2812	0.0048	0.025	118.3	14.9
FTHX-052	Staggered	1	0.4014	0.8028	1.0092	5.3226	0.115	6	205	100	0.0766	0.2069	0.0048	0.016	76.4	11.1
FTHX-053	Staggered	1	0.4047	0.8450	1.3640	5.0587	0.115	6	245	100	0.0906	0.3342	0.0051	0.030	153.5	16.8
FTHX-054	Staggered	1	0.4014	0.8059	1.2485	5.3812	0.115	6	245	100	0.0873	0.3059	0.0048	0.027	129.1	15.8
FTHX-055	Staggered	1	0.3926	0.8013	1.1713	5.0196	0.115	6	245	100	0.0766	0.2870	0.0048	0.022	105.7	13.0
FTHX-056	Staggered	1	0.4014	0.8114	1.3223	5.0098	0.115	6	245	100	0.0879	0.3240	0.0049	0.028	138.7	15.9
FTHX-057	Staggered	1	0.4014	0.8067	1.3113	5.3177	0.115	6	245	100	0.0873	0.3213	0.0048	0.028	135.7	15.9
FTHX-058	Staggered	1	0.3849	0.7758	0.9496	5.0147	0.115	6	230	100	0.0713	0.2184	0.0047	0.016	72.5	10.6
FTHX-059	Staggered	1	0.3926	0.8013	1.1713	5.3617	0.115	6	245	100	0.0813	0.2870	0.0048	0.023	112.2	14.0
FTHX-060	Staggered	1	0.4014	0.8161	1.3450	5.0489	0.115	6	245	100	0.0899	0.3295	0.0049	0.030	145.1	16.3
FTHX-061	Staggered	1	0.4014	0.8059	1.2360	5.0489	0.115	6	245	100	0.0899	0.3028	0.0048	0.027	131.7	16.0
FTHX-062	Staggered	1	0.4014	0.8028	1.0586	6.2610	0.115	6	230	100	0.0720	0.2435	0.0048	0.018	84.4	12.2
FTHX-063	Staggered	1	0.4014	0.8036	1.2289	5.3226	0.115	6	230	100	0.0860	0.2826	0.0048	0.024	117.1	14.5
FTHX-064	Staggered	1	0.4014	0.8028	1.0304	9.1153	0.115	6	205	100	0.0773	0.2112	0.0048	0.016	78.7	12.6
FTHX-065	Staggered	1	0.3926	0.7890	1.1651	5.0489	0.115	6	235	100	0.0820	0.2738	0.0047	0.022	106.2	13.3
FTHX-066	Staggered	1	0.4014	0.8059	1.2422	5.0489	0.115	6	245	100	0.0899	0.3043	0.0048	0.027	132.4	16.0
FTHX-067	Staggered	1	0.4014	0.8067	1.2477	5.0098	0.115	6	230	100	0.0879	0.2870	0.0048	0.025	122.2	14.7
FTHX-068	Staggered	1	0.4047	0.8133	1.1694	6.2708	0.115	6	230	100	0.0800	0.2690	0.0049	0.022	105.0	14.0
FTHX-069	Staggered	1	0.4014	0.8067	1.0586	6.2610	0.115	6	230	100	0.0720	0.2435	0.0048	0.018	84.8	12.2
FTHX-070	Staggered	1	0.4014	0.8059	1.2430	5.3666	0.115	6	245	100	0.0873	0.3045	0.0048	0.027	128.5	15.8
FTHX-071	Staggered	1	0.4212	0.8564	1.4147	5.3275	0.115	6	245	100	0.0899	0.3466	0.0051	0.031	160.2	18.2
FTHX-072	Staggered	1	0.4190	0.8421	1.3680	5.0489	0.115	6	245	100	0.1086	0.3351	0.0051	0.036	183.8	21.3
FTHX-073	Staggered	1	0.4025	0.8089	1.3574	5.3617	0.115	6	245	100	0.0899	0.3326	0.0049	0.030	145.2	16.6
FTHX-074	Staggered	1	0.4025	0.8089	1.3259	5.3275	0.115	6	250	100	0.0886	0.3315	0.0049	0.029	142.6	16.6
FTHX-075	Staggered	1	0.4014	0.8028	1.1096	5.3275	0.115	6	230	100	0.0766	0.2552	0.0048	0.020	94.2	12.7
FTHX-076	Staggered	1	0.4014	0.8059	1.2540	5.3666	0.115	6	245	100	0.0906	0.3072	0.0048	0.028	134.6	16.4
FTHX-077	Staggered	1	0.4014	0.8059	1.2485	5.9384	0.115	6	245	100	0.0899	0.3059	0.0048	0.028	133.0	16.6
FTHX-078	Staggered	1	0.4014	0.8059	1.2493	5.3617	0.115	6	245	100	0.0873	0.3061	0.0048	0.027	129.2	15.8
FTHX-079	Staggered	1	0.4069	0.8138	1.0731	6.2610	0.115	6	230	100	0.0720	0.2468	0.0049	0.018	86.8	12.5
FTHX-080	Staggered	1	0.4014	0.8028	1.0084	9.0762	0.115	6	205	100	0.0766	0.2067	0.0048	0.016	76.3	12.4
FTHX-081	Staggered	1	0.4366	0.8877	1.4391	5.3617	0.115	6	245	100	0.0899	0.3526	0.0053	0.032	168.9	19.5
FTHX-082	Staggered	1	0.4014	0.8067	1.2132	5.0489	0.115	6	230	100	0.0853	0.2790	0.0048	0.024	115.2	14.2
FTHX-083	Staggered	1	0.4025	0.8081	1.3259	5.0684	0.115	6	250	100	0.0873	0.3315	0.0048	0.029	140.3	16.2
FTHX-084	Staggered	1	0.4014	0.8036	1.2226	5.0196	0.115	6	245	100	0.0879	0.2995	0.0048	0.026	127.0	15.6
FTHX-085	Staggered	1	0.3926	0.7890	1.0838	5.0000	0.115	6	230	100	0.0773	0.2493	0.0047	0.019	91.2	12.1

Design Tag	Arrangement	D_o	D_i	P_l	P_t	FPI	δ_f	N_r	N_t	Passes	l	H	d	A_f	V	$V_{mat'l}$
	-	mm	mm	mm	mm	in^{-1}	mm	-	-	%	m	m	m	m^2	cm^3	cm^3
FTHX-086	Staggered	1	0.4014	0.8067	1.1096	5.0196	0.115	6	230	100	0.0766	0.2552	0.0048	0.020	94.7	12.6
FTHX-087	Staggered	1	0.4014	0.8059	1.2101	5.9384	0.115	6	245	100	0.0793	0.2965	0.0048	0.024	113.7	14.5
FTHX-088	Staggered	1	0.4025	0.8089	1.3519	5.3275	0.115	6	245	100	0.0899	0.3312	0.0049	0.030	144.6	16.6
FTHX-089	Staggered	1	0.4014	0.8059	1.2422	5.3666	0.115	6	245	100	0.0906	0.3043	0.0048	0.028	133.3	16.3
FTHX-090	Staggered	1	0.4047	0.8450	1.3656	5.0196	0.115	6	245	100	0.0906	0.3346	0.0051	0.030	153.7	16.8
FTHX-091	Staggered	1	0.4025	0.8404	1.3582	5.1271	0.115	6	245	100	0.0906	0.3328	0.0050	0.030	152.0	16.7
FTHX-092	Staggered	1	0.4036	0.8072	1.0936	5.0147	0.115	6	230	100	0.0713	0.2515	0.0048	0.018	86.9	11.8
FTHX-093	Staggered	1	0.4014	0.8059	1.2422	5.3617	0.115	6	245	100	0.0813	0.3043	0.0048	0.025	119.6	14.7

Table 33. Optimum FTHX performance and operating conditions.

Design Tag	Design Problem	Fluid	Application	V_{air}	u_{air}	$\dot{m}_{fluid}$	$T_{air,in}$	$T_{fluid,in}$	$P_{fluid,in}$	$x_{fluid,in}$	h_{air}	ΔP_{air}	ΔP_{fluid}	Q
	-	-	-	m^3/s	m/s	g/s	K	K	kPa	-	$W/m^2.K$	Pa	kPa	kW
FTHX-001	DP I	Water	Radiator	0.03	1.07	25.00	300.00	342.00	200.00	Liquid	210.38	13.19	0.926	1.003
FTHX-002	DP I	Water	Radiator	0.03	1.20	25.00	300.00	342.00	200.00	Liquid	230.32	17.24	0.870	1.005
FTHX-003	DP I	Water	Radiator	0.03	1.55	25.00	300.00	342.00	200.00	Liquid	279.15	33.20	0.860	1.011
FTHX-004	DP I	Water	Radiator	0.03	1.45	25.00	300.00	342.00	200.00	Liquid	268.94	27.52	0.974	1.015
FTHX-005	DP I	Water	Radiator	0.03	1.40	25.00	300.00	342.00	200.00	Liquid	251.09	25.98	0.895	1.008
FTHX-006	DP I	Water	Radiator	0.03	1.20	25.00	300.00	342.00	200.00	Liquid	228.96	17.70	0.987	1.005
FTHX-007	DP I	Water	Radiator	0.03	1.75	25.00	300.00	342.00	200.00	Liquid	297.84	45.69	0.890	1.013
FTHX-008	DP I	Water	Radiator	0.03	1.06	25.00	300.00	342.00	200.00	Liquid	210.55	12.94	0.926	1.001
FTHX-009	DP I	Water	Radiator	0.03	1.42	25.00	300.00	342.00	200.00	Liquid	260.52	26.14	0.897	1.006
FTHX-010	DP I	Water	Radiator	0.03	1.22	25.00	300.00	342.00	200.00	Liquid	231.17	18.45	0.987	1.011
FTHX-011	DP I	Water	Radiator	0.03	0.82	25.00	300.00	342.00	200.00	Liquid	191.30	8.37	0.974	1.072
FTHX-012	DP I	Water	Radiator	0.03	1.04	25.00	300.00	342.00	200.00	Liquid	207.86	12.62	0.908	1.007
FTHX-013	DP I	Water	Radiator	0.03	0.91	25.00	300.00	342.00	200.00	Liquid	196.27	9.92	0.877	1.041
FTHX-014	DP I	Water	Radiator	0.03	1.43	25.00	300.00	342.00	200.00	Liquid	262.99	26.90	0.977	1.007
FTHX-015	DP I	Water	Radiator	0.03	1.56	25.00	300.00	342.00	200.00	Liquid	283.92	33.80	0.956	1.017
FTHX-016	DP I	Water	Radiator	0.03	1.59	25.00	300.00	342.00	200.00	Liquid	291.35	38.77	0.876	1.033
FTHX-017	DP I	Water	Radiator	0.03	1.52	25.00	300.00	342.00	200.00	Liquid	277.19	32.13	0.875	1.017
FTHX-018	DP I	Water	Radiator	0.03	1.14	25.00	300.00	342.00	200.00	Liquid	229.05	16.23	0.928	1.028
FTHX-019	DP I	Water	Radiator	0.03	1.05	25.00	300.00	342.00	200.00	Liquid	210.43	12.70	0.934	1.004
FTHX-020	DP I	Water	Radiator	0.03	1.30	25.00	300.00	342.00	200.00	Liquid	246.91	21.37	0.936	1.018
FTHX-021	DP I	Water	Radiator	0.03	1.70	25.00	300.00	342.00	200.00	Liquid	296.83	43.20	0.797	1.016
FTHX-022	DP I	Water	Radiator	0.03	0.92	25.00	300.00	342.00	200.00	Liquid	184.85	9.81	0.633	1.013
FTHX-023	DP I	Water	Radiator	0.03	1.07	25.00	300.00	342.00	200.00	Liquid	206.28	13.68	0.927	1.005
FTHX-024	DP I	Water	Radiator	0.03	1.26	25.00	300.00	342.00	200.00	Liquid	246.65	20.33	0.925	1.025
FTHX-025	DP I	Water	Radiator	0.03	1.52	25.00	300.00	342.00	200.00	Liquid	276.46	31.99	0.865	1.017
FTHX-026	DP I	Water	Radiator	0.03	1.53	25.00	300.00	342.00	200.00	Liquid	278.16	32.62	0.867	1.016
FTHX-027	DP I	Water	Radiator	0.03	1.34	25.00	300.00	342.00	200.00	Liquid	249.53	22.46	0.927	1.007
FTHX-028	DP I	Water	Radiator	0.03	1.31	25.00	300.00	342.00	200.00	Liquid	247.49	21.73	0.908	1.012

Design Tag	Design Problem	Fluid	Application	V_{air}	u_{air}	$\dot{m}_{fluid}$	$T_{air,in}$	$T_{fluid,in}$	$P_{fluid,in}$	$x_{fluid,in}$	h_{air}	ΔP_{air}	ΔP_{fluid}	Q
	-	-	-	m^3/s	m/s	g/s	K	K	kPa	-	$W/m^2.K$	Pa	kPa	kW
FTHX-029	DP I	Water	Radiator	0.03	1.03	25.00	300.00	342.00	200.00	Liquid	209.32	12.40	0.955	1.012
FTHX-030	DP I	Water	Radiator	0.03	1.20	25.00	300.00	342.00	200.00	Liquid	227.87	17.41	0.987	1.003
FTHX-031	DP I	Water	Radiator	0.03	1.91	25.00	300.00	342.00	200.00	Liquid	331.20	62.56	0.965	1.034
FTHX-032	DP I	Water	Radiator	0.03	0.81	25.00	300.00	342.00	200.00	Liquid	187.16	7.97	0.962	1.062
FTHX-033	DP I	Water	Radiator	0.03	1.22	25.00	300.00	342.00	200.00	Liquid	229.51	17.98	0.856	1.001
FTHX-034	DP I	Water	Radiator	0.03	1.02	25.00	300.00	342.00	200.00	Liquid	208.53	12.20	0.945	1.009
FTHX-035	DP I	Water	Radiator	0.03	1.61	25.00	300.00	342.00	200.00	Liquid	291.62	39.13	0.868	1.031
FTHX-036	DP I	Water	Radiator	0.03	1.06	25.00	300.00	342.00	200.00	Liquid	210.49	12.97	0.926	1.001
FTHX-037	DP I	Water	Radiator	0.03	1.03	25.00	300.00	342.00	200.00	Liquid	208.87	12.27	0.945	1.009
FTHX-038	DP I	Water	Radiator	0.03	1.13	25.00	300.00	342.00	200.00	Liquid	224.74	15.86	0.928	1.024
FTHX-039	DP I	Water	Radiator	0.03	1.53	25.00	300.00	342.00	200.00	Liquid	275.09	32.56	0.858	1.015
FTHX-040	DP I	Water	Radiator	0.03	1.07	25.00	300.00	342.00	200.00	Liquid	214.61	13.40	0.927	1.007
FTHX-041	DP I	Water	Radiator	0.03	1.34	25.00	300.00	342.00	200.00	Liquid	246.92	22.40	0.927	1.007
FTHX-042	DP I	Water	Radiator	0.03	1.02	25.00	300.00	342.00	200.00	Liquid	208.59	12.24	0.934	1.010
FTHX-043	DP I	Water	Radiator	0.03	0.95	25.00	300.00	342.00	200.00	Liquid	193.16	10.59	0.683	1.016
FTHX-044	DP I	Water	Radiator	0.03	0.79	25.00	300.00	342.00	200.00	Liquid	184.60	7.54	0.960	1.066
FTHX-045	DP I	Water	Radiator	0.03	1.60	25.00	300.00	342.00	200.00	Liquid	289.94	38.22	0.868	1.029
FTHX-046	DP I	Water	Radiator	0.03	1.12	25.00	300.00	342.00	200.00	Liquid	226.65	15.72	0.928	1.025
FTHX-047	DP I	Water	Radiator	0.03	1.83	25.00	300.00	342.00	200.00	Liquid	283.99	53.51	0.981	1.004
FTHX-048	DP I	Water	Radiator	0.03	1.01	25.00	300.00	342.00	200.00	Liquid	206.23	11.99	0.926	1.016
FTHX-049	DP I	Water	Radiator	0.03	1.06	25.00	300.00	342.00	200.00	Liquid	208.96	13.03	0.926	1.000
FTHX-050	DP I	Water	Radiator	0.03	0.90	25.00	300.00	342.00	200.00	Liquid	184.49	9.57	0.643	1.017
FTHX-051	DP I	Water	Radiator	0.03	1.22	25.00	300.00	342.00	200.00	Liquid	232.66	18.76	0.987	1.013
FTHX-052	DP I	Water	Radiator	0.03	1.89	25.00	300.00	342.00	200.00	Liquid	320.76	58.03	0.973	1.018
FTHX-053	DP I	Water	Radiator	0.03	0.99	25.00	300.00	342.00	200.00	Liquid	200.66	11.02	0.931	1.007
FTHX-054	DP I	Water	Radiator	0.03	1.12	25.00	300.00	342.00	200.00	Liquid	223.76	15.75	0.928	1.023
FTHX-055	DP I	Water	Radiator	0.03	1.36	25.00	300.00	342.00	200.00	Liquid	253.65	23.05	0.889	1.003
FTHX-056	DP I	Water	Radiator	0.03	1.05	25.00	300.00	342.00	200.00	Liquid	210.71	12.79	0.934	1.004
FTHX-057	DP I	Water	Radiator	0.03	1.07	25.00	300.00	342.00	200.00	Liquid	211.45	13.39	0.927	1.005
FTHX-058	DP I	Water	Radiator	0.03	1.93	25.00	300.00	342.00	200.00	Liquid	335.63	63.36	0.956	1.033
FTHX-059	DP I	Water	Radiator	0.03	1.29	25.00	300.00	342.00	200.00	Liquid	245.99	20.98	0.944	1.019
FTHX-060	DP I	Water	Radiator	0.03	1.01	25.00	300.00	342.00	200.00	Liquid	205.14	11.66	0.955	1.003
FTHX-061	DP I	Water	Radiator	0.03	1.10	25.00	300.00	342.00	200.00	Liquid	227.13	15.47	0.957	1.036
FTHX-062	DP I	Water	Radiator	0.03	1.71	25.00	300.00	342.00	200.00	Liquid	291.33	43.97	0.814	1.013
FTHX-063	DP I	Water	Radiator	0.03	1.23	25.00	300.00	342.00	200.00	Liquid	234.43	18.86	0.972	1.007
FTHX-064	DP I	Water	Radiator	0.03	1.84	25.00	300.00	342.00	200.00	Liquid	284.74	54.31	0.981	1.005
FTHX-065	DP I	Water	Radiator	0.03	1.34	25.00	300.00	342.00	200.00	Liquid	253.02	22.60	0.992	1.011
FTHX-066	DP I	Water	Radiator	0.03	1.10	25.00	300.00	342.00	200.00	Liquid	225.75	15.19	0.956	1.034
FTHX-067	DP I	Water	Radiator	0.03	1.19	25.00	300.00	342.00	200.00	Liquid	230.31	17.14	0.995	1.007
FTHX-068	DP I	Water	Radiator	0.03	1.39	25.00	300.00	342.00	200.00	Liquid	249.72	25.73	0.875	1.009
FTHX-069	DP I	Water	Radiator	0.03	1.71	25.00	300.00	342.00	200.00	Liquid	291.34	43.93	0.815	1.013
FTHX-070	DP I	Water	Radiator	0.03	1.13	25.00	300.00	342.00	200.00	Liquid	225.44	15.99	0.928	1.025
FTHX-071	DP I	Water	Radiator	0.03	0.96	25.00	300.00	342.00	200.00	Liquid	193.29	10.62	0.788	1.006
FTHX-072	DP I	Water	Radiator	0.03	0.82	25.00	300.00	342.00	200.00	Liquid	193.85	8.74	0.975	1.076

Design Tag	Design Problem	Fluid	Application	V_{air}	u_{air}	$\dot{m}_{fluid}$	$T_{air,in}$	$T_{fluid,in}$	$P_{fluid,in}$	$x_{fluid,in}$	h_{air}	ΔP_{air}	ΔP_{fluid}	Q
	-	-	-	m³/s	m/s	g/s	K	K	kPa	-	W/m².K	Pa	kPa	kW
FTHX-073	DP I	Water	Radiator	0.03	1.00	25.00	300.00	342.00	200.00	Liquid	201.45	11.46	0.944	1.000
FTHX-074	DP I	Water	Radiator	0.03	1.02	25.00	300.00	342.00	200.00	Liquid	207.45	12.23	0.912	1.013
FTHX-075	DP I	Water	Radiator	0.03	1.53	25.00	300.00	342.00	200.00	Liquid	275.86	32.70	0.867	1.015
FTHX-076	DP I	Water	Radiator	0.03	1.08	25.00	300.00	342.00	200.00	Liquid	220.73	14.74	0.963	1.034
FTHX-077	DP I	Water	Radiator	0.03	1.09	25.00	300.00	342.00	200.00	Liquid	218.69	15.13	0.956	1.034
FTHX-078	DP I	Water	Radiator	0.03	1.12	25.00	300.00	342.00	200.00	Liquid	224.07	15.71	0.928	1.023
FTHX-079	DP I	Water	Radiator	0.03	1.69	25.00	300.00	342.00	200.00	Liquid	287.25	42.96	0.771	1.013
FTHX-080	DP I	Water	Radiator	0.03	1.89	25.00	300.00	342.00	200.00	Liquid	291.30	60.21	0.973	1.009
FTHX-081	DP I	Water	Radiator	0.03	0.95	25.00	300.00	342.00	200.00	Liquid	190.37	10.56	0.683	1.015
FTHX-082	DP I	Water	Radiator	0.03	1.26	25.00	300.00	342.00	200.00	Liquid	240.48	19.82	0.965	1.008
FTHX-083	DP I	Water	Radiator	0.03	1.04	25.00	300.00	342.00	200.00	Liquid	209.97	12.53	0.898	1.009
FTHX-084	DP I	Water	Radiator	0.03	1.14	25.00	300.00	342.00	200.00	Liquid	231.86	16.63	0.935	1.034
FTHX-085	DP I	Water	Radiator	0.03	1.56	25.00	300.00	342.00	200.00	Liquid	284.18	33.68	0.956	1.017
FTHX-086	DP I	Water	Radiator	0.03	1.53	25.00	300.00	342.00	200.00	Liquid	278.01	32.56	0.867	1.015
FTHX-087	DP I	Water	Radiator	0.03	1.28	25.00	300.00	342.00	200.00	Liquid	236.38	20.52	0.842	1.007
FTHX-088	DP I	Water	Radiator	0.03	1.01	25.00	300.00	342.00	200.00	Liquid	202.51	11.70	0.944	1.002
FTHX-089	DP I	Water	Radiator	0.03	1.09	25.00	300.00	342.00	200.00	Liquid	223.27	15.10	0.964	1.038
FTHX-090	DP I	Water	Radiator	0.03	0.99	25.00	300.00	342.00	200.00	Liquid	200.68	10.97	0.931	1.004
FTHX-091	DP I	Water	Radiator	0.03	1.00	25.00	300.00	342.00	200.00	Liquid	200.93	11.07	0.951	1.005
FTHX-092	DP I	Water	Radiator	0.03	1.67	25.00	300.00	342.00	200.00	Liquid	291.65	39.29	0.789	1.005
FTHX-093	DP I	Water	Radiator	0.03	1.21	25.00	300.00	342.00	200.00	Liquid	230.38	17.88	0.863	1.005

NTHX

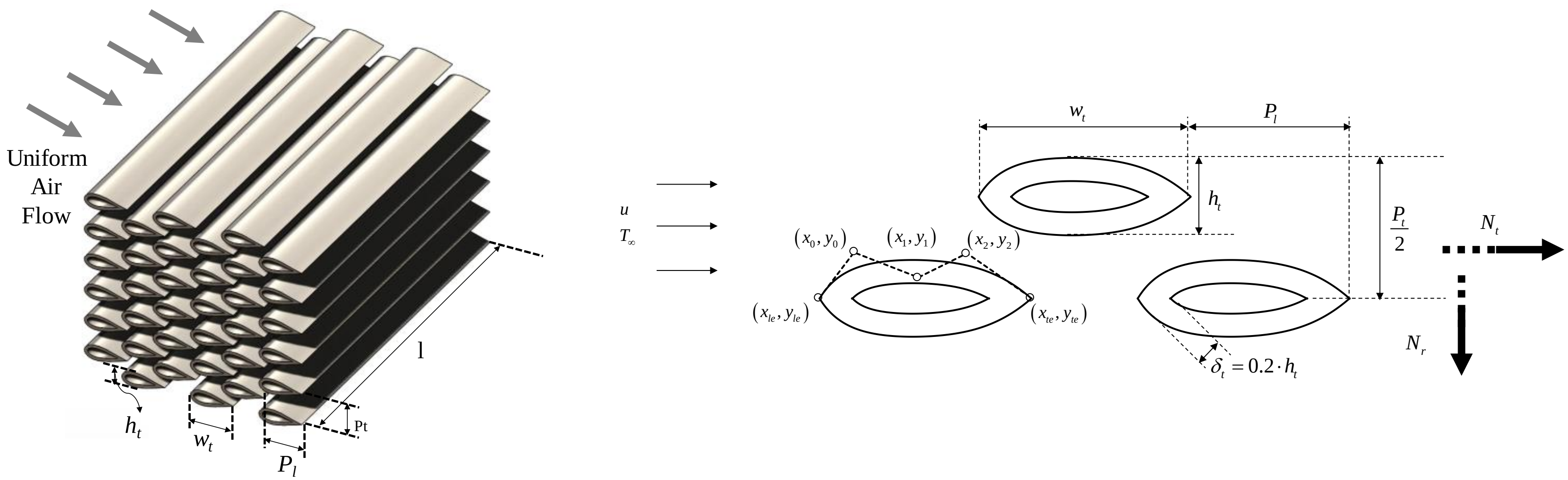

Figure 131. NTHX surface concept.

Table 34. NTHX dimensions.

Design Tag	h_t	w_t	δ_t	P_l	P_t	N_t	N_r	x_1	x_2	x_3	y_1	y_2	y_3	l	H	d	A_f	V	$V_{mat'l}$
	mm	mm	mm	mm	mm	-	-	-	-	-	-	-	-	m	m	m	m^2	cm^3	cm^3
NTHX-001	1.1000	3.0000	0.3000	2.4000	2.2000	7	45	0.00000	0.00000	0.00000	0.18000	0.36000	0.04500	0.1000	0.1000	0.0174	0.0100	174.00	46.90
NTHX-002	0.7053	1.7642	0.1411	1.5715	1.7229	5	70	0.42033	0.74194	0.07820	0.07234	0.58944	0.97752	0.1432	0.1179	0.0081	0.0169	135.90	21.78
NTHX-003	0.5684	1.4319	0.1137	1.1905	1.3886	5	79	0.81232	0.99218	0.08016	0.93255	0.67742	0.20332	0.1571	0.1075	0.0062	0.0169	104.56	17.76
NTHX-004	0.5489	1.3741	0.1098	1.1424	1.3408	5	79	0.43597	0.73998	0.06452	0.93255	0.73998	0.37537	0.1626	0.1038	0.0059	0.0169	100.33	17.81
NTHX-005	0.5489	1.3848	0.1098	1.1391	1.3408	5	79	0.42033	0.74194	0.33040	0.93255	0.74780	0.12610	0.1626	0.1038	0.0059	0.0169	100.30	17.54
NTHX-006	0.5489	1.3741	0.1098	1.1424	1.3408	5	79	0.43402	0.64614	0.06452	0.93255	0.73998	0.37537	0.1615	0.1038	0.0059	0.0168	99.62	17.67
NTHX-007	0.5684	1.4319	0.1137	1.1779	1.3886	5	79	0.93744	0.62463	0.08798	0.93255	0.73998	0.20332	0.1414	0.1075	0.0061	0.0152	93.36	15.75
NTHX-008	0.5489	1.3848	0.1098	1.1391	1.3408	5	79	0.93646	0.67742	0.08798	0.93255	0.74780	0.37537	0.1464	0.1038	0.0059	0.0152	90.29	15.74
NTHX-009	0.5489	1.4159	0.1098	1.1273	1.3408	5	79	0.93646	0.67742	0.08798	0.93255	0.74780	0.37537	0.1464	0.1038	0.0059	0.0152	90.05	16.07
NTHX-010	0.5489	1.4159	0.1098	1.0775	1.3408	5	79	0.93646	0.67937	0.08798	0.93255	0.74780	0.40665	0.1464	0.1038	0.0057	0.0152	87.02	16.14
NTHX-011	0.5489	1.4159	0.1098	1.0775	1.3408	5	79	0.81232	0.99218	0.08016	0.93255	0.74780	0.37537	0.1450	0.1038	0.0057	0.0151	86.18	16.07

Design Tag	h_t	w_t	δ_t	P_l	P_t	N_t	N_r	x_1	x_2	x_3	y_1	y_2	y_3	l	H	d	A_f	V	$V_{mat'l}$
	mm	mm	mm	mm	mm	-	-	-	-	-	-	-	-	m	m	m	m^2	cm^3	cm^3
NTHX-012	0.5489	1.4159	0.1098	1.0651	1.3065	5	79	0.81232	0.99218	0.08016	0.93255	0.74780	0.40665	0.1488	0.1011	0.0057	0.0151	85.43	16.55
NTHX-013	0.5684	1.4319	0.1137	1.1779	1.3952	5	79	0.81232	0.99022	0.08016	0.93255	0.73998	0.37634	0.1265	0.1080	0.0061	0.0137	83.91	14.71
NTHX-014	0.5489	1.3741	0.1098	1.1786	1.3472	5	79	0.81232	0.89638	0.07820	0.93255	0.68524	0.40665	0.1310	0.1043	0.0061	0.0137	83.16	14.19
NTHX-015	0.5489	1.3848	0.1098	1.1391	1.3408	5	79	0.81232	0.99218	0.08016	0.93255	0.74780	0.37537	0.1316	0.1038	0.0059	0.0137	81.15	14.29
NTHX-016	0.5489	1.4170	0.1098	1.0783	1.3387	5	79	0.93744	0.99218	0.08016	0.93255	0.74780	0.37537	0.1318	0.1036	0.0057	0.0137	78.27	14.53
NTHX-017	0.5513	1.3802	0.1103	1.0503	1.3532	5	79	0.81232	0.67742	0.08798	0.93255	0.74780	0.37537	0.1304	0.1048	0.0056	0.0137	76.23	14.13
NTHX-018	0.5489	1.3741	0.1098	1.0336	1.3140	5	79	0.81232	0.99218	0.08016	0.93353	0.74780	0.28152	0.1327	0.1017	0.0055	0.0135	74.37	14.10
NTHX-019	0.5098	1.3160	0.1020	0.9899	1.2204	5	80	0.43500	0.71065	0.08016	0.93255	0.74780	0.37537	0.1427	0.0957	0.0053	0.0137	72.06	14.05
NTHX-020	0.5489	1.3741	0.1098	1.0457	1.3483	5	70	0.81232	0.99022	0.20528	0.93646	0.74780	0.42229	0.1355	0.0922	0.0056	0.0125	69.46	13.15
NTHX-021	0.5489	1.3848	0.1098	1.0416	1.3129	5	79	0.81134	0.87488	0.08798	0.93255	0.73998	0.37537	0.1230	0.1016	0.0056	0.0125	69.40	13.34
NTHX-022	0.5489	1.3741	0.1098	1.0336	1.3140	5	80	0.81036	0.71065	0.08016	0.93255	0.74780	0.37537	0.1213	0.1030	0.0055	0.0125	68.86	13.20
NTHX-023	0.5122	1.3224	0.1024	1.0034	1.2252	5	79	0.80450	0.86706	0.07820	0.91691	0.74780	0.65689	0.1318	0.0949	0.0053	0.0125	66.70	13.05
NTHX-024	0.5489	1.3741	0.1098	1.0336	1.3140	5	70	0.81232	0.67742	0.08798	0.91691	0.59140	0.40665	0.1307	0.0899	0.0055	0.0118	64.75	12.60
NTHX-025	0.5098	1.3160	0.1020	1.0015	1.2194	5	79	0.42620	0.64614	0.06549	0.93255	0.73998	0.37537	0.1245	0.0944	0.0053	0.0118	62.56	12.09
NTHX-026	0.5098	1.2842	0.1020	0.9772	1.2194	5	79	0.42033	0.67742	0.08798	0.41642	0.74780	0.40665	0.1245	0.0944	0.0052	0.0118	61.04	11.90
NTHX-027	0.5122	1.2823	0.1024	0.9758	1.2573	5	70	0.42131	0.37048	0.26979	0.38514	0.71065	0.97067	0.1367	0.0860	0.0052	0.0118	60.95	11.87
NTHX-028	0.5098	1.3160	0.1020	0.9986	1.1556	5	79	0.80352	0.71065	0.08016	0.93255	0.73216	0.37537	0.1195	0.0895	0.0053	0.0107	56.77	11.40
NTHX-029	0.5098	1.3160	0.1020	0.9986	1.1556	5	79	0.40860	0.62463	0.26979	0.93255	0.66960	0.40665	0.1158	0.0895	0.0053	0.0104	55.02	11.53
NTHX-030	0.6540	1.7394	0.1308	1.5073	1.5508	6	65	0.99707	0.98631	0.00293	0.99707	0.33822	0.00880	0.1019	0.0999	0.0093	0.0102	94.45	14.30
NTHX-031	0.6540	1.7394	0.1308	1.5035	1.5508	6	65	0.95112	0.99316	0.01075	0.99707	0.33040	0.01662	0.1019	0.0999	0.0093	0.0102	94.26	14.39
NTHX-032	0.6540	1.7381	0.1308	1.3801	1.5508	6	70	0.95112	0.98534	0.00293	0.99316	0.33822	0.00782	0.0960	0.1061	0.0086	0.0102	87.96	14.50
NTHX-033	0.6491	1.7315	0.1298	1.3748	1.5392	6	74	0.95112	0.98729	0.00098	0.99707	0.33822	0.00880	0.0901	0.1130	0.0086	0.0102	87.62	14.23
NTHX-034	0.6491	1.7264	0.1298	1.3708	1.5392	6	74	0.95112	0.96285	0.00098	0.99707	0.33822	0.00880	0.0901	0.1130	0.0086	0.0102	87.37	14.17
NTHX-035	0.6466	1.7187	0.1293	1.3041	1.5334	6	65	0.95112	0.96285	0.00098	0.99902	0.33822	0.00489	0.1031	0.0988	0.0082	0.0102	83.90	14.09
NTHX-036	0.6149	1.6354	0.1230	1.2985	1.4581	6	65	0.95112	0.98534	0.00293	0.99707	0.33822	0.00098	0.1084	0.0939	0.0081	0.0102	82.76	13.40
NTHX-037	0.6344	1.6862	0.1269	1.2795	1.5057	6	66	0.95112	0.96481	0.00098	0.99707	0.33822	0.01662	0.1050	0.0970	0.0081	0.0102	82.31	14.12
NTHX-038	0.6075	1.6207	0.1215	1.2868	1.4407	6	65	0.95112	0.98534	0.00098	0.99707	0.46334	0.01662	0.1114	0.0914	0.0081	0.0102	82.02	13.76
NTHX-039	0.6295	1.6744	0.1259	1.2742	1.4929	6	65	0.95112	0.96676	0.00098	0.99707	0.33822	0.00098	0.1059	0.0962	0.0080	0.0102	81.92	13.70
NTHX-040	0.6075	1.6159	0.1215	1.2262	1.4419	6	65	0.95112	0.96285	0.00098	0.99707	0.33822	0.00880	0.1096	0.0929	0.0077	0.0102	78.88	13.27
NTHX-041	0.5880	1.4995	0.1176	1.1411	1.3944	6	65	0.98240	0.98534	0.00293	0.99707	0.33822	0.00098	0.1134	0.0898	0.0072	0.0102	73.37	12.33
NTHX-042	0.5880	1.4984	0.1176	1.1403	1.3944	6	65	0.98240	0.73509	0.00293	0.99707	0.33822	0.00098	0.1134	0.0898	0.0072	0.0102	73.31	12.12
NTHX-043	0.5562	1.4783	0.1112	1.1218	1.3201	6	66	0.95112	0.98534	0.00293	0.99707	0.33822	0.01662	0.1197	0.0850	0.0071	0.0102	72.16	12.40
NTHX-044	0.5880	1.5639	0.1176	1.1901	1.3944	6	64	0.95112	0.98534	0.00098	0.99707	0.31476	0.00880	0.1103	0.0870	0.0075	0.0096	72.16	12.30
NTHX-045	0.5880	1.5639	0.1176	1.1867	1.3944	6	65	0.96872	0.98631	0.00098	0.99707	0.33822	0.00098	0.1060	0.0898	0.0075	0.0095	71.41	11.98
NTHX-046	0.5880	1.5639	0.1176	1.1867	1.3944	6	65	0.94721	0.96285	0.00293	0.99707	0.33822	0.00782	0.1052	0.0898	0.0075	0.0094	70.84	11.92
NTHX-047	0.5880	1.5639	0.1176	1.1901	1.3955	6	74	0.96285	0.98534	0.00098	0.99707	0.31476	0.00880	0.0928	0.1011	0.0075	0.0094	70.44	11.95
NTHX-048	0.5904	1.5058	0.1181	1.1426	1.4002	6	65	0.96676	0.98631	0.00098	0.99707	0.32258	0.12610	0.1073	0.0902	0.0072	0.0097	69.89	12.50
NTHX-049	0.5880	1.4995	0.1176	1.1411	1.3944	6	65	0.96676	0.98631	0.00098	0.99707	0.32258	0.12610	0.1078	0.0898	0.0072	0.0097	69.76	12.45
NTHX-050	0.5880	1.4995	0.1176	1.1378	1.3944	6	65	0.96676	0.98631	0.00098	0.99707	0.32258	0.12610	0.1078	0.0898	0.0072	0.0097	69.60	12.45
NTHX-051	1.0332	2.8688	0.2066	2.1958	2.3210	7	34	0.98925	0.47312	0.01369	1.00000	0.46823	0.00098	0.1309	0.0776	0.0160	0.0102	163.01	28.50
NTHX-052	1.0039	2.7945	0.2008	2.1389	2.2551	7	43	0.99316	0.72923	0.00978	1.00000	0.46823	0.00000	0.1062	0.0957	0.0156	0.0102	158.79	28.05
NTHX-053	1.0000	2.7836	0.2000	2.1305	2.2463	7	35	0.99218	0.47898	0.01466	1.00000	0.43597	0.00000	0.1313	0.0774	0.0156	0.0102	158.17	27.53
NTHX-054	1.0000	2.7765	0.2000	2.1252	2.2463	7	35	0.99218	0.47898	0.01466	1.00000	0.43597	0.00000	0.1313	0.0774	0.0155	0.0102	157.77	27.46
NTHX-055	1.0078	2.7344	0.2016	2.0628	2.2639	7	41	0.99022	0.47898	0.01369	0.99609	0.43597	0.00000	0.1110	0.0916	0.0151	0.0102	153.54	27.05

Design Tag	h_t	w_t	δ_t	P_l	P_t	N_t	N_r	x_1	x_2	x_3	y_1	y_2	y_3	l	H	d	A_f	V	$V_{mat'l}$
	mm	mm	mm	mm	mm	-	-	-	-	-	-	-	-	m	m	m	m^2	cm^3	cm^3
NTHX-056	1.0000	2.7109	0.2000	2.0391	2.2483	7	35	0.99707	0.23069	0.01369	1.00000	0.43402	0.00000	0.1312	0.0774	0.0149	0.0102	151.85	26.43
NTHX-057	1.0000	2.7132	0.2000	2.0349	2.2483	7	34	0.99707	0.23069	0.01369	0.99804	0.46823	0.00098	0.1351	0.0752	0.0149	0.0102	151.62	26.60
NTHX-058	1.0000	2.7015	0.2000	2.0320	2.2385	7	35	0.98631	0.47898	0.01466	0.99804	0.43695	0.01564	0.1357	0.0749	0.0149	0.0102	151.33	27.96
NTHX-059	1.0000	2.7109	0.2000	2.0331	2.2463	7	43	0.99707	0.73314	0.00978	1.00000	0.49853	0.00000	0.1052	0.0953	0.0149	0.0100	149.56	27.01
NTHX-060	1.0000	2.7109	0.2000	2.0749	2.2463	7	35	0.99022	0.47898	0.01369	0.99218	0.40567	0.00000	0.1313	0.0751	0.0152	0.0099	149.53	26.78
NTHX-061	1.0000	2.7109	0.2000	2.0629	2.2463	7	35	0.99022	0.47898	0.03030	0.99022	0.43695	0.00000	0.1313	0.0751	0.0151	0.0099	148.82	26.96
NTHX-062	1.0000	2.7109	0.2000	2.0391	2.2385	7	44	0.99022	0.47898	0.01369	1.00000	0.43597	0.00000	0.1038	0.0950	0.0149	0.0099	147.41	26.71
NTHX-063	1.0000	2.7120	0.2000	2.0340	2.2385	7	35	0.99022	0.47898	0.01369	0.98925	0.43695	0.00000	0.1317	0.0749	0.0149	0.0099	147.12	26.99
NTHX-064	1.0000	2.7109	0.2000	2.0331	2.2346	7	34	0.99022	0.47898	0.00978	1.00000	0.43402	0.00391	0.1320	0.0747	0.0149	0.0099	147.06	26.28
NTHX-065	1.0000	2.7109	0.2000	2.0331	2.2385	7	35	0.99707	0.23069	0.01369	0.99609	0.43597	0.00000	0.1312	0.0749	0.0149	0.0098	146.45	26.44
NTHX-066	1.0000	2.7132	0.2000	2.0468	2.2385	7	35	0.99218	0.47898	0.01369	0.99609	0.43695	0.00000	0.1296	0.0749	0.0150	0.0097	145.46	26.55
NTHX-067	1.0000	2.7132	0.2000	2.0349	2.2346	7	34	0.95894	0.47898	0.01369	1.00000	0.46725	0.00196	0.1298	0.0747	0.0149	0.0097	144.77	25.98
NTHX-068	1.0000	2.7413	0.2000	2.0681	2.2463	7	44	0.98925	0.47898	0.01369	0.99609	0.42033	0.00000	0.1001	0.0953	0.0151	0.0095	144.60	25.97
NTHX-069	1.0000	2.7109	0.2000	2.0451	2.2463	7	44	0.98925	0.47898	0.01369	1.00000	0.43597	0.00000	0.1001	0.0953	0.0150	0.0095	142.99	25.76
NTHX-070	1.0000	2.7132	0.2000	2.0468	2.2385	7	35	0.99022	0.48094	0.00684	1.00000	0.46823	0.00000	0.1235	0.0771	0.0150	0.0095	142.82	25.37
NTHX-071	1.0000	2.7132	0.2000	2.0409	2.2385	7	34	0.99022	0.47898	0.01369	1.00000	0.43695	0.00000	0.1272	0.0749	0.0150	0.0095	142.48	25.32
NTHX-072	1.0000	2.7097	0.2000	2.0323	2.2385	7	44	0.99022	0.47898	0.01369	1.00000	0.43597	0.00000	0.1002	0.0950	0.0149	0.0095	141.96	25.78
NTHX-073	1.0000	2.7132	0.2000	2.0468	2.2385	7	35	0.99022	0.48094	0.00684	1.00000	0.46823	0.00000	0.1225	0.0771	0.0150	0.0094	141.68	25.17
NTHX-074	1.0000	2.7765	0.2000	2.0885	2.2405	7	35	0.99022	0.47898	0.01369	0.99609	0.43402	0.00000	0.1198	0.0772	0.0153	0.0092	141.52	25.05
NTHX-075	1.0000	2.7015	0.2000	2.0261	2.1935	7	35	0.99218	0.47898	0.01466	1.00000	0.43597	0.00000	0.1290	0.0734	0.0149	0.0095	140.67	26.32
NTHX-076	1.0078	2.7628	0.2016	2.0721	2.2186	7	35	0.99022	0.47898	0.01369	1.00000	0.46823	0.00000	0.1209	0.0764	0.0152	0.0092	140.49	25.49
NTHX-077	1.0000	2.7413	0.2000	2.0620	2.2023	7	41	0.98925	0.22874	0.01369	1.00000	0.43597	0.00000	0.1038	0.0891	0.0151	0.0092	139.73	24.75
NTHX-078	1.0039	2.7244	0.2008	2.0433	2.2100	7	35	0.99022	0.47898	0.01369	1.00000	0.48094	0.00000	0.1214	0.0761	0.0150	0.0092	138.53	25.20
NTHX-079	1.0000	2.7132	0.2000	2.0349	2.2014	7	35	0.99022	0.47312	0.01369	1.00000	0.46823	0.00000	0.1219	0.0758	0.0149	0.0092	137.96	25.05
NTHX-080	1.0000	2.7109	0.2000	2.0331	2.2014	7	35	0.99022	0.47898	0.01369	0.99609	0.43695	0.00000	0.1255	0.0736	0.0149	0.0092	137.85	25.70
NTHX-081	1.0000	2.7132	0.2000	2.0349	2.2014	7	35	0.98436	0.73118	0.02933	1.00000	0.46823	0.00000	0.1217	0.0758	0.0149	0.0092	137.70	25.46
NTHX-082	1.0000	2.7109	0.2000	2.0331	2.2014	7	34	0.99022	0.47898	0.00978	1.00000	0.43402	0.00391	0.1253	0.0736	0.0149	0.0092	137.58	24.95
NTHX-083	1.0000	2.7015	0.2000	2.0261	2.1935	7	35	0.99022	0.47898	0.01369	1.00000	0.49267	0.00000	0.1223	0.0756	0.0149	0.0092	137.37	25.11
NTHX-084	1.0000	2.7132	0.2000	2.0349	2.1935	7	35	0.99022	0.47898	0.01369	0.99609	0.43402	0.00000	0.1214	0.0756	0.0149	0.0092	136.89	24.86
NTHX-085	1.0000	2.7015	0.2000	2.0261	2.1935	7	41	0.99218	0.47898	0.01466	1.00000	0.43597	0.00391	0.1034	0.0887	0.0149	0.0092	136.30	24.77
NTHX-086	1.0000	2.7015	0.2000	2.0261	2.1935	7	41	0.99218	0.47898	0.01466	1.00000	0.43402	0.01662	0.1032	0.0887	0.0149	0.0092	136.04	24.90
NTHX-087	1.0000	2.7132	0.2000	2.0349	2.1935	7	35	0.98925	0.47996	0.00587	0.99609	0.43402	0.00000	0.1191	0.0756	0.0149	0.0090	134.28	24.36

Table 35. NTHX performances and operating conditions.

Design Tag	Design Problem	Fluid	Application	V_{air}	u_{air}	$\dot{m}_{fluid}$	$T_{air,in}$	$T_{fluid,in}$	$P_{fluid,in}$	$x_{fluid,in}$	h	ΔP_{air}	ΔP_{fluid}	Q
	-	-	-	m^3/s	m/s	g/s	K	K	kPa	-	$W/m^2.K$	Pa	kPa	kW
NTHX-001	DP I	Water	Radiator	0.03	3.00	25.00	300.00	350.00	200.00	Liquid	201.00	64.10	0.650	1.072
NTHX-002	DP I	Water	Radiator	0.03	1.78	25.00	300.00	349.41	200.00	Liquid	232.14	18.20	0.495	1.072
NTHX-003	DP I	Water	Radiator	0.03	1.78	25.00	300.00	348.20	200.00	Liquid	246.46	18.50	0.894	1.080
NTHX-004	DP I	Water	Radiator	0.03	1.78	25.00	300.00	348.20	200.00	Liquid	257.39	21.05	0.889	1.100

Design Tag	Design Problem	Fluid	Application	V_{air}	u_{air}	$\dot{m}_{fluid}$	$T_{air,in}$	$T_{fluid,in}$	$P_{fluid,in}$	$x_{fluid,in}$	h	ΔP_{air}	ΔP_{fluid}	Q
	-	-	-	m³/s	m/s	g/s	K	K	kPa	-	W/m².K	Pa	kPa	kW
NTHX-005	DP I	Water	Radiator	0.03	1.78	25.00	300.00	348.18	200.00	Liquid	255.05	21.09	0.942	1.098
NTHX-006	DP I	Water	Radiator	0.03	1.79	25.00	300.00	348.20	200.00	Liquid	257.12	21.43	0.905	1.096
NTHX-007	DP I	Water	Radiator	0.03	1.97	25.00	300.00	348.51	200.00	Liquid	250.04	21.93	0.974	1.041
NTHX-008	DP I	Water	Radiator	0.03	1.97	25.00	300.00	348.18	200.00	Liquid	258.15	22.84	0.984	1.051
NTHX-009	DP I	Water	Radiator	0.03	1.97	25.00	300.00	348.20	200.00	Liquid	257.14	23.15	0.936	1.060
NTHX-010	DP I	Water	Radiator	0.03	1.97	25.00	300.00	348.20	200.00	Liquid	259.53	23.57	0.911	1.064
NTHX-011	DP I	Water	Radiator	0.03	1.99	25.00	300.00	348.20	200.00	Liquid	260.98	23.79	0.805	1.063
NTHX-012	DP I	Water	Radiator	0.03	1.99	25.00	300.00	348.20	200.00	Liquid	267.00	25.22	0.810	1.086
NTHX-013	DP I	Water	Radiator	0.03	2.20	25.00	300.00	348.20	200.00	Liquid	261.83	26.22	0.640	1.002
NTHX-014	DP I	Water	Radiator	0.03	2.20	25.00	300.00	348.20	200.00	Liquid	264.44	26.42	0.763	1.005
NTHX-015	DP I	Water	Radiator	0.03	2.20	25.00	300.00	348.18	200.00	Liquid	266.01	26.73	0.766	1.013
NTHX-016	DP I	Water	Radiator	0.03	2.20	25.00	300.00	348.17	200.00	Liquid	266.09	26.82	0.773	1.025
NTHX-017	DP I	Water	Radiator	0.03	2.20	25.00	300.00	348.20	200.00	Liquid	267.58	27.73	0.824	1.010
NTHX-018	DP I	Water	Radiator	0.03	2.22	25.00	300.00	348.17	200.00	Liquid	272.30	28.18	0.836	1.025
NTHX-019	DP I	Water	Radiator	0.03	2.20	25.00	300.00	349.45	200.00	Liquid	282.45	31.79	0.950	1.094
NTHX-020	DP I	Water	Radiator	0.03	2.40	25.00	300.00	349.42	200.00	Liquid	279.28	32.20	0.807	1.013
NTHX-021	DP I	Water	Radiator	0.03	2.40	25.00	300.00	348.18	200.00	Liquid	278.88	32.67	0.733	1.002
NTHX-022	DP I	Water	Radiator	0.03	2.40	25.00	300.00	349.42	200.00	Liquid	278.21	32.95	0.755	1.023
NTHX-023	DP I	Water	Radiator	0.03	2.40	25.00	300.00	348.20	200.00	Liquid	290.51	35.35	0.829	1.035
NTHX-024	DP I	Water	Radiator	0.03	2.55	25.00	300.00	349.42	200.00	Liquid	284.82	36.65	0.880	1.005
NTHX-025	DP I	Water	Radiator	0.03	2.55	25.00	300.00	348.20	200.00	Liquid	290.12	38.90	0.867	1.006
NTHX-026	DP I	Water	Radiator	0.03	2.55	25.00	300.00	348.20	200.00	Liquid	295.74	41.81	0.875	1.001
NTHX-027	DP I	Water	Radiator	0.03	2.55	25.00	300.00	348.19	200.00	Liquid	308.25	45.80	0.972	1.008
NTHX-028	DP I	Water	Radiator	0.03	2.81	25.00	300.00	348.20	200.00	Liquid	306.29	46.61	0.952	1.009
NTHX-029	DP I	Water	Radiator	0.03	2.90	25.00	300.00	348.20	200.00	Liquid	324.31	58.00	0.693	1.024
NTHX-030	DP I	Water	Radiator	0.03	2.95	25.00	300.00	349.99	200.00	Liquid	256.14	44.95	0.400	1.006
NTHX-031	DP I	Water	Radiator	0.03	2.95	25.00	300.00	349.99	200.00	Liquid	256.51	45.26	0.393	1.007
NTHX-032	DP I	Water	Radiator	0.03	2.95	25.00	300.00	349.76	200.00	Liquid	256.76	45.27	0.353	1.009
NTHX-033	DP I	Water	Radiator	0.03	2.95	25.00	300.00	349.83	200.00	Liquid	261.06	45.30	0.316	1.014
NTHX-034	DP I	Water	Radiator	0.03	2.95	25.00	300.00	349.84	200.00	Liquid	261.08	45.37	0.322	1.013
NTHX-035	DP I	Water	Radiator	0.03	2.95	25.00	300.00	349.76	200.00	Liquid	263.05	45.53	0.429	1.015
NTHX-036	DP I	Water	Radiator	0.03	2.95	25.00	300.00	349.13	200.00	Liquid	267.15	45.84	0.550	1.011
NTHX-037	DP I	Water	Radiator	0.03	2.95	25.00	300.00	349.76	200.00	Liquid	261.38	45.94	0.467	1.019
NTHX-038	DP I	Water	Radiator	0.03	2.95	25.00	300.00	348.50	200.00	Liquid	263.55	46.09	0.568	1.001
NTHX-039	DP I	Water	Radiator	0.03	2.95	25.00	300.00	349.21	200.00	Liquid	265.71	46.10	0.495	1.010
NTHX-040	DP I	Water	Radiator	0.03	2.95	25.00	300.00	349.13	200.00	Liquid	269.93	46.34	0.587	1.016
NTHX-041	DP I	Water	Radiator	0.03	2.95	25.00	300.00	349.13	200.00	Liquid	278.92	46.37	0.764	1.013
NTHX-042	DP I	Water	Radiator	0.03	2.95	25.00	300.00	349.13	200.00	Liquid	276.96	47.38	0.892	1.008
NTHX-043	DP I	Water	Radiator	0.03	2.95	25.00	300.00	349.76	200.00	Liquid	275.45	47.46	0.892	1.048
NTHX-044	DP I	Water	Radiator	0.03	3.12	25.00	300.00	349.76	200.00	Liquid	275.11	51.39	0.691	1.017
NTHX-045	DP I	Water	Radiator	0.03	3.15	25.00	300.00	349.13	200.00	Liquid	279.77	51.57	0.646	1.000
NTHX-046	DP I	Water	Radiator	0.03	3.17	25.00	300.00	349.72	200.00	Liquid	280.47	52.60	0.636	1.010
NTHX-047	DP I	Water	Radiator	0.03	3.20	25.00	300.00	349.76	200.00	Liquid	277.88	52.71	0.502	1.007
NTHX-048	DP I	Water	Radiator	0.03	3.10	25.00	300.00	349.13	200.00	Liquid	288.14	53.04	0.640	1.003

Design Tag	Design Problem	Fluid	Application	V_{air}	u_{air}	$\dot{m}_{fluid}$	$T_{air,in}$	$T_{fluid,in}$	$P_{fluid,in}$	$x_{fluid,in}$	h	ΔP_{air}	ΔP_{fluid}	Q
	-	-	-	m^3/s	m/s	g/s	K	K	kPa	-	$W/m^2.K$	Pa	kPa	kW
NTHX-049	DP I	Water	Radiator	0.03	3.10	25.00	300.00	349.13	200.00	Liquid	288.51	53.06	0.654	1.004
NTHX-050	DP I	Water	Radiator	0.03	3.10	25.00	300.00	349.13	200.00	Liquid	288.62	53.09	0.654	1.004
NTHX-051	DP I	Water	Radiator	0.03	2.95	25.00	300.00	349.60	200.00	Liquid	206.57	42.22	0.158	1.012
NTHX-052	DP I	Water	Radiator	0.03	2.95	25.00	300.00	349.76	200.00	Liquid	212.66	42.30	0.097	1.030
NTHX-053	DP I	Water	Radiator	0.03	2.95	25.00	300.00	349.76	200.00	Liquid	210.74	42.55	0.176	1.027
NTHX-054	DP I	Water	Radiator	0.03	2.95	25.00	300.00	349.76	200.00	Liquid	210.91	42.55	0.178	1.026
NTHX-055	DP I	Water	Radiator	0.03	2.95	25.00	300.00	349.76	200.00	Liquid	211.58	42.59	0.131	1.015
NTHX-056	DP I	Water	Radiator	0.03	2.95	25.00	300.00	349.74	200.00	Liquid	208.73	42.70	0.224	1.007
NTHX-057	DP I	Water	Radiator	0.03	2.95	25.00	300.00	349.60	200.00	Liquid	208.60	42.74	0.231	1.005
NTHX-058	DP I	Water	Radiator	0.03	2.95	25.00	300.00	349.73	200.00	Liquid	207.74	43.34	0.198	1.021
NTHX-059	DP I	Water	Radiator	0.03	2.99	25.00	300.00	349.74	200.00	Liquid	216.38	43.52	0.103	1.019
NTHX-060	DP I	Water	Radiator	0.03	3.04	25.00	300.00	349.76	200.00	Liquid	208.25	44.94	0.197	1.007
NTHX-061	DP I	Water	Radiator	0.03	3.04	25.00	300.00	349.73	200.00	Liquid	208.39	45.10	0.191	1.007
NTHX-062	DP I	Water	Radiator	0.03	3.04	25.00	300.00	349.92	200.00	Liquid	211.25	45.20	0.121	1.015
NTHX-063	DP I	Water	Radiator	0.03	3.04	25.00	300.00	349.76	200.00	Liquid	209.76	45.30	0.193	1.012
NTHX-064	DP I	Water	Radiator	0.03	3.04	25.00	300.00	349.68	200.00	Liquid	216.84	45.40	0.194	1.014
NTHX-065	DP I	Water	Radiator	0.03	3.05	25.00	300.00	349.91	200.00	Liquid	206.55	45.73	0.229	1.005
NTHX-066	DP I	Water	Radiator	0.03	3.09	25.00	300.00	349.76	200.00	Liquid	211.11	46.55	0.190	1.007
NTHX-067	DP I	Water	Radiator	0.03	3.09	25.00	300.00	349.76	200.00	Liquid	217.44	46.76	0.186	1.009
NTHX-068	DP I	Water	Radiator	0.03	3.14	25.00	300.00	349.77	200.00	Liquid	212.82	47.43	0.114	1.001
NTHX-069	DP I	Water	Radiator	0.03	3.14	25.00	300.00	349.92	200.00	Liquid	213.35	47.45	0.116	1.000
NTHX-070	DP I	Water	Radiator	0.03	3.15	25.00	300.00	349.92	200.00	Liquid	218.98	47.84	0.174	1.004
NTHX-071	DP I	Water	Radiator	0.03	3.15	25.00	300.00	349.68	200.00	Liquid	219.11	47.91	0.187	1.000
NTHX-072	DP I	Water	Radiator	0.03	3.15	25.00	300.00	349.92	200.00	Liquid	214.52	47.94	0.116	1.003
NTHX-073	DP I	Water	Radiator	0.03	3.17	25.00	300.00	349.92	200.00	Liquid	219.67	48.45	0.172	1.002
NTHX-074	DP I	Water	Radiator	0.03	3.24	25.00	300.00	349.81	200.00	Liquid	220.52	50.00	0.162	1.001
NTHX-075	DP I	Water	Radiator	0.03	3.17	25.00	300.00	349.72	200.00	Liquid	218.09	50.41	0.192	1.018
NTHX-076	DP I	Water	Radiator	0.03	3.24	25.00	300.00	349.76	200.00	Liquid	224.06	51.68	0.161	1.010
NTHX-077	DP I	Water	Radiator	0.03	3.24	25.00	300.00	349.76	200.00	Liquid	220.97	51.82	0.147	1.002
NTHX-078	DP I	Water	Radiator	0.03	3.24	25.00	300.00	349.83	200.00	Liquid	224.83	51.85	0.167	1.009
NTHX-079	DP I	Water	Radiator	0.03	3.24	25.00	300.00	349.92	200.00	Liquid	225.37	51.90	0.172	1.012
NTHX-080	DP I	Water	Radiator	0.03	3.24	25.00	300.00	349.74	200.00	Liquid	219.21	51.95	0.184	1.008
NTHX-081	DP I	Water	Radiator	0.03	3.25	25.00	300.00	349.44	200.00	Liquid	228.37	51.99	0.146	1.008
NTHX-082	DP I	Water	Radiator	0.03	3.25	25.00	300.00	349.68	200.00	Liquid	226.12	52.12	0.184	1.007
NTHX-083	DP I	Water	Radiator	0.03	3.24	25.00	300.00	349.88	200.00	Liquid	226.17	52.36	0.171	1.012
NTHX-084	DP I	Water	Radiator	0.03	3.27	25.00	300.00	349.44	200.00	Liquid	227.10	52.97	0.174	1.004
NTHX-085	DP I	Water	Radiator	0.03	3.27	25.00	300.00	349.72	200.00	Liquid	227.42	53.07	0.126	1.007
NTHX-086	DP I	Water	Radiator	0.03	3.28	25.00	300.00	349.72	200.00	Liquid	227.86	53.54	0.125	1.007
NTHX-087	DP I	Water	Radiator	0.03	3.33	25.00	300.00	349.60	200.00	Liquid	228.92	54.49	0.171	1.001

WTHX

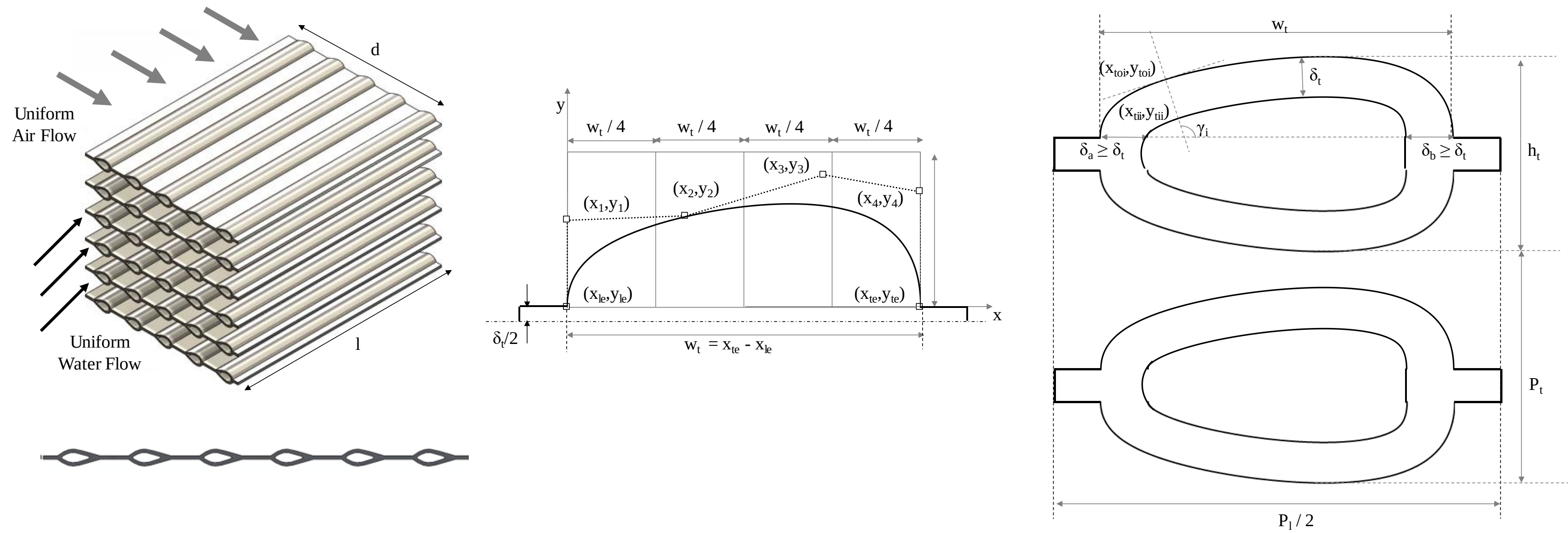

Figure 132. WTHX concept.

Table 36. WTHX dimensions.

Design Tag	h_t	w_t	δ_t	P_l	P_t	N_r	N_t	x_1	x_2	x_3	x_4	y_1	y_2	y_3	y_4	l	H	d	A_f	V
	mm	mm	mm	mm	mm	-	-	-	-	-	-	-	-	-	-	m	m	m	m^2	cm^3
WTHX-001	0.5000	1.4228	0.1000	2.2583	1.1065	6	114	0.97067	0.88270	0.07625	0.09189	0.92375	0.99218	0.8651	0.0391	0.0804	0.1266	0.0135	0.0102	137.97
WTHX-002	0.5000	1.4228	0.1000	1.8428	1.0510	6	108	0.97067	0.53861	0.07625	0.00978	0.98631	0.95894	0.8651	0.0391	0.0890	0.1140	0.0111	0.0101	112.18

Design Tag	h_t	w_t	δ_t	P_l	P_t	N_r	N_t	x_1	x_2	x_3	x_4	y_1	y_2	y_3	y_4	l	H	d	A_f	V
	mm	mm	mm	mm	mm	-	-	-	-	-	-	-	-	-	-	m	m	m	m^2	cm^3
WTHX-003	0.5264	1.5411	0.1053	2.5365	1.1722	6	108	0.97067	0.57771	0.07625	0.01760	0.92375	0.99218	0.8495	0.0391	0.0801	0.1271	0.0152	0.0102	155.01
WTHX-004	0.5029	1.3977	0.1006	2.1911	1.0993	6	108	0.97067	0.57771	0.07625	0.02933	0.92766	0.99022	0.8651	0.0547	0.0860	0.1192	0.0131	0.0103	134.78
WTHX-005	0.5000	1.4247	0.1000	1.8436	1.0518	6	108	0.97067	0.50244	0.07625	0.09189	0.99316	0.99218	0.8495	0.1017	0.0891	0.1141	0.0111	0.0102	112.41
WTHX-006	0.5000	1.3895	0.1000	2.1784	1.0929	6	124	0.97067	0.82796	0.07625	0.02542	0.92375	0.99218	0.8651	0.0078	0.0739	0.1360	0.0131	0.0101	131.46
WTHX-007	0.5000	1.3895	0.1000	2.1784	1.0929	6	110	0.97067	0.57771	0.07625	0.01760	0.92375	0.99218	0.8651	0.0078	0.0833	0.1207	0.0131	0.0101	131.45
WTHX-008	0.5000	1.3895	0.1000	2.1784	1.0920	6	108	0.98631	0.88270	0.07625	0.02542	0.89247	0.99218	0.8651	0.0078	0.0859	0.1184	0.0131	0.0102	133.03
WTHX-009	0.5264	1.5411	0.1053	2.5666	1.1722	6	108	0.97067	0.88563	0.00587	0.09189	0.93060	0.99218	0.8495	0.0391	0.0806	0.1271	0.0154	0.0103	157.88
WTHX-010	0.5000	1.3895	0.1000	2.1801	1.0929	6	109	0.98631	0.88563	0.10753	0.02542	0.92375	0.95894	0.8495	0.0078	0.0857	0.1196	0.0131	0.0103	134.10
WTHX-011	0.5264	1.5411	0.1053	2.5666	1.1722	6	108	0.97067	0.53372	0.03030	0.08407	0.93060	0.99218	0.8495	0.0391	0.0806	0.1271	0.0154	0.0102	157.74
WTHX-012	0.5000	1.4052	0.1000	1.7651	1.0373	6	111	0.99022	0.53372	0.07625	0.09189	0.99413	0.99218	0.8495	0.0391	0.0879	0.1156	0.0106	0.0102	107.66
WTHX-013	0.5000	1.4228	0.1000	1.8411	1.0501	6	108	0.97067	0.50244	0.07722	0.08016	0.93060	0.99218	0.8495	0.0391	0.0899	0.1139	0.0110	0.0102	113.13
WTHX-014	0.5000	1.4228	0.1000	1.8411	1.0510	6	108	0.97067	0.53372	0.03030	0.08407	0.99413	0.99218	0.8651	0.1017	0.0890	0.1140	0.0110	0.0101	112.07
WTHX-015	0.5000	1.4228	0.1000	1.8411	1.0510	6	108	0.97067	0.57283	0.10850	0.08407	0.92375	0.96090	0.8651	0.0391	0.0899	0.1140	0.0110	0.0102	113.15
WTHX-016	0.5000	1.4228	0.1000	2.2583	1.1065	6	108	0.98631	0.88563	0.07625	0.02933	0.92375	0.99218	0.8495	0.0078	0.0854	0.1200	0.0135	0.0103	138.91
WTHX-017	0.5000	1.4228	0.1000	1.8411	1.0510	6	108	0.99022	0.53372	0.07625	0.09189	0.99316	0.99218	0.8495	0.0391	0.0899	0.1140	0.0110	0.0103	113.24
WTHX-018	0.5000	1.3895	0.1000	2.1784	1.0929	6	114	0.97067	0.57771	0.07625	0.01760	0.92375	0.96090	0.9746	0.0000	0.0803	0.1251	0.0131	0.0101	131.36
WTHX-019	0.5000	1.3895	0.1000	2.1784	1.0929	6	120	0.97067	0.57771	0.24829	0.02639	0.92375	0.99022	0.8651	0.0391	0.0763	0.1316	0.0131	0.0100	131.34
WTHX-020	0.5000	1.4052	0.1000	1.7633	1.0373	6	123	0.98631	0.56891	0.07722	0.09189	0.92766	0.99022	0.8651	0.0391	0.0800	0.1281	0.0106	0.0102	108.36
WTHX-021	0.5000	1.4052	0.1000	1.7633	1.0373	6	111	0.99022	0.53372	0.07625	0.09189	0.99413	0.99218	0.8495	0.0391	0.0881	0.1156	0.0106	0.0102	107.73
WTHX-022	0.5000	1.4247	0.1000	1.8436	1.0518	6	108	0.97067	0.50244	0.07625	0.09189	0.99316	0.99218	0.8495	0.1017	0.0892	0.1141	0.0111	0.0102	112.64
WTHX-023	0.5000	1.3895	0.1000	2.1784	1.0929	6	172	0.99022	0.53372	0.07625	0.09189	0.92766	0.97458	0.8651	0.0391	0.0539	0.1885	0.0131	0.0102	132.76
WTHX-024	0.5000	1.4228	0.1000	2.2600	1.1065	6	196	0.98631	0.58553	0.07625	0.00978	0.92571	0.99022	0.8651	0.0391	0.0469	0.2174	0.0136	0.0102	138.11
WTHX-025	0.5000	1.4228	0.1000	1.8411	1.0510	6	108	0.97067	0.50244	0.07625	0.09189	0.99316	0.99218	0.8495	0.1017	0.0891	0.1140	0.0110	0.0102	112.26
WTHX-026	0.5029	1.4311	0.1006	1.8728	1.0571	6	108	0.97849	0.75269	0.07625	0.09189	0.92375	0.99022	0.8651	0.0391	0.0894	0.1147	0.0112	0.0103	115.24
WTHX-027	0.5264	1.4999	0.1053	2.5567	1.1722	6	126	0.97067	0.53372	0.03030	0.08407	0.92375	0.96090	0.8651	0.0391	0.0691	0.1482	0.0153	0.0102	157.14
WTHX-028	0.5000	1.3895	0.1000	2.1784	1.0929	6	148	0.97067	0.57771	0.07625	0.02933	0.92766	0.99218	0.8651	0.0078	0.0632	0.1622	0.0131	0.0103	133.99
WTHX-029	0.5000	1.3895	0.1000	2.1784	1.0929	6	108	0.97067	0.88563	0.10753	0.02542	0.92375	0.95894	0.8495	0.0391	0.0845	0.1185	0.0131	0.0100	130.95
WTHX-030	0.5000	1.3895	0.1000	2.1784	1.0929	6	110	0.97067	0.88563	0.00587	0.09189	0.93060	0.99218	0.8651	0.0078	0.0839	0.1207	0.0131	0.0101	132.30
WTHX-031	0.5000	1.4228	0.1000	1.8411	1.0510	6	109	0.97067	0.55034	0.07625	0.09189	0.99316	0.99218	0.8495	0.1017	0.0885	0.1151	0.0110	0.0102	112.48
WTHX-032	0.5000	1.3895	0.1000	2.1784	1.0929	6	109	0.93939	0.88270	0.07625	0.02542	0.89247	0.99218	0.9922	0.0078	0.0857	0.1196	0.0131	0.0103	133.99
WTHX-033	0.5000	1.4228	0.1000	1.8411	1.0518	6	108	0.98631	0.51026	0.24829	0.02639	0.99413	0.99218	0.8651	0.1017	0.0890	0.1141	0.0110	0.0102	112.12
WTHX-034	0.5000	1.3895	0.1000	1.7369	1.0176	6	108	0.97849	0.75269	0.07625	0.09189	0.92375	0.99022	0.8495	0.0391	0.0929	0.1104	0.0104	0.0103	106.88
WTHX-035	0.5029	1.4311	0.1006	1.8728	1.0571	6	161	0.97067	0.57771	0.07625	0.09189	0.92375	0.99218	0.8495	0.0000	0.0601	0.1707	0.0112	0.0103	115.20
WTHX-036	0.5000	1.4228	0.1000	2.2531	1.1065	6	109	0.97067	0.57771	0.07625	0.02933	0.92766	0.99022	0.8651	0.0391	0.0840	0.1211	0.0135	0.0102	137.58
WTHX-037	0.5000	1.3895	0.1000	2.1784	1.0929	6	109	0.97067	0.50244	0.07625	0.07625	0.99316	0.99218	0.8651	0.0078	0.0850	0.1196	0.0131	0.0102	132.83
WTHX-038	0.5000	1.4052	0.1000	1.7633	1.0373	6	170	0.97067	0.53177	0.07625	0.09189	0.98631	0.99022	0.8495	0.0391	0.0580	0.1768	0.0106	0.0103	108.46
WTHX-039	0.5000	1.4228	0.1000	1.8411	1.0518	6	108	0.97458	0.50049	0.07625	0.09189	0.99316	0.99218	0.8495	0.1017	0.0898	0.1141	0.0110	0.0103	113.23
WTHX-040	0.5000	1.3895	0.1000	2.1784	1.0929	6	172	0.97067	0.89834	0.07625	0.02542	0.89247	0.99218	0.8651	0.0391	0.0543	0.1885	0.0131	0.0102	133.87
WTHX-041	0.5000	1.3817	0.1000	2.1661	1.0929	6	172	0.97067	0.55034	0.07625	0.00978	0.99316	0.92962	0.8495	0.0391	0.0543	0.1885	0.0130	0.0102	133.12
WTHX-042	0.5000	1.4228	0.1000	2.2531	1.1065	6	109	0.97067	0.57771	0.07625	0.02542	0.92375	0.99218	0.8641	0.0078	0.0846	0.1211	0.0135	0.0102	138.46
WTHX-043	0.5337	1.5626	0.1067	2.6024	1.1885	6	108	0.97067	0.53372	0.02933	0.12317	0.93157	0.97458	0.8651	0.0391	0.0795	0.1289	0.0156	0.0103	160.08
WTHX-044	0.5000	1.4228	0.1000	1.8411	1.0501	6	120	0.98631	0.51026	0.24829	0.02639	0.92375	0.99022	0.8651	0.0391	0.0810	0.1265	0.0110	0.0102	113.13
WTHX-045	0.5000	1.4052	0.1000	1.7633	1.0373	6	123	0.98631	0.56891	0.07722	0.09189	0.92766	0.99022	0.8651	0.0391	0.0800	0.1281	0.0106	0.0103	108.47
WTHX-046	0.5000	1.3895	0.1000	2.1784	1.0929	6	161	0.97067	0.53372	0.03030	0.08016	0.92375	0.99218	0.8495	0.0000	0.0575	0.1765	0.0131	0.0101	132.61

Design Tag	h_t	w_t	δ_t	P_l	P_t	N_r	N_t	x_1	x_2	x_3	x_4	y_1	y_2	y_3	y_4	l	H	d	A_f	V
	mm	mm	mm	mm	mm	-	-	-	-	-	-	-	-	-	-	m	m	m	m^2	cm^3
WTHX-047	0.5000	1.3895	0.1000	1.7369	1.0176	6	120	0.98631	0.51026	0.20137	0.02542	0.89247	0.99022	0.8651	0.0391	0.0828	0.1226	0.0104	0.0102	105.78
WTHX-048	0.5000	1.3895	0.1000	2.1784	1.0929	6	108	0.97067	0.53861	0.07625	0.00978	0.98631	0.95894	0.8651	0.0401	0.0853	0.1185	0.0131	0.0101	132.19
WTHX-049	0.5000	1.3895	0.1000	2.1784	1.0929	6	108	0.97263	0.53372	0.03030	0.08016	0.92766	0.99022	0.8749	0.0391	0.0846	0.1185	0.0131	0.0100	131.05

Table 37. WTHX performance and operating conditions.

Design Tag	Design Problem	Fluid	Application	V_{air}	u_{air}	$\dot{m}_{fluid}$	$T_{air,in}$	$T_{fluid,in}$	$P_{fluid,in}$	$x_{fluid,in}$	h	ΔP_{air}	ΔP_{fluid}	Q
	-	-	-	m^3/s	m/s	g/s	K	K	kPa	-	$W/m^2.K$	Pa	kPa	kW
WTHX-001	DP I	Water	Radiator	0.03	2.95	25.00	300.00	350.00	200.00	Liquid	137.21	40.89	0.745	1.001
WTHX-002	DP I	Water	Radiator	0.03	2.96	25.00	300.00	350.00	200.00	Liquid	159.11	46.09	0.890	1.000
WTHX-003	DP I	Water	Radiator	0.03	2.95	25.00	300.00	350.00	200.00	Liquid	129.56	40.09	0.617	1.001
WTHX-004	DP I	Water	Radiator	0.03	2.93	25.00	300.00	350.00	200.00	Liquid	139.94	41.05	0.882	1.002
WTHX-005	DP I	Water	Radiator	0.03	2.95	25.00	300.00	350.00	200.00	Liquid	158.76	45.90	0.841	1.000
WTHX-006	DP I	Water	Radiator	0.03	2.98	25.00	300.00	350.00	200.00	Liquid	143.35	43.03	0.704	1.001
WTHX-007	DP I	Water	Radiator	0.03	2.98	25.00	300.00	350.00	200.00	Liquid	143.01	43.11	0.896	1.003
WTHX-008	DP I	Water	Radiator	0.03	2.95	25.00	300.00	350.00	200.00	Liquid	140.75	41.64	0.933	1.001
WTHX-009	DP I	Water	Radiator	0.03	2.93	25.00	300.00	350.00	200.00	Liquid	127.79	39.87	0.616	1.003
WTHX-010	DP I	Water	Radiator	0.03	2.93	25.00	300.00	350.00	200.00	Liquid	139.87	41.07	0.903	1.002
WTHX-011	DP I	Water	Radiator	0.03	2.93	25.00	300.00	350.00	200.00	Liquid	128.32	39.90	0.616	1.004
WTHX-012	DP I	Water	Radiator	0.03	2.95	25.00	300.00	350.00	200.00	Liquid	163.76	47.22	0.878	1.001
WTHX-013	DP I	Water	Radiator	0.03	2.93	25.00	300.00	350.00	200.00	Liquid	157.81	45.27	0.892	1.001
WTHX-014	DP I	Water	Radiator	0.03	2.96	25.00	300.00	350.00	200.00	Liquid	159.14	46.29	0.866	1.000
WTHX-015	DP I	Water	Radiator	0.03	2.93	25.00	300.00	350.00	200.00	Liquid	157.65	45.05	0.867	1.000
WTHX-016	DP I	Water	Radiator	0.03	2.93	25.00	300.00	350.00	200.00	Liquid	136.55	40.24	0.882	1.001
WTHX-017	DP I	Water	Radiator	0.03	2.93	25.00	300.00	350.00	200.00	Liquid	157.61	44.88	0.895	1.000
WTHX-018	DP I	Water	Radiator	0.03	2.99	25.00	300.00	350.00	200.00	Liquid	143.32	43.39	0.809	1.004
WTHX-019	DP I	Water	Radiator	0.03	2.99	25.00	300.00	350.00	200.00	Liquid	143.03	43.66	0.687	1.004
WTHX-020	DP I	Water	Radiator	0.03	2.93	25.00	300.00	350.00	200.00	Liquid	162.29	46.62	0.715	1.001
WTHX-021	DP I	Water	Radiator	0.03	2.95	25.00	300.00	350.00	200.00	Liquid	163.58	47.21	0.879	1.001
WTHX-022	DP I	Water	Radiator	0.03	2.95	25.00	300.00	350.00	200.00	Liquid	158.48	45.70	0.842	1.000
WTHX-023	DP I	Water	Radiator	0.03	2.95	25.00	300.00	350.00	200.00	Liquid	141.27	42.10	0.355	1.002
WTHX-024	DP I	Water	Radiator	0.03	2.95	25.00	300.00	350.00	200.00	Liquid	138.75	40.84	0.265	1.001
WTHX-025	DP I	Water	Radiator	0.03	2.95	25.00	300.00	350.00	200.00	Liquid	158.93	45.99	0.844	1.000
WTHX-026	DP I	Water	Radiator	0.03	2.93	25.00	300.00	350.00	200.00	Liquid	156.09	44.82	0.862	1.001
WTHX-027	DP I	Water	Radiator	0.03	2.93	25.00	300.00	350.00	200.00	Liquid	128.58	40.06	0.480	1.000
WTHX-028	DP I	Water	Radiator	0.03	2.93	25.00	300.00	350.00	200.00	Liquid	140.54	41.09	0.504	1.002
WTHX-029	DP I	Water	Radiator	0.03	2.99	25.00	300.00	350.00	200.00	Liquid	143.37	43.93	0.876	1.002

Design Tag	Design Problem	Fluid	Application	V_{air}	u_{air}	$\dot{m}_{fluid}$	$T_{air,in}$	$T_{fluid,in}$	$P_{fluid,in}$	$x_{fluid,in}$	h	ΔP_{air}	ΔP_{fluid}	Q
	-	-	-	m^3/s	m/s	g/s	K	K	kPa	-	$W/m^2.K$	Pa	kPa	kW
WTHX-030	DP I	Water	Radiator	0.03	2.96	25.00	300.00	350.00	200.00	Liquid	141.41	42.18	0.884	1.001
WTHX-031	DP I	Water	Radiator	0.03	2.95	25.00	300.00	350.00	200.00	Liquid	158.53	45.77	0.838	1.000
WTHX-032	DP I	Water	Radiator	0.03	2.93	25.00	300.00	350.00	200.00	Liquid	140.12	41.08	0.886	1.003
WTHX-033	DP I	Water	Radiator	0.03	2.96	25.00	300.00	350.00	200.00	Liquid	159.18	46.15	0.822	1.000
WTHX-034	DP I	Water	Radiator	0.03	2.93	25.00	300.00	350.00	200.00	Liquid	166.58	49.39	0.963	1.016
WTHX-035	DP I	Water	Radiator	0.03	2.93	25.00	300.00	350.00	200.00	Liquid	156.40	44.85	0.402	1.001
WTHX-036	DP I	Water	Radiator	0.03	2.95	25.00	300.00	350.00	200.00	Liquid	137.89	40.92	0.837	1.001
WTHX-037	DP I	Water	Radiator	0.03	2.95	25.00	300.00	350.00	200.00	Liquid	141.55	41.87	0.906	1.003
WTHX-038	DP I	Water	Radiator	0.03	2.93	25.00	300.00	350.00	200.00	Liquid	162.63	46.46	0.376	1.001
WTHX-039	DP I	Water	Radiator	0.03	2.93	25.00	300.00	350.00	200.00	Liquid	157.64	45.04	0.852	1.000
WTHX-040	DP I	Water	Radiator	0.03	2.93	25.00	300.00	350.00	200.00	Liquid	139.73	41.11	0.362	1.000
WTHX-041	DP I	Water	Radiator	0.03	2.93	25.00	300.00	350.00	200.00	Liquid	140.60	41.24	0.367	1.001
WTHX-042	DP I	Water	Radiator	0.03	2.93	25.00	300.00	350.00	200.00	Liquid	137.19	40.39	0.863	1.002
WTHX-043	DP I	Water	Radiator	0.03	2.93	25.00	300.00	350.00	200.00	Liquid	127.05	39.69	0.562	1.000
WTHX-044	DP I	Water	Radiator	0.03	2.93	25.00	300.00	350.00	200.00	Liquid	157.68	45.41	0.694	1.001
WTHX-045	DP I	Water	Radiator	0.03	2.93	25.00	300.00	350.00	200.00	Liquid	162.16	46.38	0.716	1.001
WTHX-046	DP I	Water	Radiator	0.03	2.96	25.00	300.00	350.00	200.00	Liquid	141.51	42.14	0.429	1.001
WTHX-047	DP I	Water	Radiator	0.03	2.96	25.00	300.00	350.00	200.00	Liquid	168.38	50.72	0.768	1.017
WTHX-048	DP I	Water	Radiator	0.03	2.97	25.00	300.00	350.00	200.00	Liquid	142.35	42.49	0.905	1.004
WTHX-049	DP I	Water	Radiator	0.03	2.99	25.00	300.00	350.00	200.00	Liquid	143.66	43.81	0.900	1.004

AFHX

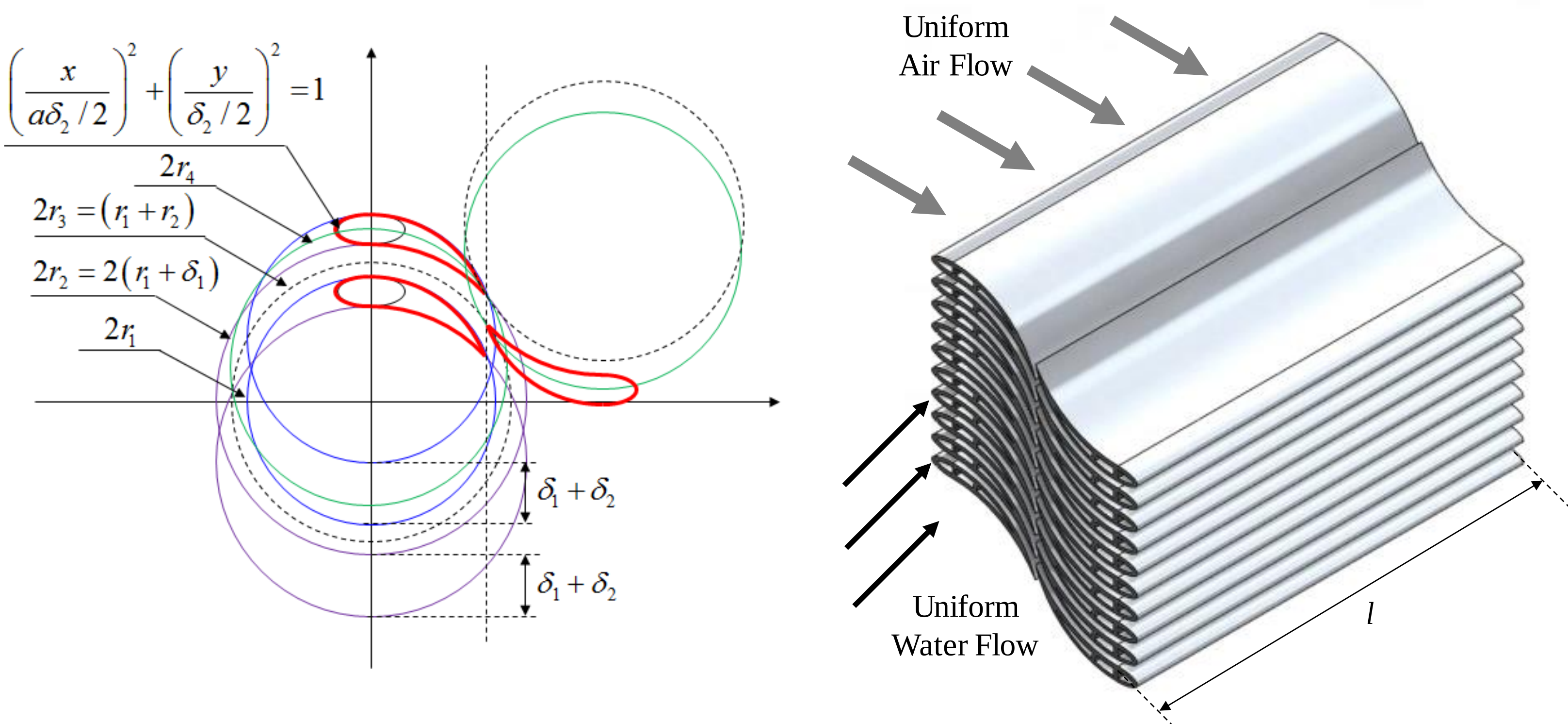

Figure 133. AFHX Concept.

Table 38. AFHX dimensions.

Design Tag	r_1	δ_1	δ_2	δ_t	a	P_t	Ports/N_t	N_t	N_r	l	H	d	A_f	V
	mm	mm	mm	mm	-	mm	-	-	-	m	m	m	m^2	cm^3
AFHX-001	23.6706	1.0450	0.5225	0.1045	2.9883	1.5674	3	2	51	0.12930	0.07929	0.01875	0.01025	192.28
AFHX-002	23.6706	1.0450	0.5225	0.1045	2.9902	1.5674	3	2	54	0.12215	0.08393	0.01875	0.01025	192.27
AFHX-003	23.6950	1.0450	0.5225	0.1045	2.9902	1.5674	3	2	54	0.12195	0.08393	0.01877	0.01024	192.15
AFHX-004	23.6950	1.0450	0.5225	0.1045	2.9902	1.5674	3	2	54	0.12195	0.08393	0.01877	0.01024	192.14
AFHX-005	23.6950	1.0450	0.5225	0.1045	2.9863	1.5674	3	2	54	0.12195	0.08393	0.01877	0.01024	192.13
AFHX-006	23.6950	1.0450	0.5225	0.1045	2.9589	1.5674	3	2	54	0.12198	0.08393	0.01877	0.01024	192.10
AFHX-007	23.6950	1.0450	0.5225	0.1045	2.9609	1.5674	3	2	54	0.12197	0.08393	0.01877	0.01024	192.09
AFHX-008	23.6950	1.0450	0.5225	0.1045	2.9589	1.5674	3	2	54	0.12195	0.08393	0.01877	0.01024	192.07
AFHX-009	23.6950	1.0450	0.5225	0.1045	2.9570	1.5674	3	2	54	0.12195	0.08393	0.01876	0.01024	192.06
AFHX-010	23.6950	1.0450	0.5225	0.1045	2.9570	1.5674	3	2	56	0.11762	0.08702	0.01876	0.01024	192.06
AFHX-011	23.6950	1.0450	0.5225	0.1045	2.9550	1.5674	3	2	54	0.12195	0.08393	0.01876	0.01024	192.06
AFHX-012	23.6950	1.0450	0.5225	0.1045	2.9550	1.5674	3	2	54	0.12195	0.08393	0.01876	0.01024	192.05
AFHX-013	23.6950	1.0450	0.5225	0.1045	2.9726	1.5674	3	2	54	0.12176	0.08393	0.01877	0.01022	191.80
AFHX-014	23.3284	1.0371	0.5186	0.1037	2.9883	1.5557	3	2	51	0.13000	0.07889	0.01854	0.01026	190.12
AFHX-015	23.3284	1.0371	0.5186	0.1037	2.9883	1.5557	3	2	51	0.12999	0.07889	0.01854	0.01026	190.12
AFHX-016	23.3284	1.0371	0.5186	0.1037	2.9922	1.5557	3	2	54	0.12276	0.08351	0.01854	0.01025	190.05
AFHX-017	23.3284	1.0371	0.5186	0.1037	2.9902	1.5557	3	2	54	0.12276	0.08351	0.01854	0.01025	190.04
AFHX-018	23.3284	1.0371	0.5186	0.1037	2.9883	1.5557	3	2	55	0.12045	0.08504	0.01854	0.01024	189.89
AFHX-019	23.3284	1.0371	0.5186	0.1037	2.9883	1.5557	3	2	51	0.12974	0.07889	0.01854	0.01024	189.75
AFHX-020	23.3284	1.0371	0.5186	0.1037	2.9863	1.5557	3	2	51	0.12974	0.07889	0.01854	0.01024	189.75
AFHX-021	23.3284	1.0371	0.5186	0.1037	2.9844	1.5557	3	2	51	0.12974	0.07889	0.01854	0.01024	189.74
AFHX-022	23.3284	1.0371	0.5186	0.1037	2.9902	1.5557	3	2	51	0.12970	0.07889	0.01854	0.01023	189.69
AFHX-023	23.3284	1.0371	0.5186	0.1037	2.9609	1.5557	3	2	51	0.12974	0.07889	0.01853	0.01024	189.68
AFHX-024	23.0841	1.0313	0.5156	0.1031	2.9550	1.5469	3	2	54	0.12327	0.08319	0.01838	0.01025	188.44
AFHX-025	23.0841	1.0313	0.5156	0.1031	2.9922	1.5469	3	2	51	0.13023	0.07860	0.01838	0.01024	188.17
AFHX-026	23.0841	1.0313	0.5156	0.1031	2.9922	1.5469	3	2	51	0.13023	0.07860	0.01838	0.01024	188.17
AFHX-027	23.3284	1.0332	0.5166	0.1033	2.9589	1.5499	3	2	51	0.12887	0.07870	0.01855	0.01014	188.11
AFHX-028	23.2796	1.0313	0.5156	0.1031	2.8944	1.5469	3	2	51	0.12930	0.07860	0.01850	0.01016	188.05
AFHX-029	23.3040	1.0313	0.5156	0.1031	2.9863	1.5469	3	2	51	0.12858	0.07860	0.01855	0.01011	187.42
AFHX-030	23.3040	1.0313	0.5156	0.1031	2.9550	1.5469	3	2	51	0.12858	0.07860	0.01854	0.01011	187.35
AFHX-031	21.9599	1.0020	0.5010	0.1002	3.0000	1.5029	3	2	54	0.12559	0.08161	0.01768	0.01025	181.22
AFHX-032	21.9599	1.0020	0.5010	0.1002	2.9980	1.5029	3	2	54	0.12548	0.08161	0.01768	0.01024	181.05
AFHX-033	21.9599	1.0020	0.5010	0.1002	3.0000	1.5029	3	2	54	0.12539	0.08161	0.01768	0.01023	180.93
AFHX-034	21.9599	1.0020	0.5010	0.1002	2.9883	1.5029	3	2	54	0.12539	0.08161	0.01768	0.01023	180.90
AFHX-035	21.8866	1.0000	0.5000	0.1000	2.9589	1.5000	3	2	54	0.12583	0.08150	0.01763	0.01025	180.75
AFHX-036	21.8866	1.0000	0.5000	0.1000	2.9550	1.5000	3	2	54	0.12583	0.08150	0.01762	0.01025	180.74
AFHX-037	21.8866	1.0000	0.5000	0.1000	2.9902	1.5000	3	2	54	0.12572	0.08150	0.01763	0.01025	180.68
AFHX-038	21.8866	1.0000	0.5000	0.1000	2.9550	1.5000	3	2	54	0.12578	0.08150	0.01762	0.01025	180.67
AFHX-039	21.8866	1.0000	0.5000	0.1000	2.9980	1.5000	3	2	54	0.12560	0.08150	0.01764	0.01024	180.52
AFHX-040	21.8866	1.0000	0.5000	0.1000	2.9980	1.5000	3	2	54	0.12557	0.08150	0.01764	0.01023	180.48
AFHX-041	21.8866	1.0000	0.5000	0.1000	2.9902	1.5000	3	2	54	0.12558	0.08150	0.01763	0.01024	180.48

Design Tag	r_1	δ_1	δ_2	δ_t	a	P_t	Ports/N_t	N_t	N_r	l	H	d	A_f	V
	mm	mm	mm	mm	-	mm	-	-	-	m	m	m	m^2	cm^3
AFHX-042	21.8866	1.0000	0.5000	0.1000	2.9589	1.5000	3	2	54	0.12564	0.08150	0.01763	0.01024	180.48
AFHX-043	21.8866	1.0000	0.5000	0.1000	2.9589	1.5000	3	2	54	0.12561	0.08150	0.01763	0.01024	180.44
AFHX-044	21.8866	1.0000	0.5000	0.1000	2.9609	1.5000	3	2	54	0.12560	0.08150	0.01763	0.01024	180.43
AFHX-045	21.8866	1.0000	0.5000	0.1000	2.9570	1.5000	3	2	54	0.12561	0.08150	0.01763	0.01024	180.43
AFHX-046	21.8866	1.0000	0.5000	0.1000	2.9589	1.5000	3	2	54	0.12560	0.08150	0.01763	0.01024	180.42
AFHX-047	21.8866	1.0000	0.5000	0.1000	2.9570	1.5000	3	2	54	0.12560	0.08150	0.01763	0.01024	180.42
AFHX-048	21.8866	1.0000	0.5000	0.1000	2.9609	1.5000	3	2	54	0.12559	0.08150	0.01763	0.01024	180.41
AFHX-049	21.8866	1.0000	0.5000	0.1000	2.9413	1.5000	3	2	54	0.12561	0.08150	0.01762	0.01024	180.39
AFHX-050	21.8866	1.0000	0.5000	0.1000	2.9609	1.5000	3	2	54	0.12555	0.08150	0.01763	0.01023	180.36
AFHX-051	21.8866	1.0000	0.5000	0.1000	2.9550	1.5000	3	2	54	0.12555	0.08150	0.01762	0.01023	180.34
AFHX-052	21.8866	1.0000	0.5000	0.1000	2.9550	1.5000	3	2	54	0.12555	0.08150	0.01762	0.01023	180.34
AFHX-053	21.9599	1.0000	0.5000	0.1000	2.9589	1.5000	3	2	54	0.12511	0.08150	0.01768	0.01020	180.28
AFHX-054	21.9599	1.0000	0.5000	0.1000	2.9589	1.5000	3	2	54	0.12506	0.08150	0.01768	0.01019	180.20
AFHX-055	21.9844	1.0000	0.5000	0.1000	2.9980	1.5000	3	2	54	0.12484	0.08150	0.01771	0.01017	180.17
AFHX-056	21.9844	1.0000	0.5000	0.1000	2.9902	1.5000	3	2	54	0.12484	0.08150	0.01771	0.01017	180.15
AFHX-057	21.9844	1.0000	0.5000	0.1000	2.9980	1.5000	3	2	54	0.12481	0.08150	0.01771	0.01017	180.13
AFHX-058	21.9844	1.0000	0.5000	0.1000	2.9883	1.5000	3	2	54	0.12483	0.08150	0.01771	0.01017	180.13
AFHX-059	21.9844	1.0000	0.5000	0.1000	2.9980	1.5000	3	2	54	0.12480	0.08150	0.01771	0.01017	180.11
AFHX-060	21.9844	1.0000	0.5000	0.1000	2.9980	1.5000	3	2	54	0.12479	0.08150	0.01771	0.01017	180.10
AFHX-061	21.9844	1.0000	0.5000	0.1000	2.9883	1.5000	3	2	54	0.12480	0.08150	0.01771	0.01017	180.09
AFHX-062	21.9844	1.0000	0.5000	0.1000	2.9883	1.5000	3	2	54	0.12479	0.08150	0.01771	0.01017	180.07
AFHX-063	21.9844	1.0000	0.5000	0.1000	2.9883	1.5000	3	2	54	0.12479	0.08150	0.01771	0.01017	180.07
AFHX-064	21.9844	1.0000	0.5000	0.1000	2.9570	1.5000	3	2	54	0.12484	0.08150	0.01770	0.01017	180.07
AFHX-065	21.9844	1.0000	0.5000	0.1000	2.9570	1.5000	3	2	54	0.12483	0.08150	0.01770	0.01017	180.06
AFHX-066	21.9844	1.0000	0.5000	0.1000	2.9883	1.5000	3	2	54	0.12475	0.08150	0.01771	0.01017	180.02
AFHX-067	21.9844	1.0000	0.5000	0.1000	2.9883	1.5000	3	2	54	0.12475	0.08150	0.01771	0.01017	180.02
AFHX-068	21.9844	1.0000	0.5000	0.1000	2.9726	1.5000	3	2	54	0.12477	0.08150	0.01770	0.01017	180.01
AFHX-069	21.9844	1.0000	0.5000	0.1000	2.9609	1.5000	3	2	54	0.12479	0.08150	0.01770	0.01017	180.00
AFHX-070	21.9844	1.0000	0.5000	0.1000	2.9609	1.5000	3	2	54	0.12479	0.08150	0.01770	0.01017	180.00
AFHX-071	21.9844	1.0000	0.5000	0.1000	2.9589	1.5000	3	2	54	0.12479	0.08150	0.01770	0.01017	179.99
AFHX-072	21.9844	1.0000	0.5000	0.1000	2.9570	1.5000	3	2	54	0.12479	0.08150	0.01770	0.01017	179.99
AFHX-073	21.9844	1.0000	0.5000	0.1000	2.9570	1.5000	3	2	54	0.12479	0.08150	0.01770	0.01017	179.99

Table 39. AFHX performance and operating conditions.

Design Tag	**Design Problem**	**Fluid**	**Application**	**V_{air}**	**u_{air}**	**$\dot{m}_{fluid}$**	**$T_{air,in}$**	**$T_{fluid,in}$**	**$P_{fluid,in}$**	**$x_{fluid,in}$**	**h**	**ΔP_{air}**	**ΔP_{fluid}**	**Q**
	-	**-**	**-**	**m^3/s**	**m/s**	**g/s**	**K**	**K**	**kPa**	**-**	**$W/m^2.K$**	**Pa**	**kPa**	**kW**
AFHX-001	DP I	Water	Radiator	0.03	2.93	25.00	300.00	350.00	200.00	Liquid	133.94	57.11	0.850	1.001
AFHX-002	DP I	Water	Radiator	0.03	2.93	25.00	300.00	350.00	200.00	Liquid	134.71	57.12	0.759	1.001
AFHX-003	DP I	Water	Radiator	0.03	2.93	25.00	300.00	350.00	200.00	Liquid	134.77	57.29	0.757	1.001
AFHX-004	DP I	Water	Radiator	0.03	2.93	25.00	300.00	350.00	200.00	Liquid	134.77	57.29	0.757	1.001
AFHX-005	DP I	Water	Radiator	0.03	2.93	25.00	300.00	350.00	200.00	Liquid	134.77	57.30	0.757	1.001
AFHX-006	DP I	Water	Radiator	0.03	2.93	25.00	300.00	350.00	200.00	Liquid	134.74	57.36	0.758	1.001
AFHX-007	DP I	Water	Radiator	0.03	2.93	25.00	300.00	350.00	200.00	Liquid	134.75	57.36	0.758	1.001
AFHX-008	DP I	Water	Radiator	0.03	2.93	25.00	300.00	350.00	200.00	Liquid	134.75	57.37	0.758	1.001
AFHX-009	DP I	Water	Radiator	0.03	2.93	25.00	300.00	350.00	200.00	Liquid	134.75	57.38	0.758	1.001
AFHX-010	DP I	Water	Radiator	0.03	2.93	25.00	300.00	350.00	200.00	Liquid	134.59	57.38	0.705	1.000
AFHX-011	DP I	Water	Radiator	0.03	2.93	25.00	300.00	350.00	200.00	Liquid	134.75	57.38	0.758	1.001
AFHX-012	DP I	Water	Radiator	0.03	2.93	25.00	300.00	350.00	200.00	Liquid	134.75	57.38	0.758	1.001
AFHX-013	DP I	Water	Radiator	0.03	2.94	25.00	300.00	350.00	200.00	Liquid	134.84	57.48	0.756	1.000
AFHX-014	DP I	Water	Radiator	0.03	2.93	25.00	300.00	350.00	200.00	Liquid	134.78	57.51	0.868	1.001
AFHX-015	DP I	Water	Radiator	0.03	2.93	25.00	300.00	350.00	200.00	Liquid	134.78	57.51	0.868	1.001
AFHX-016	DP I	Water	Radiator	0.03	2.93	25.00	300.00	350.00	200.00	Liquid	135.56	57.54	0.775	1.001
AFHX-017	DP I	Water	Radiator	0.03	2.93	25.00	300.00	350.00	200.00	Liquid	135.56	57.54	0.775	1.001
AFHX-018	DP I	Water	Radiator	0.03	2.93	25.00	300.00	350.00	200.00	Liquid	135.52	57.62	0.746	1.000
AFHX-019	DP I	Water	Radiator	0.03	2.93	25.00	300.00	350.00	200.00	Liquid	134.88	57.68	0.866	1.000
AFHX-020	DP I	Water	Radiator	0.03	2.93	25.00	300.00	350.00	200.00	Liquid	134.88	57.69	0.866	1.000
AFHX-021	DP I	Water	Radiator	0.03	2.93	25.00	300.00	350.00	200.00	Liquid	134.87	57.69	0.866	1.000
AFHX-022	DP I	Water	Radiator	0.03	2.93	25.00	300.00	350.00	200.00	Liquid	134.90	57.71	0.866	1.000
AFHX-023	DP I	Water	Radiator	0.03	2.93	25.00	300.00	350.00	200.00	Liquid	134.86	57.75	0.866	1.000
AFHX-024	DP I	Water	Radiator	0.03	2.93	25.00	300.00	350.00	200.00	Liquid	136.14	57.95	0.787	1.000
AFHX-025	DP I	Water	Radiator	0.03	2.93	25.00	300.00	350.00	200.00	Liquid	135.51	58.03	0.879	1.000
AFHX-026	DP I	Water	Radiator	0.03	2.93	25.00	300.00	350.00	200.00	Liquid	135.51	58.03	0.879	1.000
AFHX-027	DP I	Water	Radiator	0.03	2.96	25.00	300.00	350.00	200.00	Liquid	135.66	59.08	0.860	1.000
AFHX-028	DP I	Water	Radiator	0.03	2.95	25.00	300.00	350.00	200.00	Liquid	135.70	59.20	0.865	1.001
AFHX-029	DP I	Water	Radiator	0.03	2.97	25.00	300.00	350.00	200.00	Liquid	136.03	59.54	0.859	1.000
AFHX-030	DP I	Water	Radiator	0.03	2.97	25.00	300.00	350.00	200.00	Liquid	136.01	59.62	0.859	1.000
AFHX-031	DP I	Water	Radiator	0.03	2.93	25.00	300.00	350.00	200.00	Liquid	139.19	59.96	0.843	1.001
AFHX-032	DP I	Water	Radiator	0.03	2.93	25.00	300.00	350.00	200.00	Liquid	139.23	60.05	0.842	1.001
AFHX-033	DP I	Water	Radiator	0.03	2.93	25.00	300.00	350.00	200.00	Liquid	139.26	60.11	0.842	1.000
AFHX-034	DP I	Water	Radiator	0.03	2.93	25.00	300.00	350.00	200.00	Liquid	139.26	60.13	0.842	1.000
AFHX-035	DP I	Water	Radiator	0.03	2.93	25.00	300.00	350.00	200.00	Liquid	139.33	60.13	0.848	1.001
AFHX-036	DP I	Water	Radiator	0.03	2.93	25.00	300.00	350.00	200.00	Liquid	139.33	60.14	0.848	1.001
AFHX-037	DP I	Water	Radiator	0.03	2.93	25.00	300.00	350.00	200.00	Liquid	139.39	60.15	0.847	1.001
AFHX-038	DP I	Water	Radiator	0.03	2.93	25.00	300.00	350.00	200.00	Liquid	139.35	60.18	0.848	1.001
AFHX-039	DP I	Water	Radiator	0.03	2.93	25.00	300.00	350.00	200.00	Liquid	139.44	60.22	0.846	1.001
AFHX-040	DP I	Water	Radiator	0.03	2.93	25.00	300.00	350.00	200.00	Liquid	139.45	60.24	0.846	1.000
AFHX-041	DP I	Water	Radiator	0.03	2.93	25.00	300.00	350.00	200.00	Liquid	139.44	60.25	0.846	1.000

Design Tag	Design Problem	Fluid	Application	V_{air}	u_{air}	$\dot{m}_{fluid}$	$T_{air,in}$	$T_{fluid,in}$	$P_{fluid,in}$	$x_{fluid,in}$	h	ΔP_{air}	ΔP_{fluid}	Q
	-	-	-	m^3/s	m/s	g/s	K	K	kPa	-	$W/m^2.K$	Pa	kPa	kW
AFHX-042	DP I	Water	Radiator	0.03	2.93	25.00	300.00	350.00	200.00	Liquid	139.40	60.27	0.847	1.000
AFHX-043	DP I	Water	Radiator	0.03	2.93	25.00	300.00	350.00	200.00	Liquid	139.41	60.29	0.847	1.000
AFHX-044	DP I	Water	Radiator	0.03	2.93	25.00	300.00	350.00	200.00	Liquid	139.42	60.30	0.847	1.000
AFHX-045	DP I	Water	Radiator	0.03	2.93	25.00	300.00	350.00	200.00	Liquid	139.41	60.30	0.847	1.000
AFHX-046	DP I	Water	Radiator	0.03	2.93	25.00	300.00	350.00	200.00	Liquid	139.42	60.30	0.847	1.000
AFHX-047	DP I	Water	Radiator	0.03	2.93	25.00	300.00	350.00	200.00	Liquid	139.42	60.30	0.847	1.000
AFHX-048	DP I	Water	Radiator	0.03	2.93	25.00	300.00	350.00	200.00	Liquid	139.42	60.31	0.846	1.000
AFHX-049	DP I	Water	Radiator	0.03	2.93	25.00	300.00	350.00	200.00	Liquid	139.41	60.33	0.847	1.000
AFHX-050	DP I	Water	Radiator	0.03	2.93	25.00	300.00	350.00	200.00	Liquid	139.44	60.33	0.846	1.000
AFHX-051	DP I	Water	Radiator	0.03	2.93	25.00	300.00	350.00	200.00	Liquid	139.44	60.35	0.846	1.000
AFHX-052	DP I	Water	Radiator	0.03	2.93	25.00	300.00	350.00	200.00	Liquid	139.44	60.35	0.846	1.000
AFHX-053	DP I	Water	Radiator	0.03	2.94	25.00	300.00	350.00	200.00	Liquid	139.58	60.77	0.840	1.000
AFHX-054	DP I	Water	Radiator	0.03	2.94	25.00	300.00	350.00	200.00	Liquid	139.60	60.80	0.840	1.000
AFHX-055	DP I	Water	Radiator	0.03	2.95	25.00	300.00	350.00	200.00	Liquid	139.69	60.93	0.837	1.001
AFHX-056	DP I	Water	Radiator	0.03	2.95	25.00	300.00	350.00	200.00	Liquid	139.69	60.94	0.837	1.000
AFHX-057	DP I	Water	Radiator	0.03	2.95	25.00	300.00	350.00	200.00	Liquid	139.70	60.95	0.837	1.000
AFHX-058	DP I	Water	Radiator	0.03	2.95	25.00	300.00	350.00	200.00	Liquid	139.69	60.96	0.837	1.000
AFHX-059	DP I	Water	Radiator	0.03	2.95	25.00	300.00	350.00	200.00	Liquid	139.71	60.96	0.837	1.000
AFHX-060	DP I	Water	Radiator	0.03	2.95	25.00	300.00	350.00	200.00	Liquid	139.71	60.96	0.837	1.000
AFHX-061	DP I	Water	Radiator	0.03	2.95	25.00	300.00	350.00	200.00	Liquid	139.70	60.97	0.837	1.000
AFHX-062	DP I	Water	Radiator	0.03	2.95	25.00	300.00	350.00	200.00	Liquid	139.71	60.98	0.837	1.000
AFHX-063	DP I	Water	Radiator	0.03	2.95	25.00	300.00	350.00	200.00	Liquid	139.71	60.99	0.837	1.000
AFHX-064	DP I	Water	Radiator	0.03	2.95	25.00	300.00	350.00	200.00	Liquid	139.67	61.01	0.837	1.000
AFHX-065	DP I	Water	Radiator	0.03	2.95	25.00	300.00	350.00	200.00	Liquid	139.68	61.01	0.837	1.000
AFHX-066	DP I	Water	Radiator	0.03	2.95	25.00	300.00	350.00	200.00	Liquid	139.72	61.01	0.836	1.000
AFHX-067	DP I	Water	Radiator	0.03	2.95	25.00	300.00	350.00	200.00	Liquid	139.72	61.02	0.836	1.000
AFHX-068	DP I	Water	Radiator	0.03	2.95	25.00	300.00	350.00	200.00	Liquid	139.71	61.03	0.837	1.000
AFHX-069	DP I	Water	Radiator	0.03	2.95	25.00	300.00	350.00	200.00	Liquid	139.70	61.04	0.837	1.000
AFHX-070	DP I	Water	Radiator	0.03	2.95	25.00	300.00	350.00	200.00	Liquid	139.70	61.04	0.837	1.000
AFHX-071	DP I	Water	Radiator	0.03	2.95	25.00	300.00	350.00	200.00	Liquid	139.70	61.04	0.837	1.000
AFHX-072	DP I	Water	Radiator	0.03	2.95	25.00	300.00	350.00	200.00	Liquid	139.69	61.05	0.837	1.000
AFHX-073	DP I	Water	Radiator	0.03	2.95	25.00	300.00	350.00	200.00	Liquid	139.70	61.05	0.837	1.000

Table 40 – Specifications of test facility.

Item	Capacity
Coil Test Dimensions	• Max. 24" X 24" (Width X Height)
Heat Transfer Capacity	• Max. 10 kW
Max. Air Velocity	• Max. 5 m/s for the largest section (24" by 24")
Inlet Air Conditions	• -10°C to 45°C • Humidity control
Working Fluids	• Refrigerant without oil – pumped system • Refrigerant with oil – standard vapor compression system • Water - water flow rate – up to 2.5 kg/s • Brine

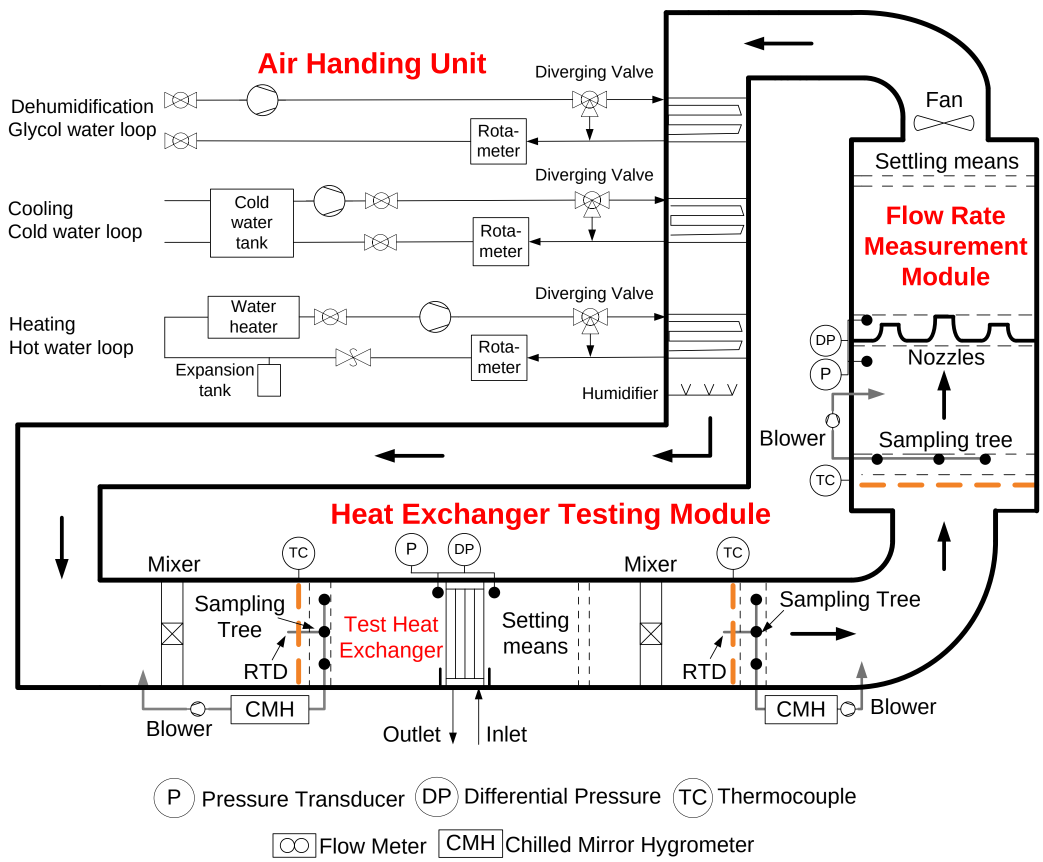

Figure 134 - Schematic diagram of air-side test facility.

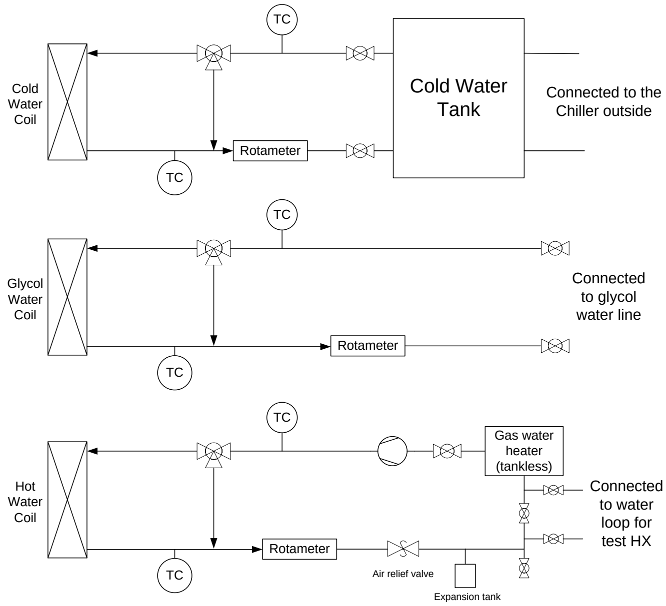

Figure 135 - Schematic of cold water loop (top), glycol water loop (middle), hot water loop (bottom) (courtesy from Zhiwei Huang).

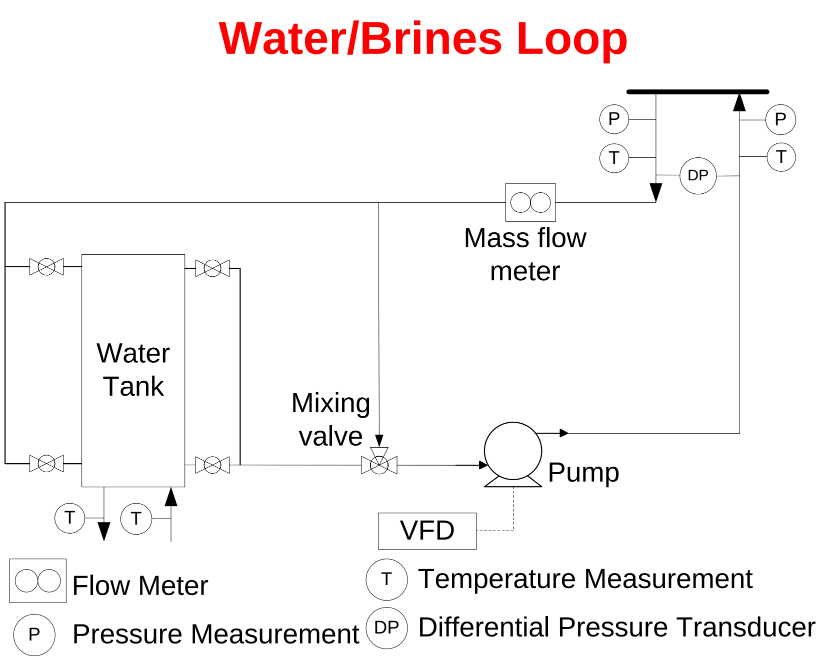

Figure 136 - Schematic diagram of water/brines system loop.

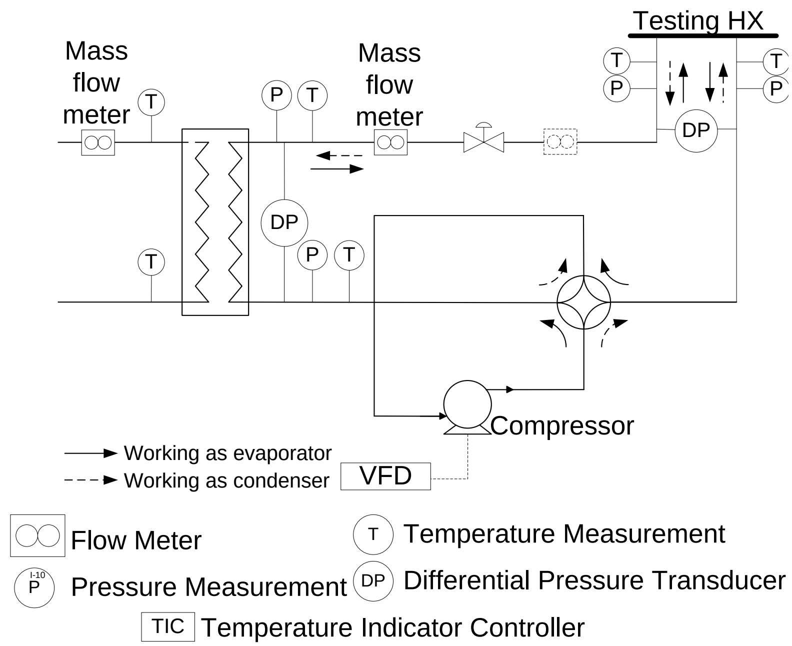

Figure 137 - Schematic diagram of refrigerant system with oil loop.

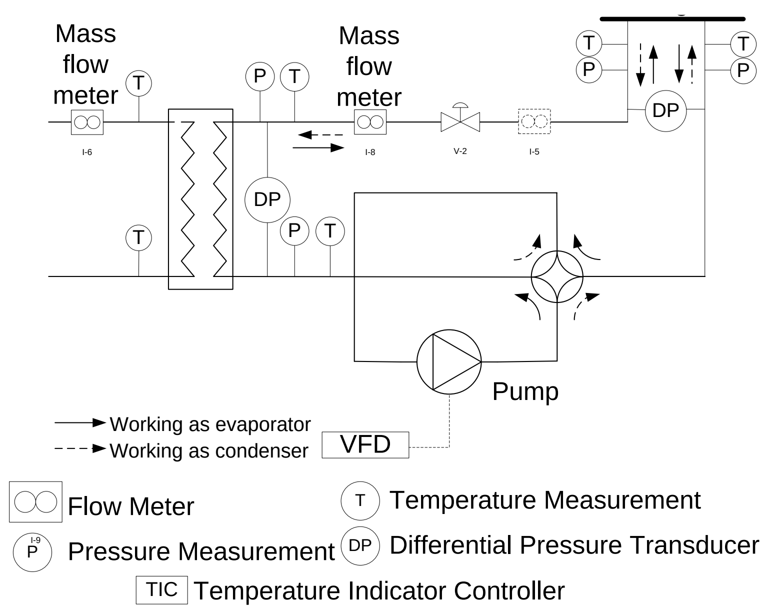

Figure 138 - Schematic diagram of refrigerant system without oil loop (courtesy from Zhiwei Huang).

Table 41 - Accuracy of every sensor of airside.

Temperature Sensor				
Type	Company	Product	Accuracy	
RTD	Omega	PR-25AP series	Class 1/10	
			-10 °C	0.03 °C
			0 °C	0.03 °C
			10 °C	0.04 °C
			20 °C	0.04 °C
			30 °C	0.05 °C
			40 °C	0.06 °C
			50 °C	0.07 °C
Dew Point Hygrometer				
Type	Company	Product	Dew Point Accuracy	
Chilled mirror hygrometer	EdgeTech	DewTrak II Chilled Mirror Transmitter	± 0.2°C dew/frost point	
Pressure Sensor				
Type	Company	Product	Accuracy	
Differential	Setra	2641005WD11T1F	± 3.11Pa	
Barometric	Setra	2781600MA1B2BT1	0-40℃	±100Pa
			‘-20 to 50 ℃	±150Pa
			’-40 to 60 ℃	±200Pa
Measurement of Nozzle Diameter				
Type			Accuracy	
ASHRAE standard nozzle			0.001D	

Table 42 - Uncertainty calculation of airside (courtesy from Zhiwei Huang).

Flow Rate	**5,000 cfm**							
ΔT	**2.5°C** (35 - 37.5°C)				**10°C** (35 - 45°C)			
	Value		Uncertainty	Relative Uncertainty	Value		Uncertainty	Relative Uncertainty
T1[°C]	35.00	±	0.06	0.17%	35.00	±	0.06	0.17%
T2 [°C]	37.50	±	0.06	0.16%	45.00	±	0.07	0.16%
P1[kPa]	100.98	±	0.10	0.10%	101.00	±	0.15	0.15%
delta_P[kPa]	0.59	±	0.00	0.52%	0.58	±	0.00	0.54%
P2[kPa]	100.38	±	0.10	0.10%	100.43	±	0.15	0.15%
delta_h[kJ/kg]	6.83	±	0.55	8.05%	30.38	±	0.70	2.31%
mdot[kg/s]	2.62	±	0.00	0.12%	2.54	±	0.00	0.13%
Q[kW]	17.88	±	1.44	**8.06%**	77.17	±	1.78	**2.31%**
Flow Rate	**70 cfm**							
ΔT	**2.5°C** (35 - 37.5°C)				**10°C** (35 - 45°C)			
	Value		Uncertainty	Relative Uncertainty	Value		Uncertainty	Relative Uncertainty
T1[°C]	35.00	±	0.06	0.17%	35.00	±	0.06	0.17%
T2 [°C]	37.50	±	0.06	0.16%	45.00	±	0.07	0.16%
P1[kPa]	100.98	±	0.10	0.10%	101.00	±	0.15	0.15%
delta_P[kPa]	0.16	±	0.00	1.98%	0.15	±	0.00	2.05%
P2[kPa]	100.82	±	0.10	0.10%	100.20	±	0.15	0.15%
delta_h[kJ/kg]	6.86	±	0.55	8.00%	30.44	±	0.70	2.30%
mdot[kg/s]	0.04	±	0.00	0.21%	0.04	±	0.00	0.22%
Q[kW]	0.27	±	0.02	**8.02%**	1.22	±	0.03	**2.31%**

Table 43. RTHX-001 Test data.

$T_{water,in}$	$T_{water,out}$	$\dot{m}_{water}$	$T_{air,in}$	$T_{air,out}$	V_{air}	u_{air}	ΔP_{air}	Q_{water}	Q_{air}	Q_{ave}	Energy Bal.
°C	°C	g/s	°C	°C	m³/s	m/s	Pa	W	W	W	%
60.01 ± 0.06	55.18 ± 0.06	29.95 ± 0.08	35.15 ± 0.15	49.83 ± 0.08	0.0317 ± 0.0005	1.39 ± 0.02	27.1 ± 1.1	605.4 ± 11.4	601.6 ± 11.3	603.5 ± 16.1	0.6
59.99 ± 0.05	54.3 ± 0.05	29.94 ± 0.09	34.93 ± 0.14	48.7 ± 0.09	0.0407 ± 0.0005	1.79 ± 0.02	39.9 ± 1.3	712.4 ± 8.8	717.2 ± 11.4	714.8 ± 14.4	-0.7
59.96 ± 0.07	53.71 ± 0.07	30.44 ± 0.07	35.04 ± 0.09	47.76 ± 0.09	0.0497 ± 0.0005	2.18 ± 0.02	54.7 ± 1.5	795.2 ± 12.4	805.8 ± 10.4	800.5 ± 16.2	-1.3
59.98 ± 0.07	53.09 ± 0.07	30.32 ± 0.07	34.93 ± 0.12	46.85 ± 0.1	0.0589 ± 0.0005	2.58 ± 0.02	71.8 ± 1.8	873.2 ± 12.6	893.6 ± 12.7	883.4 ± 17.9	-2.3
60.08 ± 0.08	52.53 ± 0.07	30.17 ± 0.08	34.94 ± 0.11	45.87 ± 0.13	0.0694 ± 0.0005	3.04 ± 0.02	95.3 ± 2	952.6 ± 13.2	971.9 ± 15.3	962.25 ± 20.2	-2
59.97 ± 0.05	56.98 ± 0.05	50.18 ± 0.09	35.18 ± 0.16	50.37 ± 0.1	0.0317 ± 0.0005	1.39 ± 0.02	27.1 ± 1.1	626.8 ± 15.5	621.6 ± 11.9	624.2 ± 19.5	0.8
59.95 ± 0.05	56.46 ± 0.05	50.26 ± 0.09	35.03 ± 0.16	49.37 ± 0.1	0.0398 ± 0.0005	1.75 ± 0.02	38.7 ± 1.3	733.6 ± 14.1	733.3 ± 12.4	733.45 ± 18.8	0.04
60.01 ± 0.08	56 ± 0.08	50.3 ± 0.09	35.1 ± 0.14	48.44 ± 0.11	0.0502 ± 0.0005	2.2 ± 0.02	55.9 ± 1.4	845 ± 22.4	852.6 ± 12.9	848.8 ± 25.8	-0.9
59.99 ± 0.05	55.52 ± 0.05	50.28 ± 0.09	34.93 ± 0.12	47.52 ± 0.09	0.0605 ± 0.0005	2.65 ± 0.02	74.8 ± 1.8	940.6 ± 15.5	956.3 ± 13.1	948.45 ± 20.3	-1.7
59.94 ± 0.05	55.13 ± 0.05	50.13 ± 0.09	35.11 ± 0.14	46.72 ± 0.13	0.07 ± 0.0005	3.07 ± 0.02	95.7 ± 2	-	-	-	-
60.01 ± 0.06	57.81 ± 0.06	70.05 ± 0.13	34.95 ± 0.12	50.62 ± 0.09	0.0317 ± 0.0005	1.39 ± 0.02	27.1 ± 1.1	646.5 ± 24	639.2 ± 11.4	642.85 ± 26.6	1.1
59.91 ± 0.05	57.33 ± 0.05	69.85 ± 0.11	34.9 ± 0.1	49.59 ± 0.09	0.0398 ± 0.0005	1.75 ± 0.02	38.7 ± 1.3	752.7 ± 21.5	750.4 ± 11	751.55 ± 24.2	0.3
59.95 ± 0.06	56.97 ± 0.06	69.82 ± 0.12	34.92 ± 0.11	48.59 ± 0.1	0.0504 ± 0.0005	2.21 ± 0.02	56.1 ± 1.5	871.2 ± 23.9	876.4 ± 11.7	873.8 ± 26.6	-0.6
60 ± 0.06	56.71 ± 0.06	69.86 ± 0.13	35.15 ± 0.13	47.78 ± 0.08	0.0603 ± 0.0005	2.64 ± 0.02	75.3 ± 1.8	961.2 ± 23.9	970 ± 13.3	965.6 ± 27.4	-0.9
60.01 ± 0.08	56.46 ± 0.08	69.96 ± 0.15	35 ± 0.18	47.28 ± 0.13	0.0695 ± 0.0005	3.05 ± 0.02	93.5 ± 2	-	-	-	-

Table 44. NTHX-001 Test data.

$T_{water,in}$	$T_{water,out}$	$\dot{m}_{water}$	$T_{air,in}$	$T_{air,out}$	V_{air}	u_{air}	ΔP_{air}	Q_{water}	Q_{air}	Q_{ave}	Energy Bal.
°C	°C	g/s	°C	°C	m³/s	m/s	Pa	W	W	W	%
60.04 ± 0.08	55.79 ± 0.09	30.2 ± 0.08	34.97 ± 0.11	47.98 ± 0.09	0.0316 ± 0.0005	1.39 ± 0.02	62.3 ± 1.5	536.8 ± 15.3	556 ± 9.8	546.4 ± 18.2	-3.5
60.02 ± 0.08	55.19 ± 0.08	30.15 ± 0.08	35 ± 0.11	46.62 ± 0.1	0.0408 ± 0.0005	1.79 ± 0.02	93.7 ± 2	609 ± 14.4	625.7 ± 9.9	617.35 ± 17.5	-2.7

$T_{water,in}$	$T_{water,out}$	$\dot{m}_{water}$	$T_{air,in}$	$T_{air,out}$	V_{air}	u_{air}	ΔP_{air}	Q_{water}	Q_{air}	Q_{ave}	Energy Bal.
°C	°C	g/s	°C	°C	m³/s	m/s	Pa	W	W	W	%
59.96 ± 0.09	54.65 ± 0.09	30.11 ± 0.09	35.01 ± 0.12	45.61 ± 0.09	0.0504 ± 0.0006	2.21 ± 0.03	129.2 ± 2.4	668.6 ± 16.2	686.1 ± 11.2	677.35 ± 19.7	-2.6
59.96 ± 0.08	54.2 ± 0.09	30.11 ± 0.09	35.02 ± 0.12	44.78 ± 0.09	0.06 ± 0.0005	2.63 ± 0.02	168.9 ± 3.2	725.3 ± 15.3	765.9 ± 12	745.6 ± 19.4	-5.4
60.08 ± 0.1	53.87 ± 0.1	29.97 ± 0.08	35.07 ± 0.07	44.08 ± 0.08	0.0701 ± 0.0005	3.07 ± 0.02	217.4 ± 3.7	778.3 ± 17.9	843.7 ± 10.1	811 ± 20.6	-8.1
59.92 ± 0.12	57.14 ± 0.11	49.9 ± 0.11	35.02 ± 0.08	48.49 ± 0.1	0.0316 ± 0.0005	1.39 ± 0.02	62.2 ± 1.5	580.2 ± 34	574.7 ± 9.8	577.45 ± 35.4	1
59.97 ± 0.08	56.79 ± 0.08	49.89 ± 0.11	34.93 ± 0.11	47.14 ± 0.09	0.0408 ± 0.0005	1.79 ± 0.02	93.6 ± 2	663.5 ± 23.7	656.4 ± 10	659.95 ± 25.7	1.1
59.99 ± 0.13	56.5 ± 0.12	50.05 ± 0.1	35 ± 0.1	46.21 ± 0.1	0.0504 ± 0.0006	2.21 ± 0.03	129.3 ± 2.5	730.5 ± 37.1	724.3 ± 11	727.4 ± 38.7	0.8
60 ± 0.09	56.21 ± 0.1	50.08 ± 0.1	35 ± 0.12	45.38 ± 0.11	0.0602 ± 0.0006	2.64 ± 0.03	169.7 ± 3	793.8 ± 28.2	814.9 ± 13.4	804.35 ± 31.2	-2.6
60.04 ± 0.11	55.96 ± 0.11	49.93 ± 0.11	35 ± 0.13	44.71 ± 0.11	0.0704 ± 0.0006	3.09 ± 0.03	217.8 ± 3.5	852 ± 32.5	909.7 ± 15.2	880.85 ± 35.9	-6.5
59.97 ± 0.08	57.85 ± 0.08	70.05 ± 0.12	35.02 ± 0.08	48.81 ± 0.08	0.0316 ± 0.0005	1.39 ± 0.02	62.4 ± 1.5	621.1 ± 33.2	587.6 ± 9.8	604.35 ± 34.6	5.5
59.93 ± 0.09	57.52 ± 0.09	69.97 ± 0.14	34.98 ± 0.08	47.36 ± 0.09	0.0409 ± 0.0006	1.79 ± 0.03	94.3 ± 1.9	705.3 ± 37.3	668.7 ± 10.4	687 ± 38.7	5.3
60.07 ± 0.12	57.41 ± 0.11	70.14 ± 0.13	35 ± 0.12	46.57 ± 0.1	0.0504 ± 0.0006	2.21 ± 0.03	129.7 ± 2.4	780.3 ± 47.8	746.8 ± 11.8	763.55 ± 49.2	4.4
59.97 ± 0.14	57.08 ± 0.13	70.07 ± 0.13	34.97 ± 0.09	45.65 ± 0.1	0.0606 ± 0.0005	2.66 ± 0.02	172 ± 3	846.9 ± 56	843.4 ± 11.5	845.15 ± 57.2	0.4
59.99 ± 0.14	56.9 ± 0.13	70.2 ± 0.12	34.99 ± 0.18	44.99 ± 0.13	0.0704 ± 0.0005	3.09 ± 0.02	218.2 ± 3.7	907.2 ± 56.1	931.1 ± 18.9	919.15 ± 59.2	-2.6

Table 45. RTHX-468 Test data.

$T_{water,in}$	$T_{water,out}$	$\dot{m}_{water}$	$T_{air,in}$	$T_{air,out}$	V_{air}	u_{air}	ΔP_{air}	Q_{water}	Q_{air}	Q_{ave}	Energy Bal.
°C	°C	g/s	°C	°C	m³/s	m/s	Pa	W	W	W	%
55.08 ± 0.08	39.99 ± 0.07	70.93 ± 0.12	30 ± 0.1	37.4 ± 0.1	0.4786 ± 0.0045	20.99 ± 0.2	47.1 ± 0.9	4478 ± 33.4	4314.2 ± 87.4	4396.1 ± 93.6	3.7
54.77 ± 0.06	42.49 ± 0.06	94.68 ± 0.16	30 ± 0.1	38.2 ± 0.1	0.4814 ± 0.0057	21.11 ± 0.25	47.1 ± 1	4859 ± 36	4731 ± 94.1	4795 ± 100.8	2.7
54.95 ± 0.06	44.38 ± 0.06	117.9 ± 0.23	30.1 ± 0.1	38.8 ± 0.1	0.4795 ± 0.0046	21.03 ± 0.2	47 ± 0.9	5210 ± 40.9	5057.2 ± 90.5	5133.6 ± 99.3	3

$T_{water,in}$	$T_{water,out}$	$\dot{m}_{water}$	$T_{air,in}$	$T_{air,out}$	V_{air}	u_{air}	ΔP_{air}	Q_{water}	Q_{air}	Q_{ave}	Energy Bal.
°C	°C	g/s	°C	°C	m^3/s	m/s	Pa	W	W	W	%
54.72 ± 0.08	45.6 ± 0.07	141 ± 0.23	30 ± 0.1	39.1 ± 0.1	0.4819 ± 0.0057	21.14 ± 0.25	47.2 ± 1	5377 ± 65.2	5245.6 ± 97.5	5311.3 ± 117.3	2.5
54.82 ± 0.06	46.76 ± 0.06	166.3 ± 0.24	30 ± 0.1	39.5 ± 0.1	0.48 ± 0.0057	21.05 ± 0.25	47 ± 0.9	5608 ± 62.1	5509.3 ± 99.5	5558.65 ± 117.3	1.8
55.08 ± 0.08	39.99 ± 0.07	70.93 ± 0.12	30 ± 0.1	37.4 ± 0.1	0.4786 ± 0.0045	20.99 ± 0.2	47.1 ± 0.9	4478 ± 33.4	4314.2 ± 87.4	4396.1 ± 93.6	3.7
54.77 ± 0.06	42.49 ± 0.06	94.68 ± 0.16	30 ± 0.1	38.2 ± 0.1	0.4814 ± 0.0057	21.11 ± 0.25	47.1 ± 1	4859 ± 36	4731 ± 94.1	4795 ± 100.8	2.7
54.95 ± 0.06	44.38 ± 0.06	117.9 ± 0.23	30.1 ± 0.1	38.8 ± 0.1	0.4795 ± 0.0046	21.03 ± 0.2	47 ± 0.9	5210 ± 40.9	5057.2 ± 90.5	5133.6 ± 99.3	3
54.72 ± 0.08	45.6 ± 0.07	141 ± 0.23	30 ± 0.1	39.1 ± 0.1	0.4819 ± 0.0057	21.14 ± 0.25	47.2 ± 1	5377 ± 65.2	5245.6 ± 97.5	5311.3 ± 117.3	2.5
54.82 ± 0.06	46.76 ± 0.06	166.3 ± 0.24	30 ± 0.1	39.5 ± 0.1	0.48 ± 0.0057	21.05 ± 0.25	47 ± 0.9	5608 ± 62.1	5509.3 ± 99.5	5558.65 ± 117.3	1.8
55.08 ± 0.08	39.99 ± 0.07	70.93 ± 0.12	30 ± 0.1	37.4 ± 0.1	0.4786 ± 0.0045	20.99 ± 0.2	47.1 ± 0.9	4478 ± 33.4	4314.2 ± 87.4	4396.1 ± 93.6	3.7
54.77 ± 0.06	42.49 ± 0.06	94.68 ± 0.16	30 ± 0.1	38.2 ± 0.1	0.4814 ± 0.0057	21.11 ± 0.25	47.1 ± 1	4859 ± 36	4731 ± 94.1	4795 ± 100.8	2.7
54.95 ± 0.06	44.38 ± 0.06	117.9 ± 0.23	30.1 ± 0.1	38.8 ± 0.1	0.4795 ± 0.0046	21.03 ± 0.2	47 ± 0.9	5210 ± 40.9	5057.2 ± 90.5	5133.6 ± 99.3	3
54.72 ± 0.08	45.6 ± 0.07	141 ± 0.23	30 ± 0.1	39.1 ± 0.1	0.4819 ± 0.0057	21.14 ± 0.25	47.2 ± 1	5377 ± 65.2	5245.6 ± 97.5	5311.3 ± 117.3	2.5
54.82 ± 0.06	46.76 ± 0.06	166.3 ± 0.24	30 ± 0.1	39.5 ± 0.1	0.48 ± 0.0057	21.05 ± 0.25	47 ± 0.9	5608 ± 62.1	5509.3 ± 99.5	5558.65 ± 117.3	1.8

Wavy Fin Correlation Coefficients Matrices

Table 46. Herringbone correlation: parameters power matrices.

$M_{NuDh,Herr,N=2\text{-}10} =$

0	0	0	0	0	0	0
1	0	0	0	0	0	0
0	1	0	0	0	0	0
0	0	1	0	0	0	0
0	0	0	1	0	0	0
0	0	0	0	1	0	0
0	0	0	0	0	1	0
0	0	0	0	0	0	1
2	0	0	0	0	0	0
1	1	0	0	0	0	0
0	2	0	0	0	0	0
1	0	1	0	0	0	0
0	1	1	0	0	0	0
0	0	2	0	0	0	0
1	0	0	1	0	0	0
0	1	0	1	0	0	0
0	0	1	1	0	0	0
0	0	0	2	0	0	0
1	0	0	0	1	0	0
0	1	0	0	1	0	0
0	0	1	0	1	0	0
0	0	0	1	1	0	0
0	0	0	0	2	0	0
1	0	0	0	0	1	0
0	1	0	0	0	1	0
0	0	1	0	0	1	0
0	0	0	1	0	1	0
0	0	0	0	1	1	0
0	0	0	0	0	2	0
1	0	0	0	0	0	1
0	1	0	0	0	0	1
0	0	1	0	0	0	1
0	0	0	1	0	0	1
0	0	0	0	1	0	1
0	0	0	0	0	1	1
0	0	0	0	0	0	2
3	0	0	0	0	0	0
1	1	1	0	0	0	0
0	2	1	0	0	0	0
1	0	2	0	0	0	0
0	1	2	0	0	0	0
0	0	3	0	0	0	0
2	0	0	1	0	0	0
1	1	0	1	0	0	0
1	0	1	1	0	0	0
1	0	0	2	0	0	0
0	0	1	2	0	0	0
0	0	0	3	0	0	0
1	0	1	0	1	0	0
0	1	1	0	1	0	0
0	0	1	1	1	0	0
0	0	1	0	2	0	0
0	0	0	1	2	0	0
2	0	0	0	0	1	0
1	1	0	0	0	1	0
0	2	0	0	0	1	0
1	0	1	0	0	1	0
0	1	1	0	0	1	0
0	0	2	0	0	1	0
1	0	0	1	0	1	0
0	1	0	1	0	1	0
0	0	1	1	0	1	0
0	0	0	2	0	1	0
0	1	0	0	1	1	0
0	0	0	0	2	1	0
1	0	0	0	0	2	0
0	1	0	0	0	2	0
0	0	1	0	0	2	0
0	0	0	1	0	2	0
2	0	0	0	0	0	1
1	1	0	0	0	0	1
1	0	1	0	0	0	1
0	1	1	0	0	0	1
0	0	2	0	0	0	1
0	1	0	1	0	0	1
0	0	0	2	0	0	1
0	1	0	0	1	0	1
0	0	0	1	1	0	1
0	0	0	0	2	0	1
1	0	0	0	0	1	1
0	1	0	0	0	1	1
0	0	0	1	0	1	1
1	0	0	0	0	0	2
0	1	0	0	0	0	2
0	0	1	0	0	0	2
0	0	0	0	1	0	2
0	0	0	0	0	0	3

$M_{NuDh,Herr,N=11\text{-}20} =$

0	0	0	0	0	0	0
1	0	0	0	0	0	0
0	1	0	0	0	0	0
0	0	1	0	0	0	0
0	0	0	1	0	0	0
0	0	0	0	1	0	0
0	0	0	0	0	1	0
0	0	0	0	0	0	1
2	0	0	0	0	0	0
1	1	0	0	0	0	0
0	2	0	0	0	0	0
1	0	1	0	0	0	0
0	1	1	0	0	0	0
0	0	2	0	0	0	0
1	0	0	1	0	0	0
0	1	0	1	0	0	0
0	0	1	1	0	0	0
0	0	0	2	0	0	0
1	0	0	0	1	0	0
0	1	0	0	1	0	0
0	0	1	0	1	0	0
0	0	0	0	2	0	0
1	0	0	0	0	1	0
0	1	0	0	0	1	0
0	0	1	0	0	1	0
0	0	0	1	0	1	0
0	0	0	0	1	1	0
0	0	0	0	0	2	0
1	0	0	0	0	0	1
0	1	0	0	0	0	1
0	0	1	0	0	0	1
0	0	0	1	0	0	1
0	0	0	0	1	0	1
0	0	0	0	0	1	1
0	0	0	0	0	0	2
2	1	0	0	0	0	0
1	2	0	0	0	0	0
0	3	0	0	0	0	0
2	0	1	0	0	0	0
1	1	1	0	0	0	0
0	2	1	0	0	0	0
1	0	2	0	0	0	0
0	1	2	0	0	0	0
0	0	3	0	0	0	0
1	1	0	1	0	0	0
0	2	0	1	0	0	0
1	0	1	1	0	0	0
0	1	1	1	0	0	0
0	0	2	1	0	0	0
1	0	0	2	0	0	0
0	1	0	2	0	0	0
0	0	1	2	0	0	0
0	0	0	3	0	0	0
2	0	0	0	1	0	0
1	0	0	0	2	0	0
0	1	0	0	2	0	0
0	0	1	0	2	0	0
2	0	0	0	0	1	0
1	1	0	0	0	1	0
1	0	1	0	0	1	0
0	1	1	0	0	1	0
1	0	0	1	0	1	0
0	1	0	1	0	1	0
0	0	1	1	0	1	0
0	1	0	0	1	1	0
0	0	0	0	2	1	0
0	0	0	0	0	3	0
1	1	0	0	0	0	1
1	0	1	0	0	0	1
0	1	1	0	0	0	1
1	0	0	1	0	0	1
0	1	0	1	0	0	1
0	0	1	1	0	0	1
0	0	0	2	0	0	1
1	0	0	0	1	0	1
1	0	0	0	0	1	1
0	1	0	0	0	1	1
0	0	1	0	0	1	1
1	0	0	0	0	0	2
0	1	0	0	0	0	2
0	0	1	0	0	0	2
0	0	0	1	0	0	2
0	0	0	0	0	0	3

$M_{Cf,Herr,N=2\text{-}10} =$

0	0	0	0	0	0	0
1	0	0	0	0	0	0
0	1	0	0	0	0	0
0	0	1	0	0	0	0
0	0	0	1	0	0	0
0	0	0	0	1	0	0
0	0	0	0	0	1	0
0	0	0	0	0	0	1
2	0	0	0	0	0	0
1	1	0	0	0	0	0
0	2	0	0	0	0	0
1	0	1	0	0	0	0
0	1	1	0	0	0	0
0	0	2	0	0	0	0
1	0	0	1	0	0	0
0	1	0	1	0	0	0
0	0	1	1	0	0	0
0	0	0	2	0	0	0
1	0	0	0	1	0	0
0	1	0	0	1	0	0
0	0	1	0	1	0	0
0	0	0	1	1	0	0
0	0	0	0	2	0	0
1	0	0	0	0	1	0
0	1	0	0	0	1	0
0	0	1	0	0	1	0
0	0	0	1	0	1	0
0	0	0	0	1	1	0
0	0	0	0	0	2	0
1	0	0	0	0	0	1
0	1	0	0	0	0	1
0	0	1	0	0	0	1
0	0	0	1	0	0	1
0	0	0	0	1	0	1
0	0	0	0	0	1	1
0	0	0	0	0	0	2
3	0	0	0	0	0	0
2	1	0	0	0	0	0
2	0	1	0	0	0	0
0	2	1	0	0	0	0
1	0	2	0	0	0	0
2	0	0	1	0	0	0
1	1	0	1	0	0	0
1	0	1	1	0	0	0
0	1	1	1	0	0	0
0	0	2	1	0	0	0
1	0	0	2	0	0	0
0	1	0	2	0	0	0
0	0	1	2	0	0	0
1	1	0	0	1	0	0
0	2	0	0	1	0	0
1	0	1	0	1	0	0
0	1	1	0	1	0	0
0	0	2	0	1	0	0
0	1	0	1	1	0	0
1	0	0	0	2	0	0
0	0	1	0	2	0	0
0	0	0	1	2	0	0
0	2	0	0	0	1	0
0	1	1	0	0	1	0
1	0	0	1	0	1	0
0	1	0	1	0	1	0
0	0	1	1	0	1	0
1	0	0	0	1	1	0
1	0	0	0	0	2	0
0	1	0	0	0	2	0
0	0	1	0	0	2	0
2	0	0	0	0	0	1
1	1	0	0	0	0	1
0	2	0	0	0	0	1
1	0	1	0	0	0	1
0	1	1	0	0	0	1
0	0	2	0	0	0	1
0	1	0	1	0	0	1
0	0	1	1	0	0	1
0	0	0	2	0	0	1
0	0	0	1	1	0	1
1	0	0	0	0	1	1
0	1	0	0	0	1	1
0	0	0	1	0	1	1
1	0	0	0	0	0	2
0	0	1	0	0	0	2
0	0	0	0	0	0	3

$M_{Cf,Herr,N=11\text{-}20} =$

0	0	0	0	0	0	0
1	0	0	0	0	0	0
0	1	0	0	0	0	0
0	0	1	0	0	0	0
0	0	0	1	0	0	0
0	0	0	0	1	0	0
0	0	0	0	0	1	0
0	0	0	0	0	0	1
2	0	0	0	0	0	0
1	1	0	0	0	0	0
0	2	0	0	0	0	0
1	0	1	0	0	0	0
0	1	1	0	0	0	0
0	0	2	0	0	0	0
1	0	0	1	0	0	0
0	1	0	1	0	0	0
0	0	1	1	0	0	0
0	0	0	2	0	0	0
1	0	0	0	1	0	0
0	1	0	0	1	0	0
0	0	1	0	1	0	0
0	0	0	1	1	0	0
0	0	0	0	2	0	0
1	0	0	0	0	1	0
0	1	0	0	0	1	0
0	0	1	0	0	1	0
0	0	0	1	0	1	0
0	0	0	0	1	1	0
0	0	0	0	0	2	0
1	0	0	0	0	0	1
0	1	0	0	0	0	1
0	0	1	0	0	0	1
0	0	0	1	0	0	1
0	0	0	0	1	0	1
0	0	0	0	0	1	1
0	0	0	0	0	0	2
2	1	0	0	0	0	0
1	2	0	0	0	0	0
2	0	1	0	0	0	0
1	1	1	0	0	0	0
0	2	1	0	0	0	0
1	0	2	0	0	0	0
2	0	0	1	0	0	0
1	1	0	1	0	0	0
0	2	0	1	0	0	0
1	0	1	1	0	0	0
1	0	0	2	0	0	0
0	1	0	2	0	0	0
2	0	0	0	1	0	0
1	0	1	0	1	0	0
0	0	2	0	1	0	0
0	0	1	0	2	0	0
1	1	0	0	0	1	0
0	1	1	0	0	1	0
1	0	0	1	0	1	0
0	1	0	0	1	1	0
0	0	1	0	1	1	0
0	0	0	1	1	1	0
0	1	0	0	0	2	0
0	0	0	0	0	3	0
2	0	0	0	0	0	1
1	1	0	0	0	0	1
0	1	0	1	0	0	1
0	0	1	1	0	0	1
0	0	0	2	0	0	1
0	0	1	0	1	0	1
0	0	0	0	2	0	1
1	0	0	0	0	0	2
0	1	0	0	0	0	2
0	0	1	0	0	0	2
0	0	0	1	0	0	2
0	0	0	0	0	1	2
0	0	0	0	0	0	3

Table 47. Herringbone correlation: coefficients arrays.

$c_{NuDh,Herr,N=2\text{-}10} =$	$c_{NuDh,Herr,N=11\text{-}20} =$	$c_{Cf,Herr,N=2\text{-}10} =$	$c_{Cf,Herr,N=11\text{-}20} =$
-4.3884	29.6938	17.8784	31.2430
3.8241	0.4421	0.0984	-3.6596
-5.5505	-0.8698	-4.1406	12.9874
6.8328	4.4086	-7.9936	-3.5077
-2.6098	1.6331	0.9576	-3.2856
0.0329	4.4418	2.4552	0.6230
-1.1233	-28.0007	-0.1146	-24.6064
1.7374	-1.1637	-5.0085	-6.4867
-0.6462	-0.4560	0.4685	1.0003
1.3482	1.9658	-0.4852	1.5960
0.0349	-0.6269	1.0845	-0.0451
-2.1053	-0.1432	-3.3757	-2.4313
2.7768	0.6684	2.1409	-0.5294
-6.2859	-6.4044	0.7065	1.2628
-0.0234	0.3081	0.0071	-0.6681
0.2687	-0.8489	-0.3017	0.4837
0.5023	-0.4941	0.4226	-0.1296
-0.6451	-0.3928	0.2527	0.3392
0.2754	1.0420	0.1028	0.6159
-0.5167	0.2411	-0.5853	0.5188
-0.8092	-0.5215	-2.7741	-1.1939
-0.3741	1.0004	0.0621	-0.6716
-0.1482	-0.2538	0.1284	0.3266
0.8253	0.5044	0.3281	0.6305
-1.3296	0.7808	-0.3773	-6.5030
0.3194	-0.3608	0.6310	-1.2588
0.1442	-1.1358	-0.1369	0.8830
-0.4880	9.0281	0.0885	0.8434
-0.1178	0.5064	-0.0921	10.5513
-0.9219	-0.0110	0.5127	1.2430
1.2285	0.2786	0.2217	-0.8330
-0.7660	-0.2996	0.4828	0.8205
0.2283	0.0725	0.0237	0.5328
-0.0099	0.2702	-0.0466	-0.1318
0.1554	0.2514	0.1258	0.6846
-0.2247	0.2106	0.6353	0.8623
0.0849	-0.3065	-0.1302	0.1633
-0.2555	0.2558	0.1589	-0.1833
-0.3418	-0.0661	-0.1541	-0.1804
0.2761	0.1316	-0.2403	-0.0977
-0.4108	-0.3520	0.6301	-0.2400
1.7931	-0.3499	-0.1232	0.5677
-0.0554	0.1945	0.1398	-0.2066
0.0616	1.7012	0.0434	0.3265
0.0608	-0.1004	0.1435	-0.1740
0.0762	0.0816	-0.2158	0.1582
0.1009	0.1131	0.1848	0.1835
-0.0712	-0.0637	-0.1618	-0.1225
-0.2624	0.1141	0.1107	0.0856
0.0965	0.0383	-0.1550	-0.3672
0.0831	-0.0478	0.1265	0.4759
-0.1091	-0.0449	-0.3860	-0.1495
-0.0279	-0.0742	0.1174	-0.2621
-0.0984	0.1513	0.6264	0.3994
0.1016	0.1741	-0.0665	0.2041
0.1421	-0.0782	-0.0796	-0.2314
-0.3254	-0.0746	-0.1753	-0.2792
0.2591	0.2177	-0.0224	0.2427
-0.3288	-0.5673	0.1808	0.9620
0.1320	0.8286	-0.1769	-1.4322
-0.1418	-0.5867	0.1315	-0.1285
0.0912	-0.1361	-0.1098	0.0561
-0.0458	0.2567	0.0918	-0.0546
-0.1132	-0.1054	0.0656	0.0814
-0.0965	-0.2954	-0.0820	0.0313
0.1953	-0.2674	0.1100	-0.0376
-0.1630	-1.1494	-0.1341	-0.0260
0.0889	0.0957	-0.1245	-0.0930
-0.1304	-0.2368	0.1035	0.0486
0.0992	0.2510	-0.1045	-0.0695
-0.1002	0.0344	0.0881	-0.0289
0.1873	-0.0405	-0.0973	-0.0468
-0.1797	0.1007	0.1147	-0.0389
0.1826	0.0180	-0.0356	
-0.0255	0.0466	0.0379	
0.0476	0.0824	0.0335	
0.0682	-0.1992	-0.0237	
0.0255	0.0993	0.0362	
0.0356	-0.0351	-0.0376	
-0.1093	0.0358	0.0439	
0.1012	-0.0684	-0.0501	
0.0357	0.0258	-0.0386	
0.0727	-0.0109	-0.0291	
-0.0722			
0.0415			
0.0173			
0.0153			

Table 48. Smooth correlation: parameters power matrices.

$M_{NuDh,Smooth,N=2\text{-}10} =$

0	0	0	0	0	0	0
1	0	0	0	0	0	0
0	1	0	0	0	0	0
0	0	1	0	0	0	0
0	0	0	1	0	0	0
0	0	0	0	1	0	0
0	0	0	0	0	1	0
0	0	0	0	0	0	1
2	0	0	0	0	0	0
1	1	0	0	0	0	0
0	2	0	0	0	0	0
1	0	1	0	0	0	0
0	1	1	0	0	0	0
0	0	2	0	0	0	0
1	0	0	1	0	0	0
0	1	0	1	0	0	0
0	0	1	1	0	0	0
0	0	0	2	0	0	0
1	0	0	0	1	0	0
0	1	0	0	1	0	0
0	0	1	0	1	0	0
0	0	0	1	1	0	0
0	0	0	0	2	0	0
1	0	0	0	0	1	0
0	1	0	0	0	1	0
0	0	1	0	0	1	0
0	0	0	1	0	1	0
0	0	0	0	1	1	0
0	0	0	0	0	2	0
1	0	0	0	0	0	1
0	1	0	0	0	0	1
0	0	1	0	0	0	1
0	0	0	1	0	0	1
0	0	0	0	1	0	1
0	0	0	0	0	1	1
0	0	0	0	0	0	2
3	0	0	0	0	0	0
1	1	1	0	0	0	0
0	2	1	0	0	0	0
0	1	2	0	0	0	0
0	0	3	0	0	0	0
2	0	0	1	0	0	0
1	1	0	1	0	0	0
1	0	1	1	0	0	0
1	0	0	2	0	0	0
0	0	1	2	0	0	0
0	0	0	3	0	0	0
1	0	1	0	1	0	0
0	0	2	0	1	0	0
0	0	1	1	1	0	0
0	0	1	0	2	0	0
0	0	0	1	2	0	0
0	2	0	0	0	1	0
1	0	1	0	0	1	0
0	1	1	0	0	1	0
0	0	2	0	0	1	0
1	0	0	1	0	1	0
0	1	0	1	0	1	0
0	0	1	1	0	1	0
0	0	0	2	0	1	0
1	0	0	0	1	1	0
0	1	0	0	1	1	0
1	0	0	0	0	2	0
0	0	1	0	0	2	0
0	0	0	1	0	2	0
2	0	0	0	0	0	1
1	1	0	0	0	0	1
1	0	1	0	0	0	1
0	1	1	0	0	0	1
0	0	2	0	0	0	1
0	1	0	1	0	0	1
0	0	0	2	0	0	1
0	0	0	1	1	0	1
0	0	0	0	2	0	1
1	0	0	0	0	1	1
0	1	0	0	0	1	1
0	0	0	1	0	1	1
0	0	0	0	1	1	1
1	0	0	0	0	0	2
0	1	0	0	0	0	2
0	0	0	1	0	0	2

$M_{NuDh,Smooth,N=11\text{-}20} =$

0	0	0	0	0	0	0
1	0	0	0	0	0	0
0	1	0	0	0	0	0
0	0	1	0	0	0	0
0	0	0	1	0	0	0
0	0	0	0	1	0	0
0	0	0	0	0	1	0
0	0	0	0	0	0	1
2	0	0	0	0	0	0
1	1	0	0	0	0	0
0	2	0	0	0	0	0
1	0	1	0	0	0	0
0	1	1	0	0	0	0
0	0	2	0	0	0	0
1	0	0	1	0	0	0
0	1	0	1	0	0	0
0	0	1	1	0	0	0
0	0	0	2	0	0	0
1	0	0	0	1	0	0
0	1	0	0	1	0	0
0	0	1	0	1	0	0
0	0	0	1	1	0	0
0	0	0	0	2	0	0
1	0	0	0	0	1	0
0	1	0	0	0	1	0
0	0	1	0	0	1	0
0	0	0	1	0	1	0
0	0	0	0	1	1	0
0	0	0	0	0	2	0
1	0	0	0	0	0	1
0	1	0	0	0	0	1
0	0	1	0	0	0	1
0	0	0	1	0	0	1
0	0	0	0	1	0	1
0	0	0	0	0	1	1
0	0	0	0	0	0	2
3	0	0	0	0	0	0
2	1	0	0	0	0	0
1	2	0	0	0	0	0
0	3	0	0	0	0	0
2	0	1	0	0	0	0
1	1	1	0	0	0	0
0	2	1	0	0	0	0
1	0	2	0	0	0	0
0	1	2	0	0	0	0
0	0	3	0	0	0	0
1	1	0	1	0	0	0
0	2	0	1	0	0	0
1	0	1	1	0	0	0
0	1	1	1	0	0	0
0	1	0	2	0	0	0
0	0	0	3	0	0	0
2	0	0	0	1	0	0
1	1	0	0	1	0	0
0	1	1	0	1	0	0
1	0	0	1	1	0	0
0	0	0	1	2	0	0
1	1	0	0	0	1	0
1	0	1	0	0	1	0
0	1	1	0	0	1	0
1	0	0	1	0	1	0
0	1	0	1	0	1	0
1	0	0	0	1	1	0
0	0	1	0	1	1	0
0	0	0	1	1	1	0
0	0	0	0	2	1	0
0	0	0	0	0	3	0
1	1	0	0	0	0	1
1	0	1	0	0	0	1
0	1	1	0	0	0	1
0	0	2	0	0	0	1
1	0	0	1	0	0	1
0	1	0	1	0	0	1
0	0	0	2	0	0	1
1	0	0	0	1	0	1
0	0	0	0	2	0	1
1	0	0	0	0	1	1
0	1	0	0	0	1	1
0	0	1	0	0	1	1
0	0	0	1	0	1	1
1	0	0	0	0	0	2
0	1	0	0	0	0	2
0	0	0	1	0	0	2

$M_{Cf,Smooth,N=2\text{-}10} =$

0	0	0	0	0	0	0
1	0	0	0	0	0	0
0	1	0	0	0	0	0
0	0	1	0	0	0	0
0	0	0	1	0	0	0
0	0	0	0	1	0	0
0	0	0	0	0	1	0
0	0	0	0	0	0	1
2	0	0	0	0	0	0
1	1	0	0	0	0	0
0	2	0	0	0	0	0
1	0	1	0	0	0	0
0	1	1	0	0	0	0
0	0	2	0	0	0	0
1	0	0	1	0	0	0
0	1	0	1	0	0	0
0	0	1	1	0	0	0
0	0	0	2	0	0	0
1	0	0	0	1	0	0
0	1	0	0	1	0	0
0	0	1	0	1	0	0
0	0	0	1	1	0	0
0	0	0	0	2	0	0
1	0	0	0	0	1	0
0	1	0	0	0	1	0
0	0	1	0	0	1	0
0	0	0	1	0	1	0
1	0	0	0	0	0	1
0	1	0	0	0	0	1
0	0	1	0	0	0	1
0	0	0	1	0	0	1
0	0	0	0	1	0	1
0	0	0	0	0	1	1
0	0	0	0	0	0	2
3	0	0	0	0	0	0
2	1	0	0	0	0	0
2	0	1	0	0	0	0
1	1	1	0	0	0	0
1	0	2	0	0	0	0
2	0	0	1	0	0	0
1	1	0	1	0	0	0
1	0	1	1	0	0	0
0	1	1	1	0	0	0
0	0	2	1	0	0	0
1	0	0	2	0	0	0
0	1	0	2	0	0	0
0	0	0	3	0	0	0
1	1	0	0	1	0	0
0	2	0	0	1	0	0
1	0	1	0	1	0	0
0	0	2	0	1	0	0
0	0	1	1	1	0	0
0	0	1	0	2	0	0
0	0	0	1	2	0	0
2	0	0	0	0	1	0
0	2	0	0	0	1	0
0	0	2	0	0	1	0
1	0	0	1	0	1	0
0	1	0	1	0	1	0
0	0	1	1	0	1	0
2	0	0	0	0	0	1
1	1	0	0	0	0	1
0	1	1	0	0	0	1
1	0	0	1	0	0	1
0	1	0	1	0	0	1
0	0	1	1	0	0	1
0	0	0	1	0	1	1
1	0	0	0	0	0	2
0	0	1	0	0	0	2
0	0	0	1	0	0	2
0	0	0	0	1	0	2
0	0	0	0	0	0	3

$M_{Cf,Smooth,N=11\text{-}20} =$

0	0	0	0	0	0	0
1	0	0	0	0	0	0
0	1	0	0	0	0	0
0	0	1	0	0	0	0
0	0	0	1	0	0	0
0	0	0	0	1	0	0
0	0	0	0	0	1	0
0	0	0	0	0	0	1
2	0	0	0	0	0	0
1	1	0	0	0	0	0
0	2	0	0	0	0	0
1	0	1	0	0	0	0
0	1	1	0	0	0	0
0	0	2	0	0	0	0
1	0	0	1	0	0	0
0	1	0	1	0	0	0
0	0	1	1	0	0	0
0	0	0	2	0	0	0
1	0	0	0	1	0	0
0	1	0	0	1	0	0
0	0	1	0	1	0	0
0	0	0	1	1	0	0
0	0	0	0	2	0	0
1	0	0	0	0	1	0
0	1	0	0	0	1	0
0	0	1	0	0	1	0
0	0	0	1	0	1	0
0	0	0	0	1	1	0
0	0	0	0	0	2	0
1	0	0	0	0	0	1
0	1	0	0	0	0	1
0	0	1	0	0	0	1
0	0	0	1	0	0	1
0	0	0	0	0	1	1
0	0	0	0	0	0	2
3	0	0	0	0	0	0
2	1	0	0	0	0	0
1	2	0	0	0	0	0
1	1	1	0	0	0	0
0	2	1	0	0	0	0
1	0	2	0	0	0	0
2	0	0	1	0	0	0
1	1	0	1	0	0	0
0	2	0	1	0	0	0
1	0	1	1	0	0	0
0	1	1	1	0	0	0
1	0	0	2	0	0	0
0	1	0	2	0	0	0
0	0	1	2	0	0	0
0	0	0	3	0	0	0
1	0	1	0	1	0	0
0	0	2	0	1	0	0
0	1	0	1	1	0	0
0	0	1	0	2	0	0
0	1	0	1	0	1	0
1	0	0	0	1	1	0
0	0	1	0	1	1	0
0	0	0	0	2	1	0
0	1	0	0	0	2	0
2	0	0	0	0	0	1
1	1	0	0	0	0	1
1	0	1	0	0	0	1
0	1	1	0	0	0	1
0	0	2	0	0	0	1
1	0	0	1	0	0	1
0	1	0	1	0	0	1
0	0	1	1	0	0	1
1	0	0	0	0	1	1
0	0	0	1	0	1	1
1	0	0	0	0	0	2
0	0	0	0	0	0	3

Table 49: Smooth correlation: coefficients arrays.

$c_{NuDh,Smooth,N=2\text{-}10} =$	$c_{NuDh,Smooth,N=11\text{-}20} =$	$c_{Cf,Smooth,N=2\text{-}10} =$	$c_{Cf,Smooth,N=11\text{-}20} =$
-5.7057	32.2699	14.9492	11.7049
0.7473	2.0889	-0.9612	1.0108
-4.5714	-3.1603	-0.4285	7.8943
6.3303	4.1082	-5.0439	-0.3384
-3.2949	0.9142	-0.4762	-2.4832
-2.4175	3.2453	3.1646	4.6503
0.9464	-35.5205	-0.1368	1.2865
0.3337	0.7006	-4.6918	-4.6596
-0.6172	-1.0000	0.5159	-0.2212
1.9777	1.6918	-0.0760	1.8546
0.0537	-0.3625	0.1598	-0.3146
-0.9572	0.0047	-2.1545	-1.5804
2.7932	1.0831	0.7870	1.4594
-6.8360	-7.6816	0.3519	-0.0988
-0.0045	-0.2817	-0.8495	-1.2066
0.3399	-0.4810	0.4980	2.1100
0.5966	0.5453	0.6811	0.1105
-0.7793	-0.4627	0.7015	0.5710
0.0933	0.0978	0.6195	0.9489
0.0596	-0.1604	-0.5583	0.0665
-0.3317	-0.9331	-1.9039	-0.9244
-0.3773	-0.0080	-0.2504	-0.1326
-0.2579	0.3454	0.1632	0.7059
1.3956	-2.1642	0.0526	-1.7413
-1.4858	1.6837	-0.5721	-4.7211
0.4491	3.1080	-0.1079	-0.8095
0.0695	-1.1988	-0.3252	0.7196
0.4728	-1.8974	0.7386	-1.1130
-0.2903	9.8103	-0.1823	-0.6272
-0.3905	0.1866	0.6262	0.4534
1.3207	-0.0075	0.2840	-0.1177
-0.1277	-0.2406	-0.3062	0.0192
0.3739	-0.1284	0.0800	0.3436
0.2949	0.2087	0.6087	0.1479
0.0615	0.6082	-0.1902	0.6544
0.0571	-0.0295	0.1648	-0.2253
0.0945	-0.1252	-0.2062	0.4438
-0.3789	0.2862	-0.2885	-0.3248
-0.4326	-0.2511	0.4604	-0.2162
-0.3846	0.1345	-0.0767	-0.2127
1.9147	-0.0775	0.1900	0.4146
-0.0462	0.1997	0.1951	-0.2267
0.0663	-0.2700	0.0818	0.5053
0.0945	-0.3423	-0.2735	-0.2157
0.0895	0.2240	0.1020	0.3168
0.1016	1.8685	-0.1274	-0.1215
-0.1016	-0.1436	0.0458	0.1229
-0.1997	0.0875	-0.1859	-0.0968
-0.1353	0.2195	0.1968	0.0773
0.0979	-0.2477	-0.3822	0.0307
-0.0975	-0.0412	0.3896	-0.1800
-0.0315	-0.0428	0.0842	0.4379
0.1976	-0.1031	-0.1322	0.1251
-0.1907	0.1234	-0.0227	-0.0899
0.1413	0.2216	-0.0641	-0.1935
-0.3685	-0.1005	0.2633	-0.2338
0.1526	-0.0485	0.1523	-0.2705
-0.1252	-0.3657	0.1703	-0.2061
0.0773	0.6953	-0.0937	0.8248
-0.0741	-0.5997	0.1492	-0.1370
0.1074	-0.1672	-0.1325	0.0679
-0.1246	0.2013	0.0748	0.0801
0.1560	-0.3093	-0.0862	-0.1531
0.1376	0.2249	0.0726	0.1493
-0.1009	-0.1340	-0.1042	0.0842
0.0863	-0.2201	0.0351	-0.1070
-0.1619	-1.2405	0.0697	0.1313
0.1194	0.0950	-0.0492	0.1652
-0.2065	-0.1990	-0.0418	-0.0729
0.1284	0.2272	-0.0137	-0.0646
-0.0394	0.1003	0.0211	-0.0324
0.0525	0.0702	-0.0259	
0.0220	-0.0540		
0.0302	0.0248		
-0.1072	0.0569		
0.0476	0.0245		
0.0245	0.1427		
-0.0458	-0.2270		
0.0407	-0.1487		
-0.0945	0.0595		
-0.0088	-0.0197		
	0.0382		
	0.0141		

Surface Optimization Study Results

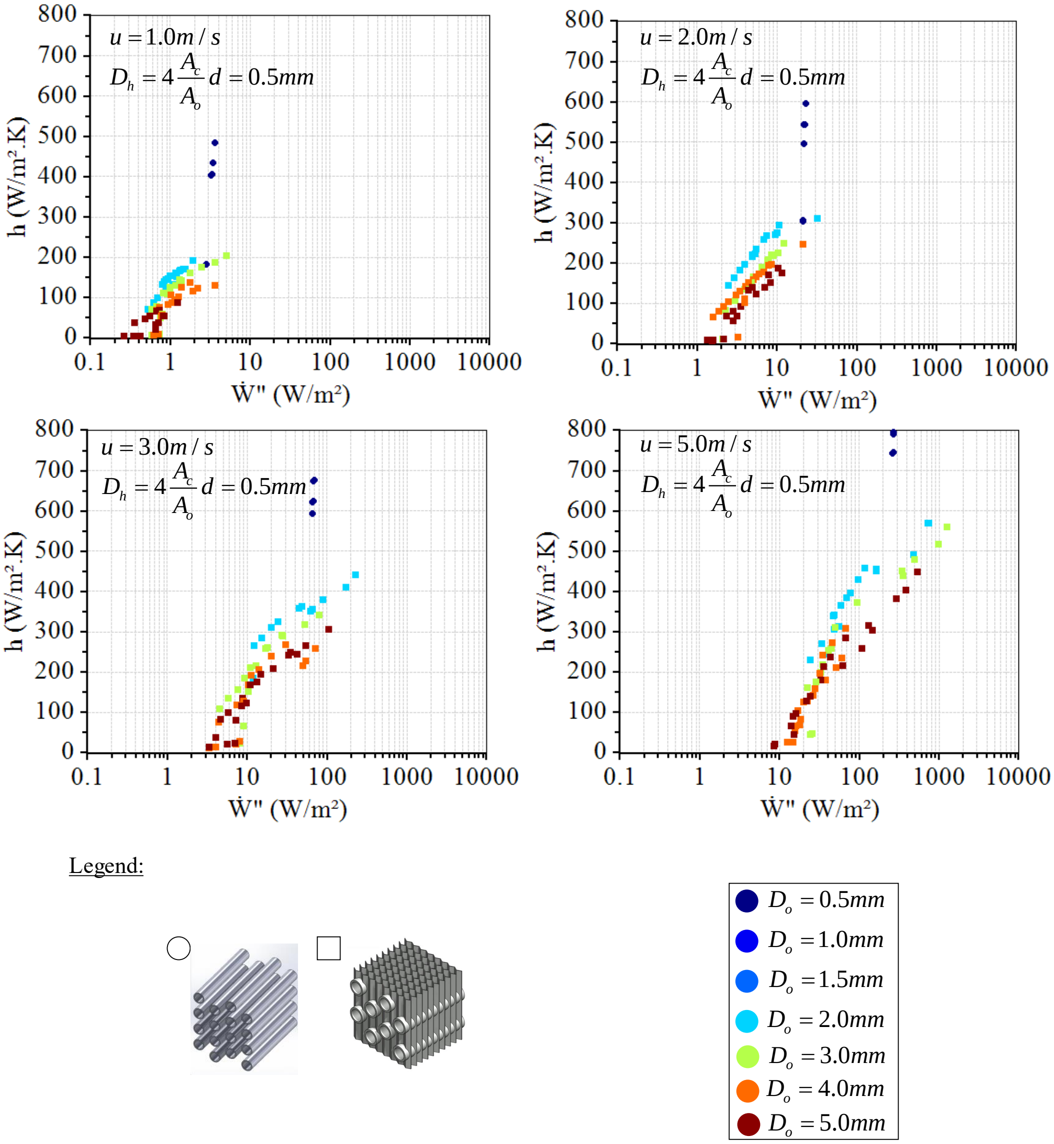

Figure 139. Surface optimization results (D_h=0.5mm).

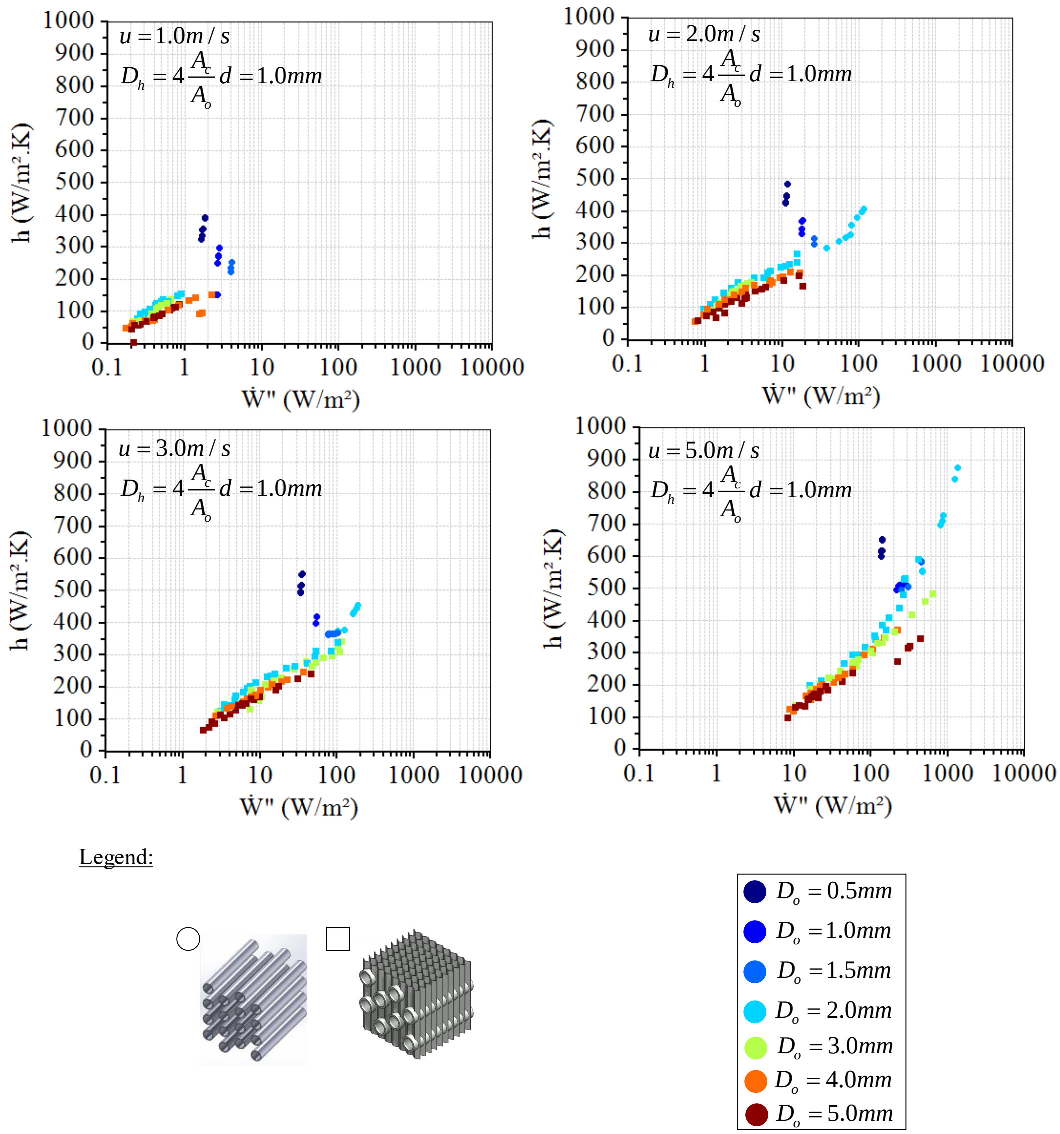

Figure 140. Surface optimization results (D_h=1.0mm).

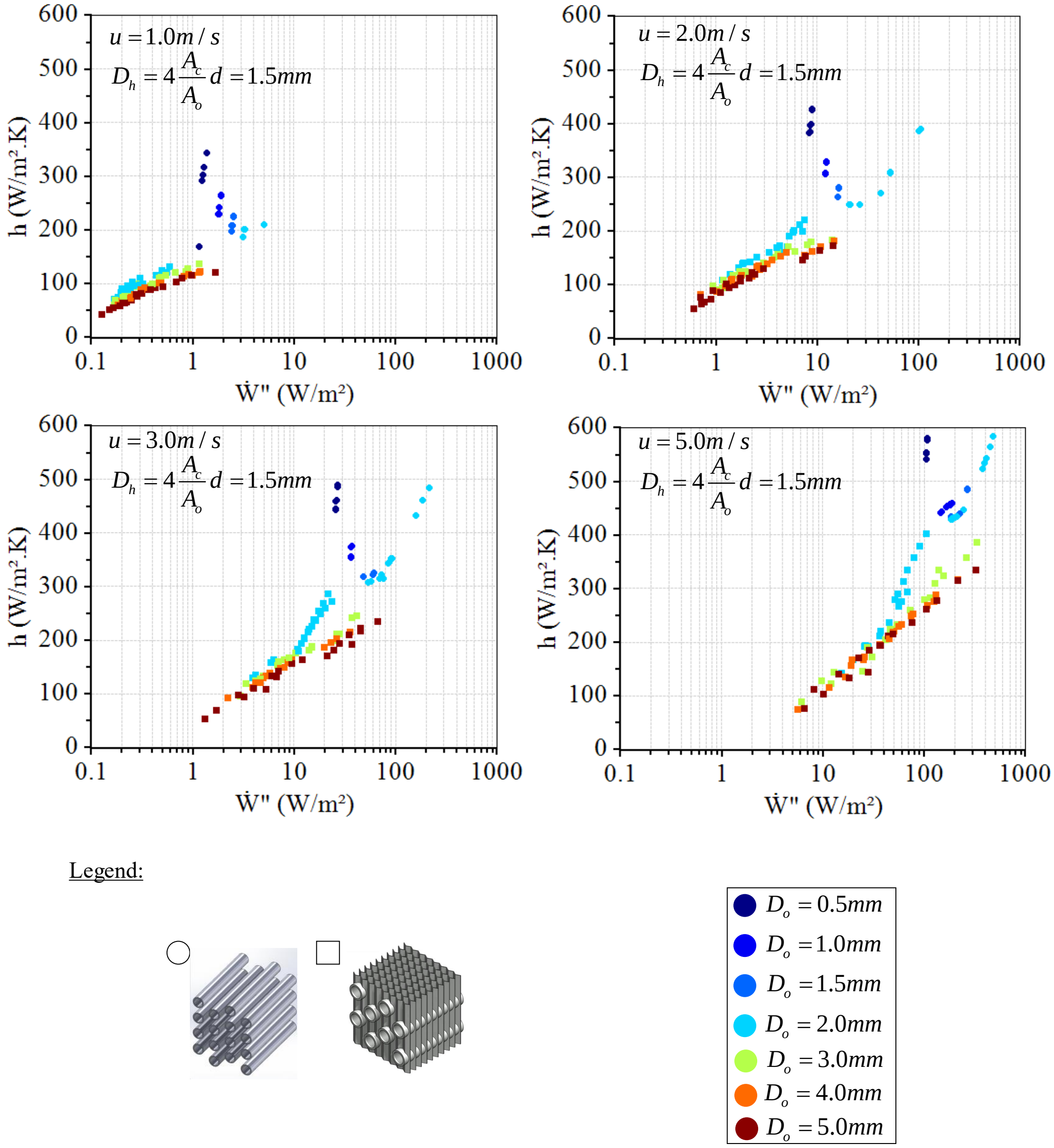

Figure 141. Surface optimization results (D_h=1.5mm).

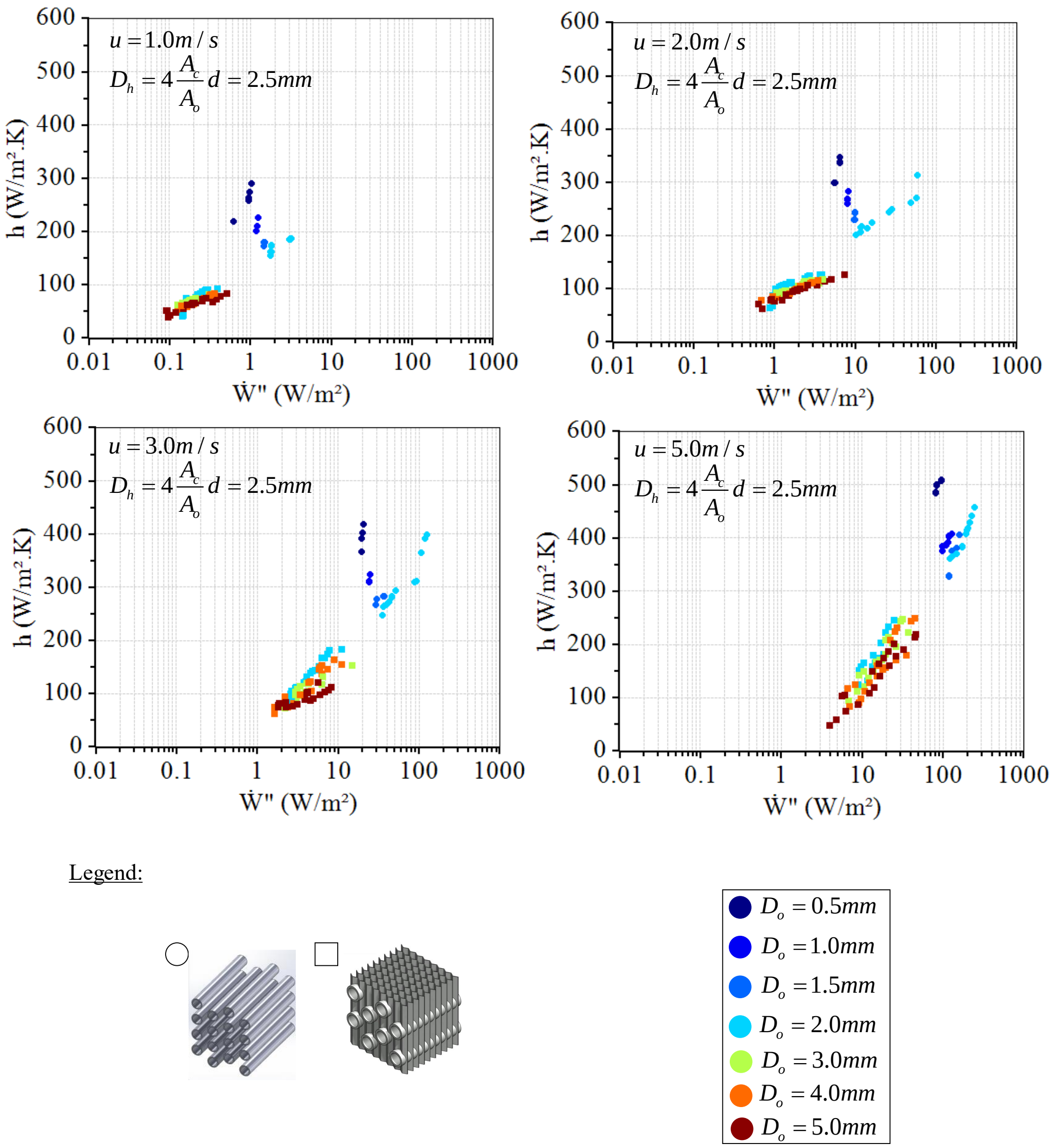

Figure 142. Surface optimization results (D_h=2.5mm).

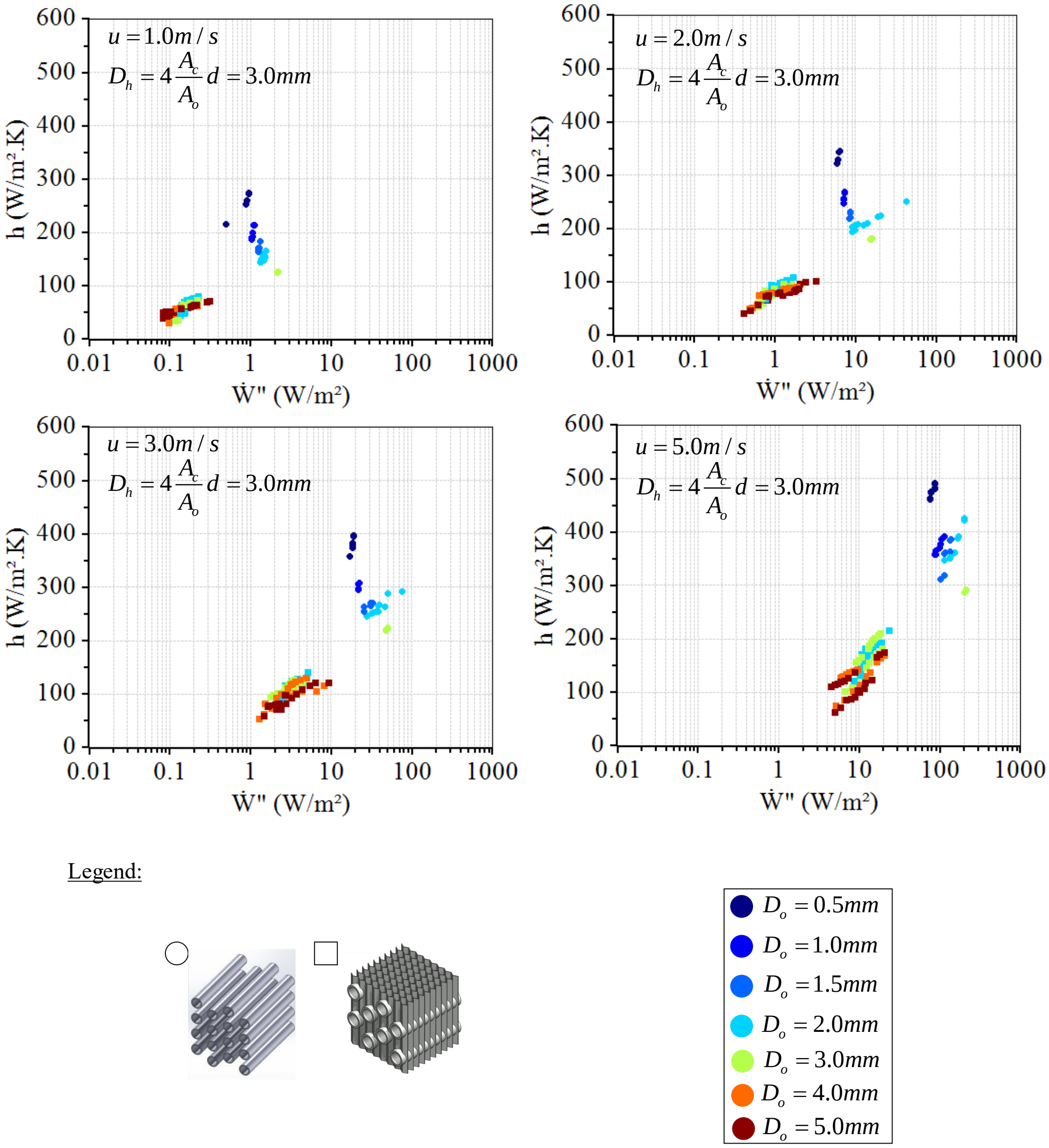

Figure 143. Surface optimization results (D_h=3.0mm).

8.3.1.2Optimum Wavy Fin Surfaces (WFTS)

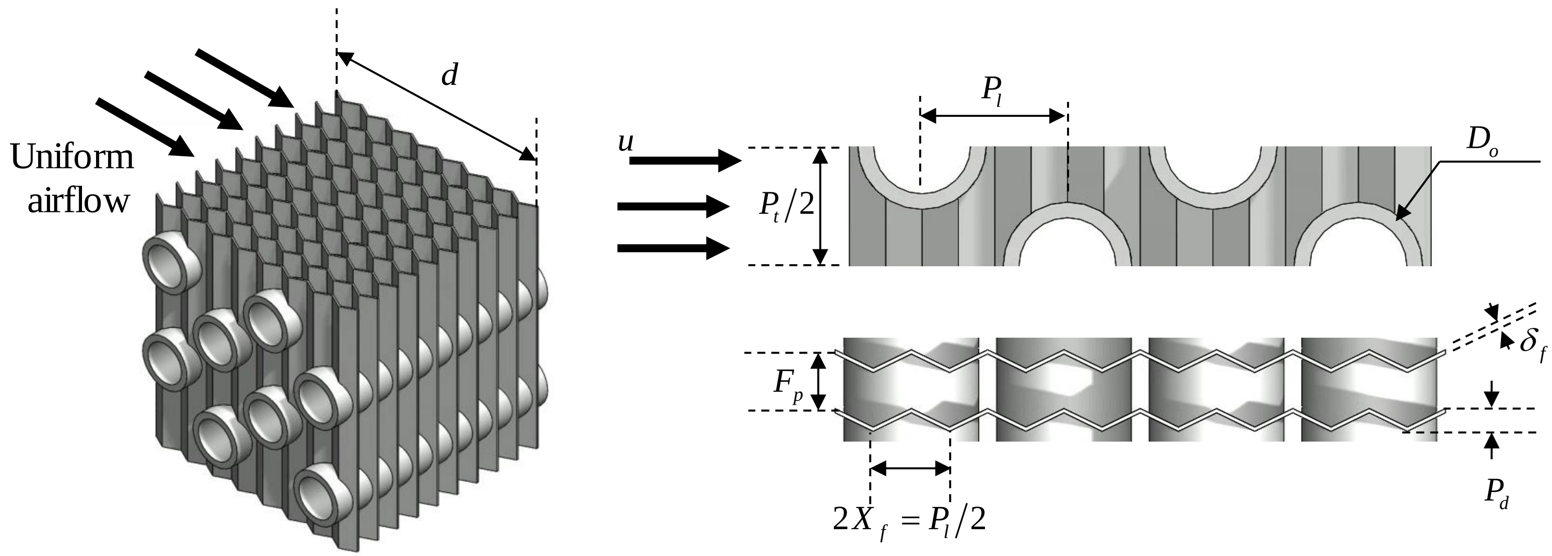

Figure 144. Wavy fin surface segment.

Table 50. WFTS Optimum designs dimensions.

TAG	D_o (mm)	P_l/D_o (-)	P_t/D_o (-)	P_t/P_l (-)	N_r (-)	F_p (mm)	FPI (in-1)	δ_f (mm)	Tanθ (-)	P_d (mm)	X_f(mm)	σ (-)	D_h (mm)	d (mm)	A_f (m^2)	A_c (m^2)	A_o (m^2)	V (cm^3)	A_o/V(cm^2/cm^3)
WFTS-001	2.00	1.25	1.73	1.38	2	0.574	44.286	0.072	0.264	0.165	0.625	0.368	0.50	5.00	2.0E-06	7.3E-07	2.9E-05	0.010	29.311
WFTS-002	2.00	1.25	1.87	1.49	8	2.534	10.024	0.051	0.324	0.202	0.625	0.455	1.51	20.00	9.5E-06	4.3E-06	2.3E-04	0.189	12.097
WFTS-003	2.00	1.25	1.87	1.49	8	2.534	10.024	0.058	0.330	0.206	0.625	0.454	1.50	20.00	9.5E-06	4.3E-06	2.3E-04	0.189	12.087
WFTS-004	2.00	1.25	1.87	1.49	8	2.534	10.024	0.068	0.330	0.206	0.625	0.452	1.50	20.00	9.5E-06	4.3E-06	2.3E-04	0.189	12.061
WFTS-005	2.00	1.25	1.87	1.49	9	2.534	10.024	0.073	0.329	0.205	0.625	0.451	1.50	22.50	9.5E-06	4.3E-06	2.6E-04	0.213	12.047
WFTS-006	2.00	1.25	1.87	1.49	9	2.534	10.024	0.083	0.330	0.206	0.625	0.450	1.50	22.50	9.5E-06	4.3E-06	2.6E-04	0.213	12.021
WFTS-007	2.00	1.25	1.87	1.49	9	2.534	10.024	0.097	0.330	0.206	0.625	0.447	1.49	22.50	9.5E-06	4.2E-06	2.6E-04	0.213	11.984
WFTS-008	2.00	1.25	1.96	1.57	2	0.528	48.119	0.094	0.341	0.213	0.626	0.403	0.50	5.01	2.1E-06	8.4E-07	3.4E-05	0.010	32.493
WFTS-009	2.00	1.26	2.35	1.86	2	0.967	26.271	0.050	0.476	0.300	0.630	0.544	1.00	5.04	4.5E-06	2.5E-06	5.0E-05	0.023	21.862
WFTS-010	2.00	1.26	2.35	1.86	3	0.999	25.435	0.067	0.511	0.323	0.632	0.536	1.00	7.58	4.7E-06	2.5E-06	7.7E-05	0.036	21.478

TAG	D_o (mm)	P_l/D_o (-)	P_t/D_o (-)	P_t/P_l (-)	N_r (-)	F_p (mm)	FPI (in-1)	δ_f (mm)	$\tan\theta$ (-)	P_d (mm)	X_f(mm)	σ (-)	D_h (mm)	d (mm)	A_f (m^2)	A_c (m^2)	A_o (m^2)	V (cm^3)	A_o/V(cm^2/cm^3)
WFTS-011	2.00	1.31	1.51	1.15	2	0.723	35.155	0.056	0.386	0.253	0.655	0.313	0.50	5.24	2.2E-06	6.8E-07	2.9E-05	0.012	25.226
WFTS-012	2.00	1.31	1.52	1.15	2	0.723	35.155	0.051	0.374	0.246	0.656	0.316	0.50	5.25	2.2E-06	6.9E-07	2.9E-05	0.012	25.224
WFTS-013	2.00	1.31	1.52	1.15	2	0.723	35.155	0.051	0.374	0.246	0.656	0.316	0.50	5.25	2.2E-06	6.9E-07	2.9E-05	0.012	25.224
WFTS-014	2.00	1.32	2.26	1.71	2	1.654	15.356	0.074	0.312	0.206	0.660	0.533	1.49	5.28	7.5E-06	4.0E-06	5.7E-05	0.040	14.359
WFTS-015	2.00	1.36	1.99	1.46	2	0.514	49.420	0.073	0.301	0.204	0.679	0.426	0.50	5.43	2.0E-06	8.7E-07	3.8E-05	0.011	33.803
WFTS-016	2.00	1.38	3.99	2.90	2	1.164	21.831	0.065	0.303	0.209	0.688	0.674	1.49	5.51	9.3E-06	6.3E-06	9.3E-05	0.051	18.094
WFTS-017	2.00	1.38	1.97	1.43	2	0.528	48.119	0.087	0.336	0.232	0.691	0.412	0.50	5.53	2.1E-06	8.6E-07	3.8E-05	0.012	33.270
WFTS-018	2.00	1.41	2.71	1.93	2	0.899	28.244	0.075	0.465	0.327	0.704	0.579	1.00	5.63	4.9E-06	2.8E-06	6.4E-05	0.028	23.252
WFTS-019	2.00	1.41	1.99	1.41	2	0.510	49.805	0.069	0.288	0.203	0.707	0.430	0.50	5.66	2.0E-06	8.7E-07	3.9E-05	0.012	34.241
WFTS-020	2.00	1.43	1.62	1.13	2	0.659	38.546	0.074	0.273	0.195	0.715	0.338	0.50	5.72	2.1E-06	7.2E-07	3.3E-05	0.012	26.801
WFTS-021	2.00	1.43	2.07	1.45	3	1.152	22.056	0.098	0.478	0.342	0.715	0.472	0.99	8.58	4.8E-06	2.3E-06	7.8E-05	0.041	18.998
WFTS-022	2.00	1.44	2.35	1.63	2	0.965	26.325	0.050	0.464	0.333	0.718	0.544	0.99	5.74	4.5E-06	2.5E-06	5.7E-05	0.026	21.944
WFTS-023	2.00	1.46	2.51	1.72	2	0.875	29.013	0.075	0.157	0.115	0.730	0.550	1.00	5.84	4.4E-06	2.4E-06	5.7E-05	0.026	22.089
WFTS-024	2.00	1.46	4.00	2.74	2	1.102	23.051	0.053	0.255	0.186	0.730	0.702	1.50	5.84	8.8E-06	6.2E-06	9.7E-05	0.052	18.772
WFTS-025	2.00	1.47	1.78	1.22	2	1.334	19.036	0.075	0.280	0.205	0.733	0.415	1.00	5.86	4.8E-06	2.0E-06	4.6E-05	0.028	16.562
WFTS-026	2.00	1.47	2.69	1.84	2	0.834	30.464	0.062	0.232	0.170	0.734	0.582	0.99	5.87	4.5E-06	2.6E-06	6.2E-05	0.026	23.409
WFTS-027	2.00	1.47	1.70	1.15	2	0.609	41.687	0.075	0.305	0.224	0.735	0.360	0.50	5.88	2.1E-06	7.5E-07	3.5E-05	0.012	29.035
WFTS-028	2.00	1.47	1.78	1.21	2	1.334	19.036	0.062	0.280	0.206	0.735	0.419	1.01	5.88	4.8E-06	2.0E-06	4.7E-05	0.028	16.615
WFTS-029	2.00	1.49	1.72	1.15	2	0.605	41.961	0.072	0.317	0.236	0.744	0.369	0.50	5.95	2.1E-06	7.7E-07	3.7E-05	0.012	29.433
WFTS-030	2.00	1.49	1.72	1.15	2	0.605	41.961	0.072	0.317	0.236	0.744	0.369	0.50	5.95	2.1E-06	7.7E-07	3.7E-05	0.012	29.433
WFTS-031	2.00	1.49	1.72	1.15	2	0.605	41.961	0.072	0.317	0.236	0.744	0.369	0.50	5.95	2.1E-06	7.7E-07	3.7E-05	0.012	29.433
WFTS-032	2.00	1.49	1.72	1.15	2	0.605	41.961	0.072	0.317	0.236	0.744	0.369	0.50	5.95	2.1E-06	7.7E-07	3.7E-05	0.012	29.433
WFTS-033	2.00	1.49	1.72	1.15	2	1.459	17.404	0.092	0.355	0.264	0.744	0.392	0.99	5.95	5.0E-06	2.0E-06	4.7E-05	0.030	15.829
WFTS-034	2.00	1.49	1.72	1.15	2	0.587	43.238	0.054	0.344	0.257	0.745	0.380	0.50	5.96	2.0E-06	7.7E-07	3.7E-05	0.012	30.541
WFTS-035	2.00	1.49	1.72	1.15	2	0.587	43.238	0.054	0.344	0.257	0.745	0.380	0.50	5.96	2.0E-06	7.7E-07	3.7E-05	0.012	30.541
WFTS-036	2.00	1.53	1.77	1.15	2	1.446	17.572	0.087	0.466	0.357	0.766	0.408	1.00	6.13	5.1E-06	2.1E-06	5.1E-05	0.031	16.286
WFTS-037	2.00	1.53	1.77	1.15	2	1.301	19.531	0.050	0.195	0.149	0.767	0.419	1.00	6.14	4.6E-06	1.9E-06	4.7E-05	0.028	16.698
WFTS-038	2.00	1.53	1.77	1.15	2	1.316	19.295	0.055	0.266	0.204	0.767	0.417	1.00	6.14	4.7E-06	2.0E-06	4.8E-05	0.029	16.715
WFTS-039	2.00	1.54	2.23	1.45	2	1.606	15.812	0.069	0.210	0.162	0.769	0.528	1.49	6.15	7.2E-06	3.8E-06	6.3E-05	0.044	14.192
WFTS-040	2.00	1.54	1.78	1.15	2	1.301	19.531	0.050	0.198	0.152	0.770	0.421	1.01	6.16	4.6E-06	2.0E-06	4.8E-05	0.029	16.695
WFTS-041	2.00	1.55	1.98	1.27	2	0.528	48.119	0.076	0.342	0.266	0.777	0.423	0.50	6.22	2.1E-06	8.8E-07	4.4E-05	0.013	34.187
WFTS-042	2.00	1.56	1.80	1.15	2	0.564	45.066	0.064	0.285	0.223	0.780	0.395	0.50	6.24	2.0E-06	8.0E-07	4.0E-05	0.013	31.543
WFTS-043	2.00	1.56	1.80	1.15	2	0.564	45.066	0.064	0.285	0.223	0.780	0.395	0.50	6.24	2.0E-06	8.0E-07	4.0E-05	0.013	31.543
WFTS-044	2.00	1.56	1.80	1.15	10	2.486	10.216	0.055	0.278	0.217	0.780	0.435	1.52	31.19	9.0E-06	3.9E-06	3.2E-04	0.279	11.483
WFTS-045	2.00	1.56	1.80	1.15	10	2.490	10.200	0.058	0.290	0.226	0.780	0.434	1.51	31.19	9.0E-06	3.9E-06	3.2E-04	0.280	11.485
WFTS-046	2.00	1.56	1.80	1.15	10	2.486	10.216	0.068	0.293	0.228	0.780	0.433	1.51	31.19	9.0E-06	3.9E-06	3.2E-04	0.279	11.476
WFTS-047	2.00	1.56	1.80	1.15	10	2.522	10.071	0.081	0.295	0.230	0.780	0.431	1.51	31.19	9.1E-06	3.9E-06	3.2E-04	0.283	11.369
WFTS-048	2.00	1.56	1.80	1.15	10	2.522	10.071	0.083	0.343	0.267	0.780	0.430	1.50	31.19	9.1E-06	3.9E-06	3.2E-04	0.283	11.447
WFTS-049	2.00	1.56	1.80	1.15	10	2.522	10.071	0.093	0.363	0.283	0.780	0.428	1.49	31.19	9.1E-06	3.9E-06	3.3E-04	0.283	11.465
WFTS-050	2.00	1.57	2.30	1.46	3	0.951	26.710	0.070	0.241	0.189	0.785	0.523	1.00	9.42	4.4E-06	2.3E-06	8.6E-05	0.041	20.953
WFTS-051	2.00	1.57	2.30	1.46	3	0.951	26.710	0.070	0.241	0.189	0.785	0.523	1.00	9.42	4.4E-06	2.3E-06	8.6E-05	0.041	20.953
WFTS-052	2.00	1.58	1.99	1.26	2	0.510	49.805	0.057	0.289	0.228	0.788	0.441	0.50	6.30	2.0E-06	8.9E-07	4.5E-05	0.013	35.036
WFTS-053	2.00	1.58	1.82	1.15	10	2.538	10.008	0.099	0.419	0.331	0.788	0.433	1.51	31.54	9.2E-06	4.0E-06	3.3E-04	0.291	11.464
WFTS-054	2.00	1.58	1.82	1.15	10	2.395	10.605	0.097	0.305	0.240	0.790	0.433	1.50	31.58	8.7E-06	3.8E-06	3.2E-04	0.276	11.584
WFTS-055	2.00	1.58	1.82	1.15	10	2.522	10.071	0.099	0.421	0.332	0.790	0.434	1.51	31.58	9.2E-06	4.0E-06	3.3E-04	0.290	11.498
WFTS-056	2.00	1.59	1.83	1.15	10	2.335	10.876	0.092	0.309	0.245	0.793	0.436	1.49	31.71	8.6E-06	3.7E-06	3.2E-04	0.271	11.737
WFTS-057	2.00	1.59	1.83	1.15	10	2.341	10.848	0.093	0.262	0.208	0.794	0.436	1.50	31.75	8.6E-06	3.8E-06	3.2E-04	0.273	11.629
WFTS-058	2.00	1.59	1.83	1.15	10	2.467	10.298	0.093	0.397	0.315	0.794	0.437	1.51	31.75	9.0E-06	4.0E-06	3.3E-04	0.287	11.563
WFTS-059	2.00	1.59	2.51	1.58	2	0.879	28.882	0.075	0.151	0.120	0.794	0.550	1.00	6.35	4.4E-06	2.4E-06	6.2E-05	0.028	22.072
WFTS-060	2.00	1.59	3.34	2.09	2	0.766	33.150	0.063	0.271	0.216	0.797	0.642	1.00	6.38	5.1E-06	3.3E-06	8.4E-05	0.033	25.757

TAG	D_o (mm)	P_l/D_o (-)	P_t/D_o (-)	P_t/P_l (-)	N_r (-)	F_p (mm)	FPI (in-1)	δ_f (mm)	Tanθ (-)	P_d (mm)	X_f(mm)	σ (-)	D_h (mm)	d (mm)	A_f (m^2)	A_c (m^2)	A_o (m^2)	V (cm^3)	A_o/V(cm^2/cm^3)
WFTS-061	2.00	1.60	1.84	1.15	10	2.286	11.112	0.056	0.283	0.226	0.798	0.446	1.50	31.92	8.4E-06	3.8E-06	3.2E-04	0.269	11.874
WFTS-062	2.00	1.60	1.84	1.15	10	2.286	11.112	0.067	0.276	0.220	0.798	0.444	1.50	31.92	8.4E-06	3.7E-06	3.2E-04	0.269	11.835
WFTS-063	2.00	1.60	1.85	1.15	2	0.530	47.938	0.050	0.210	0.168	0.799	0.415	0.50	6.39	2.0E-06	8.1E-07	4.1E-05	0.013	33.125
WFTS-064	2.00	1.60	1.85	1.15	2	0.530	47.938	0.050	0.216	0.173	0.799	0.415	0.50	6.39	2.0E-06	8.1E-07	4.2E-05	0.013	33.159
WFTS-065	2.00	1.60	1.85	1.15	2	0.550	46.206	0.059	0.277	0.222	0.799	0.409	0.50	6.39	2.0E-06	8.3E-07	4.2E-05	0.013	32.460
WFTS-066	2.00	1.60	1.85	1.15	2	0.568	44.751	0.077	0.277	0.222	0.799	0.396	0.50	6.39	2.1E-06	8.3E-07	4.2E-05	0.013	31.430
WFTS-067	2.00	1.60	1.85	1.15	2	0.570	44.594	0.087	0.277	0.222	0.799	0.388	0.50	6.39	2.1E-06	8.2E-07	4.2E-05	0.013	31.251
WFTS-068	2.00	1.60	1.62	1.01	2	0.635	39.992	0.053	0.226	0.181	0.800	0.351	0.50	6.40	2.1E-06	7.2E-07	3.7E-05	0.013	28.057
WFTS-069	2.00	1.60	1.63	1.02	2	0.651	39.016	0.065	0.263	0.211	0.800	0.346	0.50	6.40	2.1E-06	7.3E-07	3.7E-05	0.014	27.609
WFTS-070	2.00	1.60	1.85	1.15	10	2.278	11.151	0.052	0.276	0.221	0.800	0.448	1.51	32.01	8.4E-06	3.8E-06	3.2E-04	0.269	11.878
WFTS-071	2.00	1.60	1.85	1.15	10	2.282	11.132	0.076	0.276	0.221	0.800	0.444	1.50	32.01	8.4E-06	3.7E-06	3.2E-04	0.270	11.810
WFTS-072	2.00	1.61	1.86	1.15	2	0.530	47.938	0.056	0.146	0.117	0.804	0.412	0.50	6.43	2.0E-06	8.1E-07	4.2E-05	0.013	32.808
WFTS-073	2.00	1.62	1.88	1.15	2	0.512	49.612	0.052	0.090	0.073	0.812	0.420	0.50	6.50	1.9E-06	8.1E-07	4.2E-05	0.013	33.747
WFTS-074	2.00	1.63	1.89	1.15	2	0.514	49.420	0.050	0.134	0.109	0.816	0.424	0.50	6.53	1.9E-06	8.2E-07	4.3E-05	0.013	33.850
WFTS-075	2.00	1.66	1.92	1.15	2	0.512	49.612	0.052	0.095	0.079	0.829	0.429	0.50	6.63	2.0E-06	8.4E-07	4.4E-05	0.013	33.978
WFTS-076	2.00	1.66	1.92	1.15	2	0.512	49.612	0.050	0.183	0.152	0.829	0.431	0.50	6.63	2.0E-06	8.5E-07	4.5E-05	0.013	34.357
WFTS-077	2.00	1.67	1.93	1.15	2	0.556	45.711	0.086	0.299	0.249	0.834	0.406	0.50	6.67	2.1E-06	8.7E-07	4.6E-05	0.014	32.511
WFTS-078	2.00	1.72	1.98	1.15	2	0.524	48.483	0.064	0.293	0.251	0.858	0.435	0.50	6.87	2.1E-06	9.0E-07	4.9E-05	0.014	34.652
WFTS-079	2.00	1.72	1.98	1.15	2	0.524	48.483	0.064	0.293	0.251	0.858	0.435	0.50	6.87	2.1E-06	9.0E-07	4.9E-05	0.014	34.652
WFTS-080	2.00	1.74	2.00	1.15	2	0.508	50.000	0.061	0.194	0.169	0.868	0.441	0.50	6.94	2.0E-06	9.0E-07	5.0E-05	0.014	35.029
WFTS-081	2.00	1.77	2.01	1.14	2	0.510	49.805	0.057	0.289	0.256	0.884	0.446	0.50	7.08	2.1E-06	9.1E-07	5.2E-05	0.015	35.728
WFTS-082	2.00	1.77	2.07	1.17	3	1.152	22.056	0.082	0.476	0.421	0.884	0.479	1.00	10.61	4.8E-06	2.3E-06	9.7E-05	0.051	19.091
WFTS-083	2.00	1.78	2.05	1.15	2	1.811	14.025	0.058	0.279	0.248	0.888	0.496	1.51	7.11	7.4E-06	3.7E-06	7.0E-05	0.053	13.166
WFTS-084	2.00	1.78	2.05	1.15	2	1.096	23.177	0.090	0.313	0.279	0.890	0.471	0.99	7.12	4.5E-06	2.1E-06	6.1E-05	0.032	18.961
WFTS-085	2.00	1.78	2.36	1.32	2	0.901	28.182	0.050	0.193	0.172	0.890	0.544	0.99	7.12	4.3E-06	2.3E-06	6.6E-05	0.030	21.905
WFTS-086	2.00	1.79	2.07	1.15	2	1.811	14.025	0.096	0.279	0.250	0.896	0.489	1.50	7.17	7.5E-06	3.7E-06	7.0E-05	0.054	13.050
WFTS-087	2.00	1.79	2.07	1.15	2	1.811	14.025	0.099	0.328	0.294	0.897	0.489	1.49	7.18	7.5E-06	3.7E-06	7.1E-05	0.054	13.162
WFTS-088	2.00	1.80	2.08	1.15	2	0.514	49.420	0.071	0.276	0.248	0.900	0.447	0.50	7.20	2.1E-06	9.6E-07	5.5E-05	0.015	35.515
WFTS-089	2.00	1.80	2.08	1.15	2	0.514	49.420	0.075	0.309	0.278	0.900	0.443	0.50	7.20	2.1E-06	9.5E-07	5.5E-05	0.015	35.768
WFTS-090	2.00	1.80	2.08	1.15	2	0.514	49.420	0.075	0.309	0.278	0.900	0.443	0.50	7.20	2.1E-06	9.5E-07	5.5E-05	0.015	35.768
WFTS-091	2.00	1.80	2.08	1.15	2	0.514	49.420	0.075	0.309	0.278	0.900	0.443	0.50	7.20	2.1E-06	9.5E-07	5.5E-05	0.015	35.768
WFTS-092	2.00	1.80	2.08	1.15	2	0.514	49.420	0.075	0.309	0.278	0.900	0.443	0.50	7.20	2.1E-06	9.5E-07	5.5E-05	0.015	35.768
WFTS-093	2.00	1.80	2.08	1.15	2	0.524	48.483	0.080	0.308	0.278	0.902	0.440	0.50	7.22	2.2E-06	9.6E-07	5.5E-05	0.016	35.141
WFTS-094	2.00	1.80	2.08	1.15	2	0.540	47.056	0.100	0.321	0.290	0.902	0.424	0.50	7.22	2.3E-06	9.5E-07	5.6E-05	0.016	34.196
WFTS-095	2.00	1.81	3.21	1.78	2	1.175	21.610	0.054	0.213	0.193	0.903	0.657	1.49	7.23	7.6E-06	5.0E-06	9.6E-05	0.055	17.625
WFTS-096	2.00	1.81	2.09	1.15	3	1.128	22.524	0.075	0.483	0.437	0.904	0.486	1.00	10.84	4.7E-06	2.3E-06	9.9E-05	0.051	19.483
WFTS-097	2.00	1.81	2.09	1.15	3	1.128	22.524	0.075	0.483	0.437	0.904	0.486	1.00	10.84	4.7E-06	2.3E-06	9.9E-05	0.051	19.483
WFTS-098	2.00	1.82	2.11	1.15	3	1.112	22.846	0.059	0.477	0.435	0.912	0.497	1.01	10.95	4.7E-06	2.3E-06	1.0E-04	0.051	19.729
WFTS-099	2.00	1.83	2.50	1.37	2	1.438	17.668	0.073	0.260	0.238	0.913	0.569	1.50	7.30	7.2E-06	4.1E-06	8.0E-05	0.052	15.171
WFTS-100	2.00	1.83	2.53	1.38	2	1.398	18.170	0.054	0.190	0.173	0.914	0.581	1.51	7.31	7.1E-06	4.1E-06	7.9E-05	0.052	15.356
WFTS-101	2.00	1.85	3.32	1.79	2	0.762	33.322	0.061	0.185	0.171	0.927	0.642	1.00	7.42	5.1E-06	3.3E-06	9.6E-05	0.038	25.623
WFTS-102	2.00	1.88	3.99	2.12	2	1.175	21.610	0.084	0.440	0.414	0.942	0.696	1.50	7.54	9.4E-06	6.5E-06	1.3E-04	0.071	18.587
WFTS-103	2.00	1.90	2.80	1.48	2	0.826	30.758	0.061	0.232	0.220	0.949	0.595	1.00	7.59	4.6E-06	2.8E-06	8.4E-05	0.035	23.923
WFTS-104	2.00	1.90	3.07	1.62	2	1.253	20.273	0.083	0.291	0.276	0.949	0.629	1.49	7.59	7.7E-06	4.8E-06	9.9E-05	0.058	16.903
WFTS-105	2.00	1.91	3.10	1.62	2	1.251	20.305	0.081	0.319	0.305	0.954	0.633	1.49	7.63	7.8E-06	4.9E-06	1.0E-04	0.059	17.037
WFTS-106	2.00	1.93	2.53	1.31	2	0.883	28.752	0.075	0.152	0.146	0.966	0.553	1.00	7.73	4.5E-06	2.5E-06	7.7E-05	0.035	22.159
WFTS-107	2.00	1.94	1.99	1.02	2	0.510	49.805	0.057	0.111	0.108	0.970	0.442	0.50	7.76	2.0E-06	9.0E-07	5.5E-05	0.016	35.042
WFTS-108	2.00	1.94	1.99	1.02	2	0.510	49.805	0.057	0.205	0.199	0.970	0.442	0.50	7.76	2.0E-06	9.0E-07	5.6E-05	0.016	35.501
WFTS-109	2.00	1.94	2.33	1.20	9	1.507	16.854	0.059	0.250	0.243	0.970	0.549	1.50	34.94	7.0E-06	3.9E-06	3.6E-04	0.245	14.641
WFTS-110	2.00	1.94	2.33	1.20	9	1.507	16.854	0.059	0.250	0.243	0.970	0.549	1.50	34.94	7.0E-06	3.9E-06	3.6E-04	0.245	14.641

TAG	D_o (mm)	P_l/D_o (-)	P_t/D_o (-)	P_t/P_l (-)	N_r (-)	F_p (mm)	FPI (in-1)	δ_f (mm)	Tanθ (-)	P_d (mm)	X_f(mm)	σ (-)	D_h (mm)	d (mm)	A_f (m^2)	A_c (m^2)	A_o (m^2)	V (cm^3)	A_o/V(cm^2/cm^3)
WFTS-111	2.00	1.94	2.24	1.15	2	0.508	50.000	0.087	0.285	0.276	0.971	0.459	0.50	7.77	2.3E-06	1.1E-06	6.5E-05	0.018	36.539
WFTS-112	2.00	1.94	2.25	1.15	2	0.508	50.000	0.086	0.282	0.274	0.972	0.461	0.50	7.78	2.3E-06	1.1E-06	6.5E-05	0.018	36.535
WFTS-113	2.00	1.94	2.25	1.15	2	0.508	50.000	0.086	0.282	0.274	0.972	0.461	0.50	7.78	2.3E-06	1.1E-06	6.5E-05	0.018	36.535
WFTS-114	2.00	1.97	2.28	1.15	2	0.925	27.456	0.050	0.145	0.143	0.985	0.530	0.99	7.88	4.2E-06	2.2E-06	7.1E-05	0.033	21.331
WFTS-115	2.00	1.97	2.28	1.15	2	1.015	25.037	0.092	0.380	0.375	0.985	0.509	0.99	7.88	4.6E-06	2.4E-06	7.5E-05	0.036	20.581
WFTS-116	2.00	2.01	2.73	1.36	11	2.536	10.016	0.050	0.360	0.361	1.003	0.621	2.49	44.12	1.4E-05	8.6E-06	6.1E-04	0.611	9.992
WFTS-117	2.00	2.01	2.95	1.47	11	2.536	10.016	0.050	0.558	0.559	1.003	0.648	2.48	44.12	1.5E-05	9.7E-06	6.9E-04	0.659	10.435
WFTS-118	2.00	2.04	2.35	1.15	2	0.943	26.935	0.059	0.327	0.334	1.020	0.539	0.99	8.16	4.4E-06	2.4E-06	7.9E-05	0.036	21.733
WFTS-119	2.00	2.06	4.00	1.95	2	1.080	23.516	0.053	0.253	0.260	1.028	0.713	1.49	8.23	8.6E-06	6.2E-06	1.4E-04	0.071	19.091
WFTS-120	2.00	2.09	2.41	1.15	2	0.919	27.634	0.054	0.242	0.252	1.043	0.551	1.01	8.35	4.4E-06	2.4E-06	8.1E-05	0.037	21.831
WFTS-121	2.00	2.09	2.41	1.15	2	0.919	27.634	0.054	0.242	0.252	1.043	0.551	1.01	8.35	4.4E-06	2.4E-06	8.1E-05	0.037	21.831
WFTS-122	2.00	2.09	2.41	1.15	2	0.911	27.875	0.055	0.243	0.253	1.043	0.550	1.00	8.35	4.4E-06	2.4E-06	8.1E-05	0.037	21.993
WFTS-123	2.00	2.09	2.23	1.07	2	1.559	16.295	0.074	0.221	0.231	1.047	0.526	1.49	8.38	7.0E-06	3.7E-06	8.2E-05	0.058	14.132
WFTS-124	2.00	2.11	2.44	1.15	10	1.469	17.286	0.077	0.290	0.306	1.055	0.559	1.50	42.20	7.2E-06	4.0E-06	4.5E-04	0.302	14.902
WFTS-125	2.00	2.11	2.44	1.15	10	1.517	16.744	0.087	0.352	0.371	1.055	0.556	1.51	42.20	7.4E-06	4.1E-06	4.6E-04	0.312	14.720
WFTS-126	2.00	2.11	2.07	0.98	3	1.152	22.056	0.076	0.476	0.503	1.056	0.482	1.01	12.68	4.8E-06	2.3E-06	1.2E-04	0.060	19.134
WFTS-127	2.00	2.18	2.98	1.37	2	2.264	11.220	0.089	0.235	0.257	1.091	0.638	2.48	8.73	1.4E-05	8.6E-06	1.2E-04	0.118	10.299
WFTS-128	2.00	2.23	1.99	0.89	2	0.510	49.805	0.050	0.113	0.126	1.116	0.448	0.50	8.92	2.0E-06	9.1E-07	6.5E-05	0.018	35.671
WFTS-129	2.00	2.23	2.52	1.13	2	0.875	29.013	0.050	0.149	0.167	1.117	0.568	1.01	8.94	4.4E-06	2.5E-06	8.9E-05	0.039	22.505
WFTS-130	2.00	2.24	3.99	1.79	2	1.080	23.516	0.053	0.175	0.196	1.118	0.713	1.52	8.95	8.6E-06	6.2E-06	1.5E-04	0.077	18.818
WFTS-131	2.00	2.26	2.50	1.10	3	1.493	17.010	0.083	0.429	0.485	1.132	0.566	1.49	13.58	7.5E-06	4.2E-06	1.5E-04	0.101	15.173
WFTS-132	2.00	2.26	3.01	1.33	2	2.224	11.420	0.074	0.229	0.260	1.132	0.645	2.48	9.05	1.3E-05	8.6E-06	1.3E-04	0.121	10.393
WFTS-133	2.00	2.26	2.64	1.17	2	2.518	10.087	0.075	0.235	0.266	1.132	0.603	2.50	9.05	1.3E-05	8.0E-06	1.2E-04	0.120	9.638
WFTS-134	2.00	2.27	2.64	1.16	2	2.518	10.087	0.087	0.235	0.267	1.133	0.600	2.49	9.06	1.3E-05	8.0E-06	1.2E-04	0.121	9.623
WFTS-135	2.00	2.27	3.07	1.35	2	2.224	11.420	0.071	0.235	0.267	1.134	0.653	2.52	9.08	1.4E-05	8.9E-06	1.3E-04	0.124	10.379
WFTS-136	2.00	2.27	2.64	1.16	2	2.518	10.087	0.099	0.235	0.267	1.134	0.596	2.48	9.08	1.3E-05	7.9E-06	1.2E-04	0.121	9.610
WFTS-137	2.00	2.28	3.35	1.47	2	0.766	33.150	0.053	0.247	0.282	1.141	0.652	1.00	9.13	5.1E-06	3.4E-06	1.2E-04	0.047	26.037
WFTS-138	2.00	2.29	4.00	1.74	2	1.908	13.310	0.081	0.256	0.293	1.147	0.718	2.49	9.17	1.5E-05	1.1E-05	1.6E-04	0.140	11.532
WFTS-139	2.00	2.29	4.00	1.74	2	2.004	12.677	0.077	0.415	0.476	1.147	0.721	2.50	9.17	1.6E-05	1.2E-05	1.7E-04	0.147	11.528
WFTS-140	2.00	2.34	4.00	1.71	2	2.163	11.745	0.093	0.621	0.725	1.168	0.718	2.48	9.34	1.7E-05	1.2E-05	1.9E-04	0.162	11.579
WFTS-141	2.00	2.34	2.70	1.15	2	1.307	19.441	0.052	0.240	0.280	1.169	0.604	1.50	9.35	7.1E-06	4.3E-06	1.1E-04	0.066	16.173
WFTS-142	2.00	2.34	2.70	1.15	2	1.307	19.441	0.051	0.238	0.278	1.171	0.606	1.50	9.37	7.1E-06	4.3E-06	1.1E-04	0.066	16.167
WFTS-143	2.00	2.35	2.90	1.24	11	2.266	11.210	0.050	0.268	0.315	1.175	0.641	2.48	51.69	1.3E-05	8.4E-06	7.0E-04	0.680	10.337
WFTS-144	2.00	2.35	3.19	1.35	2	1.169	21.721	0.054	0.143	0.168	1.176	0.654	1.50	9.41	7.5E-06	4.9E-06	1.2E-04	0.070	17.464
WFTS-145	2.00	2.35	2.95	1.25	11	2.234	11.369	0.050	0.160	0.189	1.177	0.646	2.52	51.81	1.3E-05	8.5E-06	7.0E-04	0.682	10.254
WFTS-146	2.00	2.35	2.90	1.23	11	2.266	11.210	0.050	0.181	0.213	1.177	0.641	2.52	51.81	1.3E-05	8.4E-06	6.9E-04	0.681	10.188
WFTS-147	2.00	2.39	2.76	1.15	11	2.413	10.527	0.050	0.341	0.407	1.195	0.624	2.49	52.58	1.3E-05	8.3E-06	7.0E-04	0.700	10.046
WFTS-148	2.00	2.39	2.76	1.15	2	2.520	10.079	0.082	0.452	0.541	1.196	0.617	2.48	9.57	1.4E-05	8.6E-06	1.3E-04	0.133	9.975
WFTS-149	2.00	2.39	2.76	1.15	3	2.520	10.079	0.082	0.452	0.541	1.196	0.617	2.48	14.35	1.4E-05	8.6E-06	2.0E-04	0.200	9.976
WFTS-150	2.00	2.41	2.78	1.15	11	2.397	10.597	0.050	0.276	0.332	1.204	0.627	2.52	52.95	1.3E-05	8.4E-06	7.0E-04	0.706	9.939
WFTS-151	2.00	2.42	2.80	1.15	11	2.345	10.830	0.050	0.208	0.252	1.211	0.629	2.52	53.28	1.3E-05	8.3E-06	7.0E-04	0.699	9.970
WFTS-152	2.00	2.42	2.80	1.15	11	2.349	10.812	0.050	0.274	0.331	1.211	0.629	2.50	53.28	1.3E-05	8.3E-06	7.1E-04	0.700	10.072
WFTS-153	2.00	2.43	2.80	1.15	11	2.322	10.941	0.050	0.161	0.196	1.214	0.630	2.52	53.43	1.3E-05	8.2E-06	6.9E-04	0.696	9.977
WFTS-154	2.00	2.49	2.51	1.01	2	0.875	29.013	0.050	0.139	0.173	1.247	0.567	1.01	9.98	4.4E-06	2.5E-06	9.9E-05	0.044	22.537
WFTS-155	2.00	2.52	3.31	1.32	2	0.762	33.322	0.058	0.090	0.114	1.259	0.645	1.01	10.08	5.1E-06	3.3E-06	1.3E-04	0.051	25.605
WFTS-156	2.00	2.53	4.00	1.58	2	2.224	11.420	0.050	0.088	0.111	1.267	0.733	2.98	10.14	1.8E-05	1.3E-05	1.8E-04	0.180	9.841
WFTS-157	2.00	2.56	2.95	1.15	2	2.471	10.281	0.098	0.537	0.687	1.279	0.635	2.48	10.23	1.5E-05	9.3E-06	1.5E-04	0.149	10.230
WFTS-158	2.00	2.56	2.01	0.78	2	0.510	49.805	0.050	0.089	0.114	1.282	0.453	0.50	10.26	2.1E-06	9.3E-07	7.6E-05	0.021	36.120
WFTS-159	2.00	2.57	2.96	1.15	2	2.248	11.299	0.091	0.265	0.340	1.283	0.636	2.48	10.26	1.3E-05	8.5E-06	1.4E-04	0.137	10.235
WFTS-160	2.00	2.57	2.97	1.15	11	2.163	11.745	0.050	0.130	0.167	1.284	0.647	2.50	56.50	1.3E-05	8.3E-06	7.5E-04	0.725	10.379

TAG	D_o (mm)	P_l/D_o (-)	P_t/D_o (-)	P_t/P_l (-)	N_r (-)	F_p (mm)	FPI (in-1)	δ_f (mm)	Tanθ (-)	P_d (mm)	X_f(mm)	σ (-)	D_h (mm)	d (mm)	A_f (m^2)	A_c (m^2)	A_o (m^2)	V (cm^3)	A_o/V(cm^2/cm^3)
WFTS-161	2.00	2.57	2.97	1.15	2	0.810	31.361	0.059	0.233	0.300	1.285	0.615	1.00	10.28	4.8E-06	3.0E-06	1.2E-04	0.049	24.655
WFTS-162	2.00	2.58	3.03	1.18	4	2.532	10.031	0.096	0.644	0.831	1.289	0.644	2.48	20.62	1.5E-05	9.9E-06	3.3E-04	0.316	10.386
WFTS-163	2.00	2.60	3.01	1.15	2	2.173	11.692	0.054	0.213	0.277	1.302	0.651	2.50	10.42	1.3E-05	8.5E-06	1.4E-04	0.136	10.423
WFTS-164	2.00	2.63	3.03	1.15	2	0.792	32.069	0.050	0.230	0.302	1.313	0.628	1.00	10.51	4.8E-06	3.0E-06	1.3E-04	0.051	25.204
WFTS-165	2.00	2.63	3.98	1.51	2	2.403	10.571	0.063	0.371	0.487	1.313	0.729	3.01	10.51	1.9E-05	1.4E-05	1.9E-04	0.201	9.674
WFTS-166	2.00	2.63	2.17	0.83	2	0.528	48.119	0.091	0.171	0.225	1.315	0.447	0.50	10.52	2.3E-06	1.0E-06	8.5E-05	0.024	35.432
WFTS-167	2.00	2.63	3.04	1.15	11	2.151	11.810	0.051	0.246	0.324	1.315	0.655	2.48	57.87	1.3E-05	8.6E-06	8.0E-04	0.756	10.555
WFTS-168	2.00	2.63	3.04	1.15	11	2.151	11.810	0.051	0.246	0.324	1.315	0.655	2.48	57.87	1.3E-05	8.6E-06	8.0E-04	0.756	10.555
WFTS-169	2.00	2.63	3.04	1.15	2	0.792	32.069	0.054	0.127	0.168	1.317	0.626	1.01	10.54	4.8E-06	3.0E-06	1.3E-04	0.051	24.788
WFTS-170	2.00	2.64	3.05	1.15	2	0.792	32.069	0.050	0.266	0.350	1.319	0.629	0.99	10.55	4.8E-06	3.0E-06	1.3E-04	0.051	25.405
WFTS-171	2.00	2.64	4.00	1.52	2	2.258	11.249	0.055	0.202	0.266	1.319	0.732	2.98	10.55	1.8E-05	1.3E-05	1.9E-04	0.191	9.816
WFTS-172	2.00	2.64	3.41	1.29	11	2.532	10.031	0.050	0.305	0.403	1.321	0.693	3.00	58.14	1.7E-05	1.2E-05	9.3E-04	1.010	9.246
WFTS-173	2.00	2.69	3.11	1.15	11	2.103	12.078	0.050	0.143	0.193	1.345	0.662	2.51	59.20	1.3E-05	8.7E-06	8.2E-04	0.774	10.539
WFTS-174	2.00	2.71	3.13	1.15	2	0.782	32.476	0.058	0.207	0.281	1.354	0.629	0.99	10.83	4.9E-06	3.1E-06	1.4E-04	0.053	25.412
WFTS-175	2.00	2.73	3.15	1.15	2	1.265	20.082	0.073	0.372	0.508	1.364	0.643	1.51	10.91	8.0E-06	5.1E-06	1.5E-04	0.087	17.052
WFTS-176	2.00	2.73	3.16	1.15	2	0.814	31.208	0.052	0.395	0.540	1.367	0.640	0.99	10.94	5.1E-06	3.3E-06	1.5E-04	0.056	25.719
WFTS-177	2.00	2.76	3.41	1.24	11	2.476	10.257	0.050	0.188	0.259	1.379	0.693	3.02	60.68	1.7E-05	1.2E-05	9.4E-04	1.030	9.167
WFTS-178	2.00	2.78	4.00	1.44	2	1.086	23.389	0.053	0.218	0.302	1.388	0.713	1.51	11.11	8.7E-06	6.2E-06	1.8E-04	0.097	18.859
WFTS-179	2.00	2.80	1.70	0.61	2	0.635	39.992	0.052	0.227	0.318	1.402	0.378	0.50	11.22	2.2E-06	8.2E-07	7.3E-05	0.024	29.996
WFTS-180	2.00	2.84	1.98	0.70	2	0.528	48.119	0.052	0.107	0.152	1.422	0.445	0.50	11.38	2.1E-06	9.3E-07	8.4E-05	0.024	35.301
WFTS-181	2.00	2.91	3.36	1.15	2	2.498	10.167	0.089	0.227	0.330	1.456	0.678	2.98	11.65	1.7E-05	1.1E-05	1.8E-04	0.196	9.097
WFTS-182	2.00	2.92	3.27	1.12	2	1.183	21.465	0.078	0.233	0.340	1.460	0.649	1.49	11.68	7.7E-06	5.0E-06	1.6E-04	0.090	17.464
WFTS-183	2.00	3.02	3.21	1.06	2	1.152	22.056	0.054	0.119	0.180	1.512	0.656	1.49	12.10	7.4E-06	4.8E-06	1.6E-04	0.089	17.617
WFTS-184	2.00	3.04	2.97	0.98	11	2.131	11.920	0.050	0.135	0.206	1.522	0.647	2.50	66.95	1.3E-05	8.2E-06	8.8E-04	0.847	10.347
WFTS-185	2.00	3.05	4.00	1.31	2	1.813	14.010	0.053	0.111	0.169	1.524	0.728	2.50	12.19	1.5E-05	1.1E-05	2.1E-04	0.177	11.635
WFTS-186	2.00	3.08	3.56	1.15	2	1.906	13.324	0.057	0.101	0.155	1.542	0.698	2.50	12.34	1.4E-05	9.5E-06	1.9E-04	0.168	11.177
WFTS-187	2.00	3.14	3.62	1.15	2	0.748	33.942	0.059	0.204	0.321	1.569	0.667	1.00	12.55	5.4E-06	3.6E-06	1.8E-04	0.068	26.666
WFTS-188	2.00	3.14	3.33	1.06	2	0.762	33.322	0.062	0.088	0.137	1.571	0.643	1.00	12.57	5.1E-06	3.3E-06	1.6E-04	0.064	25.741
WFTS-189	2.00	3.15	1.70	0.54	2	0.635	39.992	0.052	0.210	0.331	1.574	0.379	0.50	12.59	2.2E-06	8.2E-07	8.2E-05	0.027	30.156
WFTS-190	2.00	3.17	3.66	1.15	2	1.910	13.296	0.051	0.165	0.262	1.585	0.708	2.52	12.68	1.4E-05	9.9E-06	2.0E-04	0.177	11.211
WFTS-191	2.00	3.18	3.67	1.15	11	2.413	10.527	0.050	0.378	0.601	1.590	0.712	2.97	69.94	1.8E-05	1.3E-05	1.2E-03	1.240	9.583
WFTS-192	2.00	3.23	3.73	1.15	2	2.264	11.220	0.059	0.113	0.182	1.616	0.713	2.98	12.93	1.7E-05	1.2E-05	2.1E-04	0.219	9.580
WFTS-193	2.00	3.25	3.75	1.15	2	1.855	13.695	0.059	0.132	0.214	1.623	0.710	2.48	12.98	1.4E-05	9.9E-06	2.1E-04	0.180	11.424
WFTS-194	2.00	3.25	3.75	1.15	2	1.855	13.695	0.059	0.132	0.214	1.623	0.710	2.48	12.98	1.4E-05	9.9E-06	2.1E-04	0.180	11.424
WFTS-195	2.00	3.25	3.75	1.15	2	1.855	13.695	0.059	0.132	0.214	1.623	0.710	2.48	12.98	1.4E-05	9.9E-06	2.1E-04	0.180	11.424
WFTS-196	2.00	3.25	3.75	1.15	3	2.375	10.694	0.084	0.800	1.299	1.625	0.708	2.50	19.50	1.8E-05	1.3E-05	3.9E-04	0.348	11.329
WFTS-197	2.00	3.26	3.76	1.15	11	1.885	13.478	0.050	0.224	0.364	1.628	0.715	2.50	71.64	1.4E-05	1.0E-05	1.2E-03	1.020	11.426
WFTS-198	2.00	3.26	3.76	1.15	3	2.375	10.694	0.084	0.802	1.306	1.629	0.708	2.50	19.55	1.8E-05	1.3E-05	4.0E-04	0.349	11.337
WFTS-199	2.00	3.26	3.27	1.00	2	1.183	21.465	0.078	0.234	0.382	1.632	0.649	1.49	13.05	7.7E-06	5.0E-06	1.8E-04	0.101	17.455
WFTS-200	2.00	3.28	3.79	1.15	2	2.417	10.510	0.088	0.366	0.599	1.639	0.709	2.99	13.11	1.8E-05	1.3E-05	2.3E-04	0.240	9.473
WFTS-201	2.00	3.28	3.79	1.15	2	2.480	10.240	0.094	0.460	0.754	1.641	0.708	2.97	13.13	1.9E-05	1.3E-05	2.4E-04	0.247	9.529
WFTS-202	2.00	3.30	3.81	1.15	11	2.294	11.074	0.052	0.197	0.325	1.651	0.721	3.02	72.64	1.8E-05	1.3E-05	1.2E-03	1.270	9.553
WFTS-203	2.00	3.32	3.33	1.00	11	2.536	10.016	0.050	0.310	0.514	1.660	0.686	3.03	73.04	1.7E-05	1.2E-05	1.1E-03	1.230	9.063
WFTS-204	2.00	3.33	3.85	1.15	2	2.417	10.510	0.090	0.416	0.693	1.667	0.713	2.97	13.34	1.9E-05	1.3E-05	2.4E-04	0.248	9.591
WFTS-205	2.00	3.34	3.85	1.15	11	1.845	13.768	0.051	0.092	0.153	1.668	0.720	2.52	73.39	1.4E-05	1.0E-05	1.2E-03	1.040	11.410
WFTS-206	2.00	3.34	2.98	0.89	2	2.137	11.887	0.064	0.235	0.393	1.669	0.645	2.48	13.36	1.3E-05	8.2E-06	1.8E-04	0.170	10.387
WFTS-207	2.00	3.34	2.98	0.89	2	2.137	11.887	0.070	0.188	0.315	1.672	0.643	2.50	13.38	1.3E-05	8.2E-06	1.8E-04	0.171	10.297
WFTS-208	2.00	3.35	4.00	1.20	2	1.082	23.475	0.053	0.207	0.347	1.673	0.713	1.51	13.39	8.7E-06	6.2E-06	2.2E-04	0.116	18.886
WFTS-209	2.00	3.37	3.89	1.15	11	2.250	11.289	0.050	0.183	0.308	1.683	0.726	3.00	74.05	1.8E-05	1.3E-05	1.3E-03	1.300	9.668
WFTS-210	2.00	3.39	3.92	1.15	11	1.837	13.828	0.050	0.157	0.266	1.697	0.725	2.52	74.67	1.4E-05	1.0E-05	1.2E-03	1.080	11.519

TAG	D_o (mm)	P_l/D_o (-)	P_t/D_o (-)	P_t/P_l (-)	N_r (-)	F_p (mm)	FPI (in-1)	δ_f (mm)	Tanθ (-)	P_d (mm)	X_f(mm)	σ (-)	D_h (mm)	d (mm)	A_f (m^2)	A_c (m^2)	A_o (m^2)	V (cm^3)	A_o/V(cm^2/cm^3)
WFTS-211	2.00	3.84	1.72	0.45	2	0.635	39.992	0.052	0.208	0.399	1.918	0.383	0.50	15.34	2.2E-06	8.3E-07	1.0E-04	0.033	30.516
WFTS-212	2.00	3.40	3.93	1.15	11	1.849	13.739	0.050	0.190	0.324	1.700	0.725	2.52	74.81	1.5E-05	1.1E-05	1.3E-03	1.090	11.509
WFTS-213	2.00	3.40	3.93	1.15	11	1.831	13.873	0.050	0.114	0.194	1.700	0.725	2.52	74.81	1.4E-05	1.0E-05	1.2E-03	1.080	11.492
WFTS-214	2.00	3.41	3.93	1.15	2	1.906	13.324	0.057	0.326	0.555	1.704	0.724	2.51	13.63	1.5E-05	1.1E-05	2.4E-04	0.204	11.524
WFTS-215	2.00	3.42	3.94	1.15	2	2.288	11.103	0.082	0.226	0.386	1.708	0.720	3.01	13.66	1.8E-05	1.3E-05	2.4E-04	0.247	9.565
WFTS-216	2.00	3.42	3.94	1.15	2	2.288	11.103	0.082	0.226	0.386	1.708	0.720	3.01	13.66	1.8E-05	1.3E-05	2.4E-04	0.247	9.565
WFTS-217	2.00	3.42	3.94	1.15	2	2.288	11.103	0.082	0.226	0.386	1.708	0.720	3.01	13.66	1.8E-05	1.3E-05	2.4E-04	0.247	9.565
WFTS-218	2.00	3.42	3.95	1.15	2	1.924	13.200	0.082	0.366	0.625	1.710	0.715	2.48	13.68	1.5E-05	1.1E-05	2.4E-04	0.208	11.537
WFTS-219	2.00	3.43	4.00	1.17	2	1.082	23.475	0.066	0.112	0.192	1.714	0.704	1.51	13.71	8.7E-06	6.1E-06	2.2E-04	0.119	18.610
WFTS-220	2.00	3.44	3.97	1.15	11	2.228	11.400	0.055	0.137	0.235	1.719	0.730	3.02	75.62	1.8E-05	1.3E-05	1.3E-03	1.340	9.662
WFTS-221	2.00	3.44	3.97	1.15	11	2.228	11.400	0.055	0.137	0.235	1.719	0.730	3.02	75.62	1.8E-05	1.3E-05	1.3E-03	1.340	9.662
WFTS-222	2.00	3.44	3.97	1.15	11	2.232	11.379	0.053	0.143	0.245	1.719	0.730	3.03	75.62	1.8E-05	1.3E-05	1.3E-03	1.340	9.654
WFTS-223	2.00	3.44	3.97	1.15	2	2.234	11.369	0.057	0.160	0.275	1.721	0.729	3.02	13.77	1.8E-05	1.3E-05	2.4E-04	0.244	9.664
WFTS-224	2.00	3.44	3.97	1.15	2	2.234	11.369	0.057	0.160	0.275	1.721	0.729	3.02	13.77	1.8E-05	1.3E-05	2.4E-04	0.244	9.664
WFTS-225	2.00	3.44	3.98	1.15	11	2.234	11.369	0.050	0.231	0.398	1.722	0.732	2.99	75.76	1.8E-05	1.3E-05	1.3E-03	1.350	9.782
WFTS-226	2.00	3.45	3.98	1.15	10	1.815	13.994	0.053	0.097	0.167	1.723	0.727	2.52	68.91	1.4E-05	1.1E-05	1.2E-03	0.995	11.549
WFTS-227	2.00	3.45	3.98	1.15	10	1.811	14.025	0.050	0.091	0.157	1.723	0.728	2.52	68.91	1.4E-05	1.1E-05	1.2E-03	0.993	11.569
WFTS-228	2.00	3.45	3.98	1.15	12	1.817	13.979	0.050	0.097	0.167	1.723	0.728	2.52	82.70	1.5E-05	1.1E-05	1.4E-03	1.200	11.540
WFTS-229	2.00	3.45	3.98	1.15	2	1.906	13.324	0.082	0.330	0.570	1.725	0.717	2.49	13.80	1.5E-05	1.1E-05	2.4E-04	0.210	11.511
WFTS-230	2.00	3.45	3.98	1.15	2	1.970	12.894	0.082	0.424	0.732	1.725	0.718	2.50	13.80	1.6E-05	1.1E-05	2.5E-04	0.217	11.494
WFTS-231	2.00	3.45	3.98	1.15	2	1.986	12.791	0.082	0.463	0.798	1.725	0.718	2.48	13.80	1.6E-05	1.1E-05	2.5E-04	0.218	11.558
WFTS-232	2.00	3.45	3.98	1.15	11	2.226	11.410	0.052	0.149	0.258	1.725	0.732	3.02	75.90	1.8E-05	1.3E-05	1.3E-03	1.350	9.681
WFTS-233	2.00	3.45	3.98	1.15	11	2.226	11.410	0.052	0.149	0.258	1.725	0.732	3.02	75.90	1.8E-05	1.3E-05	1.3E-03	1.350	9.681
WFTS-234	2.00	3.45	3.98	1.15	11	2.226	11.410	0.052	0.149	0.258	1.725	0.732	3.02	75.90	1.8E-05	1.3E-05	1.3E-03	1.350	9.681
WFTS-235	2.00	3.45	3.98	1.15	11	2.226	11.410	0.052	0.149	0.258	1.725	0.732	3.02	75.90	1.8E-05	1.3E-05	1.3E-03	1.350	9.681
WFTS-236	2.00	3.52	2.51	0.71	2	0.879	28.882	0.050	0.103	0.181	1.762	0.568	1.01	14.10	4.4E-06	2.5E-06	1.4E-04	0.062	22.507
WFTS-237	2.00	3.66	3.38	0.92	2	0.776	32.726	0.081	0.088	0.160	1.829	0.631	0.99	14.63	5.3E-06	3.3E-06	2.0E-04	0.077	25.363
WFTS-238	2.00	3.66	4.00	1.09	2	2.230	11.390	0.052	0.202	0.369	1.829	0.733	3.02	14.63	1.8E-05	1.3E-05	2.5E-04	0.261	9.706
WFTS-239	2.00	3.73	4.00	1.07	2	1.789	14.196	0.053	0.120	0.224	1.866	0.728	2.49	14.93	1.4E-05	1.0E-05	2.5E-04	0.214	11.686
WFTS-240	2.00	3.83	4.00	1.04	2	2.226	11.410	0.055	0.182	0.349	1.915	0.732	3.03	15.32	1.8E-05	1.3E-05	2.6E-04	0.273	9.664
WFTS-241	2.00	3.83	4.00	1.04	2	2.226	11.410	0.055	0.182	0.349	1.915	0.732	3.03	15.32	1.8E-05	1.3E-05	2.6E-04	0.273	9.664
WFTS-242	2.00	3.83	4.00	1.04	2	2.226	11.410	0.055	0.182	0.349	1.915	0.732	3.03	15.32	1.8E-05	1.3E-05	2.6E-04	0.273	9.664
WFTS-243	2.00	3.90	3.33	0.85	2	0.770	32.979	0.059	0.090	0.176	1.949	0.645	1.01	15.59	5.1E-06	3.3E-06	2.1E-04	0.080	25.612
WFTS-244	2.00	3.93	3.48	0.89	2	1.908	13.310	0.054	0.112	0.219	1.964	0.693	2.51	15.71	1.3E-05	9.2E-06	2.3E-04	0.209	11.056
WFTS-245	2.00	3.95	2.51	0.64	2	0.879	28.882	0.050	0.092	0.181	1.974	0.567	1.01	15.80	4.4E-06	2.5E-06	1.6E-04	0.070	22.522
WFTS-246	2.00	3.97	3.48	0.88	2	1.908	13.310	0.055	0.118	0.234	1.985	0.692	2.50	15.88	1.3E-05	9.2E-06	2.3E-04	0.211	11.056
WFTS-247	2.00	4.00	4.00	1.00	2	2.161	11.756	0.050	0.089	0.178	2.000	0.733	2.99	16.00	1.7E-05	1.3E-05	2.7E-04	0.277	9.796
WFTS-248	3.00	1.44	2.37	1.64	2	1.392	18.248	0.087	0.337	0.365	1.083	0.541	1.49	8.66	9.9E-06	5.4E-06	1.3E-04	0.086	14.550
WFTS-249	3.00	1.64	1.82	1.11	2	0.508	50.000	0.054	0.155	0.191	1.230	0.403	0.50	9.84	2.8E-06	1.1E-06	8.9E-05	0.027	32.495
WFTS-250	3.00	2.06	2.38	1.15	2	1.446	17.572	0.076	0.398	0.614	1.544	0.549	1.51	12.35	1.0E-05	5.7E-06	1.9E-04	0.127	14.529
WFTS-251	3.00	2.07	2.39	1.15	3	0.889	28.560	0.067	0.291	0.450	1.550	0.537	0.99	18.61	6.4E-06	3.4E-06	2.6E-04	0.118	21.651
WFTS-252	3.00	2.07	2.39	1.15	3	0.953	26.655	0.065	0.467	0.724	1.550	0.542	1.01	18.61	6.8E-06	3.7E-06	2.7E-04	0.127	21.455
WFTS-253	3.00	2.11	1.85	0.88	2	0.532	47.759	0.050	0.238	0.376	1.583	0.415	0.50	12.66	3.0E-06	1.2E-06	1.2E-04	0.037	33.294
WFTS-254	3.00	2.15	2.49	1.15	11	2.427	10.466	0.050	0.330	0.533	1.615	0.585	2.51	71.06	1.8E-05	1.1E-05	1.2E-03	1.290	9.321
WFTS-255	3.00	2.19	2.53	1.15	11	2.300	11.045	0.050	0.145	0.238	1.641	0.591	2.52	72.19	1.7E-05	1.0E-05	1.2E-03	1.260	9.392
WFTS-256	3.00	2.19	2.53	1.15	11	2.300	11.045	0.050	0.145	0.238	1.641	0.591	2.52	72.19	1.7E-05	1.0E-05	1.2E-03	1.260	9.392
WFTS-257	3.00	2.23	2.58	1.15	2	2.429	10.458	0.100	0.381	0.638	1.675	0.587	2.51	13.40	1.9E-05	1.1E-05	2.4E-04	0.252	9.354
WFTS-258	3.00	2.33	2.69	1.15	3	0.844	30.106	0.069	0.291	0.510	1.750	0.578	1.00	21.01	6.8E-06	3.9E-06	3.3E-04	0.143	23.137
WFTS-259	3.00	2.41	4.00	1.66	2	2.161	11.756	0.071	0.187	0.337	1.804	0.725	2.99	14.44	2.6E-05	1.9E-05	3.6E-04	0.374	9.701
WFTS-260	3.00	2.46	4.00	1.63	2	1.779	14.276	0.070	0.208	0.384	1.843	0.720	2.49	14.74	2.1E-05	1.5E-05	3.7E-04	0.315	11.588

TAG	D_o (mm)	P_l/D_o (-)	P_t/D_o (-)	P_t/P_l (-)	N_r (-)	F_p (mm)	FPI (in-1)	δ_f (mm)	Tanθ (-)	P_d (mm)	X_f(mm)	σ (-)	D_h (mm)	d (mm)	A_f (m^2)	A_c (m^2)	A_o (m^2)	V (cm^3)	A_o/V(cm^2/cm^3)
WFTS-261	3.00	2.48	4.00	1.61	2	2.161	11.756	0.056	0.183	0.340	1.859	0.730	3.01	14.87	2.6E-05	1.9E-05	3.7E-04	0.386	9.694
WFTS-262	3.00	2.49	2.88	1.15	11	2.540	10.000	0.050	0.165	0.308	1.870	0.640	3.00	82.27	2.2E-05	1.4E-05	1.5E-03	1.800	8.537
WFTS-263	3.00	2.51	2.90	1.15	11	2.540	10.000	0.050	0.191	0.360	1.883	0.642	3.00	82.84	2.2E-05	1.4E-05	1.6E-03	1.830	8.562
WFTS-264	3.00	2.51	2.90	1.15	11	2.540	10.000	0.050	0.227	0.426	1.883	0.642	2.98	82.84	2.2E-05	1.4E-05	1.6E-03	1.830	8.613
WFTS-265	3.00	2.51	2.90	1.15	11	2.540	10.000	0.050	0.144	0.272	1.884	0.642	3.02	82.91	2.2E-05	1.4E-05	1.6E-03	1.830	8.507
WFTS-266	3.00	2.51	2.90	1.15	11	2.540	10.000	0.050	0.250	0.471	1.884	0.642	2.97	82.91	2.2E-05	1.4E-05	1.6E-03	1.830	8.650
WFTS-267	3.00	2.53	2.92	1.15	11	2.032	12.503	0.050	0.088	0.166	1.894	0.641	2.51	83.34	1.8E-05	1.1E-05	1.5E-03	1.480	10.216
WFTS-268	3.00	2.57	3.75	1.46	2	1.785	14.228	0.051	0.092	0.177	1.927	0.712	2.50	15.42	2.0E-05	1.4E-05	3.5E-04	0.310	11.390
WFTS-269	3.00	2.58	2.98	1.15	11	2.492	10.191	0.050	0.143	0.277	1.934	0.651	3.02	85.11	2.2E-05	1.5E-05	1.6E-03	1.890	8.614
WFTS-270	3.00	2.63	1.82	0.69	2	0.572	44.440	0.068	0.149	0.294	1.970	0.397	0.50	15.76	3.1E-06	1.2E-06	1.6E-04	0.049	31.497
WFTS-271	3.00	2.63	3.04	1.15	11	2.413	10.527	0.050	0.118	0.232	1.975	0.657	2.98	86.88	2.2E-05	1.5E-05	1.7E-03	1.910	8.808
WFTS-272	3.00	2.66	3.07	1.15	11	2.413	10.527	0.050	0.188	0.374	1.994	0.660	2.97	87.73	2.2E-05	1.5E-05	1.7E-03	1.950	8.878
WFTS-273	3.00	2.68	3.09	1.15	2	2.014	12.614	0.091	0.231	0.463	2.007	0.646	2.48	16.06	1.9E-05	1.2E-05	3.1E-04	0.300	10.435
WFTS-274	3.00	2.69	3.11	1.15	11	2.411	10.535	0.050	0.105	0.212	2.020	0.664	3.03	88.87	2.3E-05	1.5E-05	1.8E-03	2.000	8.783
WFTS-275	3.00	2.82	3.26	1.15	11	2.341	10.848	0.050	0.094	0.199	2.117	0.678	3.03	93.13	2.3E-05	1.6E-05	1.9E-03	2.130	8.962
WFTS-276	3.00	2.84	3.91	1.38	2	2.169	11.713	0.057	0.140	0.297	2.129	0.725	3.03	17.03	2.5E-05	1.8E-05	4.2E-04	0.433	9.572
WFTS-277	3.00	2.86	3.30	1.15	2	0.746	34.032	0.052	0.101	0.217	2.142	0.648	1.01	17.14	7.4E-06	4.8E-06	3.3E-04	0.127	25.723
WFTS-278	3.00	2.96	3.42	1.15	2	0.752	33.762	0.071	0.103	0.228	2.218	0.640	1.00	17.75	7.7E-06	4.9E-06	3.5E-04	0.137	25.586
WFTS-279	3.00	2.96	3.42	1.15	2	0.752	33.762	0.071	0.103	0.228	2.218	0.640	1.00	17.75	7.7E-06	4.9E-06	3.5E-04	0.137	25.586
WFTS-280	3.00	2.97	1.78	0.60	2	0.572	44.440	0.054	0.092	0.205	2.228	0.398	0.50	17.82	3.1E-06	1.2E-06	1.7E-04	0.055	31.719
WFTS-281	3.00	2.97	3.43	1.15	11	2.274	11.171	0.050	0.100	0.223	2.231	0.693	3.03	98.17	2.3E-05	1.6E-05	2.1E-03	2.300	9.163
WFTS-282	3.00	2.97	3.43	1.15	11	2.278	11.151	0.050	0.132	0.295	2.231	0.693	3.02	98.17	2.4E-05	1.6E-05	2.1E-03	2.300	9.179
WFTS-283	3.00	2.99	3.45	1.15	2	1.118	22.723	0.078	0.115	0.257	2.241	0.660	1.50	17.93	1.2E-05	7.6E-06	3.7E-04	0.207	17.581
WFTS-284	3.00	3.00	3.47	1.15	2	1.144	22.211	0.065	0.280	0.632	2.254	0.671	1.51	18.03	1.2E-05	8.0E-06	3.8E-04	0.215	17.741
WFTS-285	3.00	3.17	3.66	1.15	2	2.224	11.420	0.087	0.193	0.458	2.379	0.699	2.97	19.04	2.4E-05	1.7E-05	4.4E-04	0.465	9.404
WFTS-286	3.00	3.17	3.66	1.15	2	2.224	11.420	0.087	0.193	0.458	2.379	0.699	2.97	19.04	2.4E-05	1.7E-05	4.4E-04	0.465	9.404
WFTS-287	3.00	3.17	3.66	1.15	2	2.224	11.420	0.087	0.193	0.458	2.379	0.699	2.97	19.04	2.4E-05	1.7E-05	4.4E-04	0.465	9.404
WFTS-288	3.00	3.17	2.70	0.85	2	0.818	31.056	0.061	0.088	0.208	2.381	0.583	1.00	19.05	6.6E-06	3.9E-06	3.0E-04	0.126	23.430
WFTS-289	3.00	3.18	3.67	1.15	4	1.108	22.926	0.066	0.276	0.658	2.386	0.685	1.50	38.17	1.2E-05	8.4E-06	8.5E-04	0.466	18.311
WFTS-290	3.00	3.19	3.69	1.15	4	1.096	23.177	0.082	0.106	0.254	2.396	0.674	1.50	38.33	1.2E-05	8.2E-06	8.3E-04	0.465	17.951
WFTS-291	3.00	3.22	3.72	1.15	2	1.813	14.010	0.068	0.189	0.457	2.417	0.704	2.48	19.33	2.0E-05	1.4E-05	4.4E-04	0.391	11.332
WFTS-292	3.00	3.23	3.73	1.15	2	1.823	13.934	0.077	0.206	0.498	2.420	0.701	2.48	19.36	2.0E-05	1.4E-05	4.5E-04	0.394	11.304
WFTS-293	3.00	3.27	3.78	1.15	11	2.159	11.767	0.050	0.153	0.375	2.452	0.718	2.99	107.89	2.4E-05	1.8E-05	2.5E-03	2.640	9.605
WFTS-294	3.00	3.31	3.54	1.07	2	1.120	22.683	0.076	0.162	0.402	2.486	0.669	1.51	19.89	1.2E-05	8.0E-06	4.2E-04	0.237	17.715
WFTS-295	3.00	3.33	3.84	1.15	11	2.159	11.767	0.050	0.118	0.294	2.497	0.723	3.03	109.88	2.5E-05	1.8E-05	2.6E-03	2.740	9.556
WFTS-296	3.00	3.38	3.90	1.15	2	1.783	14.244	0.067	0.110	0.280	2.536	0.716	2.52	20.29	2.1E-05	1.5E-05	4.8E-04	0.424	11.376
WFTS-297	3.00	3.39	3.91	1.15	11	2.159	11.767	0.050	0.176	0.447	2.542	0.727	3.02	111.86	2.5E-05	1.8E-05	2.7E-03	2.840	9.621
WFTS-298	3.00	3.41	3.94	1.15	2	2.099	12.101	0.050	0.093	0.239	2.558	0.728	2.98	20.47	2.5E-05	1.8E-05	5.0E-04	0.508	9.771
WFTS-299	3.00	3.44	3.97	1.15	11	2.095	12.124	0.050	0.106	0.273	2.581	0.730	2.98	113.57	2.5E-05	1.8E-05	2.8E-03	2.840	9.795
WFTS-300	3.00	3.44	3.97	1.15	11	2.159	11.767	0.050	0.235	0.607	2.581	0.731	3.01	113.57	2.6E-05	1.9E-05	2.8E-03	2.920	9.719
WFTS-301	3.00	3.49	3.98	1.14	2	1.779	14.276	0.070	0.112	0.292	2.617	0.719	2.52	20.94	2.1E-05	1.5E-05	5.1E-04	0.445	11.396
WFTS-302	3.00	3.78	1.90	0.50	2	0.574	44.286	0.078	0.177	0.501	2.839	0.410	0.50	22.71	3.3E-06	1.3E-06	2.4E-04	0.074	32.806
WFTS-303	3.00	3.83	1.83	0.48	2	0.572	44.440	0.050	0.139	0.399	2.873	0.412	0.50	22.98	3.1E-06	1.3E-06	2.4E-04	0.072	32.725
WFTS-304	3.00	3.95	3.80	0.96	2	1.054	24.094	0.054	0.089	0.264	2.964	0.699	1.49	23.71	1.2E-05	8.4E-06	5.3E-04	0.285	18.712
WFTS-305	4.00	1.73	2.00	1.15	2	0.528	48.119	0.100	0.303	0.525	1.734	0.406	0.50	13.87	4.2E-06	1.7E-06	1.9E-04	0.059	32.469
WFTS-306	4.00	1.75	2.39	1.37	2	1.303	19.501	0.098	0.177	0.310	1.750	0.538	1.49	14.00	1.3E-05	6.7E-06	2.5E-04	0.175	14.404
WFTS-307	4.00	1.75	2.39	1.37	2	1.303	19.501	0.098	0.177	0.310	1.750	0.538	1.49	14.00	1.3E-05	6.7E-06	2.5E-04	0.175	14.404
WFTS-308	4.00	1.98	2.28	1.15	11	2.528	10.047	0.051	0.430	0.851	1.977	0.551	2.50	86.98	2.3E-05	1.3E-05	1.8E-03	2.010	8.818
WFTS-309	4.00	2.25	2.60	1.15	2	0.842	30.177	0.095	0.118	0.267	2.254	0.546	1.00	18.03	8.8E-06	4.8E-06	3.5E-04	0.158	21.913
WFTS-310	4.00	2.35	2.71	1.15	11	2.540	10.000	0.050	0.259	0.609	2.351	0.619	2.97	103.45	2.8E-05	1.7E-05	2.4E-03	2.850	8.339

TAG	D_o (mm)	P_l/D_o (-)	P_t/D_o (-)	P_t/P_l (-)	N_r (-)	F_p (mm)	FPI (in-1)	δ_f (mm)	$\tan\theta$ (-)	P_d (mm)	X_f(mm)	σ (-)	D_h (mm)	d (mm)	A_f (m^2)	A_c (m^2)	A_o (m^2)	V (cm^3)	A_o/V(cm^2/cm^3)
WFTS-311	4.00	2.35	2.72	1.15	3	1.271	19.989	0.100	0.285	0.670	2.353	0.582	1.50	28.24	1.4E-05	8.0E-06	6.0E-04	0.390	15.487
WFTS-312	4.00	2.36	2.72	1.15	2	1.271	19.989	0.100	0.285	0.671	2.358	0.583	1.51	18.86	1.4E-05	8.1E-06	4.0E-04	0.261	15.490
WFTS-313	4.00	2.43	2.80	1.15	4	1.271	19.989	0.100	0.380	0.923	2.426	0.593	1.49	38.82	1.4E-05	8.4E-06	8.8E-04	0.553	15.958
WFTS-314	4.00	2.56	2.95	1.15	2	0.780	32.559	0.067	0.095	0.243	2.558	0.605	1.01	20.46	9.2E-06	5.6E-06	4.5E-04	0.189	24.025
WFTS-315	4.00	2.59	2.99	1.15	2	0.762	33.322	0.054	0.088	0.229	2.592	0.619	1.01	20.74	9.1E-06	5.7E-06	4.7E-04	0.189	24.614
WFTS-316	4.00	2.61	1.87	0.72	2	0.538	47.230	0.059	0.093	0.244	2.608	0.413	0.50	20.86	4.0E-06	1.7E-06	2.7E-04	0.084	32.759
WFTS-317	4.00	2.76	3.19	1.15	2	0.764	33.236	0.067	0.119	0.329	2.762	0.626	1.01	22.09	9.8E-06	6.1E-06	5.4E-04	0.215	24.819
WFTS-318	4.00	2.94	3.39	1.15	2	2.224	11.420	0.064	0.088	0.257	2.938	0.685	3.02	23.51	3.0E-05	2.1E-05	6.4E-04	0.710	9.080
WFTS-319	4.00	2.97	3.43	1.15	2	1.813	14.010	0.050	0.088	0.260	2.973	0.689	2.51	23.78	2.5E-05	1.7E-05	6.5E-04	0.592	10.970
WFTS-320	4.00	3.06	2.97	0.97	2	0.792	32.069	0.075	0.091	0.279	3.057	0.601	1.00	24.45	9.4E-06	5.7E-06	5.5E-04	0.230	23.946
WFTS-321	4.00	3.14	4.00	1.27	11	2.057	12.346	0.050	0.088	0.274	3.137	0.732	3.00	138.03	3.3E-05	2.4E-05	4.4E-03	4.540	9.759
WFTS-322	4.00	3.18	3.67	1.15	11	1.779	14.276	0.051	0.106	0.336	3.177	0.707	2.52	139.78	2.6E-05	1.8E-05	4.1E-03	3.650	11.197
WFTS-323	4.00	3.18	3.67	1.15	2	2.121	11.976	0.068	0.088	0.278	3.177	0.704	2.97	25.42	3.1E-05	2.2E-05	7.5E-04	0.791	9.481
WFTS-324	4.00	3.18	4.00	1.26	2	2.065	12.298	0.050	0.088	0.278	3.177	0.732	3.01	25.42	3.3E-05	2.4E-05	8.2E-04	0.840	9.723
WFTS-325	4.00	3.19	2.46	0.77	2	0.862	29.481	0.065	0.111	0.354	3.186	0.549	1.00	25.48	8.5E-06	4.7E-06	4.7E-04	0.216	21.942
WFTS-326	4.00	3.21	3.70	1.15	11	1.781	14.260	0.050	0.181	0.580	3.207	0.709	2.51	141.11	2.6E-05	1.9E-05	4.2E-03	3.720	11.299
WFTS-327	4.00	3.21	3.71	1.15	2	2.113	12.021	0.069	0.088	0.281	3.213	0.707	2.97	25.71	3.1E-05	2.2E-05	7.7E-04	0.806	9.513
WFTS-328	4.00	3.21	3.71	1.15	2	2.113	12.021	0.069	0.088	0.281	3.213	0.707	2.97	25.71	3.1E-05	2.2E-05	7.7E-04	0.806	9.513
WFTS-329	4.00	3.21	3.71	1.15	2	2.113	12.021	0.069	0.088	0.281	3.213	0.707	2.97	25.71	3.1E-05	2.2E-05	7.7E-04	0.806	9.513
WFTS-330	4.00	3.21	3.71	1.15	2	2.113	12.021	0.069	0.088	0.281	3.213	0.707	2.97	25.71	3.1E-05	2.2E-05	7.7E-04	0.806	9.513
WFTS-331	4.00	3.23	3.73	1.15	2	1.779	14.276	0.071	0.088	0.285	3.229	0.702	2.51	25.83	2.7E-05	1.9E-05	7.7E-04	0.685	11.175
WFTS-332	4.00	3.24	3.74	1.15	3	0.750	33.852	0.094	0.120	0.388	3.239	0.641	1.00	38.87	1.1E-05	7.2E-06	1.1E-03	0.436	25.672
WFTS-333	4.00	3.24	3.74	1.15	3	0.750	33.852	0.094	0.120	0.388	3.239	0.641	1.00	38.87	1.1E-05	7.2E-06	1.1E-03	0.436	25.672
WFTS-334	4.00	3.25	3.75	1.15	11	1.761	14.420	0.050	0.088	0.284	3.248	0.713	2.52	142.90	2.6E-05	1.9E-05	4.3E-03	3.780	11.290
WFTS-335	4.00	3.25	3.75	1.15	11	1.761	14.420	0.050	0.088	0.284	3.248	0.713	2.52	142.90	2.6E-05	1.9E-05	4.3E-03	3.780	11.290
WFTS-336	4.00	3.25	3.75	1.15	2	1.070	23.736	0.083	0.094	0.306	3.250	0.677	1.49	26.00	1.6E-05	1.1E-05	7.6E-04	0.418	18.158
WFTS-337	4.00	3.25	1.77	0.54	2	0.585	43.384	0.063	0.088	0.287	3.253	0.388	0.50	26.02	4.1E-06	1.6E-06	3.3E-04	0.108	30.830
WFTS-338	4.00	3.30	3.81	1.15	2	2.097	12.112	0.052	0.088	0.289	3.297	0.719	3.00	26.38	3.2E-05	2.3E-05	8.1E-04	0.842	9.585
WFTS-339	4.00	3.30	3.81	1.15	2	0.510	49.805	0.095	0.804	2.653	3.300	0.600	0.50	26.40	7.8E-06	4.7E-06	9.8E-04	0.205	47.684
WFTS-340	4.00	3.31	4.00	1.21	2	2.065	12.298	0.050	0.088	0.289	3.307	0.732	3.01	26.45	3.3E-05	2.4E-05	8.5E-04	0.874	9.723
WFTS-341	4.00	3.36	3.87	1.15	11	2.097	12.112	0.050	0.107	0.358	3.355	0.724	3.02	147.64	3.3E-05	2.4E-05	4.6E-03	4.800	9.601
WFTS-342	4.00	3.37	3.89	1.15	3	1.070	23.736	0.057	0.241	0.812	3.366	0.704	1.51	40.39	1.7E-05	1.2E-05	1.3E-03	0.672	18.641
WFTS-343	4.00	3.37	3.89	1.15	11	2.099	12.101	0.050	0.099	0.332	3.370	0.725	3.03	148.30	3.3E-05	2.4E-05	4.6E-03	4.850	9.585
WFTS-344	4.00	3.37	3.89	1.15	13	0.508	50.000	0.095	0.814	2.746	3.373	0.605	0.50	175.38	7.9E-06	4.8E-06	6.7E-03	1.390	48.220
WFTS-345	4.00	3.42	3.95	1.15	11	2.097	12.112	0.050	0.130	0.446	3.424	0.729	3.03	150.66	3.3E-05	2.4E-05	4.8E-03	5.000	9.626
WFTS-346	4.00	3.42	3.95	1.15	11	2.097	12.112	0.050	0.133	0.456	3.424	0.729	3.03	150.66	3.3E-05	2.4E-05	4.8E-03	5.000	9.629
WFTS-347	4.00	3.42	3.95	1.15	11	2.105	12.067	0.050	0.168	0.577	3.424	0.729	3.03	150.66	3.3E-05	2.4E-05	4.8E-03	5.020	9.643
WFTS-348	4.00	3.43	3.96	1.15	11	2.097	12.112	0.050	0.148	0.507	3.433	0.730	3.03	151.04	3.3E-05	2.4E-05	4.9E-03	5.020	9.648
WFTS-349	4.00	3.43	3.96	1.15	11	2.109	12.044	0.050	0.177	0.608	3.433	0.730	3.03	151.04	3.3E-05	2.4E-05	4.9E-03	5.050	9.639
WFTS-350	4.00	3.44	3.97	1.15	11	2.127	11.943	0.050	0.251	0.862	3.437	0.730	3.01	151.23	3.4E-05	2.5E-05	5.0E-03	5.110	9.699
WFTS-351	4.00	3.44	3.97	1.15	11	2.121	11.976	0.050	0.224	0.772	3.441	0.731	3.02	151.42	3.4E-05	2.5E-05	4.9E-03	5.100	9.670
WFTS-352	4.00	3.45	3.98	1.15	11	2.113	12.021	0.050	0.202	0.695	3.450	0.731	3.03	151.80	3.4E-05	2.5E-05	4.9E-03	5.110	9.662
WFTS-353	4.00	3.68	2.51	0.68	11	0.554	45.874	0.065	0.760	2.796	3.680	0.531	0.50	161.92	5.6E-06	3.0E-06	3.8E-03	0.901	42.264
WFTS-354	4.00	3.70	2.47	0.67	2	0.877	28.948	0.070	0.088	0.324	3.702	0.548	1.01	29.61	8.7E-06	4.8E-06	5.6E-04	0.257	21.705
WFTS-355	4.00	3.74	4.00	1.07	2	2.065	12.298	0.050	0.088	0.327	3.737	0.732	3.01	29.89	3.3E-05	2.4E-05	9.6E-04	0.988	9.723
WFTS-356	4.00	3.90	3.38	0.87	3	1.084	23.432	0.050	0.091	0.355	3.898	0.672	1.49	46.77	1.5E-05	9.9E-06	1.2E-03	0.686	17.991
WFTS-357	4.00	3.93	3.06	0.78	2	0.774	32.809	0.059	0.097	0.381	3.927	0.622	1.00	31.42	9.5E-06	5.9E-06	7.4E-04	0.298	24.863
WFTS-358	4.00	3.94	1.77	0.45	2	0.597	42.519	0.064	0.088	0.345	3.941	0.388	0.50	31.53	4.2E-06	1.6E-06	4.1E-04	0.133	30.827
WFTS-359	4.00	3.95	3.87	0.98	2	1.787	14.212	0.087	0.119	0.471	3.952	0.705	2.52	31.61	2.8E-05	2.0E-05	9.8E-04	0.874	11.180
WFTS-360	4.00	3.99	2.52	0.63	12	0.550	46.206	0.052	0.782	3.117	3.987	0.546	0.50	191.36	5.5E-06	3.0E-06	4.6E-03	1.060	43.276

TAG	D_o (mm)	P_l/D_o (-)	P_t/D_o (-)	P_t/P_l (-)	N_r (-)	F_p (mm)	FPI (in-1)	δ_f (mm)	$\tan\theta$ (-)	P_d (mm)	X_f(mm)	σ (-)	D_h (mm)	d (mm)	A_f (m^2)	A_c (m^2)	A_o (m^2)	V (cm^3)	A_o/V(cm^2/cm^3)
WFTS-361	4.00	3.99	2.17	0.54	2	0.514	49.420	0.065	0.311	1.240	3.987	0.471	0.50	31.89	4.5E-06	2.1E-06	5.4E-04	0.142	37.848
WFTS-362	4.00	3.99	2.17	0.54	2	0.514	49.420	0.065	0.311	1.240	3.987	0.471	0.50	31.89	4.5E-06	2.1E-06	5.4E-04	0.142	37.848
WFTS-363	4.00	3.99	4.00	1.00	2	2.065	12.298	0.050	0.088	0.350	3.995	0.732	3.01	31.96	3.3E-05	2.4E-05	1.0E-03	1.060	9.722
WFTS-364	4.00	4.00	2.15	0.54	2	0.613	41.417	0.069	0.747	2.984	3.997	0.474	0.50	31.98	5.3E-06	2.5E-06	6.4E-04	0.168	37.787
WFTS-365	4.00	4.00	2.15	0.54	2	0.613	41.417	0.069	0.747	2.984	3.997	0.474	0.50	31.98	5.3E-06	2.5E-06	6.4E-04	0.168	37.787
WFTS-366	4.00	4.00	4.00	1.00	11	2.077	12.228	0.050	0.091	0.364	3.997	0.732	3.03	175.88	3.3E-05	2.4E-05	5.7E-03	5.850	9.673
WFTS-367	5.00	1.98	2.29	1.15	4	1.342	18.923	0.094	0.230	0.569	2.474	0.523	1.50	39.58	1.5E-05	8.0E-06	8.5E-04	0.607	13.927
WFTS-368	5.00	2.45	2.83	1.15	3	1.158	21.944	0.062	0.103	0.315	3.060	0.612	1.50	36.72	1.6E-05	1.0E-05	9.8E-04	0.601	16.258
WFTS-369	5.00	2.48	2.87	1.15	3	0.802	31.672	0.085	0.104	0.324	3.103	0.582	1.01	37.23	1.2E-05	6.7E-06	9.9E-04	0.428	23.097
WFTS-370	5.00	2.52	4.00	1.59	11	2.036	12.479	0.050	0.089	0.280	3.145	0.731	3.02	138.39	4.1E-05	3.0E-05	5.5E-03	5.630	9.703
WFTS-371	5.00	2.54	2.94	1.15	2	1.938	13.106	0.096	0.089	0.283	3.181	0.627	2.49	25.45	2.9E-05	1.8E-05	7.3E-04	0.725	10.071
WFTS-372	5.00	2.59	2.99	1.15	2	1.906	13.324	0.075	0.089	0.288	3.235	0.639	2.50	25.88	2.9E-05	1.8E-05	7.6E-04	0.737	10.243
WFTS-373	5.00	2.61	2.85	1.09	2	0.774	32.809	0.059	0.088	0.288	3.259	0.599	1.00	26.08	1.1E-05	6.6E-06	6.9E-04	0.287	23.971
WFTS-374	5.00	2.61	3.01	1.15	2	0.520	48.854	0.094	0.736	2.399	3.261	0.548	0.50	26.09	7.8E-06	4.3E-06	8.9E-04	0.204	43.637
WFTS-375	5.00	2.63	3.03	1.15	2	1.162	21.868	0.098	0.088	0.290	3.283	0.613	1.50	26.26	1.8E-05	1.1E-05	7.5E-04	0.462	16.303
WFTS-376	5.00	2.72	3.03	1.12	2	1.146	22.172	0.073	0.088	0.299	3.394	0.627	1.51	27.15	1.7E-05	1.1E-05	7.8E-04	0.471	16.567
WFTS-377	5.00	2.72	4.00	1.47	2	1.028	24.699	0.068	0.088	0.298	3.401	0.701	1.50	27.20	2.1E-05	1.4E-05	1.0E-03	0.560	18.653
WFTS-378	5.00	2.91	3.37	1.15	2	0.762	33.322	0.082	0.105	0.383	3.643	0.627	1.01	29.15	1.3E-05	8.0E-06	9.3E-04	0.374	24.842
WFTS-379	5.00	2.92	3.37	1.15	2	1.084	23.432	0.069	0.101	0.368	3.649	0.659	1.49	29.19	1.8E-05	1.2E-05	9.4E-04	0.533	17.661
WFTS-380	5.00	2.92	3.38	1.15	4	1.108	22.926	0.093	0.136	0.497	3.654	0.645	1.49	58.46	1.9E-05	1.2E-05	1.9E-03	1.090	17.352
WFTS-381	5.00	2.94	1.56	0.53	2	0.671	37.861	0.050	0.182	0.667	3.673	0.332	0.50	29.38	5.2E-06	1.7E-06	4.1E-04	0.154	26.374
WFTS-382	5.00	3.02	3.49	1.15	2	1.783	14.244	0.079	0.092	0.347	3.778	0.682	2.48	30.22	3.1E-05	2.1E-05	1.0E-03	0.940	10.994
WFTS-383	5.00	3.06	3.53	1.15	11	1.761	14.420	0.050	0.089	0.340	3.823	0.697	2.50	168.22	3.1E-05	2.2E-05	5.8E-03	5.230	11.136
WFTS-384	5.00	3.09	3.57	1.15	2	1.811	14.025	0.090	0.092	0.355	3.864	0.684	2.52	30.91	3.2E-05	2.2E-05	1.1E-03	0.999	10.842
WFTS-385	5.00	3.16	3.64	1.15	2	2.135	11.898	0.075	0.088	0.345	3.944	0.700	3.01	31.55	3.9E-05	2.7E-05	1.1E-03	1.230	9.289
WFTS-386	5.00	3.17	3.66	1.15	11	0.522	48.668	0.099	0.831	3.294	3.963	0.588	0.50	174.37	9.6E-06	5.6E-06	7.8E-03	1.670	46.897
WFTS-387	5.00	3.17	3.67	1.15	16	0.508	50.000	0.090	0.838	3.325	3.968	0.599	0.50	253.98	9.3E-06	5.6E-06	1.1E-02	2.360	48.340
WFTS-388	5.00	3.17	3.67	1.15	2	0.508	50.000	0.089	0.832	3.301	3.968	0.600	0.50	31.75	9.3E-06	5.6E-06	1.4E-03	0.296	48.202
WFTS-389	5.00	3.23	2.46	0.76	11	0.516	49.230	0.056	0.648	2.613	4.032	0.529	0.50	177.42	6.4E-06	3.4E-06	4.8E-03	1.130	42.324
WFTS-390	5.00	3.23	2.44	0.75	2	0.852	29.825	0.052	0.089	0.360	4.042	0.553	1.01	32.34	1.0E-05	5.7E-06	7.4E-04	0.335	21.974
WFTS-391	5.00	3.32	3.84	1.15	2	1.738	14.619	0.070	0.088	0.363	4.154	0.709	2.51	33.23	3.3E-05	2.4E-05	1.3E-03	1.110	11.315
WFTS-392	5.00	3.33	3.84	1.15	2	1.722	14.754	0.061	0.088	0.364	4.162	0.714	2.50	33.30	3.3E-05	2.4E-05	1.3E-03	1.100	11.420
WFTS-393	5.00	3.34	2.35	0.70	4	0.530	47.938	0.061	0.594	2.480	4.173	0.508	0.50	66.77	6.2E-06	3.2E-06	1.7E-03	0.415	40.216
WFTS-394	5.00	3.35	3.87	1.15	2	2.065	12.298	0.068	0.088	0.367	4.192	0.717	2.99	33.53	4.0E-05	2.9E-05	1.3E-03	1.340	9.601
WFTS-395	5.00	3.36	3.88	1.15	2	2.065	12.298	0.074	0.088	0.368	4.202	0.716	2.98	33.62	4.0E-05	2.9E-05	1.3E-03	1.350	9.600
WFTS-396	5.00	3.37	3.89	1.15	2	1.783	14.244	0.098	0.162	0.681	4.208	0.702	2.52	33.66	3.5E-05	2.4E-05	1.3E-03	1.170	11.134
WFTS-397	5.00	3.37	3.89	1.15	3	1.783	14.244	0.098	0.161	0.678	4.208	0.702	2.52	50.49	3.5E-05	2.4E-05	2.0E-03	1.750	11.132
WFTS-398	5.00	3.39	1.56	0.46	2	0.673	37.749	0.050	0.088	0.371	4.241	0.332	0.50	33.93	5.3E-06	1.7E-06	4.7E-04	0.178	26.506
WFTS-399	5.00	3.39	1.56	0.46	2	0.673	37.749	0.050	0.088	0.371	4.241	0.332	0.50	33.93	5.3E-06	1.7E-06	4.7E-04	0.178	26.506
WFTS-400	5.00	3.39	1.56	0.46	2	0.673	37.749	0.050	0.088	0.371	4.241	0.332	0.50	33.93	5.3E-06	1.7E-06	4.7E-04	0.178	26.506
WFTS-401	5.00	3.40	3.03	0.89	2	1.146	22.172	0.073	0.088	0.375	4.251	0.627	1.50	34.01	1.7E-05	1.1E-05	9.9E-04	0.590	16.760
WFTS-402	5.00	3.42	3.95	1.15	11	1.696	14.978	0.050	0.143	0.613	4.272	0.724	2.48	187.97	3.4E-05	2.4E-05	7.3E-03	6.290	11.673
WFTS-403	5.00	3.42	3.43	1.00	2	1.104	23.009	0.076	0.088	0.375	4.281	0.660	1.51	34.25	1.9E-05	1.3E-05	1.1E-03	0.648	17.469
WFTS-404	5.00	3.43	3.96	1.15	2	2.065	12.298	0.055	0.088	0.375	4.288	0.728	3.03	34.31	4.1E-05	3.0E-05	1.4E-03	1.400	9.609
WFTS-405	5.00	3.44	3.98	1.15	11	2.059	12.334	0.050	0.091	0.392	4.304	0.730	3.03	189.39	4.1E-05	3.0E-05	7.5E-03	7.750	9.641
WFTS-406	5.00	3.44	3.98	1.15	11	2.063	12.310	0.050	0.124	0.532	4.304	0.730	3.03	189.39	4.1E-05	3.0E-05	7.5E-03	7.770	9.655
WFTS-407	5.00	3.44	3.98	1.15	11	2.063	12.310	0.050	0.150	0.646	4.304	0.730	3.02	189.39	4.1E-05	3.0E-05	7.5E-03	7.770	9.687
WFTS-408	5.00	3.50	1.94	0.56	12	0.649	39.135	0.057	0.777	3.396	4.372	0.443	0.50	209.84	6.3E-06	2.8E-06	4.7E-03	1.320	35.354
WFTS-409	5.00	3.50	1.94	0.56	12	0.649	39.135	0.057	0.777	3.396	4.372	0.443	0.50	209.84	6.3E-06	2.8E-06	4.7E-03	1.320	35.354
WFTS-410	5.00	3.61	2.37	0.66	4	0.580	43.830	0.057	0.825	3.727	4.516	0.521	0.50	72.26	6.9E-06	3.6E-06	2.1E-03	0.497	41.309

TAG	D_o (mm)	P_l/D_o (-)	P_t/D_o (-)	P_t/P_l (-)	N_r (-)	F_p (mm)	FPI (in-1)	δ_f (mm)	Tanθ (-)	P_d (mm)	X_f(mm)	σ (-)	D_h (mm)	d (mm)	A_f (m^2)	A_c (m^2)	A_o (m^2)	V (cm^3)	A_o/V(cm^2/cm^3)
WFTS-411	5.00	3.65	3.96	1.08	11	1.716	14.804	0.050	0.108	0.493	4.563	0.725	2.52	200.78	3.4E-05	2.5E-05	7.8E-03	6.820	11.510
WFTS-412	5.00	3.76	3.81	1.01	2	1.044	24.323	0.068	0.088	0.412	4.704	0.690	1.49	37.63	2.0E-05	1.4E-05	1.4E-03	0.749	18.583
WFTS-413	5.00	3.84	2.44	0.63	2	0.856	29.686	0.051	0.088	0.420	4.795	0.555	1.00	38.36	1.0E-05	5.8E-06	8.8E-04	0.400	22.125
WFTS-414	5.00	3.85	3.97	1.03	2	2.097	12.112	0.093	0.088	0.421	4.815	0.715	3.02	38.52	4.2E-05	3.0E-05	1.5E-03	1.600	9.474
WFTS-415	5.00	3.90	2.09	0.54	3	0.546	46.542	0.094	0.213	1.038	4.869	0.431	0.50	58.43	5.7E-06	2.5E-06	1.2E-03	0.333	34.495
WFTS-416	5.00	3.90	2.60	0.67	11	0.530	47.938	0.081	0.630	3.068	4.872	0.521	0.50	214.38	6.9E-06	3.6E-06	6.2E-03	1.480	41.672
WFTS-417	5.00	3.93	4.00	1.02	2	2.049	12.394	0.050	0.088	0.430	4.909	0.732	3.02	39.27	4.1E-05	3.0E-05	1.6E-03	1.610	9.696
WFTS-418	5.00	3.94	2.04	0.52	2	0.985	25.794	0.054	0.089	0.438	4.926	0.482	1.01	39.41	1.0E-05	4.8E-06	7.6E-04	0.396	19.136
WFTS-419	5.00	3.99	3.96	0.99	2	1.716	14.804	0.050	0.088	0.436	4.987	0.725	2.52	39.89	3.4E-05	2.5E-05	1.6E-03	1.350	11.506
WFTS-420	5.00	3.99	1.98	0.49	12	0.647	39.256	0.050	0.819	4.085	4.990	0.455	0.50	239.51	6.4E-06	2.9E-06	5.6E-03	1.530	36.705

Table 51. WFTS optimum designs performance.

TAG	u (m/s)	Re (-)	C_{min} (W/K)	$\dot{W}''$ (W/m^2)	ΔP (Pa)	f (-)	h ($W/m^2.K$)	Nu (-)	j (-)	η (-)	η_o (-)	NTU (-)
WFTS-001	2.000	63.743	0.005	10.624	77.852	0.113	296.680	5.805	0.037	0.993	0.994	1.828
WFTS-002	3.000	286.340	0.034	12.484	100.680	0.074	205.430	12.037	0.021	0.991	0.996	1.395
WFTS-003	3.000	285.751	0.034	13.866	111.740	0.082	220.910	12.917	0.023	0.992	0.996	1.499
WFTS-004	3.000	285.199	0.034	15.611	125.520	0.091	238.620	13.927	0.024	0.992	0.997	1.616
WFTS-005	3.000	284.990	0.034	17.336	156.630	0.100	255.150	14.880	0.026	0.992	0.997	1.942
WFTS-006	3.000	284.419	0.034	19.213	173.220	0.110	270.450	15.741	0.028	0.993	0.997	2.055
WFTS-007	3.000	283.659	0.034	21.763	195.600	0.122	287.940	16.715	0.029	0.994	0.997	2.181
WFTS-008	5.000	157.348	0.012	117.030	381.080	0.104	463.150	8.948	0.025	0.988	0.990	1.262
WFTS-009	3.000	189.322	0.016	15.809	58.100	0.160	245.060	9.494	0.030	0.981	0.985	0.750
WFTS-010	3.000	189.870	0.017	21.934	119.040	0.213	261.480	10.160	0.032	0.985	0.988	1.186
WFTS-011	3.000	94.293	0.008	48.619	214.250	0.094	366.050	7.018	0.026	0.991	0.994	1.355
WFTS-012	3.000	95.291	0.008	44.778	197.640	0.089	360.350	6.978	0.026	0.990	0.993	1.335
WFTS-013	3.000	95.291	0.008	44.778	197.640	0.089	360.350	6.978	0.026	0.990	0.993	1.335
WFTS-014	1.000	94.147	0.009	0.594	4.500	0.153	131.970	7.628	0.048	0.993	0.995	0.842
WFTS-015	2.000	63.974	0.005	7.457	68.441	0.123	270.110	5.304	0.039	0.989	0.990	2.075
WFTS-016	1.000	94.452	0.011	0.301	3.002	0.157	113.610	6.588	0.052	0.971	0.975	0.933
WFTS-017	5.000	156.946	0.012	96.447	354.670	0.092	435.950	8.401	0.024	0.984	0.986	1.337
WFTS-018	2.000	126.207	0.012	4.353	28.518	0.179	195.890	7.589	0.038	0.982	0.985	1.068
WFTS-019	2.000	63.670	0.005	6.786	65.711	0.115	260.960	5.100	0.038	0.987	0.989	2.113
WFTS-020	1.000	31.993	0.003	1.913	29.331	0.126	194.230	3.815	0.045	0.994	0.996	2.506
WFTS-021	5.000	315.204	0.028	113.530	370.130	0.163	356.090	13.781	0.023	0.986	0.990	0.971
WFTS-022	3.000	188.523	0.016	14.194	59.616	0.144	240.260	9.269	0.030	0.976	0.981	0.837
WFTS-023	1.000	63.145	0.005	0.528	6.816	0.150	137.990	5.349	0.052	0.989	0.991	1.490
WFTS-024	1.000	94.838	0.010	0.253	2.776	0.149	107.340	6.249	0.051	0.965	0.969	0.964
WFTS-025	2.000	127.093	0.011	6.996	33.954	0.106	215.510	8.408	0.030	0.992	0.994	0.879
WFTS-026	2.000	126.064	0.011	2.702	18.566	0.113	180.900	7.000	0.036	0.979	0.982	1.032
WFTS-027	2.000	62.908	0.005	10.050	85.756	0.100	277.730	5.321	0.034	0.990	0.992	1.988
WFTS-028	2.000	127.955	0.011	6.500	31.758	0.102	210.140	8.254	0.030	0.990	0.993	0.862

TAG	u (m/s)	Re (-)	C_{min} (W/K)	$\dot{W}''$ (W/m²)	ΔP (Pa)	f (-)	h (W/m².K)	Nu (-)	j (-)	η (-)	η_o (-)	NTU (-)
WFTS-029	2.000	63.506	0.005	9.441	82.737	0.100	273.750	5.291	0.034	0.989	0.991	2.011
WFTS-030	2.000	63.506	0.005	9.441	82.737	0.100	273.750	5.291	0.034	0.989	0.991	2.011
WFTS-031	2.000	63.506	0.005	9.441	82.737	0.100	273.750	5.291	0.034	0.989	0.991	2.011
WFTS-032	2.000	63.506	0.005	9.441	82.737	0.100	273.750	5.291	0.034	0.989	0.991	2.011
WFTS-033	3.000	188.246	0.018	28.216	88.655	0.107	265.090	10.160	0.023	0.992	0.995	0.701
WFTS-034	3.000	94.715	0.007	24.386	148.050	0.084	329.080	6.292	0.028	0.983	0.986	1.666
WFTS-035	3.000	94.715	0.007	24.386	148.050	0.084	329.080	6.292	0.028	0.983	0.986	1.666
WFTS-036	2.000	127.157	0.012	9.586	47.827	0.139	225.410	8.750	0.031	0.992	0.995	0.946
WFTS-037	1.000	63.566	0.005	0.811	8.314	0.101	149.170	5.784	0.042	0.990	0.994	1.284
WFTS-038	1.000	63.282	0.006	0.897	9.195	0.111	156.490	6.042	0.044	0.991	0.994	1.349
WFTS-039	1.000	94.344	0.008	0.501	4.373	0.125	124.970	7.238	0.045	0.990	0.993	0.916
WFTS-040	1.000	63.914	0.005	0.801	8.239	0.101	148.890	5.804	0.042	0.990	0.993	1.286
WFTS-041	5.000	156.933	0.012	78.011	331.500	0.080	403.680	7.778	0.023	0.978	0.981	1.422
WFTS-042	3.000	95.120	0.007	20.257	132.880	0.078	315.320	6.050	0.028	0.983	0.986	1.724
WFTS-043	3.000	95.120	0.007	20.257	132.880	0.078	315.320	6.050	0.028	0.983	0.986	1.724
WFTS-044	5.000	480.117	0.053	51.686	370.270	0.058	282.130	16.478	0.017	0.982	0.991	1.693
WFTS-045	5.000	479.420	0.053	54.956	393.780	0.061	293.390	17.113	0.017	0.983	0.991	1.761
WFTS-046	5.000	477.772	0.053	61.851	442.840	0.068	316.050	18.384	0.018	0.984	0.992	1.897
WFTS-047	5.000	480.022	0.054	68.799	487.990	0.075	338.090	19.776	0.020	0.986	0.992	2.012
WFTS-048	5.000	476.283	0.054	79.010	564.230	0.085	360.700	20.928	0.021	0.985	0.992	2.160
WFTS-049	5.000	473.716	0.054	90.011	643.820	0.096	382.960	22.105	0.022	0.986	0.992	2.298
WFTS-050	5.000	316.155	0.026	45.412	179.250	0.088	271.500	10.539	0.019	0.977	0.982	0.889
WFTS-051	5.000	316.155	0.026	45.412	179.250	0.088	271.500	10.539	0.019	0.977	0.982	0.889
WFTS-052	2.000	63.850	0.005	5.535	61.098	0.101	239.590	4.696	0.036	0.982	0.984	2.200
WFTS-053	5.000	478.945	0.055	104.310	754.270	0.115	405.220	23.638	0.024	0.985	0.992	2.457
WFTS-054	2.000	189.676	0.021	5.914	108.170	0.102	202.840	11.760	0.030	0.992	0.996	3.123
WFTS-055	2.000	191.299	0.022	7.484	135.880	0.130	221.960	12.975	0.033	0.992	0.996	3.391
WFTS-056	2.000	188.345	0.020	5.793	107.790	0.102	198.620	11.431	0.029	0.992	0.995	3.110
WFTS-057	2.000	190.272	0.020	5.293	97.711	0.093	190.680	11.089	0.028	0.992	0.996	2.963
WFTS-058	2.000	191.755	0.021	6.711	123.200	0.119	212.580	12.453	0.031	0.991	0.995	3.283
WFTS-059	1.000	63.219	0.005	0.493	6.913	0.140	132.410	5.139	0.049	0.987	0.989	1.553
WFTS-060	3.000	189.666	0.018	6.181	33.839	0.103	190.520	7.395	0.028	0.960	0.965	0.851
WFTS-061	3.000	285.827	0.030	12.475	157.630	0.070	203.790	11.826	0.020	0.986	0.992	2.160
WFTS-062	3.000	285.332	0.030	13.727	172.890	0.076	217.750	12.625	0.022	0.987	0.993	2.302
WFTS-063	1.000	31.754	0.002	0.998	21.145	0.121	156.430	3.018	0.044	0.988	0.990	2.772
WFTS-064	1.000	31.721	0.002	1.008	21.374	0.122	156.960	3.025	0.044	0.988	0.990	2.784
WFTS-065	1.000	31.963	0.002	1.176	24.398	0.137	163.820	3.185	0.045	0.989	0.991	2.848
WFTS-066	1.000	31.922	0.002	1.356	27.245	0.143	169.300	3.294	0.045	0.991	0.993	2.855
WFTS-067	1.000	31.502	0.002	1.471	29.392	0.146	172.090	3.306	0.045	0.992	0.993	2.888
WFTS-068	1.000	31.736	0.002	1.300	23.342	0.096	166.480	3.244	0.040	0.991	0.993	2.508
WFTS-069	1.000	31.814	0.003	1.521	26.866	0.107	173.170	3.382	0.041	0.992	0.994	2.570
WFTS-070	3.000	287.101	0.030	11.705	148.350	0.066	195.240	11.376	0.020	0.985	0.992	2.075
WFTS-071	3.000	285.617	0.030	14.810	186.640	0.081	227.600	13.215	0.023	0.988	0.993	2.409
WFTS-072	1.000	31.866	0.002	0.934	19.688	0.111	149.170	2.892	0.041	0.989	0.991	2.635
WFTS-073	1.000	31.538	0.002	0.836	18.323	0.105	135.490	2.599	0.038	0.989	0.991	2.488
WFTS-074	1.000	31.742	0.002	0.849	18.759	0.110	142.490	2.748	0.041	0.988	0.990	2.635
WFTS-075	1.000	32.005	0.002	0.795	17.928	0.107	134.000	2.606	0.039	0.988	0.990	2.528
WFTS-076	1.000	31.813	0.002	0.879	20.037	0.120	146.710	2.832	0.042	0.987	0.988	2.794
WFTS-077	5.000	158.467	0.013	76.585	332.080	0.070	402.940	7.692	0.022	0.978	0.981	1.449
WFTS-078	3.000	95.539	0.007	15.227	120.770	0.079	291.790	5.585	0.028	0.976	0.979	1.915

TAG	u (m/s)	Re (-)	C_{min} (W/K)	$\dot{W}''$ (W/m²)	ΔP (Pa)	f (-)	h (W/m².K)	Nu (-)	j (-)	η (-)	η_o (-)	NTU (-)
WFTS-079	3.000	95.539	0.007	15.227	120.770	0.079	291.790	5.585	0.028	0.976	0.979	1.915
WFTS-080	3.000	95.841	0.007	12.140	98.434	0.066	272.490	5.228	0.027	0.975	0.978	1.827
WFTS-081	2.000	63.348	0.005	4.870	61.555	0.092	221.470	4.306	0.034	0.977	0.980	2.318
WFTS-082	5.000	318.335	0.028	85.174	345.150	0.128	325.270	12.713	0.021	0.976	0.981	1.093
WFTS-083	2.000	191.045	0.018	3.384	15.832	0.088	162.140	9.398	0.027	0.983	0.988	0.634
WFTS-084	5.000	315.004	0.027	57.676	155.640	0.082	297.360	11.316	0.019	0.980	0.984	0.667
WFTS-085	3.000	188.746	0.015	7.468	38.818	0.076	206.880	7.991	0.025	0.967	0.972	0.884
WFTS-086	2.000	190.120	0.018	3.945	18.450	0.098	170.780	9.888	0.028	0.989	0.992	0.670
WFTS-087	2.000	188.383	0.018	4.278	20.205	0.106	174.780	10.026	0.029	0.989	0.992	0.692
WFTS-088	2.000	63.865	0.005	4.947	63.266	0.094	224.320	4.317	0.033	0.980	0.982	2.381
WFTS-089	2.000	62.852	0.005	5.402	69.575	0.100	227.850	4.319	0.034	0.980	0.982	2.437
WFTS-090	2.000	62.852	0.005	5.402	69.575	0.100	227.850	4.319	0.034	0.980	0.982	2.437
WFTS-091	2.000	62.852	0.005	5.402	69.575	0.100	227.850	4.319	0.034	0.980	0.982	2.437
WFTS-092	2.000	62.852	0.005	5.402	69.575	0.100	227.850	4.319	0.034	0.980	0.982	2.437
WFTS-093	5.000	158.822	0.013	58.082	294.700	0.067	375.390	7.125	0.022	0.970	0.973	1.567
WFTS-094	5.000	157.168	0.013	69.205	341.690	0.072	394.370	7.436	0.022	0.975	0.977	1.609
WFTS-095	2.000	188.966	0.018	1.672	10.644	0.101	135.470	7.858	0.030	0.963	0.968	0.706
WFTS-096	2.000	126.509	0.011	6.486	68.500	0.158	202.590	7.755	0.033	0.982	0.986	1.783
WFTS-097	2.000	126.509	0.011	6.486	68.500	0.158	202.590	7.755	0.033	0.982	0.986	1.783
WFTS-098	2.000	127.803	0.011	5.788	62.494	0.151	197.250	7.598	0.033	0.977	0.982	1.768
WFTS-099	2.000	190.259	0.017	2.553	14.138	0.100	154.010	8.994	0.030	0.980	0.984	0.710
WFTS-100	2.000	191.819	0.017	2.175	12.212	0.091	144.710	8.521	0.029	0.974	0.979	0.673
WFTS-101	2.000	127.131	0.012	1.742	16.556	0.098	151.500	5.912	0.033	0.959	0.963	1.172
WFTS-102	3.000	284.686	0.033	6.299	29.415	0.133	171.850	10.012	0.027	0.951	0.956	0.648
WFTS-103	2.000	126.186	0.011	2.184	19.828	0.098	165.720	6.419	0.034	0.966	0.970	1.234
WFTS-104	5.000	471.973	0.045	25.692	65.932	0.087	197.750	11.460	0.017	0.964	0.970	0.416
WFTS-105	5.000	471.180	0.046	26.442	68.787	0.091	200.060	11.574	0.017	0.962	0.968	0.426
WFTS-106	1.000	63.322	0.005	0.422	7.237	0.122	120.240	4.674	0.045	0.982	0.985	1.715
WFTS-107	2.000	63.893	0.005	3.452	46.957	0.063	186.630	3.660	0.028	0.977	0.979	2.101
WFTS-108	2.000	63.067	0.005	3.983	54.892	0.073	201.510	3.901	0.030	0.975	0.977	2.295
WFTS-109	5.000	475.015	0.042	36.385	372.220	0.082	217.730	12.698	0.016	0.965	0.973	1.833
WFTS-110	5.000	475.015	0.042	36.385	372.220	0.082	217.730	12.698	0.016	0.965	0.973	1.833
WFTS-111	5.000	159.142	0.013	48.511	275.460	0.064	353.960	6.698	0.021	0.966	0.968	1.646
WFTS-112	5.000	159.903	0.013	47.496	269.950	0.063	351.580	6.682	0.021	0.965	0.968	1.635
WFTS-113	5.000	159.903	0.013	47.496	269.950	0.063	351.580	6.682	0.021	0.965	0.968	1.635
WFTS-114	3.000	189.008	0.015	6.940	38.892	0.065	203.520	7.630	0.024	0.964	0.969	0.935
WFTS-115	3.000	188.255	0.016	12.418	67.144	0.103	235.430	8.890	0.027	0.977	0.980	1.055
WFTS-116	3.000	472.968	0.049	7.807	114.720	0.118	188.310	18.226	0.026	0.950	0.964	2.256
WFTS-117	3.000	471.960	0.053	11.221	172.200	0.192	192.360	18.578	0.028	0.943	0.957	2.388
WFTS-118	3.000	188.786	0.016	8.853	52.315	0.087	222.500	8.311	0.026	0.961	0.967	1.075
WFTS-119	1.000	94.680	0.010	0.226	3.552	0.139	101.220	5.884	0.049	0.948	0.953	1.280
WFTS-120	1.000	63.965	0.005	0.426	7.771	0.121	125.780	4.825	0.046	0.973	0.977	1.893
WFTS-121	1.000	63.965	0.005	0.426	7.771	0.121	125.780	4.825	0.046	0.973	0.977	1.893
WFTS-122	1.000	63.349	0.005	0.431	7.906	0.121	126.070	4.792	0.046	0.974	0.977	1.912
WFTS-123	1.000	94.401	0.008	0.435	5.149	0.108	117.680	6.820	0.042	0.983	0.987	1.163
WFTS-124	5.000	475.363	0.042	37.141	467.170	0.088	226.650	12.859	0.017	0.965	0.972	2.343
WFTS-125	5.000	478.659	0.044	45.144	560.920	0.105	242.440	13.871	0.018	0.967	0.974	2.479
WFTS-126	5.000	319.476	0.028	70.312	341.110	0.107	304.140	11.930	0.020	0.964	0.970	1.210
WFTS-127	1.000	157.149	0.016	0.251	2.260	0.111	87.058	8.399	0.038	0.982	0.986	0.652
WFTS-128	2.000	63.718	0.005	2.897	46.112	0.055	168.800	3.302	0.026	0.968	0.971	2.205

TAG	u (m/s)	Re (-)	C_{min} (W/K)	$\dot{W}''$ (W/m²)	ΔP (Pa)	f (-)	h (W/m².K)	Nu (-)	j (-)	η (-)	η_o (-)	NTU (-)
WFTS-129	1.000	63.978	0.005	0.353	7.100	0.110	109.380	4.296	0.042	0.969	0.972	1.808
WFTS-130	1.000	96.023	0.010	0.201	3.387	0.124	95.085	5.605	0.046	0.945	0.950	1.285
WFTS-131	3.000	283.830	0.026	10.862	74.606	0.124	189.090	10.983	0.024	0.967	0.973	1.068
WFTS-132	1.000	157.358	0.016	0.240	2.261	0.110	85.226	8.233	0.037	0.977	0.982	0.666
WFTS-133	1.000	158.556	0.016	0.276	2.409	0.103	89.463	8.708	0.037	0.981	0.986	0.650
WFTS-134	1.000	158.011	0.016	0.286	2.493	0.105	91.190	8.846	0.037	0.983	0.987	0.664
WFTS-135	1.000	159.424	0.016	0.233	2.194	0.110	83.982	8.219	0.037	0.975	0.981	0.656
WFTS-136	1.000	157.314	0.016	0.296	2.578	0.106	92.606	8.943	0.038	0.985	0.989	0.675
WFTS-137	3.000	190.602	0.018	4.681	37.087	0.082	172.760	6.738	0.026	0.925	0.931	1.077
WFTS-138	2.000	315.819	0.036	1.199	6.342	0.094	109.700	10.635	0.027	0.956	0.962	0.472
WFTS-139	2.000	317.226	0.038	1.541	8.149	0.123	116.400	11.334	0.029	0.951	0.958	0.498
WFTS-140	2.000	314.260	0.041	2.406	13.017	0.189	124.520	12.012	0.030	0.955	0.961	0.547
WFTS-141	2.000	189.524	0.017	1.853	14.015	0.087	145.750	8.142	0.029	0.953	0.960	0.895
WFTS-142	2.000	190.019	0.017	1.834	13.890	0.087	145.240	8.125	0.029	0.952	0.959	0.892
WFTS-143	3.000	471.694	0.047	5.737	102.180	0.095	159.530	15.399	0.023	0.938	0.952	2.286
WFTS-144	2.000	189.993	0.018	1.386	11.385	0.082	126.000	7.348	0.028	0.947	0.953	0.834
WFTS-145	3.000	479.033	0.047	4.594	81.336	0.078	144.980	14.212	0.021	0.942	0.954	2.071
WFTS-146	3.000	478.387	0.047	4.817	84.736	0.080	150.020	14.686	0.022	0.941	0.954	2.129
WFTS-147	3.000	472.720	0.047	7.434	130.880	0.114	183.790	16.904	0.025	0.936	0.951	2.601
WFTS-148	2.000	313.753	0.033	2.566	12.243	0.128	126.040	11.867	0.026	0.971	0.978	0.497
WFTS-149	2.000	313.753	0.033	2.706	19.367	0.135	126.590	11.918	0.026	0.971	0.978	0.749
WFTS-150	3.000	479.737	0.047	6.315	110.780	0.098	176.590	16.493	0.024	0.937	0.951	2.491
WFTS-151	5.000	799.403	0.078	21.367	227.020	0.072	250.000	22.887	0.020	0.913	0.933	2.095
WFTS-152	5.000	791.322	0.078	24.861	266.850	0.084	263.770	23.819	0.021	0.909	0.929	2.225
WFTS-153	5.000	799.878	0.077	19.677	209.770	0.067	237.810	21.834	0.019	0.916	0.935	2.004
WFTS-154	1.000	63.825	0.005	0.325	7.300	0.101	102.180	4.004	0.039	0.964	0.968	1.880
WFTS-155	2.000	127.752	0.012	1.342	17.305	0.077	132.130	5.181	0.029	0.938	0.942	1.357
WFTS-156	2.000	377.717	0.042	1.251	6.242	0.105	107.130	12.421	0.027	0.921	0.934	0.422
WFTS-157	1.000	157.377	0.017	0.394	4.119	0.171	95.137	9.020	0.040	0.977	0.981	0.826
WFTS-158	2.000	63.601	0.005	2.449	45.365	0.048	150.740	2.943	0.023	0.961	0.964	2.276
WFTS-159	1.000	157.453	0.016	0.254	2.672	0.111	89.259	8.463	0.038	0.976	0.981	0.778
WFTS-160	5.000	790.751	0.076	17.206	201.810	0.063	218.350	19.631	0.018	0.908	0.926	2.005
WFTS-161	3.000	189.691	0.017	4.924	41.610	0.072	183.550	6.673	0.024	0.931	0.937	1.228
WFTS-162	2.000	314.615	0.036	3.857	41.307	0.219	129.750	12.530	0.028	0.966	0.972	1.142
WFTS-163	1.000	158.315	0.015	0.220	2.392	0.103	83.857	7.896	0.036	0.962	0.969	0.746
WFTS-164	1.000	63.164	0.006	0.304	8.052	0.128	102.170	3.777	0.042	0.950	0.953	2.180
WFTS-165	1.000	191.020	0.023	0.188	1.907	0.123	77.786	9.122	0.039	0.951	0.958	0.640
WFTS-166	5.000	159.874	0.014	33.527	249.840	0.041	283.690	5.569	0.017	0.952	0.955	1.707
WFTS-167	3.000	471.922	0.046	5.239	106.680	0.093	154.120	14.003	0.021	0.928	0.941	2.496
WFTS-168	3.000	471.922	0.046	5.239	106.680	0.093	154.120	14.003	0.021	0.928	0.941	2.496
WFTS-169	1.000	64.016	0.006	0.261	6.810	0.109	95.434	3.594	0.039	0.955	0.958	2.020
WFTS-170	1.000	62.787	0.006	0.322	8.630	0.136	103.400	3.795	0.042	0.948	0.952	2.230
WFTS-171	1.000	188.986	0.021	0.151	1.560	0.100	73.691	8.550	0.037	0.946	0.954	0.615
WFTS-172	3.000	570.151	0.061	5.173	92.686	0.108	152.080	17.744	0.024	0.909	0.926	2.132
WFTS-173	3.000	477.778	0.046	4.109	85.447	0.075	140.880	12.950	0.020	0.928	0.940	2.329
WFTS-174	5.000	313.990	0.029	16.117	88.725	0.055	216.220	7.620	0.017	0.908	0.914	0.920
WFTS-175	3.000	286.777	0.028	5.847	36.256	0.098	168.540	9.331	0.023	0.937	0.943	0.834
WFTS-176	5.000	315.198	0.030	22.507	126.610	0.080	237.230	8.223	0.018	0.888	0.896	1.011
WFTS-177	3.000	574.638	0.060	3.847	71.329	0.080	138.370	16.271	0.022	0.911	0.927	2.010
WFTS-178	1.000	95.859	0.010	0.197	4.121	0.121	89.610	5.273	0.043	0.928	0.933	1.481

TAG	u (m/s)	Re (-)	C_{min} (W/K)	$\dot{W}''$ (W/m²)	ΔP (Pa)	f (-)	h (W/m².K)	Nu (-)	j (-)	η (-)	η_o (-)	NTU (-)
WFTS-179	1.000	31.991	0.003	0.687	23.094	0.063	100.750	1.979	0.026	0.977	0.979	2.805
WFTS-180	5.000	159.972	0.012	24.159	194.040	0.029	245.990	4.832	0.015	0.930	0.935	1.561
WFTS-181	1.000	188.852	0.020	0.196	2.081	0.104	78.659	8.876	0.035	0.968	0.973	0.686
WFTS-182	3.000	282.461	0.027	4.167	28.330	0.072	144.670	8.362	0.021	0.936	0.941	0.783
WFTS-183	2.000	188.776	0.017	1.162	12.386	0.070	116.730	6.764	0.026	0.924	0.931	0.979
WFTS-184	3.000	475.972	0.045	3.965	91.555	0.068	132.830	12.938	0.019	0.917	0.930	2.412
WFTS-185	3.000	475.877	0.051	2.979	14.089	0.072	121.360	11.818	0.020	0.892	0.903	0.438
WFTS-186	2.000	316.516	0.032	1.140	7.863	0.082	111.190	10.071	0.025	0.923	0.932	0.604
WFTS-187	3.000	190.121	0.019	3.470	38.718	0.065	163.190	5.704	0.022	0.893	0.898	1.383
WFTS-188	2.000	126.661	0.012	1.159	18.749	0.065	119.450	4.644	0.026	0.923	0.927	1.515
WFTS-189	1.000	31.844	0.003	0.611	23.193	0.056	89.697	1.754	0.023	0.974	0.976	2.810
WFTS-190	2.000	319.989	0.033	1.019	7.245	0.077	107.930	9.765	0.024	0.911	0.921	0.597
WFTS-191	5.000	942.392	0.105	23.537	315.500	0.116	253.010	24.868	0.021	0.825	0.849	2.435
WFTS-192	2.000	377.489	0.040	1.148	7.107	0.088	105.040	11.308	0.024	0.918	0.929	0.511
WFTS-193	1.000	157.497	0.016	0.163	2.415	0.099	78.316	7.145	0.036	0.937	0.944	0.927
WFTS-194	1.000	157.497	0.016	0.163	2.415	0.099	78.316	7.145	0.036	0.937	0.944	0.927
WFTS-195	1.000	157.497	0.016	0.163	2.415	0.099	78.316	7.145	0.036	0.937	0.944	0.927
WFTS-196	2.000	316.681	0.042	3.716	41.050	0.280	134.800	12.225	0.030	0.925	0.933	1.175
WFTS-197	5.000	792.748	0.084	13.752	225.150	0.068	208.960	17.427	0.017	0.839	0.857	2.478
WFTS-198	2.000	316.757	0.042	3.722	41.251	0.281	134.930	12.232	0.030	0.924	0.932	1.179
WFTS-199	3.000	282.594	0.027	3.921	29.779	0.067	139.280	8.054	0.020	0.926	0.932	0.833
WFTS-200	2.000	379.467	0.043	1.401	8.702	0.106	109.660	12.085	0.025	0.938	0.946	0.545
WFTS-201	2.000	376.817	0.044	1.691	10.580	0.128	114.310	12.522	0.026	0.939	0.947	0.572
WFTS-202	3.000	574.163	0.062	3.268	75.578	0.077	138.820	14.603	0.020	0.880	0.895	2.430
WFTS-203	3.000	575.494	0.060	5.085	112.190	0.103	145.480	17.133	0.023	0.880	0.898	2.438
WFTS-204	1.000	188.352	0.022	0.230	2.942	0.141	82.938	9.174	0.038	0.951	0.957	0.858
WFTS-205	3.000	479.946	0.050	2.662	74.316	0.063	116.030	10.295	0.017	0.892	0.903	2.474
WFTS-206	1.000	157.415	0.015	0.220	3.049	0.100	81.119	7.839	0.036	0.951	0.958	0.911
WFTS-207	1.000	158.309	0.015	0.210	2.897	0.095	79.747	7.750	0.035	0.955	0.962	0.893
WFTS-208	1.000	95.726	0.010	0.182	4.605	0.112	81.041	4.763	0.039	0.913	0.918	1.591
WFTS-209	5.000	952.153	0.103	12.028	172.230	0.063	215.900	21.312	0.018	0.823	0.844	2.207
WFTS-210	5.000	797.311	0.085	10.545	181.400	0.055	195.450	16.246	0.016	0.832	0.849	2.413
WFTS-211	1.000	31.797	0.003	0.521	24.403	0.050	74.139	1.447	0.019	0.968	0.970	2.847
WFTS-212	3.000	479.223	0.052	3.072	88.162	0.074	125.020	10.922	0.018	0.879	0.891	2.702
WFTS-213	5.000	799.625	0.085	9.579	164.710	0.050	186.730	15.644	0.016	0.837	0.853	2.316
WFTS-214	3.000	477.493	0.053	3.746	19.611	0.089	135.590	11.851	0.020	0.883	0.894	0.537
WFTS-215	1.000	190.786	0.021	0.163	2.124	0.103	76.272	8.511	0.036	0.946	0.953	0.803
WFTS-216	1.000	190.786	0.021	0.163	2.124	0.103	76.272	8.511	0.036	0.946	0.953	0.803
WFTS-217	1.000	190.786	0.021	0.163	2.124	0.103	76.272	8.511	0.036	0.946	0.953	0.803
WFTS-218	2.000	314.222	0.036	1.377	10.867	0.107	116.760	10.471	0.026	0.922	0.930	0.724
WFTS-219	1.000	95.973	0.010	0.167	4.256	0.099	76.293	4.495	0.037	0.930	0.934	1.536
WFTS-220	5.000	957.414	0.105	10.638	155.440	0.056	197.420	19.848	0.017	0.836	0.855	2.086
WFTS-221	5.000	957.414	0.105	10.638	155.440	0.056	197.420	19.848	0.017	0.836	0.855	2.086
WFTS-222	5.000	958.998	0.105	10.646	155.430	0.056	201.570	20.166	0.017	0.830	0.850	2.114
WFTS-223	2.000	382.661	0.042	0.919	6.113	0.076	102.950	11.057	0.023	0.903	0.914	0.529
WFTS-224	2.000	382.661	0.042	0.919	6.113	0.076	102.950	11.057	0.023	0.903	0.914	0.529
WFTS-225	5.000	948.065	0.105	13.513	200.280	0.072	225.760	21.852	0.019	0.810	0.831	2.352
WFTS-226	5.000	797.597	0.085	8.985	143.020	0.047	140.980	12.179	0.012	0.870	0.882	1.674
WFTS-227	5.000	797.660	0.085	8.867	141.370	0.046	141.700	12.158	0.012	0.863	0.876	1.673
WFTS-228	5.000	799.688	0.086	9.065	173.020	0.048	176.520	14.813	0.015	0.839	0.855	2.434

TAG	u (m/s)	Re (-)	C_{min} (W/K)	$\dot{W}''$ (W/m^2)	ΔP (Pa)	f (-)	h ($W/m^2.K$)	Nu (-)	j (-)	η (-)	η_o (-)	NTU (-)
WFTS-229	2.000	315.730	0.036	1.272	10.103	0.099	114.620	10.321	0.026	0.922	0.929	0.715
WFTS-230	2.000	316.630	0.037	1.532	12.150	0.120	119.850	10.791	0.027	0.919	0.926	0.744
WFTS-231	2.000	314.970	0.037	1.653	13.184	0.130	121.980	10.913	0.028	0.918	0.925	0.761
WFTS-232	3.000	574.829	0.063	2.713	66.439	0.067	130.900	13.664	0.019	0.873	0.887	2.405
WFTS-233	3.000	574.829	0.063	2.713	66.439	0.067	130.900	13.664	0.019	0.873	0.887	2.405
WFTS-234	3.000	574.829	0.063	2.713	66.439	0.067	130.900	13.664	0.019	0.873	0.887	2.405
WFTS-235	3.000	574.829	0.063	2.713	66.439	0.067	130.900	13.664	0.019	0.873	0.887	2.405
WFTS-236	1.000	63.927	0.005	0.244	7.743	0.076	80.087	3.143	0.031	0.947	0.951	2.042
WFTS-237	3.000	189.162	0.019	3.044	37.665	0.048	134.410	5.203	0.019	0.913	0.917	1.289
WFTS-238	1.000	191.375	0.021	0.142	2.020	0.095	68.992	8.106	0.034	0.912	0.921	0.763
WFTS-239	3.000	473.538	0.051	2.571	14.948	0.062	113.280	10.977	0.019	0.864	0.876	0.488
WFTS-240	1.000	191.920	0.021	0.140	2.067	0.093	67.975	8.009	0.034	0.912	0.921	0.783
WFTS-241	1.000	191.920	0.021	0.140	2.067	0.093	67.975	8.009	0.034	0.912	0.921	0.783
WFTS-242	1.000	191.920	0.021	0.140	2.067	0.093	67.975	8.009	0.034	0.912	0.921	0.783
WFTS-243	2.000	127.790	0.012	0.964	19.238	0.055	105.160	4.125	0.023	0.901	0.905	1.606
WFTS-244	2.000	317.771	0.031	0.964	8.370	0.068	96.418	9.405	0.023	0.893	0.904	0.640
WFTS-245	1.000	63.876	0.005	0.221	7.850	0.069	73.471	2.881	0.028	0.940	0.944	2.087
WFTS-246	2.000	317.517	0.031	0.957	8.398	0.067	95.650	9.322	0.022	0.894	0.905	0.642
WFTS-247	2.000	379.213	0.041	0.903	7.079	0.075	97.131	11.306	0.024	0.862	0.875	0.563
WFTS-248	3.000	283.050	0.035	10.246	43.038	0.102	180.440	10.452	0.022	0.976	0.980	0.628
WFTS-249	3.000	94.329	0.010	10.959	116.790	0.045	218.040	4.209	0.020	0.964	0.968	1.901
WFTS-250	3.000	287.348	0.037	8.861	53.002	0.092	175.690	9.856	0.021	0.947	0.954	0.848
WFTS-251	5.000	314.447	0.038	28.407	228.860	0.060	240.450	8.618	0.016	0.921	0.928	1.520
WFTS-252	5.000	319.983	0.040	39.989	319.250	0.086	262.930	9.507	0.018	0.912	0.920	1.633
WFTS-253	3.000	94.810	0.010	9.264	130.170	0.042	195.340	3.790	0.018	0.938	0.943	2.187
WFTS-254	5.000	796.170	0.107	31.493	417.190	0.086	275.360	24.177	0.020	0.872	0.898	2.770
WFTS-255	5.000	797.628	0.103	19.443	263.660	0.055	230.070	20.424	0.017	0.883	0.906	2.391
WFTS-256	5.000	797.628	0.103	19.443	263.660	0.055	230.070	20.424	0.017	0.883	0.906	2.391
WFTS-257	2.000	318.202	0.044	2.365	14.818	0.102	117.040	11.078	0.023	0.962	0.969	0.601
WFTS-258	5.000	316.519	0.040	21.859	212.460	0.057	220.540	7.736	0.016	0.896	0.903	1.636
WFTS-259	1.000	189.562	0.031	0.146	2.046	0.095	68.173	7.934	0.034	0.927	0.935	0.754
WFTS-260	1.000	157.624	0.025	0.161	2.749	0.102	72.914	7.056	0.036	0.919	0.926	0.975
WFTS-261	1.000	191.045	0.031	0.139	2.000	0.092	66.176	7.761	0.033	0.908	0.918	0.740
WFTS-262	5.000	949.966	0.130	15.043	211.310	0.054	228.750	23.024	0.017	0.835	0.863	2.344
WFTS-263	5.000	950.632	0.131	15.832	224.580	0.057	234.080	23.439	0.018	0.830	0.858	2.408
WFTS-264	5.000	945.023	0.131	17.443	248.900	0.063	241.710	23.966	0.018	0.826	0.855	2.492
WFTS-265	5.000	957.287	0.131	14.194	200.210	0.051	223.260	22.630	0.017	0.835	0.862	2.296
WFTS-266	5.000	941.378	0.131	18.638	267.340	0.067	246.310	24.260	0.018	0.823	0.852	2.545
WFTS-267	3.000	477.151	0.063	3.363	95.421	0.056	125.680	11.128	0.017	0.892	0.907	2.734
WFTS-268	2.000	317.150	0.048	0.950	8.338	0.073	93.889	9.140	0.023	0.870	0.882	0.615
WFTS-269	5.000	957.762	0.132	13.439	197.040	0.050	218.170	21.925	0.016	0.828	0.855	2.311
WFTS-270	3.000	95.877	0.011	7.594	125.640	0.030	167.440	3.285	0.015	0.938	0.942	2.205
WFTS-271	3.000	567.451	0.078	3.128	79.796	0.056	136.270	14.085	0.018	0.871	0.890	2.616
WFTS-272	3.000	565.645	0.079	3.532	91.710	0.064	142.420	14.557	0.019	0.864	0.883	2.760
WFTS-273	1.000	156.927	0.022	0.208	3.479	0.095	77.908	7.167	0.033	0.949	0.955	1.054
WFTS-274	3.000	575.266	0.080	2.955	76.899	0.055	133.810	13.932	0.018	0.866	0.884	2.603
WFTS-275	3.000	575.722	0.081	2.663	74.070	0.052	128.250	13.180	0.017	0.854	0.872	2.631
WFTS-276	1.000	191.958	0.030	0.133	2.161	0.086	63.691	7.506	0.031	0.896	0.906	0.795
WFTS-277	1.000	63.908	0.009	0.210	9.269	0.097	75.058	2.674	0.030	0.904	0.908	2.540
WFTS-278	3.000	190.374	0.027	2.815	42.607	0.047	140.640	4.774	0.018	0.866	0.871	1.568

TAG	u (m/s)	Re (-)	C_{min} (W/K)	$\dot{W}''$ (W/m²)	ΔP (Pa)	f (-)	h (W/m².K)	Nu (-)	j (-)	η (-)	η_o (-)	NTU (-)
WFTS-279	3.000	190.374	0.027	2.815	42.607	0.047	140.640	4.774	0.018	0.866	0.871	1.568
WFTS-280	3.000	95.385	0.011	5.739	108.150	0.023	145.870	2.847	0.013	0.917	0.921	2.141
WFTS-281	5.000	959.125	0.139	9.241	166.230	0.042	193.840	18.414	0.015	0.783	0.807	2.378
WFTS-282	5.000	957.509	0.139	9.782	176.280	0.044	199.700	18.849	0.015	0.779	0.803	2.443
WFTS-283	2.000	190.412	0.027	0.926	14.590	0.057	108.010	5.695	0.022	0.897	0.902	1.298
WFTS-284	3.000	287.823	0.042	3.341	35.619	0.064	139.600	7.074	0.018	0.852	0.860	1.083
WFTS-285	1.000	188.352	0.029	0.149	2.670	0.086	68.679	7.386	0.030	0.923	0.930	0.967
WFTS-286	1.000	188.352	0.029	0.149	2.670	0.086	68.679	7.386	0.030	0.923	0.930	0.967
WFTS-287	1.000	188.352	0.029	0.149	2.670	0.086	68.679	7.386	0.030	0.923	0.930	0.967
WFTS-288	5.000	315.343	0.039	10.650	95.058	0.029	159.790	6.187	0.013	0.843	0.851	1.026
WFTS-289	5.000	474.032	0.072	12.786	178.750	0.056	178.040	8.421	0.013	0.804	0.813	1.710
WFTS-290	5.000	476.251	0.072	9.649	132.780	0.040	150.290	7.518	0.012	0.849	0.855	1.496
WFTS-291	1.000	157.428	0.024	0.146	3.188	0.086	72.223	6.323	0.031	0.898	0.906	1.212
WFTS-292	1.000	157.149	0.024	0.152	3.322	0.089	72.401	6.384	0.031	0.907	0.914	1.224
WFTS-293	3.000	568.592	0.087	2.220	76.674	0.052	122.530	11.710	0.016	0.805	0.821	2.939
WFTS-294	1.000	95.795	0.014	0.167	5.869	0.085	66.336	3.901	0.030	0.908	0.912	1.802
WFTS-295	3.000	575.266	0.088	1.955	68.406	0.046	119.310	11.479	0.016	0.801	0.817	2.885
WFTS-296	1.000	159.532	0.025	0.125	2.891	0.078	70.686	6.186	0.031	0.886	0.894	1.232
WFTS-297	3.000	574.924	0.090	2.228	79.939	0.054	125.480	11.866	0.017	0.787	0.804	3.059
WFTS-298	2.000	377.946	0.059	0.740	7.403	0.061	101.890	9.767	0.021	0.812	0.826	0.712
WFTS-299	3.000	567.185	0.089	1.790	66.387	0.044	116.780	10.928	0.016	0.790	0.806	2.952
WFTS-300	3.000	572.033	0.091	2.620	96.416	0.064	131.040	12.147	0.017	0.775	0.792	3.228
WFTS-301	1.000	159.995	0.025	0.125	2.986	0.079	62.400	6.129	0.030	0.883	0.891	1.121
WFTS-302	5.000	158.410	0.019	22.343	332.900	0.021	181.730	3.535	0.010	0.880	0.884	2.024
WFTS-303	3.000	95.810	0.011	4.567	114.510	0.020	122.880	2.409	0.011	0.879	0.884	2.303
WFTS-304	5.000	473.494	0.071	6.077	53.921	0.028	121.150	7.043	0.012	0.732	0.741	0.674
WFTS-305	5.000	158.521	0.025	46.209	416.230	0.042	289.920	5.332	0.015	0.942	0.945	2.086
WFTS-306	3.000	284.210	0.044	5.763	38.736	0.057	144.140	8.383	0.018	0.954	0.959	0.786
WFTS-307	3.000	284.210	0.044	5.763	38.736	0.057	144.140	8.383	0.018	0.954	0.959	0.786
WFTS-308	5.000	791.449	0.137	45.034	690.900	0.102	285.950	24.278	0.019	0.843	0.874	3.240
WFTS-309	5.000	316.142	0.052	14.480	114.440	0.032	182.900	6.432	0.012	0.901	0.906	1.107
WFTS-310	3.000	564.770	0.098	4.824	138.700	0.072	150.320	15.021	0.018	0.842	0.865	3.160
WFTS-311	5.000	476.599	0.082	19.430	169.940	0.052	186.310	9.795	0.013	0.890	0.898	1.238
WFTS-312	5.000	477.011	0.082	18.755	109.580	0.050	173.290	9.171	0.012	0.896	0.904	0.773
WFTS-313	5.000	470.705	0.084	25.561	316.700	0.072	196.370	10.033	0.014	0.876	0.884	1.818
WFTS-314	2.000	127.689	0.022	1.072	26.335	0.050	109.370	3.775	0.020	0.876	0.881	2.001
WFTS-315	1.000	63.737	0.011	0.210	10.722	0.085	69.460	2.439	0.026	0.894	0.898	2.690
WFTS-316	2.000	63.959	0.009	2.118	72.349	0.032	99.712	1.958	0.014	0.924	0.927	2.670
WFTS-317	3.000	191.876	0.035	2.651	48.463	0.041	129.710	4.262	0.015	0.831	0.837	1.677
WFTS-318	1.000	191.229	0.036	0.135	2.878	0.074	66.638	6.925	0.027	0.875	0.885	1.064
WFTS-319	3.000	477.797	0.088	2.203	19.157	0.045	118.630	9.146	0.015	0.773	0.789	0.688
WFTS-320	2.000	127.233	0.022	0.961	28.132	0.044	88.292	3.448	0.018	0.861	0.866	1.892
WFTS-321	3.000	570.208	0.117	1.489	66.833	0.037	82.941	9.678	0.014	0.739	0.755	2.377
WFTS-322	5.000	800.005	0.154	6.724	210.480	0.032	165.790	11.609	0.011	0.695	0.713	3.128
WFTS-323	2.000	376.602	0.074	0.715	8.609	0.053	92.193	8.852	0.018	0.818	0.831	0.780
WFTS-324	2.000	381.622	0.078	0.627	7.753	0.052	77.080	9.029	0.019	0.749	0.764	0.615
WFTS-325	1.000	63.407	0.010	0.205	11.436	0.057	59.013	2.297	0.022	0.907	0.911	2.542
WFTS-326	5.000	795.949	0.156	8.200	261.460	0.040	178.170	12.106	0.012	0.677	0.695	3.339
WFTS-327	1.000	188.339	0.037	0.119	2.912	0.071	66.216	6.611	0.027	0.854	0.864	1.182
WFTS-328	1.000	188.339	0.037	0.119	2.912	0.071	66.216	6.611	0.027	0.854	0.864	1.182

TAG	u (m/s)	Re (-)	C_{min} (W/K)	$\dot{W}''$ (W/m²)	ΔP (Pa)	f (-)	h (W/m².K)	Nu (-)	j (-)	η (-)	η_o (-)	NTU (-)
WFTS-329	1.000	188.339	0.037	0.119	2.912	0.071	66.216	6.611	0.027	0.854	0.864	1.182
WFTS-330	1.000	188.339	0.037	0.119	2.912	0.071	66.216	6.611	0.027	0.854	0.864	1.182
WFTS-331	2.000	318.709	0.063	0.696	10.039	0.051	94.718	7.650	0.019	0.815	0.826	0.954
WFTS-332	5.000	316.329	0.066	8.973	179.090	0.032	157.100	4.822	0.011	0.786	0.790	2.095
WFTS-333	5.000	316.329	0.066	8.973	179.090	0.032	157.100	4.822	0.011	0.786	0.790	2.095
WFTS-334	3.000	480.041	0.094	1.642	88.280	0.037	96.003	7.326	0.012	0.764	0.777	3.391
WFTS-335	3.000	480.041	0.094	1.642	88.280	0.037	96.003	7.326	0.012	0.764	0.777	3.391
WFTS-336	2.000	189.017	0.038	0.708	16.706	0.047	98.645	4.761	0.019	0.826	0.832	1.637
WFTS-337	2.000	63.822	0.010	1.852	74.294	0.023	87.146	1.707	0.011	0.911	0.915	2.703
WFTS-338	2.000	380.380	0.076	0.639	8.078	0.050	97.187	8.808	0.018	0.761	0.776	0.806
WFTS-339	5.000	159.576	0.046	20.031	504.240	0.059	163.030	2.481	0.010	0.774	0.777	2.694
WFTS-340	2.000	381.660	0.078	0.602	7.745	0.050	75.884	8.890	0.019	0.739	0.755	0.622
WFTS-341	5.000	956.146	0.192	5.966	169.120	0.031	190.130	14.857	0.012	0.644	0.666	3.033
WFTS-342	3.000	287.043	0.059	2.239	56.205	0.049	125.360	5.421	0.015	0.728	0.736	1.958
WFTS-343	3.000	575.399	0.116	1.535	72.711	0.037	110.090	9.654	0.013	0.728	0.745	3.284
WFTS-344	5.000	158.965	0.047	12.410	2099.000	0.037	27.860	0.510	0.002	0.937	0.937	3.734
WFTS-345	5.000	960.234	0.196	6.132	177.860	0.032	197.310	15.144	0.013	0.629	0.651	3.150
WFTS-346	5.000	960.044	0.196	6.174	179.140	0.033	198.800	15.201	0.013	0.627	0.649	3.163
WFTS-347	5.000	958.650	0.197	6.954	202.050	0.037	206.340	15.647	0.013	0.622	0.644	3.265
WFTS-348	5.000	959.030	0.197	6.442	187.760	0.034	202.610	15.377	0.013	0.622	0.645	3.218
WFTS-349	5.000	960.076	0.198	7.110	207.030	0.038	209.880	15.815	0.013	0.617	0.639	3.302
WFTS-350	5.000	954.688	0.200	9.065	265.930	0.048	224.690	16.545	0.014	0.605	0.628	3.501
WFTS-351	5.000	957.699	0.199	8.306	243.240	0.044	219.360	16.313	0.014	0.610	0.632	3.435
WFTS-352	5.000	959.379	0.199	7.640	224.100	0.041	216.150	16.098	0.014	0.610	0.632	3.389
WFTS-353	3.000	95.594	0.020	4.017	916.410	0.038	15.958	0.312	0.002	0.964	0.964	2.968
WFTS-354	1.000	63.952	0.010	0.174	11.163	0.048	52.500	2.061	0.020	0.900	0.904	2.578
WFTS-355	2.000	381.622	0.078	0.530	7.702	0.044	71.876	8.420	0.018	0.713	0.728	0.643
WFTS-356	5.000	473.145	0.087	5.637	94.878	0.023	110.410	6.414	0.010	0.661	0.671	1.055
WFTS-357	2.000	126.789	0.022	0.732	28.592	0.037	72.819	2.834	0.015	0.789	0.794	1.909
WFTS-358	2.000	63.875	0.010	1.561	75.838	0.019	75.208	1.475	0.010	0.893	0.897	2.770
WFTS-359	3.000	479.908	0.098	1.615	19.022	0.036	78.289	7.688	0.013	0.785	0.794	0.619
WFTS-360	3.000	95.881	0.020	3.322	917.070	0.034	13.592	0.267	0.002	0.956	0.957	3.034
WFTS-361	3.000	94.656	0.016	4.424	177.990	0.029	91.105	1.765	0.010	0.838	0.841	2.607
WFTS-362	3.000	94.656	0.016	4.424	177.990	0.029	91.105	1.765	0.010	0.838	0.841	2.607
WFTS-363	2.000	381.673	0.078	0.492	7.640	0.041	69.463	8.138	0.017	0.697	0.712	0.650
WFTS-364	5.000	159.076	0.031	16.806	406.160	0.024	128.960	2.519	0.008	0.798	0.802	2.114
WFTS-365	5.000	159.076	0.031	16.806	406.160	0.024	128.960	2.519	0.008	0.798	0.802	2.114
WFTS-366	3.000	575.532	0.118	1.307	74.129	0.032	76.996	9.068	0.013	0.677	0.693	2.557
WFTS-367	5.000	476.187	0.091	22.698	250.230	0.044	187.390	9.974	0.012	0.901	0.910	1.590
WFTS-368	3.000	286.112	0.058	2.820	56.105	0.041	117.640	5.772	0.014	0.829	0.838	1.658
WFTS-369	5.000	319.476	0.068	10.479	180.230	0.028	158.300	5.165	0.010	0.826	0.832	1.915
WFTS-370	3.000	573.307	0.144	1.469	65.767	0.036	78.420	9.200	0.013	0.733	0.750	2.224
WFTS-371	2.000	315.717	0.067	0.935	11.981	0.049	89.305	7.762	0.017	0.888	0.897	0.868
WFTS-372	2.000	316.402	0.067	0.906	12.008	0.050	91.350	7.695	0.017	0.856	0.867	0.888
WFTS-373	5.000	316.754	0.065	8.361	104.520	0.024	125.590	4.884	0.010	0.765	0.773	1.026
WFTS-374	5.000	159.101	0.046	21.806	496.540	0.049	156.360	2.509	0.010	0.819	0.822	2.473
WFTS-375	1.000	95.364	0.021	0.166	7.114	0.065	59.760	3.499	0.025	0.907	0.911	1.971
WFTS-376	1.000	95.960	0.021	0.152	6.859	0.064	58.071	3.421	0.025	0.876	0.882	1.947
WFTS-377	3.000	285.693	0.073	1.718	29.056	0.037	93.162	5.447	0.015	0.734	0.741	0.988
WFTS-378	3.000	191.990	0.046	2.360	56.963	0.037	115.390	3.621	0.013	0.794	0.799	1.880

TAG	u (m/s)	Re (-)	C_{min} (W/K)	$\dot{W}''$ (W/m^2)	ΔP (Pa)	f (-)	h ($W/m^2.K$)	Nu (-)	j (-)	η (-)	η_o (-)	NTU (-)
WFTS-379	2.000	189.157	0.043	0.702	18.093	0.043	95.090	4.425	0.017	0.794	0.801	1.661
WFTS-380	5.000	470.927	0.111	8.075	163.820	0.029	143.430	6.529	0.010	0.780	0.787	1.937
WFTS-381	1.000	31.893	0.006	0.478	37.062	0.030	51.390	1.006	0.012	0.931	0.934	3.145
WFTS-382	3.000	471.789	0.110	1.847	20.449	0.037	103.720	7.980	0.013	0.786	0.797	0.774
WFTS-383	5.000	792.875	0.184	6.136	229.880	0.028	157.840	10.257	0.010	0.650	0.668	3.337
WFTS-384	2.000	319.989	0.076	0.638	10.691	0.043	86.141	6.990	0.017	0.817	0.826	1.008
WFTS-385	1.000	191.064	0.046	0.103	3.021	0.060	62.533	6.132	0.025	0.826	0.836	1.295
WFTS-386	2.000	63.618	0.023	1.334	545.400	0.058	9.162	0.174	0.002	0.972	0.973	3.080
WFTS-387	5.000	157.089	0.055	8.550	2099.300	0.025	17.450	0.318	0.001	0.945	0.945	3.424
WFTS-388	5.000	157.669	0.055	16.044	491.030	0.047	128.680	1.882	0.008	0.753	0.756	2.515
WFTS-389	3.000	94.978	0.023	3.335	834.680	0.031	13.914	0.270	0.002	0.957	0.958	2.820
WFTS-390	3.000	191.457	0.037	2.202	52.171	0.023	98.077	3.843	0.012	0.758	0.766	1.505
WFTS-391	1.000	158.943	0.039	0.094	3.550	0.057	64.476	5.053	0.025	0.795	0.803	1.646
WFTS-392	1.000	158.442	0.039	0.092	3.491	0.057	65.989	5.012	0.025	0.771	0.781	1.656
WFTS-393	5.000	159.979	0.037	14.117	758.220	0.025	80.488	1.581	0.006	0.814	0.817	2.986
WFTS-394	1.000	189.436	0.047	0.091	2.923	0.057	64.028	5.934	0.025	0.787	0.797	1.389
WFTS-395	1.000	189.043	0.047	0.092	2.959	0.057	63.218	5.929	0.025	0.798	0.808	1.394
WFTS-396	3.000	479.490	0.123	1.810	22.614	0.039	95.427	7.397	0.012	0.781	0.790	0.796
WFTS-397	3.000	479.471	0.123	1.842	34.510	0.040	99.550	7.666	0.012	0.776	0.785	1.238
WFTS-398	1.000	31.741	0.006	0.355	31.909	0.022	42.088	0.820	0.009	0.924	0.928	2.968
WFTS-399	1.000	31.741	0.006	0.355	31.909	0.022	42.088	0.820	0.009	0.924	0.928	2.968
WFTS-400	1.000	31.741	0.006	0.355	31.909	0.022	42.088	0.820	0.009	0.924	0.928	2.968
WFTS-401	1.000	94.851	0.021	0.128	7.286	0.054	50.587	2.946	0.022	0.846	0.851	2.074
WFTS-402	5.000	786.727	0.198	5.590	245.320	0.029	173.630	10.022	0.010	0.581	0.598	3.849
WFTS-403	2.000	191.489	0.045	0.602	18.010	0.037	71.136	4.181	0.016	0.773	0.780	1.403
WFTS-404	1.000	191.945	0.048	0.084	2.771	0.055	66.459	5.914	0.025	0.743	0.755	1.399
WFTS-405	5.000	960.203	0.242	4.546	165.990	0.024	191.290	13.108	0.011	0.561	0.581	3.432
WFTS-406	5.000	958.903	0.243	4.983	182.210	0.026	197.130	13.384	0.011	0.556	0.577	3.515
WFTS-407	5.000	955.639	0.243	5.422	198.950	0.029	202.850	13.623	0.012	0.552	0.572	3.602
WFTS-408	1.000	31.782	0.007	0.346	256.370	0.051	4.611	0.090	0.001	0.988	0.988	2.858
WFTS-409	1.000	31.782	0.007	0.346	256.370	0.051	4.611	0.090	0.001	0.988	0.988	2.858
WFTS-410	3.000	95.985	0.024	4.061	404.030	0.036	43.410	0.853	0.005	0.864	0.866	3.163
WFTS-411	5.000	798.896	0.201	4.804	222.010	0.025	100.540	9.862	0.010	0.564	0.580	2.278
WFTS-412	3.000	282.385	0.071	1.304	30.404	0.027	78.116	4.514	0.012	0.678	0.685	1.055
WFTS-413	3.000	190.640	0.037	1.866	52.781	0.020	88.609	3.457	0.011	0.713	0.722	1.529
WFTS-414	1.000	191.305	0.049	0.084	3.066	0.052	47.686	5.601	0.023	0.805	0.813	1.196
WFTS-415	5.000	158.531	0.034	14.608	588.820	0.016	111.490	2.170	0.007	0.812	0.816	3.100
WFTS-416	5.000	158.391	0.041	8.871	1585.000	0.017	22.456	0.437	0.002	0.929	0.930	3.155
WFTS-417	2.000	382.560	0.097	0.408	7.775	0.034	61.939	7.274	0.015	0.637	0.652	0.650
WFTS-418	2.000	127.626	0.024	0.814	30.678	0.019	75.803	2.970	0.012	0.790	0.798	1.929
WFTS-419	5.000	799.181	0.201	3.995	36.673	0.021	81.233	7.971	0.008	0.578	0.592	0.373
WFTS-420	1.000	31.460	0.008	0.260	228.310	0.042	3.999	0.077	0.001	0.985	0.985	2.927

8.3.1.3Round Finless Tube Surface (RFTS)

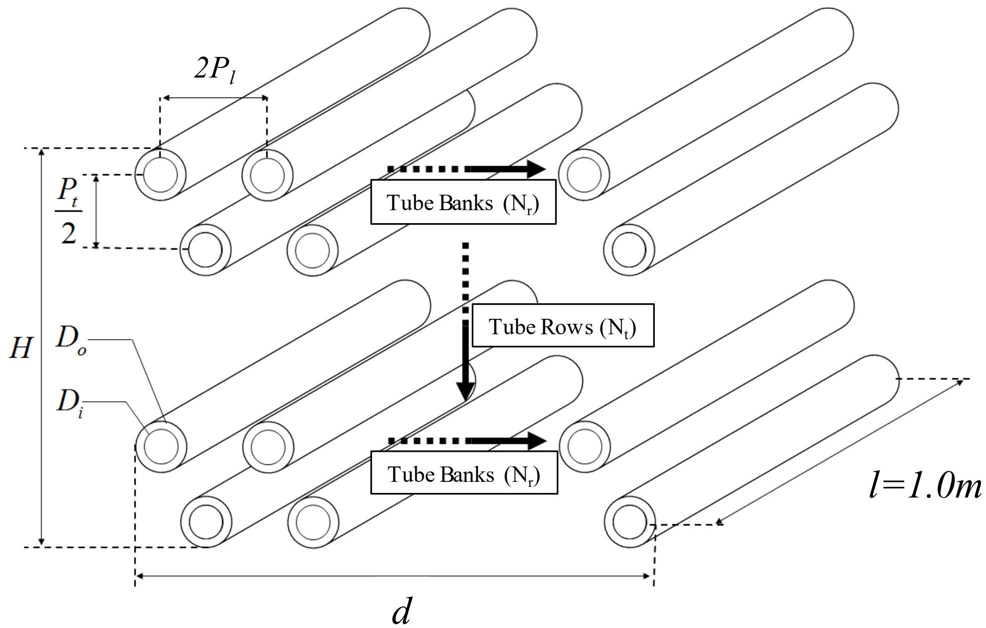

Figure 145. RFTS Segment.

Table 52. RFTS Optimum designs dimensions.

TAG	Type (-)	D_o (mm)	P_l/D_o (-)	P_t/D_o (-)	P_t/P_l (-)	N_t (-)	σ (-)	D_h (mm)	d (mm)	A_f (m^2)	A_c (m^2)	A_o (m^2)	A_o/V (cm^2/cm^3)
RFTS-001	1	0.50	1.37	1.58	1.15	4	0.37	0.50	2.73	7.9E-04	2.9E-04	6.3E-03	29.11
RFTS-002	1	0.50	1.37	1.58	1.15	4	0.37	0.50	2.73	7.9E-04	2.9E-04	6.3E-03	29.11
RFTS-003	1	0.50	1.37	1.58	1.15	4	0.37	0.50	2.73	7.9E-04	2.9E-04	6.3E-03	29.11
RFTS-004	1	0.50	1.36	1.57	1.15	4	0.36	0.50	2.73	7.9E-04	2.9E-04	6.3E-03	29.30
RFTS-005	1	0.50	1.36	1.57	1.15	3	0.36	0.50	2.04	7.9E-04	2.9E-04	4.7E-03	29.30
RFTS-006	1	0.50	1.36	1.57	1.15	2	0.36	0.50	1.36	7.9E-04	2.9E-04	3.1E-03	29.30
RFTS-007	1	0.50	1.37	1.58	1.15	4	0.37	0.50	2.73	7.9E-04	2.9E-04	6.3E-03	29.11

TAG	Type (-)	D_o (mm)	P_l/D_o (-)	P_t/D_o (-)	P_t/P_l (-)	N_t (-)	σ (-)	D_h (mm)	d (mm)	A_f (m^2)	A_c (m^2)	A_o (m^2)	A_o/V (cm^2/cm^3)
RFTS-008	1	0.50	1.37	1.58	1.15	4	0.37	0.50	2.73	7.9E-04	2.9E-04	6.3E-03	29.11
RFTS-009	1	0.50	1.37	1.58	1.15	3	0.37	0.50	2.05	7.9E-04	2.9E-04	4.7E-03	29.11
RFTS-010	1	0.50	1.37	1.58	1.15	3	0.37	0.50	2.05	7.9E-04	2.9E-04	4.7E-03	29.11
RFTS-011	1	0.50	1.36	1.57	1.15	3	0.36	0.50	2.04	7.9E-04	2.9E-04	4.7E-03	29.30
RFTS-012	1	0.50	1.36	1.57	1.15	3	0.36	0.50	2.04	7.9E-04	2.9E-04	4.7E-03	29.30
RFTS-013	1	0.50	1.36	1.57	1.15	3	0.36	0.50	2.04	7.9E-04	2.9E-04	4.7E-03	29.30
RFTS-014	1	0.50	1.37	1.58	1.15	2	0.37	0.50	1.37	7.9E-04	2.9E-04	3.1E-03	29.11
RFTS-015	1	0.50	1.37	1.58	1.15	2	0.37	0.50	1.37	7.9E-04	2.9E-04	3.1E-03	29.11
RFTS-016	1	0.50	1.36	1.57	1.15	2	0.36	0.50	1.36	7.9E-04	2.9E-04	3.1E-03	29.30
RFTS-017	1	0.50	1.37	1.58	1.15	3	0.37	0.50	2.05	7.9E-04	2.9E-04	4.7E-03	29.11
RFTS-018	1	0.50	1.37	1.58	1.15	3	0.37	0.50	2.05	7.9E-04	2.9E-04	4.7E-03	29.21
RFTS-019	1	0.50	1.37	1.58	1.15	3	0.37	0.50	2.05	7.9E-04	2.9E-04	4.7E-03	29.21
RFTS-020	1	0.50	1.37	1.58	1.15	3	0.37	0.50	2.05	7.9E-04	2.9E-04	4.7E-03	29.21
RFTS-021	1	0.50	1.37	1.58	1.15	3	0.37	0.50	2.05	7.9E-04	2.9E-04	4.7E-03	29.21
RFTS-022	1	0.50	1.37	1.58	1.15	2	0.37	0.50	1.37	7.9E-04	2.9E-04	3.1E-03	29.11
RFTS-023	1	0.50	1.37	1.58	1.15	2	0.37	0.50	1.37	7.9E-04	2.9E-04	3.1E-03	29.11
RFTS-024	1	0.50	1.37	1.58	1.15	2	0.37	0.50	1.37	7.9E-04	2.9E-04	3.1E-03	29.11
RFTS-025	1	0.50	1.37	1.58	1.15	2	0.37	0.50	1.37	7.9E-04	2.9E-04	3.1E-03	29.11
RFTS-026	1	0.50	1.36	1.57	1.15	2	0.36	0.50	1.36	7.9E-04	2.9E-04	3.1E-03	29.30
RFTS-027	1	0.50	1.37	1.58	1.15	40	0.37	0.50	27.34	7.9E-04	2.9E-04	6.3E-02	29.11
RFTS-028	1	0.50	1.36	1.57	1.15	40	0.36	0.50	27.26	7.9E-04	2.9E-04	6.3E-02	29.30
RFTS-029	1	0.50	1.36	1.57	1.15	40	0.36	0.50	27.26	7.9E-04	2.9E-04	6.3E-02	29.30
RFTS-030	1	0.50	1.37	1.58	1.15	5	0.37	0.50	3.42	7.9E-04	2.9E-04	7.9E-03	29.11
RFTS-031	1	0.50	1.37	1.58	1.15	5	0.37	0.50	3.42	7.9E-04	2.9E-04	7.9E-03	29.11
RFTS-032	1	0.50	1.37	1.58	1.15	5	0.37	0.50	3.42	7.9E-04	2.9E-04	7.9E-03	29.11
RFTS-033	1	0.50	1.37	1.58	1.15	5	0.37	0.50	3.42	7.9E-04	2.9E-04	7.9E-03	29.11
RFTS-034	1	0.50	1.37	1.58	1.15	3	0.37	0.50	2.05	7.9E-04	2.9E-04	4.7E-03	29.11
RFTS-035	1	0.50	1.36	1.57	1.15	3	0.36	0.50	2.04	7.9E-04	2.9E-04	4.7E-03	29.30
RFTS-036	1	0.50	1.36	1.57	1.15	2	0.36	0.50	1.36	7.9E-04	2.9E-04	3.1E-03	29.30
RFTS-037	1	0.50	1.68	1.94	1.15	5	0.49	1.01	4.20	9.7E-04	4.7E-04	7.9E-03	19.24
RFTS-038	1	0.50	1.68	1.94	1.15	4	0.49	1.01	3.36	9.7E-04	4.7E-04	6.3E-03	19.24
RFTS-039	1	0.50	1.68	1.93	1.15	4	0.48	1.00	3.35	9.7E-04	4.7E-04	6.3E-03	19.39
RFTS-040	1	0.50	1.68	1.94	1.15	3	0.49	1.01	2.52	9.7E-04	4.7E-04	4.7E-03	19.24
RFTS-041	1	0.50	1.68	1.94	1.15	3	0.49	1.01	2.52	9.7E-04	4.7E-04	4.7E-03	19.24
RFTS-042	1	0.50	1.68	1.93	1.15	3	0.48	1.00	2.51	9.7E-04	4.7E-04	4.7E-03	19.39
RFTS-043	1	0.50	1.68	1.93	1.15	3	0.48	1.00	2.51	9.7E-04	4.7E-04	4.7E-03	19.39
RFTS-044	1	0.50	1.68	1.94	1.15	2	0.49	1.01	1.68	9.7E-04	4.7E-04	3.1E-03	19.24
RFTS-045	1	0.50	1.68	1.94	1.15	2	0.49	1.01	1.68	9.7E-04	4.7E-04	3.1E-03	19.24
RFTS-046	1	0.50	1.68	1.93	1.15	2	0.48	1.00	1.68	9.7E-04	4.7E-04	3.1E-03	19.39
RFTS-047	1	0.50	1.68	1.94	1.15	4	0.49	1.01	3.36	9.7E-04	4.7E-04	6.3E-03	19.24
RFTS-048	1	0.50	1.68	1.93	1.15	4	0.48	1.00	3.35	9.7E-04	4.7E-04	6.3E-03	19.39
RFTS-049	1	0.50	1.68	1.94	1.15	3	0.49	1.01	2.52	9.7E-04	4.7E-04	4.7E-03	19.24
RFTS-050	1	0.50	1.68	1.94	1.15	3	0.49	1.01	2.52	9.7E-04	4.7E-04	4.7E-03	19.24
RFTS-051	1	0.50	1.67	1.93	1.15	3	0.48	0.99	2.51	9.7E-04	4.7E-04	4.7E-03	19.44
RFTS-052	1	0.50	1.67	1.93	1.15	3	0.48	0.99	2.51	9.7E-04	4.7E-04	4.7E-03	19.44
RFTS-053	1	0.50	1.67	1.93	1.15	3	0.48	0.99	2.51	9.7E-04	4.7E-04	4.7E-03	19.44
RFTS-054	1	0.50	1.68	1.94	1.15	2	0.49	1.01	1.68	9.7E-04	4.7E-04	3.1E-03	19.24
RFTS-055	1	0.50	1.68	1.94	1.15	2	0.49	1.01	1.68	9.7E-04	4.7E-04	3.1E-03	19.24
RFTS-056	1	0.50	1.67	1.93	1.15	2	0.48	0.99	1.67	9.7E-04	4.7E-04	3.1E-03	19.44
RFTS-057	1	0.50	1.68	1.94	1.15	4	0.49	1.01	3.36	9.7E-04	4.7E-04	6.3E-03	19.24

TAG	Type (-)	D_o (mm)	P_l/D_o (-)	P_t/D_o (-)	P_t/P_l (-)	N_t (-)	σ (-)	D_h (mm)	d (mm)	A_f (m^2)	A_c (m^2)	A_o (m^2)	A_o/V (cm^2/cm^3)
RFTS-058	1	0.50	1.68	1.94	1.15	4	0.48	1.00	3.35	9.7E-04	4.7E-04	6.3E-03	19.34
RFTS-059	1	0.50	1.68	1.94	1.15	3	0.49	1.01	2.52	9.7E-04	4.7E-04	4.7E-03	19.24
RFTS-060	1	0.50	1.68	1.94	1.15	3	0.49	1.01	2.52	9.7E-04	4.7E-04	4.7E-03	19.24
RFTS-061	1	0.50	1.67	1.93	1.15	3	0.48	0.99	2.51	9.7E-04	4.7E-04	4.7E-03	19.44
RFTS-062	1	0.50	1.67	1.93	1.15	3	0.48	0.99	2.51	9.7E-04	4.7E-04	4.7E-03	19.44
RFTS-063	1	0.50	1.68	1.94	1.15	2	0.49	1.01	1.68	9.7E-04	4.7E-04	3.1E-03	19.24
RFTS-064	1	0.50	1.68	1.94	1.15	2	0.49	1.01	1.68	9.7E-04	4.7E-04	3.1E-03	19.24
RFTS-065	1	0.50	1.68	1.94	1.15	2	0.49	1.01	1.68	9.7E-04	4.7E-04	3.1E-03	19.24
RFTS-066	1	0.50	1.67	1.93	1.15	2	0.48	0.99	1.67	9.7E-04	4.7E-04	3.1E-03	19.44
RFTS-067	1	2.00	1.35	1.29	0.95	40	0.22	0.99	108.26	2.6E-03	5.8E-04	2.5E-01	9.01
RFTS-068	1	2.00	1.33	1.30	0.97	40	0.23	1.00	106.51	2.6E-03	5.9E-04	2.5E-01	9.11
RFTS-069	1	2.00	1.65	1.24	0.75	40	0.19	1.00	132.34	2.5E-03	4.8E-04	2.5E-01	7.67
RFTS-070	1	2.00	1.65	1.24	0.75	40	0.19	1.00	132.34	2.5E-03	4.8E-04	2.5E-01	7.67
RFTS-071	1	2.00	1.30	1.30	1.00	40	0.23	1.01	103.88	2.6E-03	6.1E-04	2.5E-01	9.28
RFTS-072	1	2.00	1.30	1.30	1.00	40	0.23	1.01	103.88	2.6E-03	6.1E-04	2.5E-01	9.28
RFTS-073	1	2.00	1.74	1.23	0.70	40	0.19	1.01	139.35	2.5E-03	4.5E-04	2.5E-01	7.35
RFTS-074	1	0.50	1.68	1.94	1.15	4	0.49	1.01	3.36	9.7E-04	4.7E-04	6.3E-03	19.24
RFTS-075	1	0.50	1.68	1.94	1.15	4	0.49	1.01	3.36	9.7E-04	4.7E-04	6.3E-03	19.24
RFTS-076	1	0.50	1.68	1.94	1.15	3	0.49	1.01	2.52	9.7E-04	4.7E-04	4.7E-03	19.24
RFTS-077	1	0.50	1.68	1.94	1.15	3	0.48	1.00	2.52	9.7E-04	4.7E-04	4.7E-03	19.29
RFTS-078	1	0.50	1.67	1.93	1.15	3	0.48	0.99	2.51	9.7E-04	4.7E-04	4.7E-03	19.44
RFTS-079	1	0.50	1.67	1.93	1.15	3	0.48	0.99	2.51	9.7E-04	4.7E-04	4.7E-03	19.44
RFTS-080	1	0.50	1.68	1.94	1.15	2	0.49	1.01	1.68	9.7E-04	4.7E-04	3.1E-03	19.24
RFTS-081	1	0.50	1.68	1.94	1.15	2	0.49	1.01	1.68	9.7E-04	4.7E-04	3.1E-03	19.24
RFTS-082	1	0.50	1.68	1.94	1.15	2	0.49	1.01	1.68	9.7E-04	4.7E-04	3.1E-03	19.24
RFTS-083	1	0.50	1.67	1.93	1.15	2	0.48	0.99	1.67	9.7E-04	4.7E-04	3.1E-03	19.44
RFTS-084	1	2.00	1.53	1.39	0.90	40	0.28	1.51	122.71	2.8E-03	7.7E-04	2.5E-01	7.39
RFTS-085	1	0.50	1.93	2.23	1.15	4	0.55	1.51	3.86	1.1E-03	6.2E-04	6.3E-03	14.57
RFTS-086	1	0.50	1.93	2.23	1.15	4	0.55	1.51	3.86	1.1E-03	6.2E-04	6.3E-03	14.57
RFTS-087	1	0.50	1.93	2.23	1.15	3	0.55	1.51	2.90	1.1E-03	6.2E-04	4.7E-03	14.57
RFTS-088	1	0.50	1.93	2.22	1.15	3	0.55	1.50	2.89	1.1E-03	6.1E-04	4.7E-03	14.67
RFTS-089	1	0.50	1.92	2.22	1.15	3	0.55	1.49	2.88	1.1E-03	6.1E-04	4.7E-03	14.74
RFTS-090	1	0.50	1.92	2.22	1.15	3	0.55	1.49	2.88	1.1E-03	6.1E-04	4.7E-03	14.74
RFTS-091	1	0.50	1.93	2.23	1.15	2	0.55	1.51	1.93	1.1E-03	6.2E-04	3.1E-03	14.57
RFTS-092	1	0.50	1.93	2.23	1.15	2	0.55	1.51	1.93	1.1E-03	6.2E-04	3.1E-03	14.57
RFTS-093	1	0.50	1.93	2.23	1.15	2	0.55	1.51	1.93	1.1E-03	6.2E-04	3.1E-03	14.57
RFTS-094	1	0.50	1.92	2.22	1.15	2	0.55	1.49	1.92	1.1E-03	6.1E-04	3.1E-03	14.77
RFTS-095	1	0.50	2.33	2.69	1.15	25	0.63	2.51	29.13	1.3E-03	8.5E-04	3.9E-02	10.02
RFTS-096	1	0.50	2.33	2.69	1.15	25	0.63	2.50	29.08	1.3E-03	8.4E-04	3.9E-02	10.06
RFTS-097	1	0.50	2.33	2.69	1.15	25	0.63	2.50	29.08	1.3E-03	8.4E-04	3.9E-02	10.06
RFTS-098	1	0.50	2.33	2.70	1.15	5	0.63	2.52	5.84	1.3E-03	8.5E-04	7.9E-03	9.98
RFTS-099	1	0.50	2.33	2.70	1.15	5	0.63	2.52	5.84	1.3E-03	8.5E-04	7.9E-03	9.98
RFTS-100	1	0.50	2.33	2.70	1.15	5	0.63	2.52	5.84	1.3E-03	8.5E-04	7.9E-03	9.98
RFTS-101	1	0.50	2.33	2.69	1.15	4	0.63	2.50	4.65	1.3E-03	8.4E-04	6.3E-03	10.06
RFTS-102	1	0.50	2.33	2.69	1.15	3	0.63	2.50	3.49	1.3E-03	8.4E-04	4.7E-03	10.06
RFTS-103	1	0.50	2.33	2.70	1.15	2	0.63	2.52	2.33	1.3E-03	8.5E-04	3.1E-03	9.98
RFTS-104	1	0.50	2.33	2.69	1.15	2	0.63	2.50	2.33	1.3E-03	8.4E-04	3.1E-03	10.06
RFTS-105	1	0.50	2.33	2.69	1.15	25	0.63	2.51	29.13	1.3E-03	8.5E-04	3.9E-02	10.02
RFTS-106	1	0.50	2.32	2.68	1.15	25	0.63	2.48	28.99	1.3E-03	8.4E-04	3.9E-02	10.11
RFTS-107	1	0.50	2.32	2.68	1.15	25	0.63	2.48	28.99	1.3E-03	8.4E-04	3.9E-02	10.11

TAG	Type (-)	D_o (mm)	P_l/D_o (-)	P_t/D_o (-)	P_t/P_l (-)	N_t (-)	σ (-)	D_h (mm)	d (mm)	A_f (m^2)	A_c (m^2)	A_o (m^2)	A_o/V (cm^2/cm^3)
RFTS-108	1	0.50	2.32	2.68	1.15	25	0.63	2.48	28.99	1.3E-03	8.4E-04	3.9E-02	10.11
RFTS-109	1	0.50	2.33	2.69	1.15	4	0.63	2.52	4.67	1.3E-03	8.5E-04	6.3E-03	10.00
RFTS-110	1	0.50	2.33	2.69	1.15	4	0.63	2.52	4.67	1.3E-03	8.5E-04	6.3E-03	10.00
RFTS-111	1	0.50	2.33	2.69	1.15	4	0.63	2.52	4.67	1.3E-03	8.5E-04	6.3E-03	10.00
RFTS-112	1	0.50	2.33	2.69	1.15	4	0.63	2.50	4.66	1.3E-03	8.4E-04	6.3E-03	10.04
RFTS-113	1	0.50	2.32	2.68	1.15	4	0.63	2.48	4.64	1.3E-03	8.4E-04	6.3E-03	10.11
RFTS-114	1	0.50	2.32	2.68	1.15	3	0.63	2.48	3.48	1.3E-03	8.4E-04	4.7E-03	10.11
RFTS-115	1	0.50	2.33	2.69	1.15	25	0.63	2.52	29.16	1.3E-03	8.5E-04	3.9E-02	10.00
RFTS-116	1	0.50	2.33	2.69	1.15	25	0.63	2.50	29.10	1.3E-03	8.4E-04	3.9E-02	10.04
RFTS-117	1	0.50	2.33	2.69	1.15	25	0.63	2.50	29.10	1.3E-03	8.4E-04	3.9E-02	10.04
RFTS-118	1	0.50	2.33	2.69	1.15	4	0.63	2.52	4.67	1.3E-03	8.5E-04	6.3E-03	10.00
RFTS-119	1	0.50	2.33	2.69	1.15	4	0.63	2.52	4.67	1.3E-03	8.5E-04	6.3E-03	10.00
RFTS-120	1	0.50	2.33	2.69	1.15	4	0.63	2.50	4.65	1.3E-03	8.4E-04	6.3E-03	10.06
RFTS-121	1	0.50	2.32	2.68	1.15	3	0.63	2.48	3.48	1.3E-03	8.4E-04	4.7E-03	10.11
RFTS-122	1	0.50	2.32	2.68	1.15	3	0.63	2.48	3.48	1.3E-03	8.4E-04	4.7E-03	10.11
RFTS-123	1	0.50	2.33	2.69	1.15	2	0.63	2.52	2.33	1.3E-03	8.5E-04	3.1E-03	10.00
RFTS-124	1	0.50	2.32	2.68	1.15	2	0.63	2.49	2.32	1.3E-03	8.4E-04	3.1E-03	10.08
RFTS-125	1	0.50	2.33	2.70	1.15	3	0.63	2.52	3.50	1.3E-03	8.5E-04	4.7E-03	9.98
RFTS-126	1	0.50	2.32	2.68	1.15	3	0.63	2.48	3.48	1.3E-03	8.4E-04	4.7E-03	10.09
RFTS-127	1	0.50	2.32	2.68	1.15	3	0.63	2.48	3.48	1.3E-03	8.4E-04	4.7E-03	10.09
RFTS-128	1	0.50	2.32	2.68	1.15	3	0.63	2.48	3.48	1.3E-03	8.4E-04	4.7E-03	10.09
RFTS-129	1	0.50	2.33	2.69	1.15	2	0.63	2.52	2.33	1.3E-03	8.5E-04	3.1E-03	10.00
RFTS-130	1	0.50	2.33	2.69	1.15	2	0.63	2.52	2.33	1.3E-03	8.5E-04	3.1E-03	10.00
RFTS-131	1	0.50	2.33	2.69	1.15	2	0.63	2.50	2.33	1.3E-03	8.4E-04	3.1E-03	10.06
RFTS-132	1	0.50	2.33	2.69	1.15	2	0.63	2.50	2.33	1.3E-03	8.4E-04	3.1E-03	10.06
RFTS-133	1	0.50	2.33	2.69	1.15	10	0.63	2.52	11.66	1.3E-03	8.5E-04	1.6E-02	10.00
RFTS-134	1	0.50	2.33	2.69	1.15	10	0.63	2.50	11.63	1.3E-03	8.4E-04	1.6E-02	10.06
RFTS-135	1	0.50	2.51	2.90	1.15	25	0.65	3.03	31.36	1.4E-03	9.5E-04	3.9E-02	8.65
RFTS-136	1	0.50	2.49	2.88	1.15	25	0.65	2.98	31.14	1.4E-03	9.4E-04	3.9E-02	8.77
RFTS-137	1	0.50	2.49	2.88	1.15	25	0.65	2.98	31.14	1.4E-03	9.4E-04	3.9E-02	8.77
RFTS-138	1	0.50	2.50	2.89	1.15	4	0.65	3.02	5.01	1.4E-03	9.5E-04	6.3E-03	8.68
RFTS-139	1	0.50	2.50	2.89	1.15	4	0.65	3.02	5.01	1.4E-03	9.5E-04	6.3E-03	8.68
RFTS-140	1	0.50	2.50	2.89	1.15	4	0.65	3.02	5.01	1.4E-03	9.5E-04	6.3E-03	8.68
RFTS-141	1	0.50	2.49	2.88	1.15	4	0.65	2.98	4.98	1.4E-03	9.4E-04	6.3E-03	8.77
RFTS-142	1	0.50	2.49	2.88	1.15	3	0.65	2.98	3.74	1.4E-03	9.4E-04	4.7E-03	8.75
RFTS-143	1	0.50	2.51	2.90	1.15	2	0.65	3.03	2.51	1.4E-03	9.5E-04	3.1E-03	8.65
RFTS-144	1	0.50	2.49	2.88	1.15	2	0.65	2.98	2.49	1.4E-03	9.4E-04	3.1E-03	8.77
RFTS-145	1	0.50	2.50	2.88	1.15	4	0.65	3.00	5.00	1.4E-03	9.4E-04	6.3E-03	8.72
RFTS-146	1	0.50	2.49	2.88	1.15	4	0.65	2.98	4.99	1.4E-03	9.4E-04	6.3E-03	8.75
RFTS-147	1	0.50	2.50	2.89	1.15	3	0.65	3.02	3.76	1.4E-03	9.5E-04	4.7E-03	8.68
RFTS-148	1	0.50	2.50	2.88	1.15	3	0.65	2.99	3.74	1.4E-03	9.4E-04	4.7E-03	8.74
RFTS-149	1	0.50	2.49	2.88	1.15	3	0.65	2.98	3.74	1.4E-03	9.4E-04	4.7E-03	8.75
RFTS-150	1	0.50	2.49	2.88	1.15	3	0.65	2.98	3.74	1.4E-03	9.4E-04	4.7E-03	8.75
RFTS-151	1	0.50	2.51	2.90	1.15	2	0.65	3.03	2.51	1.4E-03	9.5E-04	3.1E-03	8.65
RFTS-152	1	0.50	2.51	2.90	1.15	2	0.65	3.03	2.51	1.4E-03	9.5E-04	3.1E-03	8.65
RFTS-153	1	0.50	2.51	2.90	1.15	2	0.65	3.03	2.51	1.4E-03	9.5E-04	3.1E-03	8.65
RFTS-154	1	0.50	2.49	2.88	1.15	2	0.65	2.98	2.49	1.4E-03	9.4E-04	3.1E-03	8.75
RFTS-155	1	0.50	2.51	2.90	1.15	25	0.65	3.03	31.36	1.4E-03	9.5E-04	3.9E-02	8.65
RFTS-156	1	0.50	2.49	2.88	1.15	25	0.65	2.98	31.14	1.4E-03	9.4E-04	3.9E-02	8.77
RFTS-157	1	0.50	2.49	2.88	1.15	25	0.65	2.98	31.14	1.4E-03	9.4E-04	3.9E-02	8.77

TAG	Type (-)	D_o (mm)	P_l/D_o (-)	P_t/D_o (-)	P_t/P_l (-)	N_t (-)	σ (-)	D_h (mm)	d (mm)	A_f (m^2)	A_c (m^2)	A_o (m^2)	A_o/V (cm^2/cm^3)
RFTS-158	1	0.50	2.51	2.89	1.15	4	0.65	3.02	5.01	1.4E-03	9.5E-04	6.3E-03	8.66
RFTS-159	1	0.50	2.50	2.89	1.15	4	0.65	3.00	5.00	1.4E-03	9.4E-04	6.3E-03	8.71
RFTS-160	1	0.50	2.51	2.90	1.15	3	0.65	3.03	3.76	1.4E-03	9.5E-04	4.7E-03	8.65
RFTS-161	1	0.50	2.49	2.88	1.15	3	0.65	2.98	3.74	1.4E-03	9.4E-04	4.7E-03	8.77
RFTS-162	1	0.50	2.49	2.88	1.15	3	0.65	2.98	3.74	1.4E-03	9.4E-04	4.7E-03	8.77
RFTS-163	1	0.50	2.51	2.90	1.15	2	0.65	3.03	2.51	1.4E-03	9.5E-04	3.1E-03	8.65
RFTS-164	1	0.50	2.49	2.88	1.15	2	0.65	2.98	2.49	1.4E-03	9.4E-04	3.1E-03	8.77
RFTS-165	1	0.50	2.51	2.90	1.15	3	0.65	3.03	3.76	1.4E-03	9.5E-04	4.7E-03	8.65
RFTS-166	1	0.50	2.49	2.88	1.15	3	0.65	2.98	3.74	1.4E-03	9.4E-04	4.7E-03	8.77
RFTS-167	1	0.50	2.49	2.88	1.15	3	0.65	2.98	3.74	1.4E-03	9.4E-04	4.7E-03	8.77
RFTS-168	1	0.50	2.51	2.89	1.15	2	0.65	3.02	2.51	1.4E-03	9.5E-04	3.1E-03	8.66
RFTS-169	1	0.50	2.49	2.88	1.15	2	0.65	2.98	2.49	1.4E-03	9.4E-04	3.1E-03	8.77
RFTS-170	1	0.50	2.51	2.90	1.15	9	0.65	3.03	11.29	1.4E-03	9.5E-04	1.4E-02	8.65
RFTS-171	1	0.50	2.50	2.89	1.15	9	0.65	3.00	11.25	1.4E-03	9.4E-04	1.4E-02	8.71
RFTS-172	1	0.50	2.49	2.88	1.15	9	0.65	2.98	11.21	1.4E-03	9.4E-04	1.4E-02	8.77
RFTS-173	1	0.50	2.51	2.90	1.15	10	0.65	3.03	12.54	1.4E-03	9.5E-04	1.6E-02	8.65
RFTS-174	1	0.50	2.49	2.88	1.15	10	0.65	2.98	12.46	1.4E-03	9.4E-04	1.6E-02	8.77

Table 53. RFTS optimum designs performance.

TAG	u (m/s)	Re (-)	C_{min} (W/K)	$\dot{W}''$ (W/m^2)	ΔP (Pa)	f (-)	NTU (-)	h ($W/m^2.K$)	Nu (-)	j (-)
RFTS-001	1.000	86.453	0.001	3.273	26.051	0.274	2.720	404.240	7.923	0.101
RFTS-002	1.000	86.453	0.001	3.273	26.051	0.274	2.720	404.240	7.923	0.101
RFTS-003	1.000	86.453	0.001	3.273	26.051	0.274	2.720	404.240	7.923	0.101
RFTS-004	1.000	86.940	0.001	3.318	26.498	0.273	2.738	405.600	7.854	0.100
RFTS-005	1.000	86.940	0.001	3.409	20.416	0.281	2.198	434.060	8.405	0.107
RFTS-006	1.000	86.940	0.001	3.599	14.371	0.296	1.635	484.440	9.381	0.120
RFTS-007	3.000	259.360	0.003	65.509	173.820	0.203	1.333	594.280	11.647	0.049
RFTS-008	3.000	259.360	0.003	65.509	173.820	0.203	1.333	594.280	11.647	0.049
RFTS-009	3.000	259.360	0.003	65.966	131.270	0.204	1.047	622.500	12.200	0.052
RFTS-010	3.000	259.360	0.003	65.966	131.270	0.204	1.047	622.500	12.200	0.052
RFTS-011	3.000	260.820	0.003	66.862	133.490	0.204	1.054	624.620	12.095	0.052
RFTS-012	3.000	260.820	0.003	66.862	133.490	0.204	1.054	624.620	12.095	0.052
RFTS-013	3.000	260.820	0.003	66.862	133.490	0.204	1.054	624.620	12.095	0.052
RFTS-014	3.000	259.360	0.003	67.658	89.759	0.210	0.756	674.220	13.214	0.056
RFTS-015	3.000	259.360	0.003	67.658	89.759	0.210	0.756	674.220	13.214	0.056
RFTS-016	3.000	260.820	0.003	68.568	91.261	0.209	0.761	676.590	13.101	0.056
RFTS-017	5.000	432.270	0.005	263.790	314.960	0.177	0.750	743.180	14.566	0.037
RFTS-018	5.000	433.500	0.005	265.550	317.590	0.176	0.753	744.420	14.501	0.037
RFTS-019	5.000	433.500	0.005	265.550	317.590	0.176	0.753	744.420	14.501	0.037
RFTS-020	5.000	433.500	0.005	265.550	317.590	0.176	0.753	744.420	14.501	0.037
RFTS-021	5.000	433.500	0.005	265.550	317.590	0.176	0.753	744.420	14.501	0.037
RFTS-022	5.000	432.270	0.005	266.840	212.400	0.179	0.533	791.520	15.513	0.039
RFTS-023	5.000	432.270	0.005	266.840	212.400	0.179	0.533	791.520	15.513	0.039
RFTS-024	5.000	432.270	0.005	266.840	212.400	0.179	0.533	791.520	15.513	0.039
RFTS-025	5.000	432.270	0.005	266.840	212.400	0.179	0.533	791.520	15.513	0.039

TAG	u (m/s)	Re (-)	C_{min} (W/K)	$\dot{W}''$ (W/m²)	ΔP (Pa)	f (-)	NTU (-)	h (W/m².K)	Nu (-)	j (-)
RFTS-026	5.000	434.700	0.005	270.380	215.920	0.178	0.536	794.230	15.379	0.039
RFTS-027	2.000	172.910	0.002	20.987	835.280	0.220	10.252	304.690	5.972	0.038
RFTS-028	2.000	173.880	0.002	21.274	849.440	0.219	10.314	305.550	5.917	0.038
RFTS-029	2.000	173.880	0.002	21.274	849.440	0.219	10.314	305.550	5.917	0.038
RFTS-030	2.000	172.910	0.002	21.602	107.470	0.226	2.085	495.840	9.718	0.062
RFTS-031	2.000	172.910	0.002	21.602	107.470	0.226	2.085	495.840	9.718	0.062
RFTS-032	2.000	172.910	0.002	21.602	107.470	0.226	2.085	495.840	9.718	0.062
RFTS-033	2.000	172.910	0.002	21.602	107.470	0.226	2.085	495.840	9.718	0.062
RFTS-034	2.000	172.910	0.002	21.972	65.586	0.230	1.369	542.510	10.633	0.068
RFTS-035	2.000	173.880	0.002	22.273	66.700	0.229	1.378	544.380	10.541	0.067
RFTS-036	2.000	173.880	0.002	23.091	46.100	0.238	1.008	596.920	11.559	0.074
RFTS-037	1.000	65.340	0.001	1.654	13.378	0.321	2.204	322.330	12.646	0.106
RFTS-038	1.000	65.340	0.001	1.670	10.808	0.324	1.830	334.410	13.120	0.110
RFTS-039	1.000	65.614	0.001	1.686	10.956	0.323	1.843	335.490	13.005	0.110
RFTS-040	1.000	65.340	0.001	1.716	8.327	0.333	1.453	354.020	13.889	0.117
RFTS-041	1.000	65.340	0.001	1.716	8.327	0.333	1.453	354.020	13.889	0.117
RFTS-042	1.000	65.614	0.001	1.732	8.442	0.332	1.463	355.250	13.771	0.117
RFTS-043	1.000	65.614	0.001	1.732	8.442	0.332	1.463	355.250	13.771	0.117
RFTS-044	1.000	65.340	0.001	1.818	5.884	0.353	1.064	388.860	15.256	0.128
RFTS-045	1.000	65.340	0.001	1.818	5.884	0.353	1.064	388.860	15.256	0.128
RFTS-046	1.000	65.614	0.001	1.836	5.965	0.352	1.072	390.340	15.131	0.128
RFTS-047	2.000	130.680	0.002	11.158	36.105	0.270	1.163	425.160	16.680	0.070
RFTS-048	2.000	131.230	0.002	11.265	36.594	0.270	1.171	426.520	16.534	0.070
RFTS-049	2.000	130.680	0.002	11.336	27.510	0.275	0.914	445.460	17.477	0.073
RFTS-050	2.000	130.680	0.002	11.336	27.510	0.275	0.914	445.460	17.477	0.073
RFTS-051	2.000	131.410	0.002	11.482	28.010	0.274	0.923	447.480	17.277	0.073
RFTS-052	2.000	131.410	0.002	11.482	28.010	0.274	0.923	447.480	17.277	0.073
RFTS-053	2.000	131.410	0.002	11.482	28.010	0.274	0.923	447.480	17.277	0.073
RFTS-054	2.000	130.680	0.002	11.813	19.112	0.286	0.660	482.310	18.923	0.079
RFTS-055	2.000	130.680	0.002	11.813	19.112	0.286	0.660	482.310	18.923	0.079
RFTS-056	2.000	131.410	0.002	11.964	19.457	0.285	0.666	484.690	18.714	0.079
RFTS-057	3.000	196.020	0.003	33.964	73.266	0.244	0.899	493.220	19.351	0.054
RFTS-058	3.000	196.570	0.003	34.178	73.922	0.243	0.904	494.260	19.236	0.054
RFTS-059	3.000	196.020	0.003	34.269	55.443	0.246	0.701	512.800	20.119	0.056
RFTS-060	3.000	196.020	0.003	34.269	55.443	0.246	0.701	512.800	20.119	0.056
RFTS-061	3.000	197.110	0.003	34.703	56.439	0.245	0.708	515.080	19.887	0.056
RFTS-062	3.000	197.110	0.003	34.703	56.439	0.245	0.708	515.080	19.887	0.056
RFTS-063	3.000	196.020	0.003	35.348	38.126	0.254	0.501	549.280	21.550	0.060
RFTS-064	3.000	196.020	0.003	35.348	38.126	0.254	0.501	549.280	21.550	0.060
RFTS-065	3.000	196.020	0.003	35.348	38.126	0.254	0.501	549.280	21.550	0.060
RFTS-066	3.000	197.110	0.003	35.793	38.808	0.253	0.506	551.920	21.309	0.060
RFTS-067	5.000	2837.600	0.015	892.760	17426.000	0.135	11.975	725.690	27.986	0.022
RFTS-068	5.000	2776.500	0.015	847.550	16439.000	0.137	11.650	710.480	27.725	0.022
RFTS-069	5.000	3293.600	0.015	1249.900	25368.000	0.121	14.433	841.150	32.856	0.022
RFTS-070	5.000	3293.600	0.015	1249.900	25368.000	0.121	14.433	841.150	32.856	0.022
RFTS-071	5.000	2718.700	0.015	808.860	15590.000	0.139	11.344	696.210	27.231	0.022
RFTS-072	5.000	2718.700	0.015	808.860	15590.000	0.139	11.344	696.210	27.231	0.022
RFTS-073	5.000	3421.100	0.015	1367.000	27991.000	0.118	15.137	874.430	34.320	0.022
RFTS-074	5.000	326.700	0.006	138.280	178.980	0.214	0.655	598.340	23.475	0.039
RFTS-075	5.000	326.700	0.006	138.280	178.980	0.214	0.655	598.340	23.475	0.039

TAG	u (m/s)	Re (-)	C_{min} (W/K)	$\dot{W}''$ (W/m^2)	ΔP (Pa)	f (-)	NTU (-)	h ($W/m^2.K$)	Nu (-)	j (-)
RFTS-076	5.000	326.700	0.006	138.280	134.230	0.214	0.505	615.290	24.140	0.041
RFTS-077	5.000	327.150	0.006	138.700	134.810	0.214	0.506	615.950	24.070	0.041
RFTS-078	5.000	328.520	0.006	140.000	136.610	0.214	0.510	617.950	23.859	0.040
RFTS-079	5.000	328.520	0.006	140.000	136.610	0.214	0.510	617.950	23.859	0.040
RFTS-080	5.000	326.700	0.006	140.770	91.099	0.218	0.355	649.020	25.463	0.043
RFTS-081	5.000	326.700	0.006	140.770	91.099	0.218	0.355	649.020	25.463	0.043
RFTS-082	5.000	326.700	0.006	140.770	91.099	0.218	0.355	649.020	25.463	0.043
RFTS-083	5.000	328.520	0.006	142.500	92.701	0.217	0.359	652.020	25.174	0.043
RFTS-084	5.000	2275.400	0.016	483.510	8767.000	0.142	8.962	584.640	34.308	0.022
RFTS-085	5.000	287.140	0.007	104.850	118.100	0.240	0.515	540.380	31.850	0.041
RFTS-086	5.000	287.140	0.007	104.850	118.100	0.240	0.515	540.380	31.850	0.041
RFTS-087	5.000	287.140	0.007	104.900	88.617	0.240	0.394	552.240	32.549	0.041
RFTS-088	5.000	287.940	0.007	105.500	89.429	0.239	0.397	553.640	32.319	0.041
RFTS-089	5.000	288.470	0.007	105.910	89.979	0.239	0.398	554.580	32.168	0.041
RFTS-090	5.000	288.470	0.007	105.910	89.979	0.239	0.398	554.580	32.168	0.041
RFTS-091	5.000	287.140	0.007	107.050	60.289	0.245	0.275	577.210	34.021	0.043
RFTS-092	5.000	287.140	0.007	107.050	60.289	0.245	0.275	577.210	34.021	0.043
RFTS-093	5.000	287.140	0.007	107.050	60.289	0.245	0.275	577.210	34.021	0.043
RFTS-094	5.000	288.750	0.007	108.280	61.400	0.243	0.278	580.440	33.558	0.043
RFTS-095	1.000	50.432	0.002	0.621	18.123	0.262	5.421	219.710	21.448	0.094
RFTS-096	1.000	50.489	0.002	0.625	18.265	0.262	5.434	219.820	21.354	0.094
RFTS-097	1.000	50.489	0.002	0.625	18.265	0.262	5.434	219.820	21.354	0.094
RFTS-098	1.000	50.375	0.002	0.943	5.496	0.399	1.272	258.300	25.339	0.110
RFTS-099	1.000	50.375	0.002	0.943	5.496	0.399	1.272	258.300	25.339	0.110
RFTS-100	1.000	50.375	0.002	0.943	5.496	0.399	1.272	258.300	25.339	0.110
RFTS-101	1.000	50.489	0.002	0.950	4.445	0.399	1.045	264.170	25.662	0.113
RFTS-102	1.000	50.489	0.002	0.971	3.408	0.408	0.811	273.540	26.572	0.117
RFTS-103	1.000	50.375	0.002	1.024	2.387	0.433	0.571	289.960	28.445	0.124
RFTS-104	1.000	50.489	0.002	1.029	2.407	0.432	0.575	290.880	28.257	0.124
RFTS-105	2.000	100.860	0.003	5.558	81.111	0.293	3.694	299.410	29.228	0.064
RFTS-106	2.000	101.150	0.003	5.621	82.417	0.294	3.717	299.900	28.919	0.064
RFTS-107	2.000	101.150	0.003	5.621	82.417	0.294	3.717	299.900	28.919	0.064
RFTS-108	2.000	101.150	0.003	5.621	82.417	0.294	3.717	299.900	28.919	0.064
RFTS-109	2.000	100.810	0.003	6.415	14.963	0.339	0.663	336.170	32.898	0.072
RFTS-110	2.000	100.810	0.003	6.415	14.963	0.339	0.663	336.170	32.898	0.072
RFTS-111	2.000	100.810	0.003	6.415	14.963	0.339	0.663	336.170	32.898	0.072
RFTS-112	2.000	100.920	0.003	6.429	15.024	0.338	0.665	336.580	32.777	0.072
RFTS-113	2.000	101.150	0.003	6.457	15.147	0.337	0.669	337.400	32.535	0.072
RFTS-114	2.000	101.150	0.003	6.545	11.515	0.342	0.516	346.960	33.457	0.074
RFTS-115	3.000	151.210	0.005	19.421	188.760	0.304	3.011	366.460	35.863	0.052
RFTS-116	3.000	151.380	0.005	19.493	189.820	0.304	3.019	366.710	35.712	0.052
RFTS-117	3.000	151.380	0.005	19.493	189.820	0.304	3.019	366.710	35.712	0.052
RFTS-118	3.000	151.210	0.005	19.709	30.649	0.308	0.515	391.590	38.322	0.056
RFTS-119	3.000	151.210	0.005	19.709	30.649	0.308	0.515	391.590	38.322	0.056
RFTS-120	3.000	151.470	0.005	19.771	30.834	0.308	0.517	392.290	38.108	0.056
RFTS-121	3.000	151.720	0.005	19.989	23.447	0.310	0.398	401.580	38.724	0.057
RFTS-122	3.000	151.720	0.005	19.989	23.447	0.310	0.398	401.580	38.724	0.057
RFTS-123	3.000	151.210	0.005	20.552	15.980	0.321	0.274	417.550	40.863	0.059
RFTS-124	3.000	151.550	0.005	20.640	16.110	0.321	0.276	418.790	40.583	0.059
RFTS-125	5.000	251.880	0.008	81.177	56.754	0.275	0.286	483.680	47.449	0.041

TAG	u (m/s)	Re (-)	C_{min} (W/K)	$\dot{W}''$ (W/m²)	ΔP (Pa)	f (-)	NTU (-)	h (W/m².K)	Nu (-)	j (-)
RFTS-126	5.000	252.720	0.008	81.678	57.428	0.274	0.289	485.510	46.935	0.041
RFTS-127	5.000	252.720	0.008	81.678	57.428	0.274	0.289	485.510	46.935	0.041
RFTS-128	5.000	252.720	0.008	81.678	57.428	0.274	0.289	485.510	46.935	0.041
RFTS-129	5.000	252.020	0.008	83.080	38.759	0.281	0.197	498.560	48.790	0.043
RFTS-130	5.000	252.020	0.008	83.080	38.759	0.281	0.197	498.560	48.790	0.043
RFTS-131	5.000	252.440	0.008	83.334	38.989	0.280	0.198	499.620	48.534	0.043
RFTS-132	5.000	252.440	0.008	83.334	38.989	0.280	0.198	499.620	48.534	0.043
RFTS-133	5.000	252.020	0.008	95.109	221.850	0.321	1.002	507.950	49.709	0.043
RFTS-134	5.000	252.440	0.008	95.461	223.310	0.321	1.006	508.710	49.417	0.043
RFTS-135	1.000	48.399	0.002	0.495	13.418	0.236	4.940	215.520	25.403	0.096
RFTS-136	1.000	48.580	0.002	0.506	13.805	0.238	4.984	215.890	24.997	0.096
RFTS-137	1.000	48.580	0.002	0.506	13.805	0.238	4.984	215.890	24.997	0.096
RFTS-138	1.000	48.444	0.002	0.876	3.807	0.417	0.926	251.970	29.569	0.112
RFTS-139	1.000	48.444	0.002	0.876	3.807	0.417	0.926	251.970	29.569	0.112
RFTS-140	1.000	48.444	0.002	0.876	3.807	0.417	0.926	251.970	29.569	0.112
RFTS-141	1.000	48.580	0.002	0.881	3.848	0.415	0.934	252.810	29.272	0.112
RFTS-142	1.000	48.557	0.002	0.898	2.941	0.424	0.720	260.240	30.201	0.115
RFTS-143	1.000	48.399	0.002	0.945	2.050	0.451	0.501	273.220	32.204	0.121
RFTS-144	1.000	48.580	0.002	0.952	2.079	0.449	0.507	274.800	31.819	0.122
RFTS-145	2.000	97.024	0.003	5.967	13.000	0.353	0.593	321.970	37.530	0.071
RFTS-146	2.000	97.113	0.003	5.978	13.045	0.353	0.595	322.320	37.406	0.071
RFTS-147	2.000	96.887	0.003	6.027	9.822	0.358	0.453	328.860	38.592	0.073
RFTS-148	2.000	97.069	0.003	6.048	9.891	0.358	0.456	329.660	38.342	0.073
RFTS-149	2.000	97.113	0.003	6.053	9.908	0.357	0.456	329.860	38.281	0.073
RFTS-150	2.000	97.113	0.003	6.053	9.908	0.357	0.456	329.860	38.281	0.073
RFTS-151	2.000	96.799	0.003	6.282	6.813	0.375	0.315	343.430	40.479	0.076
RFTS-152	2.000	96.799	0.003	6.282	6.813	0.375	0.315	343.430	40.479	0.076
RFTS-153	2.000	96.799	0.003	6.282	6.813	0.375	0.315	343.430	40.479	0.076
RFTS-154	2.000	97.113	0.003	6.321	6.897	0.373	0.318	345.100	40.049	0.076
RFTS-155	3.000	145.200	0.005	16.899	152.730	0.299	2.732	357.560	42.145	0.053
RFTS-156	3.000	145.740	0.005	17.121	155.830	0.299	2.757	358.360	41.494	0.053
RFTS-157	3.000	145.740	0.005	17.121	155.830	0.299	2.757	358.360	41.494	0.053
RFTS-158	3.000	145.260	0.005	18.308	26.497	0.323	0.458	374.580	44.054	0.055
RFTS-159	3.000	145.470	0.005	18.353	26.632	0.322	0.460	375.180	43.832	0.056
RFTS-160	3.000	145.200	0.005	18.422	19.979	0.325	0.349	380.700	44.872	0.056
RFTS-161	3.000	145.740	0.005	18.547	20.257	0.324	0.353	382.500	44.289	0.056
RFTS-162	3.000	145.740	0.005	18.547	20.257	0.324	0.353	382.500	44.289	0.056
RFTS-163	3.000	145.200	0.005	19.065	13.785	0.337	0.241	394.780	46.532	0.059
RFTS-164	3.000	145.740	0.005	19.194	13.976	0.335	0.244	396.900	45.956	0.059
RFTS-165	5.000	242.000	0.009	75.595	49.192	0.288	0.254	461.480	54.394	0.041
RFTS-166	5.000	242.900	0.009	76.085	49.860	0.287	0.257	463.580	53.677	0.041
RFTS-167	5.000	242.900	0.009	76.085	49.860	0.287	0.257	463.580	53.677	0.041
RFTS-168	5.000	242.110	0.009	77.383	33.599	0.295	0.174	472.770	55.602	0.042
RFTS-169	5.000	242.900	0.009	77.820	33.998	0.294	0.175	474.900	54.988	0.042
RFTS-170	5.000	242.000	0.009	85.687	167.280	0.327	0.793	480.580	56.645	0.043
RFTS-171	5.000	242.440	0.009	85.933	168.340	0.326	0.797	481.310	56.231	0.043
RFTS-172	5.000	242.900	0.009	86.184	169.430	0.325	0.801	482.050	55.816	0.043
RFTS-173	5.000	242.000	0.009	87.036	188.790	0.332	0.898	489.460	57.691	0.044
RFTS-174	5.000	242.900	0.009	87.743	191.670	0.331	0.907	491.170	56.872	0.044

Appendix G - Performance Evaluation Criteria Analysis

Excerpt from Purdue publication:

Bacellar, D., Aute, V., Radermacher, R., Performance Evaluation Criteria Analysis of Compact Air-to-Refrigerant Heat Exchangers and Selection Utility Function for Single Phase Applications, 16th International Refrigeration and Air Conditioning Conference at Purdue, July 11-14, 2016.

<u>*Introduction*</u>

The research on heat transfer augmentation (HTA) relentlessly seeks developing highly compact heat exchangers (CHX) with high performance surfaces. A CHX is the definition of high surface-to-volume ratio [4]. The definition of high-performance surface, however, is more subject to interpretations, particularly when evaluating a full-sized HX. The sole evaluation of the thermal-hydraulic ratio of a surface do not necessarily portray the broader characteristics in the context of the HX, including overall size, face area and degradation aspects. The literature on HX Performance Evaluation Criteria (PEC) is quite extensive. There are two main approaches to assess the HX PEC: a) energy-based (first law of thermodynamics); b) entropy-based (second law of thermodynamics).

Cowell (1990) revised the main categories within the energy-based PEC. The first, known as “area goodness” factor, is a typical way of evaluating surfaces and HX’s, and is simply defined as the ratio of j and f factors (equation 1). The main advantage of such metric is the non-dimensional aspect, which allows one to compare surfaces regardless the geometrical scale, particularly the surface hydraulic diameter.

Although it well represents the surface characteristics, it leads to potential skewed evaluation of the HX or even biasing the search made by an optimizer. The simplified form shows the dependency to the thermal conductance and the inverse of the pressure drop and the square of the minimum free flow area. In other words, this metric can only have some meaning either if the thermal hydraulic ratio is fixed or if the minimum free flow area is fixed. Furthermore, the general knowledge is that this factor is inversely proportional to the Reynolds number, which is not necessarily desired to be relatively low. The reason for this is that the pressure drop and face area (assuming constant flow rate) terms are more sensitive to the variation in velocity than for the thermal conductance. If one uses this metric as an optimization objective there is a possibility the optimizer will search for either low-pressure drop and/or small face area designs instead of lower thermal resistance.

$$\frac{j}{f}=\left[\frac{h}{\rho u_c c_p}\mathrm{Pr}^{2/3}\right]\Bigg/\left[\frac{2A_c\Delta P}{A_o\rho u_c^2}\right]=K\,\frac{1}{A_c^2}\,\frac{N_{tu}}{\Delta P},\quad K=\frac{\dot{m}^2\,\mathrm{Pr}^{2/3}}{2\rho} \tag{96}$$

$$\Delta P\propto u_c^m, m>1.0;\quad h\propto u_c^n, 0.0<n<1.0;\quad A_c\propto u_c^{-1} \tag{97}$$

The second category is the “volume goodness”, also described by London (1964) but discussed in other relevant publications including Kays and London (1984), Webb and Kim (2005) and Shah (1978). This category evaluates the dimensioned heat transfer coefficient and pressure drop (in the form of pumping power per surface area) (equation 3). The common observation with regards to these metrics is their dependency to the hydraulic diameter, thus in order for one to make a fair comparison between two or more designs they must have the same hydraulic diameters [90, 92, 93, 94]. Additionally, the reduction in pressure drop is usually simpler to obtain instead of improving the heat transfer coefficient, thus normally resulting in large face area designs.

$$\frac{h}{\dot{W}''} = \frac{h}{\Delta P \cdot \dot{V} / A_o} = \left(\frac{c_p \mu}{\Pr^{2/3}} \frac{j \operatorname{Re}}{D_h} \right) \Big/ \left(\frac{\mu^3}{2\rho^2} \frac{f \operatorname{Re}^3}{D_h^3} \right) = \frac{2 j \rho^2 c_p D_h^2}{f \mu^2 \Pr^{2/3} \operatorname{Re}^2}$$

(98)

The third main category identified by Cowell (1990) include the 12 scenario design method [95] , which are at most limited to one or more fixed parameters, in addition to fixed hydraulic diameters. Such category was not intended to be applied to actual variable geometry HX's, much less comparing multiple HX's with very different surface types.

The fourth category, and Cowell's (1990) own method, account for methods that are either of diffusive interpretation, very particular or by any means extendable to a more general method, or a variation of the previous categories.

In spite of the particular issues and limitations, the common denominator to all energy-based PEC metrics is the premise that the performance degradation is solely due to the hydraulic resistance. When one thinks of degradation, it can be flatly interpreted as the direct energy cost for driving the fluid through the HX. Alternatively, the degradation can be interpreted as everything that can cause a negative impact not only on the overall HX performance but also to a larger control volume including a system of sub components (Shah, 2006). For the second interpretation, the entropy-based PEC (or thermodynamic) approach is more appropriate. Additionally, in many cases the entropy generation due to the finite temperature difference is significantly larger than it is for the pressure drop.

McClintock (1951) introduced the concept of irreversibility to HX design, which was later formalized by Bejan (1977) where he defined the concept of Number of Entropy Generation Units (N_S) as an evaluation metric. His work culminated in the idealization of the Entropy Generation Minimization (EGM) for broad applications of finite-size systems and finite-time processes (Bejan et al., 1996).

$$N_S = \frac{\dot{S}_{gen}}{C_{\min}} \tag{99}$$

According to the literature, it is well established that the tradeoff between energy-based and entropy-based approaches comprises balancing out the HX size and production costs directly for savings in energy degradation (irreversibilities) (Bejan, 1977) further down the process. It is also a common sense that a larger and “more expensive” HX is more thermodynamically efficient (Bejan, 1977), and better heat transfer performance does not lead to minimum entropy generation (Bejan & Pfister, 1980; Seculik & Herman, 1986).

The evolution of computational tools (such as CFD), optimization algorithms, storage capacities, processing speed and manufacturing technologies enable a large number of novel ideas and concepts establishing new frontiers.

Unfortunately, while the more novel heat transfer types and shapes are being developed the less clear their consequences are to a full HX design. Furthermore, it is becoming harder to compare and select an optimum HX on a fair basis.

In this paper, we propose the use of a set of comprehensive metrics attempting to address the challenges from the common PEC approaches. We show how the optimization outcomes can be shifted when using different objectives and demonstrate why one metric should be chosen over the other.

HX Evaluation Criteria

Performance-Degradation Number

Considering the brief literature review in the previous section, it should be clear that we want to find a metric that, not only carries quantitative and qualitative information regarding the performance and degradation aspects, but also it has to be sufficiently general so one can compare multiple HX types fairly.

Bejan (1982) first studied the relationship between the Number of Entropy Generation Units (Ns) and the Number of Transfer Units (Ntu) for a balanced counter flow HX with no pressure drop. He encountered what was called the "entropy generation paradox" when the Ns went to zero for either Ntu = 0 or ∞, but reached a maximum at an intermediate Ntu. Shah & Skiepko (2004) interpreted such behavior as the irreversibility tend to zero whenever the heat transfer potential is zero; i.e. at NTU = 0 there is no heat flow thus, from the Second Law, S_{gen} has to be zero for it cannot be negative. When NTU $\rightarrow \infty$ the hot and cold stream temperatures approach to the same value, thus nulling the heat transfer potential. Ogiso (2003) defined the dimensionless "entropy generation index" (Ns/Ntu) and showed that the Bejan's paradox can be Shah & Skiepko (2004) since the index is not defined at NTU = 0 or NTU → ∞.

This metric satisfies the criteria we looked for since it provides the information on the thermal performance (Ntu), the degradation factors (Ns) and is non-dimensional. In this paper, we use the inverse and call it the performance-degradation number (equation 5). The reason is merely convenience; to have a number, which higher values are better.

$$\psi = \frac{N_{tu}}{N_s} \tag{100}$$

For purposes of this paper, all analysis will focus on the airside. With this assumption, we can use the ideal gas model to calculate ψ.

$$\Delta s = \int \frac{\partial q}{T} + s_{gen} \rightarrow s_{gen} \approx c_p \ln\left(\frac{T_o}{T_i}\right) - \frac{q}{\bar{\bar{T}}} - R\ln\left(\frac{P_o}{P_i}\right) \tag{101}$$

$$N_s = N_{s,\Delta T} + N_{s,\Delta P}, \quad N_{s,\Delta T} = \frac{\dot{S}_{gen,\Delta T}}{C} = \ln\left(\frac{T_o}{T_i}\right) - \frac{N_{tu}\Delta T_{ml}}{\bar{\bar{T}}}, \quad N_{s,\Delta P} = \frac{s_{gen,\Delta P}}{R} = \ln\left(\frac{P_o + \Delta P}{P_o}\right)$$

(102)

$$\psi = \frac{N_{tu}}{\ln\left(\dfrac{T_o\left(P_o + \Delta P\right)}{T_i P_o}\right) - \dfrac{N_{tu}\Delta T_{ml}}{\bar{\bar{T}}}} = \frac{N_{tu}}{\ln\left(\dfrac{T_o\left(P_o + \Delta P\right)}{T_i P_o}\right) - \dfrac{\varepsilon \Delta T_{\max}}{\bar{\bar{T}}}}$$

(103)

On equation (8) it is clear that the performance degradation number has on its denominator, in addition to the pressure drop, the finite temperature difference contribution.

HX Compactness and Face Area

Typically, when using EGM or any other entropy-based PEC for designing a HX the trade-off between size and low entropy generation is always an issue. In reality, the larger HX's actually have larger heat transfer surfaces in order to reduce the overall thermal resistance. For conventional surface types and dimensions, larger area will naturally result in larger volumes, thus the reference to the HX size. However, the next generation of HX's is shifting to novel shapes and towards smaller tube sizes, which result in surfaces that are more compact. Additionally, smaller sized surfaces have higher heat transfer coefficients. In other words, these novel HX's have the potential to reduce thermal resistance in a smaller envelope compared to conventional HX's, but not proportionally increasing the surface area once the heat transfer coefficient is higher. Additionally, the term "size" is normally used loosely, i.e. most studies do not qualify what aspect of the size is the most relevant. In many applications, the envelope volume is not much of an issue as long as the design can satisfy potential limitations on tube length, face area and/or aspect ratio. The face area can be more critical since it can affect the cross section of an air duct, size of an equipment casing, or the size of the front of a car.

Ultimately, the metrics that better evaluate the geometrical aspects of a HX are the face area and the surface hydraulic diameter (equation 9), since it represents the inverse of compactness.

$$D_h = 4A_c/A_o d = 4\sigma V/A_o \quad (104)$$

<u>HX Design</u>

In this paper, we study the design of a 1.0 kW air-to-water HX in cross flow. We investigate two different HX surfaces: a) round bare tubes in staggered arrangement with diameters below 2.0mm (RTHX), b) Webbed NURBS tube (NURBS shaped channels connected by a longitudinal web) (WTHX). Here we investigate how the different performance metrics affect the optimization results. For this study, we solve three multi-objective optimization problems targeting minimizing face area and maximizing ψ, j/f, and h/ΔP, respectively for each problem.

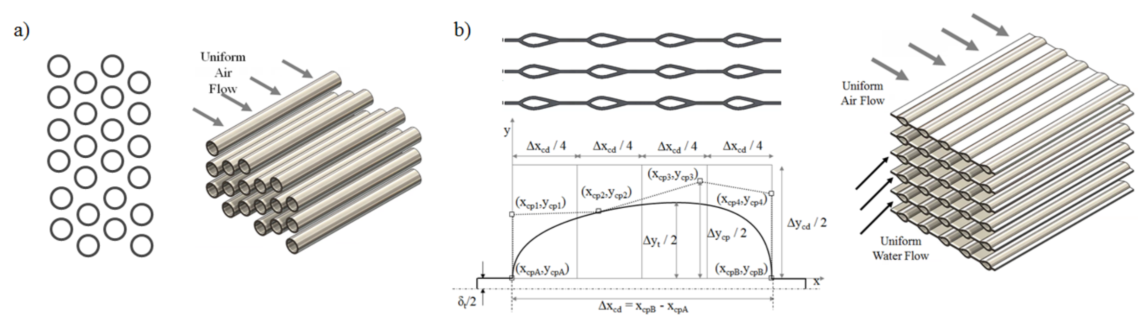

Figure 146: HX surface types: a) RTHX; b) WTHX.

Table 54: Optimization Problem.

Optimization	OPT01	OPT02	OPT03
Objectives	min A_f max h/ΔP	min A_f max j/f	min A_f max ψ
Constraints		$1.0 < Q < 1.01$kW $V_{HX} \leq V_{HX,\ baseline}$ $\Delta P_{air} \leq \Delta P_{air,\ baseline}$ $\Delta P_{water} \leq \Delta P_{water}$ $0.61 < AR < 1.61$	
Parameters		$\dot{m}_{air}$ = fixed $\dot{m}_{water}$ = fixed $0.5 \leq u_{air} \leq 7.0$m/s $0.8\ \Delta T_{in\_baseline} \leq \Delta T_{in} \leq \Delta T_{in\_baseline}$	

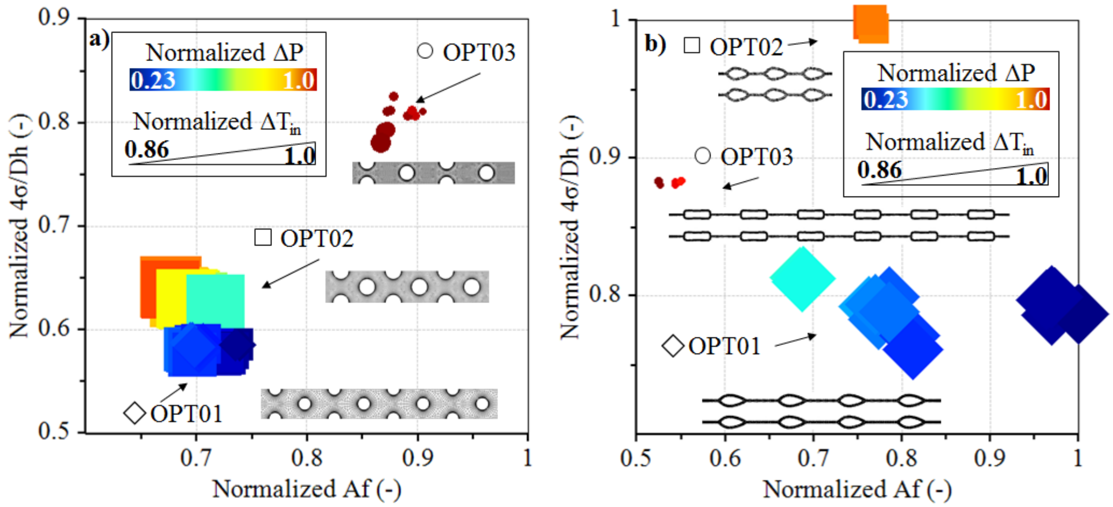

Figure 147: HX Design results: a) RTHX; b) WTHX.

Figure 147 presents the optimization results on a compactness vs. face area plot, where the shading indicates the pressure drop and the symbol size the inlet approach temperature. The symbol type indicates the optimization problem from

Table 54. On both surface types, the OPT03 resulted in designs with relatively higher-pressure drop and lower approach temperature, as expected. Additionally, for the RTHX both OPT01 and OPT02 resulted in designs with longitudinal pitch larger than the transverse pitch, unlike the conventional tube arrangements. Furthermore, the OPT03 results have satisfactory geometrical characteristics; for the RTHX surface, it resulted in the most compact designs with relatively small face area, whereas for the WTHX it resulted in designs with the smallest face area with relatively high compactness. Figure 148 shows how, for this application, the entropy generation due to finite temperature difference is significantly larger than for pressure drop.

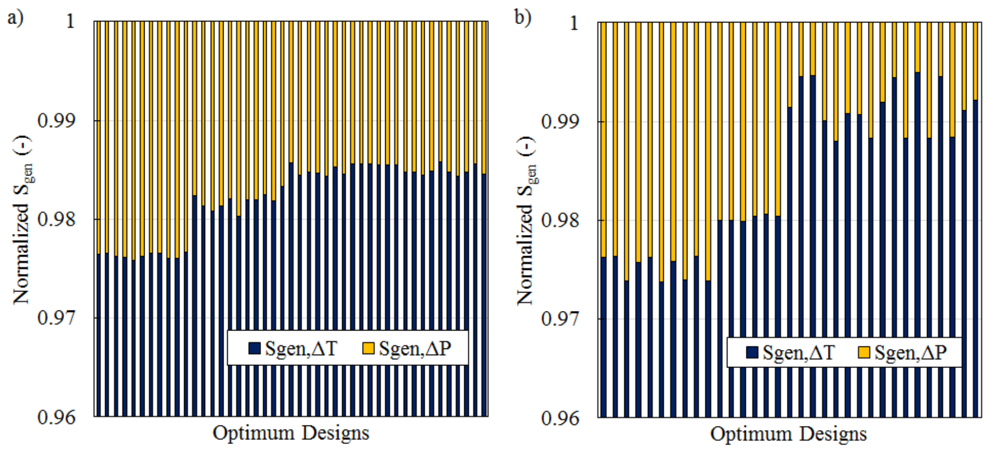

Figure 148: Entropy Generation: a)RTHX; b) WTHX.

References

[1] U. E. I. Administration, "Annual Energy Outlook 2015," U.S. Department of Energy, Washington, DC, 2015.

[2] D. Westphalen, K. Roth and J. Brodrick, "Heat transfer enhancement," *ASHRAE Journal*, vol. 48, no. 4, pp. 68-70, 2006.

[3] R. Shah and D. Sekulic, Fundamentals of Heat Exchanger Design, Hoboken, NJ: John Wiley & Sons, 2003.

[4] W. Kays and A. London, Compact heat exchangers, 3rd ed., New York: McGraw-Hill, 1984.

[5] R. Webb and N. Kim, Principles of enhanced heat transfer, New York: Taylor&Francis, 2005.

[6] D. Huang, R.-J. Zhao, Y. Liu and D.-B. Yi, "Effect of fin types of outdoor fan-supplied finned-tube heat exchanger on periodic frosting and defrosting performance of a residential air-source heat pump," *Applied Thermal Engineering*, vol. 69, pp. 251-260, 2014.

[7] W. Kays, "The basic heat transfer and flow friction characteristics of six compact high-performance heat transfer surfaces," *Journal of Engineering for Power*, vol. 82, no. 1, pp. 27-34, 1960.

[8] A. M. Jacobi and R. K. Shah, "Air-side flow and heat transfer in compact heat exchangers: a discussion of enhancement mechanisms," *Heat Transfer Engineering*, vol. 19, no. 4, pp. 29-41, 1998.

[9] T. Cowell, M. Heikal and A. Achaichia, "Flow and Heat Transfer in Compact Louvered Fin Surfaces," *Experimental Thermal and Fluid Science*, vol. 10, pp. 192-199, 1995.

[10] K. Atkinson, R. Drakulic, M. Heikal and T. Cowell, "Two! and three!dimensional numerical models of fow and heat transfer over louvred fin arrays in compact heat exchangers," *International Journal of Heat and Mass Trasfer,* vol. 41, pp. 4063-4080, 1998.

[11] C.-C. Wang, Y.-M. Tsai and D.-C. Lu, "Comprehensive Study of Convex-Louverand Wavy Fin-and-Tube Heat Exchangers," *Journal of Thermophysiscs and Heat Transfer,* vol. 12, no. 3, pp. 423-430, 1998.

[12] J. Yun and K. Lee, "Investigation of heat transfer characteristics on various kinds of fin-and-tube heat exchangers with interrupted surfaces," *International Journal of Heat and Mass Transfer* , vol. 42, pp. 2375-2385, 1999.

[13] D. Tafti, G. Wang. and W. Lin, "Flow transition in a multilouvered fin array," *International Journal of Heat and Mass Transfer,* vol. 43, pp. 901-919, 2000.

[14] J. Leu, M. Liu, J.-S. Liaw and C.-C. Wang, "A numerical investigation of louvered fin-and-tube heat exchangers having circular and oval tube configurations," *International Journal of Heat and Mass Transfer,* vol. 44, pp. 4235-4243, 2001.

[15] M. Kim and C. Bullard, "Air-side thermal hydraulic performance of multi-louvered fin aluminum heat exchangers," *International Journal of Refrigeration,* vol. 25, pp. 390-400, 2002.

[16] T. Perrotin and D. Clodic, "Thermal-hydraulic CFD study in louvered fin-and-flat-tube heat exchangers," *International Journal of Refrigeration,* vol. 27, pp. 422-432, 2004.

[17] C.-T. Hsieh and J.-Y. Jang, "3-D thermal-hydraulic analysis for louver fin heat exchangers with variable louver angle," *Applied Thermal Engineering,* vol. 26, pp. 1629-1639, 2006.

[18] C. T'Joen, H. Huisseune, H. Caniere, H. Steeman, A. Willockx and M. De Paepe, "Interaction between mean flow and thermo-hydraulic behaviour in inclined

louvered fins," *International Journal of Heat and Mass Transfer,* vol. 54, pp. 826-837, 2011.

[19] N. DeJong and A. Jacobi, "Localized flow and heat transfer interactions in louvered-fin arrays," *International Journal of Heat and Mass Transfer,* vol. 46, pp. 443-455, 2003.

[20] W. Tao, Y. Cheng and T. Lee, "3D numerical simulation on fluid flow and heat transfer characteristics in multistage heat exchanger with slit fins," *Heat and Mass Transfer,* vol. 44, pp. 125-136, 2007.

[21] J. Li, S. Wang, J. Chen and Y.-G. Lei, "Numerical study on a slit fin-and-tube heat exchanger with longitudinal vortex generators," *International Journal of Heat and Mass Transfer,* vol. 54, pp. 1743-1751, 2011.

[22] J.-Y. Yun and K.-S. Lee, "Influence of design parameters on the heat transfer and flow friction characteristics of the heat exchanger with slit fins," *International Journal of Heat and Mass Transfer* , vol. 43, pp. 2529-2539, 2000.

[23] M. Fujii, Y. Seshimo and G. Yamanaka, "Heat transfer and pressure drop of perforated surface heat exchanger with passage enlargement and contraction," *International Journal of Heat and Mass Transfer,* vol. 31, pp. 135-142, 1988.

[24] X. Liu, J. Yu and G. Yan, "A numerical study on the air-side heat transfer of perforated finned-tube heat exchangers with large fin pitches," *International Journal of Heat and Mass Transfer,* vol. 100, pp. 199-207, 2016.

[25] W. M. Kays, "The basic heat transfer an flow friction characteristics of six compact high-performance heat transfer surfaces," *Journal of Engineering for Power,* vol. 82, no. 1, pp. 27-34, 1960.

[26] C. Wang, J. Chang and N. Chiou, "Effects of Waffle Height on the Air-Side Performance of Wavy Fin-and-Tube Heat Exchangers," *Heat Transfer Engineering,* p. 20, 1999.

[27] B. Lotfi, M. Zeng, B. Sunden and Q. Wang, "3D numerical investigation of flow and heat transfer characteristics in smooth wavy fin-and-elliptical tube heat exchangers using new type vortex generators," *Energy,* vol. 73, pp. 233-257, 2014.

[28] H. Mohammed, P. Gunnasegaran and N. Shuaib, "Influence of channel shape on the thermal and hydraulic performance of microchannel heat sink," *International Communications in Heat and Mass Transfer,* vol. 38, pp. 474-480, 2011.

[29] Y. Sui, C. teo, P. Lee, Y. Chew and C. Shu, "Fluid flow and heat transfer in wavy microchannels," *International Journal of Heat and Mass Transfer,* vol. 53, pp. 2760-2772, 2010.

[30] D. Silva, C. Hermes and C. Melo, "Experimental study of frost accumulation on fan-supplied tube-fin evaporators," *Applied Thermal Engineering,* pp. 1013-1020, 2011.

[31] D. Huang, R.-J. Zhao, Y. Liu and D.-B. Yi, "Effect of fin types of outdoor fan-supplied finned-tube heat exchanger on periodic frosting and defrosting performance of a residential air-source heat pump," *Applied Thermal Engineering,* pp. 251-260, 2014.

[32] A. Gholami, M. A. Wahid and H. A. Mohammed, "Heat transfer enhancement and pressure drop for fin-and-tube compact heat exchangers with wavy rectangular winglet-type vortex generators," *International Communications in Heat and Mass Transfer,* vol. 54, p. 132–140, 2014.

[33] H. Huisseune, C. T'Joen, P. De Jaeger, B. Ameel, S. De Schampheleire and M. De Paepe, "Performance enhancement of a louvered fin heat exchanger by using delta winglet vortex generators," *International Journal of Heat and Mass Transfer,* vol. 56, p. 475–487, 2013.

[34] L. Salviano, D. Dezan and J. Yanaghiara, "Thermal-hydraulic performance optimization of inline and staggered fin-tube compact heat exchangers applying

longitudinal vortex generators," *Applied Thermal Engineering,* vol. 95, pp. 311-329, 2016.

[35] A. Arora, P. Subbarao and R. Agarwal, "Development of parametric space for the vortex generator location for improving thermal compactness of an existing inline fin and tube heat exchanger," *Applied Thermal Engineering,* vol. 98, pp. 727-742, 2016.

[36] S. Tiwari, D. Maurya, G. Biwas and V. Eswaran, "Heat transfer enhancement in cross-flow heat exchangers using oval tubes and multiple delta winglets," *International Journal of Heat and Mass Transfer,* vol. 46, pp. 2841-2856, 2003.

[37] A. Jacobi and R. Shah, "Heat transfer surface enhancement through the use of longitudinal vortices," *Experimental Thermal and Fluid Sciences,* vol. 11, no. 3, pp. 295-309, 1995.

[38] S. Paitoonsurikarn, N. Kasagi and Y. Suzuki, "Optimal design of micro bare-tube heat exchanger," in *Proceedings of Symposium on Energy Engineering in the 21st Century*, Hong Kong, 2000.

[39] N. Kasagi, Y. Suzuki, N. Shikazono and T. Oku, "Optimal design and assessment of high performance micro bare-tube heat exchangers," in *Proc. 4th Int. Conf. on Compact Heat Exchangers and Enhancement Technologies for the Process Industries*, Crete, Greece, 2003.

[40] D. Bacellar, V. Aute, O. Abdelaziz and R. Radermacher, "Design of Novel Air-to-Refrigerant Heat Exchangers Using Approximation Assisted Optimization," in *ASME 2014 Verification & Validation Symposium*, Las Vegas, NV, 2014.

[41] D. Bacellar, J. Ling, O. Abdelaziz, V. Aute and R. Radermacher, "Multi-scale modeling and Approximation Assisted Optimization of bare tube heat exchangers," in *Multi-scale modeling and approximation assisted optimization of bare tube heat*

exchangers, Proceedings of the 15th International Heat Transfer Conference, IHTC-15, Kyoto, Japan, 2014.

[42] N. Saji, S. Nagai, K. Tsuchiya, H. Asakura and M. Obata, "Development of a compact laminar flow heat exchanger with stainless stell micro-tubes," *Physica C,* vol. 354, pp. 148-151, 2001.

[43] H.-T. Chen, Y.-S. Lin, P.-C. Chen and J.-R. Chang, "Numerical and experimental study of natural convection heat transfer characteristics for vertical plate fin heat exchangers with various diameters," *International Journal of Heat and Mass Transfer,* vol. 100, pp. 320-331, 2016.

[44] J. Min and R. L. Webb, "Numerical analyses of effects of tube shape on performance of a finned tube heat exchanger," *Journal of Enhanced Heat Transfer,* vol. 11, no. 1, pp. 61-73, 2004.

[45] A. Joardar and A. Jacobi, "Impact of leading edge delta-wing vortex generators on the thermal performance of a flat tube, louvered-fin compact heat exchanger," *International Journal of Heat and Mass Transfer,* vol. 48, p. 1480–1493, 2005.

[46] D. Tuckerman and R. Pease, "High-performance heat sinking for VLSI," *IEEE Electron Device Letters,* vol. 2, no. 5, pp. 126-129, 1981.

[47] S. Kandlikar, "History, advances, and challenges in liquid flow and flow boiling heat transfer in microchannels: a critical review," in *Proceedings of the 14th International Heat Transfer Conference*, Washington, DC, 2010.

[48] S. Kandlikar, "A roadmap for implementing microchannels in refrigeration and air-conditioning systems-current status and future directions," *Heat Transfer Engineering,* vol. 28, no. 12, pp. 973-985, 2007.

[49] L. Huang, V. Aute and R. Radermacher, "A model for air-to-refrigerant microchannel condensers with variable tube and fin geometries," *International Journal of Refrigeration,* vol. 40, pp. 269-281, 2014.

[50] Z. Li, J. H. Davidson and S. Mantell, "Heat Transfer Enhancement Using Shaped Polymer Tubes: Fin Analysis," *Journal of Heat Transfer,* vol. 126, pp. 211-218, 2004.

[51] A. M. Lavasani, H. Bayat and T. Maarefdoost, "Experimental study of convective heat transfer from in-line cam shaped tube bank in crossflow," *Applied Thermal Engineering,* vol. 65, pp. 85-93, 2014.

[52] A. Nouri-Borujerdi and A. M. Lavasani, "Experimental study of forced convection heat transfer from cam shaped tube in cross flows," *International Journal of Heat and Mass Transfer,* vol. 50, pp. 2605-2611, 2007.

[53] G.-M. Zhang, M.-C. Tian, N.-X. Zhou, W. Li and D. Kukulka, "Analysis of Flow and Heat Transfer Characteristics Around an Oval-Shaped Cylinder," *Journal of Heat Transfer,* vol. 136, 2014.

[54] H. Sobieczky, "Parametric airfoils and wings," *Notes on Numerical Fluid Mechanics,* vol. 68, pp. 71-88, 1998.

[55] J. Hajek, "Parameterization of airfoils and its application in aerodynamic optimization," in *WDS'07 Proceedings of Contributed Papers*, 2007.

[56] H. Onishi, A. Yamamoto, Y. Tada and A. Takimoto, "Heat transfer performance of finless heat exchanger using airfoil-shaped tubes with extended leading or trailing edge section," in *Proceedings of the 15th International Heat Transfer Conference*, Kyoto, Japan, 2014.

[57] Y. Ito, N. Inokura and T. Nagasaki, "Conjugate heat transfer in air-torefrigerant airfoil heat exchangers," *Journal of Heat Transfer,* vol. 136, pp. 08170301-08170312, 2014.

[58] E. Nobile, F. Pinto and G. Rizzetto, "Geometric parameterization and multiobjective shape optimization of convective periodic channels," *Numerical Heat Transfer, Part B: Fundamentals,* vol. 50, pp. 425-453, 2006.

[59] K. Foli, T. Okabe, M. Olhofer, Y. Jin and B. Sendhoff, "Optimization of micro heat exchanger: CFD, analytical approach and multi-objective evolutionary algorithms," *International Journal of Heat and Mass Transfer,* vol. 49, pp. 1090-1099, 2006.

[60] M. Cavazzuti and M. Corticelli, "Optimization of heat exchanger enhanced surfaces thorugh multiobjective genetic algorithms," *Numerical Heat Transfer,* vol. 54, pp. 603-624, 2008.

[61] E. Stalio and M. Piller, "Direct Numerical Simulation of heat transfer in converging-diverging wavy channels," *Journal of Heat Transfer,* vol. 129, pp. 769-777, 2006.

[62] G. Fabbri, "A genetic algorithm for fin profile optimization," *International Journal of Heat and Mass Transfer,* vol. 40, no. 9, pp. 2165-2172, 1997.

[63] G. Fabbri, "Heat transfer optimization in internally finned tubes under laminar flow conditions," *International Journal of Heat and Mass Transfer,* vol. 41, no. 10, pp. 1243-1253, 1998.

[64] E. Duplain and B. R. Baliga, "Computational optimization of the thermal performance of internally finned ducts," *International Journal of Heat and Mass Transfer*, vol. 52, p. 3929–3942, 2009.

[65] J. Lee and K.-S. Lee, "Correlations and shape optimization in a channel with aligned dimples and protrusions," *International Journal of Heat and Mass Transfer,* vol. 64, p. 444–451, 2013.

[66] R. Hilbert, G. Janiga, R. Baron and D. Thevenin, "Multi-objective shape optimization of a heat exchanger using parallel genetic algorithms," *International Journal of Heat and Mass Transfer,* vol. 49, p. 2567–2577, 2006.

[67] P. Ranut, G. Janiga, E. Nobile and D. Thevenin, "Multi-objective shape optimization of a tube bundle in cross-flow," *International Journal of Heat and Mass Transfer,* vol. 68, pp. 585-598, 2014.

[68] R. Shah, "Advances in science and technology of compact heat exchangers," *Heat Transfer Engineering,* vol. 27, no. 5, pp. 3-22, 2006.

[69] C. J. Roy and W. L. Oberkampf, "A comprehensive framework for verification, validation, and uncertainty quantification in scientific computing," *Computational Methods Applied to Mechanical Engineering,* vol. 200, p. 2131–2144, 2011.

[70] ASME, Standard for verification and validation in Computational Fluid Dynamics and heat transfer - ASME V&V 20-2009, New York: ASME, 2009.

[71] P. J. Roach, "Quantification of Uncertainty in Computational Fluid Dynamics," *Annual Review of Fluid Mechanics,* vol. 29, p. 123–160, 1997.

[72] O. Abdelaziz, S. Azarm, V. Aute and R. Radermacher, "Approximation-Assisted Optimization for Novel Compact Heat Exchanger Designs," *HVAC&R Research,* vol. 16, no. 5, pp. 707-728, 2010.

[73] T. Xioping, L. Huahe and L. Xiangfei, "CFD simulation and experimental study on airside performance for MCHX," in *International Refrigeration and Air Conditioning Conference,* Lafayette, IN, 2010.

[74] D. Taler and P. Oclon, "Thermal contact resistance in plate fin-and-tube heat exchangers, determined by experimental data and CFD simulations," *International Journal of Thermal Sciences,* vol. 84, pp. 309-322, 2014.

[75] S. Pantakar, Numerical heat transfer and fluid flow, McGraw-Hill, 1980.

[76] O. Abdelaziz, V. Aute, S. Azarm and R. Radermacher, "Approximation-Assisted Optimization for novel compact heat exchangers," *HVAC&R Research*, vol. 16, no. 5, pp. 707-728, 2010.

[77] O. Abdelaziz, Development of multi-scale, multi-physics, analysis capability and its application to novel heat exchanger design and optimization, College Park, MD: PhD Thesis presented to the Department of Mechanical Engineering at the University of Maryland, 2009.

[78] D. Bacellar, O. Abdelaziz, V. Aute and R. Radermacher, "Novel heat exchanger design using Computational Fluid Dynamics and Approximation Assisted Optimization," in *ASHRAE Winter Conference*, Chicago, 2015.

[79] K. Saleh, O. Abdelaziz, V. Aute, R. Radermacher and S. Azarm, "Approximation assisted optimization of headers for new generation of air-cooled heat exchangers," *Applied Thermal Engineering*, vol. 61, pp. 817-824, 2013.

[80] C. Hedderich, M. Kellher and G. Vanderplaats, "Design and optimization of air-cooled heat exchangers," *Journal of Heat Transfer*, vol. 104, no. 4, pp. 683-690, 1982.

[81] D. Mayne and E. Polak, "Feasible directions algorithms for optimization problems with equality and inequality constraints," *Mathematical Programming*, pp. 67-80, 1976.

[82] M. Hestenes, "Multiplier and gradient methods," *Journal of OPtimization, Theory and Applications*, vol. 4, no. 5, pp. 303-320, 1969.

[83] K. Deb, "Genetic algorithms for optimization," KanGAL Report No. 2001002, Kanpur, India, 2001.

[84] L. Gosselin, M. Tye-Gingras and F. Mathieu-Potvin, "Review of utilization of genetic algorithms in heat transfer problems," *International Journal of Heat and Mass Transfer*, vol. 52, pp. 2169-2188, 2009.

[85] L. Huang, V. Aute and R. Radermacher, "A survey of optimization formulations and techniques for the design of heat exchangers using lower GWP refrigerants," in *ASHRAE Winter Conference*, Chicago, IL, 2015.

[86] N. Queipo, R. Devarakonda and J. Humphrey, "Genetic algorithms for thermosciences research: application to the optimized cooling of electronic components," *International Journal of Heat and Mass Transfer,* vol. 37, no. 6, pp. 893-908, 1994.

[87] G. Fabbri, "Optimum profiles for asymmetrical longitudinal fins in cylindrical ducts," *International Journal of Heat and Mass Transfer,* vol. 42, pp. 511-523, 1999.

[88] N. Cressie, Statistics for Spatial Data, New York: John Wiley & Sons, 1993.

[89] G. Wang and S. Shan, "Review of metamodeling techniques in support of engineering design and optimization," *Transactions of the ASME,* vol. 129, pp. 370-380, 2007.

[90] R. Webb and N. Kim, Principles of enhanced heat transfer, 2005.

[91] V. Zimparov and N. Vulchanov, "Performance evaluation criteria for enhanced heat transfer surfaces," *International Journal of Heat and Mass Transfer,* vol. 37, no. 12, pp. 1807-1816, 1994.

[92] T. A. Cowell, "A general method for the comparison of compact heat transfer surfaces," *Journal of Heat Transfer,* vol. 112, no. 2, pp. 288-294, 1990.

[93] K. Stone, "Review of literature on heat transfer enhancement in compact heat exchangers," Air Conditioning and Refrigeration Center at Univerity of Illinois, Urbana, IL, 1996.

[94] A. London, "Compact Heat Exchangers," *Mechanical Engineering ASME,* vol. 86, pp. 31-34, 1964.

[95] A. Bergles, A. Bllumenkrantz and J. Taborek, "Performance evaluation criteria for enhanced heat transfer surfaces," *Heat Transfer*, pp. 234-238, 1973.

[96] A. Bergles, R. Bunn and G. Junkhan, "Extended performance evaluation criteria for enhanced heat transfer surfaces," *Letters of Heat and Mass Transfer*, vol. 1, pp. 113-120, 1974.

[97] R. Webb, "Performance evaluation criteria for use of enhanced heat transfer surfaces in heat exchangers design," *International Journal of Heat and Mass Transfer*, vol. 24, no. 5, pp. 715-726, 1981.

[98] R. Shah, "Compact heat exchanger surface selection methods," in *Heat Transfer*, Toronto, CA, 1978.

[99] F. McClintock, "The design of heat exchnager for minimum irreversibility," in *ASME Annual Meeting, Paper No. 51-A-108*, 1951.

[100] A. Bejan, "The concept of irreversibility in heat echanger design: counterflow heat exchangers for gas-to-gas applications," *Journal of Heat Transfer*, vol. 99, pp. 374-380, 1977.

[101] A. Bejan, Entropy generation through heat and fluid flow, New York, NY: Wiley & Sons, 1982.

[102] A. Bejan, Entropy Generation Minimization: The Method of Thermodynamic Optimization of Finite-Size Systems and Finite-Time Processes, CRC Press, 1995.

[103] A. Bejan, G. Tsatsaronis and M. Moran, Thermal Design and Optimization, John Wiley & Sonos, 1996.

[104] A. Bejan and P. Pfister, "Evaluation of heat transfer augmentation techniques based on their impact on entropy generation," *Letters in Heat and Mass Transfer*, vol. 7, pp. 97-106, 1980.

[105] D. Seculic' and C. Herman, "One approach to irreversibility minimization in compact crossflow heat exchanger design," *International Communications in Heat and Mass Transfer,* vol. 13, pp. 23-32, 1986.

[106] B. Chen and W. Huang, "Performance evaluation criteria for enhanced heat transfer surfaces," *International Communications in Heat and Mass Transfer,* vol. 15, pp. 59-72, 1988.

[107] A. Bejan, "Second-Law analysis in heat transfer and thermal Design," *Advances in Heat Transfer,* vol. 15, pp. 1-58, 1982.

[108] R. Shah and T. Skiepko, "Entropy generation extrema and their relationship with heat exchanger effectivenss-number of transfer unit behavior for complex flow arrangements," *Journal of Heat Transfer,* vol. 126, pp. 994-1002, 2004.

[109] K. Ogiso, "Duality of heat exchanger performance in balanced counter-flow systems," in *Proceedings of the International Symposium on Compact Heat Exchangers*, 2002.

[110] K. Ogiso, "Duality of heat exchanger performance in balanced counter-flow systems," *Journal of Heat Transfer,* vol. 125, no. 3, pp. 530-532, 2003.

[111] C. J. Hermes, "Conflation of e-Ntu and EGM design methods for heat exchangers," *International Journal of Heat and Mass Transfer,* vol. 55, pp. 3812-3817, 2012.

[112] A. Gheorghian, A. Dobrovicescu, L. Popescu, M. Cruceru and B. Diaconu, "Entropy generation assessment criterion for compact heat transfer surfaces," *Applied Thermal Engineering,* vol. 87, pp. 137-149, 2015.

[113] Z. Guo, H. Zhu and X. Liang, "Entransy - a physical quantity describing heat transfer ability," *International Journal of Heat and Mass Transfer,* vol. 50, pp. 2545-2556, 2007.

[114] A. Bejan, ""Entransy" and its lack of content in physics," *Journal of Heat Transfer*, vol. 136, pp. 1-6, 2014.

[115] J. F. Guo and M. Xu, "The Application of Entransy Dissipation Theory in Optimization Design of Heat Exchanger," *Applied Thermal Engineering*, vol. 36, pp. 227-235, 2012.

[116] W. Kays, M. Crawford and B. Weigand, Convective Heat and Mass Transfer, New York, NY: McGraw-Hill, 1993.

[117] L. T. Bergman, A. S. Lavine, F. P. Incropera and D. P. DeWitt, Fundamentals of heat and mass transfer - 7th Edition, John Wiley & Sons, 2011.

[118] E. Grimison, "Correlation and utilization of new data on flow resistances and heat transfer for cross flow of gases over tube banks," *Transactions ASME*, vol. 59, pp. 583-594, 1937.

[119] A. Žukauskas, "Heat Transfer from Tubes in Cross Flow," in *Advances in Heat Transfer*, New York, Academic Press, 1972.

[120] B. Launder and T. Massey, "The numerical prediction of viscous flow and heat transfer in tube banks," *Journal of Heat Transfer*, vol. 100, pp. 565-571, 1978.

[121] O. Bergelin, G. Brown and S. Doberstein, "Heat transfer and fluid friction across banks of tubes - IV," *Transactions ASME*, vol. 74, pp. 953-960, 1952.

[122] M. Fujii, T. Fujii and T. Nagata, "A numerical analysis of laminar flow and heat transfer of air in an in-line tube bank," *Numerical Heat Transfer*, vol. 7, pp. 89-102, 1984.

[123] H. Hausen, Heat Transfer in Counter Flow, Parallel Flow and Cross Flow, New York: McGraw-Hill, 1983.

[124] J. Tabokek, G. Hewitt and N. Hamdia, Heat Exchangers : Theory and Practice, Washington: Hemisphere, 1983.

[125] E. Gaddis and V. Gnielinski, "Pressure drop on the shell side of shell-and-tube heat exchangers with segmental baffles," *Chemical Engineering and Processing*, vol. 36, pp. 149-159, 1997.

[126] T. Wung and C. Chen, "Finite Analytic Solution of Convective Heat Transfer for Tube Arrays in Crcssflow: Part I-Flow Field Analysis," *Journal of Heat Transfer*, vol. 111, pp. 633-640, 1989.

[127] T. Wung and C. Chen, "Finite analytic solution of convective heat transfer for tube arrays in crossflow: Part II - Heat transfer analysis," *Journal of Heat Transfer*, pp. 641-648, 1989.

[128] M. Dhaubhadel, J. Reddy and D. Telionis, "Finite element analysis of fluid flow and heat transfer for staggered banks of cylinders in crossflow," *International Journal of Numerical Methods Fluids*, vol. 7, pp. 1325-1342, 1987.

[129] S. Beale and D. Spalding, "A numerical study of unsteady fluid flow in in-line and staggered tube banks," *Journal of Fluids and Structures*, vol. 13, pp. 723-754, 1999.

[130] A. Wilson and M. Bassiouny, "Modeling of heat transfer for flow across tube banks," *Chemical Engineering and Processing*, vol. 39, pp. 1-14, 2000.

[131] E. Buyruk, "Numerical study of heat transfer characteristics on tandem cylinder, inline and staggered tube banks in crossflow of air," *International Communications of Heat and Mass Transfer*, vol. 29, pp. 355-366, 2002.

[132] W. Khan, J. Culham and M. Yovanovich, "Convection heat transfer from tube banks in crossflow: Analytical approach," *International Journal of Heat and Mass Transfer*, vol. 49, p. 4831–4838, 2006.

[133] F. McQuiston, "Correlation of heat, mass and momentum transport coefficients for plate-fin-tube heat transfer surface," *ASHRAE Transactions*, vol. 84, no. 1, pp. 294-308, 1978.

[134] D. Gray and R. Webb, "Heat transfer and friction correlations for plate finned-tube heat exchangers having plain fins," in *Proc. 8th. Heat Transfer Conference*, 1986.

[135] R. L. Webb, "Air-side heat transfer correlations for flat and wavy plate fin-and-tube geometries," *ASHRAE Transaction,* vol. 96, no. 2, pp. 445-449, 1990.

[136] N. H. Kim, B. Youn and R. L. Webb, "Air-side heat transfer and friction correlations for plain fin-and-tube heat exchangers with staggered tube arrangements," *Journal of Heat Transfer*, vol. 121, pp. 662-667, 1999.

[137] C. Wang, K. Chi and C. Chang, "Heat transfer and friction characteristics of plain fin-and-tube heat exchangers, part II: Correlation," *International Journal of Heat and Mass Transfer,* vol. 43, pp. 2693-2700, 2000.

[138] N.-H. Kim, J.-H. Yun and R. L. Webb, "Heat transfer and friction correlations for wavy plate fin-and-tube heat exchangers," *Journal of Heat Transfer,* vol. 119, no. 3, pp. 560-567, 1997.

[139] C. C. Wang, W. L. Fu and C. T. Chang, "Heat transfer and friction characteristics of typical wavy fin-and-tube heat exchangers," *Experimental Thermal and Fluid Science,* vol. 14, pp. 174-186, 1997.

[140] C.-C. Wang, J.-Y. Jang and N.-F. Chiou, "A heat transfer and friction correlation for wavy-fin-and-tube heat exchangers," *International Journal of Heat and Mass Transfer,* pp. 1919-1924, 1999.

[141] C. Wang, Y. Hwang and Y. Lin, "Empirical correlations for heat transfer and flow friction characteristics of herringbone wavy fin-and-tube heat exchangers," *International Journal of Refrigeration,* vol. 25, pp. 673-680, 2002.

[142] C. C. Wang, C.-L. Lee, C.-T. Chang and S.-P. Lin, "Heat transfer and friction correlation for compact louvered fin-and-tube heat exchangers," *International Journal of Heat and Mass Transfer,* vol. 42, pp. 1945-1956, 1999.

[143] C. Wang, W. Lee and W. Sheu, "A comparative study of compact enhanced fin-and-tube heat exchangers," *International Journal of Heat and Mass Transfer* , vol. 44, pp. 3565-3573, 2001.

[144] C. T'Joen, Y. Park, Q. Wang, A. Sommers, X. Han and A. Jacobi, "A review on polymer heat exchangers for HVAC&R applications," *International Journal of Refrigeration,* vol. 32, pp. 763-799, 2009.

[145] L. Cheng and C. W. M. Van Der Geld, "Experimental Study of Heat Transfer and Pressure Drop Characteristics of Air/Water and Air-Steam/Water Heat Exchange in a Polymer Compact Heat Exchanger," *Journal of Heat Transfer,* vol. 26, no. 2, pp. 18-27, 2007.

[146] C. Harris, K. Kelly, T. Wang, A. McCandless and S. Motakef, "Fabrication, Modeling, and Testing of Micro-Cross-Flow Heat Exchangers," *Journal of Microelectromechanical Systems,* vol. 11, no. 6, pp. 726-735, 2002.

[147] C. Harris, M. Despa and K. Kelly, "Design and Fabrication of a Cross Flow Micro Heat Exchanger," *Journal of Microelectromechanical Systems,* vol. 9, no. 4, pp. 502-508, 2000.

[148] J. Cevallos, A. Bar-Cohen and D. C. Deisenroth, "Thermal Performance of a Polymer Composite Webbed-Tubbe Heat Exchanger," *International Journal of Heat and Mass Transfer,* vol. 98, pp. 845-856, 2016.

[149] R. Felber, G. Nellis and N. Rudolph, "Design and Modeling of 3D Printed Air-Cooled Heat Exchangers," in *16th International Refrigeration and Air Conditioning Conference at Purdue,* West Lafayette, IN, 2016.

[150] M. Arie, Air Side Heat Transfer Enhancement in Heat Exchangers Utilizing Innovative Designs and the Additive Manufacturing Technique, College Park, MD: PhD Thesis Submitted to the Department of Mechanical Engineering at the University of Maryland, 2016.

[151] T. Shih and J. Zhu, "A new Reynolds stress algebraic equation model," NASA Lewis Research Center, Cleveland, OH, 1994.

[152] U. Schumann, "Realizability of Reynolds-stress turbulence models," *Physics of Fluids,* vol. 20, no. 5, pp. 721-725, 1977.

[153] T. Schmidt, "Heat transfer calculations for extended surfaces," *Refrigerating Engineering,* pp. 351-357, 1949.

[154] T. Ypma, "Historical development of the Newton-Raphson method," *SIAM Review,* vol. 37, no. 4, pp. 531-551, 1995.

[155] W. Oberkampf and G. Trucano, "Verification and validation in computational fluid dynamics," Sandia National Laboratories, Albuquerque, NM, 2002.

[156] W. Oberkampf and C. Roy, Verification and validation in scientific computing, Cambridge, UK: Cambridge University Press, 2010.

[157] P. L. Tiller, The NURBS book, New York: Springer, 1995.

[158] F. Incropera, D. Dewitt, T. Bergman and L. A.S., Fundamental of heat and mass transfer, Wiley, 2011.

[159] H. Jiang, V. Aute and R. Radermacher, "CoilDesigner: A general purpose simulation and design tool for air-to-refrigerant heat exchangers," *International Journal of Heat and Mass Transfer,* vol. 29, pp. 601-610, 2006.

[160] M. Shewry and H. Wynn, "Maximum entropy sampling," *Journal of Applied Statistics,* vol. 14, no. 2, pp. 165-170, 1987.

[161] M. McKay, R. Beckman and W. Conover, "A comparison of three methods for selecting values of input variables in the analysis of output from a computer code," *Technometrics,* vol. 21, pp. 239-245, 1979.

[162] J. Koplow, "A Fundamentally New Approach to Air-cooled Heat Exchangers," Sandia National Laboratories, Albuquerque, New Mexico 87185 and Livermore, California 94550, 2010.

[163] *Private Communications*, 2010.

[164] M. E. Steinke and S. G. Kandlikar, "Single-phase liquid friction factors in microchannels," *International Journal of Thermal Sciences,* vol. 45, p. 1073–1083, 2006.

[165] M. E. Steinke and S. G. Kandlikar, "Single-phase liquid heat transfer in microchannels," in *Proceedings of the 3rd International Conference on Microchannels and Minichannels, ICMM2005*, Toronto, ON, 2005.

[166] J. Winkler, V. Aute and R. Radermacher, "Comprehensive Investigation of Numerical Methods in Simulating a Steady-State Vapor Compression System," *International Journal of Refrigeration,* vol. 31, no. 5, pp. 930-942, 2008.

[167] C. C. Wang, W.-H. Tao and C.-J. Chang, "An investigation of the airside performance of the slit fin-and-tube heat exchangers," *International Journal of Refrigeration,* vol. 22, pp. 595-603, 1999.

[168] M. Beshr, V. Aute and R. Radermacher, "Multi-objective optimization of a residential air source heat pump with small-diameter tubes using genetic algorithms," *International Journal of Refrigeration,* vol. 67, pp. 134-142, 2016.

[169] D. Bacellar, V. Aute, J. Ling and R. Radermacher, "Integrated air-to-refrigerant heat exchanger and impeller". United States of America Patent 62/264692 (Provisional), 06 October 2014.